AD NUMBER
AD379232
CLASSIFICATION CHANGES
TO: unclassified
FROM: confidential
LIMITATION CHANGES
TO: Approved for public release, distribution unlimited
FROM: Distribution authorized to U.S. Gov't. agencies and their contractors; Administrative/Operational Use; 30 JUN 1965. Other requests shall be referred to Federal Aviation Administration, Washington, DC.
AUTHORITY
FAA ltr, 10 Oct 1972; FAA ltr, 10 Oct 1972

SECURITY MARKING

The classified or limited status of this report applies to each page, unless otherwise marked. Separate page printouts MUST be marked accordingly.

THIS DOCUMENT CONTAINS INFORMATION AFFECTING THE NATIONAL DEFENSE OF THE UNITED STATES WITHIN THE MEANING OF THE ESPIONAGE LAWS, TITLE 18, U.S.C., SECTIONS 793 AND 794. THE TRANSMISSION OR THE REVELATION OF ITS CONTENTS IN ANY MANNER TO AN UNAUTHORIZED PERSON IS PROHIBITED BY LAW.

NOTICE: When government or other drawings, specifications or other data are used for any purpose other than in connection with a definitely related government procurement operation, the U. S. Government thereby incurs no responsibility, nor any obligation whatsoever; and the fact that the Government may have formulated, furnished, or in any way supplied the said drawings, specifications, or other data is not to be regarded by implication or otherwise as in any manner licensing the holder or any other person or corporation, or conveying any rights or permission to manufacture, use or sell any patented invention that may in any way be related thereto.

Best Available Copy

Best
Available
Copy

NOTICES

When Government drawings, specifications, or other data are used for any purpose other than in connection with a definitely related Government procurement operation, the United States Government thereby incurs no responsibility nor any obligation whatsoever; and the fact that the Government may have formulated, furnished, or in any way supplied the said drawings, specifications, or other data, is not to be regarded by implication or otherwise as in any manner licensing the holder or any other person or corporation, or conveying any rights or permission to manufacture, use, or sell any patented invention that may in any way be related thereto.

Copies have been placed in the DDC collection. U.S. Government agencies may obtain copies from DDC. Other qualified DDC users may request, by submission of a DDC Form 1, through:

Director of Supersonic Transport Development
Federal Aviation Agency
Washington, D.C. 20553

Defense Documentation Center release to the Clearinghouse for Federal, Scientific, and Technical Information (CFSTI) and foreign announcement and dissemination are not authorized. The distribution of this report is limited because it contains technology identifiable with items excluded from export by the Department of State (U S. Export Control Act of 1949 as amended).

CONFIDENTIAL

Report No. PWA-2600 Volume 2
Date: 30 June 1965

SUPERSONIC TRANSPORT AIRCRAFT ENGINE

PHASE II-B DEVELOPMENT PROGRAM

FINAL REPORT (U)

Prepared Under Contract FA-SS-65-18

Period Covered 1 January through 30 June 1965

PWA-E. H. Document Control
Eng. Sub-Control Station

JUN 25 1965

Number: C63-5-C276-B

This document contains information affecting the national defense of the United States within the meaning of the Espionage Laws, Title 18 U S C, Sections 793 and 794. Its transmission or the revelation of its contents in any manner to an unauthorized person is prohibited by law.

Reproduction, distribution and use of this document are limited as specified in the contract under which it was prepared. Use for other than U. S. Governmental purposes is subject to prior approval of United Aircraft Corporation.

Approved by [illegible] C. W. Bristol, Jr.
Project Engineer

Pratt & Whitney Aircraft DIVISION OF UNITED AIRCRAFT CORPORATION

EAST HARTFORD • CONNECTICUT

FAA SECURITY CONTROL
NO. [illegible]

COPY NO.

DOWNGRADED AT 3 YEAR INTERVALS
DECLASSIFIED AFTER 12 YEARS
DOD DIR 5200.10

CONFIDENTIAL

ITEM 2A

STF219 TURBOFAN

ITEM 2 - DESIGN

OBJECTIVE

The contractor shall resolve critical problem areas in the preliminary engine configuration and undertake the design of the STF219 duct heating turbofan engine properly sized to the requirements of the supersonic transport aircraft. The contractor is also submitting design information and a preliminary layout of the STJ227 turbojet engine.

A. STF219 ENGINE

1. OVERALL ENGINE DESIGN

The general engine configuration arrived at during Phase IIA of the SST contract was retained during Phase IIB. However, the detailed design of the powerplant has resulted in refinement and changes in the details of the engine components.

a. Aerodynamic Design

The largest change was in the low pressure turbine and low pressure turbine exhaust case. These changes were necessary in order to provide efficient operation at both the 2200°F cruise turbine inlet temperature (required for the prototype and basic production rating) and at 1900°F cruise temperature which is the expected level at the start of commercial airliner operation. In order to accomplish this objective the exit annulus of the turbine was increased slightly and an efficient diffusing section was added downstream of the turbine to accept the higher turbine exit Mach numbers at the 2000°F TAKE OFF rating without excessive losses.

Further studies of the fan and high compressor rig results from testing conducted during Phase IIA indicated that lower specific inlet flows were necessary for both the fan and the high compressor. Although some weight increase is inherent in this approach the performance gains which were indicated justified the revisions. The specific designs still retain the advanced light-weight characteristic required by the S. S. T. powerplant.

The windmilling brake has been moved from the fan exit section to the inlet of the high compressor. This change is justified by detailed analytical studies conducted during Phase IIB.

These changes are discussed in detail in the following sections of this report.

The detailed design of the STF219 Fan Engine is continuing.

b. Mechanical Design

To obtain the maximum benefit from the Phase IIB design effort, four areas of the STF219 engine design were featured. It was necessary to resolve the many design trade-offs to determine the best component designs for the high compressor, high turbine, duct heater, and ejector-reverser in order to be ready to perform the complete engine detail design when the airframe's engine requirements are established. The design work which has been performed may be applied to the engine required when such important features as engine airflow, secondary airflow, location and angle of exhaust nozzle cant, mounting requirements, and accessory arrangements are established.

The ejector-reverser design has evolved from the Phase IIA twelve (12) element round design to the present eight (8) element octagonal configuration with a translating shroud ejector. This has resulted in improved mechanical features fewer parts, reduced seal leakage area, and a better secondary airflow path while providing improved installation compatibility for the various operating conditions. Airframe installation requirements have introduced a downward cant of the engine centerline at approximately the fan nozzle station.

c. Updated Engine Elevation

Figure 2A-0 represents the STF219 engine defined in this section of the report.

2. FAN

a. Aerodynamic Turbofan Studies

(1) Introduction

The Phase II-A study contract ended with the design of a fan engine which satisfied the performance and design objectives of the STF219 engine. This fan design was based on parametric studies and data from a limited number of transonic fan test rigs.

A detailed analytical study of test results from these and other transonic stage fans was undertaken and completed during the Phase II-A study contract. These rig results covered the range of aerodynamics required of the STF219 fan. The results of these transonic tests were then used to determine the final fan configuration during the Phase II-B detailed design. This resulted in some changes in the fan flow path from that shown in Phase II-A.

The original requirements of the fan were defined by the engine cycle studies. Subsequent discussions and changes during the detailed design resulted in a two-stage fan having the following parameters:

$\frac{W\sqrt{\theta_{T2}}/\delta_{T2}}{A}$	40.0
Pressure Ratio (avg)	2.62
Pressure Ratio Duct	2.70
Pressure Ratio Engine	2.50
Hub/Tip Ratio	0.412
Corrected Tip Speed (ft/sec)	1552

Other general requirements which influenced the fan design were:

1. No inlet guide vane - This decision was made largely to reduce the fan weight and noise level.

2. Fan bypass ratio of 1.3 - STF219 engine cycle performance requirements.

3. The Mach number leaving the duct and engine were specified.

(2) Discussion of Design

(a) Flow Path - The original aerodynamic design requirements stated in the Phase II-A contract determined the general fan elevation. The inlet specific flow $W\sqrt{\theta}/\delta A$, hub/tip ratio and tip speed set the inlet elevation. These parameters were varied somewhat during the early part of the design but the small advantages to be gained did not warrant any appreciable deviation from the original design

The exit diameter of the fan was made compatible with the STF219 high-pressure compressor, although some increase in exit diameter could have been used advantageously. This increase in diameter was held to a minimum so that the radial inflow of gas along the inner wall of the intermediate case would not be excessive.

The specific flow from the engine portion of the fan was set at 37.0 lb/sec/ft^2 to be compatible with the inlet flow to the high-pressure compressor. The second-stage stator was designed to remove only the exit swirl necessary to make it compatible with the inlet of the high-pressure compressor. The duct exit guide vane (DEGV) discharge Mn was set at 0.45. This level of Mn considered the amount of diffusion and associated diffusion losses necessary to lower the fan Mn to an acceptable level in the duct heater.

An IBM program using flow streamline definition and radial equilibrium evaluated a number of different flow paths and the effects of the following parameters:

1. stage pressure ratio variation
2. stage spanwise pressure slope
3. entrance swirl to second-stage stator
4. flow path overall convergence
5. flow path wall curvature
6. wheel speed
7. inlet hub/tip ratio

The airfoil loadings (D_{factor} and $\Delta P/q$) and approach Mn were the most influential parameters in determining an acceptable flow path. Transonic stage rig studies indicated that rotors could tolerate higher loading levels than stators without as large a stage efficiency loss. Therefore, rotor D_f's were limited to about 0.6 while stator D_f's were limited to about 0.5. The stator approach Mn was limited to a maximum of 0.85 to avoid choking and excessive losses.

The final flow path as shown in Figure 2A-1 has a tip speed of 1550 ft/sec, a compromise between stress and aerodynamic loading. No inlet swirl was used at the entrance to the second stage since the study showed no advantage for this effect.

As much overall flow path convergence as possible was used to reduce loadings without exceeding Mach numbers and specific flow limits. More convergence was put into the stators than rotors.

The wall radii of curvature was designed to be at least 0.5 feet to prevent severe distortions of the flow pattern.

Positive work slopes were included in both rotors to reduce root loadings to acceptable levels resulting in an engine Pr of 2.50 and a duct pressure ratio of 2.70. The individual rotor pressure ratios of this design are shown in Figures 2A-2, 2A-3 and 2A-4. Figures 2A-5 through 2A-24

show the important aerodynamic parameters of this design. The following table summarizes the maximum levels of Mach number and loadings:

	Mn	$\Delta P/q$	"D_f"
Rotor 1	1.52 (tip)	0.77	0.59
Stator 1	0.80 (root)	0.45	0.52
Rotor 2	1.39 (tip)	0.79	0.61
Stator 2	0.85	0.49	0.525
DEGV	0.68	0.59	0.54

To obtain the proper level of loadings on the DEGV and second stator, an IBM program was used which allowed the simulation of a flow splitter behind the second rotor. The splitter nose was set close to the rotor trailing edge and slightly inward radially from a neutral location. Previous engine experience has shown that this will cause a convergence of the stream tubes through the second rotor root and will unload the rotor root section.

The proximity of the splitter nose to the rotor trailing edge tends to prevent the rotor root section load from fluctuating to a large extent during off-design operation.

The rotor and stator losses assumed are shown in Figures 2A-25 and 2A-26. These values were estimated from data obtained from the transonic rigs.

All aerodynamic studies were conducted with effective wall diameters with no provisions for boundary layer growth or rotor shroud blockage. For the final mechanical flow path, adjustments were made for both of these effects. The sum total of the boundary layer correction for both walls was about 0.5% of the passage height at the first rotor inlet to 1.4% at the second rotor exit.

The blades were designed to have part span shrouds at the 50% and 85% radial locations. To compensate for the shroud blockage effect on the flow area, an area equivalent to one-third of the shroud blockage was assumed to extend forward to the blade leading edge and an equivalent area of two-thirds of the blockage to the blade trailing edge. This correction amounted to approximately 1.1% and 2.4% change in passage height at the first rotor leading and trailing edge stations respectively and 1.5% and 3.3% in passage height at the second rotor stations. A new wall was faired through these rotor diameters to retain the original wall curvatures.

The shroud angles were set to align the shrouds with the average meridional flow angle through the blading at the shroud spanwise location.

(b) Airfoil Type - The high Mach numbers at the rotor tip indicated a high Mn airfoil should be used. Test data to date indicates that "J" blades have lower losses than circular arc (C. A.) airfoils in the supersonic range. For this reason a "J"-type airfoil section was used from about the 1.1 Mn streamline out to the tip. Circular arc airfoils were used at the root sections and in all stators.

A gradual transition from C. A. to "J" section was made with an s/b of 0.5 at the tip.* This s/b was felt to be a reasonable level in view of the Mach number. Enough cambered section was retained, however, to prevent extremely high deviations which might occur with a higher s/b, which concentrates all of the turning at the trailing edge.

* s/b is the ratio of straight section length to total chord length for the "J" blade.

All airfoil thicknesses were made as thin as was practical. The blade thicknesses (t/b) were set to 0.08 at the root and 0.03 at the tip, based on the chord along the streamlines. The blade root spacing (τ /b) was set slightly less than 0.5, and the taper ratio was set as high as res reasonable from a stress consideration. A root τ/b of much less than 0.5 was not felt to be possible based on blade attachment considerations.

The first stator was tapered to provide a tighter τ/b at the tip while the second stator and the DEGV have constant chords. The thickness ratio (t/b) variation of the first and second stators is 0.05 to 0.07 from the root to the tip. Local thickness increases at the end walls to reduce the stress levels to approximately 30,00(psi at the design point.

(c) Airfoil Angles - The design program defines all required air triangles in a plane perpendicular to the engine axis. Since the airfoil leading and trailing edges normally do not lie in this plane but in a plane canted to the engine axis, air angles had to be corrected to adjust them to the same axial location as the leading and trailing edges.

(d) Incidence - Studies from the transonic stage rigs determined the amount of incidence used in the initial design of the rotor blades. After checking the blades for choking tendencies, the incidence

was adjusted. The final rotor incidence is shown in Figure 2A-27 for the first and second stage rotors. Incidence is defined as an angle measured relative to the surface of the airfoil (ISS). At these incidence levels the average blade throat A/A* and the worse streamline A/A* are:

	A/A*(ave)	A/A* min
Rotor 1	1.09	1.05
Rotor 2	1.08	1.06

The first stator incidence was initially set at the minimum loss angle at the design point but was later adjusted to reduce the amount of acceleration from the free stream to the throat in the mean-to-tip region. The final incidence is shown in Figure 2A-28.

The second stator incidence was set at -1° at the root and +1.5° at the tip to give a smooth reduction in inlet Mach number entering the stator. The DEGV incidence was set at +2° from root to tip.

(e) Deviation - Regardless of how the airfoil section itself was defined, the air turning along the streamlines would be used to define the amount of deviation between the gas exit angle and the blade metal angle. It was found that Carter's rule did not estimate sufficient deviation for the type of blading used. A correlation of the deviation from the transonic stage rigs is shown in Figure 2A-29. This was used in the design of the rotor blades.

The stator deviations from Pratt & Whitney Aircraft C. A. airfoil correlations were found to be up to 1° greater than those calculated by Carter's rule. The final stator deviations were set by these correlations.

(f) Choking - The choking tendencies of all airfoils were investigated. The first and second rotors and the first stator were checked for choking by three-dimensional analysis. This involved determining the location of the minimum channel passage area as calculated from the channel width and stream tube height. The large amount of annular convergence and the streamline curvature caused the minimum area to be rearward of the leading edge.

(g) Defining Airfoils - The actual airfoils to be manufactured were defined along cylindrical surfaces instead of stream tubes or conical surfaces. The definition of the cylindrical airfoil was obtained by rotating the metal angles from the meridonally defined airfoil through the flow slope angle. This set the metal angles relative to a cylindrical surface.

In determining the final rotor blade shapes, the center of gravity of all airfoil sections were stacked in a radial line. This stacking line was then tilted about the root stacking point to reduce the gas bending stresses. This tilt was sufficient to just equalize the gas bending stresses.

The leading and trailing edge thickness of all airfoils were standard, except the rotors were thickened somewhat to make them less susceptible to foreign object damage.

b. Mechanical Description

(1) General Description

The STF219 engine includes a two-stage fan and a five-stage axial flow high pressure compressor (see Figure 2A-1). Air flows into the fan from the inlet and is subsequently split into two streams, one which flows through the high pressure compressor, and one which passes into the discharge ducting.

The fan and compressor sections are separated by an intermediate section which supports the fan and compressor sections, and provides space and support for the number 1 and 2 thrust bearings.

(2) Fan

Analytical studies of transonic stage fans undertaken during Phase II-B have resulted in small changes to the fan flowpath. The required changes were incorporated, and the Phase II-A mechanical configuration checked to determine the effects of these changes. The required flowpath changes did not require altering of the basic rotor structure.

The Phase II-A design configuration with the fan hub supporting both fan stages overhung from a single thrust bearing and the second stage disk with an integrally flanged spacer fastened to the first stage basically has not changed. The aerodynamic revisions mentioned in the preceding section have been incorporated, and the aerodynamic brake system has been removed from the fan section and relocated at the inlet to the high compressor.

The first and second stage fan blades have dovetailed roots which are inserted into conforming slots into the disk rim to constrain the blades radially. A tab on the forward side of the blade root prevents the blade from being driven rearward by the impingement of any ingested foreign objects. The first stage blades are prevented from moving forward by the nose cone attachment spacer. Forward movement of the second

stage blade is prevented by a ring with tabs which lock into machined slot in the blade attachment.

The second stage interstage seal has been made integral with the lockring. This combination seal-lockring is riveted to a flange on the rear of the second stage disk. The disk flange is also used for balancing by inserting the necessary weights between scallops in the lockring flange.

Airfoils with two shrouds have been incorporated in both fan stages. These shrouds are placed at specific locations along the airfoil span to insure structural integrity of the blade and disk system.

The shrouds are protrusions integral with the blades which are linked together by the contacting bearing surfaces of adjacent shrouds when the blades are assembled on the rotor disks. Vibrations normal to the plane of contact are restricted by the mechanical stiffness of adjacent blades, and vibrations parallel to the contact surface are dampened by frictional drag. The frictional force potential is obtained by the natural untwisting tendency of the twisted airfoil, as described in Fan Structural Analysis. The contact areas are flame-plated with tungsten carbide, and sufficient bearing area is provided to keep friction wear to acceptable levels. The airfoils are offset forward of the center of the dovetail attachment so that a centrifugal moment is induced to counteract the moment caused by the gas loading and to insure optimum uniform attachment loading.

The first and second stage disk and blade assemblies are statically balanced to specified limits by adding balance weights to flanges on the disks. The disks are then dynamically balanced together to minimize rotor vibration. Suitable fits between mating parts are obtained to resist separation during all critical steady-state and transient operating conditions. This insures maintaining alignment and concentricity for dynamic balance.

Radial loads from the rotor are transmitted to the number 1 bearing through the fan hub, which is supported by the thrust bearing and has mating splines to transmit torque loads to the low-speed turbine drive shaft. The splines are forward of the thrust bearing to insure continued spline engagement and to prevent uncoupling of the fan and turbine rotors and the subsequent serious turbine overspeeding should a major bearing failure occur.

A positive pressure differential is maintained across the front bearing compartment seal to prevent the possibility of oil leakage from the compartment. Pressurized air for this purpose is bled from behind the second stage rotor, channeled up the side of the intermediate case, and

vented through holes in the seal ring to a compartment outside of the carbon seal. The pressure in the compartment is maintained by a pair of knife-edge seals between the fan rotor hub and the thrust bearing support structure. An additional seal is located on the rear of the second stage disk to reduce the thrust loading on the number 1 bearing and consequently to increase the bearing life.

One interstage seal is used between the first and second fan stages. This seal is riveted to a flange on the integral conical spacer of the second stage disk and rotates in close proximity to the stator seal ring. The clearance between the seal and seal ring is as small as possible while still providing for the maximum tolerance buildup, the maximum radial differential thermal expansion encountered during steady-state operation, and elastic radial deflections during high-performance operations. These provisions will permit light, non-destructive rubbing during transient thermal or overspeed operation.

Blade tip clearances were similarly established with provisions made for the maximum tolerance buildup, the maximum differential radial and axial thermal growths anticipated during transient operation, the radial elastic disk and blade growths during normal high-temperature operation, the anticipated effects of surge, and foreign object ingestion. To permit small clearances, an abradable material is used inside the fan case. This will prevent severe blade-to-case rubbing resulting from blade deflections caused by foreign object ingestion and will permit light, non-destructive rubbing during operation at the maximum adverse conditions.

Axial gaps between the forward side of the rotating parts and the adjacent stationary parts are established by providing for the maximum total tolerance accumulation, the maximum axial differential thermal growths during transient operations, the maximum net end-play accumulation, the computed net intermediate case deflection, the maximum anticipated forward blade tip deflections resulting from foreign object ingestion, and the deflection encountered during surges.

The axial gaps and seal land lengths between the rear side of rotating and adjacent stationary parts provide for the maximum total tolerance accumulation, the maximum axial differential thermal growths during transient operation, the maximum net end-play accumulation, the estimated fan rotor hub net rearward deflection resulting from centrifugal loading, the maximum forward stator vane deflection resulting from gas loads during steady-state operation, the maximum rearward blade tip deflection resulting from foreign object ingestion, the maximum deflection during surges, and the maximum forward seal support diaphragm deflections resulting from steady-state pressure loads.

The first stage stator is made of forged titanium (PWA 1202). Integral platforms are forged at the inner and outer ends of the vanes to form the flowpath and to facilitate vane attachment. The vane is attached to the front fan case by a flange extension at the rear of the platform and is held in place by an annular ring integral with the fan case at the front of the platform. The inner rear feet are riveted to an annular ring, and the inner forward feet are riveted to an annular diaphragm integral with the seal ring.

Since the location of the aerodynamic brake has been changed, (Refer to Aerodynamic Brake), the second stage vanes which were previously used as an aerodynamic brake have been redesigned using titanium strip stock (PWA 1202). Box shroud construction at the foil root and tip sections has been utilized. The splitter ring has been redesigned so that it is separate and removable from the second stage vane assembly. The vane assembly intermediate shroud and outer shroud are piloted to the intermediate case. The inner vane assembly shroud and the second stage seal land are bolted to the front inner flange of the intermediate case. Vane torque loads are absorbed by the bolts holding the inner shroud and by machined lugs at the outer shroud. This type of construction gives sufficient mechanical flexibility to absorb large radial and axial thermal expansions.

The fan cases and support cases were altered where necessary to conform to flowpath changes and to contain the redesigned blades. The fan cases, mount ring, and support cases are made of titanium (A-110) and are cantilevered from the front flange of the intermediate case. Within the fan cases space has been allowed for a liner configuration suitable for either abradable material, honeycomb, or a combination of the two. The liner thicknesses and construction is determined by the amount of blade tip excursion under adverse conditions. Use of honeycomb construction as a liner back-up ring permits lightweight construction while maintaining the relative stiffness needed for large diameter rings. A stiff back-up ring will resist liner buckling if hard blade tip rubs should occur.

The selected configuration allows easy liner replacement in the field and easy interchangeability for testing new liner materials under development.

c. Structural Analysis

(1) Introduction

Extensive turbofan engine experience over the past years at Pratt & Whitney Aircraft has led to the formulation of a series of necessary

structural criteria for fan designs. Some of the more significant items considered in the structural design of the STF219 fan section are as follows:

1. Airfoil flutter margin
2. Blade and disk resonant vibrations
3. Bird ingestion capabilities
4. Centrifugal stresses
5. Blade attachment stresses
6. Shroud locking forces

Details of each category, as applied to the STF219, are discussed below.

(2) Airfoil Flutter Problems

The Phase II-A STF219 proposal featured high aspect ratio blades (4.5 first stage and 5.5 second stage) with one shroud per stage in an attempt to obtain minimum weight. Subsequent test experience with rigs of similar geometry and a review of Pratt & Whitney Aircraft fan flutter experience in general led to the use of double shrouds and a more modest 4.5 aspect ratio on the second rotor blade. The resultant design will incorporate adequate flutter margin and still be an advanced, lightweight concept compared to present production fans. A comparison of fan parameters is given in Table 1.

Double-shrouded fan blades have been used successfully in the C-5A program for the JTF14F demonstrator engine. This engine has similar aspect ratios and blade series as the STF219 (see Table 1). Limited running on this engine has indicated no flutter or resonant frequency problems.

(3) Blade and Disk Resonant Vibrations

The predicted resonances shown in Figure 2A-30 indicate that both rotors will be free of 2E resonance within the engine running range. The 2E margin is well within the 7 1/2 percent vibration considered allowable, based on previous Pratt & Whitney Aircraft compressor and fan experience.

TABLE 1

FAN BLADE PARAMETERS

	Engine & Stage				
Parameter	TF33-P-7 Stage 1	JT8D-1 Stage 1	JTF14F Stage 1	STF219 Stage 1	STF219 Stage 2
t/b* Root	0.091	0.104	0.07	0.086	0.086
t/b Inner Shroud	0.049	0.050	0.046	0.052	0.052
t/b Outer Shroud	-	-	0.028	0.032	0.032
L/b Root (Aspect Ratio)	4.26	4.2	4.48	4.56	4.5
Inner Shroud Station (% of Length)	63	60	50	50	50
P/A Stress at Design Speed (psi)	45,600	38,300	51,300	46,000	32,000
Blade Series	Modified Circ. arc	Circ. arc	J	J	J
No. of Shrouds	1	1	2	2	2
Chord at Root	3.79	3.08	5.50	3.70	2.41

* Blade section maximum thickness to chord ratio

(4) Bird Ingestion Capabilities

The bird ingestion capability of the STF219 first stage fan blade is shown in Figure 2A-31 where a bending stressparameter is plotted vs. blade length. This parameter is used on a comparative basis with other Pratt & Whitney Aircraft engines which have exhibited adequate margin in this respect.

As can be seen, the STF219 is in the marginal range for pin-jointed and single-shrouded blades. The use of two shrouds will, however, increase bird ingestion resistance into the safe range. Again, the JTF14F is in a similar position and any test experience gained with it will be useful to the STF219 development program.

Bird ingestion was not considered for the second stage fan blade, since Pratt & Whitney Aircraft experience has shown that only first stage rotors must be designed to withstand this hazard.

(5) Centrifugal Stresses

The P/A stresses in the STF219 fan are in the same range as other engines (see Table 1 and 2). Adequate creep and yield margin exists for AMS 4928 titanium at the Mn 2.7 cruise condition for 6,000 hour life.

TABLE 2

STF219 CENTRIFUGAL STRESS

	Stage 1	Stage 2
SLTO Condition		
P/A Stress* (psi)	49,000	34,000
Blade Temp Root (°F)	100	190
0.2% Y.S. AMS 4928 (psi)	107,000	101,000
MN 2.7 65,000 feet		
P/A Stress* (psi)	41,000	28,500
Blade Root Temp (°F)	518	584
1% Creep, 6000 Hrs., AMS 4928	76,000	70,000

* Maximum Deteriorated Speed

(6) Blade Attachments

Although no detailed design work has been completed in this area, a preliminary analysis indicates that there is adequate pitch in the disk rim to accomodate the use of conventional dovetail attachments to support the blades.

(7) Shroud Locking

The conventional single-shrouded compressor blade is usually assembled line-on-line or with slight interference at the contact surfaces. Under the influence of the centrifugal forces the blade tends to untwist toward the root stagger angle and the shrouds lock against each other. This action causes the shroud to act as one continuous ring in resisting blade motion. The STF219 second stage has a negligible change in chord angle (α c) between shrouds and, therefore, blade twist alone is insufficient to

effectively lock both shrouds. To provide an adequate locking force the blade will be preloaded at assembly with about 5° pretwist making the shroud locking load compatible with existing fan stages (see Table 3). Since the second blade is very flexible, the forces to cause this pretwist are quite small (about 65 in./lbs.). Hence, no assembly problems are anticipated.

The structural design of the fan blades and disks is continuing at present.

TABLE 3

FAN SHROUD LOCK LOAD COMPARISON

Engine	Stage	Shroud Locking Parameter (FR/Zb^3)
JT3D-1	1	8.2
	2	4.0
JT8D	1	6.9
JTF10 A-20	1	12.4
	2	8.5
JTF14F	1	4.9 (Sum of 2 shrouds)
STF219	2	5.0 (Sum of 2 shrouds)

* F = shroud contact force
R = radius to shroud
Z = number of blades
b = average chord

Note: High value of parameter indicates high shroud locking force.

3. INTERMEDIATE SECTION

a. General Description

The structure between the fan and high pressure compressor is called the intermediate section. This section is largely a single, welded AMS 5616 stainless-steel structure as seen in Figure 2A-1. It incorporates sections of the fan duct outer wall, the compressor flow path inner wall, and the high compressor flow splitter. Eight radial struts extend from the outer wall to the inner wall. The fan exit guide vanes

are incorporated just forward of these struts. The fan rotating parts are overhung in front, and the gas generator is cantilevered from the rear of the splitter ring. In general the structure provides:

1. Support for the fan and gas generator

2. Housing and supports for the number 1 and 2 bearing compartment

3. Power take-off at the top vertical centerline for airframe drive

4. Power drive at the left horizontal centerline for the engine gearbox (shifted 45° downward for the Lockheed engine)

5. Tachometer drive scavenge pump and drain for the number 1 bearing compartment at bottom vertical center line.

Four of the eight radial struts are of thicker construction to provide access to the number 1 and 2 bearing compartment for external power drives. These struts are located on the engine horizontal and vertical centerlines as shown in Figure 2A-32. A schematic view of this area is presented in Figure 2A-33. A detailed discussion of this spacing is presented in the Aerodynamics section. One strut houses an air line to pressurize the labyrinth seal in front of the number 1 thrust bearing.

In the Phase II-A design the tachometer drive was located on the right horizontal centerline and the engine accessory gearbox mounted on the bottom vertical centerline. These positions have been changed to remove units containing combustible fluids from the bottom of the engine as a landing safety factor.

In the new locations positioning of the external scavenge sump and pump remained at the bottom vertical centerline for gravity drainage and space considerations. Provisions were made to incorporate the tachometer drive at this same position. Scavenge oil from the number 1 compartment drains through a sleeve surrounding the tachometer drive. The scavenge pump and tachometer are mounted in the sump.

A box structure inside the compressor flowpath inner wall provides flanges on the front and rear inner section to mount the number 1 and number 2 bearings. This box structure also supports the bearings for the towershaft drive. A detailed description of this system explaining changes from the Phase II-A design report is given in the Bearing section.

The bearings are lubricated and cooled by oil injected under the races. Number 1 bearing oil is picked up from a jet by an oil scoop just aft of the bearing. Number 2 bearing oil is collected in an internal groove which is an integral part of the accessory gear retaining nut. This groove previously was in a separate ring, but for simplicity and lower weight and cost the integral design was adopted during Phase II-B. The oil then flows through a series of holes in the bearing liner to an annulus cooling the inner race. It then flows radially to the bearing compartment through a series of holes in the seal rub plate.

Part of the oil also flows outward through a series of holes in the bearing liner to an annulus at the split inner race of the number 2 bearing. The inner race has radial slots which centrifugally force the oil into the bearing lubricating the balls.

The bearing compartment contains three carbon face seals, all supported by the intermediate case. Two seals are between the ends of the compartment and the low and high shafts, and the third is a double seal between the compartment and the intershaft annulus. The carbon face seal forward of the number 1 bearing has an oil-cooled face plate which utilizes oil from the number 1 bearing cooling passages. A three-lip labyrinth seal, pressurized by fan discharge air, is employed for controlling air leakage in case of carbon seal malfunction. Fan discharge air at a higher pressure than that maintained within the breather compartment will always flow into the compartment. This prevents contamination of the cabin pressurizing air from oil leakage past the seal face. The double carbon seal used between the intershaft annulus and the bearing compartment is protected from excessive air flow by a four-lip labyrinth seal. The front seal plate of the double seal is cooled by oil from the number 1 bearing oil scoop. The oil-cooled rear seal face plate of the double seal is supplied with oil from an internal groove fed by a jet. The carbon face seal behind the number 2 bearing is cooled by oil from the number 2 bearing cooling passages. A three-lip labyrinth seal protects this area. The basic design concepts used for seals were described in Volume E-VI of the Phase I proposal.

Two towershafts transmit power radially from the high compressor shaft front hub to the power take-off and accessory drive pads. A third towershaft is required to transmit the rotational speed from the fan rotor hub to a tachometer drive pad (AND 20005XVB). The established power requirements are the same as quoted in the Phase II-A specifications.

The power take-off pads are being designed to accomodate both the Boeing and Lockheed installations with the same requirements as the Phase II-A proposal. The Lockheed installation will have a right-angle drive on the top of the intermediate case, while the Boeing installation will have a plain pad. The side mounted gearbox pad will have a 310 H.P drive for Boeing and a 150 H.P. drive for Lockheed. Power for these towershafts is supplied by a spiral bevel gear integral with the number 2 bearing sleeve fitted to the compressor hub. The tachometer towershaft is driven from the rotor hub through spur and bevel gears.

The spiral bevel pinions for the drives are supported by a ball and roller bearing assembly bolted into the inner box structure. The shaft is connected to a stub shaft by a double spline coupling at the lower end. Loose fits at the coupling and at the shaft supports provide for possible misalignments.

Convoluted tubes are mechanically attached with tight pilots and puller groove provisions to the outer portion of the outer towershaft bearing support, and at the pedestals at the outer portion of the case. These tubes previously brazed. However, to accommodate repair or salvage of parts the mechanical scheme was devised. The convoluted tubes protect the struts and inner compressor wall from oil and, in conjunction with flanged bosses on the outside of the intermediate case, provide sealed passageways to the accessory gearbox and power take-off.

The intermediate case is attached to the rear cases at four locations. The outer fan duct wall provides a flange front and rear for mounting to the outer duct wall. The inner wall extends rearward to support the high compressor inlet vanes and the splitter structure extends rearward to support the inner gas generator. A flange joint is provided on the forward inner box assembly to support the inner fan exit guide vanes.

The splitter ring is located at approximately the 50% span position of the struts. It separates the engine flow from the fan flow and provides an attachment ring to support the gas generator through the outer high compressor case. This system allows the loads resulting from the overhung inner engine to be fed into the structure in a manner which most efficiently reduces local deformation and discontinuity. A load diagram for the intermediate section is shown in Figure 2A-34.

b. Fabrication

Experience gained during development of current high TBO Pratt & Whitney Aircraft turbojet engines was utilized in designing the intermediate case. The use of butt-welded construction throughout the basic structure reduces weld shrinkage, distortion, and built-in stress concentration points. This method of fabrication greatly facilitates inspection and quality control, and provides greater reliability in the structural integrity of the assembly.

Between the outer fan duct wall and the inner compressor wall are eight hollow machined struts. The compressor outer wall and fan duct wall are formed by welding sheet stock to contoured ribs on the sides of these struts.

The case is fabricated from Greek Ascoloy material. This material has been used very successfully in similar structures on several Pratt & Whitney engines. The low thermal coefficient of expansion of Greek Ascoloy reduces the thermal incompatibility of the steel case and the adjoining titanium cases.

c. Vibration

The intermediate case struts will produce wakes (both fore and aft) and possible excitation of the compressor blading. This has been taken into consideration in the blade design for each applicable compressor stage. This will be accomplished by blade frequency selection or friction damping.

d. Aerodyanmics

(1) Fan Duct - Duct Burner Section

Aerodynamic design of the duct intermediate case started at the strut leading edge and was carried through as part of the complete duct burner diffuser design. The flow area occupied by the strut cross sections have been accounted for by diverging the annulus walls to yield an equivalent diffusion conical angle of 9.2° and a diffusion area ratio of 1.27. This was included in the complete design of the duct burner diffuser, so that the intermediate case exit annulus is mated to the duct with no discontinuities in the flowpath.

(2) Fan Duct - High Compressor Inlet Section

Originally this portion of the intermediate case was required to provide a constant area duct to the inlet of the high pressure compressor. To relieve a cascade choke problem at the root of the high compressor first rotor and stator, it was found necessary to lower the specific flow into the high compressor. This change was made by reducing the high compressor inlet inner diameter 1.18 inches and necessitated a redesign of the intermediate case flowpath. To insure that the thick strut fairings would not unfavorably alter the diffusion rate required in the duct passage, three I.D. contours were examined in detail relative to the diffusion conical angle, the diffusion area ratio and the area distribution each contour yielded. The three I.D. contours were positioned between two axial stations which were considered inviolate; the fan rotor exit and the high compressor rotor inlet. Strut blockage was accounted for with each flowpath and the diffusion conical angle, the maximum diffusion conical angle, and the maximum diffusion area ratio were as follows:

Contour I.D.	Diffusion Conical Angle	Maximum Area Ratio
A	9.4	1.1437
B	9.35	1.1618
C	9.38	1.1307

I.D. Contour C was chosen for the design because it yielded the lowest maximum diffusion area ratio without compromising the diffusion conical angle.

(3) Diffuser Conical Angle

The struts in the engine portion of the intermediate case are staggered 75°, as shown in Sections A-A and B-B of Figure 2A-32, to alleviate a marginal choke problem and to reduce the turning required from the fan exit stator. The stator was originally designed at a low gap/chord ratio so that all the fan root swirl could be removed with one row of stators. Two factors interferred with this approach: the low gap/chord yielded a low choke margin at sea level take-off flow and, because of high compressor design, it was no longer desirable to turn the flow axially at the fan exit. For these reasons the fan exit stator gap/chord ratio was increased, and its turning was reduced to exit at 75°. To maintain this swirl the struts were oriented to align with the flow and to continue the fan exit swirl into the high pressure compressor. The

four struts are structurally and aerodynamically larger than necessary to accomodate accessory and lubrication requirements. These struts are placed around the duct circumference alternately with the thinner struts to minimize asymmetrical distortion.

e. Structures

Two cones provide support for the number 1 and 2 bearings. Both cones are connected together at their O.D. and I.D. to stiffen the structure and to reduce axial deflections caused by rotor thrust loads. The important feature in this structure is the included angle or apex angle of these cones. The smaller the angle, the stiffer this shell becomes.

The forward or number 1 bearing cone carries most of the thrust load for both the number 1 and 2 bearings. Maximum axial deflection is expected to be between 0.010 and 0.020 inches, depending on the final thrust balance loads, and maximum stress less than 50,000 psi. Attention was given to transition pieces in the bearing support structure. Since local high stresses will develop at the ends of the cones, the section transition or connecting shells were thickened locally. The sections were butt-welded to secure the best possible joint. This design should keep manufacturing costs and weight low.

The struts and support rings were structurally analyzed for the engine loads shown in Figure 2A-34. These loads are bearing loads, inner engine thrust load, maneuver loads, and aerodynamic loads. The most efficient design from a weight standpoint results when the rings supporting the main engine flowpath struts are as stiff as possible. The bearing support cones provide considerable stiffness to the inner rings. The outer rings are stiffened by the axial beams connecting the forward and aft rings. This feature makes this section act as a large box section, which is very efficient for the torsional loading induced by the strut reactions. The support rings were kept as close as possible to the leading and trailing edge of the struts to provide as much moment arm as possible. Also, the strut chord length was kept large to minimize the ring stresses and deflections. A solid connection between the struts and support rings is also provided. Thus, the weight of the struts and rings are kept to a minimum while the flexibility of manufacturing and structural integrity is maintained.

4. AERODYNAMIC BRAKE

a. Introduction

At high flight speeds where a high inlet-to-exit pressure ratio is imposed on the engine, the rotor speeds are nearly independent of throttle

setting. That is, flight idle or even windmilling operation does not significantly reduce rotor speeds because of the high inlet-to-exit pressure ratios imposed on the engine. In the event of an in-flight shutdown, low shaft speeds are required to reduce the possibility of damage to the engine. A windmilling throttle valve is required to provide for this speed reduction.

b. Discussion

The preliminary studies in Phase II-A indicated that some throttling would be required in both the duct and engine streams. This was to be accomplished by closing the exit vane of the fan.

A more detailed analysis of this problem was carried out in Phase II-B. This analysis consisted of establishing a computer program using engine component characteristics and "flying" the engine over a range of Mach numbers with two basic throttling schemes. The first scheme is described above, the second throttled only the gas generator. The second scheme showed that with the fan duct exit nozzle fully closed the low spool rpm can be reduced to 1500 rpm with a high spool rpm of 2000 at cruise Mach number. This combination of speeds is adequate to maintain oil pressure and low enough to eliminate engine damage. The second scheme has another advantage in that the gas generator valve will be the inlet vane to the high compressor. This same mechanism can be used as an aerodynamic variable inlet vane during development. The characteristics of this scheme are shown in Figures 2A-35, 36, and 37.

As noted in the previous discussion, the basic concept and control of the aerodynamic brake has been changed from that described in the Phase II-A Report, although its basic functions remain the same. The fan exit vanes are now stationary and the inlet guide vanes of the high pressure compressor serve two functions - aerodynamic brake and variable inlet guide vane. When the braking system is actuated, airflow through the compressor is decreased and rotor speeds are reduced to a range which has proven safe for subsonic windmilling engines.

To withstand the high stresses produced by aerodynamic braking, the compressor inlet guide vanes are made from PWA 1202 (Type 811 Titanium Alloy).

As shown in Figure 2A-38, the inlet guide vanes are pivoted on steel-backed carbon sleeve bushings at the outer intermediate case and the split inner intermediate flange. The vanes are rotated by a unison

ring connected by levers to the shaft extension on each vane. The unison ring is located between the outer intermediate case and the inner duct burner case, and is guided and supported by the vane connecting levers. Two pneumatic actuators, spaced 180° apart on the outside of the intermediate case and each operating a bellcrank and torque rod, move the unison ring tangentially and permit rotation of the vanes. The two torque rods are inserted through fan diffuser case struts located 180° apart. Torque from these rods is transmitted to the unison ring by levers and a slip joint.

Power for the actuators will be provided by engine bleed air during normal engine operation while the vanes are operating as inlet guide vanes. When the vanes are required to operate as an aerodynamic brake, power for the actuators will be provided by high pressure gas bottles, provided in the airframe for emergency control system power.

5. HIGH PRESSURE COMPRESSOR

a. Aerodynamic Design

(1) Introduction

During Phase II-A a high compressor was defined that accomplished an overall pressure ratio of 4.4 in five stages with a target efficiency of 86%. Since that time some changes have occurred which have slightly altered the design approach. The detailed design of the fan indicated advantages were to be gained by lowering the fan root pressure ratio from 2.7 to 2.5. This meant that the high compressor would have to be increased in pressure ratio to maintain a constant overall engine match point. In addition, more detailed information was accumulated from the five stage rig indicating changes in the early aerodynamic approach.

The design goals of the STF219 high pressure compressor are now:

	Sea Level Static	Cruise
Pressure Ratio P_{T4}/P_{T3}	4.77	2.84
Corrected Flow (lb/sec)	130	97.5
Adiabatic Efficiency	0.86	0.86

These goals are consistent with a 650 lb/sec turbofan engine with a bypass ratio of 1.3.

The detailed aerodynamic design was based on the following general ground rules:

1) The average exit Mn from the compressor should not exceed 0.38.

2) The compressor average aerodynamic loading should be limited to a $\Delta P/q$ of approximately 0.43.

3) A constant mean diameter design should be maintained.

4) The total work required of the high compressor should be accomplished in five stages.

After some preliminary studies a general design approach was defined as follows:

1. Maximum stator Mn's were limited to 0.8 and maximum rotor Mn's to 1.0.

2. Stage choking margins were to be kept within present experience levels.

3. Negative work slopes (higher stage work at root than at tip) were to be used to aid in setting adequate surge margin and cruise performance.

4. The last stage was designed to give the desired diffuser profile.

5. Rotor and stator incidences were to be compromised for full- and part-speed requirements.

6. The final airfoil series were to be chosen based on inlet Mach numbers as follows:

Mn	Airfoil Series
Above 0.8	Circular Arc
0.6 to 0.8	65
0.4 to 0.6	400

(2) Discussion of Detailed Design

(a) RPM Selection - Having established inlet and exit diameters based on specific flow and exit Mach number requirements, it was possible

to estimate the rpm required for the desired average loading of $P/q = 0.43$. This was done based on nondimensional work and flow coefficients correlated with loading. The required high compressor speed was found to be 8140 rpm.

(b) Work Distribution - The STF219 high compressor requirements are very similar to the JT11D-20 fifth through ninth stages with the exception of the higher required loadings. Because of this similarity and the success of the JT11D-20 compressor, the same general design philosophy was used in the design of this compressor. The stage work distribution was selected based on balanced loadings and incidence ranges required of a specific stage. The resulting stage pressure ratio distribution is shown in Figure 2A-39.

Radial work distribution was chosen to maintain high velocities along the I.D. wall. This was done for two reasons:

- First, part speed operation tends to shift flow toward the tip sections of the compressor leaving the roots with low velocity air (commonly called a root defect). This root defect occurs primarily in the front stages and causes incidence mismatch and poor compressor efficiency. Higher root velocities at design point, however, tend to reduce this problem.

- Second, as the surge line is approached along a constant speed line, the flow tends to shift from the roots causing the root sections to separate before the tips. This separation occurs primarily in rear stages at high corrected speed and eventually leads to compressor surge. Greater root velocities improve compressor high speed surge margin.

The last stage radial work distribution was determined by the required velocity profile into the diffuser. This profile was biased toward the cruise condition because the compressor exit Mach number is highest at this flight condition. The resulting exit profiles are shown in Figure 2A-40.

(c) Incidence Selection - Incidence selection was based on a balance between full- and part- speed requirements. Cascade loss buckets were examined at the two extreme conditions, and, wherever possible, incidences were selected to minimize losses. Rear stage roots were biased slightly toward the full-speed surge line. The resulting mid-span incidences at full- and part-speed are shown in Figures 2A-41 and 2A-42.

(d) Chord Selection - In selecting the chords for the STJ219 turbofan engine the following parameters were considered:

1. Stress
2. Aerodynamic Wall Loading
3. Aspect Ratio
4. Reynolds Number

Combined P/A and bending stresses were not allowed to exceed 57% of 0.2% yield on rotors or 85% of 0.2% yield on stators.

An aerodynamic loading limit was applied to this design as a discipline on chord selection. This loading limit was derived from data obtained during the development of the JT11D-20 compressor.

Aspect ratios were compared to other successful compressors and were determined acceptable. The Reynolds Numbers were also found acceptable.

The final chords chosen for the compressor design are shown in Figure 2A-43. The first three stages on the curve are approaching the stress limit level, and the last two chords were set by aerodynamic wall loading.

(e) Reaction Optimization - The ground rules previously stated limiting rotor and stator Mach numbers dictated the reaction of the first two stages. Where there was a choice to be made, consideration was given to the incidence range and peak loading required on that stage.

Experience indicates that rotor's can stand higher loadings than stators. Stators, however, are more tolerant to incidence because of lower Mach numbers. This reasoning forces the design toward higher reaction levels.

The final stage reaction distribution is shown in Figure 2A-44.

(f) Choke Margin - A preliminary design estimate of 40 $lb/sec/ft^2$ was used in sizing the inlet of the high pressure compressor. However, after analyzing the detailed design of the first rotor, it became apparent that the choke margin of this stage was not sufficient.

Figure 2A-45 is an experience plot of choking area/available area as a function of inlet relative Mach number. This correlation is used only for compressors with relatively high hub/tip ratios. In general, designs on or below this curve have been successful in attaining their specific flow, but the majority of the compressors designed above the curve fall short of their goal. This curve should not be considered as an absolute

barrier, since some compressors operate slightly outside this curve. Designs which are far above this curve, however, would not be expected to meet their specific flow requirements with good efficiency.

With a specific flow of 40 $lb/sec/ft^2$ into the compressor the first rotor choke parameter was located at point A in Figure 2A-45. Three design approaches were studied in an attempt to improve this condition.

The first approach studied the effect of increasing design incidence shown by points B, C, D and E, which are for incidences of 1, 2, 3, and 4 degrees, respectively. Increased incidence effectively staggers the blade open which increases its minimum area. However there were problems encountered in this procedure. The losses due to incidence mismatch begin to rise sharply past 2° and, in order to have some margin for error, 1° was considered the maximum allowable value. Also at the cruise flight condition this incidence becomes higher and is detrimental to compressor efficiency.

A lower inlet guide vane exit angle was then investigated. This improved the choke margin by opening the blading and reducing the inlet relative Mach number. Point F indicates the result of decreasing the angle from 75° to 70°. This procedure, however, increased the first stator root Mach number. An IGV angle of 70° was the minimum allowable to keep the first stator root Mach number below 0.8.

The third approach was to increase the annulus area of the compressor in the first two stages. This was accomplished by decreasing the I.D. as any O.D. changes would affect engine envelope. Points G, H and I show the effect of decreasing the inside radius by 0.5, 0.7, and 1.5 inches, respectively. The increased area resulted in higher stage loadings and an increased divergence angle in the fan high compressor intermediate case. Analysis showed that the 0.5 inch radius decrease would be acceptable.

By combining the acceptable portions of the three design approaches, the choke parameter was moved to point J in Figure 2A-45. This resulted in a design with marginal choke capability in an area which has previously been attained.

The stage elevations for the resulting design are shown in Figure 2A-46.

(g) Aerodynamic Loading Distribution - The preliminary design estimate on compressor average $\Delta P/q$ was 0.43. After completing the detailed

design the average loading was 0.437. Although this is a relatively high loading, recent results with the SST five stage rig and the STF200 high compressor indicate this value is attainable.

Another important loading parameter which was considered was the NACA derived diffusion factor. This parameter is advantageous over $\Delta P/q$ because it contains the effect of gap/chord ratio. Both parameters were considered with $\Delta P/q$ being used primarily as a measure of wall loading and with the D-factor used to limit balde and vane loading.

As a result of data from the SST five stage rig and because of the relatively high $\Delta P/q$ values, gap/chord ratios were set at approximately 0.7 at the mid-span location to maintain reasonable diffusion factors. The resulting stage loadings are shown in Figure 2A-47 and 2A-48.

(h) Inlet Guide Vane Design - Analysis of the STF219 windmilling characteristics indicates that the high compressor inlet guide vane could be used as an aerodynamic brake. By rotating the vanes closed the engine airflow can be maintained at the level required for a desirable windmilling rotational speed.

Since this vane has variable stagger capability, it will be used for performance improvements or aerodynamic flutter tolerance during the development process.

(j) Stresses - Figures 2A-49 and 2A-50 show the maximum P/A plus restored bending stresses and allowable stresses for each blade and vane row.

(3) Vibration Analysis

The design of the STF219 compressor has been set to eliminate the primary mode blade-disk resonances from the engine running range.

Figures 2A-51 through 2A-54 show the expected frequency responses from the various compressor stages. Slight variations in these values may be necessary as the design progresses to insure adequate resonance margin on each stage.

In addition to frequency selection, extended root damping was employed on the third stage blades to overcome the effects of flow disturbances caused by the intermediate struts. The seventh stage blades also incorporate extended root damping to minimize blade stresses caused by the upstream excitation of the compressor exhaust section. This damping is accomplished by centrifugally-forced toggle weights bearing

on the blade platforms and the disk coverplates. Rubbing contact caused by the motion of the blade platform relative to the disk creates damping forces which are optimized by the selection of toggle damper weights. Similar damping can be incorporated on fourth, fifth and sixth stage, with only slight modifications if necessary.

The vibration analysis of the high compressor disks and blades is proceeding.

b. Mechanical Description

(1) Introduction

As discussed in the Structural Analysis section which follows thermal stress and low cycle fatigue life operation experience from the JT11D-20 engine were applied to the analysis of the basic rotor construction undertaken during the Phase II-B program. The resulting configuration, shown in Figure 2A-1, is the current design approach to the solution of the rotor thermal stress problems.

(2) Discussion

The rotating portion of the high compressor consists of five rows of blades and their supporting disks and shafts. The fourth through seventh stages are joined and positioned axially by three cylindrical inner and outer spacers. The third stage is overhung forward and positioned axially by a spacer bolted to the front face of the fourth disk at the outer spacer diameter.

Cover plates are presently being studied to reduce the low cycle fatigue (LCF) of the third through sixth rotor. The plates channel hot compressor discharge air to the disk rims and reduce the thermal gradient from bore to rim. Radial knife-edge seals are included on the cover plates to provide the sealing required between stages. The cover plate on the third rotor also serves as the support for damping weights required on that stage. The third rotor front cover plate is bolted in place with the support spacer and the rear cover plate is piloted on a flange and retained by a bolted spacer. The next three cover plates are piloted on flanges and held in place by the outer bolted spacer. The blades have dovetail roots inserted in slots machined into the disk rims. Mechanical damping devices and extended blade roots are employed on the third through seven stages to reduce the effects of blade vibrations. Damping weights are attached to cover plates on the third rotor and to

riveted damper support plates on the seventh rotor. Extended roots on the fourth, fifth and sixth stages are used to improve the LCF life of the disk rim by reducing bore-to-rim thermal gradients. Axial movement of the blades is restrained by cover plates in the third through sixth stages and by damper support plates on the seventh stage. The compressor blades, hubs, disks, spacers and cover plates are to be fabricated of Waspaloy (PWA 1007) nickel alloy.

Each disk and blade assembly and the front hub are statically balanced. The rotor shaft is dynamically balanced. The rotor assembly is then dynamically balanced as a unit by adding weights to flanges provided on the third stage disk and the seventh stage seal disk. Throughout the rotor structure, fillet radii, careful blending of intersecting surfaces, and the use of rounded or chamfered corners are provided to reduce stress levels in locations where stress concentrations occur.

The thrust loading on the rotor is transmitted to the number 2 bearing from the outer spacers through the disks and conical front hub. Radial loads are tranmitted to the number 2 bearing through the front hub and to the number 3 bearing through a conical shaft secured by the tiebolts to the rear side of the seventh stage disk. This shaft extends rearward to engage a spline on the high speed turbine shaft.

The cold static radial clearances of all knife-edge seals in the high pressure compressor were made as small as possible while providing for the maximum tolerance build-up, the maximum radial differential thermal growths during steady-state operation, and the maximum elastic radial deflections during operation. Light, non-destructive rubbing will occur during thermal transient or overspeed during initial operation.

Blade tip radial clearances were established to provide for the maximum tolerance build-up, the maximum differential radial and axial thermal growth during transient operation, and radial elastic blade and disk growths at normal high temperature operating speeds.

Axial gaps on the forward side of all rotating parts and adjacent stationary parts provide for the maximum total tolerance accumulation, the maximum axial differential thermal growths during transient operation, the estimated net forward deflection of the end bell resulting from centrifugal action, the maximum forward blade tip deflections resulting from the steady-state gas loads, and the maximum forward blade tip deflection resulting from surge gas loads.

The axial gaps and the seal land lengths between the rear of the rotating parts and the adjacent stationary parts provide for the maximum tolerance

accumulation, the maximum axial differential thermal growths during transient operation, the maximum net thrust bearing end play, the maximum disk rim deflection resulting from surge gas loads, the maximum forward stator vane deflections resulting from steady-state gas loads, and the maximum forward seal support diaphragm deflections resulting from steady-state static pressure loads.

c. Structural Analysis

(1) Introduction

The preliminary design effort conducted during Phase II-A on the high pressure compressor resulted in a structural design concept which utilized lightweight disk construction in combination with a double spacer arrangement to maintain overall rotor rigidity. Detailed design work during Phase II-B has resulted in the definition of a disk stress problem which may warrant a change in this design approach. The problem arose as a result of the high average disk stress level resulting from the lightweight construction and an initial Phase II-B thrust balance system which circulated hot gases through the bores of the high compressor disks. The hot gases on the bore resulted in an inverse thermal gradient (i.e. bore temperatures higher than rim temperatures) on some of the disks. This inverse gradient is accentuated by the deceleration from high flight Mach numbers, where the disk rims respond quickly to the resultant decrease in gas temperature while the disk bores lag. The overall result of these two effects (i.e. high average stresses and inverse thermal gradient) is to increase the rim tangential stress above normal. This stress level is further increased by a stress concentration factor resulting from rim discontinuities at the blade attachment slots. The resultant local stresses at the blade attachment slots are forced well over the yield stress of the disk material. This stress cycle, repeated once on each flight, would result in ultimate cracking of the disk at a stress concentration point. This problem though less severe, is common to all turbojet engines and is termed low cycle fatigue (LCF). The design objective of the STF219 engine is 8000 LCF cycles.

(2) Discussion

One approach to the problem would be to lower the average disk tangential stress level by increasing disk thickness. The effect of this approach on a typical disk weight is shown in Figure 2A-55. This figure illustrates the prohibitive weight increase resulting from this approach.

Three other approaches are now being investigated to resolve this problem. They are as follows:

1. Reduction of stress concentration factors at blade attachment slots.
2. Elimination of the inverse thermal gradient by circulating cooler gases around and through the disk bores.
3. Elimination of the inverse thermal gradient by thermally shielding the disk rims with "coverplates".

Laboratory test programs have been initiated to determine a means of reducing disk rim stress concentration factors. One program involves a photoelastic analysis to determine the effects on the concentration factor of an elliptical (rather than circular) radius in the blade attachment slot. Another program is investigating the optimum disk slot-to-neck width ratio by use of an electrical analog. A third program is investigating the improvements in the concentration factor to be gained by shot-peening the attachment slots. The second approach is discussed in detail in the Thrust Balance section of this report.

Since the third approach is the only scheme involving major mechanical changes, it was studied in some detail during Phase II-B. The coverplate approach provides for hot gas circulation around the rims of all compressor stages and, thereby, eliminates the inverse thermal gradient. In addition, the plates provide a barrier between the disk rims and the static stator walls, further reducing heat transfer rates. This effect decreases the rim response to thermal transients.

A final approach resolving this LCF problem has not been chosen. Studies are continuing to produce a high compressor structural configuration which will meet the stated requirements of the Supersonic Transport powerplant.

d. Stator and Case Design

(1) Discussion

The high compressor stator and case design as presented in the STF219 Phase II-A report was further studied and has been revised in several respects. It was established that the provisions for an abradable shroud were not sufficient therefore, the design was revised to incorporate a recessed tip seal cavity. This seal cavity can be used to house various types of tip seals and has had successful application in the JT11D-20 turbojet engine.

A second area revision was a method of retaining the outer ends of the vanes. A change was made to the double outer, or box, shroud construction, shown on Figure 2A-1. This revision was necessitated by the axial tolerance build-up within the flanged portions of the individual vanes in the Phase II-A design.

The first attempt to change the Phase II-A design is presented in Figure 2A-56. This scheme incorporates a blade tip seal cavity and eliminates the flanged portion of the forged vane. The flange section of vane is replaced by a separate one-piece flange with provisions on the I. D. to retain the vanes of that stage and hold the seal in place. An alternate case profile is also shown which reduces the discontinuities in the outer case wall section. This design was considered an improvement relative to the Phase II-A design but it was not carried further because the preliminary weight estimates indicated other configurations under study promised to be lighter.

It was felt that the design of the stators and cases could be made lighter by using a JT-3 and JT-4 engine outer case design, consisting of a single outer case to take engine loads with the vanes and seals piloted on the I. D. of this case. This type of case is shown in Figure 2A-57. It was found that with this design the individual rings required to take the vane bending moment could not take the buckling loads imposed on them.

A strip stock fabricated vane was then investigated to save weight and reduce manufacturing costs. The resulting schemes had apparent structural deficiencies, probable susceptibility to long-term crack formation, and wear problems. The studies of this design scheme have been curtailed.

Further studies indicated that the individually replaceable vanes increased weight, therefore it was decided to concentrate on the lightest weight design.

Figure 2A-1 is a design similar to that used in the JT11D-20 engine. The compressor outer wall is formed by stacking a combined short case and stator assembly together, one for each of five stages. Each case and stator assembly provides a seal cavity into which many types of blade tip seals may be tested. A box structure to which the outer ends of the forged vanes are brazed is provided at the other end of the seal cavity case. The inner ends of the vanes have integral tabs riveted to a diaphragm. This diaphragm supports the interstage seal rings b, rivets and spacers in radially-slotted holes to accommodate thermal growth. The seventh stage stators and exit guide vanes are

made of rolled strip stock inserted into pre-punched slots in the outer shroud ring. They are twisted and forced into the inner shroud ring and are located radially by rings at the I.D. and O.D. The inner shroud ring is bolted to the adjoining diffuser case flange. The outer shroud ring is supported by the seventh stage compressor outer case with provisions for thermal expansion and fabrication tolerances.

A study was made of a revision to the preceding design whereby the intermediate flanges were eliminated and the cases held by tierods. This was an attempt to eliminate the intermediate flanges and their small bolts. The new design would replace them with tierods which would have greater energy absorbtion ability. It turned out that 32 tierods of 0.375 inch diameter were required. This increased the design weight to 20 lbs. over than the reference design.

Also, an attempt was made to incorporate a single outer case design, similar to Figure 2A-57, but with box shroud stator construction. This turned out heavier than the tierod design.

The design of Figure 2A-1 was evaluated as the most promising and is incorporated in the current engine assembly.

To save additional weight, it may be possible to revise the design and make the third and fourth stage vanes of titanium in a small independent box structure contained in steel cases. The outer cases would be lighter using steel because they are buckling-limited.

6. DIFFUSER CASE

(a) Mechanical Description

The current diffuser case is an Inconel 718 weldment consisting of an inner and outer machined forged ring connected by sixteen equally spaced struts butt-welded to the rings. The weldment provides an outer sheet metal manifold with various welded accessory bosses. The case weldment also provides the necessary passages and supports for the accessory air requirements, number 3 bearing oil and air lines, fuel nozzles, and forward burner can support.

Figure 2A-1 shows a typical cross section through a strut of the present case. Although the general purpose and requirements of the diffuser case have remained the same, many differences have evolved from

the Phase II-A design. The more apparent changes in the diffuser case are listed below:

a. General flow path size and shape have changed.

b. The Phase II-B case has 16 struts. The Phase II-A case had 12 struts.

c. The Phase II-B case has 32 fuel nozzles. The Phase II-A case had 24 nozzles.

d. The Phase II-B case fuel nozzle plane is behind the strut. The Phase II-A case fuel nozzles plane was between the struts.

e. The Phase II-A case provided inner bleed air passages for seventh stage compressor and turbine cooling air. The present case does not provide this feature.

f. The present external two compartment manifold bleeds high compressor discharge total pressure air from each strut leading edge for aircraft cabin air bleed, aircraft anti-icing and the duct heater fuel turbopump. It also bleeds discharge static air from the sides of each strut for the duct flameholder. The Phase II-A case provided cabin air bleed from the leading edge of each strut and other aircraft air from the outer wall. The duct flameholder air was bled from the burner outer case wall.

g. General fabrication and structural changes are reflected in the Phase II-B design as a result of above changes in requirements.

Changes "a" through "d" were primarily the result of a reduction in engine size, additional test rig data, and further evaluation of the ram inductor burner. These studies demonstrated that it is possible to reduce the size of the forward portion of the burner can. This allows the diffuser to be resized to provide better diffusion characteristics with reduced flow losses.

The number of fuel nozzles was increased to 32 to improve flame uniformity. This increase required a change in the number of struts as it was desired to maintain equally spaced struts for even stress distribution, uniformity of flame pattern, and vibration considerations. To limit strut width (wake size limitation) and provide adequate strut cross sectional area (for the number 3 bearing lines and manifold air), it was found necessary to provide a minimum of 16 struts.

With the large number of struts and nozzle required, it was then found necessary to place the nozzle plane behind the struts to provide sufficient clearance for the nozzle swirlers (Figure 2A-58). The Main Combustion Chamber section describes the burner requirements more fully.

Continuing thrust balance and turbine cooling air studies indicate that the inner bleed air passages of the Phase II-A case should be omitted (change e). It was found that by ducting compressor air along the inner burner wall through holes in the rear end of the liner air could be fed to turbine cooling passages at a higher total pressure than through tubes, as originally specified in Phase II-A. The latest thrust balance and compressor disk cooling schemes indicate that compressor total discharge pressure from the center of the flowpath is not required. The studies also indicate that the original scheme could lead to compromises in compressor efficiency. The removal of this ducting simplifies and lightens the diffuser case.

It was decided to bleed the fan duct flameholder air from the side walls of the diffuser case strut because at this location the effects of variations in the percentage of bleed flow and also completely shutting off the bleed would be common to both the inner and outer burner annuli. If bled only from the outer burner case wall, flow variations and bleed air shut-off would affect the outer burner annulus flow only, and would probably alter the burner discharge temperature pattern. The discharge bosses for flameholder air are placed to the rear of the plane of the fuel nozzles and behind the oil lines to simplify the manifolding and to provide as much room as possible for other lines going through the area. It was decided to take all high compressor discharge total pressure bleed air through the strut leading edge for the following reasons:

a. It provides the clean air necessary for cabin air.

b. It provides the required air without promising size or configuration.

c. It has simpler manifolding and fabrication than the Phase II-A design.

d. It results in a lighter, easier to fabricate configuration.

The Phase II-A turning vanes incorporated in the cabin bleed struts were omitted for simplicity. They can be added if initial engine testing indicates that they are needed for pressure recovery. Figures 2A-59 and 2A-60 show typical fabrication techniques considered for the diffuser

case. The inner and outer cases are supported by struts and strengthened at the four corners by circumferential ring flanges to support and distribute the loads imposed by the inner duct (number 3 bearing loads and axial pressure loads on the number 3 bearing wall). Integral gussets machined in the inner and outer case walls opposite the strut attachment projections aid in distributing the loads between the struts and the inner and outer cases and their stiffening flanges. Figures 2A-59 and 2A-60 show the various methods of fabricating this configuration. Figure 2A-59 shows a one-piece machined inner and outer ring with fabricated struts (forgings and sheet metal) butt-welded to the rings at airfoil contoured projections machined integral with the rings. Figure 2A-60 provides preassembled fabricated struts with integral feet welded to cutouts in the inner and outer rings to provide for the struts. An additional configuration not shown is similar to Figure 2A-6 except that the struts are cast as one piece. The emphasis in each design is in the elimination of fillet and lap welds which have disadvantages for long life structural joints due to their cracking formation tendency and the difficulties in inspecting and repairing. All of the above schemes depend exclusively on butt-welding techniques.

The first design, Figure 2A-59, is proposed for the Phase II-B design for the following reasons:

a. It provides for minimum weld distortion of the final assembly.

b. It provides the least amount of welding in highly stressed areas.

c. The additional cost of this design would be overcome by the advantages.

d. Consideration of the cast struts was deferred until more experience has been gained in casting and welding complex weldments with cast Inconel 718 components.

Inconel 718 nickel alloy (PWA 1009 and 1033) in forged and sheet forms was chosen because of its high strength at the operating temperature and its relative ease of weldability and repair. Waspaloy was not considered, since the engine is now limited to Mach 2.7 operation and the higher temperature strength of Waspaloy is not considered necessary.

(b) Structural Analysis

The major loads on the diffuser case assembly are caused by aircraft maneuvers, thermal gradients between the inner and outer walls, and

gas pressure differentials. Of these, the pressure differential across the inner wall produces the predominate load on the structure. This load is transferred from the inner wall to the diffuser struts, and hence to the outer wall which is reinforced with continuous rings and local connecting ribs. The pressure differential on the inner wall causes a collapsing load on the structure resulting in a buckling-limited case. The limiting circumferential and axial stresses are 46,500 and 85,500 psi, respectively. The actual stresses are 16,000 and 30,200 psia.

To keep local stresses low and structure stiffness high, the diffuser struts were used as a bridge between the two pairs of support rings. One pair of rings was located at the I.D. and the other at the O.D. of the case. The rings were placed over the leading and trailing edge of the strut to give a direct connection between the structures. Upon determining the loads, the support rings were sized accordingly and the stresses in the struts checked. NASA technical notes TN D-400 and TN D-402 were used for the ring structural analysis. Creep and stress rupture life was checked to determine if this criteria was limiting. It was found, however, that a yield criterion is limiting at sea level ram conditions. Therefore, the rings were sized accordingly.

The basic design provides flexibility of manufacture and process. Several alternate designs were investigated from a manufacturing viewpoint, however, the fabricated design shown was chosen as being the most practical and least expensive.

7. MAIN COMBUSTION CHAMBER

a. General Description

The main combustion chamber section encompasses that part of the engine between the compressor exit and the turbine inlet. This includes the compressor discharge air diffuser, the inner and outer combustion chamber cases, the single annular combustion chamber, the transition duct into the turbine, a fuel supply system, an ignition source, and seals. These features are shown in Figure 2A-61.

The combustion chamber is an advanced-design annular ram induction burner. The annular burner permits the maximum utilization of available engine space by combining the burner and diffuser in a common volume. The ram induction burner is basically as proposed in Phase II-A with minor modifications for differences in the engine flowpath and the increased number of diffuser case struts. As in the Phase II-A design, airflow into the ram induction burner is accomplished by

ram pressure. The use of velocity head for penetration requires less diffusion between the compressor and combustion area, thus lowering diffuser pressure loss. The high momentum of the compressed air is utilized to inject primary and secondary air into the combustion chamber and to mix fuel vapors, burned gases, and dilution air. In conventional systems, the penetration and turbulence are a function of the static pressure differential at the holes in the combustion chamber liner. With the same burner, however, the use of total pressure rather than static pressure permits greater control over mixing characteristics without incurring a significant pressure loss.

High velocity diffuser discharge air is introduced into the combustion chamber through a series of small ram air scoops in the primary zone. Additional rows of larger scoops in the secondary zone provide further mixing of the air and gases. Fuel is injected directly into the combustion chamber by means of swirl atomizing nozzles. Since the ram air scoops provide a high level of turbulence and mixing, adequate fuel preparation can take place in the primary section of the combustion chamber. Consequently, the primary scoop arrangement provides a mechanical method of fuel preparation and eliminates requirements for heat cone premixing.

The ram induction burner also provides certain structural advantages. First, because this type of burner does not rely upon a static pressure differential across the combustion chamber liner as does the conventional combustion chamber, the pressure loading of the liner is much lower. Second, the high velocity flow over the liner and through the ram air scoops provides basic cooling by convection. Supplementary film cooling is utilized to cool the surfaces which are exposed to the hot gases. Figure 2A-62 shows a detailed section of a scoop with film-cooled louvers on the portion exposed to the hot gas.

Downstream of the secondary scoop section is the transition duct section of the combustion chamber. The convectively-cooled inner and outer transition ducts serve to channel the burned gases into the turbine inlet. Air supply for transition duct cooling is taken from between the combustion chamber walls and liners. The pressure gradient between the forward and aft ends of the transition duct liner accelerates the cooling air between the concentric walls of the liner. This air is discharged at the turbine inlet, thus film cooling the shrouds of the first stage turbine vane.

The extensive use of convective cooling in the combustion chamber section significantly reduces the amount of transpiration and film cooling required. Consequently, a greater portion of the airflow is available to tailor the burner exit profile than in a liner using other cooling methods.

(1) Compressor Discharge Air Diffuser

The diffuser flowpath between the compressor exit vanes and ram air scoops shown in the Phase II-A report was primarily a scaled version of the STF200 engine combustor diffusion section. The fairing on the front of the inner burner case extended into the flared rear section of the compressor to the strut leading edge. This formed two parallel diffusers with entry and exit ducting. A smaller central diffuser in the nose of the extended burner can fairing diffused the initial primary air before dumping into the cavity where it feeds the vane swirler.

The diffuser flowpaths were carefully analyzed to determine local regions of excessive diffusion on each surface due to wall and flow curvature as well as expected diffuser inlet flow profiles. Other situations which could cause local flow separation or diffuser instability (i.e. mechanical tolerances and thermal displacements of mating wall surfaces, unavoidable leakage into and out of the diffuser, the wakes shed from the struts and fuel nozzle supports, the effect on the flow through the primary scoops and, in turn, the combustor, and the thick boundary layer on the inner burner case wall) were analyzed. As a result of this study, the diffuser flowpath underwent several changes to insure stable and unseparated flow to the ram air scoops at all flight conditions with good recovery efficiency and low flow losses.

More recent combustor rig testing has indicated that combustor flow areas need not be as great in the mixing region as the burning zone. By reducing combustor inlet size, the amount of divergence of the diffuser was reduced and the diffuser inlet wall curvature problems were greatly reduced.

The suppression of strut wakes and the elimination of boundary feeding into the primary scoops was accomplished by taking the primary scoop air and swirler cup air through the central diffuser. The swirler air bleeds into the combustor while the remainder is accelerated through a nozzle to feed the primary scoops. The air passing through the main diffuser then supplies secondary scoop air and turbine cooling air.

(2) Inner and Outer Combustion Chamber Cases

The outer combustion chamber case consists of two sections. The front section of the outer case attaches to the rear flange of the diffuser case. The rear flange of the rear section joins with the turbine case and the end of the outer transition duct. The outer case is pressure-limited and

was designed to withstand the pressure differential between the high pressure compressor discharge air and the lower fan duct pressure. At sea level, Mach 0.7 this pressure will be 159.5 psi. The flange was designed to creep no more than 0.5% in 6000 hours at Mach 2.7 at 65,000 feet. Both sections of the outer case are flow-turned from Waspaloy (PWA 1030) with an integral front flange. The front outer combustion case contains six welded engine bleed ports and a flange to support the actuator ring of the duct flameholder valves. Both the front and rear cases have welded rear flanges.

The inner combustion case also consists of two Waspaloy sections. The front flange of the forward section attaches to the rear of the diffuser case and the Number 3 bearing support flange. Number 3 bearing loads are channeled directly into the diffuser case, thus eliminating the requirement of a reinforced forward inner case as employed in the Phase II-A design. The rear flange of the rear section joins with the turbine first stage vane support flange. The allowable stress for the inner case was calculated to provide a 1.3 buckling margin. This allowance has been found adequate in other Pratt & Whitney Aircraft engines.

The rear outer combustion case flanges permit rearward movement over the turbine case for hot section inspection. The rear flange of the case and its mating turbine case flange are scalloped to interlock over a common internal flange for assembly of the cases. The inner and outer walls of the transition duct can be moved forward over the primary and secondary ram air scoop sections. At this point, the first stage turbine vane retaining segments may be unbolted and moved forward for vane replacement. The inner rear combustion chamber case was designed to move forward over the front section presenting a five-inch access to the Number 3 bearing rear labyrinth seal supports. With the release of these seals, the first stage turbine rotor and shaft may be removed as a unit. Further design studies of the Number 3 bearing compartment and compressor-to-turbine shaft assembly may make it possible to remove the turbine without going through the rear section of the combustion chamber. In this case, the inner combustion chamber case may be a single segment.

The alternate design for an axially split combustor presented in the Phase II-A report has been studied and discontinued. The factor of maintenance accessibility was weighed against compromises in cost, performance, and development effort required. An axially split combustion chamber and outer combustion chamber case would be more expensive to fabricate. The case would be more difficult to seal

against external air leakage and would have lower allowable stresses than the present flow-turned design in which hoop stresses do not cross longitudinal welded joints. More elaborate fixtures and hoisting equipment would be required for the non-split design to prevent damage to adjacent sliding parts. The alternate scheme will be investigated during the next phase.

(3) Annular Combustion Chamber

The annular combustion chamber is divided axially into two sections. The first or forward section is the primary injection section. Air is injected into this section through a series of ram air scoops to provide a stoichiometric air/fuel mixture in the combustion chamber. There are three axially staggered primary scoops in both the inner and outer combustion chamber walls for each fuel nozzle. These scoops are formed of sheet metal and are welded into the chamber walls. The secondary or aft section of the combustion chamber is located immediately behind the last row of primary injection scoops. The secondary scoops are shaped to insure uniform mixing and dilution of the burning primary gases and furnish both a suitable temperature and temperature profile to the turbine. There are two axially staggered secondary scoops on the chamber walls for each fuel nozzle. Fabrication of the secondary section is similar to the primary except for the inclusion of tab-ended cascade vanes which are punched and welded into the side of the secondary scoops.

The scoop walls in both the primary and secondary sections are convectively cooled by air flowing through the scoops. Combustion chamber wall cooling is achieved by a boundary layer film produced by a series of louvers in the walls between the scoops. Fabrication of the scoops by casting, as mentioned in the Phase II-A report, has undergone further study. It was found that while costing less a cast scoop would also have to be welded into the chamber walls as do the formed scoops. The low loading on each scoop along with convectively-cooled walls, dictated a thin scoop wall. This could not be achieved by casting without a considerable amount of casting process refinement which would in turn increase the cost.

A single sheet metal wall is placed between each combustion chamber scoop wall and the adjoining combustion chamber case. The wall serves to maintain the air velocity supplying the ram air scoops and to minimize radiation.

The short front section of the combustion chamber around the fuel nozzle discharge is a single wall construction cooled both internally and externally. Internally, the wall is boundary layer film-cooled with air issuing

from holes located in the vicinity of the nozzle face. Externally, the wall is convectively-cooled by initial air which is accelerated from the forward cavity into the ram air scoop feed passages. Development of the front section of the chamber has moved the fuel nozzle aft from earlier designs, thus eliminating the Phase II-A requirement of a double wall for transpiration cooling.

The swirl cup is the forwardmost part of the combustion chamber. The cup is installed by sliding tabs through mating gaps in the collar on the forward section of the combustion chamber. The cup is then turned 90° and is held in place by tabs on the lockring. The lockring is then tack-welded to the combustion chamber collar making the swirl cup replaceable. When the lockring and swirl cup are in position, they form a radial groove which receives the fuel nozzle swirler flange.

The combustion chamber section containing the swirl cup and lockring assembly and the primary and secondary scoops is held in place by eight radial pins. The pins are inserted from the outside of the diffuser case and pass within the trailing edge of the diffuser struts into inserts in the combustion chamber front section. The pins take the thrust load on the combustion section and also position it axially and concentrically with the diffuser discharge. A radial clearance gap at each pin allows for differential thermal expansion and tolerance accumulation between the diffuser case and the combustion section.

The basic sheet metal of the combustion section including ram air scoops, combustion chamber walls, and the front section of the combustion chamber is Hastelloy X (AMS 5536) nickel alloy. L-605 (AMS 5537) was considered for the above applications as yield and rupture strengths of L-605 are superior to those of Hastelloy X at the temperatures to which it will be subjected. The oxidation resistance of this material is, however, inferior. The air guide swirlers are cast Stellite 31 (AMS 5382) cobalt alloy. Combustion chamber retaining pins are Waspaloy (PWA 1004) nickel alloy and the retaining inserts on the front section of the combustion chamber are L-605 (AMS 5759).

(4) Transition Duct

The rear or transition duct section of the combustion section is an annular passage which further mixes the burned combustion gases and leads them into the turbine section. The transition duct is composed of independent inner and outer shells, each of which is fabricated with double-wall construction. The walls are formed sheet metal (Hastelloy X AMS 5536) weldments. The wall is convectively cooled with air taken in at diffuser discharge pressure at the forward end of the wall and discharged at the aft

end just forward of the turbine inlet guide vanes at turbine inlet pressure. Analysis has shown that an excessive amount of air would be required to boundary layer film cool the duct and that a porous wall construction, as proposed in Phase II-A, would not have the desired durability. The cool, shielded skin of each wall provides the structural support to withstand the pressure gradient while the skin exposed to the combustion gases provides the channel for convection cooling. The transition duct walls are held rigidly with respect to each other at the forward end. The aft ends of the inner and outer skin of each wall are held concentric, but are free to allow for radial and axial differential thermal growth.

(5) Fuel System

The fuel system for the annular ram induction combustion chamber consists of 32 individually removable dual orifice nozzles having a turndown ratio of 60:1. The pressurizing valves for the dual orifice system are incorporated in the nozzle housing as close as possible to the orifices to avoid coking effects which might occur in the interconnecting passages when the valves are located farther from the nozzles. Each nozzle and swirler are an integral assembly which slides radially inward through the diffuser case to engage a positioning groove. As described earlier, the groove is formed when the swirl cup and lockring were tack welded to the front section of the combustion chamber. The integral nozzle/swirler provides excellent concentricity between swirl air and injected fuel, thus insuring more uniform mixing. The assembly also allows removal of the nozzle and swirler for inspection or replacement. The nozzle support has an airfoil-shaped sheet metal heatshield attached where it passes through the compressor discharge air annulus. The fuel nozzles are retained by flanges bolted to the outer wall of the diffuser case.

(6) Ignition System

Ignition is provided by two electrical igniters which penetrate into the front section of the combustion chamber. These igniters and their extended torque tubes pass through the fan discharge duct and are individually removable without removing the duct, as in the Phase II-A design.

(7) Seals

Large diameter seals (30 to 40 inches) are required at three locations in the main combustion chamber of the engine. The first two locations are

at the joints between the inner and outer scoops and their respective transition duct walls. The third location is at the aft end of the outer transition duct. The main problem in the design of these seals was not the pressure gradient, but the high radial and axial thermal displacements. For this reason, the seals must have good flexibility and must be able to withstand temperatures in the 1200 F to 1800 F range.

Two types of seals have been studied for use with the annular combustion chamber. These seals are shown in Figure 2A-63. The first seal is similar to the JT11 combustion chamber seal. The sealing ability of this configuration has proven accpetable. However, extensive testing has shown that the durability of the seal will require extensive development. The second seal is similar to that used in the STF200. This seal has undergone a considerable amount of testing and has shown promise of having adequate durability.

The second seal consists of two adjacent conical sheet metal strips and an annular rub ring. The outer edges of the seal are riveted to their support, while the inner edges are joined by folding one strip over the other. The adjacent strips contain alternating slots which begin at the folded edge of the seal and end just short of the rivet drill holes. The alternating slots in the two strips eliminate a direct leakage path into the combustion chamber and, at the same time, allow relative circumferential movement between the two strips as the folded edge of the seal undergoes radial displacement. A finger pattern in each strip results from cutting the slots. When the folded edge of the seal is displaced radially, the fingers are stressed as cantilevers and are thus more durable than a hoop configuration. The remainder of the seal is the annular rub ring against which the folded edge is preloaded at assembly. Variations of this seal are being studied for use in three locations mentioned above.

STF200 testing is being carried out on an Inconel X (AMS 5542) nickel alloy seal with silver-plating (AMS 2410) on the rubbing edge. The rub ring is Incoloy 901 (AMS 5660) nickel alloy. The higher turbine inlet temperature in the STF219 engine results in higher seal temperatures and consequently more durable materials are required. Materials selected for the STF219 seals are Astroloy (PWA 1013) nickel seals plated in the rubbing area with PWA 586-1 moly-disulfide. The rub ring is L-605 (AMS 5759) cobalt alloy.

b. General Combustor Configuration

During Phase II-B, testing of the ram induction burner has progressed through several modifications. Testing has shown that this type of burner

is very tolerant to changes in inlet flow profile. In addition, the testing has shown that turbine inlet temperature profile can be changed substantially without major burner redesign. Both of these characteristics are very desirable, since experience has shown that the final burner hole and scoop configuration can be developed only on an engine. The burner configuration showing the best test results, Modification #2-7, was used as the model for the STF219 combustor design.

Figures 2A-64 through 2A-66 show the estimated pressures, flow areas, and Mach numbers through the combustor section. Overall combustion chamber length from compressor exit to turbine inlet is 28 inches while the actual burning length is 20.8 inches.

The general parameters for this burner are as follows:

	Sea Level	Cruise
Space Heating Rate	5.5×10^6 Btu/ft^3/hr atmospheric	
Shroud Mn	0.21	0.255
Liner Velocity (ft/sec)	113	
Burner Pressure Loss ($\Delta P/P_t$)	6.0	8.3
Ratio of Maximum Burner ΔT to Average ΔT	1.11	

8. TURBINE DESIGN

a. Introduction

The turbine design work conducted in the Phase II-B SST contract period was directed toward the selection of the turbine configuration best suited to fulfilling the basic objective established in Phase II-A. This objective is the design of an engine with an Initial Rating of 2000°F TIT and the capability of eventual development to the Basic Rating of 2300°F TIT. In addition the Initial design must have the capability of meeting a 2300°F Turbine Inlet Temperature FTS rating.

In the selection of the turbine designs, a strong consideration has been given to state-of-the-art in terms of background experience. At any given time, high performance, low TBO military fighter engines operate with higher turbine temperatures than transport aircraft engines which require much longer part life. At the same time, development engines experiment with and prove out designs and materials for the next logical advancement for reliable flight operation. In each new design, judgment must be exercised to determine how much to extend the design beyond the current state-of-the-art with respect to turbine inlet temperature levels and coolant flow requirements so that an acceptable balance of engine performance and durability can be achieved. The STF219 turbine design represents a reasonable extrapolation of past engine experience.

A three stage turbine consisting of a single high pressure stage and two low pressure stages was selected for the STF219 engine as a result of optimization studies performed under the Phase II-A study contract. These studies evaluated the weight, diameter, efficiency, and life trade-off factors necessary to set the turbine flowpath for the optimum engine.

b. Discussion of Detailed Design

The objectives stated in the previous section are satisfied by the turbine flowpath shown in Figure 2A-67. This flowpath does not deviate to any large extent from that developed during Phase II-A.

During the Phase II-B detailed design of the turbine, several design changes were made to the preliminary turbine flowpath to assure attainment of the final engine performance requirements. The most significant change was the decision to design a turbine flowpath that would assure the required efficiency at maximum turbine inlet temperatures ranging from 2000°F (initial rating) to 2300°F (basic rating). This temperature rise must be accomplished without major mechanical changes to the turbine hardware. Since the compressor and fan match point will remain the same throughout this turbine inlet temperature range, the 2000°F rating represented the more difficult aerodynamic

design task. For this reason a new design point was established having the following parameters:

Airflow (lbs/sec)	650
Maximum T.I.T. (°F)	2000
Work (Btu/lbs)	
High Pressure Turbine	113.4
Low Pressure Turbine	104.0
Rim Velocity Ratio	
High Pressure Turbine	0.44
Low Pressure Turbine	0.42
Rotor Speed (rpm)	
High Pressure	8140
Low Pressure	6160
Efficiency (%)	
High Pressure Turbine	88
Low Pressure Turbine	87.2
Turbine Exit Mn	0.58
Turbine Exit Hub/Tip Ratio	0.562
Last Stage Tip Diameter (in.)	43.7
Required Life (hrs.)	3000

(1) Velocity Ratio

The efficiency level of a turbine is determined primarily by the velocity ratio and the through flow gas velocity to rim wheel speed ratio. Since low weight and minimum tip diameter were desirable, a high through flow gas velocity (Mach number) and relatively low velocity ratio turbine were desired. A number of turbine flowpaths with varying inner wall diameters were investigated in an attempt to obtain the minimum velocity ratio which would achieve the desired efficiency levels. Some compromise was necessary between the high pressure and low pressure turbines. The high pressure turbine required a substantially larger diameter than the low pressure turbine to obtain the design efficiency level. This resulted in a steep inner wall angle which was limited to a 17° slope initially so that the flow would remain attached to the inner wall. Subsequent changes in the design reduced this wall angle slightly.

(2) Mach Number

The high axial Mach number in all stages reduced the turbine tip diameters and helped keep the blade centrifugal stresses low. The rpm of both the high and low pressure turbines was set by the high compressor and the fan, although there was some consideration for the high pressure turbine stresses in setting the high rotor speed.

(3) Turbine Inlet Temperature Effect on Mach Number

Changing the match temperature of the engine changes the expansion ratio of the turbine significantly, since the work requirement is constant at both 2000°F and 2300°F turbine inlet temperature. The lower temperature match requires the greater expansion ratio and, therefore, a greater volume flow at the turbine exhaust. A higher Mach number occurs for a given turbine exit annulus area.

At the turbine diameters indicated in the Phase II-A report, the lower turbine match temperature increased the turbine exit Mach number to unacceptably high levels. The last stage turbine tip diameter and annulus area was increased so that the exit Mach number was reduced to approximately 0.6. This resulted in an exit Mach level of 0.5 at the higher temperature match, somewhat below that quoted in the Phase II-A study.

(4) Turbine Cooling Losses

The effects of cooling air on turbine efficiency were also investigated during Phase II-B. In addition to the thermodynamic effects on the overall engine cycle performance, there are some aerodynamic effects on the turbine performance. These effects are stated below:

a. Cooling air injected into the turbine gas stream requires some portion of the main stream energy to accelerate the cooling air-to-main gas stream velocity levels. Turbine tests have been run indicating desirable methods of introducing this cooling air into the gas path with a minimum loss.

b. Compromises in the airfoil design (mainly leading and trailing edge thicknesses) required to effectively cool and protect the airfoils from low cycle fatigue, creep and erosion add some losses to the turbine.

c. Pumping losses in the blades also add to the turbine work requirements.

These losses were estimated to result in a total high turbine efficiency loss of approximately 1.5%. Even with these losses, the required turbine efficiency of 88% is maintained.

c. Turbine Exhaust Section

The major change resulting from the decision to design a 2000°F turbine with growth potential to 2300°F without major mechanical change occurs in the turbine exhaust section. The high exit Mn at the lower turbine inlet temperature requires a diffusing section before the air is turned to enter the nozzle in an axial direction. This has increased the length of the turbine exhaust section approximately 11 inches. As the engine is updated to the final turbine inlet temperature, the exit Mach number will drop, further increasing the efficiency of this section.

Figure 2A-68

TURBINE MEAN LINE AERODYNAMICS
AT 1900°F CRUISE CONDITION

Stage	1	2	3
Vane			
Inlet Velocity (ft/sec)	577.9	1063.	997.1
Inlet Mach number at 1900°F	-	0.5153	0.5079
Axial Velocity	577.9	963.1	933.6
Swirl Velocity	-	450.	350.
Gas Inlet Angle (deg.)	90.0	64.96	69.45
Exit Velocity (ft/sec)	2100.8	1569.2	1516.0
Exit Mach number	0.9731	0.7796	0.7935
Axial Velocity (ft/sec)	800.4	941.5	996.3
Swirl Velocity (ft/sec)	1942.4	1255.4	1142.7
Gas Exit Angle (deg.)	22.39	36.87	41.08
Blade			
Inlet Relative Velocity (ft/sec)	1926.6	1028.3	1041.8
Inlet Relative Mach number	0.4958	0.5109	0.5453
Axial Velocity (ft/sec)	800.4	941.5	996.3
Relative Swirl Velocity (ft/sec)	710.6	413.5	304.4
Inlet Wheel Speed (ft/sec)	1231.7	841.9	838.3
Inlet Relative Gas Angle (deg.)	48.4	66.29	73.01
Exit Relative Velocity (ft/sec)	1926.6	1510.4	1709.0
Exit Relative Mach number	0.9339	0.7694	0.9341
Axial Velocity (ft/sec)	963.1	933.6	1179.7
Relative Swirl Velocity (ft/sec)	1668.6	1187.3	1236.6
Exit Wheel Speed (ft/sec)	1218.6	837.3	836.6
Exit Relative Gas Angle (deg.)	29.99	38.18	43.65
Stage Work (Btu/lb)	113.4	53.0	51.0

d. Aerodynamics

The mean line gas velocity triangles and some of the more important thermodynamic properties of the turbine design are listed in Figure 2A-68. Since the detailed design work is only 50% complete, the root and tip velocity triangles are not listed. The airfoil design will be completed by 1 July 1965.

e. Design Evaluation of the Turbine Rotors

Detailed studies of designs to meet the requirements of a high performance, high temperature turbine were undertaken at the beginning of Phase II-B.

To achieve the desired flow through the blades, it was necessary to provide air to the blades at as high a pressure as feasible. The design goal was to provide cooling air at 90% of the compressor exit pressure. This requirement dictated a minimum pressure loss system to duct the air from the compressor exit into the blades. The air was to be supplied to the turbine compartment forward of the first disk through an annular duct, providing minimum flow losses.

The basic design problem was to provide a minimum loss passage for the air from the forward turbine compartment to the blades, and still meet the rotor life and overall engine performance requirements.

At this point in the design of the engine, neither the turbine flowpath nor the number of blades or airfoil geometry had been established. A general study was therefore undertaken to investigate different configurations meeting the basic design requirements.

A configuration introducing cooling air to the bore of the first stage disk and conducting it to the blade roots through radial passages is shown in Figure 2A-69. Accompanying design features include extended root blades with air sealing plugs between blades at the "fir-tree" root connections to prevent leakage from the air distribution annulus in the disk rim. Blade sealing extensions on the disk rim also support vibration damping weights at the rear end of each blade root platform. Possible advantages of this configuration are: lower pressure loss, introduction of cooling air into the rotating disk, benefits from disk pumping action, uniform disk cooling, and an effective sealing system between the blade roots and the disk rim.

Variations of this basic design were also studied, including connecting the front and rear half of the disk by radial ribs to provide airflow passages. As the turbine detailed design work progresses, this configuration will be analyzed as an alternate design. The suitability of this design is highly influenced by the final number of turbine blades and the required cooling airflow per blade. Other areas of design investigation are machining methods and costs, forgeability of the disk and hub, and possible methods of weight reduction.

A parallel study was made for a more conventional disk and blade cooling system, (drawing upon background J58 engine experience) with cover plates at the disk rim. This study evolved into the design shown in Figure 2A-70. In this design, cover plates are fastened on the front and rear of the disk rim by through bolts and cooling air is introduced through holes in the front plate.

In the double cover plate design, the sealing at the front of the first cover plate is accomplished by a single knife edge on the I. D. of the seal land and by a double knife edge with spoiler on the O. D. of the seal land. The front cover plate of this design is slotted radially from the I. D. to the cooling air feed holes. The seal land is a full hoop. The rear cover plate acts as a full diaphragm to prevent circulation of air between the extended necks and carries the damper weights. Studies of this approach are still being carried out. This design is shown on the general engine arrangement drawing, as preliminary weight calculations indicate that it is lighter than the Phase II-A design.

The major changes on the low turbine rotor from the original Phase II-A design are:

a. The disks and disk-to-blade attachments are sized. This includes LCF calculations, and the second stage change to a solid disk.

b. The second stage blades are damped by tip shrouds instead of an extended root type damping scheme.

c. The low rotor labyrinth seal diameters have been changed to revise the thrust balance.

Disks were sized for various turbines which have been considered in this study (2300°F and 2000°F inlet temperatures, various exit Mach numbers, etc). The fir tree root attachments selected for the last turbine considered (2000°F inlet temperature, approximately 4.5 percent total cooling air) were the J58 Model 1 first and second stage roots for the low rotor second and third stages. The latest temperature estimates

for these attachments are lower than the original estimates, therefore the disk rim widths were set at minimum value (1/2 blade root chord). When the final turbine configuration is set, these attachments can be optimized. Another factor which will affect the second stage root is the consideration of cooling the second stage blades. Two designs are now being investigated. The first utilizes an uncooled, root-damped, shroudless blade, the second approach utilizes a cooled shrouded design. Both designs will be capable of long time operation at 2000°F T.I.T. and short time operation at 2300°F as an initial requirement.

The second stage disk was made solid when the disk synthesis runs on a bored disk showed high tangential stresses at the bore. When the bore diameter was increased to obtain acceptable bore stresses, the cone angles of the shafts became large and excessively heavy cone wall thickness were requied to meet the shaft critical speed. All subsequent turbine sketches show a solid disk with cooling air holes as required.

The second and third stage disks are both fabricated of Waspaloy. The second stage disk is LCF limited. Currently the same LCF allowances are used for Astroloy and Waspaloy, therefore the slight weight saving because of density differences would not offset the cost factor. An Incoloy 901 third stage disk was investigated and rejected because it was too heavy.

Preliminary weight investigations has shown some weight advantages for a tip shrouded design for the second stage blades. Most of this weight difference was in the blade extended necks, which have to be long enough to provide a disk rim-to-damped surface length of 1/4 of the airfoil length. If the second stage blades are cooled, the weight difference is smaller. The second stage blades are hollow to reduce stresses during thermal shocks and to reduce weight.

The low rotor labyrinth seal diameters were increased to obtain a thrust balance system which would keep the bearing out of the skid range at all times. The critical condition for the seal was SLTO.

The cone attaching the third stage disk to the second stage was originally integral with the third stage disk. This part was changed to a two piece design to simplify forging.

The second-to-third stage rim spacer-seal support was securely bolted at both ends. This was accomplished by moving it outward during the thrust balance changes previously mentioned and bringing it conveniently close to the existing disk bolt circles. On occasion JT11D-20 spacers which are held only by snaps have shifted.

All labyrinth seals are designed with sufficient axial clearance to allow the low rotor to shift aft far enough to destroy blade airfoils in case of failure of the forward shaft. This is a safety feature to prevent over-speeding of an unloaded rotor and possible subsequent bursting of disks.

f. Turbine Structural Analysis

(1) General Description

The STF219 engine uses a single-stage high pressure turbine and a two-stage low pressure turbine, as seen in Figure 2A-70. It is enclosed in a forged two-piece case bolted together at interlocking scalloped flanges. Relative to the Phase II-A design, there are dimensional changes resulting from changes in the engine size and in the turbine flowpath. More detailed changes are discussed within each component.

(2) Turbine Cases

The outer turbine case consists of two sections, both of which are one-piece forgings of Waspaloy (PWA 1004). The front turbine case is flanged at the front and rear and contains two conical sections which meet at the minimum diameter. The front flange is scalloped to inter-lock with the scalloped rear flange of the outer combustion chamber case. The rear turbine case is a conical section flanged at the front and rear. The third stage vane retention ring is sandwiched between the rear flange of the rear turbine case and the front flange of the turbine exhaust case. The three flanges involved are all deeply scalloped to reduce thermal stresses, to reduce weight, and to provide clearance for tubes passing over the flanges. Grooves and flanges integral with both turbine cases provide support for the turbine stators.

(3) First Stage Vanes

It is now planned to cast the first stage turbine vanes from B1900 (PWA 663), a nickel base alloy with moderate high temperature strength and creep properties and excellent thermal shock resistance. Other material types are still being considered for this application. The decision to use this material instead of WI-52, as proposed in the Phase II-A report, was based on high temperature experience with B1900 vanes in the J58 and other Pratt & Whitney Aircraft engines. The vanes are air cooled and structurally supported at the end platform attachment points to withstand airfoil gas loads. This attachment scheme is shown in Figure 2A-71. The inner and outer attachments are locked in such a way that, in event of a vane airfoil failure,

the broken end will be retained and will not pass through the turbine. The inner support for the first vane consists of the inner turbine nozzle vane case and the inner vane retaining plate. At the outer platform the vane feet are inserted into a circumferential groove on the rear of the turbine case and into slots on the front of the first vane outer retaining plates. At the inner vane platform, the attachment takes thrust and side loads, but allows free radial movement between the vane and the inner support case. This radial looseness allows for thermal differentials between the inner and outer case and prevents the number 3 bearing loads from being transmitted through the vanes. The inner support case also supports an assembly of labyrinth seals to reduce the leakage of cooling air into the turbine gas stream.

The first stage vanes are cooled by internal impingement and convection. Air enters the vane through an internal distribution tube from a plenum between the outer platform and turbine case. The cooling air from compressor discharge reaches the vane by passing between the combustion chamber outer liner and outer case and through holes in the outer vane retaining plates. The air distribution tube inside the vane airfoil has a number of small holes which direct air to impingement cool the inside of the leading edge and to convectively cool the sides of the airfoil. Small protrusions on the sides of the tube control the gap between the tube and the airfoil inner wall. They help maintain effective convective cooling as the air flows around the tube and exits through slots in the trailing edge of the airfoil.

(4) Second and Third Stage Vanes

The second and third stage vanes are cast from a nickel base alloy (PWA 658) and are cantilevered from the turbine case. The vanes are subjected to loading by gas pressure on the airfoils and inner vane supports. They are secured front and rear by feet integral with the vane platforms and engage circumferential grooves in the turbine cases. The tangential shear loads are transferred to lugs on the first and second stage tip seals. The inner platforms of the second and third stage vanes are provided with lugs which engage mating lugs in an annular channel-shaped inner support fabricated from Waspaloy (PWA 687). Rings carrying knife-edge seal lips are riveted to the forward inner edges of the annular channels. Both second and third vanes are uncooled; the second stage vanes can be readily cooled by air admitted to their outer shroud annulus as development proceeds to higher gas temperatures.

(5) Blade Tip Shrouds

The blade tip seals are fabricated from Hastelloy X because of its high oxidation resistance and strength. The first stage blade tip seal is held in place by the outer support of the first stage vanes and by the second stage vanes. The seal is cooled by compressor discharge air traveling between the seal and the outer turbine case, and by a flow of air which is metered through holes in the outer support. The second stage blade seal is held in place by the second and third stage vanes. The first stage blade tip seal has a pressurized axial seal ring in a groove at its forward edge which bears against the inner flange of the first stage vane outer support. Replaceable wear rings are sandwiched between the first and second stage seal rear edges and the forward surfaces of the second and third stage vanes respectively. In addition, the first and second stage blade tip seals have torque lugs at the rear which engage grooves in the turbine case and then extend rearward into the flow passage in the outer front foot of the following vane. Adequate radial and axial clearances have been provided between the seal lugs and case lugs to ensure that the relative thermal expansion of the parts will not constrain the seals during steady-state or transient operation. The third stage blade tip seal is held in place by the third stage vane retention ring and by a shoulder on the turbine exhaust case grooved to engage the seal torque lugs. Also, the contact surfaces between the vanes and the seals are hardfaced to prevent galling.

(6) Fail-Safe Features and Blade Containment

Each of the vanes is secured at both ends to prevent any part of a fractured or burned vane from being carried downstream. In addition, the knife-edge seals have been designed to allow unrestricted rearward travel of the rotor. Hence, in the event of a shaft failure the rotor shifts axially into the stator. This dissipates the stored rotational energy within the engine and batters the airfoils to reduce their torque input to the rotor. Containment of broken blades is provided partially by the turbine cases and the duct heater cases. Additional containment is provided with the minimum addition of weight by the heatshield liner located just inside the duct heater outer case. The total containment thicknesses were based on the strength and toughness factors for each different containment material at their maximum operating temperatures.

(7) Turbine Hot-Parts Inspection

Provision has been made for the inspection of the first stage vanes and the first stage turbine blades without a complete disassembly of the

engine. The outer combustion chamber can be moved aft after the oil and cooling air tubes to the number 4 bearing compartment are removed from the turbine case. The combust on chamber outer liner then is moved forward exposing the vanes. ndividual vanes may be removed by sliding the inner combustion chamber liner forward and removing the inner and outer vane retaining plates. Visual inspection of the first stage blades is possible after the vanes are removed.

g. Description of Rotating Parts

As discussed in the Design Evolution of the Turbine Rotors, the high pressure rotor consists of the first stage disk and blade assembly, the first stage rear seal ring, and the first stage turbine front shaft. The disk and blade assembly includes the disk front and rear cover plates and the front cover plate cover.

The self-supporting disk seals shown in the Phase II-A final design report have been replaced by cover plates supported on pilot diameters of the main disk for reduced weight.

The disk and blade assembly and the rear inner seal ring are bolted to the rear flange of the turbine front shaft by 16 hollow tiebolts (5/8 inch). The front and rear cover plates and the front cover plate cover are mounted on snap diameters on the disk and retained by 50 bolts (1/4 inch). Cooling air for the rear face of the first disk flows through the hollow tiebolts.

The disk front cover plate fulfills two functions. First, it provides a sealing surface for the knife-edge seals mounted on the first stator inner support, and second it acts as a feeder plate to distribute cooling air to the first stage blades.

Elliptical holes in the front cover plate are aligned with cooling air passages in the front of the extended necks of the blades. To prevent leakage of blade cooling air, the blades are held against the rear face of the front cover plate by the tight axial fit of the blades between the front and rear cover plates. The front cover plate is slotted radially from the inside diameter to the seal ring. This reduces the thermal stresses due to temperature gradients. The front cover plate cover prevents cooling air leakage through the slots in the front cover plate. The rear cover plate retains the blades, provides a mount for the blade vibration damping weights, and acts as an air baffle preventing the circulation of hot turbine gases past the blade necks and platforms. The rear cover plate is conical in shape and offsets the gas pressure loads by centrifugal force. The rear cover plate is slotted from the

outside diameter inward to reduce thermal stresses. The slots are aligned with extensions on rear face of the blade necks which serve to prevent leakage through the slots.

Air sealing at the rear of the first disk and the front of the second disk is provided by a number of knife-edge seals, all of which are supported by the second stage stator inner shroud. To assure a uniform temperature across the first disk, a chamber is formed at the rear of the disk by a seal at the first blade platform, and another at a seal ring mounted at the tiebolt circle. This chamber is pressurized by air passing through the hollow cover plate bolts. Sealing at the front of the second disk is provided by a double knife-edge and seal ring bolted to the second stage disk and a single knife-edge seal at the second blade platform.

The low pressure rotor consists of the second stage disk and blade assembly, the interstage spacer and seal support, the second stage front seal, the third stage disk support cone, the third stage disk and blade assembly, the third stage disk rear seal, the low pressure turbine rear hub, and the low pressure turbine front shaft.

The rear flange of the low pressure turbine front shaft, the second disk and blade assembly, the low pressure turbine rear hub, and the third disk support cone are bolted together with 18 tiebolts (5/8 inch). The third disk support cone rear flange, the interstage spacer and seal support, and the third disk and blade assembly are bolted together with 24 tiebolts (3/8 inch).

The cylindrical interstage spacer and seal support provides disk stiffening and raises the resonant vibration frequency of the third stage disk. This brings the disk out of the frequency range excited by the upstream flow pattern of the turbine exhaust struts. In addition, the spacer supports the knife-edge seals which mate with the seal surface mounted on the third stage stator inner shroud.

In all turbine stages, the blade roots are attached to the disk by a multiple serration "fir tree" root. This provides an attachment that withstands fatigue and stresses resulting from centrifugal forces and aerodynamically excited vibrations. Experience has shown that this method of attachment is reliable and efficient. Extended blade roots, similar to the J58 engine in which the blade neck extends between the platform and root attachment, are used on the first stage blades to displace the disk rim and attachment away from the hot turbine gas stream and to facilitate their cooling. Cooling air enters the blade through an elliptical hole in the front of the extended neck just outboard of the root attachment and passes through the hollow neck to the airfoil. The first stage blades are retained by

bolted front and rear cover plates. The second and third blades are uncooled and have their root attachment immediately adjacent to the platform for minimum weight. The second and third blades are retained by rivets through the apex of the fir tree.

Vibration damping for the first stage blades is provided by damper weights riveted to the first disk rear cover plate. Centrifugal force causes the weights to bear against the blade platform and a surface on the cover plate to provide frictional damping of blade vibrations. The change to the riveted type damper instead of the Phase II-A pin type was based on extensive experience with the J58 engine.

The second and third stage blades have interlocking tip shrouds to control blade vibrations. The tip shroud bearing surfaces are hardfaced to prevent excessive wear. The shrouds also carry two knife-edge seals which mate with a stepped seal ring mounted in the turbine case. The second stage blades airfoils are hollow for reduced weight and greater resistance to thermal shock. The alternate second stage blade design without tip shrouds will utilize extended roots and friction damping.

(1) Blade Platform

All turbine blades have integral platforms at the root which extend to form cylindrical surfaces to mate with stationary interstage knife-edge seals. These seals prevent the hot turbine gases from circulating into the cavities between the disks, and therefore the temperature gradient between the disk bore and rim is reduced together with the resultant thermal stresses. The outer surfaces of the platform form the inner boundary for the gas path.

(2) Disk Material Selection

The primary element in the design of a satisfactory life turbine disk is the selection of materials with the necessary properties to meet the requirements dictated by the levels of stress and temperature under which the disk must operate. The determination of the mechanical properties of these materials has been accomplished largely by Pratt & Whitney Aircraft, although some data were supported by material published by material producers, government agencies, research corporations, and full scale spin testing.

Nickel alloy (PWA 1013) has been selected for the first stage turbine disk and another nickel alloy (PWA 1007) for the first disk cover plates. The second and third stage disk are also PWA 1007. Experience with

these materials in Pratt & Whitney Aircraft engines indicates that they will provide satisfactory life at the temperature and stress levels predicted for the STF219.

h. Turbine Stress Analysis

Computer programs were utilized to accurately determine the stresses in the rotating components. These programs analyzed both symmetrical and asymmetrical shapes with both symmetrical and asymmetrical loading The analyses provided information needed to determine burst speed, low cycle fatigue capabilities, creep growth, and disk blade resonance.

To ensure that the best disk material would be chosen for each stage, three different materials were considered: Inconel 901, Waspaloy, and Astroloy. In selecting the material for a stage the designs in the three materials were judged on the basis of optimum weight, shape and cost.

By utilizing Astroloy's high creep and stress rupture properties the lightest disk with an optimum sized root attachment was designed for the first disk. The disk is burst limited.

FIRST TURBINE DISK STRESS SUMMARY

Material	Astroloy
Average Temperature (°F)	1120
Maximum Gradient (°F)	125
Average Tangential (psi)	71,300
yield margin (%)	18
burst margin (%)	30
Low Cycle Fatigue Life (hrs)	
bore	50,000
main bolt circle	35,000
coverplate bolt circle	90,000
rim	35,000

Waspaloy was chosen for the second turbine disk because of its excellent low cycle fatigue properties.

SECOND TURBINE DISK STRESS SUMMARY

Material	Waspaloy
Average Temperature (°F)	1160
Maximum Gradient (°F)	70
Average Tangential (psi)	66,100
yield margin (%)	14
burst margin (%)	38
Low Cycle Fatigue Life (hrs)	
center	8,000
main bolt circle	30,000
rim spacer	30,000
rim	30,000

The third stage disk material was changed to Waspaloy to provide a light-weight disk at reasonable cost. This disk is burst limited.

THIRD TURBINE DISK STRESS SUMMARY

Material	Waspaloy
Average Temperature (°F)	1130
Maximum Gradient (°F)	45
Average Tangential (psi)	75,300
yield margin (%)	7
burst margin (%)	30
Low Cycle Fatigue Life (hrs)	
bore	100,000
main bolt circle	20,000
rim spacer	20,000
rim	9,000

Blade-to-disk fir tree attachments are either the same or similar to those which have many hours of successful experience at similar temperatures in the JT11D-20. The allowable stress ratios have been derived from both the JT11D-20 engine program and other applicable experience. The following is a stress summary of a typical root attachment:

Disk Material	Waspaloy
Attachment Temperature (°F)	1200
Blade Material	IN-100

DISK STRESSES

	Stress	Allowable	Ratio (Stress/Allowable)
P/A (First Neck)	32,000	54,500 (65% 6000 Hr. S. R.)	.59
MC/I (First Tooth)	23,500	33,600 (40% " " ")	.70
Shear (First Tooth)	20,900	25,300 (30% " " ")	.83
Combined (First Neck)	55,500	88,200 (105% " " ")	.63
Bearing (First Tooth)	61,700	63,300 (80% x .2% yield)	.98

BLADE STRESSES

	Stress	Allowable	Ratio (Stress/Allowable)
P/A (First Neck)	44,800	50,200 (60% 6000 Hr. S. R.)	.89
MC/I (First Tooth)	22,100	33,400 (40% " " ")	.66
Shear (First Tooth)	20,500	25,100 (30% " " ")	.82
Combined (First Neck)	66,000	83,500 (100% " " ")	.79
Bearing (First Tooth)	56,200	56,200 (80% x .2% yield)	1.0

(1) Blade Material

Pratt & Whitney Aircraft turbine blade materials are selected to achieve the best combination of ductility, corrosion resistance, and high tensile and stress rupture properties to satisfy the design requirements Inconel 100 (PWA 658) was chosen as the blade material for all three turbine stages. Based on current engine experience, this material shows promise of demonstrating satisfactory blade attachment life at predicted temperatures and attachment stress levels.

(2) Turbine Cooling

Cooling air for turbine parts is obtained from the last stage of the compressor, and arrives at the turbine via two routes. The outer portion of the first stage disk and blades is fed through holes in the inner burner case into the plenum at the front of the first disk. A small portion of this air is metered through the first disk by means of hollow cover plate bolts to cool the rear face of the first disk. Cooling air for the first turbine blades is supplied from the plenum. The remainder of

this air is lost through leakage past the knife-edge seals at the front cover plate. The second source of turbine cooling air from the seventh stage compressor discharge leaks past the knife-edge seals at the rear of the compressor seventh disk, flows through holes in the high speed compressor rear hub, passes through the annulus between the high and low speed turbine shafts, and then passes between the bore of the first stage turbine disk and the low speed turbine shaft. This air establishes the bore temperature of the first stage disk and cools all of the low speed turbine rotor. From the plenum in front of the second stage disk, the air splits into three paths. Part is lost past the knife-edge seals at the front of the second stage disk; part passes through holes in the second disk, cools the rear face of this disk and the inter-stage spacer and seal support, then leaks past the knife-edge seals at the second and third blade platforms; the remainder passes through holes in the low speed shaft, through holes in the solid second disk, through holes in the low rotor rear hub to cool the third stage turbine disk, and leaks past the knife-edge seal at the rear of the third blade platform. Very little pressure differential exists across the inner seal at the rear of the first stage disk and the direction of flow past this seal may reverse at some flight conditions. The primary function of this seal is to separate the high rotor cooling air from the low rotor cooling air and to assure a uniform air temperature on both sides of the first stage disk. Experience on the JT11D-20 has shown that temperature gradients across a disk can be very troublesome as they may produce high bending stresses in the disk web. Base cooling the first disk and the second and third stages with compressor fourth stage air, as proposed in Phase II-A, was abandoned because the resultant radial thermal gradients in the disks produced unsatisfactory low cycle fatigue life.

The first stage blade is cooled convectively by air flowing radially through the airfoil. The air enters the root extended neck and flows through a relatively large hollow neck to the airfoil. A series of baffles in the airfoil core passage begin at approximately midspan to restrict the flow and to increase the gas velocity for more effective cooling. The tip of the airfoil is extended slightly on the high pressure side insuring that the exiting cooling air will exhaust to the low pressure side. This baffle type hollow blade has been used successfully on the JT11 turbine.

(3) Turbine Rotor Balance

Before assembly, the high speed front turbine shaft is dynamically balanced by removing material from the rear flange and by inserting plugs into holes provided in the front of the shaft. The first stage disk and blade assembly is statically balanced by pairing blades by moment

weight during assembly, by mounting the front and rear cover plates with heavy sides opposite, and by subsequently inserting plugs into holes provided between the tiebolts in the disk. The plugs are trapped after assembly by adjacent flanges.

The turbine rotor is assembled together with the number 3 bearing compartment and support, the combustion chamber inner and outer cases, the first stage turbine stators, and all associated hardware. The entire assembly is then balanced using nuts on the high speed turbine tiebolts which are classed by weight and by adding riveted weights on an extension of the seventh stage compressor seal disk. The system of weight classed nuts has been proved satisfactory for JT11D-20 turbine rotor balancing.

The low speed turbine front shaft is balanced by machining corrections in the flange provided just behind the high pressure compressor and by machining the outside of the rear flange. The second stage disk and blade assembly is balanced in the manner described for the first stage. The third stage disk and blade assembly is rough balanced by the blade pairing moment weight method.

The low speed rotor is then assembled with the turbine rear case and the third stage stators and inner shroud. The rotor is also balanced by using classed nuts on the tiebolts at the rear of the third stage turbine disk and the tiebolts at the low rotor turbine shaft rear flange. This method of turbine rotor balancing was selected over the riveted weights-extension system used in Phase II-A to simplify the disk forging.

j. Turbine Vibrations

(1) First Stage

The first stage turbine incorporates damped extended root blades because of high blade buffeting excitations from the burner. Damping similar to the J58 first stage is accomplished by the use of centrifugal toggle weights. The toggles contact the aft blade platforms and a land on the coverplate. Each toggle can adjust radially, but is retained by a rivet to the aft disk coverplate. Relative motion between the blade platforms and coverplate is provided by a flexible blade root extension. In the fundamental blade vibration modes, friction forces caused by the toggles rubbing on the contact surfaces dampen the motion and reduce stresses. Damping effectiveness is sensitive to the friction forces. Optimum friction force was achieved by properly sizing the toggle weights.

The first stage blade and disk assembly exhibits no resonance in the running range. Figure 2A-72 shows the bladed disk coupled mode. A seven nodal diameter mode lies in the running range, but this mode should have very little excitation.

(2) Second and Third Stage

The second and third stage blades are tip-shrouded to increase blade stiffness and blade resonance above 2E at speed. The alternate unshrouded second stage blades utilize extended roots and friction damping for vibration control. Blade stresses are reduced by positioning the shroud angle parallel to the blade bending motion in the fundamental vibration mode. Damping is thus assured in the modes where maximum stresses are expected. A disk spacer was necessary to stiffen the disk to provide the 2E margin in the bladed disk coupled vibrations mode. Figures 2A-73 and 2A-74 show the disk blade coupled frequencies.

A rim spacer was used on these stages because it was found impractical to extend the bolt circle of the shaft radially outward enough to lend sufficient stiffness to the disk for 2E margin. With a rim spacer the location of the shaft bolt spacer has little effect on disk stiffness. Straight through bolting of the shaft is then possible. This yields a lighter, stiffer turbine shaft for critical speed purposes.

9. TURBINE COOLING ANALYSIS

a. Introduction

Design emphasis has been placed on the efficient use of cooling air within the demonstrated state of the art of cooling techniques, materials and erosion-corrosion preventative coatings. The blade and vane designs proposed for the Initial Engine operation use current production engine materials, coatings and cooling techniques. The Basic Engine blade and vane designs use current production engine materials and coatings. The effectiveness of the advanced cooling techniques has been documented on Turbine Development Engines.

The blade and vane coolant airflow requirements for the Initial Engine and Basic Engine cruise conditions are summarized in the table below. The design coolant airflows for this conservative approach limit the maximum local metal temperatures to levels consistent with current experience (1735°F). As a result, flows at the Basic Engine cruise condition are somewhat higher than desired for good thermodynamic performance. Cooling flow requirements are expected to be eased

substantially during the development of the Basic Engine as a result of advances that have been made, but not proven in long time production engine service, in erosion-corrosion preventative coatings and in the use of materials such as PWA 664, the directionally-solidified-grain casting process for Mar M-200.

Blade and Vane Design Cooling Flow
Requirements Based on Current State of the Art

	Initial Engine Cruise	Basic Engine Cruise
First Stage Vane	1.5%	4.0%
First Stage Blade	1.0%	3.9%
Second Stage Vane	0.0%	1.25%
	2.5%	9.15%

Some of the effort expended in Phase II-B has been used in the development and calibration of new analytical techniques needed in the design of advanced cooling schemes and in obtaining and interpreting data employed to describe the physical properties used in design work. The areas in which this work is most important are basic heat transfer, the performance properties of materials, and cooling configurations. Any changes from the techniques and data used in Phase II-A are noted in the specific sections below as they are incorporated into the design. Also reflected in the design described is a basic difference from Phase IIa in that the Basic Rating at 2300°F is actually a specific design to be arrived at through an ordered process of development-evolution. In Phase II-A a single design was proposed which would be essentially operating at an "off design" condition at the initial turbine inlet temperature.

b. Design Requirements

- The TBO goal for turbine blades and vanes is 3000 hrs.

- Blades and vanes designed for initial engine TIT of 2000° at take-off for a 3000 hour TBO and for capability of meeting a 2300°F Turbine Inlet Temperature FTS rating.

- Burner temperature profiles - Average radial profile requirement is shown Figure 2A-75. The peak average gas temp. is 2070°F for take-off condition. The burner design objective is $\Delta TVR = \frac{T_{max.}}{T_{avg.}} = 1.11$ for the 2300°F TIT engine. The initial engine blade and vane design is predicated on a ΔTVR of 1.18 to ensure adequate design margin.

- Hot spot vane peak gas temperature of 2240° at 2000°F TIT take-off condition. This would give a hottest vane metal temperature about 110°F higher than average vane maximum temperature.

- Structural requirements - the design must satisfy the following structural requirements for 3000 hr. TBO.

  Stress Rupture and Creep
  Erosion - Corrosion
  Thermal Fatigue
  High Frequency Fatigue
  Impact

- Performance - Cooling flow quantity must be minimized and the method of injection into the turbine flow path must not seriously affect turbine efficiency.

- Weight and cost are minimized consistent with structural, life and performance requirements.

- Growth Capability - The vane and blade configurations will permit the required increases in TIT without radical changes in cooling supply pressure, vane or blade construction and with comparable life.

c. Blade and Vane Design Choice

The first stage turbine vane designs chosen for the STF219 engines are summarized below.

The impingement cooled vane design was chosen for the Initial Engine. The vane configuration is used in the JT11D-20 and the turbine development engines. This vane has adequate margin for 2140°F TIT transport operation with 3000 hour design life, and for 2300°F TIT development operation with at least 500 hours engine life.

The Basic Engine vane design utilizes a highly refined version of impingement cooling which is a development of the initial vane design to provide additional cooling for long time operation at 2300°F TIT.

A film cooled vane was designed as a backup for the Basic Engine convectively cooled vane and to permit growth in turbine inlet temperature.

The following design possibilities were considered:

(1) Vane Design Selection

A. The vane design chosen for the initial engine is shown in Figure 2A-7o with the impingement cooled leading edge and convectively cooled pedestal-core trailing edge. This configuration is the one developed for and used by the JT11D-20 engine with very satisfactory results at turbine inlet temperatures substantially in excess of initial STF219 engine requirements.

In this design, coolant is introduced into a dead ended coolant tube. The coolant impinges on the vane leading edge through holes in the tube, flows around the tube toward the trailing edge, and is injected into the gas path through a trailing edge pedestal supported slot. This configuration has several significant features:

(a) The span wise gradient, Figure 2A-77, is low because the coolant flow direction is chordwise and coolant, at essentially constant minimum temperature, is introduced to all parts of the span simultaneously.

(b) Leading edge metal temperatures are low because the impingement coolant heat transfer coefficients are very high.

(c) Ejection of coolant into the flow path is through a trailing edge slot with minimum aerodynamic loss.

The material chosen for the vane is B-1900 (PWA663). The alternate material selected for this vane is PWA664. The vane design life limit of 3000 hours is met at the design coolant flow.

Growth capability is excellent, the only modification required being the enlargement of the coolant feed spigot to provide additional air. Figure 2A-78 shows the growth capability of this configuration at the design flow and at the maximum flow possible without part reoperation. The vane is erosion limited and growth limits are shown based on results of current Pratt & Whitney Aircraft experience with the PWA45 coating.

B. The vane design shown for the Basic Rating of the engine for operation at 2300°F TIT is shown in Figure 2A-79, with the impingement cooled leading edge with leading edge coolant air ejected at the vane O.D. and the convectively cooled finned mid-chord

section with a pedestal core trailing edge slot. This configuration is a modification of the one used by the JT11D-20 engine and proposed for the initial STF219 engines.

In this design, the coolant used to protect the leading edge is introduced at the vane I.D. The coolant used to protect the mid-chord and trailing edge is introduced as required along the chord and finally injected into the gas path through the trailing edge slot. This configuration has the following features:

1. The spanwise gradient, Figure 2A-80, is comparable to that of the initial engine configuration even at the very high gas temperatures as a result of the introduction of coolant at constant minimum temperature to all parts of the span simultaneously.

2. Leading edge cooling requirements are more severe than those of the initial engine configuration. This configuration permits the high impingement velocities to be realized at increased mass flows that are required. This design allows the use of a high pressure ratio across the impingement tube insuring that maximum cooling can be obtained.

The material chosen for the vane is PWA664. The alternate material is B-1900 (PWA663). The vane design life limit of 3000 hours is met at the design coolant flow.

Growth capability of this scheme is shown in 2A-81. The vane is erosion limited and growth limits are shown based on results of current Pratt & Whitney Aircraft experience with the PWA45 coating. Additional growth margin (100°F or more) will be realized as the new coatings are proven, such as the Tantalum enriched AlCo coating system now being tested.

C. An alternate vane design is shown in Figure 2A-82 for the basic rating at 2300°F TIT. The leading edge is impingement cooled with coolant ejected at the vane O.D. The trailing edge and mid chord are film cooled. The configuration has the advantage that the spanwise gradient, Figure 2A-83, is very flat, even at the very high gas temperatures as a result of the leading edge impingement cooling and the protection of the air film over the mid chord and trailing edge.

PWA664 was chosen as the vane material. The vane design life limit of 3000 hours is met at the design coolant flow.

Growth capability of this scheme is shown in Figure 2A-84. The vane erosion limits and growth limits are shown based on results of current Pratt & Whitney Aircraft experience with PWA45 and PWA47 coatings.

(2) Blade Design Selection

The first stage turbine blade designs chosen for the STF219 engines are summarized below.

A three-cavity convectively cooled blade design was chosen for the Initial Engine. This blade in PWA658 (IN 100) has growth margin for 2110°F TIT transport operation with 3000 hours engine life.and for 2300°F TIT development operation with at least 400 hour life.

A baffled passage, single cavity, convectively cooled blade was designed as an alternate for the Initial Engine. This configuration is the proven JT11D-20 cooling scheme and has adequate margin for 2075°F TIT transport operation, and for 2300°F TIT development operation with at least 300 hour life.

The Basic Rating blade design is a modification of the Initial Engine design to provide additional cooling for long time operation at 2300°F TIT and above. This blade uses a showerhead leading edge, convectively cooled midchord and film cooled trailing edge.

A. The blade design chosen for the initial engine is shown in Figure 2A-85. This blade has a three cavity, convectively cooled foil with metered flow to each cavity. Leading and trailing edge cavities flow coolant at a higher mass flow rate than the mid-chord cavity. The mass cross-section distribution and the coolant flow are adjusted to provide the required erosion life at the leading and trailing edges without creating the chordwise thermal gradients which would create a cyclic life problem. This blade has a 400 Hour life capability at 2300°F TIT.

This blade configuration has the advantage of good growth margin as a convectively cooled blade with the built in capability of being converted to the Basic Rating engine blade, Figure 2A-86, by the addition of film cooling provisions.

Figure 2A-87 shows the first turbine blade metal temperature for the 2000°F TIT take-off condition. The allowable metal temperatures are based on the creep strength of IN-100.

IN-100 (PWA658) was chosen as the blade material, and B-1900 (PWA663) was chosen as an alternate material. The blade design life limit of 3000 hours is met at the design coolant flow with either IN-100 or B-1900 material.

Growth capability is excellent, the only modification required is to open the flow metering restrictions to permit higher coolant airflow. Figure 2A-88 shows the growth capability of this configuration at the design flow and at the maximum flow possible.

The blade in IN-100 (PWA-658) or B-1900 (PWA663) is cyclic fatigue limited with approximately a 60°F temperature margin, allowing an initial growth to 2060°F takeoff TIT. Approximately 100°F additional TIT margin could be obtained by the direct material substitution of PWA664, Mar M-200 material cast with directionally solidified grain oriented along the blade span. The PWA664 blade with very high thermal cyclic fatigue strength is essentially erosion limited as the cyclic fatigue limit approaches the erosion limit.

B. An alternate blade design for the Initial Engine is shown in Figure 2A-89. This blade is convectively cooled, single cavity with baffles arranged to direct the coolant toward the leading and trailing edges. This configuration is one developed for and used in the J58 engine with very satisfactory results and at turbine inlet temperatures in excess of initial STF219 engine requirements.

Figure 2A-90 shows the first turbine blade metal temperature for the 2000°F TIT takeoff condition. The allowable metal temperatures are based on the creep strength of IN-100.

The blade material selected is IN-100, with B-1900 as an alternate. The blade design life limit of 3000 hours is met at the design coolant flow in either material.

Growth capability is moderately good, the only modification required is to open the flow metering restrictions to permit higher coolant airflow. Figure 2A-91 shows the growth capability of this configuration at the desired flow and at the maximum flow possible.

C. The blade design chosen for the Basic Rating of the engine for operation at 2300°F TIT is shown in Figure 2A-86. This blade uses a "showerhead" leading edge, convectively cooled midchord and a film cooled trailing edge. The coolant flow is metered to provide the desired chordwise and spanwise temperature distributions.

Figure 2A-92 shows the blade metal temperature for the 2300°F TIT takeoff condition. The allowable metal temperatures are based on the creep strength of PWA658 (In-100).

The blade material selected is IN-100, with B-1900 as an alternate. The blade design life limit of 3000 hours is met at the design coolant flow in either material. Additional growth potential can be had either in TIT or blade life with the use of PWA664, the directionally solidified grain casting process using Mar M-200 materials.

Flat chordwise temperature profiles are desired for good thermal fatigue life. Figure 2A-93 shows the maximum chordwise thermal gradients at 8.0 seconds as a result of an 8.0 second acceleration from idle to 2300°F takeoff TIT. The thermal gradients shown here are conservatively high to ensure the margin needed for manufacturing tolerances. Measured maximum transient thermal gradients on similar film cooled hardware in the Turbine Development Engine are shown in Figure 2A-94 at 7.0 seconds during a 2 second acceleration from idle to 2330°F TIT. The thermal gradients are less severe than the design gradients.

d. <u>The Effect of Combustor Design on Turbine Life</u>

Turbine durability is influenced to a great degree by combustor performance. To provide maximum life, the combustor must deliver a specified radial temperature profile and, at the same time, minimize circumferential temperature distortion in the form of local hot spots. An improper radial profile can cause excessive blade creep and excessive distress on turbine disc rims and case attachment areas. Local hot

spots reduce life by causing excessive local oxidation, erosion, and creep. The annular combustor proposed for the STF219 engine has been designed to deliver an optimum radial temperature profile with minimum hot spots.

The proposed STF219 engine is being designed for a initial turbine inlet temperature of 2000°F at sea level takeoff and 1900°F at Mn 2.7 cruise. Ultimately, the turbine will be developed for operation at turbine inlet temperatures of 2300°F and 2200°F for SLTO and cruise respectively. It is apparent that temperature distortion becomes a more critical problem as turbine inlet temperatures are increased and the development of a 2300°F turbine will depend on the development of a combustor which exhibits a distortion level which is somewhat less than current engines are demonstrating. The 2000°F turbine design is based on a conservative distortion level which represents a small improvement over current commercial engines but well within the demonstrated performance of the JT11D-20.

Pratt & Whitney Aircraft's nomenclature for this temperature distortion is ΔTVR, which is defined as:

$$\frac{\text{Maximum Combustor Temperature Rise}}{\text{Average Combustor Temperature Rise}} = \frac{T_{T5\ max} - T_{T4\ avg}}{T_{T5\ avg} - T_{T4\ avg}}$$

The following table presents the ΔTVR target value for the STF219 engine compared with two other production engines.

Engine	ΔTVR
JT8D-1	1.20
JT11D-20	1.145
STF219	1.11*

* Vane and blade design margin provides for ΔTVR = 1.18 at 2000°F initial design point.

The JT8D-1 has been used as an example of current commercial engine combustor performance. This engine is currently in production and represents Pratt & Whitney Aircraft's latest engine model in wide scale commercial use. It normally operates at turbine inlet temperatures of approximately 1800°F at sea level takeoff. It can be seen that the immediate goal for the STF219 engine represents a nominal improvement over the JT8D-1 current design. The JT11D-20 engine, designed for Mach numbers in excess of SST requirements, and turbine inlet temperatures in excess of 2000°F, has a combustor performance comparable to STF219 requirements. The STF219 annular configuration, which provides a smooth transition between the compressor and turbine, is a major factor contributing to the planned improvement. All airflow is in the axial direction with no requirement for transition from the annular configuration of the compressor to a can-annular combustor and subsequent transition back to an annular turbine. Elimination of transition areas minimizes maldistribution of airflow which is a factor contributing to temperature distortion. This change to an annular configuration should provide the indicated ΔTVR at the 2000°F level with substantial margin. Further reduction to a ΔTVR of 1.11 at 2300°F will be achieved through development which will optimize finer details such as fuel nozzle and swirler design and liner air injector geometries.

Another important requirement of the combustor is that it deliver a specified radial temperature profile to the turbine. The radial temperature profile must be controlled to provide cool gas at the gas path inner and outer diameters and to place the peak temperature near the middle of the gas path where airfoil stresses are low. The gas must be cool at the I.D. and O.D. of the turbine annulus to keep the turbine disc rims and case attachment regions at a low temperature. The peak temperature must be kept at a radial location which will not create excessive local creep on the blades. The control of a radial profile has never presented any problem in current systems so no difficulty in achieving the desired profile in the STF219 is anticipated.

Testing conducted by Pratt & Whitney Aircraft has indicated that the desired combustor performance can be achieved in the type of annular combustor proposed for the STF219 engine. A ΔTVR as low as 1.10 has been measured in a 72° segment rig at a combustor temperature rise in excess of 1800°F. (The temperature rise required to attain a turbine inlet temperature of 2300°F at S.L.T.O. is less than 1700°F.) In addition, radial temperature profile tailoring has produced profiles which approach those required for the engine design. Figure 2A-97 shows a comparison between the optimum profile for a 2000°F S.L.T.O.

design point and a profile measured in the test rig. A more detailed discussion of combustor testing is presented elsewhere.

o Turbine Blade and Vane Anlysis for Initial 2000°F TIT

Turbine blades and vanes are designed to meet structural requirements which result from engine cycle and engine mission requirements. The engine cycle sets:

- engine operating speed
- engine operating temperatures
- blade-hub-tip ratio
- blade solidity

The engine mission sets the life requirements:

- time at take-off, climb, and cruise temperatures
- cyclic life

The cycle and mission together define an environment which creates turbine blade requirements for

- centrifugal loads - vary with power setting
- time at temperature - set by desired life
- rapid changes of temperature - rapid power changes
- integral order and random vibratory excitations
- gas bending loads - vary with thrust
- corrosive and erosive environment

The modes of failure which result from exposure to the above environment are outlined below.

Blade and vane creep and stress rupture failure is characterized by the time-temperature dependent deformation of these components. Maximum local creep limits are established for blades to avoid excessive strains which might lead to tip rubs and/or material stress rupture. Vane limits are expressed in terms of vane bow and material stress rupture.

Erosion-corrosion of blade and vane surfaces is a defined degree of distress. Erosion limits are set to limit replacement at overhaul for poor appearance, prevent intergranular corrosion of blade or vane base metal and to limit performance losses due to blade contour changes.

Thermal fatigue of turbine blades and vanes is a result of temperature gradients in the foils caused by rapid gas temperature changes during operation. These gradients can become large enough to produce fatigue cracks before the blade stretch or vane bow would require replacement.

Vibratory fatigue is an important design factor in turbine blades. Turbine blades are subjected to two important types of excitation: wakes from stationary structures and "random" excitation resulting from turbulence induced by combustion. Blade tuning to avoid stationary wake excitation and damping to control "random" excitation will permit trouble free operation.

Impact damage is encountered in the design of turbine blades and vanes. Little can be done to reduce significantly the probability of foreign object ingestion. The vane and blade damage can however be affected by the structural design of the vane or blade.

(1) 2000°F TIT Initial Engine Design

As stated in the introduction the object of these design studies was to produce a detailed turbine design for initial flight operation at 2000°F and capable of escalation to the basic rating of 2300°F. The general turbine configuration was established to meet both of these objectives without major mechanical changes. The blades and vanes designed for the Initial Rating of 2000°F will be capable of meeting prototype durability requirements at the Basic Rating of 2300°F.

The performance penalties associated with blade and vane cooling combined with the cost increases attributed to these foils made the use of uncooled foils attractive if their structural integrity can be assured. The decision was therefore made to cool a minimum number of stages in the initial 2000°F engine but provide the physical spacing and sizing that would be required to cool other stages should this be required.

The STF219 turbine is a three stage design consisting of one high pressure stage and two low pressure stages. In the 2000°F design the first blade and vane require cooling. The first vane is a conventional simply supported design. The first blade uses an extended root with friction damping to assure good vibration control with maximum cooling scheme flexibility and growth potential. The remaining stages use O.D. cantilevered stators and tip shrouded blades. A alternate second stage blade design without tip shrouds will utilize extended roots and friction damping. Stress distributions are given in Figure 2A-98 through 2A-103. These blade stresses are generated for IN-100 material.

The following sections describe the STF219 design approach to each of the failure modes and uses analytical techniques correlated with engine experience to substantiate the 2000°F design configuration. The STF219 first blades and vanes are used as models to illustrate the analytical techniques used in this and other Pratt & Whitney Aircraft design projects. The results of the STF219 analysis is then compared to the analysis and performance of current production engines.

(2) Blade Stretch

Overall blade elongation is used as a measure of blade distress resulting from a combination of:

- Centrifugal stresses
- Gas bending stresses
- Time at temperature
- Thermal stresses resulting from rapid temperature change

Overall blade elongation is a weighted average of local distress along the blade since stresses, material strength and metal temperature vary along the span. The greater part of the stretch results from creep caused by centrifugal stresses. Gas bending and vibratory stresses have a negligible effect on overall blade stretch.

Table I tabulates first turbine blade centrifugal stress for the STF219 and for three current production engines. Stresses are shown for the critical section of each blade for the flight conditions that are of interest. STF219 first turbine blade stress levels are substantially lower than those of current transport engines, ranging from 69% to 80% of present engine stress levels, at the most severe design condition.

TABLE I

Tabulation of First Turbine Blade Centrifugal Stress at 50% Span - The Critical Section

SLTO

	Stress (psi)	TIT (°F)	Metal Temperature (°F)
JT3C-7	16,300	1610	1520
JT4A-9	19,000	1675	1515
TF33P-7	18,000	1675	1560
STF219			
(IN-100)	15,900	2000	1370
(B-1900)	15,000	2000	1370

Cruise - Normal Rated Power

	Stress (psi)	TIT (°F)	Metal Temperature (°F)
JT3C-7	14,200	1420	1390
JT4A-9	17,600	1335	1200
TF33-P-7	17,500	1500	1395
STF219			
(IN-100)	15,000	1900	1500
(B-1900)	15,900	1900	1500

Table II compares blade mid-span section gas bending stresses for three current production engines and the STF219. The gas bending stress (no correction for tilt, creep or centrifugal restortion) is compared with the actual initial bending stress (correction for initial tilt and centrifugal restortion) and with the actual bending stress after one hour and 10 hours of engine operation. The relaxed gas bending stresses are not significant after a short period of engine operation and have a negligible effect on blade stretch.

Gas bending stresses are deliberately minimized by tilting the blade stacking line to induce centrifugal moments which counter the gas bending moments. Any significant initial residual bending stress relaxes with time as the blade seeks a bending-stress-free shape.

TABLE II

Tilt Stress Minus Gas-Bending Stress

Engine	Pure Gas Bending	Cent. Rest. Tilt Bending	Resultant	After 1 Hr.	After 10 hrs.
JT3C-7	11,300 psi	6,100 psi	5,200 psi	3,900 psi	2,000 psi
JT4A-9	8,500 psi	4,000 psi	4,500 psi	3,900 psi	2,100 psi
TF33P-7	13,000 psi	7,000 psi	6,000 psi	5,200 psi	2,800 psi
STF219	19,500 psi	15,000 psi	4,500 psi	3,900 psi	2,200 psi

Figure 2A-104 shows a representative relaxation curve for superalloys at turbine blade temperature. Since initially the stress is combined bending plus tension, the relaxation is very rapid.

Vibratory stresses do not accelerate the blade stretch rate. The work of Lazan (1) indicates that vibratory stress may in fact tend to inhibit blade creep or stretch. Figure 2A-105 shows a normalized modified Goodman diagram for a typical superalloy showing that vibratory stresses must exceed the design limit before significant damage can result.

(1) F. H. Vitovec, and B. J. Lazan, WADC TR 56-181, 1956

The effect of temperature on this phenomenon is shown in Figure 2A-106. It should be noted that the conventionally assumed linear relation is approached at low temperatures but that at turbine blade temperatures creep life is not appreciably affected by reasonable vibratory stresses.

Turbine blade materials considered during the design of an engine must permit operation for the required time with an acceptable amount of blade stretch. A number of materials such as B-1900, IN-100, U-700 and INCO-713 are suitable for use in high performance, high turbine inlet temperature engines and differ primarily in the amount of coolant necessary to achieve the desired life.

The degree of cooling required is determined by considering:

- blade stress
- blade material creep strength
- gas temperature profile
- mission requirements (time at temp. and stress)

Figure 2A-107 shows the most critical midspan centrifugal stress for a number of Pratt & Whitney Aircraft engines as a function of tip speed and hub/tip ratios. Turbine tip speed and hub/tip ratios are ordinarily determined by the engine cycle. Once these parameters are set the blade centrifugal stress is established within the reasonable limits.

The gas temperature profile is controlled by the burner aerodynamics and is adjusted to provide a profile which favors the blade root, placing the critical section at about mid-span.

Examples of materials considered for blades are, INCO-713, U-700, IN-100, and B-1900. The creep characteristics for each of these materials are usually summarized on plots where stress, temperature and time relationships are defined for several levels of creep.

A comparison of the creep strength temperature margin of the various materials shows the relative strength of the various alloys. See Figure 2A-108. B-1900 and IN-100 have about a 100°F temperature margin on U-700 and INCO-713 and about a 200°F temperature margin on Waspaloy.

For any given engine mission and life requirements, the time at temperature and blade material properties can be used to define curves of allowable creep stress vs. span. Pratt & Whitney Aircraft practice is to present the integrated effect of take-off, climb and cruise as allowable stress at the most severe condition. Table III shows a summary of the method of calculation performed.

This method of presentation permits a rapid evaluation of the blade strength margin since a blade which operates to the given stress for a weighted time at one segment of the mission will operate satisfactorily for the desired engine life.

TABLE III

First Blade Creep Life Mission Integration

Flight Condition	T.I.T.	Time for 3000 Hr. Life	Stress at Critical Section	Temp. at Critical Section	Life For 1% Creep	% Life	Cruise Life
SLTO	2000°F	900 Hr.	15,000 psi	1370°F	10^7(1)	$.1 \times 10^{-4}$	8 Hrs.
Transonic Accel.	2000°F	100 Hr.	14,400 psi	1450°F	10^7(1)	$.1 \times 10^{-4}$	8 Hrs.
Alt. and Mn Cruise	1900°F	2000 Hr	15,000 psi	1590°F	800,000(1)	$.25 \times 10^{-2}$	2000

Total Equivalent
Time at Cruise = 2016 Hrs.

(1) Note that these creep lives are arrived at by extrapolations of log-log plots of 1% creep data to demonstrate the relative effect of the flight conditions on the overall creep damage to the foil.

(3) Vane Bow

Vane "bow" is the term used to describe either or both of the following types of deformation:

> Overall bending of the vane as a beam under the influence (primarily) of the aerodynamic loads.
>
> Uncambering of the airfoil at the trailing edge under the influence of the aerodynamic loads and the thermally induced (or "thermal ratcheting") loads.

Vane bow is normally measured at the trailing edge during overhaul inspections, and vanes with bow exceeding a limiting value are withdrawn from service. The amount of permissible bow is determined on the basis of the performance deterioration characteristics of the engine and in general has a different value for each engine model.

Engine experience has shown that most aircraft engine vanes show deflection patterns which are characteristic of a combination of the two types of deformation described above. An investigation of vane bow in experimental engines has shown a rather complex relationship between mechanical properties and bow resistance. This relationship involves both creep strength and yield strength. Creep strength is a measure of the resistance to steady aerodynamic loads and is most important at high temperature steady state operation while yield strength is a measure of the resistance to "thermal ratcheting" and predominates at lower operating temperatures. "Thermal racheting" is a process of successively yielding the trailing edge, in compression during acceleration, and in tension during deceleration. Vane bow resistance can be improved if required, by (1) increased material strength, substituting PWA664 (directionally solidified grain Mar M 200) for PWA 663 (B-1900); (2) modifying the thermal gradients by modifying the vane cooling; (3) increasing the "uncambering" stiffness of the vane by trailing edge thickness changes; (4) lowering the temperature level of the vane trailing edge by increasing the trailing edge cooling.

The correlation between trailing edge bow predictions made using this complex strength parameter and values measured in experimental engines is shown in Figure 2A-109. It can be seen from the figure that the deformation mechanism is strongly temperature dependent. It therefore follows that the bow life of a particular vane design and mission can be extended by the use of cooling as a means of lowering the vane metal temperature. This has been accomplished in production engines in both the TF30 and J58 first stage vane designs.

The benefits of vane cooling with regard to trailing edge bow resistance have been investigated thoroughly on experimental engines, two examples of which are shown in Table IV.

TABLE IV

Effect of Vane Cooling on Trailing Edge Bow

	Engine	Test	Vane Configuration & Material		Coolant Flow	Avg. T.E. bow*
1)	JT4	1000 LCF Cycles to 1810°F T.I.T.	uncooled	SM 302	-	.042"
			Film cooled T.E. only	SM 302	.5%	.013
2)	JT4	1000 LCF cycles to 1810°F T.I.T.	uncooled	SM 302	-	.046
			Impingement cooled L.E. and film cooled T.E.	SM 302	.5%	.017

* Average of 1/2 set of vanes.

The degree of improvement is readily apparent even on these early designs which used coolant flows below the optimum for maximum bow resistance. It is through tests such as these that the direct relationship between average metal temperature and vane bow resistance was established.

The pertinent vane metal temperature and stress information is tabulated in Table V for the STF219 and two commercial engines with vane bow life in excess of 5000 hrs.

TABLE V

Average Vane Temperatures and Gas Bending Stresses for the STF219 and Typical Commercial Engines

	JT3C-7	JT4A-9	STF219
Max bending stress	840 psi	3920 psi	4000 psi
Avg. vane metal temp	1730°F	1720°F	1625°F
Material	W152 (1)	W152 (1)	B-1900 (2)

(1) PWA 45 coated
(2) PWA 47 coated

From Table V it can be seen that the bow life of the STF219 is at least equal to that of the JT3C-7 or JT4A-9.

(4) Erosion-Corrosion Limits

Turbine blades and vanes must be designed to resist corrosion and erosion. Turbine blade erosion-corrosion limits are affected by:

- blade metal surface temperature
- operating time at temperature
- gas stream velocity
- erosive elements - carbon and dirt particle and concentration corrosive elements - sulphides, halides, oxygen
- effectiveness of blade coating
- resistance of blade base metal and its compatibility with the coating

The gas stream velocity and erosive and corrosive elements do not vary in any significant amount for any of the modern aircraft gas turbine engines using JP type fuels. For aircraft gas turbine engines, surface erosion is determined by the blade surface temperature and the exposure time for any given blade material-coating combination.

An erosion-corrosion limit is a definition of degree of distress. Turbine blades which are "erosion" limited are not failed in the usual sense of the word. Ordinarily the blade is still structurally sound and capable of doing the work it was designed to do. The degree of "erosion" must, however, be controlled to:

- limit replacement at overhaul for poor appearance
- prevent intergrannular corrosion of blade base metal
- limit performance losses due to blade contour changes.

The rate of weight loss (either through corrosion or erosion) is much lower in coated parts than in uncoated parts. The weight loss versus time curve for a coated part may be divided into two regions, one in which the coating remains intact and protective and in which the slope of the curve is low, and the other in which the coating has begun to break down and in which the slope is increasing rapidly. These regions are identified in Figure 2A-110 which shows the results of an erosion corrosion test of a coated B-1900 sample carried well beyond the point of failure of the coating. It should be noted that the 2000°F

test metal temperature is comparable to that of an uncooled first turbine blade at 2150°F TIT. The coating finally failed after 440 hours at this condition.

Additional examples of erosion-corrosion tests of coated B-1900 are shown in Figure 2A-111. This type of data, once generated, furnished the transition (or coating failure) point for the coating as a function of time at temperature and can be cross-plotted on a time-temperature plot to produce a design curve. Figure 2A-111 shows that at 1830°F metal temperature and 2000 hours of testing the coating is still undergoing the surface oxide build up, which precedes the erosion of the coating. Such long time erosion-corrosion tests are very pertinent as they give a graphic picture of the design erosion-corrosion margin built into the STF219.

The 2000°F data in Figure 2A-110 has been included in Figure 2A-111 to give a quantitative idea of the excellence of the coating at 1830°F compared to the very satisfactory 440 hr. performance at 2000°F and the short time coating capability at 2100°F metal temperature. Pratt & Whitney currently has under investigation and development several coatings which will increase the erosion-corrosion temperature capabilities. These coatings, when developed, could be used on the STF219 and would, of course, provide an even more substantial erosion-corrosion margin than that of the present PWA47 and PWA45 coating systems.

Erosion-corrosion data as shown in Figures 2A-110 and 2A-111 can be cross-plotted on a time-temperature plot to produce a design curve. Such a design curve is shown for PWA45 and 47 coatings in Figure 2A-112. It has been shown in laboratory tests that the erosion life of a coated specimen is a function primarily of time, temperature, and coating and only secondarily of specimen configuration and base alloy. It is therefore possible to plot on the same curve points representing commercial and military service experience on parts from various engine and of various materials as a means of verifying the validity of the plot as a design curve. The design curve of Figure 2A-112 includes the results of laboratory tests, some run for times as long as 2000 hours, points which represent the more than 130,000 hours of low to moderate turbine temperature experience gained during the industrial use of J57 and J75 type engines, points which represent the more than 50,000,000 hours of current transport and commercial experience, and points which represent Pratt & Whitney Aircraft R/D engine turbine blade and vane experience. Turbine blade and vane experience gained as a result of J58 engine development was available at the higher temperatures.

The erosion life of a coated part may be predicted using the information in Figure 2A-112 as follows:

1. The metal temperatures and times-at-temperature (in hrs/engine hour) are determined for each significant portion of the flight cycle.

2. The erosion life for each operating condition is determined by entering 2A-112 with the appropriate metal temperature.

3. The ratio of time-at-temperature to erosion life is determined for each operating condition. These ratios are then added together and the reciprocal of the sum taken. This reciprocal is the calculated erosion life.

The procedure is illustrated in Table VI using the STF219 first stage blade with PWA47 coating as an example.

TABLE VI

Summary of Method Used to Determine Integrated Erosion Life

Engine Power Setting	Time at Power	T.I.T.	Tm	Erosion Life	Time Life
SLTO	.300 hr.	2000°F	1525°F	21000 hr.	1.43×10^{-5} hr.$^{-1}$
Transonic Acceleration	.033 hr.	2000°F	1535°F	19000 hr.	$.174 \times 10^{-5}$ hr.$^{-1}$
Altitude Mn Cruise	.667 hr.	1900°F	1575°F	13000 hr.	5.14×10^{-5} hr.$^{-1}$
					6.744×10^{-5} hr.$^{-1}$

$$\text{Life} = \frac{1}{6.744 \times 10^{-5}} = 14,800 \text{ hrs.}$$

The "life" predicted in this calculation is the life of the coating, not the part itself. It is important to bear in mind that failure of the coating does not constitute failure of the part nor, in fact, does it indicate that the performance of the part has been compromised to any appreciable extent.

The design life of the coating represents the time at which the coating will have ceased to provide adequate oxidation, corrosion, and erosion protection to the part and loss of metal and depth of intergranular penetration will proceed at an accelerated rate. Coated parts which are removed from service prior to complete coating failure can be stripped and re-coated and returned to service. This procedure has been followed for several years on nozzle guide vanes in commercial service and has been demonstrated on blades in service tests of JT3C and JT4A parts. The procedure had also been put into practice on JT8D-1 blades and vanes.

TABLE VII

First Stage Turbine Metal Temperature Comparison

Engine	Max. Turbine Inlet Temp. °F	Max. Metal Temp. for Average Vane or Blade °F	Max. Metal Temp. for Hottest Vane °F
JT3C-7 1st vane	1650°	1730°	1840°
JT4A-9 1st vane	1665°	1720°	1855°
TF33-P-7 1st vane	1745°	1815°	1865°
STF219 1st vane	2000°	1665°	1775°
STF219 1st blade	2000°	1525°	1525°

(5) Vibratory Fatigue Limits

Fatigue strength is an important design factor in turbine blades. Turbine blades are subjected to two important types of excitation: wakes from stationary structures upstream and randomly varying forces resulting from turbulence created or amplified during the combustion process.

Wakes from stationary structures, such as turbine nozzle vanes, burner cans or fuel nozzles, and struts are seen by the turbine blade as integral order disturbances. Each type of disturbance excites the turbine rotor blade an integral number of times each revolution and the frequency of the excitation is proportional to the rotor speed.

The turbine rotor blade sees significant levels of randomly varying gas bending loads (buffeting). These buffet loads are caused by local gas stream turbulence generated during the combustion process and swept downstream through the blade (some small part of the buffet load may be attributed to the radiated noise generated in the burner).

Pratt & Whitney Aircraft controls the blade response to these two types of excitation by tuning and by damping the blade. Acceptable turbine blade designs are carefully tuned to avoid the integral order resonances which result from fuel nozzle, burner can or strut wakes. Figure 2A-113 shows the result of the frequency calculation for the STF219 first turbine blade. Note that no important resonance occurs in the engine operating range. The calculations were made using modified Prohl type solutions to include effects of centrifugal stiffening, coupled bending-torsion and blade damper action.

Minor resonances in the operating speed range and the random buffet loads are controlled by tip shrouds or by root dampers, as the application warrants. Tip shrouds are effective damping devices which have been used extensively in current commercial and transport engines. Blade root dampers are used where high inlet temperature requirements dictate cooled foils and extended root blades, as in the J58 and STF219 first stage turbines.

Typical turbine blade vibratory stress levels are shown in Figure 2A-114. Figure 2A-115 shows stress levels measured on the JT3C engine with and without turbine tip shrouds. As indicated, shrouded blade resonances show low stresses and are sparsely distributed. The undamped unshrouded blades have unacceptably high resonant stress levels superimposed on a buffet stress which increases rapidly with increases in engine power level.

Table VII showed a typical modified Goodman diagram for superalloy materials operating at turbine temperatures encountered by the first stage turbine blades. The shape of the Goodman diagram is relatively unaffected by specific blade materials in this temperature range. Maximum first turbine blade stress levels are indicated for the JT3C-7, JT4 and TF33-P-7. STF219 first turbine blades will have the same margin, assured by design to the standards developed for other engines.

(6) Thermal Stress Fatigue

The improvements in the creep and stress rupture strength of superalloys and the use of component cooling have placed emphasis on the importance of the thermal cyclic properties of turbine blades and vanes. The thermal cyclic fatigue problem is created by the rapid application and reduction of power which is both characteristic of, and necessary to, the normal operation of aircraft power plant. One of the goals of the Phase II-B design study was to provide a turbine

design capable of meeting full power requirements at take-off and for a full reverse stop at each landing for each mission. This section outlines the design studies which resulted in the selection of the STF219 cooling scheme to meet these goals.

Pratt & Whitney Aircraft has developed an analytical method of designing for thermal fatigue, the method is described in considerable detail in Reference 1. Briefly, this system is a numerical solution of the spanwise stress-strain variations of the blade or vane when cycled between various steady state power conditions. The analysis is founded primarily on principles which have been reported in the literature (2-5). The analysis takes into account the material properties and their variations with temperature, the Bauschinger effect, and the prior strain history of the part. The analysis is similar to that presented by Mendelson and Manson (NACA Technical Report R-28, 1959) but has been extended to allow the solution of transient problems.

The fatigue life of a material has been shown by a number of investigations (8, 9, 10) to be related directly to the cyclic strain range imposed on it. Using the analytical method above and strain-life data for a material, an accurate prediction of the full cyclic life may be made.

Any adequate analysis of thermal fatigue requires the accurate calculation of transient temperatures and the resulting temperature gradients. Pratt & Whitney Aircraft has developed analytical methods of predicting steady state and transient temperatures for uncooled, convection cooled, and film cooled turbine blades. Figure 2A-116 shows the results of transient measurements which were made on convectively cooled blades on the JT4 high temperature turbine development engine (7).

(1) Vogel, Spaeth, Waring, Martens, Donachie, ASME Preprint 65 GTP-17, 1965.
(2) J. Padlog, R. D. Huff, and G. F. Holloway, WADD Technical Report 60-271, 1960.
(3) A. Mendelson, and S. S. Manson, NACA Technical Report R-28, 1959.
(4) S. S. Manson, Machine Design, August 7, 1958, pp 100-107.
(5) E. Z. Stowell, NACA Technical Note 2073.
(6) J. F. Tavernelli, and L. F. Coffin, Jr., ASME Journal of Basic Engr., December 1962, pp 533-541.
(7) The high rotor of a JT4 (J75) has been used as a turbine development engine test blade and vane cooling system. The high rotor

is operated as a single spool turbojet engine. An air preheater is supplied so that the design temperature conditions into the high pressure compressor are duplicated. This assures that the engine will run at the correct speed and therefore produce engine blade stresses.

(8) L. F. Coffin, ASME Paper 53-A-76, 1963.
(9) S. S. Manson, NACA Tr-1170, 1952.
(10) A. E. Cardon, ASME Paper 64-Met-2, 1964.

It may be seen by superimposing the data points from Figure 2A-116 upon Figure 2A-117 that the estimate (solid curves Figure 117) of the minimum blade strength for this material is conservative. From a curve of material strength and the strain range calculated and shown in Figure 2A-117 it may be shown that the first turbine blade life is greater than 6,000 cycles for the 2000°F TIT design. Similar curves for the first stage vane are shown in Figure 2A-118. The first stage vane has a cyclic life of approximately 8,000 cycles for the 2000°F design.

Engine substantiation of cyclic fatigue strengths of the useful turbine blade materials is a continuing process in all Pratt & Whitney Aircraft development programs. Engine experience is extensive and varied. Cyclic predictions made for the STF219 are based on the results of documented tests involving different engine models, different turbine blade materials and a wide range of turbine inlet temperatures. Figure 2A-119 shows the results of testing to date for three of the important turbine blade alloys, clearly showing the superior fatigue strength of the B-1900 and IN-100 type materials. Note the very good correlation between engine test failures and calculated failures.

(7) Impact Damage

Experience in both military and commercial service has shown that the blades and vanes of turbine engines are subject to impact damage as a result of foreign objects passing through the engine or carbon particles formed in the combustor. The rotating blades strike these objects as they exit at a relatively slow velocity from the vane; this impact in turn imparts a high velocity to the object in the direction of the suction side of the vanes, exposing these stationary parts to impact.

Service experience has also shown that current production blades are adequate for long periods between overhaul with only occasional in-flight shutdown attributed to impact damage. Impact damage has, however, been reflected in service maintenance cost and, with the introduction of air cooled foils to this environment, the problem of impact damage assumes more importance.

Since impact loading is of a random nature the actual design loading is not an absolute value in the sense that the gas loading of the blade is. The method used to assure adequate impact strength for the STF219 blade and vane has been to compare the strength of these cooled foils to those of the uncooled JT4 foils which have had extensive long-time service and are now operating to 6200 hr. TBO. Figure 2A-120 shows the first blade and vane tip section of both the STF219 and the JT4. A comparison of these two designs shows the increased blade thickness of the STF219 air cooled parts. This increase in thickness results in an increase in cross-sectional inertia for the cooled parts even though they are hollow.

Experience and analysis has shown that most blade impacts result in leading edge damage at approximately twenty percent of the chord and near the tip section of the blade.

At this span and chord location the increased thickness of the STF219 first blade makes this foil approximately 2.5 times stronger in chord-wise bending (that is bending which tends to break the leading edge from the blade midsection). At the operating temperature of the two blades, the STF219 material has slightly higher material strength and a higher resistance to impact than the already proven JT4 foil.

The basic three cavity foil cooling scheme is inherently resistant to cooling scheme damage since the internal cooling passage is divided into three small passages which keeps the length of unsupported wall to a minimum. The result of this compartmenting is that impact loads on the suction side of the blade do not have to be transmitted to the leading and trailing edges before the pressure side of the foil can share the load. This proved to be a problem in an early TF30 single cavity design where impact caused permanent deflections large enough to close a portion of the cavity. The cores of the three cavity blade are placed closer to the pressure side permitting thick walls in the area of impact. From Figure 2A-120 it can be seen that by locating the cavities properly it is possible to make the suction side wall of the leading edge approximately the same thickness as the entire JT4 tip section.

The same type of comparison may be made for the first stage nozzle vanes of the STF219 and the JT4. Most vane impact damage occurs from high velocity objects striking the suction side of the vane trailing edge. As can be seen in Figure 2A-121, the vane trailing edge is separated to form the trailing edge air passage with wall thicknesses comparable to JT4 vanes.

Engine experience with JT11D-20 vanes having this trailing edge configuration has been good. In one turbine development engine the failure of an experimental transpiration cooled blade afforded an opportunity for the vanes to be impacted by sections of blade core as large as one fourth of an entire blade. Inspection showed the pedestal core trailing edge vanes to be in at least as good condition as solid trailing edge parts which had experienced approximately the same failure conditions in an earlier test. The condition of these cooled vanes was termed excellent. None were sufficiently damaged to have caused termination of engine operation and a majority were reinstalled for further testing.

(8) First Turbine Vane Thermal Analysis, 2000°F TIT Design

The first turbine vane geometry is shown in Figure 2A-122 and incorporates a sheet metal insert centered inside the cast hollow vane cavity. Cooling air enters the vane at the vane inner diameter and flows into the insert and is ejected thru holes at the leading edge of the insert. The coolant impinges on the inner surface of the leading edge then splits with one half the coolant flowing along each side of the vane between the inner vane wall and the insert. At the trailing edge of the insert, the two coolant streams rejoin and continue flowing thru a pedestal cored trailing edge slot.

At the Mn 2.70 condition, the vane coolant flow is 1.5% engine flow and requires an 80 percent compressor discharge supply pressure. The average vane temperature for this condition is shown in Figure 2A-123 for a vane subjected to the average and hotspot gas profile. Both the average and hotspot vanes are below the required 2000°F vane stress rupture limit for 3,000 hour life. At the SLTO condition, the coolant flow increases to 2.10%; this increase is the result of coolant Mach number and Reynold's number effects. For these flows, the average vane temperatures are as shown in Figure 2A-124 for average and hotspot foils.

The local metal temperatures for the first stage vane are shown in Figure 2A-125 for 1900°F cruise and 2000°F SLTO. The average vane maximum temperature is below the 1735°F, 3000 hour design erosion life limit at the cruise condition; the hotspot vane is erosion limited and has a design life of at least 1500 hours consistent with present engine design practice. At SLTO the equivalent maximum design allowable metal temperature is 1680°F; the maximum temperature on the average vane is below this limit and the hotspot vane is erosion limited with 1500 hours life to significant coating damage and required repair.

A typical transient response for the first vane is shown in Figure 2A-126 for the average vane; the hotspot vane gradients are somewhat more severe. With these hotspot gradients, the hotspot vane LCF life is in excess of the required 3000 cycles.

(9) First Turbine Blade

The first turbine, three cavity blade cross section is shown in Figure 2A-127. Cooling air is fed into each of the three cavities at the root attachment. Both the leading edge and trailing edge cavities are sized to remove the maximum amount of heat from these regions. Since the midchord region does not require as much cooling as the leading and trailing edges, the flow to the center cavity is metered at the entrance to the foil attachment. By using the three cavity concept, the two end cavities do the maximum amount of cooling and the midchord blade wall temperature is controlled independently of leading and trailing edge temperature. There is also considerable mass removed from the midchord region of the three cavity foil. The combination of midchord temperature control and mass removal has led to a long cyclic fatigue life for this type of foil.

The estimated spanwise average and allowable metal temperatures are shown in Figure 2A-128 for IN-100 (PWA658) material at the cruise condition and in Figure 2A-129 for the SLTO condition. At both conditions, there is considerable creep life margin and the blade is capable of running in excess of 10,000 hours. At cruise, the design coolant flow is 1.0 percent engine flow with .40 percent flowing thru each of the leading and trailing edge cavities and .20 percent coolant thru the midchord cavity. For SLTO, the total flow increases to 1.40 percent engine flow.

The local metal temperatures are shown in Figure 2A-130; at both cruise and SLTO conditions, these temperatures are well below the 1735°F cruise and 1680°F SLTO erosion limits for 3000 hours.

The convectively cooled first turbine blade is cyclic life limited. With the transient gradients shown in Figure 2A-131, the blade has an LCF life in excess of 6000 cycles.

(10) Convectively Cooled Blade Design Substantiating Test Data

During November of 1964 the JT4 High Temperature Turbine development test was run with instrumented convectively cooled blades. The

object of the test was to measure cooled blade temperatures which could be compared against analytical predictions.

Description of Airfoils Tested - Three different convectively cooled blades were tested:

1 - 11 hole blade - mid span cross section shown in Figure 2A-132
2 - 0.020" sawtooth blade - Figure 2A-133
3 - 0.030" sawtooth blade - Figure 2A-134

Test Conditions - The engine was run through a cycle which simulated a typical ground idle condition followed by an acceleration to full power. After airfoil temperatures were stabilized at the full power condition the power was cut rapidly inducing a "snap" deceleration. The turbine inlet temperature varied between 1240°F and 2240°F and the blade coolant temperature varied between 425°F and 900°F. A typical cycle is shown in Figure 2A-135.

During this cycle blade temperatures were measured and recorded. The temperatures were measured at the leading edge, trailing edge and midchord regions on both pressure and suction surfaces. A photograph showing a typical instrumented blade is shown in Figure 2A-136.

Results - Following the running of the engine the operating temperatures, pressures, and acceleration rates were determined and an analytical study of blade temperatures was conducted at exactly the same conditions run by the engine. The results of these analyses are shown in Figure 2A-137, 2A-138 and 2A-139 for the three different blades along with the temperatures measured in the engine. It can be seen that the analytical predictions agree faborably with the test data. Some deviation exists at the trailing edge because the trailing edges radiate to a cool exhaust case and these radiation losses were not taken into account in the analysis. The coolant flow rates for the different blades are listed below:

Blade	Coolant Flow
1 - 11 hole	1% of engine airflow
2 - 0.020" sawtooth	2% of engine airflow
3 - 0.030" sawtooth	2% of engine airflow

The curves also indicate that an appreciable gradient exists between the leading or trailing edge and the mid-chord region. This is a result of overcooling the mid-chord relative to the leading and trailing

edges because the flow rate of coolant was equally distributed along the chord.

Conclusion:

Based on the results of this test it was concluded that the analytical prediction of convectively cooled blade temperatures is accurate. This same analytical system was used in the design of the three cavity convectively cooled blade proposed for the STF219 engine. The conclusions based on temperature analysis drawn concerning both cyclic and steady state blade life can, therefore, be assumed to be accurate.

f. Basic Engine Turbine Structural Design

(1) Introduction

The three cavity convectively cooled blade becomes cyclic life limited at approximately 2060°F takeoff temperature as shown in Figure 2A-140. For operation to 2300°F take-off turbine inlet temperature the STF219 first stage blades and vanes incorporate additional leading and trailing edge cooling. A detailed description of the cooling schemes considered follows in the heat transfer section. The second stage vane also requires cooling at these temperatures: A simple convective cooling scheme is incorporated into the same second stage vane air foil used in the 2000°F design. The remainder of the turbine cooling configuration is unchanged from the 2000°F design.

(2) Creep and Stress Rupture

The STF219 Basic Engine first turbine blade is of the "shower head" type with multiple rows of holes through to the foil leading edge surface and connecting this outer surface with an inner leading edge

passage running the length of the foil. The trailing edge is film cooled by a series of slots on both the suction and pressure side of the foil forward of the trailing edge. This cooling scheme is shown in Figure 2A-162. The small holes and slots required for proper cooling at high turbine inlet temperature also cause stress concentrations which modify to some extent the creep and stress rupture properties of the superalloys used.

Steady load stress rupture testing has actually shown that the stress rupture life of some materials is increased when notched. Examples of this phenomenon have been reported in the literature[1] and are shown in the test data presented in Figure 2A-141. The increase in time to failure for notched stress rupture failures has been attributed to the generation of triaxial stress patterns which inhibit the failure mechanisms associated with this mode of failure. In any case, the high local stress pattern around a notch is rapidly relaxed as the strain patterns are reduced to low stress configurations.

The material properties used to determine the creep and stress rupture margins and the creep-allowable metal temperature limits are conservatively chosen. No design credit is taken for notched-stress-rupture life increases. The creep-allowable temperatures used for these foils are based on the same design philosophy used on all other Pratt & Whitney Aircraft engines. The creep and stress rupture margins for each stage are shown in Figures 2A-142 through 2A-147. Figures 2A-142 and 2A-143 show the large creep limit temperature margin of the first blade and vane which result from the high effectiveness of these cooling schemes designed primarily to reduce chordwise gradients. The adequate creep margin of the low pressure turbine stages may be seen in Figures 2A-144, 2A-145, 2A-146 and 2A-147.

(3) Thermal Cyclic Fatigue

Thermal cyclic fatigue endurance is a major design consideration. A properly designed turbine blade will have a mass distribution which minimizes thermal-induced stresses during transient operation and a cooling configuration which can meet steady state metal temperature limits set by erosion-corrosion and blade stretch requirements. Long

[1] WADC TR 54-175 Part 1, 2, and 3
Notch sensitivity of heat resistant alloys at elevated temperatures.
Vourhees, Freeman

As-Cast Mar M 200 Stress Rupture Data

Heat	Condition	Temp.	Stress	Time to Rupture	Elong.	R. A.	Remarks
P5624	as-cast	1200	115 ksi	8.1 hrs.	7%	28.5%	
P5626	as-cast	1200	115	289.7	discontinued		Notched K_t 3.8
P5625	as-cast	1400	92	0.7	6.6	27	
P5626	as-cast	1400	92	329.6	discontinued		Notched K_t 3.8
A-64	as-cast	1400	95	73.1	0.4	2.2	
P5417	as-cast	1400	95	9.0	2.1	4.4	
P5417	as-cast	1400	95	15.0	-	-	Notched K_t 3.8
A-64	as-cast	1400	110	2.4	2	6	
P5417	as-cast	1600	60	5.7	1.2	2.0	
P5417	as-cast	1600	60	167.6	-	-	Notched K_t 3.8
A-64	as-cast	1600	60	66.8	1.0	6.0	
A-64	as-cast	1600	65	26.1	1.0	4.0	
P5423	as-cast	1800	27.5	69.2	6.45	13.8	
P5424	as-cast	1800	27.5	29.2	3.0	3.0	
P5424	as-cast	1800	27.5	67.2	2.0	5.0	Porosity in gage section
P5425	as-cast	1800	27.5	74.6	5.0	7.0	
P5425	as-cast	1800	27.5	69.3	7.0	6.0	
P5417	as-cast	1800	25	45	8.5	17.5	
P541,	as-cast	1800	25	305.2	discontinued	-	Notched K_t 3.8
XA137	as-cast	1800	25	36.3	4.2	16.5	
A-80	as-cast	1800	24	252.3	4.1	4.8	

MAR M200 STRESS RUPTURE DATA

time 2300°F turbine inlet temperature operation of the STF219 is made possible by film cooled or showerhead (a form of transpiration cooling) turbine blades. These blades with their cooling holes and slots are more sensitive to the transient thermal-induced stresses than the usual convectively cooled blades.

The effects of local stress concentrations must be taken into account where they exist. This is most effectively done by making these local stress concentrations a feature of the experimental determination of the relation between strain amplitude and cyclic life. When handled this way, then, even transverse holes may be dismissed when considering the analytical procedure to be used in arriving at the applicable value of strain per cycle. This technique is particularly valuable since it assures that the effect of the hole manufacturing operation on the material fatigue strength is documented. The preferential attack of the ECM (electrochemical machining) process on components in the alloy; the thin remelted and perhaps cracked hole surface produced by EB (electron beam), Laser, or EDM (electrical discharge machining); or the locally work hardened surface in a drilled hole all have an effect on the fatigue strength of materials that is difficult to evaluate analytically.

The trends associated with notched effects or the low cyclic fatigue of the candidate superalloys has been investigated through the testing of smooth and notched specimens at comparable conditions. Standard LCF specimens were drilled and the reduction in area accounted for in the calculated stresses. Results of these tests are discussed in section 5H1 and 5H2 of this report.

Elementary analyses of the stress field around a hole show effective theoretical stress concentrations at least twice as high as experimental testing has shown. Table VIII below shows the results for comparison. Note the SCF (stress concentration factor) change as one hole is replaced by a row of holes (-8%) or by several rows of holes (-20%). From this, one can conclude that any engine design with its multiple holes will see less SCF than an LCF specimen with its single hole in the gage area.

A significant decrease in SCF (-33%) can be made merely by substituting elliptical holes (b/a = 2, 0.010" by 0.020") for the circular holes (0.015" dia.) in the STF219 first turbine blade. Analysis to date indicates that this refinement is not necessary to get the desired cyclic fatigue life, but it is available if required.

TABLE VIII

Stress Concentrations at Cooling Hole

	Theoretical[2] SCF	Superalloy Test SCF
One hole in a sheet	3.0	-
One hole in a LCF specimen	2.5-2.7	1.2
One row of holes in a sheet (Pitch/diameter = 5.0)	2.75	-
Many rows of holes in a sheet (Pitch/diameter = 5.0)	2.42	-
One ellipse in a sheet (b/a = 2, major axis along span)	2.0	-

2. Stress Concentration Design Factors, R. E. Peterson, Wiley & Sons 1953.

The good notched low cyclic fatigue properties demonstrated for B 1900, Mar M 200 are not suprising considering the low notch sensitivity of these materials in high cyclic fatigue and tensile testing. It has been noted elsewhere that the effect of notching on HFF strength of a material is also reflected in the LCF region of the S-N curve[2]. One explanation for apparent lack of correlation of test and analytical results in any of

the elementary analytical methods of accounting for strain concentrations such as holes[3] is that cast superalloys have a tendency toward microporosity and therefore all specimens both smooth and notched are actually compromised to some degree.

Engine and rig experience has shown that the empirical method of establishing design limits for materials and configurations in which the fatigue specimens are prepared to simulate the desired components gives good correlation. Although this testing is both time consuming and expensive it is the only method to date which has demonstrated the accuracy required.

Even though the candidate superalloys have shown these excellent notched properties care has been taken in the sizing and spacing and the selection of shapes for the film cooling holes for the STF219 2300°F design. The spacing of the blade leading-edge holes was made to give the lowest possible concentration factors and interaction consistent with Ref. 2 without compromising the cooling scheme effectiveness.

The transient response curves for temperature and strain are shown in Figure 2A-148 and 2A-150. Using the test experience and reasoning given above to substantiate the use of specimen data reproduced in Figure 2A-151 for life predictions of the first blade and vane of the 2300°F design a life more than 10,000 cycles for the first blade and of approximately 10,000 cycles for the vane may be seen.

(4) Vibratory Fatigue Limits

Blade vibration problems and the design requirements of the 2300°F version of the STF219 turbine are similar to those of the 2000°F version. The primary difference in these two designs with respect to vibratory fatigue limits is the inclusion of film cooling holes and slots in the foil.

Detailed analysis of this problem has led to two areas for concentration of effort in order to increase the design operating margin for vibration stress associated with these factors. The first area of investigation has been into the relative smooth and notched fatigue strength of various turbine materials. Figure 2A-152 shows both notched and smooth runout fatigue strengths for AMS5382 (X40), Waspaloy (PWA686), and IN 100.

3. E. A. Stowell - NACA Technical Note 2073

This curve of vibratory stress allowables also shows the relative notch sensitivity of these three different generation turbine materials. The notch sensitivity of IN 100 is seen to be very low to nonexistent in the operating temperature range of the STF219 first turbine blade. The same trend in fatigue strength is also characteristic of SM200 and B1900. IN 100 unshrouded, root damped first turbine blades used in the J58 Bill of Materials have never experienced a vibration induced blade failure. JT4 high spool engine testing of undamped, unshrouded "shower head" blades has been very successful. Fatigue failures have not occurred. JT4 vibration surveys on unshrouded, undamped turbine blades have shown vibratory stresses as high as 7500 psi. These surveys are shown in Figure 2A-153.

The second area of investigation aimed at increasing film cooled blade vibratory fatigue life is vibration control. The STF219 first turbine blade is an extended root, friction damped design similar to that used in the J58. This design offers both cooling scheme flexibility and excellent vibration control, which has been documented in the J58, the JT12 material evaluation turbine, the light weight turbojet study engine, and the experimental J52. Stress surveys have shown buffeting stresses of extended root friction damped blades to be reduced by 50-70 percent of that of similar blades undamped and with unextended roots. Blade stress surveys made to date on the JTF14 have indicated that the buffeting stresses as a result of the turbulence created by the annular combustor are less than the turbulence created by present commercial and military engine can-annular burners. The STF219 with an annular combustor comparable to that of the JTF14 is expected to have buffeting stresses below those of previous engines and well within the blade capability.

(5) First Vane Thermal Analysis

2300°F Take-off TIT and 2200°F Cruise TIT Design Point

The first stage Basic Engine vane employs an impingement cooled leading edge, convection cooled midchord region and a convection cooled pedestal-core trailing edge. Figure 2A-154 shows the vane geometry. The main structural portion of the vane consists of a cast hollow airfoil section with a pedestal-core trailing edge. The hollow cavity is divided into two cooling compartments. Burner secondary air is supplied at the vane I.D. to the distribution tube in the leading edge compartment and is ejected at high velocity through slots onto the internal surface of the leading edge which has chordwise cooling fins. These fins provide an internal cooling area of two times that of the external heating area, resulting in excellent cooling

effectiveness. After impinging on the leading edge, the air flows chordwise along the vane to an exhaust manifold which vents the air to the vane O.D. A sheet metal insert is placed into the rear central hollow cavity to provide a cooling air supply manifold and to form a regulating flow passage on both suction and pressure surface of the airfoil. The flow passage is formed by fins cast into the side walls of the vane and the outer wall of the sheetmetal insert. The fins, as before, increase the internal heat transfer area, increasing the heat transfer to the coolant. Burner secondary air fed into the insert is ejected through slots at the leading edge of the insert, flows rearward in a chordwise direction convectively cooling both surfaces of the airfoil, and is ejected through the pedestal core trailing edge thus cooling the trailing edge.

At the cruise condition the vane total coolant requirement is 3.9 percent engine flow; 1.5 percent leading edge impingement flow, 1.0 percent flow along the suction surface, and 1.4 percent flow along the pressure surface. The combined suction and pressure surface flows through the pedestal core trailing edge. At these flows the required coolant supply pressure is 95 percent of compressor discharge.

Curves showing the average vane temperature at the 2200°F Mn 2.70 altitude condition are shown in Figure 2A-155. At these temperatures both the average vane and the hotspot vane are well below the allowable metal temperature for 3,000 hour creep life.

For the 75 percent span location the local metal temperatures are shown in Figure 2A-156 at the Mn 2.7 condition. At a maximum local metal temperature of 1725°F for a vane subjected to the average gas profile the erosion life is greater than 3,000 hours. The hotspot vane local maximum temperature is 1780°F which provides at least 1500 hours erosion life. The vane temperature response for the idle to 2300°F SLTO transient acceleration is shown in Figure 2A-157.

The alternate for the first stage Basic Engine vane employs impingement cooling on the leading edge and film cooling on the pressure side and suction side. The trailing edge is both film cooled and convection cooled. Figure 2A-158 shows the vane geometry. Burner secondary air is supplied at the vane I.D. to the distribution tube in the leading edge compartment, and the hollow cavity in the midchord region of the vane. The distribution tube ejects the air at high velocity through slots into the internal surface of the leading edge which has chordwise fins. The fins increase the cooling area to twice that of the external area. After impinging on the leading edge, the air flows chordwise along the vane to the exhaust manifold which vents the air to the vane

O.D. The air from the hollow cavity supplies the four film slots through feed holes, and supplies the pedestal trailing edge. Each slot is continuous from root to tip. The flow is metered by varying the number of feed holes supplying each slot. The metered slot provides a continuous slot, hence a continuous film and complete coverage from root to tip.

At the cruise condition the vane total coolant requirement is 4.0 percent engine flow; 1.5 percent leading edge impingement flow, 0.5 percent pedestal trailing edge, 1.1 percent film flow on the suction surface, and 0.90 per cent film flow on the pressure surface. At these flows the required coolant supply pressure is 95 percent of compressor discharge.

Curves showing the average vane temperature at the 2200°F Mn 2.70 altitude condition are shown in Figure 2A-159. At these temperatures both the average vane and the hotspot vane are well below the allowable temperature for 3,000 hour creep life. The coolant film temperature used in calculating the average vane temperatures are based on a 50% effective film; this means that theoretically only 50% of the coolant flow is needed to obtain the desired film temperature. It is expected that more effective films will be developed with continued experience in film cooling. As these improved film techniques develop the required coolant flow will decrease.

For the 75% span location the local metal temperatures are shown in Figure 2A-160 at the Mn 2.7 condition. At a maximum local metal temperature of 1725°F for a vane subjected to the average gas profile the erosion life is greater than 3,000 hours. The hotspot vane local maximum temperature is 1780°F which results in approximately 1500 hours design erosion life.

The vane temperature response for the idle to 2300°F SLTO transient acceleration is shown in Figure 2A-161.

(6) First Blade Thermal Analysis

2300°F Takeoff TIT and 2200°F Cruise TIT Design Point.

The first blade employs a showerhead leading edge, convective midchord and a film cooled trailing edge. The blade geometry is shown in Figure 2A-162. The cooling air is supplied to the three blade cavities through the extended root attachment. At the leading edge, cooling is accomplished by convection in the radial passage and in the showerhead holes.

The showerhead holes are angled at 30° to increase the convection area. Both the trailing edge and midchord cavities cool convectively and feed coolant to the film cooling slots.

The trailing edge cavity employs wall to wall cast pedestals to provide structural integrity and a means of controlling coolant flow areas. The pedestals act as fins and turbulence generators and serve to increase the internal heat transfer coefficient, and therefore the cooling efficiency.

At the 2200°F TIT cruise condition the total blade coolant flow is 3.9% of engine air flow with 2.00% flowing thru the showerhead leading edge, .90% thru the combination convection and pressure surface film slots and 1.0% thru the combination convection and suction surface film slots. This blade requires 90% compressor discharge coolant supply pressure.

The average blade temperatures are shown in Figure 2A-163 for the 2200°F Mn 2.70 cruise condition. At these conditions the average blade temperature is below the 1750°F design blade creep limit. In calculating the blade average temperature no credit was taken for any film cooling from the showerhead leading edge; tests to date have not indicated any appreciable film effect for the showerhead configuration.

Along the film cooled suction and pressure surfaces a 50% effective film has been used. It is expected that the coolant flow requirements will decrease with improved film cooling techniques and experience. The local blade temperatures are listed in Figure 2A-164 for the 50% span location. At the 2200°F Mn 2.70 cruise point the maximum local blade metal temperature is below the 1735°F design erosion limit.

Figure 2A-165 illustrates the blade temperature response for the idle to 2300°F SLTO transient acceleration and deceleration.

(7) Second Vane Thermal Analysis

2300°F TIT Takeoff and 2200°F TIT Cruise Design Point

The second turbine vane geometry is shown in Figure 2A-166 and incorporates a sheet metal insert centered inside the cast hollow vane cavity. Cooling air enters the vane at the vane O. D., flow into the insert and is ejected at high velocity into the inner surface of the leading edge. The coolant then splits and flows chordwise between the insert and the vane wall. The two coolant streams come together and flow through the pedestal trailing edge. The second stage vane requires 1.25 percent coolant flow at the Mn 2.7 2200°F cruise condition.

The average vane temperatures are shown in Figure 2A-167 for both the average vane and the hotspot vane for 2200°F and Mn 2.70. Both the average and hotspot second stage vane temperatures are below the creep allowable limit for a 3,000 hour engine.

The maximum metal temperatures for the second vane as shown in Figure 2A-168. The average and hotspot vanes have maximum temperature below the allowable erosion limit for a 3,000 hour engine life.

The LCF life is adequate for a 3,000 hour engine. Typical transient gradients for idle to 2300°F SLTO are shown in Figure 2A-169.

g. <u>SST Convectively Cooled and Film Cooled Vane Design Substantiating Test Data</u>

(1) Introduction

Pratt & Whitney Aircraft has conducted a series of tests to evaluate the cooling capabilities of convectively and film cooled foils. These tests have been conducted primarily in vane cascade rigs where accurate measurements at coolant flows and gas temperatures could be made.

(2) Description of Airfoils Tested

The following vanes have been evaluated in connection with the SST engine design:

- Impingement cooled leading edge, convectively cooled T. E. (Figure 2A-170).
- Radial hole convectively cooled leading edge, convectively cooled trailing edge (Figure 2A-171).
- Showerhead cooled leading edge, convection cooled midchord and film cooled trailing edge (Figure 2A-172).
- Detached leading edge film cooled (Figure 2A-173).
- Film cooled trailing edge (Figure 2A-174).

(3) Test Conditions

The vanes were tested in cascade rigs which provided a realistic representation of the engine gas path. Gas path pressure levels and temperatures were varied to simulate those levels which would be encountered in

the STF219 engine. The cascade rigs contain three vanes, the middle vane being the test vane. This arrangement insures that the environment surrounding the vane will be similar to that environment in an engine. The vanes are instrumented with surface thermocouples as shown in Figure 2A-175. A measured quantity of coolant is supplied to the vane and the external gas temperatures are measured just upstream from the vane leading edge.

(4) Impingement Cooled Vane

Test data shown in Figure 2A-165 was obtained from a JT11D-20 vane similar to that proposed for the 2000°F takeoff turbine inlet temperature STF219 engine. Air is supplied to the vane through a sheet metal tube. The air impinges against inside surface of the leading edge and flows rearward through a pedestal supported trailing edge slot. In the STF219 engine the impingement tube has been replaced by an airfoil-shaped baffle which forces the cooling air over the pressure and suction surfaces as it passes toward the rear of the vane. This will insure that these surfaces are protected by convective cooling. Figure 2A-176 shows that the JT11D-20 vane is cooled approximately 200°F using 1.21 percent of engine airflow. The STF219 vane will be cooled approximately the same amount using 1.5 percent of airflow at cruise. More coolant is required for the STF219 because the coolant temperature at cruise is almost 100° hotter while the gas temperature at midspan is only 50° colder than the point for which the test vane was run.

(5) Pedestal Trailing Edge Vanes

The radial hole convectively cooled leading edge and convection cooled pedestal vane is a parallel flow vane; the coolant enters at the vane tip then splits with approximately one half the coolant flowing thru the radial holes and the remainder thru the pedestal trailing edge. The vane is available and is currently used for hot turbine development work in the JT4 size engine. Since the STF219 engine first turbine vane uses a pedestal core trailing edge cooling system similar to this one, extensive heat transfer tests were conducted on this vane in the UAC High Pressure Cascade. The pedestal trailing edge vane was run at 2300°F gas stream temperature for two different pressure levels, 30 PSIA and 175 PSIA. The 30 PSIA with a 1200°F coolant supply simulates a Mn 3.0 cruise condition while the 175 PSIA with 650°F coolant simulates a SLTO condition. Thermocouple data for both these conditions at three different coolant flow rates are shown in Figure 2A-176A. The higher temperature readings at the 30 PSIA point indicate the

severity of the cruise condition relative to SLTO. At the trailing edge, the pedestal convection scheme is capable of maintianing local metal temperatures below the 1735°F design erosion limit for SST foils. The test data also shows that the radial hole pattern used in this design is incapable of maintaining leading edge temperatures at the simulated cruise condition below the desired 1735°F limit.

(6) Showerhead Vanes

The showerhead vane is a reoperated JT4 radial hole vane. The leading edge section with its five radial holes were removed from the parent vane; a solid leading edge section with an identical outer contour was welded onto the parent vane. Showerhead holes were then EDM machined into suction and pressure surface to provide film cooling. The coolant entering the vane splits, a portion of it flowing through the midchord radial holes, another portion flowing into the film coolant manifold feeding the rear set of suction side slots, and the remainder of the coolant flowing into the midcore cavity feeding the leading edge showerhead holes and the film slots on the suction and pressure surfaces. These heat transfer tests were conducted to evaluate the film cooling provided by the showerhead leading edge and film cooled trailing edge. The vane was tested in 2300°F gas stream environment and three pressure levels 10, 45 and 175 PSIA; test results are shown in Figure 2A-177 for the different coolant flows. The leading edge thermocouple data indicates that there is no appreciable film cooling effect from the showerhead. This particular showerhead runs too hot and is unacceptable for SST conditions. Designs aimed at better using the convection cooling capability of the showerhead holes have resulted in schemes that are acceptable for SST conditions. The results of a preliminary comparison of measured and calculated temperatures on this vane indicates the trailing edge film is 75-100 percent effective. The level of the trailing edge temperatures is too high to be acceptable for SST condition at the airflows used.

(7) Detached Leading Edge Vanes

The detached leading edge vane is also a reoperated JT4 radial hole vane. The radial hole leading edge section was replaced with an impingement cooled detached leading edge section. The midchord and trailing section were identical to the showerhead vane; the coolant flow path was also identical to the showerhead vane. These tests were conducted to evaluate the film cooling provided by the detached leading edge vane. Thermocouples were not used for recording vane temperatures on the vane; an optical system measuring infrared radiation level

was used. With this instrumentation the leading edge and a portion of the forward pressure surface were scanned and foil temperatures recorded. Figure 2A-178 compares the measured vane temperature and predicted vane temperatures for no film. The test data lies 200°F below the zero film predictions for the film cooled region downstream of the shield and indicate the film is 72% effective. The above comparison is for the design point pressure ratio with 3.8% coolant flow at 2400°F mainstream gas and 900°F coolant temperature. The impingement cooled leading edge data is in good agreement with predictions.

For the STF219 engine cruise condition the calculated theoretical leading edge temperatures and the measured data indicate that leading edge temperatures are low enough to provide adequate erosion life. The data indicates that the detached leading edge provides a highly effective coolant film.

(8) Film Cooled Trailing Edge Vanes

A film cooled trailing edge vane was tested to determine the effectiveness of trailing edge film cooling schemes. The vane was a reoperated JT4 uncooled vanes with film cooling holes EDM machined at a 30° angle to the vane surface. Since only the trailing edges of the foil were cooled, the test was conducted at low mainstream gas temperatures. The vane had film injection on the suction surface above the gage point approximately 1.0 inch from the trailing edge. The trailing edge temperatures were recorded with the infrared optical system; the detector scanned the suction surface of the vane from the trailing edge to a point .45 inches upstream of the trailing edge.

The data, Figure 2A-179, indicate that the vane trailing edge temperature was reduced to a level approximately 200°F below the surrounding hot gas temperature. The results are shown superimposed over the analytical estimate for convective cooling. The estimate labeled "convective cooling" indicates the amount of cooling expected if no film was established over the surface. The temperature reduction was due only to convective cooling from the coolant flowing through the manifold system. The test results indicate that approximately 100°F of film cooling was achieved and a stable film was established over the entire trailing edge region.

h. SST Film Cooling Background

Film cooling provides protection for turbine airfoils exposed to high temperatures by insulating the metal surface from the hot gas with a

layer of coolant. Numerous studies have been conducted to evaluate film cooling (Ref. 4-10). Of these the investigations which most closely approximate the turbine airfoils are summarized in Ref. 4. Preliminary SST film cooled airfoil designs were based on the film effectiveness data presented in this report. However, the accuracy of the design procedure was questioned because the test data had been obtained in an environment which was not representative of the environment which exists in an engine. Most of the previous film cooling testing was conducted in large scale ducts, at low temperatures, and with low turbulence levels. In an engine, the free stream turbulence level is relatively high due to the combustion process. In addition, the gas temperatures are high and the injection slots are extremely small, ranging from 0.008 to 0.020 inches in thickness. To evaluate the effect of the turbulence, temperature and size effects on film cooling, Pratt & Whitney Aircraft constructed a flat plate test rig (Fig. 2A-180) which is supplied with hot gas from an engine-type burner and which is used to test specimens constructed with engine materials and slot sizes.

4. "Velocity Distributions, Temperature Distributions, Effectiveness and Heat Transfer in Cooling of a Surface With a Pressure Gradient", J. P. Hartnett, R. C. Birkebak, E. R. G. Eckert, 1961 Int. H. T. Conference, Part IV, ASME

5. "The Effects of Slot Geometry on Film Cooling", E. R. G. Eckert, R. C. Birkebak, HTL TR No. 41, March 1962

6. "Velocity Distributions, Temperature Distributions, Effectiveness and Heat Transfer for Air Injected through a Tangential Slot into a Turbulant Boundary Layer", J. P. Hartnett, R. C. Birkebak, E. R. G. Eckert, Journal of H. T. August 1961

7. "Experimental Investigation of Air Film Cooling Applied to An Adiabatic Wall by Means of an Axially Discharging Slot", S. S. Papell, A. U. Trout, NACA TND9, August 1959

8. "Effect on Gaseous Film Cooling of Coolant Injection Through Angled Slots and Normal Holes", S. S. Papell, NACA TD 299

9. "Comparison of Effectiveness of Connection, Transpiration and Film Cooling Methods With Air as Coolant", E. R. G. Eckert, J. N. B. Livingood, NACA Report 1182, 1954

10. "Investigation of Slot Configurations for Film Cooled Turbine Blades by Flow Visualization Methods", E. R. G. Eckert, T. W. Jackson, A. C. Francisco, NACA RM E50K01, January 1951

A series of test specimens containing film injection slots of various configurations were run in this rig and the measured temperatures were compared with temperatures predicted by the data presented in Ref. 4. Figure 2A-181 shows a typical comparison for a specimen run in a study program.

The good comparison between the PWA test and the previous experimental data (Ref. 4) at constant pressure indicates that good agreement will probably be found with static pressure gradients. Testing with pressure gradients will be conducted in future tests as part of the film cooling study program.

j. SST Film Cooled Blade Design Substantiating Test Data

(1) Introduction

During March of 1965 the JT4 High Spool Engine was run with instrumented film cooled blades. The object of the test was to compare several different blade configurations and to provide verification of analytical temperature predictions. In addition, instrumented convectively cooled blades were also tested to provide a direct comparison between the cooling capability of film cooled and convectively cooled airfoils.

(2) Description of Airfoils Tested

Five different blade designs were tested; four film cooled and two convectively cooled (sawtooth designs); The leading edges of the film cooled blades were a "showerhead" design and the remaining portions of the chord wise sections were cooled by film injected from rows of holes. In addition some convective cooling was provided in the mid-chord section. The blade geometries are listed below:

1. 0.020" Sawtooth
2. 0.030" Sawtooth
3. 3 row leading edge showerhead. 0.008" Dia holes 90° Fig. 2A-182*
4. 3 row leading edge showerhead. 0.013" Dia holes 30° Fig. 2A-183*
5. 3 row leading edge showerhead. 0.013" Dia holes 90° Fig. 2A-184*
6. 1 row leading edge showerhead. 0.030" Dia holes 30° Fig. 2A-185*

(* angles are measured from the radial direction)

(3) Test Conditions

The JT4 engine was run through a cycle similar to that explained in the section on convection cooled blades. The turbine inlet temperature was varied between 1550°F and 2435°F as shown in Figure 2A-186.

(4) Results

The results of the test indicated that analytical temperature estimates compare favorably with measured test data as shown in Figure 2A-187. In addition the test indicated that the film cooling system was considerably more effective than the convectively cooled blade in cooling the blade leading and trailing edges. This can be seen by comparing Figure 2A-187 to Figure 2A-188, which shows temperatures measured on a sawtooth blade during the same test. All the film cooled blades indicated better cooling at the leading and trailing edges as shown below:

Foil	Leading Edge ($T_{gas}-T_{metal}$)	Trailing Edge ($T_{gas}-T_{metal}$)	Coolant Flow
1 Uncooled	0°F	0°F	0% Wae
2 Sawtooth	540	520	4%
3 0.008"/90° 3 Row	850	700	3.5%
4 0.013"/30° 3 Row	740	700	3.5%
5 0.013"/90° 3 Row	660	700	3.5%
6 0.030"/30° 1 Row	650	700	3.5%

The major factor contributing to the increased cooling effectiveness at the leading edge is the increased surface area within the blade available for convective cooling. This concept begins to approach transpiration cooling. In addition to this convective cooling additional protection is provided by the ejected coolant in the form of a film. The mechanism of film formation after injection through leading edge holes is an unknown factor at this time. The analytical and actual temperatures are shown in Figures 2A-138 and 2A-189. Cooling formation of a cooling film. The exact reason why one hole configura-

formation of a cooling film. The exact reason why one hole configuration should indicate this while other similar blades do not has not yet been determined. However, further testing is being carried out to determine which parameters have any significant effect on film formation. The following variables are being studied:

- Hole diameter
- Angle of injection
- Number of rows of holes
- Pressure ratio across holes

Testing will be conducted both in engines and rigs.

Figures 2A-188 and 2A-189 also show that film cooling is more effective than convection cooling for protecting the blade and aft portions of the chord. Analytical predictions were made assuming various degrees of film cooling effectiveness. The effectiveness has been arbitrarily defined as the rate of mixing of coolant with hot gas relative to a baseline film-mixing correlation.[4] The effectiveness in establishing midchord and trailing edge film is indicated to vary between 70 and 100 percent of the effectiveness predicted in the reference paper.[4] The high degree of effectiveness indicates that film cooled blades can be used in the STF219 engine to provide the required life at advanced engine ratings.

(5) Conclusions

Based on the early testing conducted by Pratt & Whitney Aircraft it can be concluded that the "showerhead" leading edge blade shows cooling capability which exceeds that of convectively cooled blades. The degree to which this system is capable of establishing effective film cooling has not yet been determined and further testing will be required before an exact engine configuration can be designed. In addition, the effect of coolant injection on engine performance must be evaluated and given consideration in the choice of an optimum design. However, the testing to date indicates that the "showerhead" film cooled blades will be capable of providing the cooling required for the Basic Rating of the STF219 engine.

10. TURBINE EXHAUST

a. General Description

The turbine exhaust section of the STF219 turbofan engine serves a dual purpose. Aerodynamically it diffuses the gas generator exhaust stream and directs it through 16 exit guide vanes. This eliminates the tangential swirl of the exhaust gases before they enter a convergent annulus which directs the flow through the primary nozzle. Structurally it supports the number 4 bearing and the exhaust tailcone.

As discussed under Turbine Aerodynamic Design, the exhaust section was lengthened and the exhaust struts moved rearward to permit operation at 2000°F turbine inlet temperature. No annular area change occurs through the exit vanes. The diffuser is of minimum length commensurate with stable, efficient diffusion over the expected range of turbine exit conditions. This information is based upon annular diffuser experience gained on Pratt & Whitney Aircraft production engines.

b. Physical Structure

The flowpath through the turbine exhaust section (Figure 2A-190) is an annulus defined by an inner and outer case. The inner and outer cases are weldments fabricated from Hastelloy X reinforced sheet (AMS 5536) and Waspaloy (AMS 5706 and AMS 5544) respectively. The inner shroud to which the vanes attach is also Waspaloy (AMS 5706). The sixteen exit guide vanes of cast Inconel 713 (PWA 655) will be heatshielded with a sheet of Hastelloy X (AMS 5536) to cut down on transient temperature differentials. The vanes are attached to the inner and outer cases by dowel bolts. Eight of the vanes are also bolted to the bearing support cylinder to transmit maneuver loads to the outer case. Some of the vanes will require a greater thickness to permit the use of flattened tubes through their hollow core. These tubes will provide an oil supply and return line, a breather line, and a labyrinth seal air supply and return lines to the number 4 bearing compartment.

A tailcone is bolted to the inner shroud aft of the exit guide vanes. An outer rear case is bolted to the turbine exhaust case to form a converging annulus, the primary nozzle throat, and its diffuser section.

Experience gained during development of the JT11D-20 turbojet engine was used extensively in designing the turbine exhaust section and exit guide vane system. Experience on the JT11D-20 has shown that a high thermal gradient exists in the exit guide vane system during engine starting due to the rapid heating of the vane. On a long life engine

this could result in low cycle fatigue problems in the vane and vane support rings. The thermal gradient has been reduced in the SST design by wrapping a heat shield (Hastelloy X) around the exit guide vane to reduce the rate of vane temperature response during transient conditions. This heat shield is also beneficial in reducing the effects of thermal shock and hot spots.

The number 4 bearing support and exit guide vane system was designed to sustain the load resulting from a turbine failure equivalent to a 10% blade loss. It is assumed that after a blade loss the rotor will rotate about a new center of gravity. The number 4 bearing support and exit guide vane system were therefore designed to keep stresses below the yield strength of the material when subjected to loads imparted by a 10% blade loss. This was accomplished by making the system's spring rate as low as critical speed requirements allowed.

c. Turbine Shafts

As in the Phase II-A design, the high speed turbine shafts tie the high pressure compressor to the high speed turbine. The two shafts are coupled at the number 3 bearing by means of a coupling nut and lock located just ahead of the first stage disk. The low speed turbine shaft couples the low speed turbine to the fan hub at the number 1 bearing coupling nut. Besides transmitting torque and axial load, the two shafts form an annulus to carry cooling air from the compressor to the turbine. The number 4 bearing provides support for the low speed turbine rotor through the low turbine rear hub.

(1) Physical Structure

The rear section of the high speed turbine shaft is flanged and bolted to the high speed turbine disk. The shaft at this flange is conical in shape. It becomes cylindrical, however, aft of the number 3 bearing and terminates forward of the number 3 bearing compartment. Material is provided adjacent to the flange for detail balancing of the shaft. The cylindrical portion of the rear section is splined to drive the forward section of the shaft which is flanged at the forward end and bolted to the rear disk of the high pressure compressor. A shoulder on the inside of the rear section behind the splined section provides a bearing surface for the coupling nut which screws onto the end of the forward section. The shaft sections form a double shaft which passes through the number

3 bearing compartment and provides protection against turbine overspeeding in case of an outer shaft failure. Ahead of the number 3 bearing compartment the forward section of the shaft tapers outward to match the rear high speed compressor disk pilot diameter.

The low speed turbine shaft is flanged at the rear and is bolted to the front face of the first low speed turbine disk. The shaft is cylindrical at the flange and extends forward to couple with the fan hub just forward of the number 1 bearing. The shaft is splined at the forward end on the outside to drive the fan hub which is splined on the inside. The hub and shaft are tied together by a threaded coupling which screws into the turbine shaft and pulls against a shoulder on the hub. Fitting spacers are placed between the end of the shaft and the hub shoulder to absorb accumulated tolerances and accurately position the low speed turbine rotor. Material is provided just aft of the forward hub of the high speed compressor and at the shaft rear flange for detail balancing of the low rotor shaft.

The low speed turbine shaft and fan hub form a double shaft that passes through the number 1 bearing compartment. This shaft provides protection against turbine overspeeding in case of a failure in the hub adjacent to the bearing.

The low speed turbine hub front flange is bolted to the rear face of the first low turbine disk. It is conical in shape aft of the flange and becomes cylindrical prior to passing through the number 4 bearing.

d. Stress Analysis Summary

The shafts and hub are designed to withstand the stress produced by a 10% blade loss load. They were evaluated for torsional yield stress, creep stress, buckling stress, and critical speed. In all cases critical speed was the limiting factor. The shafts and hub for the STF219 turbofan engine provide for a stiff bearing critical speed margin of 20%. This assures that the rotors will not have any vibration modes in the operating range of the engine with significant rotor bending when coupled to the bearing support structure and cases.

11. DUCT HEATER DIFFUSER

a. General Description

The current design of the fan duct diffuser is aerodynamically similar to the Phase II-A design, adjusted to the latest 650 lb/sec. airflow and

fan flow path. The mechanical design features have been modified relative to Phase II-A as discussed under Design Philosophy. A schematic drawing of the diffuser is shown on Figure 2A-191.

The purpose of this part of the engine is to diffuse the fan duct airflow to the lower velocities compatible with the duct combustion system and to deliver a stable profile to the duct combustor at all flight conditions. The flow path is offset to connect the fan exit at the intermediate case with the duct combustor which is at a larger diameter. The diffuser duct must clear the main gearbox on the outer diameter while bending outward as rapidly as possible to provide maximum clearance between the diffuser case and the high compressor case. This clearance is required for assembly and inspection purposes, and for the fuel, lubricant, bleed air and instrumentation lines which enter the cavity through struts in the fan duct diffuser. These struts also act as aerodynamic fairings for the intermediate case support struts and structural members of the diffuser case assembly.

The composite duct diffuser is composed of three conventional diffusers connected by two sets of annular cascades which turn the air radially as well as support cascade diffusion. The rate of diffusion in the individual annular sections has been based on Pratt & Whitney production engine diffusers and on rig tests of this configuration run during Phase II-A. These rates allow the diffuser to operate at good recovery efficiency considering the expected inlet flow profile and boundary layer conditions. A streamline analysis has been made of the diffuser flowpath to assist in leading edge alignment of the cascades. Incidence and camber of the NACA 65-series airfoils will be selected with Pratt & Whitney cascade tunnel data modified to reflect diffuser side wall effects.

The inner duct diffuser wall will be bled for duct combustion inner wall cooling. The bleed will be located to provide some boundary layer control on the inner duct diffuser wall at the location which future testing shows to be optimum.

Early concepts for the duct diffuser envisioned essentially constant area turning vanes feeding an annular diffuser whose meanline moved out radially at 40-45 degrees. The flow was then turned axially by another constant area turning cascade. This diffuser was, in philosophy, somewhere between the conventional annular diffuser of near constant mean diameter and the vaneless radial diffuser (without swirl) used on centrifugal compressors. The axial length was shortened considerably

by this technique. However, early model testing showed the amount of diffusion called for in the STF219 fan duct (A_2/A_1 = 2.8) was too great for the single diffuser.

The present design allows diffusion in the turning cascades similar to that occurring in stators of axial flow compressors. The design employs the concept of D factor and $\Delta P/q$ as vane loading parameters. The first outward bend of the diffuser had to begin several inches downstream of the diffuser inlet to clear the main gearbox. This first passage was designed as an annular diffuser since ample length was available. The bend in the outer diameter wall of the diffuser case at the first turn was reduced (as was the Mach number) into the first cascade which should reduce cascade losses and outer wall loading.

Diffusion in the passage between the cascades was reduced to reasonable limits, with the remaining diffusion taken by the rear cascade and annular diffuser at the rear of the rear cascade. A smooth increase of area through the various diffuser sections was maintained and blockage by the support struts was accounted for in the actual flow area sizing.

b. Physical Structure

The fan air diffusion is accomplished in three sections; the intermediate case, the fan duct diffuser case, and the duct formed by the forward duct case and the front inner liner. These sections also route the gas generator plumbing to the outside of the engine and provide easy access to the annulus formed by the outer wall of the gas generator and the inner wall of the fan duct diffuser. This annulus contains most of the gas generator plumbing.

The intermediate case houses the first section of the fan duct diffuser. Eight hollow airfoil shaped struts provide space for the plumbing to the number one and two bearing compartment and for the tower shafts for the gearbox and power takeoffs. A flange is provided on the rear of the outer wall of the intermediate case to attach the outer front flange of the duct diffuser case. A pilot diameter is provided on the rear of the inner wall to mate with the pilot diameter on the inner diffuser duct. Other constructional details of the intermediate case are discussed in the Intermediate Case section of this report.

The fan duct diffuser case is fabricated from AMS 4910 and AMS 4966 titanium alloy with butt-welded construction utilized throughout. The diffuser case consists of an inner and outer case joined by eight hollow

airfoil-shaped struts. These struts serve as fairings behind the intermediate case struts and also house the plumbing routed from the outer engine to the annulus formed by the gas generator and the fan duct diffuser case.

The outer diffuser case consists of a front and rear forged-ring welded to a formed sheet metal center section. The front and rear rings have machined mounting attachments for the cascades, strut attachments, and flanges to mount the diffuser case to the intermediate case and the forward duct case.

The inner diffuser case is made up of a front and rear forged-ring welded to a formed sheet metal center section. The front and rear rings have machined strut attachments and inner diameters that are piloted on the intermediate case and the inner duct burner case. The inner diffuser case is supported by the eight struts.

The forward duct case is fabricated from AMS 4910 and AMS 4966 titanium alloy with butt-weld construction utilized. The forward duct case consists of a front and rear forged-ring welded to a center section of formed sheet metal. Provisions were made to mount the access panels, zone 1 and zone 2 sprayrings, the gas generator spark igniters, and the duct heater igniters. The front and rear rings have machined flanges to attach to the fan duct diffuser case, the intermediate mount, and the duct combustion chamber case.

The front inner liner is fabricated from AMS 4910 and AMS 4966 titanium alloy with butt-weld construction. The front inner liner is composed of a front, intermediate and rear forged ring welded to connecting formed sheet metal sections. Provisions were made to mount the access panels, and openings were provided for the gas generator igniters and flameholders.

c. Design Philosophy

(1) Access Panels

An access to the annulus between the gas generator and the inner fan duct is provided without having to remove the fan duct burner or fan duct diffuser case. This access is necessary to reduce the elapsed time in inspecting plumbing, components, and fuel nozzles mounted in this annulus. Also, provisions were made for boroscope inspection of the compressor without engine teardown by means of removable plugs opening access passages extending radially inward through the

diffuser strut fairings. By removing the duct burner and disconnecting the fan diffuser case from the intermediate case, access to the front flange of the high compressor is obtained. This enables the entire low compressor to be removed as a unit, and the number 1 and 2 bearings replaced without turbine teardown.

Several methods of providing this accessibility were studied. These methods included splitting the fan duct diffuser case; splitting the forward duct case with removable panels in the front inner liner; utilizing removable panels in the fan duct diffuser between the struts; and utilizing removable panels in the forward duct case and front inner liner. The split case design was discarded for the following reasons:

- More complicated case construction.
- Greater difficulty in sealing the outer cases.
- Components and outer plumbing would have to be removed to pull the case.
- With increased fuel nozzle line requirements the concept of running the fluid lines through the two split struts is less practical and might require that the case be split in four places.

The method selected to provide access to the inner annulus consists of rectangular shaped access panels in the forward duct case and front inner liner as shown on Figures 2A-191 and 2A-192. The advantages of this method of access are as follows:

- No components and a minimum of outside plumbing have to be removed to remove access panels.
- No special tooling is necessary to support the engine while panels are removed.
- Panels are located to allow replacement of fuel nozzles and to check most plumbing connections.

The disadvantage of access panels is the difficulty in controlling outer duct wall leakage. Closely spaced panel fasteners or development of a gasket material capable of withstanding 650-700°F will be required to control the leakage.

(2) Cascades

Several methods of attaching the front and rear cascades to the fan duct diffuser case were studied. Mechanical attachment of the cascades to

the diffuser case allows flexibility in cascade design during development and a damaged cascade may be replaced without any rework on the case. The front and rear cascades and supporting pylons are fabricated from AMS 4966 titanium alloy. The cascade airfoil shape is machined in the supporting pylon and, when the cascade is installed in the pylon, the two are fillet-welded together. The mounting bracket at the base of the support pylon is mechanically attached to the diffuser case.

12. DUCT HEATER

a. General Description

Thrust augmentation for the STF219 turbofan engine is provided by a fan duct combustion system commonly referred to as a duct heater. To initiate and maintain combustion in the relatively cool fan air stream, an aerodynamic or "jet flameholder" is used. Combustion continues along the entire length of the duct heater combustion section and exhausts through a variable area exit nozzle. Ignition will be provided by either a torch or spark type igniter located upstream of the duct fuel sprayrings. The duct heater is shown in Figure 2A 193.

The burner length was set at 60 inches, the distance from the aerodynamic flameholder centerline to the nozzle exit plane. Extensive small scale rig data has demonstrated that the required efficiency of 95% at simulated cruise conditions can be achieved with sections 60 inches in length. The duct burner cross sectional area of 1950 sq. in. was set to give a maximum duct burner inlet Mach number on the typical climb path of 0.175. The critical design point for this area occurs at Mn 2.0, 55,000 ft. Small scale rig test results indicated that at this velocity combustion could be sustained and that the required combustion efficiencies could be obtained. At higher velocities the combustion becomes less efficient and the probability of blow-out begins to increase. The centerline of the aerodynamic flameholder is located 12 inches downstream of the intermediate case strut trailing edge. This is about four times the maximum strut thickness and is, therefore, approximately at the trailing edge of the wake generated by the strut. Placing the flameholder in this position prevents the flame from propagating upstream into this wake.

b. Aerodynamic Flameholder Design

The aerodynamic flameholder concept was selected because of its ability to sustain combustion over a wide operating range with low blockage

pressure losses. It has an additional feature during non-duct burning conditions of a high pressure air shut off which further reduces the cold losses. The V-gutter flameholder concept was discarded because of its inability to sustain combustion at low duct inlet temperatures. The soundness of the aerodynamic flameholder approach has been demonstrated by extensive small scale and full scale rig testing. The required efficiencies have been demonstrated using a 60 inch burner length at simulated flight conditions with aerodynamic flameholders. The air flow through these flameholders has been targeted at 3% of the gas generator flow.

The overall design of the flameholder calls for a ring midway between the duct O.D. and I.D. with 12 radial struts passing from the I.D. to the O.D. Provisions are to be made in both the struts and the ring for air injection into the duct stream. These injected streams of air form the aerodynamic flameholder.

Burner bleed air is to be supplied to the I.D. of each of the radial struts. A gap of 0.1 inch has been allowed between the flameholder outer tip and the duct outer liner to prevent streaking of the outer liner in the wake of the flameholder strut. The width of the flameholder was limited to one inch to keep blockage down to 10% of the duct passage. Inside areas were sized to insure uniform distribution of air throughout the flameholder system at all flight conditions.

c. Spraybar Configuration

The fuel injection system for the STF219 is broken up into two zones. The first zone (Zone I) will be developed to give the required 95% combustion efficiency during cruise. The second zone (Zone II) will supplement Zone I to provide a combustion efficiency of 93% during acceleration. The overall shape of the Zone I spraybars is that of the flameholder; that is, it consists of 12 radial struts and a circular ring midway between the duct O. D. and I. D. Fuel is supplied from the manifold outside the outer wall to each of the twelve struts. The centerlines of the assembly are located one inch upstream of the leading edges of the flameholder. Test results have confirmed that with the Zone I flameholder in this location the required efficiencies can be achieved without fuel coking or plugging of the nozzles in the spraybar. The I.D. of the spraybars was set at 0.5 inches to insure adequate fuel distribution to all sections of the spraybar assembly during maximum fuel flow conditions.

Zone II supplies fuel to virtually all of the remaining duct air not supplied by Zone I. For this reason, these spraybars are located further upstream and are designed to cover the area between the flameholders and the inner and outer walls. This is accomplished with four spray rings and sixteen radial struts. Eight of the struts are supplied by a fuel manifold outside the duct outer wall with the eight remaining supports for structural purposes only. The inside diameter of the spray rings was set at 0.25 inches to insure uniform fuel distribution throughout the Zone II spray bar system. The axial displacement between the Zone II spray ring and the flameholder was set at 2.8 inches. This is the length used in small scale testing where high combustion efficiencies have been demonstrated.

d. Cooling Liner

The duct heater discussed in the Phase II-A final design report incorporated a rigimesh liner. As a currently preferred alternate to this concept, the design effort during Phase II-B has been directed towards providing a perforated cooling liner for the inner wall and a convectively cooled liner for the outer wall. A perforated inner liner would have more predictable cooling and structural characteristics, although it would, however, require slightly more cooling airflow, since its cooling efficiency is lower than that of rigimesh. The outer liner could be convectively cooled with nozzle flap cooling air. This method would eliminate any need for transpiration air on the outer liner. A final conclusion has not been reached, but for the purposes of this report all configurations shown are based on a perforated inner liner and a convectively cooled outer liner.

The outer liner shown in Figure 2A-193 contains a double-walled liner beginning at 2/3 of the liner length. The purpose of this feature is to increase local cooling air velocities where the burner gases are hottest. The inner liner is in tension because the cooling air is at a higher pressure than that of the duct air. This simplifies the inner liner structural problems and makes rigimesh more attractive here than on the outer liner. The higher cooling air pressure on the outer liner would impose a buckling load on a circular liner. To circumvent this difficulty a segmented or scalloped outer liner, as shown in Figure 2A-193, Sections A-A and B-B, is being studied.

e. Fuel System Requirements

(1) Overall Duct Fuel-Flow Range

Setting of the fuel-flow range is determined by the range of fuel/air ratio requirements. The lowest f/a setting was found to be 0.008 for ignition. This level is predicated on three considerations: (a) avoidance of fan surge; (b) engine inlet stability; and (c) passenger comfort during light-off was considered. The maximum value of fuel/air ratio required is found to be 0.054 during acceleration at Mn 0.7, sea level.
The fuel flow variation is further increased by the large range of duct air flow. The minimum air flow is 75 lb/sec at Mn 2.0, 75,000 ft., while the maximum airflow is 476 lb/sec at Mn 0.7, sea level. From the above the required turndown ratio of the fuel system may be determined as follows:

$$\text{Turndown ratio} = \frac{\text{Max fuel flow}}{\text{Min fuel flow}} = \frac{0.054}{0.008} \times \frac{476}{75} = 42.8$$

This equation states the overall variation in the fuel flow requirement. To determine what can be achieved by a single spray ring with a single set of fixed geometry nozzles, the nozzle ΔP upper and lower limits must be evaluated. The maximum available ΔP based on fuel pump pressures and line losses is estimated to be 800 psi. The minimum pressure drop is 15 psi. This is the lowest allowable ΔP for which adequate fuel penetration can be achieved. The turndown ratio available from a single set of fixed geometry nozzles is the square root of the ratio of the maximum ΔP to the minimum ΔP, i.e. $\sqrt{800/15}$ or 7.4. Comparing the available turndown ratio with the required ratio indicates that more than one set of nozzles or a variable nozzle must be used.

Combustion efficiency is a second performance requirement of the duct burner that affects the design of the fuel system. This efficiency has been specified over two narrow f/a ranges as indicated.

	Cruise	Acceleration
Required f/a	0.018 - .025	0.048 - .054
Required efficiency	95%	93%
Fuel zones in operation	I	I & II

With these two efficiency targets in mind Zone I is designed and will be developed to meet cruise operating requirements. To meet the acceleration specification Zone II is added to supplement Zone I. The

feasibility of this two zone approach was demonstrated by test data presented in the Phase II-A report.

(2) Fuel Flow Requirements of Zones I and II

The turndown ratio of each zone is evaluated by a study of Figure 2A-194. During ignition only Zone I will be in operation. The f/a of Zone I then increases with power lever angle from a level of .008 to a level of 0.026 which is just above the cruise requirement. At this point additional power lever movement simultaneously lowers the Zone I fuel flow and turns fuel on to Zone II. This schedule is designed to keep the total fuel continuous during transition into or out of 2 zone operation.

Also, any fuel flow discontinuities that do result will take place outside the range of normal operation. During Zone II operation, the Zone I f/a is set at about 0.015. This value was selected because test experience indicates Zone I should run a little lean when operating with a second zone. Under these conditions the level of 0.015 f/a will give near optimum combustion efficiencies. A summary of these considerations and a calculation of the turndown ratio for each zone is included in Figure 2A-194. For Zone I the turndown ratio is 20.6 and for Zone II it is 22.5. In both instances the limiting turndown ratio of 7.3, discussed above, is exceeded. Both zones, must, therefore, be "duplex", that is each must have a means for scheduling the fuel flow other than by a single set of fixed geometry nozzles.

A number of systems for extending the fuel flow range of each zone are under study. One system being considered consists of two identical sets of spraybars in each zone, one upstream of the other. One set of spraybars would be used for the entire fuel range of the zone, while the second set of spraybars would be used for the higher levels of fuel flow for the particular zone. The selection of the high flow range could be scheduled either by a pressurizing valve operated by the pressure level in the base spraybars, or by pressure level in the aerodynamic air bleed. Another approach to the fuel variation problem is the use of variable area spraybar nozzles. Studies to complete the fuel system design are continuing.

f. Physical Structure

The duct heater consists of the duct heater cases and liners, the aerodynamic flameholder and its air supply system and valves, the fuel sprayrings, and the ignition system.

The duct heater case consists of three sections. The forward duct case and the intermedia e mount and duct combustion case are made from Titanium alloys (PWA 1202). The rear duct case is made from stainless steel (AMS 5616 and AMS 5508) to withstand the slightly higher temperature present in this area. Each of the cases is cylindrical and fastens to the adjacent sections at flanges. The forward duct case has provisions for the installation of the main engine igniter torque tubes, Zone I and Zone II sprayrings, access panels, igniters, and fuel drain plug.

Access to the inner plumbing and fuel nozzles is provided by removing panels in the forward duct heater case and in the front inner liner. The intermediate mount and duct combustion case includes the rear engine mount ring. Both the intermediate mount and duct combustion case and the rear duct case have attaching points to support the exhaust nozzle and ejector-reverser hardware.

The three major sections of the duct heater inner liner are the front liner, the perforated screech and cooling liner, and the exhaust nozzle cone. The three sections of the outer liner are the fuel baffle, the single-walled segmented front section, and the double-walled segmented rear section.

The inner front liner and the outer conical fuel baffle form the forward sections of the liners and prevent fuel from entering the inner and outer cooling flow annular areas. The section of the inner liner immediately downstream of the flameholder is the screech liner. Many small holes are drilled in this liner until the open area is a predetermined percentage of the total area. A cross section of the outer liner in this same area shows a series of valleys and arches beneficial for screech suppression. This section absorbs the periodic combustion energy fluctuations and prevents random pressure fluctuations from developing into cyclic vibrations of large amplitudes.

To the rear of this screech section there is an inner cooled liner fabricated from perforated sheet with an additional smaller diameter wall for increased cooling air velocity and heat transfer capacity. The outer liner in this section is also double-walled for the same reasons as the inner wall, but does not require any transpiration cooling except at the extreme end. These liners protect the outer duct and engine cases from the high temperatures of the burning gases by forming the inner wall of the annulus which carries fan discharge cooling air to the duct heater exhaust nozzle at the outer end of the fan duct discharge air passage. They also form the outer wall of the annulus which carries

fan discharge cooling air to the engine exhaust nozzle at the inner extremity of the fan discharge passage. Fan discharge air is carried between the liners and the inner and outer cases through a series of liner supports that have graduated orifices to allow the desired flow to every section of the liner, case, and nozzle. The orifice areas are based on hole area only, and are unaffected by gaps between the outer liner and supports. At the end of the outer combustion case, cooling air is directed at the nozzle flaps to keep them from overheating, and at the end of the inner case, air is discharged into the exhaust stream.

High temperature compressor discharge static air for the aerodynamic flameholder is controlled by 12 piston-shuttle type valves. These valves are supported by the main engine combustion chamber outer case and are remotely controlled by the duct fuel control. With the fuel control in the "off" position, a two-way valve permits engine diffuser air to pass into one chamber of the control valve and actuate the piston to shut off the airflow. Moving the fuel control to the "on" position causes the two-way valve to vent the diffuser air overboard, allowing combustion chamber air to enter the opposite end of the control valve. This air actuates the control valve to direct high temperature compressor discharge air into the aerodynamic flameholder ring and subsequently into the duct stream.

g. Stress Analysis

The duct heater cases are sized to resist buckling when subjected to maneuver loading with a safety factor of 1.3. The flanges were designed to resist blow-off and maneuver loading with a medium design stress equal to 80% of the 0.2 percent yield strength. The rear mount ring was designed to permit a displacement of the outer case from the normal position no greater than 0.2 inch.

In the segmented liner configuration, both liner and duct are under net tensile loads which are predictable. The bending loads imposed by the liner attachments on the duct are controlled by the number and spacing of the attachment points, i.e., by the number of liner segments. It is felt that 30 evenly spaced attachment points is a minimum number. The present design contemplates the use of 36. The segmented liner has other merits. The segments are individually replaceable if damaged. Handling of smaller segments requires no special tooling or fixtures. The relatively small size of the segment compared with the size of a sheet of material required for a complete cylinder makes obtaining material of consistent quality easier.

13. DUCT HEATER NOZZLE

After reviewing the design requirements of the duct heater nozzle, it was decided that a "balanced flap" design should be considered. A balanced flap design has proven satisfactory in the JT11D-20 engine, therefore a study was initiated to determine if this type system could be used in the STF219 engine.

The balanced flap system, as shown by Figure 2A-195, uses a conventional unison ring to synchronize the flaps. The flaps are connected directly to the ring. A roller is attached to the back side of each flap directly opposite the center of pressure of the flap. The roller of each flap is guided by its own roller track. Moving the unison ring fore and aft causes the nozzle to open and close.

Investigations have shown, however, that this system could not be used for the STF219 turbofan because the track assembly interfered with the "blow-in" doors of the ejector/reverser assembly. The necessary clearance could be obtained by moving the hinge point of the doors aft, but this would restrict the area requirements of the ejector.

After this study indicated that the balanced flap system could not be used, a bellcrank linkage system similar to that used on the TF30 engine was investigated. Early studies of this system showed that a flap actuating scheme of this type could be compatible with the blow-in door ejector assembly.

Investigation of this system led to a 12-sided nozzle design compatible with the 12-sided ejector assembly being considered at that time. Each of the 12 flaps was actuated by a bellcrank mounted on the top (inboard) surface of each ejector axial support strut. The nozzle flaps were connected to the bellcranks through ball-joints. Links which connected the bellcrank to the unison ring were located along the inboard surface of each strut. This arrangement provided clearance for the blow-in doors.

As studies progressed, it was felt that satisfactory ejector performance was dependent on controlling the flow of secondary air as it entered the ejector. The object was to direct the flow of secondary air into the hot gas stream just aft of the duct heater flap tips (Figure 2A-196). This system was designed primarily to improve the aerodynamic performance of the ejector, but it also offered the advantage of providing an adequate flow of cooling air for the nozzle flaps. Studies concurrently conducted with the "blow-in" door ejector show that the "ducted" flap scheme would not be necessary.

A new study was begun which led to the configuration as it appears in the present design. The only major change involved using an 8-sided ejector in lieu of the original 12-sided ejector.

The basic problem necessitating the duct heater nozzle investigation was that of physically placing the necessary mechanism in the space allowed. Stress levels, temperatures, and weights were considered. Operating experience with the JT11D-20 engine was relied upon in designing the exhaust nozzle system.

During the design of the duct nozzle system, the major problem encountered was that of finding space for the necessary mechanism. The unison ring presented the major problem due to its size and shape. A study was started to investigate a synchronizing system rather than the conventional unison ring.

The system investigated a bellcrank-linkage scheme for synchronization as shown in Figure 2A-197. Bellcranks are mounted forward on the struts in such a manner that they can be connected by links running perpendicular to the struts. This system would use less space than the translating unison ring, but it did have several disadvantages. First, there are no provisions to allow for thermal expansions of the links. Also, in going through the complete actuating stroke, the tierods must pull the bellcrank lever arms at an angle producing large bending loads in the lever arm. An alternate system was considered which replaced the tierods with a continuous ring, but this approach also had disadvantages. The basic problem for this scheme was providing adequate support for the rotating ring.

In all designs, the actual nozzle flaps and seals were of a design similar to the type used in the JT11D-20 engine. This was based on the proven success of these flaps and the fact that the STF219 and the JT11D-20 will have similar operating conditions.

Two flap/seal concepts were considered but were soon discarded for several reasons. The first scheme is shown in Figure 2A-198. In this design, the triangular-shaped seal was attached to one flap edge using a "piano" type hinge. The other edge of the seal was then free to rest against the adjacent flap. The major disadvantage of this seal is the possibility of the hinge joint seizing and not allowing the seal to rest against the adjacent flap.

The other flap/seal arrangement is shown in Figure 2A-199. This system uses eight flaps and seals of nearly the same size creating a 16-sided

nozzle. This system produced high loads on the seals due to the size and pressure acting on them. This load would produce high wear rates at the interface between the seal and flaps.

The final duct heater nozzle design combined the best features of the designs previously studied into the configuration shown on Figures 2A-200 and 2A-201.

The duct heater nozzle controls fan rotor speeds by varying the nozzle area from 3.2 to 10.9 sq. ft. Nozzle areas are scheduled by the duct fuel control as a function of engine inlet temperature and pressure.

The nozzle is octagonal in shape and consists of 8 flap-type segments with 8 interflap seals. The flap segments are operated by a bellcrank-linkage system and a unison ring to ensure synchronization. The unison ring is actuated by 8 hydraulic cylinders. Engine fuel is used as the hydraulic fluid, and a bleed circulation system maintains a continual flow of cool fuel through the actuation system.

The flap segments and seals are corrosion and heat resistant nickel base alloy. Stiffening ribs are cast on the back side of both the flaps and seals. The flap and seals may be individually removed from the duct heater for inspection or replacement.

A "slave" link forged from a nickel base alloy is attached to the rear of the main flaps on the same axis as the seals. Cam follower rollers mounted on the slave link fit into a mating channel track located on the outer edge of each flap. As the slave link is actuated, the roller transfer the force into the two adjacent flaps. The geometry of the flaps and "slave" link is such that the cam follower rolls in the track and maintains line contact at the mating surfaces.

The slave link and seal segments are pinned on the same axis. The seals are then free to rest on the front face of the flaps and provide the sealing surface at the corner of the octagon shaped nozzle.

Each seal is positioned by the pin at the base and by a tab-slot arrangement located on the slave link. This system allows the seal a certain amount of freedom so that it can adjust to any alignment irregularities between adjacent flaps. The tab-slot system also keeps the upper seals from falling out of position when the engine is not operating. During normal engine operation the gas stream flowing through the nozzle forces the seal against the flaps. This slave link-flap system also tends to synchronize all eight flaps.

Each slave link is connected to its bellcrank by a forged connecting rod. This link is forged from a nickel based alloy with a threaded clevis on one end to provide the necessary adjustment during assembly.

The bellcrank is pivoted on a mounting located on the inside of each of the struts. These eight struts are trapezoidal in section with a slot cut in the inboard face to allow clearance for the bellcrank and connecting rod. Since the bellcrank linkage is located on the inside of the strut, access holes are provided on the side for assembly.

Each bellcrank is actuated by a link connected to the unison ring. The unison ring is fabricated from sheet metal with stiffeners added to which adjustable cam followers are mounted. The rollers are guided by channel section tracks which are integral parts of the struts. The ring is positioned between the struts and the O. D. of the duct heater. Eight equally spaced arms extend radially from the unison ring into the center of each strut. Tierods extend rearward to the radial arms connecting the unison ring with the bellcrank and forward to the hydraulic actuator. Slots are cut in the struts to allow proper clearance.

The advantage of this system is that normal actuator loads are not transmitted through the unison ring. The ring is loaded only in the event of unbalanced actuation forces or unbalanced flap loads.

The actuators are of conventional design and are mounted on the forward face of the mount ring. Under normal cruise conditions all nozzle linkages (except the slave link connecting rod) are loaded in tension. This eliminates the buckling problem normally found in long tierods.

The eight struts supporting the ejector assembly are also an integral part of the duct heater nozzle assembly. The nozzle system can be installed and the engine operated without having the ejector/reverser in place.

14. EJECTOR-REVERSER

a. Preliminary Studies

The ejector design reported in Phase IIA was a circular, 12 blow-in door configuration. The reverser system consisted of 12 doors with a unique linkage system to fold the door tips under in the stowed position. Trailing edge flaps for this system were of the conventional flap and seal design.

Preliminary investigations indicated difficulty in actuating the blow-in doors for reversing and in defining the linkage system on the reverser doors on this particular design. Single line kinematic sketches analyzing relative motion, mechanical advantage, loads, and sequencing were then started to study the problem area. However, before any of these sketches were concrete enough for starting a layout study, new information was received that called for revisions to the preliminary work in progress. Aerodynamic and design studies indicated that the ejector diameter could be revised. In addition, variable geometry to utilize higher secondary airflows and pressures was to be incorporated. The combination of these changes called for a new overall evaluation of the ejector.

Due to the reduction in area between the fan duct O.D. and nacelle, secondary flow passages were restricted below allowable limits and interference occurred between the blow-in doors and the fan duct nozzle flaps. This new configuration also eliminated the possibility of actuating the blow-in doors as in the Phase IIA system. Several "latching" schemes were then studied that would hold the doors once they were in the "blow-in" condition. Also, doors that were closed on reversal were left free and depended upon the pressure loads of the reverse gas stream to aerodynamically close them.

Before this concept could be pursued, a change in turbine exhaust diffuser length eliminated some of the problems. The increased length allowed the fan duct nozzle to be relocated and resolved the blow-in door fan nozzle interference problem. The front hinges on the blow-in doors were located under the engine mount ring, allowing more area for secondary air flow passage. The problem of designing a blow-in door actuating system, a reverser door linkage system, and a reverser door/blow-in door synchronizing system still existed.

A new concept consisting of an octagonal shaped ejector, having a circumferential set of torque tubes interconnected by universal joints was devised. The tubes operate and synchronize the reverser and blow-in doors by connecting cables and pulleys running down the struts. This system was studied in detail for mechanical feasibility and weight. This concept proved to be over 300 lbs. heavier than the original Phase II A ejector mainly because of the actuation system. During the study, however, many advantages were foreseen in the octagonal shape. An optimization study was then initiated which combined the best features of both ejector designs and also incorporated some new concepts.

b. Octagonal Ejector-Reverser "Fixed Shroud"

The term "fixed shroud" as used in this section indicates that the entire shroud does not move or translate. However, a portion of the shroud has variable geometry capability.

An octagonal ejector-reverser design incorporating internal variable geometry at the forward part of the shroud evolved from the preceding studies. This design was directed toward improving the engine/airframe installation, toward more efficient utilization of energy available from the engine and secondary air streams, and toward reduction of minimum wrap.

In the Boeing installation, it became necessary to reduce the base drag area between the ejector and the wing. The octagonal ejector, with its flat sides, offered the possibility of entirely eliminating the objectionable base drag. A design study was therefore made which applied the octagonal ejector concept to the round Phase IIA ejector-reverser. This study included the Boeing canting requirements. The design is shown in Figure 2A-202.

(1) General Description

Conceptually, the octagonal ejector-reverser is similar to the Phase IIA design in that the system incorporates a set of blow-in doors, trailing edge flaps, thrust reversal flaps, and a structural shroud attached to the engine by integral axial struts. In addition, the system incorporates secondary airflow control panels. These panels reduce the gap between the ejector shroud leading edge and the duct heater nozzle flaps during cruise to utilize more efficiently the secondary and primary air streams. The differences between the Phase IIA ejector design and the above design and revisions to the duct heater nozzle are discussed in the following paragraphs. The material requirements of both designs are similar.

(a) Duct Heater Nozzle - The octagonal ejector-reverser concept requires that the primary and duct heater nozzle planes be octagonal in shape. The duct heater nozzle consists of 8 large, flat panels hinged to the duct case. Each panel forms one side of an eight-sided truncated pyramid with the smaller end forming the nozzle. The varying gaps between the flaps are sealed with sheet metal segments which are hinged to the duct case and interlocked with lugs along the sides of adjacent flaps.

The nozzle actuation system was similar to the Phase IIA design, but was revised to make it more compact. One of the design objectives was to reduce the radial distance between the O.D. of the duct heater case and the outer surface of the ejector longitudinal support struts to permit the use of a smaller ejector reverser equivalent diameter. This was accomplished by placing the nozzle actuators aft of the rear mount ring as close as possible to the duct heater case O.D. and moving the unison ring and support struts closer to the duct heater case. The structural ring at the nozzle hinge plane was incorporated into the hinge support structure and connected to the longitudinal support struts by short radial tie members.

Moving this ring inward and changing its shape from circular to octagonal permitted the blow-in doors and the other components of the ejector to be moved inward while still satisfying the aerodynamic blow-in door flow area requirements, with resulting size and weight advantages

The flaps are actuated by eight hydraulic pistons which move the unison ring. This ring is then coupled to bell-crank linkages which in turn move the flaps. The unison ring distributes the actuating loads uniformly and insures proper functioning of the nozzle flaps in the event of asymmetrical loading. The hydraulic actuators are pin-mounted to brackets attached to the axial struts.

The unison ring is a short sheet metal cylinder stiffened at both ends by square cross-section rings. Eight sets of rollers are equally spaced around the outside of the ring and are attached to the stiffening rings. These rollers straddle the ejector shroud support struts and prohibit circumferential motion, while permitting axial motion of the ring with low friction. The roller system is designed to prevent cocking and binding of the ring when subjected to asymmetrical loading. Integral flanges on the axial support struts guide the rollers.

(b) Ejector-Reverser Shroud - The octagonal shroud is the structural and load transmitting component of the ejector system. It provides storage and support for the secondary airflow control panels, the reverser flaps and their actuation mechanism, and attachment for the trailing edge flaps. Structurally, the shroud consists of a forward and aft octagonal ring joined by flat panels forming the outer surface of the shroud. The shroud is attached to the engine case by eight trapezoidal cross-section struts. The support struts contain the secondary airflow control panel actuators and the blow-in door positioning links. Removable structural panels form the outer surface of the strut and allow access to the interior of the strut. Lips on the outer edges of the support struts and the leading edge of the shroud provide support for the edges of the blow-in doors.

(c) Secondary Airflow Control Panels - In the Phase IIB study, it was determined that for the high Mach number cruise condition some means of controlling the gap between the duct heater nozzle flaps and the leading edge of the ejector shroud should be incorporated to insure maximum thrust benefit from the secondary airflow. This is accomplished by incorporating movable folding panels which in the retracted position form the leading edge of the ejector shroud. The panels are extended by an arm which is rotated by a torque tube connected to an actuator within the support struts. The arm positions a cam attached to the rear panel and is connected to the forward panel via a push rod. In the extended position, the arm rides in the cam slot and maintains the rear panel in a fixed position. By modulation, sufficient force is supplied to the forward panel to maintain contact with the spacer cam on the duct heater nozzle flap. This provides an almost constant area for secondary air flow during cruise. The cam has been set up to allow the forward panel to follow the duct heater nozzle through a nozzle variation of +5% to -15% of nominal nozzle area required for Mn 2.7 cruise. If the nozzle area exceeds +5%, the secondary airflow control panels will automatically retract into the leading edge of the shroud.

(d) Blow-In Doors - Eight blow-in doors are located around the ejector periphery ahead of the shroud and between the support struts. During normal operation, the blow-in doors are self-actuating (free floating). Below Mach 1.0, the doors are generally open, and above Mach 1.3 the doors are closed. During reverser operation the doors are normally held open to exhaust the reversed gases, but selected doors can be closed to prevent impingement of hot gases on vital airframe structures.

Each blow-in door is fabricated of a forward and a rear section which are hinged together. The use of two sections allows the doors to assume appropriate angles for inlet flow and yet return to a closed configuration for supersonic flight, providing a smoothly faired nacelle. Positions of the doors are controlled by the linkage system shown in Figure 2A-202, (links A, B, and C). For those doors which remain open during reversing, links A, B, and C are interconnected; and for the doors which are held closed during reversing, only links B and C are interconnected, with link A acting only as a positioning cam. For forward flight, link A is held in the position shown and provides a "ground" point for the linkage system. This allows the blow-in doors to seek any equilibrium position from full closed to full open. The link system has been set so that the rear section rotates through its travel proportionally faster than the forward panel. For the doors that are open during reversing, link A rotates to the reverse position

pulling links B and C with it. The action forces the forward door closed and opens the rear panel providing further reverser area. The linkage geometry allows adjacent doors that are open for reverse operation to overlap. This provides sufficient reverser area, without interference between the sides of the doors at their trailing edges. The sharp break at the panel joint provides an aerodynamic trip which keeps the reverser gases from attaching to the nacelle skin and being re-ingested by the inlet. For the doors that are held closed during reversing, link A rotates to the position shown to close the forward door, while links B and C close the rear door. Link A is operated by a torque tube actuated by a hydraulic cylinder within the strut. This also is shown in Figure 2A-202, Sections D and E.

Operation of the blow-in doors is sequenced with the action of the reverser panels through hydraulic valves, i.e. the blow-in doors assume their reverse positions before the valves permit flow to the actuators which provide operation of the reverser panels.

(e) Thrust Reverser - The reverser concept considered is identical to the Phase IIA design, except the actuators are positioned within the shroud rather than within the axial struts. The articulated flap design is capable of ground or inflight reversing and null thrust, and also to targeting control on the ground to prevent the exhaust jet from striking vulnerable objects. These functions are achieved by activating the reverser flaps in unison or singly, either fully or partially as required.

The reverser flap assembly consists of a main flap, a tip flap (not shown in Figure 2A-202) incorporating a cascade similar to the Phase II-A ejector, an A-frame link which attaches to the main flap, a link from the A-frame to the tip flap, two adjustable stabilizing links from the A-frame to the rear ring of the shroud, and an actuator link from the A-frame to a track and roller assembly which guides the mechanism and the actuator. The hinge line of the tip flap is canted to retract the panel along the actuator.

Each flap is operated separately by its own actuator. Incorporated into the actuator is an inflight lock mechanism to hold the flaps in the retracted position when not in use. The locking mechanism consists of a locking pin, piston, and spring. The pin engages a groove in the head of the piston to lock the piston in place. The locking stroke and holding load is provided by the spring, hence, if hydraulic pressure is lost, the reverser flaps will remain locked in the stowed position.

When the actuator is pressurized, the pressurizing fluid (fuel) enters the locking pin piston and disengages the pin. At the same time, the piston opens the port to the actuator cylinder. A control valve in the locking cylinder ensures that the locking pin is removed before the actuator is pressurized.

An important characteristic of the articulated flap design is that the tip flap is rapidly extended and retracted. Hence, the major segment of the reverser is nearly fully extended before the tip section protrudes into the gas stream. This design permits the reverser flaps and actuating mechanism to be subjected to lower stresses during extension than would be encountered if the tip were extended earlier.

Loading from the reverser flaps is transferred to the ejector shroud at the forward ring through the flap hinges and through the link to the roller and track assembly mounted in the shroud. Loading is transferred to the rear ring through the stabilizing links of the mechanism. These links are located so that the load reaction is taken through the shear section of the rear ring. Maximum loading occurs when the flap is fully extended and the flap and link mechanism is at its maximum mechanical advantage. Maximum stresses occur in the flaps at the attachment to the links and at the hinge fittings. The maximum stress in the A-frame is bending, whereas the maximum stress in the other links is compressive.

One important feature of the reverser system is its ability to deflect the exhaust jet by actuating only a portion of the thrust reverser flaps to protect vulnerable areas from engine exhaust gases during reversing. A mechanical lock in the actuator can be supplied to hold the reverser flap in a partially extended position for deflection purposes. The exhaust deflection capability adds no appreciable weight to the exhaust system.

Another important feature of the reverser is the cascade contained in the articulating flap. This cascade spoils the forward thrust component produced by the hot inner engine gas stream. The hot gases are deflected against the inner nozzle wall during reverse operation, while the cooler fan air is discharged forward through the open blow-in doors. This minimizes the temperature of any exhaust gas which might be reingested.

(f) Trailing Edge Flaps - Eight trailing edge trapezoidal flaps are attached to the rear ring of the ejector shroud. The free-floating flaps are actuated by the pressure differential on their inner and

outer surfaces and vary the exit nozzle area within preset limits. The flaps are synchronized through paired radius arms. The arms are hinged to adjacent flaps near the flap hinge at the forward end and to each other through a ball joint at the rear end. This synchronization insures unified motion of the eight flaps and maintains an aerodynamically symmetrical nozzle even against side gust loads. When fully extended, the flaps are restrained by tiebolts. At the maximum inner position, the flaps rest against forged stops.

Sealing between adjacent flaps is accomplished by a modified H section seal positioned centrally between the flaps by pins on the radius arm ball joint and a hinge at the forward end.

The octagonal ejector-reverser with flap control of secondary air offered a performance improvement relative to the Phase II-A design, however it was still mechanically complex.

c. Octagonal Ejector-Reverser "Translating Shroud"

From the continuing studies and more detail engine design a new ejector configuration evolved. It consisted of an octagonal blow-in door ejector-reverser with a translating shroud.

This configuration, as shown in Figure 2A-203, had shortened blow-in doors which "tuck" behind the fan duct nozzle hinge, allowing maximum blow-in door area. The translating feature allowed the use of separate cascades for reversing, thus eliminating the blow-in door actuation system required for reversing. In addition, the ejector throat was moved forward and made smaller, providing a means for more efficient secondary air control at supersonic cruise. The translating shroud served as a synchronizing ring to position the reverser doors, and the octagonal shape, combined with the translating feature, allowed a "balanced flap" reverser door design. The high reverser loads were transmitted by links to the fixed structure, reducing actuation loads to a point where only "failsafe" requirements dictate the actuation force.

A new synchronized trailing edge flap concept was incorporated to connect the corner flaps mechanically to the flat flaps by a universal joint system. In addition, a damping scheme was devised, using a fluid powder dash-pot system to prevent flutter and to act as a mechanical stop to limit flap positions to the desired inner and outer limits.

The fixed support structure was changed to a crossbraced framework with a rigid end ring. The struts extend forward from this framework

and are connected by ball joints to the engine mount ring. This system eliminated strut bending at the attachment points and a second stiff ring at the fan nozzle. It also allowed the struts to become pure tension, compression members. The crossbracing at the aft end of the structure transmits ejector loads uniformly to all the struts. The translating shroud, being rigid itself, applies loads to the structure at the roller points which are within the crossbraced section, thereby, reducing bending loads on the struts to short span sections. The links on the reverser doors apply the reverser load normal to four of the eight sides. This eliminates bending in the end ring as the alternate sides are only in tension.

d. Translating Shroud and Cascade Ejector-Reverser

Before detailed layout studies could be started on this ejector, the engine airflow size was decreased from 700 lb/sec to 650 lb/sec, reducing the ejector equivalent diameter. Analytical studies of ejector performance were made, and a new set of aerodynamic requirements dictating the ejector shape were complied with. The final result was a 3-position shroud configuration; supersonic cruise, subsonic cruise, and reverse. To achieve this and still retain complete control over reverser flow targeting, the cascades in the shroud were made moveable and translated opposite to the shroud movement so as to provide the proper open cascade area in the region normally occupied by the open blow-in doors. This was accomplished by a double rack and idler pinion mounted between struts. This configuration is shown schematically in Figure 2A-204 with details of the rack and pinion arrangement in Figure 2A-205, and details of the actuation system in Figure 2A-206. The engine general arrangement drawing, Figure 2A-0, also shows the shroud in three positions.

A full size detail layout was made incorporating this new translating cascade feature. Also, a 1/4 scale working model was made to provide a three-dimensional check on the design concept and to show the operating principles. Photographs of the model are shown in cruise position (Figure 2A-207), loiter position (Figure 2A-208), and reverse position (Figure 2A-209 and 2A-210).

(1) General Description

The system incorporates a crossbraced octagonal strut framework supporting a translating shroud assembly and the free floating blow-in doors. The translating shroud assembly consists of the reverser doors, reverser cascade, and the free floating trailing edge flaps.

(a) Support System - Eight crossbraced struts of the stationary framework form the support for the ejector-reverser assembly. Each strut is trapezoidal in cross-section, and occupies 10 degrees of circumference. Lips on the outer edges of the struts provide support and sealing for the blow-in doors, and add an additional degree of blockage making a total circumferential blockage of 88 degrees.

The struts provide roller tracks for the translating shroud and reverser cascade. The shroud actuators are housed inside the struts and are cooled by small amounts of secondary air which bleed through the strut passages.

(b) Shroud - The ejector shroud contains the reverser system and floating trailing edge flaps. The internal shroud surface is composed of a lightweight liner "floating" on a skeleton structure. Thermal problems are minimized because the liner shields the shroud assembly and is free to expand.

An end ring attached to the shroud framework provides an attachment point for the floating trailing edge flaps. The outer skin is also attached to the shroud framework which rolls on the strut surfaces to provide translation. The roller supports are positioned to assure that all loads are transmitted to the rigid framework allowing the outer skin to be a lightweight, simply supported shell.

(c) Actuation System - The actuation system for shroud translation and reverser door operation consists of three-position, hydraulic actuators mounted on ball joints at the rod end of each actuator housing. The ball joint connects to the aft end of the struts, with the rod connected to the end frame of the translating shroud. The actuator body is housed entirely within the strut. The actuators are fabricated primarily of AMS 5643 stainless steel to provide the proper strength and wear characteristics. Fuel, cooled by a continuous recirculation system, is supplied to the cylinders from the augmentation control.

Sealing is accomplished by a two-section shaft seal with a drain between the sections. The seal housing protects the seals from high temperatures by recirculating fuel. The seals are protected from contaminants by a cast iron bushing which has two grooves to trap contaminants. The actuator cylinders and seal housing are designed to withstand fluid pressure surges.

( ) Reverser Doors and Cascade - The reverser system consists of the reverser doors and the cascade. Four large doors comprise approximately 75 percent of the blocked area, and four small doors make up the remaining 25 percent. The doors are hinged aft of the minimum shroud diameter and are rotated into position by connecting links. The links are attached to the doors slightly below the door's center of pressure in the reverse condition. The other end of the link is guided in a track attached to the shroud framework. This allows the shroud to translate initially with no reverser door movement. The link end buttons into the fixed framework (when shroud translation to the reverse condition is accomplished), and rotates the doors into the reverse position. The cascade is essentially in position before any appreciable amount of the stream is reversed, thus insuring correct targeting.

The translating cascades are supported on rollers and mounted between adjacent struts. Each side of the cascade has an integral rack running the full cascade length. An idler pinion is mounted on the side wall and is driven by a rack attached to the shroud framework. This arrangement permits balanced blow-off loads between the shroud and reverser cascade.

(e) Blow-in Doors - Eight free floating, double hinged blow-in doors are attached to hinges on the rear engine mount and are supported in the closed position along their full length by lips on the strut edges. The door is fabricated from honeycomb material with reinforced hinge and trailing edge sections. Stops are provided to limit door travel when opening, and at maximum open position the doors rest on supports just ahead of the fan nozzle attachment point. Air leakage around the door periphery is minimized by a flat sealing surface around the doors.

(f) Trailing Edge Flaps - The trailing edge flap assembly consists of eight flat flaps and eight corner flaps interlocked at each joint with seal faces integral with the corner flaps. Each flap is separately hinged to the main shroud structure, and the entire assembly is synchronized so that movement of one flap will drive the adjacent flaps.

Individual flaps are of skin and shear web construction with inner and outer surfaces free to move relative to one another for thermal differential expansion.

Several damping schemes are currently being investigated to insure that flap "flutter" will not occur during floating flap operation.

(2) Materials Selection

Materials selected for the ejector nozzle and reverser provide light weight and maximum strength in the required areas. The materials are summarized in the listing below:

Item	Material	Limiting Stress
Translating Structure	Waspaloy	Creep
Inner Shield	Hastelloy X	Creep
Outer Skin	Titanium	Yield
Floating Flaps	Waspaloy and Hastelloy	Creep Creep
Cascades	Waspaloy	Yield
Blow-in Doors	Titanium	Yield
Reverser Doors	Waspaloy	Yield or Stress Rupture
Support Structure	Waspaloy	Buckling

(3) Operation

During supersonic and cruise operation, the shroud is in the forward position for optimum expansion of the engine, fan and secondary air gas streams. The blow-in doors will be closed and the trailing edge flaps will be in the maximum open position. For flight operation below Mach 1.3, the shroud is translated rearward to the mid-position, and the cascade moves forward to direct external air to the interior of the ejector, along with the blow-in doors. When less than the maximum area is required, the blow-in doors are partially or fully closed as the flight condition requires.

The position control need only be a two-position type (excluding reversal) sensing flight Mach number. During this condition the trailing edge flaps will be in the closed position.

For reverse operation the shroud is translated an additional distance aft by a signal from the pilot to position the reverser doors and cascade. As soon as reverse flow is established the blow-in doors close,

and check valves prevent forward flow of the hot gas stream in the secondary air passage.

(4) Design Features

Several unique features have been incorporated into the ejector-reverser design to produce an efficient exhaust nozzle system. The octagonal shape was selected to permit minimum thickness at hinge lines, easy fabrication of parts, improved installation characteristics relative to the airframe, and reduced complexity. The system of cross braces and octagonal sections provides a stable support system with short axial members whose trapezoidal box section provides adequate buckling margin and torsional strength. The translating shroud concept permits good aerodynamic performance over the range of flight conditions and simultaneously provides a simple method of obtaining thrust reversal. The translating shroud eliminates the need for a separate unison ring by uniformly transmitting actuator loads to the reverser flaps and cascades, even in the event of an actuator failure.

The design also provides a failsafe feature in that should failure occur, the shroud will assume a forward flight position with only small losses in performance. The translating concept and cascade reverser also allows greater target capabilities. Portions of the cascade may be blocked, and the cascades may have directional vanes added to them to alter the issuing flow to a direction other than radially outward.

All sketches shown are for uncanted nozzles; however, some preliminary investigation has been completed on canted nozzles. Canting may impose aerodynamic and mechanical problems. Cooling problems which arise from hot gas flow impinging on duct walls at bend locations will require local cooling control (baffles and orifices) to increase cooling air flow where needed.

The reversed flow for this design may be discharged out of any of the eight flat segments. With two panels beneath the wings blocked, the flow is distributed around six segments. Proper positioning of the panels allows approximately 50 percent of the reverse flow from two segments of the reverser cascade in installations where this might be a requirement.

(5) Cooling

The ejector-reverser will be cooled at cruise conditions by inlet or secondary air and at loiter flight conditions by air entering through the blow-in doors. In both cooling methods air enters upstream of the throat and film cools the throat and tail feathers. Metal temperatures can therefore be maintained within realistic limits.

During reversing, the temperature of the ejector-reverser will not exceed cruise metal temperatures because of the lower hot gas temperatures and the relatively short duration.

e. Other Ejector-Reverser Concepts

Other concepts studied included a ten flap articulated ejector, a blow-in door reverser with a translating internal plug to act as the fan duct nozzle, and several designs using various methods of changing the ejector inner wall contours. Weight, sealing, mechanical, and performance deficiencies eliminated these concepts from further consideration.

15. ASSEMBLY OF MAJOR COMPONENTS

a. Fan Assembly (See Figure 2A-211)

The fan stages are assembled from the intermediate case forward and may be assembled either vertically or horizontally, provided proper fixturing is provided.

A separate, removable splitter nose is provided for splitter nose angle adjustment during development. This nose is bolted to the fan exit guide vane assembly before this assembly is attached to the intermediate case by indexing and rotating the vane and splitter sub-assembly into the slotted intermediate case splitter flange. The shroud and outer case sections are then bolted to the intermediate case flange. The second stage disk is snapped onto the front hub. The front outer case section is slipped over the front shroud case, which contains riveted-in first stage vanes, prior to assembly with the other cases. The first stage disk and the mount ring may then be installed.

Note that with the mount ring removed and a fixture holding the shaft concentric with the outer cases and the cases concentric with each other, the fan section may be removed as a unit leaving only the duct and fan stators attached to the intermediate case.

b. Intermediate Section Assembly

The intermediate case is assembled as a separate component as follows: The airframe power take-off, main gearbox power take-off, and N_1 tachometer-scavenge pump drives are installed into the case. The N_2 forward main engine thrust bearing and rear seal assembly is mounted on a removable bearing support and secured to the intermediate case by a bolted flange.

The intermediate case and N_2 bearing assembly is installed on the engine with the compressor and turbine already built up. The nut on the N_2 shaft is secured along with the gas generator mount flange. This flange is reached through the duct diffuser case.

The N_1 hub, seal and bearing support, N_1 tachometer-scavenge drive, and N_1 to N_2 shaft seal assembly are assembled as a complete unit and installed into the intermediate case as a complete unit (less fan). The top forward flange on the intermediate case is secured along with the nut which connects the low rotor shafts together.

The engine is now ready for the fan installation.

c. Aerodynamic Brake and High Compressor Assembly

The aerodynamic brake vanes are inserted into the intermediate case outer compressor flange from the inside.

The intermediate case split inner compressor flange is then bolted into place to retain the inner end of the vanes. The vane actuating bellcranks and synchronization ring are assembled outside the intermediate case outer compressor flange. Assembly of the compressor can now be completed. After the fan duct diffuser is installed, the two torque rods for aerodynamic brake actuation are bolted into place through two of the fan duct diffuser struts. Actuators are attached outside the fan diffuser.

The high-compressor as a unit consists of the front hub with a labyrinth seal, all the rotor and stator stages and their associated hardware, and the rear hub with a fitting spacer.

The high-compressor unit can be built either from the front rearward or the rear forward.

Starting with a hub, disk, blades and cover plates, spacers, cases with stators, and then outer shrouds are built up stage by stage until all stages are assembled. With the compressor unit made up and balanced, it can be joined to the rear and front portions of the engine.

With the main diffuser, burner, No. 3 bearing compartment, and high-turbine rotor made up, the rear hub of the compressor can be inserted through the No. 3 bearing compartment and can be bolted to the high-turbine disk front hub. The rearmost flange of the compressor cases can now be attached to the front flange of the main diffuser case.

The compressor, now attached to the rear portion of the engine, can be assembled to the intermediate case. The duct diffuser, which was in position when the compressor and intermediate case were put together, can be moved rearward until the front flange of the compressor and the rear inner flange of the intermediate case are mated, finishing this portion of the assembly.

d. High Pressure Compressor and First Stage Turbine Assembly

The first stage tie bolts and their retaining rings are assembled on the flange of the high speed turbine shaft. The rear labyrinth seal-spacer is installed over the turbine shaft. The rear compartment case, rear labyrinth seal ring, rear labyrinth seal assembly, insulation assembly, and the rear face seal assembly are slid over the spacer. The rear face seal plate, the inner race and rollers of the number 3 bearing, the oil scoop, the forward face seal plate, and the front labyrinth seal and spacer are installed over the high pressure turbine hub. The retaining nut is threaded on the turbine shaft and torqued to the prescribed value.

To start the assembly of the diffuser burner section, the number 3 bearing front compartment insulation and the compartment external support (which contains the bearing outer race, spanner nut, tab washer and flange seal) are slid over and assembled to the front face seal support assembly. The front labyrinth seal assembly is then piloted onto the front face seal support. Countersunk screws will be used to hold the forward compartment together prior to completion of assembly procedures.

The compressor seventh stage rotor seal assembly is bolted to the front inner flange of the diffuser case. The combustion chamber inner front and rear cases may be bolted together as an assembly prior to joining with the number 3 bearing compartment support. The combustion chamber inner front case is attached to the number 3 bearing compartment support with counter sunk screws for holding during completion of the assembly. The number 3 bearing front compartment subassembly is piloted onto the diffuser case inner rear flange and bolted to it. All tubing between the diffuser case and the bearing compartment is installed

The oil lines inside the number 3 bearing front compartment are installed. The flange seal is installed on the bearing support. The bearing front and rear compartments are bolted together, along with the high turbine shaft, bearing, and seal rotating parts. Access to these bolts is obtained by sliding the rear compartment outer cover case in the rearward direction. The rear compartment case is then attached to the bearing support by flange bolts.

The front section of the annular burner is inserted in the rear section of the diffuser case and retained by radial pins assembled through the diffuser case. The combustion chamber outer front case is bolted to the diffuser case rear flange. The combustor inner and outer transition ducts are slid forward on the front burner section. The turbine nozzle inner case is assembled to the combustion chamber inner rear case with flange bolts. The nozzle vanes are inserted into the vane inner and outer support rings. A segmented, bolted ring is used to retain the vanes in the outer support ring.

The burner inner transition duct is slid to the rear and the holes in the segmented ring which retain the turbine vane inner feet are aligned with the gang channel self-locking nuts riveted to the turbine vane inner support ring. The radial bolts are installed through the scalloped trailing edge of the inner burner transition duct and tightened. The burner outer transition duct is slid to the rear and assembled to the turbine case forward flange. The combustion chamber rear outer case is slid forward and assembled to the combustion chamber outer forward case and to the forward flange of the turbine case.

The high pressure compressor exit guide vane assembly and seventh stage seal land are bolted to the diffuser case inner front flang . The exit guide vane outer shroud torque lugs engage mating slots in the flange in the diffuser case.

A classified spacer which positions the turbine rotor axially is installed on the compressor rotor rear hub. The compressor assembly and classified spacer are installed by engaging the compressor rear hub spline with that of the turbine. The spanner nut is installed on the compressor hub. The spanner nut is then tightened to a prescribed torque value, the tab lock washer is inserted and the retaining ring is installed. The turbine disk and blade assembly is installed on the turbine hub. The complete assembly of the high pressure compressor and turbine is dynamically balanced by adding weights on the third stage compressor disk and by installing weight classified nuts on the turbine tie bolts.

e. Low Speed Turbine Assembly

The second stage turbine disk front seal ring and the second to third stage interstage spacer and seal support are bolted to the second stage disk and blade assembly. The second stage disk and blade assembly, the turbine rear hub, and the third disk conical support are assembled to the low-pressure turbine front shaft using temporary nuts on the second stage tiebolts. The second stage blade outer seal shroud and wear ring are installed in the turbine rear case. The second stage rotor subassembly is inserted into the turbine rear case. The third stage vane inner shroud and seal support is placed in position and the third stage vanes are installed in the inner shroud and the turbine rear case. The third stage outer retaining ring and the outer front turbine exhaust case are bolted to the turbine rear case. The third stage blade outer seal shroud is sandwiched between the turbine exhaust case and the third stage vane outer retaining ring. The third stage disk and blade assembly is bolted to the second stage rotor subassembly and retained with temporary nuts. Axial and radial positioning of the low speed rotor relative to the stationary members, prior to final engine assembly, is accomplished by the use of temporary fixtures. The rotor is dynamically balanced by replacing the temporary nuts on the second and third stage tiebolts with permanent weight classed nuts.

The first stage blade outer tip shroud and wear ring are installed in the front turbine case. The second stage vane inner shroud and seal support is positioned and the second stage vanes are installed into the inner shroud and into the turbine front case. The second vane inner rear retaining plate is bolted to the inner shroud and seal support. The low speed rotor assembly is inserted behind the second stag vanes and installed with the turbine rear case bolted to the front case. The low-rotor rear bearing, carbon seals, and spacers are installed on the turbine rear hub and are retained by the scavenge pump drive gear which is bolted to the hub.

f. Turbine Exhaust Assembly and Number 4 Bearing Compartment

The outer bearing support including the exit guide vanes, inner case, and outer case is assembled as a subassembly as follows: The exit guide vane feet are inserted into pockets in the intermediate outer case where they are bolted in place with the outer heatshielding. The front inner case, the shroud rings, and the rear inner case are bolted to the I.D feet of the exit guide vanes. The I.D. feet of adjoining vanes overlap each other and are riveted together. The outer bearing support cylinder is mounted to 8 support vanes at the I.D. by bolts. At this point the bearing compartment is assembled around the front flange of

the outer support cylinder as follows: The front labyrinth seal assembly includes one seal at the rear hub and another at the number 3 turbine disk plus front compartment heatshielding placed on the front face of the flange on the outer bearing support. The bearing compartment subassembly, consisting of front carbon liner assembly, inner bearing support and rear oil sump, is installed on the rear face of the outer bearing support using bolts which engage nuts anchored to the front labyrinth seal assembly. The bearing outer race is installed on the inner bearing support. The oil scavenge pump is attached to the pump support which is bolted to the rear side of the bearing support. The pump support also retains the bearing outer race. All lines to the number 4 compartment through the exit guide vanes are installed except the oil out line which is installed through the exit guide vane but cannot be connected to the bearing compartment until the rear cover plate is put on the bearing compartment. The rear compartment insulation and heatshielding is installed.

The front outer turbine exhaust case is bolted to the rear turbine case with the third stage vane retainer and blade seal sandwiched between the case flanges. The turbine exhaust assembly slides into place engaging the No. 4 bearing outer race over the bearing rollers and is bolted to the front outer case. The bearing compartment rear cover plate is bolted on, the plumbing to it is attached and the cover plate insulation and heatshielding is installed. The tail cone is bolted in place and the outer rear exhaust case forming the primary nozzle is attached. Note: Fixtures will be required to axially retain the low-speed rotor prior to assembly of the fan section to the intermediate case assembly.

g. Fan Duct Diffuser Case Assembly

The fan duct diffusercase assembly consists of the fan duct diffuser case, and the front and rear cascades which are mechanically attached to the outer diffuser duct. After the fan, intermediate case, and compressor are assembled, the fan diffuser is installed. The fan duct diffuser case assembly outer front flange is attached to the rear flange of the intermediate case. The forward end of the inner duct is piloted on the surface provided on the intermediate case. The gas generator fluid lines are routed through the struts of the fan duct diffuser case and are installed after the gas generator is assembled and before the duct heater is installed. External oil, breather, and fuel lines are connected, fuel nozzles and manifolds installed, and seal pressurizing air lines connected.

h. Duct Heater Section Assembly

The forward case section of the duct heater is fixed to the completed fan duct diffuser section. The forward duct case inner liner is attached to the aft end of the diffuser thru a piloted slip joint. The outer case is then bolted to the diffuser providing the mounts for the duct heater. The duct heater spray rings are next attached to the outside case while the flameholder is fixed to the inside case.

The duct inner liner section is added to the forward liner section and extends rearward to the sliding joint at the front end of the primary exhaust nozzle cone supporting flange.

The entire outer duct case can now be installed as an assembly to the bolted flange just aft of the flameholder. The outer case is an assembly which contains the rear engine mount ring, liners for the duct heater and the transition section at the rear used to mount the variable duct heater nozzle.

The 8 nozzle flaps and 8 seals of the nozzle are attached to the joint which is bolted to the transition section of the duct.

Structurally, the variable nozzle is an integral part of the blow-in-door ejector assembly. After the 8 struts and unison ring have been attached to the rear mount, the nozzle linkage can then be connected. The bellcranks and tierods are located on the inside of the struts. Access holes are provided in the struts to allow assembly of the linkage.

i. Ejector - Reverser Assembly

The main ejector support structure assembly prior to mounting on the engine will have the actuators for the reverser mounted in the rear of the struts with hydraulic lines extending to the front of the struts. The fan duct nozzle synchronizing ring along with the bellcranks and internal connecting links will be installed on the struts. The front end of the struts containing the ball joint connections will be held in position during assembly and installation by a removable mounting fixture.

With the above components in place, the reverser cascades are mounted on the strut rollers, and the blow-in-doors are placed in position between struts. Removable clamps hold the blow-in-doors in position until they are connected to hinges on the rear mount ring at assembly.

The entire assembly is then assembled from the rear, over the fan duct and connected by 8 pins at the ball joint connections on the rear engine mount ring. The strut mounting fixture is then removed.

The blow-in-doors are connected to the hinges on the rear mount ring. The fan nozzle actuation system is connected to the internal links and bellcranks. The basic supporting structure is now complete.

With cascades positioned by a gage fixture, the outer shroud is slid forward over the support structure, the racks on the shroud engage idler pinions and lock the cascades into a translating system. This system is checked for operation before assembling the inner shroud to the main assembly.

After the translating system is checked out, the reverser door links are set into stop points on the struts. The inner shroud assembly, containing the main structure, liner and reverser doors, is slid over the main support structure. With the shroud in full reverse position, door links are connected to their respective doors. Actuator rod ends and the O.D. shroud are connected to the shroud support system end ring.

The trailing flaps are assembled in a loose holding fixture. They are then connected to hinges on the shroud support end ring. Trailing flap O.D. seal plates are installed.

The trailing flap holding fixture and blow-in-door clamps are removed at completion of the installation.

This completes the normal assembly procedure. Disassembly is essentially the reverse of the assembly procedure.

16. CRITICAL SPEEDS

The rotor shafts, hubs, and spacers for the STF219 turbofan engine are designed for stiff bearing critical speeds to occur 20% above the maximum deteriorated rotor speeds. Rotor shafting, cones, and spacers are designed for minimum weight while insuring that 20% margin is met. Bearing locations on the low rotor are placed as close as possible to cantilevered disks to keep overhang at a minimum. Figures 2A-212 and 2A-213 show the calculated preliminary mode shapes for the rotors.

Bearing support structures for the number 3 and 4 bearings are designed for low spring rates. Relatively stiff rotors, coupled with the soft number 3 and 4 bearing structure, achieve a combination of rotor stiffness to support stiffness which insures that the coupled rotors and case do not have critical rotor bending modes in the operating range. Further analyses of the complete engine critical speeds are being undertaken to verify minimum rotor induced vibration. Results of these analyses will also be used to study the effects of 10% blade loss.

Shaft clearances and blade-to-case clearances have been designed based on a preliminary analysis of the deflection caused by blade loss. In the turbine section at least 0.3 inch clearance is provided for shaft deflections in the event of blade loss.

Transient and steady-state analyses of rotor and case response to blade loss will be used to confirm the preliminary analysis. Rotors and bearing structure stress analyses will be based on rotor shears, moments, and reactions to insure structural integrity.

The critical speed studies are continuing and will be updated as the engine enters the final design configuration.

17. BEARING DESIGN

a. Introduction

Consumable vacuum melt M-50 (PWA-725) material will be used for the fan and compressor thrust bearings, both towershaft ball bearings, and the tachometer drive ball bearings. Rower 315 (PWA-724) will be used for the roller bearings on both main shafts and both towershafts. Fatigue tests on main shaft size bearings made from M-50 have shown a considerable life improvement over that predicted by standard methods. All bearings will utilize a steel cage of AMS 6415 and will be stabilized for minimum distortion at the operating temperature. Pratt & Whitney Aircraft has demonstrated the increase in bearing reliability using these improved materials in the JT11D-20 and the JT8D engines.

The internal geometries of the fan and compressor thrust bearings were optimized for maximum fatigue life and for elimination of skidding damage. The optimum internal geometries for both bearings were based on a design study utilizing an IBM bearing dynamic analysis and experience gained on previous engine mainshaft thrust bearings. The

fan thrust bearing has a predicted B-10 life of 15,000 hours based on a calculated mean effective thrust load at maximum shaft speed. The bore diameter of the fan bearing was sized from critical speed criteria. The predicted B-10 life of the compressor thrust bearing is presently estimated to be 7,100 hours based on a calculated mean effective thrust load at maximum shaft speed. No skidding problems are expected in either bearing.

The predicted B-10 lives of the fan and turbine roller bearings are well above 10,000 hours. The compressor roller bearing will be radially preloaded by utilizing an out-of-round outer race. The preload is needed to prevent skidding due to the light radial loads and the high DN value* of this bearing. Pratt & Whitney Aircraft has successfully used DN product to determine if a roller bearing should be preloaded. The turbine roller bearing is also lightly loaded, but no preload is required because the DN value is relatively low. The housing support can be altered with a minor design change to provide for a preload, if necessary.

Split inner race angular-contact ball bearings with one-piece cages are recommended for both towershafts because of the high shaft speeds and radial and thrust loads. Radial deep-groove bearings in these positions would be adequate for fatigue life but would require two-piece riveted cages. The split inner race bearing permits the use of a considerably stronger one-piece cage necessary for high speed operation. This design is presently used in the JT11D-20 and JTF10 towershafts and has experienced no problems from cage failures. The fatigue lives of all towershaft bearings are well in excess of 10,000 hours. The high B-10 lives are a result of sizing the bearings for critical speed and not for fatigue criteria.

The intermediate tachometer drive bearings will be of the radial deep-groove design and will be preloaded by wave washers to minimize skid possibilities. The tachometer drive bearings will also be radial deep-groove; however, no preload is necessary because of the low shaft speed. All tachometer bearings are very lightly loaded and fatigue is not a problem.

---

* DN value is defined as the product of the bore diameter in millimeters and shaft speed rpm.

b. Number 1 and 2 Bearing Compartment

The number 1 and 2 bearing compartment underwent many design changes which should result in increased durability, better maintainability, and lower weight. These changes are shown in Figure 2A-1.

During Phase II-B a more intensive study was made of the sealing arrangement between the N_1 low-speed and N_2 high-speed shafts. In the Phase II-A design a carbon face seal backed up with a rotating bellows was used, since it was felt that it would provide an adequate lightweight seal. Further studies of temperatures and pressures revealed that this design has limitations and unknown factors such as fatigue and radial loads possibly imposed by bellows eccentricities. A further complication is thermal stresses introduced by the large differential temperature supplied by the hot bleed air from aft of the compressor seventh stage knife-edge seal leakage.

This seal was replaced with a design incorporating a carbon face seal for each shaft with a series of springs loading the seals against the face plates. This unit also incorporates two sliding piston rings which provide a sealed sliding joint between the shafts. These piston rings are backed up with a set of pressurized knife-edge seals. The bearing compartment seal arrangement incorporates a wet-face seal plate to provide cooler seal face temperatures and increased carbon seal life.

A positive pressure differential is maintained across the front bearing compartment seal to prevent oil leakage from the compartment. Pressurized air for this purpose is supplied from fan discharge and vented to ambient. The pressure in the compartment is maintained by a pair of knife-edge seals between the fan rotor hub and the thrust bearing support structure. An additional seal is located on the rear of the second stage disk to reduce the thrust loading on the number 1 bearing.

Further design studies were also made on the high compressor thrust bearing support. In the early stages of design an integral support seemed to be the lightest; however, this required that the intermediate case be threaded for the high rotor thrust bearing outer race retaining nut. Replacing the case would be very expensive if this thread were damaged. The additional weight was warranted, since the design now has a smaller rear intermediate case flange and an integral seal bearing support. The seal package O. D. was also reduced. This allowed the first stage compressor disk bore diameter to be decreased.

reducing the disk weight by approximately 10 pounds. This alone was a substantial weight reduction, but, in addition, the bearing support can be replaced without replacing the entire intermediate case.

Airframe manufacturer requirements to remove accessories containing combustible fluids from the bottom of the engine led to a preliminary selection of the left horizontal position for the engine accessory tower-shaft for the Boeing installation, and 45° below horizontal for Lockheed, as discussed in the Installation Coordination section of this report. The horizontal location is a more difficult design because of its associated oil scavenge problems, therefore the Phase II-B design effort was concentrated on the horizontal shaft arrangement. This required revising the oil pressurizing system and the oil scavange system for the compartment. Originally, scavenge oil was drained into the gearbox on the bottom of the engine and returned to the oil system with the gearbox scavenge pump.

With the side-mounted gearbox, oil could no longer be returned to the gearbox by gravity drainage because of its location; therefore, various schemes of locating a scavenge pump in the compartment were studied. These schemes included both gear and jet type pumps. The final design, Figure 2A-32, eliminates internal pumps within the intermediate case and locates the pump externally for easy maintenance. This permits the N_1 tachometer shaft now located at the bottom of the engine to serve a dual purpose of driving the scavenge pump as well as the N_1 tachometer.

With a scavenge pump on the bottom of the engine there is no longer a need for a separate scavenge pump in the gearbox. The gearbox and the intermediate case bearing compartment now drain into a sump on the bottom of the engine. Oil is then returned to the tank from this sump by the scavenge pump.

Various schemes for oiling the Number 1 and 2 bearing compartment were considered. The oil for this system is piped into the compartment through a strut located at 45° in the upper quadrant looking aft. It enters a central fitting which diverts the oil flow to the compartment with minor internal plumbing. This central oiling fitting incorporates a final filter to catch any dirt which may have gotten into the system and which could clog the small orifices. The top portion of this fitting is removable for ease of engine disassembly. This allows the screen to be replaced or cleaned without removing the main portion of the fitting from the intermediate case.

Consideration was also given to the ease of assembly and disassembly of the engine. The forward portion of the compartment was redesigned

allowing the fan hub, seals, bearing support, and tachometer drive to be assembled as a separate unit and installed or removed as a unit. This reduced the exterior size of the compartment. The intermediate case can also be removed from the main engine without disassembly of the compressor or turbine providing access to the high compressor thrust bearing.

Additional features incorporated in the compartment design are:

- Radial loads from the rotor are transmitted to the number 1 bearing through the fan hub, which is supported by the thrust bearing and has mating splines to transmit torque loads to the low speed turbine drive shaft. The splines are forward of the thrust bearings to ensure continued spline engagement and positive coupling of the fan and low turbine rotors to prevent serious turbine overspeeding should a major failure of the bearing occur.

- Bearing retaining nuts are located so that thrust loads act against integral structure and not the threaded nut. In addition, all nuts, where possible, are secured with a lock washer and ring wire. This insures a positive locking feature for highly loaded nuts.

- Metal conical seals are used for all flanges where sealing was required. These seals have a very good service record at elevated temperatures.

- Blanket type insulation enclosed in metal foil is used to protect the compartment from high surrounding temperatures and to reduce heat rejection to the oil system.

c. <u>Number 3 Bearing Compartment</u>

Number 3 bearing compartment design is similar to that proposed in Phase II-A, with detail revisions to account for changes in engine size, thrust balance system, and adjacent assemblies. Figure 2A-214 shows details of this design. The STF219 employs an overhung turbine design for the high speed rotor, supported by a conical case bolted to the aft inner flange of the diffuser case. The number 3 bearing is a preloaded roller bearing with inner race, cage and rollers pressed on the turbine rotor shaft. The bearing material is high temperature consumable-electrode melted tool steel (Bower 315). The outer diameter of the outer race is elliptically ground. When the race is pressed

into a round housing, the inner diameter of the outer race assumes an elliptical shape. The minor diameter then eliminates the bearing clearance thus preloading the rollers. This preloading is done in lightly loaded high speed bearings to reduce roller skidding.

The compartment is sealed fore and aft with spring-loaded carbon face seals having two cast iron static piston rings per seal. The carbon seals are shrink-threaded into the seal retainer. The threads are opposite to the direction of shaft rotation therefore friction at the seal rubbing surface tends to tighten the carbon in its holder. The spring and torque pin centerlines are different, preventing incorrect installation.

The seal plates are separate and are the wet-face type. The rubbing face is washed continuously with oil for cooling and low wear rate characteristics. Test experience has indicated longer life and better sealing with this type of seal.

The compartment has back-up labyrinth seals at both ends pressurized with fan discharge air which is vented to ambient. The fan discharge air is piped through the diffuser case struts and into the inner pressurizing compartment. The cooling air is routed to both ends of the compartment. The outer pressurized compartment is vented to ambient by lines routed back out through the diffuser struts. Labyrinth seals separate the various pressurized compartments to limit flow.

The inner bearing compartment is surrounded by foil covered blanket type insulation to reduce environmental heat transfer to the oil. The fan discharge air and ambient air are routed through the outer compartments by a series of internal lines.

Crushed washer type static seals have been incorporated at the bearing support flange. Development experience indicates that the conical seals are superior to the chevron type seals in sealing capability with the thermal distortions present in a high temperature environment. Also, the conical seal does not require a deep machined groove; therefore, a thinner, lighter flange is allowable.

Because of the high temperature environment it was necessary to provide protection to the bearing compartment in the event of air leakage due to a carbon seal failure. For an unprotected system, excessive leakage of high temperature compressor discharge air into the compartment could cause an oil fire and possible failure of the shaft. A common breather system connects all bearing compartments. The in-rush of high pressure air following a number 3 carbon seal failure would overpressurize all compartments and cause oil leakage past the

seals into the engine air stream. If the number 3 compartment were surrounded with high pressure air, the resulting high seal loads would greatly accelerate wear on seals not designed for normal operation at high pressures. The increased frictional heat generation would contribute heavily to the overall oil heat rejection problem.

To reduce these hazards, the seals are pressurized with relatively cool, low pressure fan discharge air. The original thrust balance scheme vented the forward plenum to fan inlet pressure and the fan discharge air just dumped into this area. However, later schemes pressurized this area to seventh stage (high rotor fifth stage) seal leakage which made it necessary to add an additional section to the bearing compartment to provide for venting.

The innermost section is vented to breather pressure which varies from ambient pressure to 5.5 psia. The section adjacent to this at both ends is pressurized with fan discharge air, and the outer compartment is vented to ambient pressure. During normal operation labyrinth seals between each section limit the flow of fan discharge, compressor discharge, and compressor rear seal leakage into the ambient pressurized section. If any oil should leak past the carbon seals, it would be harmlessly vented overboard instead of causing coking or possible fire inside the engine. In the event of a carbon seal failure the flow of fan discharge air into the compartment is limited by a set of four lip labyrinth seals. The outside air would not be able to reach the inner compartment due to large vent line sizes. The pressurizing and exhaust air is piped out of the area through the struts in the gas generator diffuser case. Figure 2A-215 shows the pressurizing and vent system in schematic form.

An additional safety feature of this design is the location of the number 3 bearing on the turbine rotor forward of the torque spline. If the bearing should fail and cut the outer shaft in two, the turbine would still be connected to the compressor by the inner shaft, preventing turbine runaway and subsequent possible disk burst. There are other small detail features in the design such as the use of step diameters on the shaft to prevent incorrect assembly of the components which contribute to the overall reliability and safety of the engine.

The bearings and seals are lubricated and cooled by oil (lubrication primarily by oil mist and cooling by convection to the flowing oil) as shown on Figure 2A-216. The oil passes through a diffuser case strut into a central fitting in the compartment where it is manifolded to the main jets and the scavenge pump primary jet. This central fitting contains a removable oil screen to catch any particles which may have gotten into the line before they reach the jets. The inlet, scavenge, and breather lines are sealed from the surrounding air by Harrison "K"

seals, which are replaceable at teardown. The oil is distributed through 3/8 inch diameter tubing to two jet holders located 180° apart. Each jet holder has two removable jets, one for forward seal plate cooling and one for the bearing inner race and aft seal plate. The oil from the forward jet impinges on the forward radial scoop, is captured in an annulus and is fed axially forward to the seal plate. The cooling oil is then thrown outward by centrifugal force through a series of radial holes which carry the oil across the rubbing surface and into the compartment. The oil from the other jet is captured by the aft scoop and is fed axially rearward through a series of slots on the inner race of the bearing, cooling the inner race before being collected in the seal plate annulus and thrown outward through radial holes similar to the forward seal plate. The oil coming off the seal plates forms a mist which lubricates the bearing and the sliding surfaces in the seals. The axial passages are slanted slightly outward so that centrifugal force keeps the oil flowing axially.

An ejector type pump was selected for scavenging the compartment for several reasons. A jet pump has no moving parts which eliminates the wear problem and it is inherently lightweight compared to an equivalent capacity gear pump. Test experience with jet scavenge pumps indicate a very high resistance to cavitation damage. This is highly desirable in a pump with inlet conditions approaching oil vapor pressure. Another advantage of the jet pump is the ability to pass ingested foreign objects that would damage a gear type pump. The jet pump does increase the size of the main oil pump to provide the recirculation or primary flow necessary to aspirate the scavenge flow. The oil that is not fed through the scoops as coolant is brought to the scavenge pump as primary flow. The pump is sized to operate on the ratio of secondary flow/primary flow = 2. This means that the primary flow will scavenge twice its own flow rate. Since the jet pump capacity is rated at twice the cooling flow for safety reasons, the primary flow approximately equals the cooling flow. Test data on the STF200 jet pumps has been directly applied to the STF219 number 3 bearing compartment pump.

The aft face seal and labyrinth seals are captured on the turbine rotor by the bearing inner race and seal plate. To remove the bearing for replacement it is necessary to slide the burner inner and outer transition cases forward, remove the outer compartment shroud and slide it aft, and remove the bolts which hold the aft seal assembly. The location of the outer compartment shroud bolt flange was moved forward to make the bolts more accessible from the outside.

There are several maintainability features provided in the number 3 bearing compartment design. All the labyrinth seal lands are attached to the cases by rivets for easy replacement if for some reason the seals bottom and score the surface. Similarly all the labyrinth seals are separate from the scoops or seal plates to lower the cost of replacement in case of labyrinth seal damage. Both seal plates are separate parts because they are subject to wear and possible replacement. The air and oil lines between the compartment and diffuser case are replaceable in case of a tubing failure. All fittings are removable and no threaded parts are permanently attached to the expensive compartment shells or bearing support.

d. Number 4 Bearing Compartment

The number 4 turbine rear bearing at the close of Phase II-A featured a hairpin spring bearing support positioned directly beneath the bearing and inside the oil sump. An initial study and layout of the bearing compartment and its individual components indicated that the compartment could be made smaller in diameter by placing the spring outside of the oil sump. The increased operating temperature of the spring necessitated an increase in section and weight to retain the required spring rate as determined by rotor critical speed requirements. The justification for the increased weight was a decrease in heat rejection to the lubricating oil. The total compartment area exposed to the high temperature turbine exhaust environment was considerably reduced. The redesigned compartment is shown in Figure 2A-217.

The engine operating characteristics were changed requiring the turbine exit guide vanes to be moved farther to the rear of the turbine. This changed the required bearing support from a stiff cone to a long flexible cylinder. An analysis indicated that the hairpin spring would no longer be required for rotor critical speed reasons; therefore, it was discarded.

Heat rejection to the lubricating oil was lowered by increasing the insulation thickness around the bearing compartment. Gold paint which was highly effective against radiant heat on the JT11D-20 was added to the insulation cover heatshield, the oil-in oil-out, breather lines and fittings. The heatshield forward of the compartment inside the hub cone was revised to decrease heat input from that direction. Coking inside the hub had been a problem on the JT11D-20 and an efficient heatshield was required. The provision for supplying fan discharge air around the outer front half of the bearing compartment was retained. This 700°F air is 550°F cooler than the normal compartment environment.

Emphasis in Phase II-B was placed on a design incorporating minimum heat rejection to the lubricating oil. The limited heat sink capacity of the supersonic transport places an upper limit on the total amount of heat that can be absorbed from the powerplants. Any reduction in this cooling load is highly desirable.

Several criteria were used in the selection of the number 4 roller bearing with past experience on long TBO commercial engines and high Mach number military engines governing the choice. The material used for the bearing is vacuum-melted PWA 724 low alloy steel for both rollers and races. The bearing size is 130 x 190 mm; however, it would be preferable from a weight and seal rubbing speed viewpoint to use a smaller bearing. A bearing larger than this would improve the rotor critical speed and either a larger or smaller bearing would be suitable from a load-life viewpoint. The DN value is 800,000 and preloading is not to be used. The bearing has an inner land riding cage and an axial floating outer race. This combination has proven best for long life operation.

A complicating factor in design of the bearing compartment is the large relative axial movement possible between the rotating and stationary members. The size of the engine and its extreme operating temperature range necessitate axial clearances of approximately 0.400 inches both fore and aft. Transient thermal conditions, thrust bearing axial clearance and mechanical tolerances were considered in arriving at the required clearances.

A gear-driven oil scavenge pump was designed for the low speed rotor. The pump was based on Pratt & Whitney Aircraft developed standard construction and sized to handle twice the required oil flow at engine idle speed. The pump was mounted off the bearing support for minimum tolerance build-up between the drive and the pump gears. Gear backlash may easily be checked after installation prior to bolting on the rear compartment cones.

The double set of back-to-back carbon seals designed for Phase II-B were retained with only minor dimensional changes. Oil routed into a groove between the seal land and support remove heat produced by carbon seal friction.

The problems of reducing heat rejection to the lubricating oil (as discussed previously) and providing long life carbon seals led to an alternate sealing scheme. This approach is presented in Figure 2A-218. Hydrostatic seals have the advantages of little heat generation, little wear and long life. A program is now underway testing hydrostatic

seals for the JT11D-20 turbine rear bearing compartment. The STF219 application is very similar and the results of the JT11D-20 program will be directly applicable.

The preceding compartment sealing configurations are being designed for initial engine operation while a hydrostatic type seal will be developed for long life engines. This is a face seal which rides on a thin cushion of air a few ten-thousandths of an inch off the seal plate. The cushion of air is provided by an air supply from a pressure source greater than that to be encountered on either side of the seal.

The advantages of the hydrostatic seal over a carbon faced seal are:

- Reduced heat generation and lube side heat input. The lube side heat input could be reduced as much as 25%.
- Long life because of the air cushion effect.
- Fail-safe design, such that it will operate as a carbon face seal if the air supply should fail.

A hydrostatic seal similar to that shown on Figure 2A-218 has been successfully tested for 150 hours on a rig simulating high Mach number conditions. At the conclusion of the test this seal exhibited no measurable wear and the seal faces were absolutely clean. However, this seal does require a sophisticated pressure balance system which will require development.

The hydrostatic seal was designed to fit within the space occupied by the back-to-back ring seal system. New parts required for a retrofit (other than the seal and related parts) would be the turbine rear hub and the number 4 bearing compartment housing-bearing support. The hydrostatic seal is similar to the spring-loaded face seals used in the forward bearing compartments. It has a carbon ring for axial sealing and two piston rings for radial sealing. The carbon ring is mounted on its carrier with a shrink fit. A ring is shrunk on the I.D. overlapping both carbon and carrier to seal the gap. Air at a higher pressure than either the bearing compartment inner or outer environment is introduced between the piston ring seals to the inside of the carbon carrier. Metering holes then lead the air to the carbon face or sealing surface. This face has circumferential and radial slots which distribute the air for uniform pressure across the surface. Fan discharge air is used to pressurize the seal. This air is brought through the turbine exit guide vane through the number 4 bearing support flange into a plenum formed by the double wall of the bearing compartment forward section. Each

wall supports a piston ring seal land and creates a passageway to the back of the carbon carrier assembly. A failure of the fan discharge air supply would not cause a catastropic seal failure. The carbon seal assembly is spring-loaded against the mating rub ring. An air supply failure would therefore cause the seal to operate as a standard type face seal.

A computer program was utilized to investigate stability, pressure requirements, air flow, and performance throughout the flight envelope. The results show that low air flows to the bearing compartment are possible with a hydrostatic seal. The seal insures that leakage from the bearing compartment does not enter the surrounding chamber. The wear problem is practically eliminated except during start and shutdown. Analytically, the hydrostatic seal appears to be a good backup design for the number 4 bearing compartment.

18. BEARING THRUST BALANCE SYSTEM

a. Introduction

The proposed mission profile of the Supersonic Transport encompasses a wide range of Mach numbers, altitudes, and engine power settings which result in large variations in engine pressure ratio, pressure levels, and operating temperatures. These effects, in turn, tend to subject the rotor thrust bearings to extreme load changes and induce transient thermal gradients in much of the engine structure.

To cope with these problems, a secondary flow system must be designed to provide a workable thrust balance range for long bearing life and to insure the aerodynamic and structural integrity of the other engine components. Specifically, the ground rules established for the secondary flow system are:

1. The integrated rotor thrust loads over the mission profile must satisfy a 10,000 hour bearing life requirement. In addition, a minimum and maximum load of approximately 2,000 and 15,000 pounds respectively must be obtained to satisfy the incipient skid and load capacity limits of the candidate simplex thrust bearings.

2. A maximum long-time carbon seal environment of 700°F must be provided to insure long seal life.

3. The turbine blade cooling air supply pressure of 90% P_{t4} must be supplied to the first turbine disk. In addition, the turbine

disk cooling air must be supplied at sufficient pressure to satisfy disk cooling requirements and to prevent the backflow of hot gases.

4. Radial inflow of air to the compressor inlet must not exceed current experience levels (about 0.5% of engine flow).

5. The system should provide the flexibility to flow relatively cool air over the bores of the high compressor disks. This option may be required to resolve a structural problem in the high compressor.

In addition to these ground rules, three design points were selected on the basis of the following thrust balance considerations:

Mn 0.7 sea level acceleration - Maximum forward or rearward thrust due to the maximum pressure level effect.

Mn 1.2 45,000 feet acceleration - Minimum rearward thrust due to the combined effects of maximum pressure ratio with minimum pressure level.

Mn 2.7 65,000 feet cruise - Typical long-time bearing load condition. Minimum forward thrust for normal cruise altitude due to minimum pressure ratio and low pressure level effects. Higher cruise altitudes will produce still lower thrust levels.

Further study of the externally vented system proposed in Phase II-A of the SST program uncovered two major problem areas. First, a detailed study of the diffuser struts indicated that insufficient flow area was available to vent the rear compressor compartment to the low pressure required and, secondly, that the high rotor thrust balance was extremely sensitive to the rear compressor seal clearance which controls the pressure level.

Based on these findings, numerous alternate systems were studied during Phase II-B in an attempt to satisfy the ground rules with as simple and reliable a mechanical configuration as possible. At present, the final decision on the thrust balance system is unresolved due to structural problems in the high compressor. Studies are continuing to see if the requirement for cool air over the high compressor disks must be incorporated into the thrust balance system.

b. Summary

Figure 2A-219 presents a summary of the five thrust bearing systems studied during Phase II-B of the SST program. System E, shown schematically in Figure 2A-220, is the only system which fulfills all the ground rules set forth in the introduction and, therefore, is currently the system being investigated in depth. Figure 2A-221 shows the seal locations, piston areas, and characteristic pressures for System E.

Figures 2A-222 and 2A-223 are curves of bearing thrust versus bias pressure* for the high and low rotors respectively. The slope of these curves is indicative of the sensitivity of the bearing thrust to variations in seal clearances which may effect the bias pressure levels. Figures 2A-224 and 2A-225 show the bearing thrust versus typical mission time for the high and low rotors respectively.

---

* The term "bias pressure" denotes the internal compartment pressure which is of primary concern in controlling the thrust load on a rotor.

c. Technical Discussion

(1) Design Considerations

To achieve an acceptable thrust balance system over the entire SST operating envelope, it is fundamental that the rotors be negatively (rearward) biased for three reasons:

Minimum Thrust Range
Optimum Thrust at Cruise Conditions
No Thrust Reversal

As shown in Figure 2A-226, a rearward directed (negatively biased) thrust balance system has a narrower range of thrust loads than a positive system due to the interaction of pressure ratio and pressure level effects. In going from sea level - ram to altitude cruise conditions, both the compressor pressure ratio and overall engine pressure levels decrease. This decrease in compressor pressure ratio effectively increases the rearward loading of the rotor, since the turbine pressure ratio is essentially constant at all normal rated conditions. The decrease in pressure level, however, has a scalar effect which simply reduces the magnitude of the thrust irrespective of direction. Therefore, if the rotors are negatively biased initially at the sea level - ram condition, these two effects will

tend to cancel. This results in a more nearly equal thrust at the cruise condition (i.e. the decreasing pressure ratio will tend to increase the rearward loading whereas the decreasing pressure level will tend to relax the loading). With a positively biased system these two effects would be additive, necessitating a very high loading at the sea level - ram condition to maintain a minimum "skid-limited" loading at the altitude cruise condition. Herein lies the second advantage of a negatively biased system, in that the minimum load condition occurs at a short time transonic acceleration condition (Mn 1.2 - 45,000 feet maximum pressure ratio and minimum pressure level) and not at the long-time cruise condition. Consequently, if the rotors are negatively biased to skirt the skid limit (2000 lbs.) transonically, then the normal cruise thrust will be 3,500-6,000 lbs., which is safely out of the skid region yet well within the load range for long bearing life.

The third advantage of the negatively biased system is the absence of a thrust reversal during the idle descent from supersonic cruise conditions.

When the engine is throttled back from cruise to idle power, the back pressure on the turbine, particularly the low rotor turbine, decreases far more than any of the other engine pressures and results in a sudden increase in rearward thrust loading. With a positively biased system, this rearward loading is sufficient to reverse the rotor thrust load which subjects the bearings to a transient skidding condition. This transition from cruise to idle power should be relatively rapid with a very short skidding period and should not cause any significant bearing problems. The main concern arises when the aircraft has decelerated to much lower flight Mach numbers and the rotor thrust tends back toward the positive direction. At this point the bearings will again be subjected to a "no-load" condition, but of much longer duration than the initial reversal condition. This will undoubtedly result in short time bearing failures.

From this discussion, it is obvious that a negatively biased system will not result in thrust reversals and thereby avoids the attendant bearing problems.

The question of sensitivity and thrust balance control is another important consideration. The major thrust contributors are generally the piston areas which are acted upon by some intermediate bias pressure. This bias pressure results from a flow balance between various combinations of seals, orifices, and other flow restrictors. To insure thrust balance control, two approaches can be taken:

1. Make the system insensitive to variations in bias pressures by subjecting equal and opposite piston areas to the same bias pressure or,

2. Make the bias pressure itself insenstive to variations in seal clearances by referencing it to some fixed gas path pressure via a very low resistance path.

Both of these approaches were applied in the Phase II-B studies. For example, the opposed piston scheme was used in the high rotor to subject both the front and rear compressor hubs to a common bias pressure, whereas the fan disks and outer portions of the turbine disks are referenced to local gas path static pressures.

During the development program, it will be desirable to trim the thrust levels by changing a metering hole size or increasing a seal clearance. By design intent, the thrust balance will be relatively insensitive to minor changes of this nature and will require repositioning of a seal to affect a final "production" fix. However, appreciable blockage of the compressor hub holes to upset the pressure balance between the front and rear compressor faces or a slight change in the turbine cooling air supply system are temporary trims that can be used during development to define the final seal locations.

To achieve a rearward bias on the low rotor, a high counter-balancing load on the forward side of the low turbine is required, since the absence of an inlet case precludes the use of the forward side of the fan as a counter-balancing thrust piston. To counteract the varying ram pressure force which acts on the front face of the fan, both the rear face of the fan and low turbine must be subjected to a similar pressure force or else the thrust range is too large. Fan discharge pressure is satisfactory for this purpose; however, this requires a low resistance flow path between the fan exit and rear turbine compartment.

The problems of carbon seal protection and radial inflow to the high compressor inlet must be considered in setting the allowable level of the high rotor bias pressure.

(2) Systems Investigated

The following alternate systems were investigated during Phase II-B. The systems are discussed in the chronological order in which they evolved.

System A, shown schematically in Figure 2A-227, was a logical extension of the Phase II-A scheme. Instead of external venting, a seal was

added to the front of the compressor and the rear compressor compartment was then internally "short-circuited" to the forward compressor compartment via holes in the hubs. This eliminated the diffuser vent requirement and desensitized the rotor to variations in the bias pressure level. The system was further simplified by accepting a forward biased low rotor which eliminated the need for an intershaft seal and the venting provisions behind the fan hub.

These changes resulted in a very clean mechanical configuration with excellent high rotor thrust balance provisions, but an unacceptable thrust range on the low rotor (2,000 to 22,000 lbs. positive). At this point, a fan bias on the rear of the low turbine was studied to reduce the load range and System B (Figure 2A-228) was evolved. This configuration is essentially the same as System A, except that the holes in the low turbine front hub were deleted and a diaphragm was added to the front fan hub utilizing the low shaft to supply the fan bias to the turbine. An acceptable range in low rotor thrust was obtained (2,000 to 15,000 lbs), but the system still suffered from potential skidding during long-time cruise and thrust reversals during idle descent. Since these problems are inherent with a positively biased rotor, all subsequent studies were redirected at a negatively biased low rotor.

The simplest approach to achieve a negatively biased rotor was to move the low turbine front seal to its maximum radius and increase the bias pressures (P_4 and P_6) to 60% P_{t4} as shown in Figure 2A-229 (System C). The resulting low rotor thrust range is good (2000 to 12,000 lbs.), but the sensitivity to variations in the bias pressure is very poor. In addition, all the problems associated with a high bias pressure were encountered.

To reduce the sensitivity and high bias objections, an intershaft seal was added and the low rotor bias pressure (P_6) was referenced to the turbine cooling supply plenum (90% P_{t4}) as shown in Figure 2A-230(System D). This permitted the low turbine front seal to be reduced to an intermediate radius and the high rotor bias pressure to be reduced to any desired level by a vent line to the fan duct in parallel with the front compressor seal. This system meets all the ground rules set forth for the design, except it does not provide for compressor disk bore cooling. Since this option may be required to solve the structural problems in the compressor rotor, System E is currently being studied in greater depth.

(3) System Currently Being Studied

In System E, shown schematically in Figure 2A-220, the holes in the rear compressor hub are eliminated and the front and rear compressor compartments are short-circuited via holes through the compressor disk webs. Also, the #2 bearing vent system is eliminated and the holes in the front compressor hub are relocated inside the seal to permit the cool fan pressurizing air to flow rearward over the disk bores. The flow area between the shafts and through the low turbine front hub is inadequate and requires that holes be added through the low rotor shaft to provide a parallel flowpath between the high compressor drum and the low turbine rear compartment. This requirement, however, is somewhat offset by eliminating the need for the fan hub diaphragm scheme needed in Systems B, C, and D for supplying the fan discharge bias to the low turbine rear compartment.

Figure 2A-221 shows the piston areas, pressure characteristics, and seal clearances used in the System E.

Figures 2A-222 and 2A-223 are curves of bearing thrust versus bias pressure for the high and low rotors respectively. The slope of these curves is indicative of the sensitivity of the bearing thrust to variations in seal clearances which may affect the bias pressure levels. The circled points are the predicted operating pressures for the system. Figures 2A-224 and 2A-225 show the bearing thrust versus typical mission time for the high and low rotors respectively.

19. OIL HEAT REJECTION

a. Introduction

The oil heat rejection problem was studied in greater depth during Phase II-B of the SST program. A detailed analysis of the lubrication system was performed to refine the estimates previously used for the oil system heat pick-up. In addition, the fuel pump temperature rise and hydraulic system environmental heating characteristics were updated. These revisions were based on vendor-supplied pump data and a better definition of the engine configuration and performance requirements.

The fuel and oil system shown in Figure 2-64 of the Phase II-A Preliminary Design Report is still proposed for the STF219 engine. All major features of the system, such as two separate coolers located upstream of their respective fuel controls and a return line to the airframe for

supplementary cooling, have been retained. One possible change, however, has been considered. This revision would shunt hydraulic circuit fuel to the duct heater system. The necessity for this change is dependent on a final definition of the end of cruise operating conditions.

b. Summary

The results of the more detailed Phase II-B studies indicate that the engine fuel temperature will not exceed the 325°F fuel supplied at cruise conditions, based on 250°F fuel supplied to the engine pumps and no supplementary cooling. For cruise altitudes above 72,000 feet, a revision to the fuel system may be necessary.

During idle descent or sustained supersonic windmilling conditions, supplementary cooling via a return fuel flow to the airframe must be provided.

c. Discussion

It is estimated that by the end of cruise at a normal altitude of 72,000 feet, the fuel in the main engine system could be worked to its thermal limit by virtue of the energy inputs of the boost pump, main pump, hydraulic actuator system, and environmental heating (assuming 250°F fuel is supplied from the airframe). Thus, the ample heat sink capacity of the duct heater fuel supply must be utilized to the greatest extent possible. With properly designed fuel-oil coolers, no additional controls will be required to achieve this oil system heat rejection split.

Any increase in operating altitude with an attendant decrease in main engine fuel flow, however, would tend to overheat the main fuel system. The allowable fuel temperature limits can still be met by the addition of another control valve. The valve would shunt the hydraulic system fuel (and hence its energy input) to the duct heater circuit. When the duct heater is not in operation, (e.g. idle descent) the valve would return the fuel to the main engine circuit as shown in Figure 2-64 of the Phase II-A Preliminary Design Report.

The breakdown of the engine oil system heat generation is shown in Table I. This estimate is consistent with current design practice for carbon seals, ball bearings, and roller bearings. This engine oil system heat rejection will result in a somewhat lower total engine system heat rejection than used in Phase II-A, but will not change the basic fuel-oil heat rejection system.

TABLE I

OIL FLOWS

Jet Pump Not Included   ΔT Oil = 50°F

Front Bearing Compartment	Q BTU/Min	w PPM	Scoop Efficiency %	w' PPM	Excess Oil -
Front Seal	171	5.7	70	8.1	2.4
Rear Seal	260	8.7	90	9.8	1.1
Middle Forward Seal	134	4.5	70	6.4	1.9
Middle Rear Seal	177	5.9	90	6.6	0.7
Front Bearing	160	5.3	70	7.6	2.3
Rear Bearing	490	15.0	90	16.6	1.2
M.E. Gear - Top	255	8.5	-	8.5	-
M.E. Gear - Side	130	4.3	-	4.3	-
A.C. T.S. Ball Brg.	25	0.8	-	0.8	-
A.C. T.S. Roller Brg.	50	1.6	-	1.6	-
M.E. T.S. Ball Brg.	25	0.8	-	0.8	-
M.E. T.S. Roller Brg.	50	1.6	-	1.6	-
Amb. & Conduction	177	5.9	-	-	-
Tower Shaft Cont'd.	142	4.7	-	-	-
TOTAL	2206	-	-	72.70	9.6

Total Flow = 163 PPM

Total Q = 4659 BTU/Min

MIDDLE BEARING COMPARTMENT

Front Seal	294	9.8	70	14.0	4.2
Rear Seal	294	9.8	70	14.0	4.2
Roller Bearing	230	7.7	70	11.0	3.3
Amb. & Conduction	104	3.5	-	-	-
TOTAL	922	-	-	39.0	11.7

REAR BEARING COMPARTMENT

Seals	150	5.0	-	5.0	-
Roller Bearing	30	1.0	-	1.0	-
Amb. & Conduction	250	8.3	-	8.3	-
TOTAL	430	-	-	14.3	-
Main G/B	751	25.0	-	25.0	-
Rt. Hnd. G/B	300	10.0	-	10.6	-
Oil Tank Amb.	50	1.6	-	1.6	-

20. TUBING SYSTEM DESIGN

a. Introduction

The Phase II-B design effort was largely concentrated on internal tubing and the general method of transferring lines from the gas generator section of the engine through the fan duct diffuser struts to the outer duct. The routing of the external tubing is so dependent upon airframe nacelle configurations and accessory requirements, neither of which is final at this time, that it is premature to design in this area.

A schematic diagram of the flow systems required to be passed through the fan duct diffuser struts is shown in Figure 2A-231, and is referred to frequently in the detailed description of the following fluid systems.

The materials used for tubing, brackets, and seals are based on experience gained from the design and operation of the JT11D-20 engine. PWA 770 tubing is used for all lines which do not exceed 800°F. Heatshield brazing on these tubes was accomplished in accordance with PWA Spec 2666, silver. Tubes which exceed 800°F are fabricated from Inconel tubing (PWA 1060) with heatshield spacer brazing per PWA 90, gold nickel. The tubing connections employ a modified AN threaded connector with ferrules machined as an integral part of the tube. Tubes with integral ferrules have a higher fatigue strength and reliability than brazed ferrules because the only variables, upsetting and machining, are subject to strict quality control.

A highly effective seal is produced by a nickel gasket compressed between the ferrule and the male connector. This arrangement permits rapid replacement of engine tubes and components, and allows complete inspection of plumbing prior to installation. This system is particularly effective for high pressure plumbing.

Tubing is supported by fully heat treated Inconel X brackets, spaced at calculated intervals to provide a firm foundation for tube clamp points. Where required, brackets are slotted to allow one-plane movement to relieve thermal stresses. Wear resistant materials and coatings are also used at these locations. At clamp locations on high pressure tubing, where thermal and maximum vibratory movements are in the same plane, a vibration damper is used. This permits thermal movement, but restricts vibratory movement.

b. Bleed Air

Non-contaminated air is drawn from the gas generator diffuser case and routed through fan duct diffuser struts to flanged bosses on the fan duct outer case as shown on Figure 2A-232. Six bosses are provided in sets of two at three locations. These sets are axially arranged. The forward boss is supplied by a 2.25 inch diameter tube, and the rearward boss by a 2.0 inch diameter tube. These two tubes branch from a 3.0 inch main supply tube.

A sliding type joint is provided in the 3.0 inch diameter section of the duct to allow freedom in all directions for installation tolerances and thermal deflections. Metal seal rings are used in the joint to prevent leakage. One feature of the sliding joint is that it allows the bleed air ducts to be installed on the case subassemblies for ease of installation. The sliding joint is then installed during the final engine build-up.

The 3.0 inch duct branches into two smaller ducts to reduce its thickness in passing through the fan duct diffuser strut. An internal type gland nut is used to attach the tubes to the two bosses. The same nut is used for both the forward and rear bosses and the nuts are locked to the bosses with tab washers. An anti-torque device is incorporated to prevent the nut tightening torque from being transmitted to the twin tube assembly. The manifold is additionally supported at the inboard side of the strut. This support provides restraint and prevents bending loads on the manifold. The support does, however, allow freedom for thermal growth.

c. Fuel System

Fuel to the main burner will pass through the outer wall of the fan duct diffuser at four locations in 0.750 inch diameter stainless steel tubes (PWA 770). These tubes have an integral bulkhead type fitting as seen in Figure 2A-233 (typical strut). The four supply manifolds will then be supported at the inner wall of the fan duct diffuser by an Inconel X (AMS 5542) sliding bracket to provide added support for the bulkhead connector and to prevent chafing. Using an expansion leg to absorb the thermal differentials and locational tolerances, the supply manifolds are then supported at the forward flange of the main diffuser by Inconel X sliding brackets. The supply manifolds are each then split into two 0.500 inch diameter stainless steel tubes (PWA 770) by means of tee connections. Figure 2A-234 shows a typical quadrant installation of the fuel manifolds.

The tee will be a standard mechanical tee requiring conical seals. The tubes will have integral ferrules and will use gold coating for heat rejection.

The two tubes then carry the fuel directly to two nozzles of an eight nozzle quadrant where 0.500 inch PWA 770 jumper tubes carry the fuel to the other nozzles in the quadrant.

All fittings are integral and located within the fan diffuser duct access doors. One configuration jumper tube can be used in all but two locations. Here an "S" type jumper tube is required to accommodate the two ignitors. The jumper tubes lie close to the diffuser case and pass plumbing over the tubes and between the nozzles. This allows all 32 fuel nozzles to be removed without disassembling any plumbing other than the nuts on the jumper tubes.

d. Lubricating Oil Lines for the Number 3 and 4 Bearings

The number 3 and 4 bearing lubrication system consists of oil supply, scavenge and breather plumbing.

Lubricating oil is carried externally from the oil pump to the heater duct #8 strut. The heater duct oil line is mounted to the strut flange by means of a bulkhead type fitting which is an integral part of the tube (Figure 2A-233). This 0.750 inch diameter line passes thru the #8 duct diffuser strut and is bracketed with a solid clamp to the fifth stage compressor case flange. An expansion loop is provided between the heater duct and the gas generator tube mounting points. A tee-connection is made to the lines which supply oil to the number 3 and 4 bearings. The 0.500 inch number 3 bearing oil line from the tee is connected to a male fitting on the #14 strut on the diffuser case. The line is then routed through the diffuser case strut to the number 3 bearing compartment. A similar oil line for the number 4 bearing is routed aft through the annulus between the heater duct and gas generator to the turbine exhaust duct strut fitting. An expansion loop is also provided in this line to reduce thermal stresses.

The oil pressure tubing incorporates integral ferrules and is gold-plated for heat rejection. Nickel conical washer seals are used on mechanical joints at tee and strut connections. The oil pressure tubing is fabricated from 0.035 inch wall stainless steel (PWA 770). The joints at the tee and diffuser duct are made before the aft heater duct is assembled. Scavenge oil is brought from the number 4 bearing compartment by a 0.500 inch diameter line through the exhaust duct

strut to a tee located near the diffuser duct #8 strut. An expansion loop is incorporated in this line. Scavenge oil from the number 3 bearing compartment is routed to a connection on the #8 diffuser duct strut. A 0.750 inch diameter line from the fitting on #8 diffuser duct flange is routed to the tee. The scavenge oil is then routed in a 0.875 inch diameter tube from the tee through the fan diffuser duct #6 strut to the strut flange. An integral, tube bulkhead type fitting is utilized at this joint as shown in Figure 2A-233.

A second scavenge oil line, with the same diameter dimensions, is routed from the number 3 bearing compartment to a fitting on the #9 diffuser duct strut. From the fitting on the strut flange, a 0.750 inch diameter line is routed through the fan diffuser duct #6 strut to the flange with an integral bulkhead fitting. An expansion loop is provided for both scavenge lines between the gas generator and the heater duct to reduce thermal stresses. All lines are supported by Inconel X (AMS 5542) brackets with solid clamps to the gas generator near the tee.

The oil scavenge lines incorporate integral ferrules and are gold-plated for heat rejection. Nickel conical washer seals are used at all mechanical joints. Tubing material for the scavenge lines is stainless steel (PWA 770) with 0.035 inch walls. The joints at the struts and tee are made before the aft heater duct is assembled.

e. Number 3 and 4 Bearing Seal Air Pressurizing Lines

The pressurizing air for the number 3 and 4 bearing compartments is brought from flanges, located on the inner wall of the duct heater, through 1.00 inch diameter tubes to connections on #1, #5 and #13 diffuser case struts. The air is then routed to three locations in the number 3 bearing compartment. Five 1.000 inch diameter vent tubes from the number 3 bearing compartment are routed to fittings on the diffuser struts. Two lines are routed from diffuser case struts #15 and #16 to the heater duct strut #8 outer flange. The remaining lines are routed as follows: One line from diffuser case strut #12 to heater duct strut #6, one line from diffuser case strut #7 through heater duct strut #4, and one line from diffuser case strut #4 through heater duct strut #2.

Thermal expansion loops are provided in the tubes between the fan duct and the gas generator. Bulkhead type fittings are used for all tubes at the heater duct strut outer flange. Tube connections are made before the aft fan duct is assembled.

In a similar system, number 4 bearing seal pressurizing air is run aft in a line connecting to one of the turbine exhaust struts. This line is routed through the strut to a connecting line to the number 4 bearing compartment mounting flange, and from the flange into the compartment upstream of the carbon seals. Leakage past the labyrinth seal flows to the rear of the third stage disk and out the rear inner seal into the exhaust stream.

f. Hydraulic Lines

Two hydraulic line systems are located within the inner annulus. They are the proposed starting bleed valve system (requirements, six valves and two actuators) and the aerodynamic flameholder air valve system (requirements twelve valves and three actuators). The starting bleed system is not a firm requirement. This system, however, has been designed to insure that a spare will be available for the lines and actuators, if engine testing indicates the need.

The starting bleed actuators, if required,will be located in the upper quadrants of the engine near the rear flange of the main burner case. The actuators require opening and closing pressure manifolds. Both manifolds are routed along the rear flange of the main burner case and tee into supply manifolds which run forward to the fan duct diffuser struts (Figure 2A-2[illegible]). Both supply manifolds have expansion loops near the intermediate flange of the main burner case, and mechanical connectors in the area of the fan duct diffuser access doors. The "open" pressure manifold passes through the fan duct diffuser strut #2, and the "close" pressure manifold passes through strut #3 (Figure 2A-233, typical strut connections).

The aerodynamic flameholder actuators are equally spaced around the engine in the same plane as the start bleed actuators. They also require "open" and "close" pressure manifolds. The "open" and "close" manifolds are routed from the #1 and #3 actuators around the bottom of the engine, aft of the rear flange of the main burner. They are joined to the #2 actuator and the supply manifolds by mechanical tees. The supply manifolds extend forward to the fan duct diffuser struts as shown in Figure 2A-231. The manifolds incorporate expansion loops near the intermediate flange of the main burner case and mechanical connectors in the area of the fan duct diffuser access doors. The "open" pressure manifold passes through fan duct diffuser strut #4 and the "close" pressure manifold passes through strut #6.

Both actuator systems have 0.375 inch diameter stainless steel integral fittings, and "open" and "close" pressure plumbing supported from the gas generator by Inconel X brackets.

The drain manifold is routed from the #1 starting bleed actuator and the #3 flameholder actuator to the bottom of the engine along the rear flange of the main burner case. The #1 and #2 aerodynamic flameholder actuators and the main burner fuel drain are joined to the #2 start bleed actuator by mechanical tees. An overboard drain line is then routed through fan duct diffuser strut #5. All of the drain lines are Inconel (PWA 1060) and are supported from the gas generator by Inconel X (AMS 5542) brackets.

21. WEIGHT ANALYSIS

The Phase IIA report presented the STF219, duct-burning turbofan engine, in sizes specified by Boeing and Lockheed. During Phase IIB the STF219 was studied at a 650 lb/sec size. The estimated weights for the Boeing and Lockheed engines are given in Tables I and II including a sectional weight breakdown.

During Phase IIB two changes have been incorporated that increase the engine weight. They are: (1) lower fan specific flow which increases the fan outer diameter and (2) redesign of the turbine section to provide for the required turbine efficiency level to be met at both the Basic Rating and the Initial Rating.

TABLE I

Boeing Installation - Weight Summary

650 lb/sec flow
Base flow schedule
Basic and Initial Rating

Fan rotor, stator, case and front mount	795
Intermediate case	655
High pressure compressor rotor, stator, case	615
Diffuser and burner	981
Turbine rotor, stator, and shaft	1,377
Turbine exhaust	396
Ducts, liners, and variable area nozzle	1,767
Ejector reverser	1,880
Accessories drive	184
Components and plumbing	910
Total estimated dry engine weight	9,560
*Additional equipment and installation features	540
Total Engine Weight	10,100 lbs.

*Additional equipment and installation features are based on Phase IIA requirements.

TABLE II

Lockheed Installation - Weight Summary

650 lb/sec flow
Base flow schedule
Basic and Initial Rating

Fan rotor, stator, case and front mount	762
Intermediate case	655
High pressure compressor rotor, stator, case	615
Diffuser and burner	981
Turbine rotor, stator, and shaft	1,377
Turbine exhaust	396
Ducts, liners, and variable area nozzle	1,730
Ejector reverser	1,880
Accessories drive	184
Components and plumbing	910
Total estimated dry engine weight	9,490
*Additional equipment and installation features	180
Total Engine Weight	9,670 lbs.

*Additional equipment and installation features are based on Phase IIA requirements except for addition of weight increase due to canting the ejector reverser 4° from engine centerline.

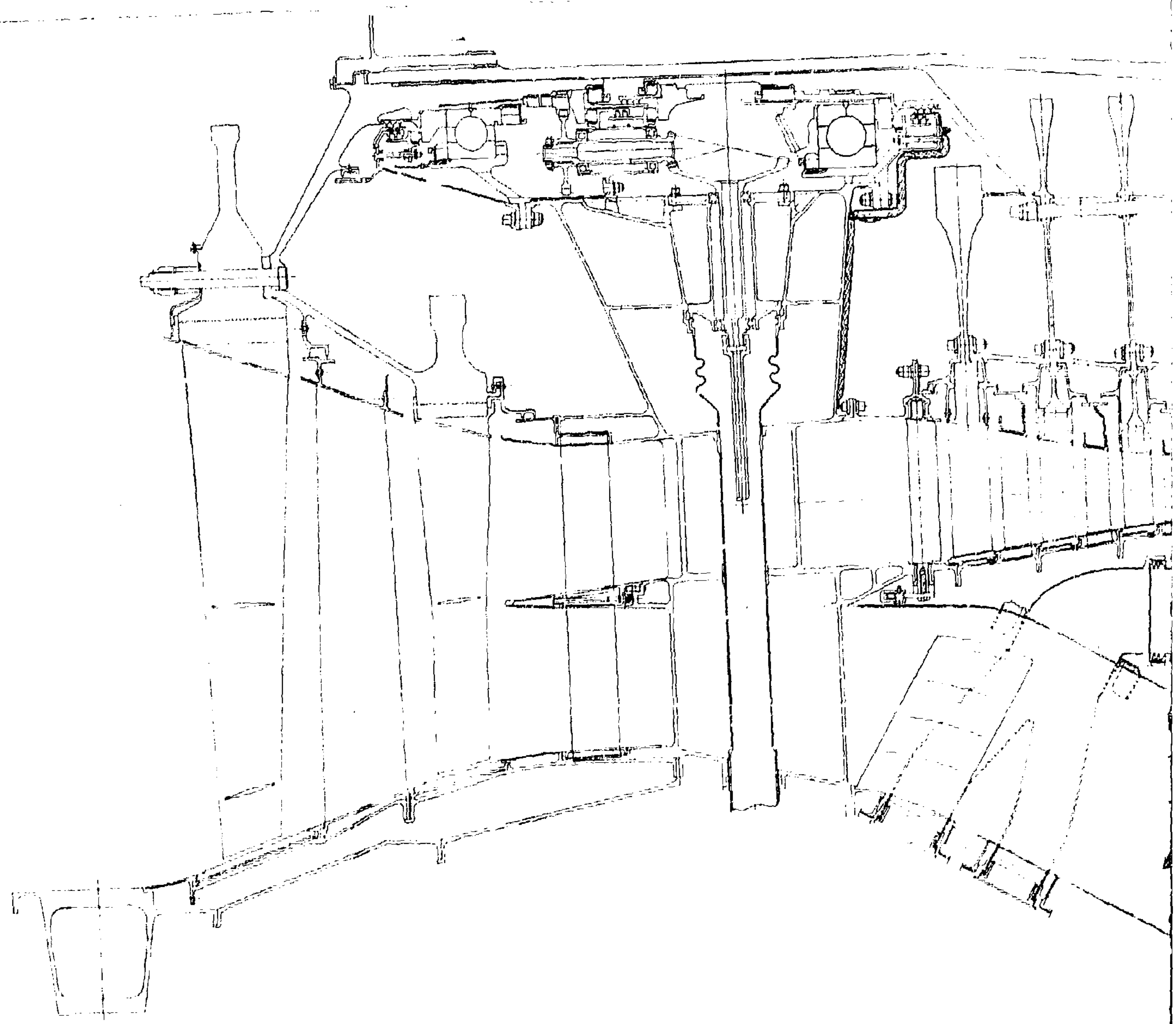

1

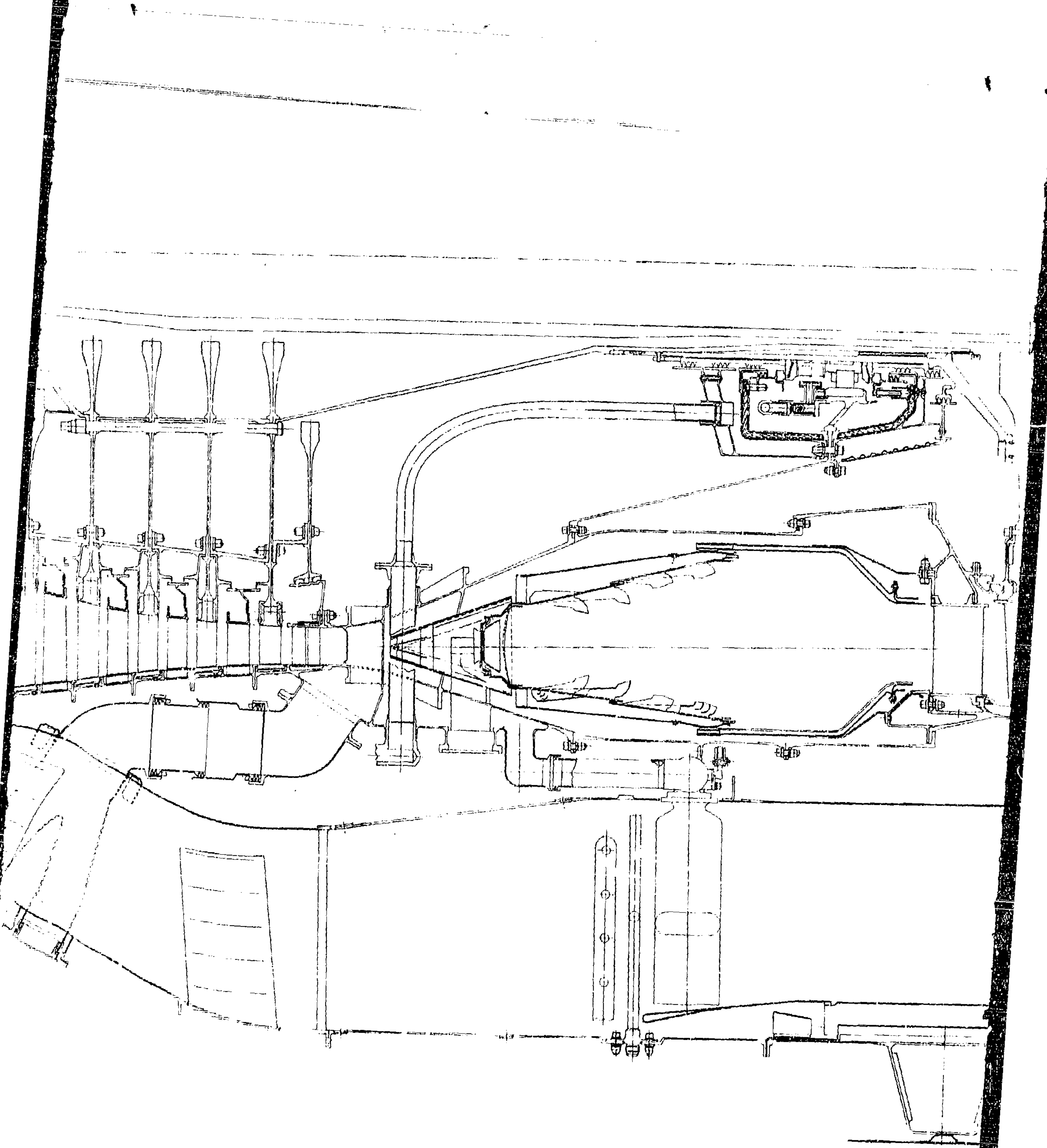

2

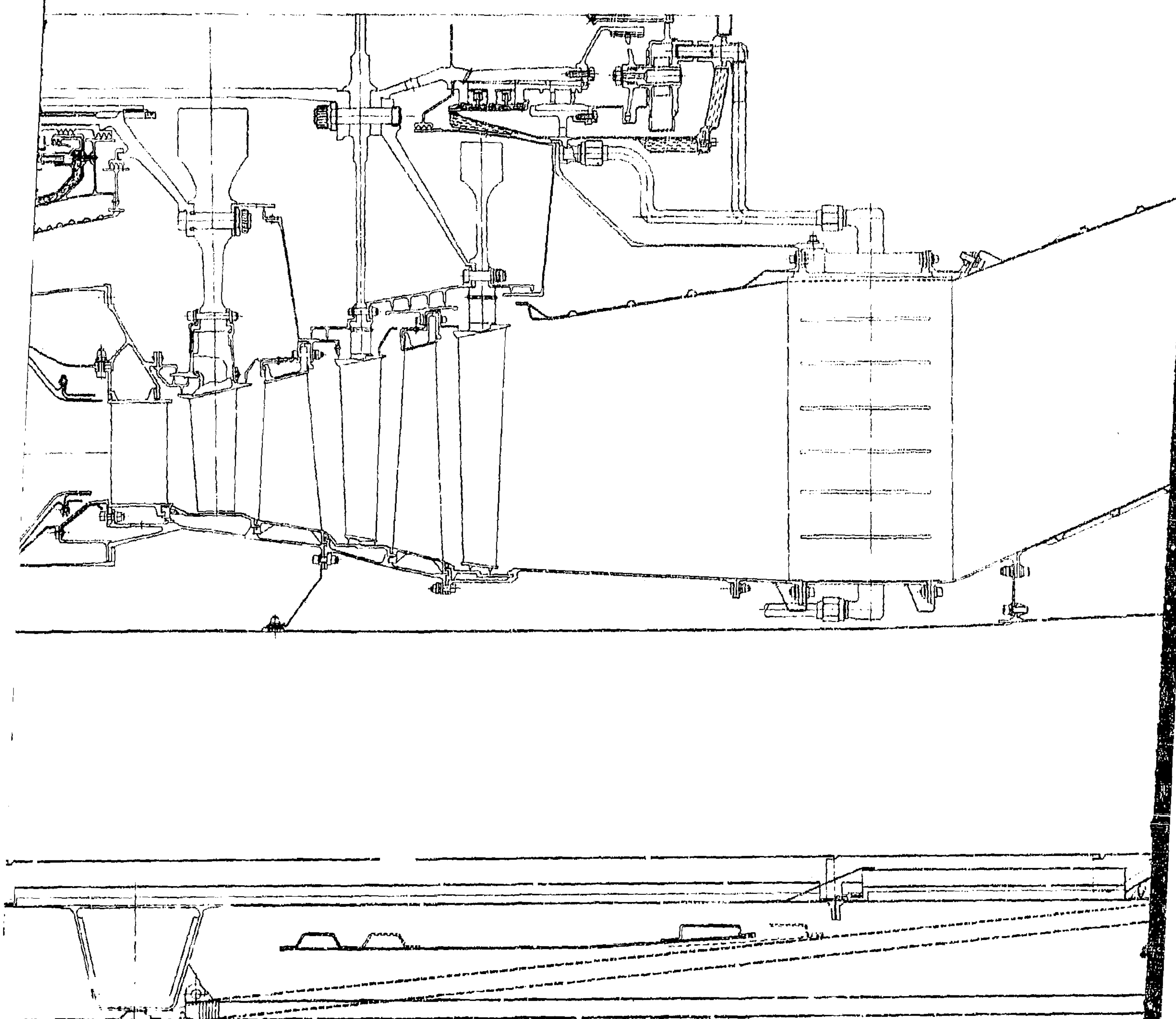

3

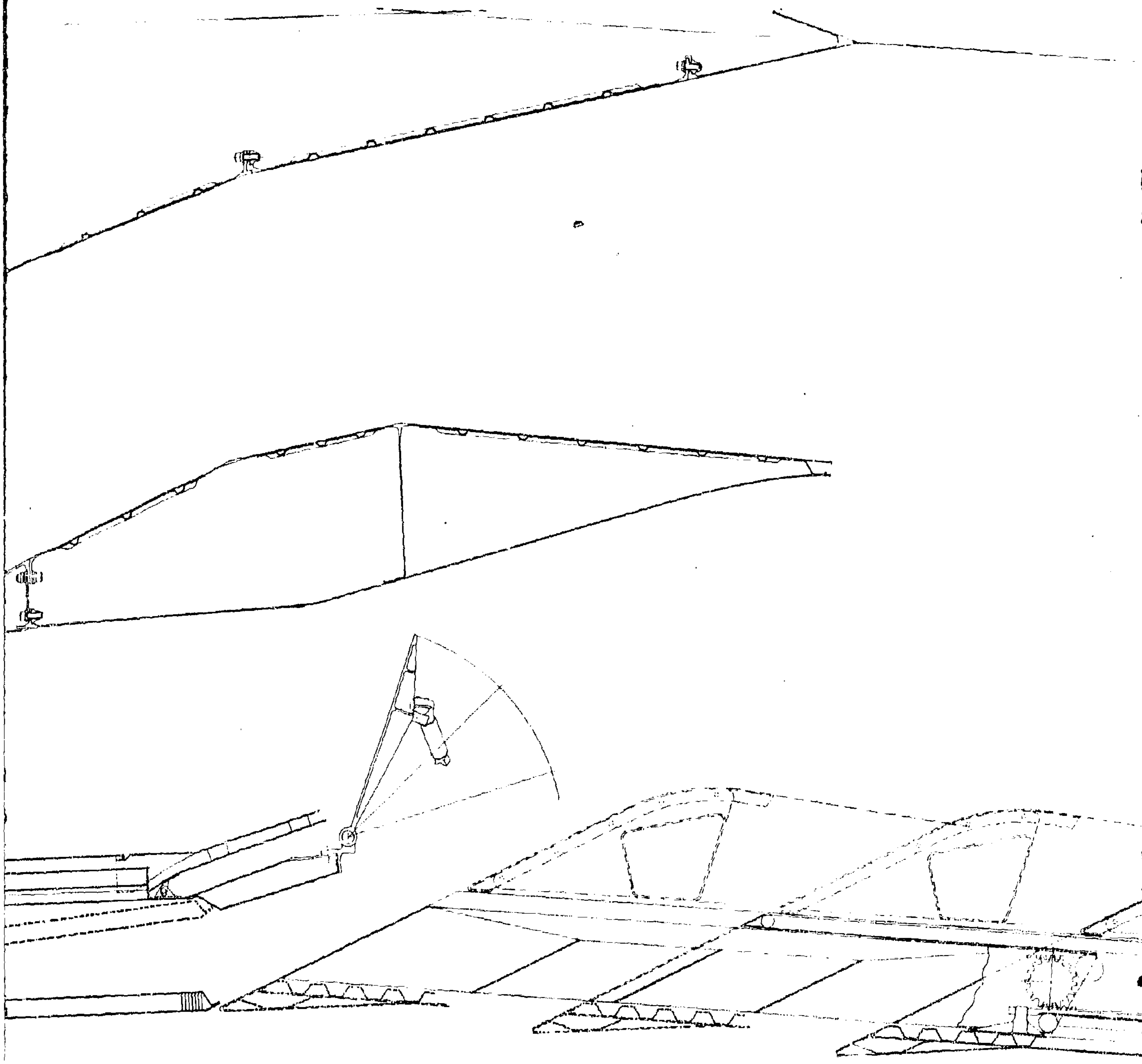

4

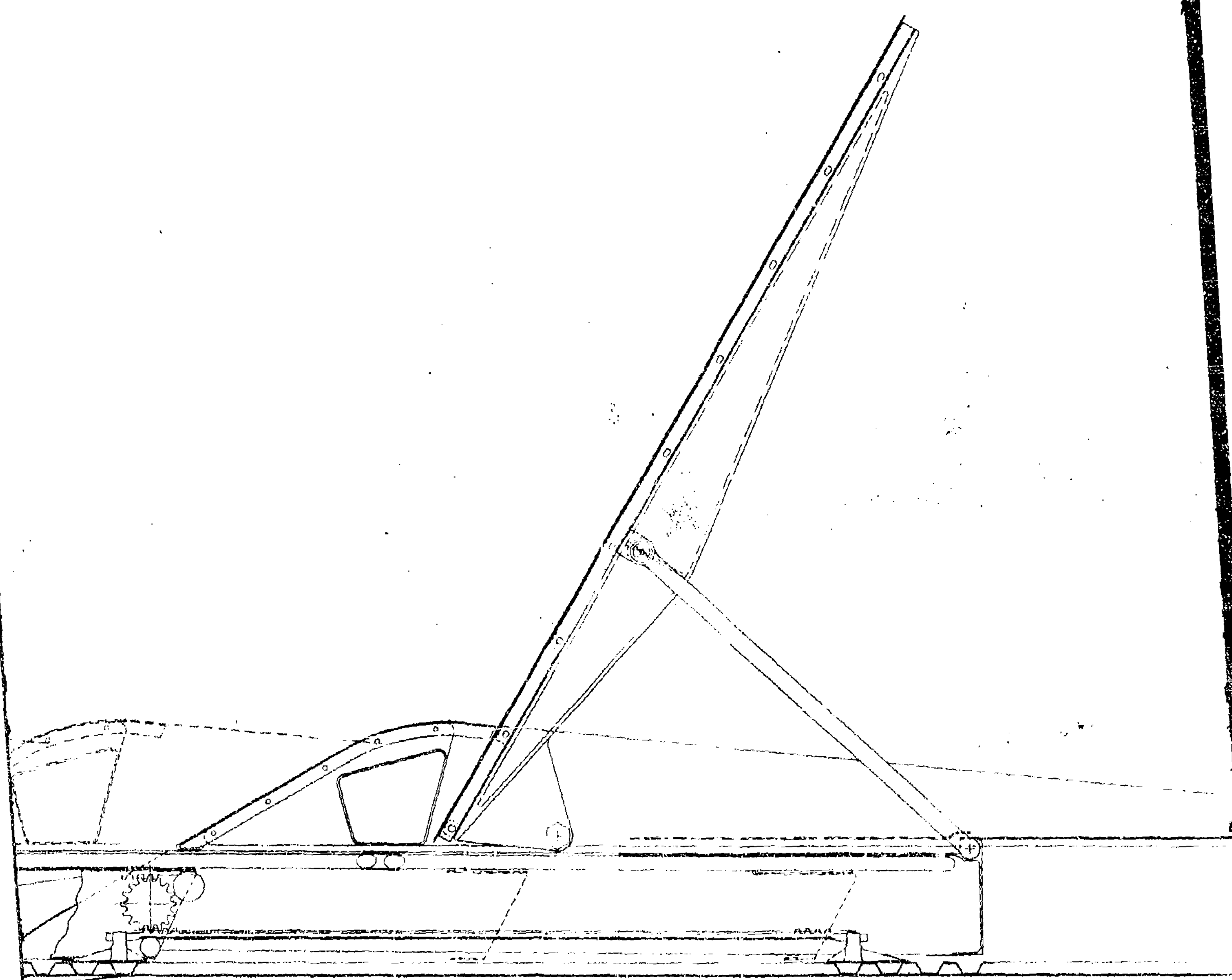

5

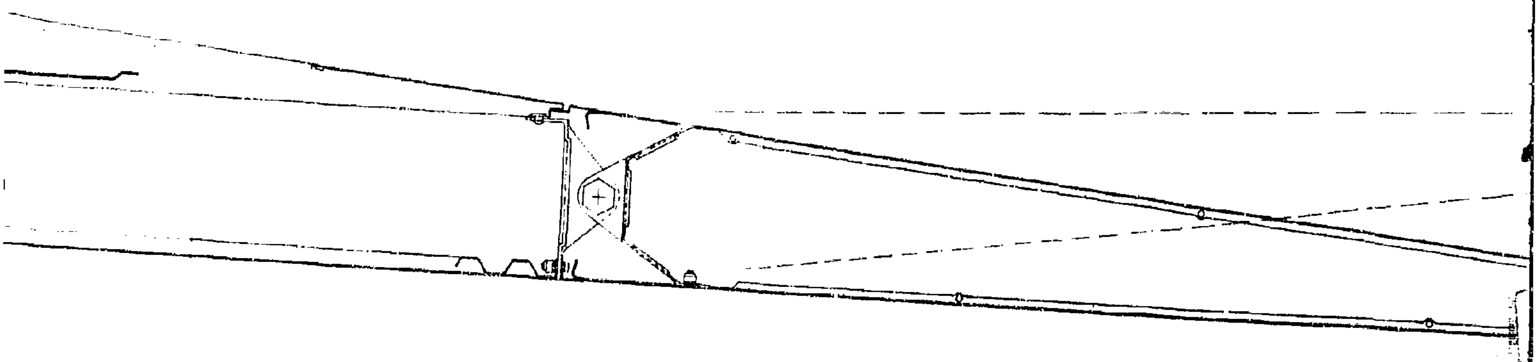

STF219 GENERAL ENGINE ARI

6

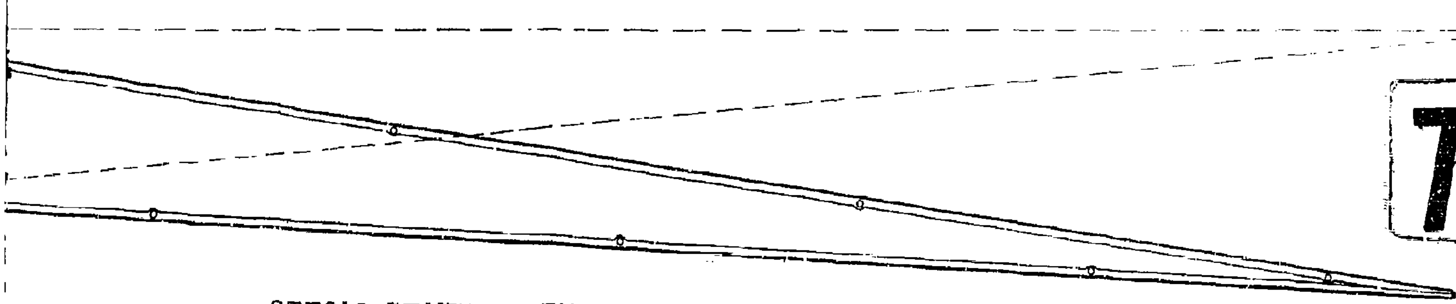

7

STF219 GENERAL ENGINE ARRANGEMENT

Figure 2A-0

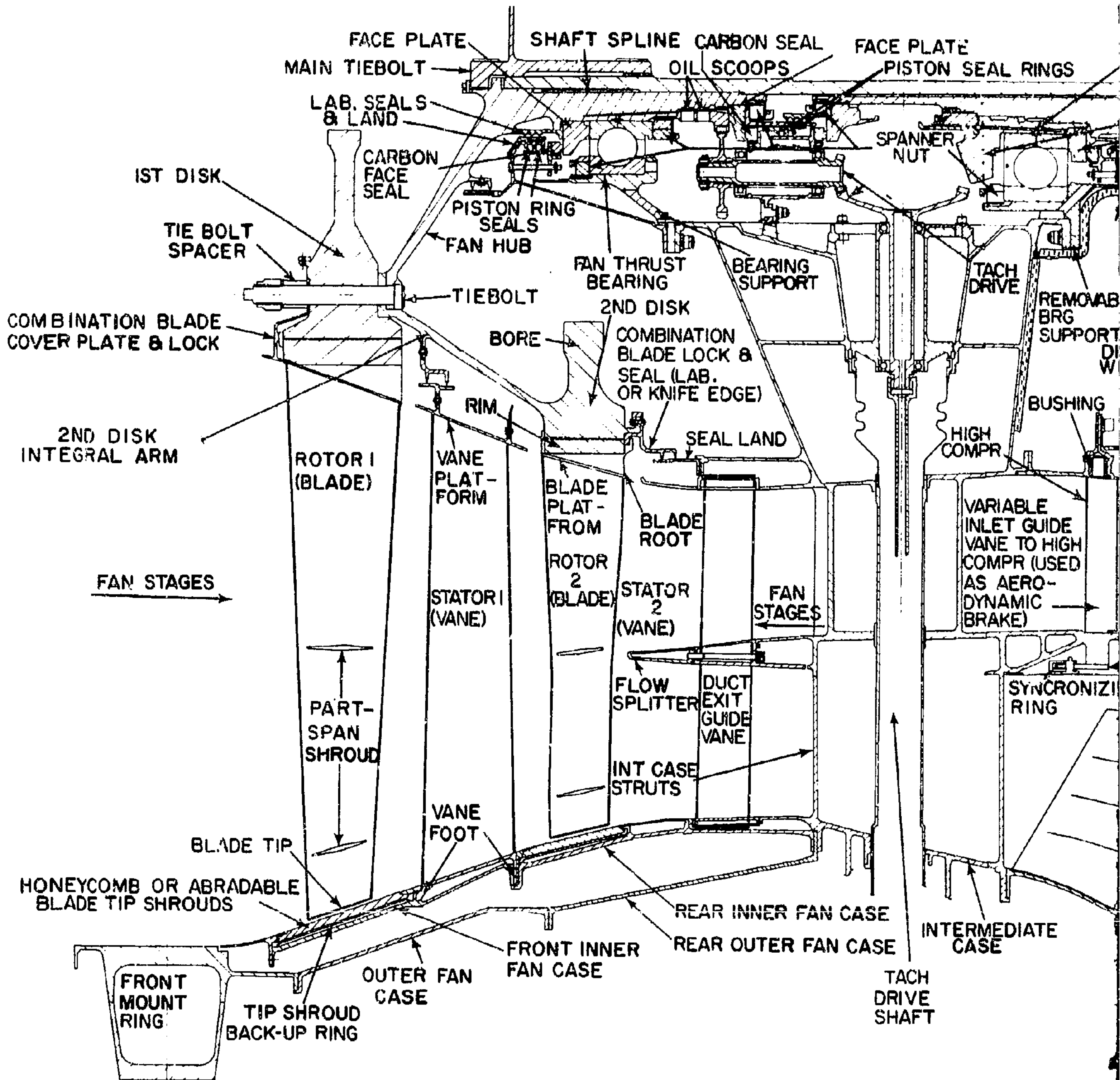
FACE PLATE
SHAFT SPLINE
CARBON SEAL
FACE PLATE
MAIN TIEBOLT
OIL SCOOPS
PISTON SEAL RINGS
LAB. SEALS & LAND
SPANNER NUT
CARBON FACE SEAL
IST DISK
PISTON RING SEALS
TIE BOLT SPACER
FAN HUB
FAN THRUST BEARING
BEARING SUPPORT
TACH DRIVE
TIEBOLT
2ND DISK
COMBINATION BLADE COVER PLATE & LOCK
BORE
COMBINATION BLADE LOCK & SEAL (LAB. OR KNIFE EDGE)
REMOVAB
BRG
SUPPORT
RIM
BUSHING
2ND DISK INTEGRAL ARM
SEAL LAND
HIGH COMPR
ROTOR I (BLADE)
VANE PLAT-FORM
BLADE PLAT-FROM
BLADE ROOT
VARIABLE INLET GUIDE VANE TO HIGH COMPR (USED AS AERO-DYNAMIC BRAKE)
ROTOR 2 (BLADE)
FAN STAGES
STATOR I (VANE)
STATOR 2 (VANE)
FAN STAGES
FLOW SPLITTER
DUCT EXIT GUIDE VANE
SYNCRONIZI
RING
PART-SPAN SHROUD
INT CASE STRUTS
VANE FOOT
BLADE TIP
HONEYCOMB OR ABRADABLE BLADE TIP SHROUDS
REAR INNER FAN CASE
REAR OUTER FAN CASE
INTERMEDIATE CASE
FRONT INNER FAN CASE
OUTER FAN CASE
FRONT MOUNT RING
TIP SHROUD BACK-UP RING
TACH DRIVE SHAFT

ST
SE

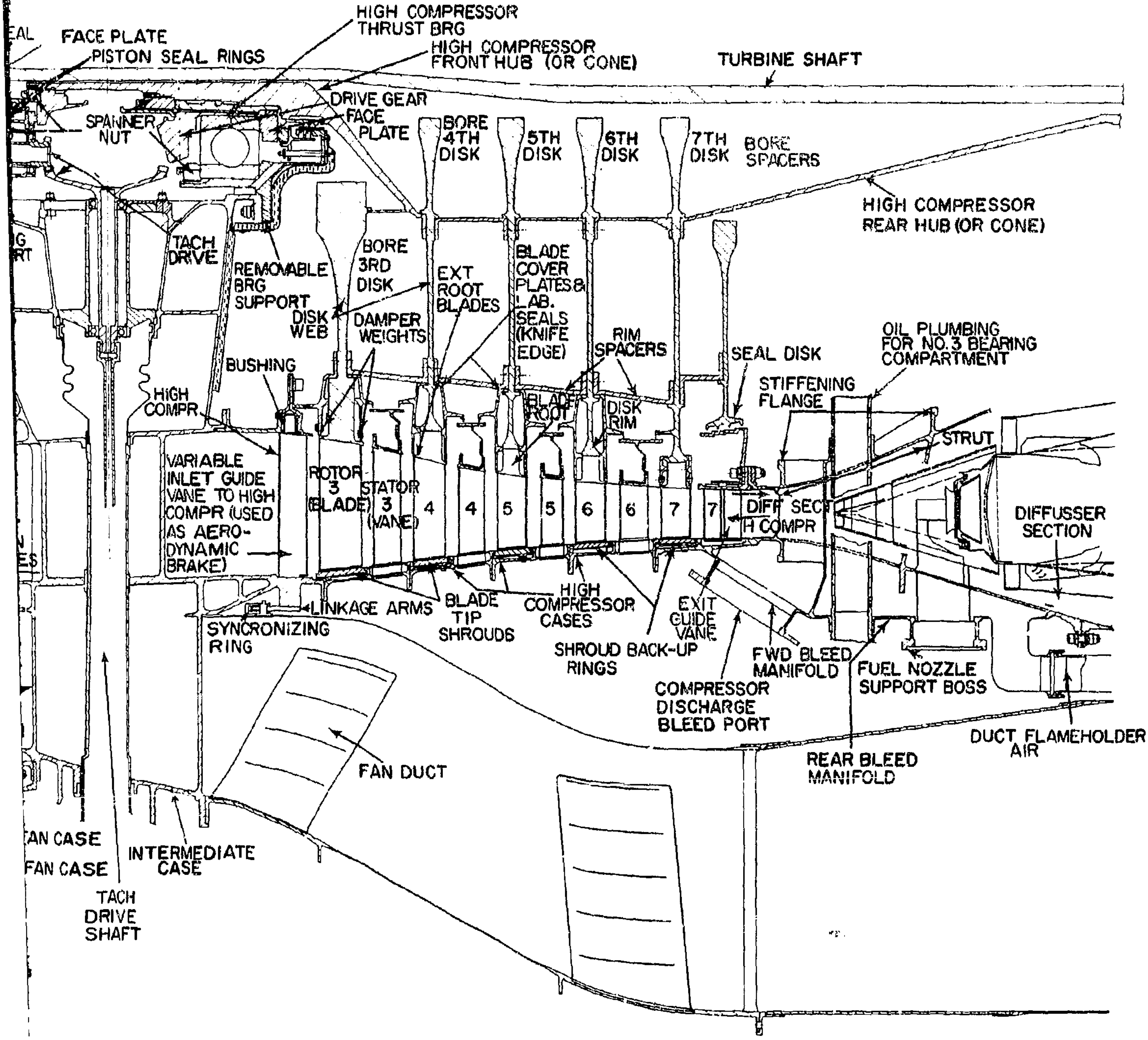

STF219 FAN, INTERMEDIATE CASE, AND HIGH PRESSURE COMPRESSOR SECTIONS

Figure 2A-1

2

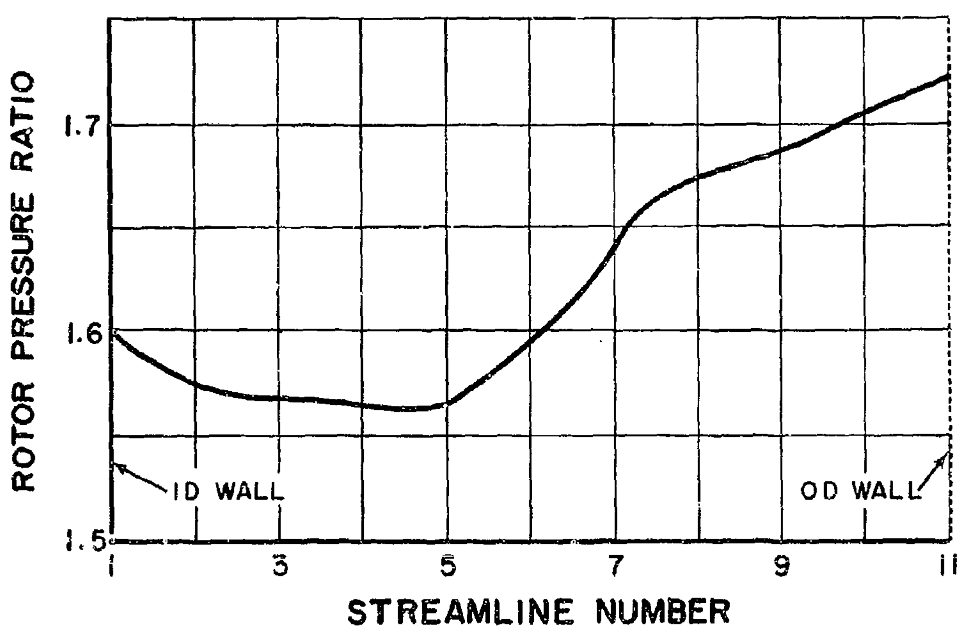

STF219 FAN AERODYNAMIC DESIGN ROTOR ONE PRESSURE RATIO

Figure 2A-2

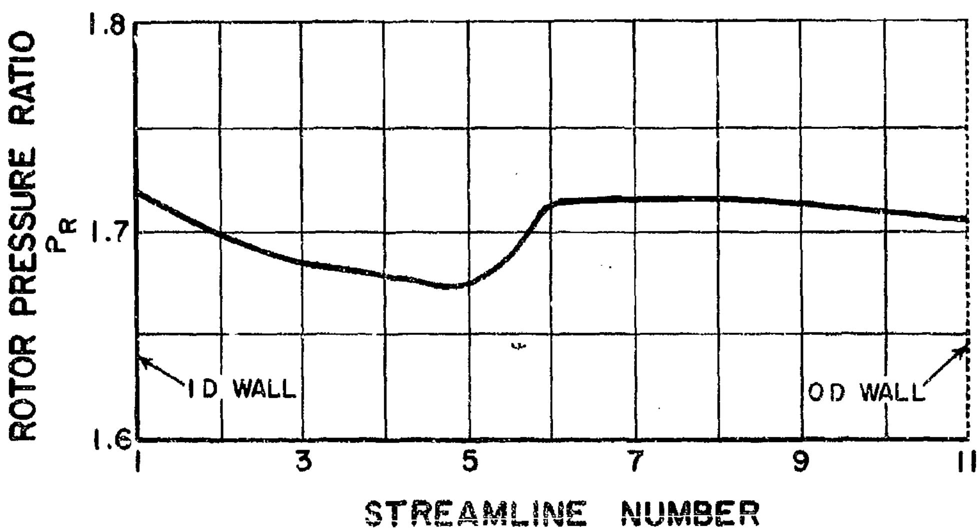

STF219 FAN AERODYNAMIC DESIGN ROTOR TWO PRESSURE RATIO

Figure 2A-3

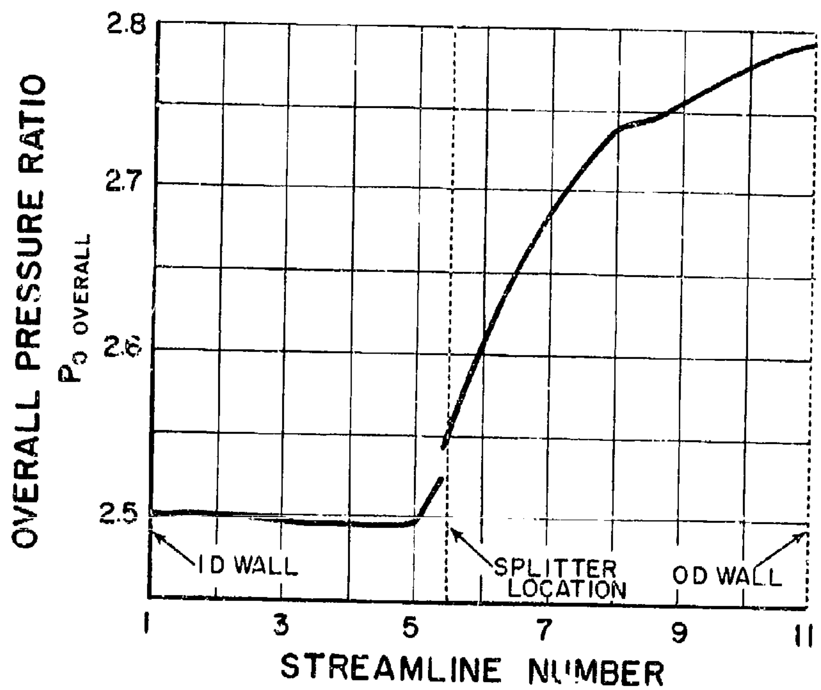

STF219 FAN AERODYNAMIC OVERALL PRESSURE RATIO

Figure 2A-4

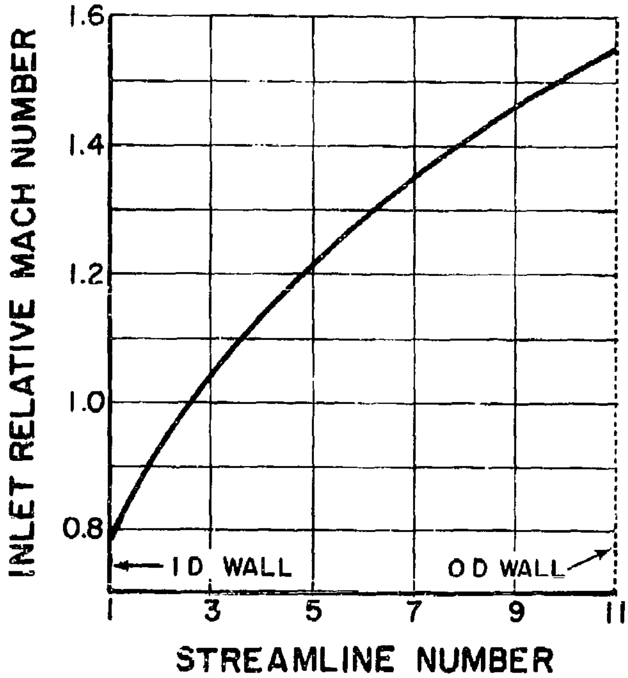

STF219 FAN AERODYNAMIC DESIGN STAGE ONE ROTOR INLET MACH NUMBER

Figure 2A-5

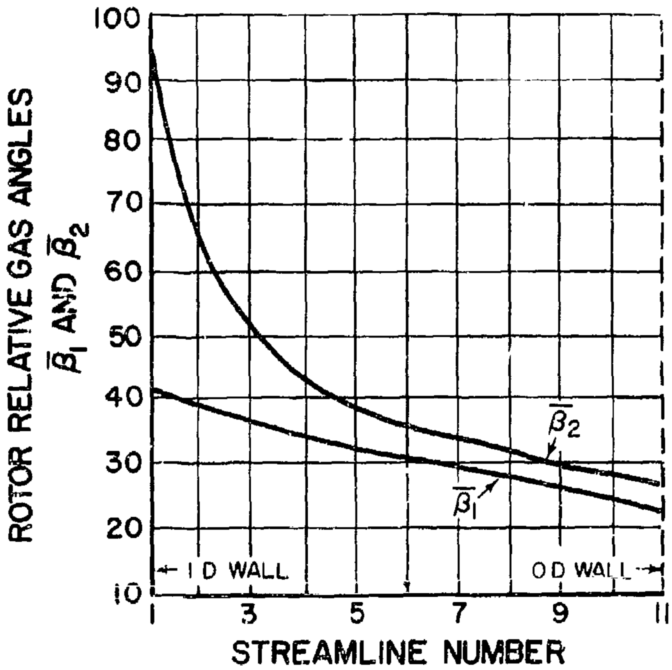

STF219 FAN AERODYNAMIC DESIGN STAGE ONE ROTOR RELATIVE GAS ANGLES

Figure 2A-6

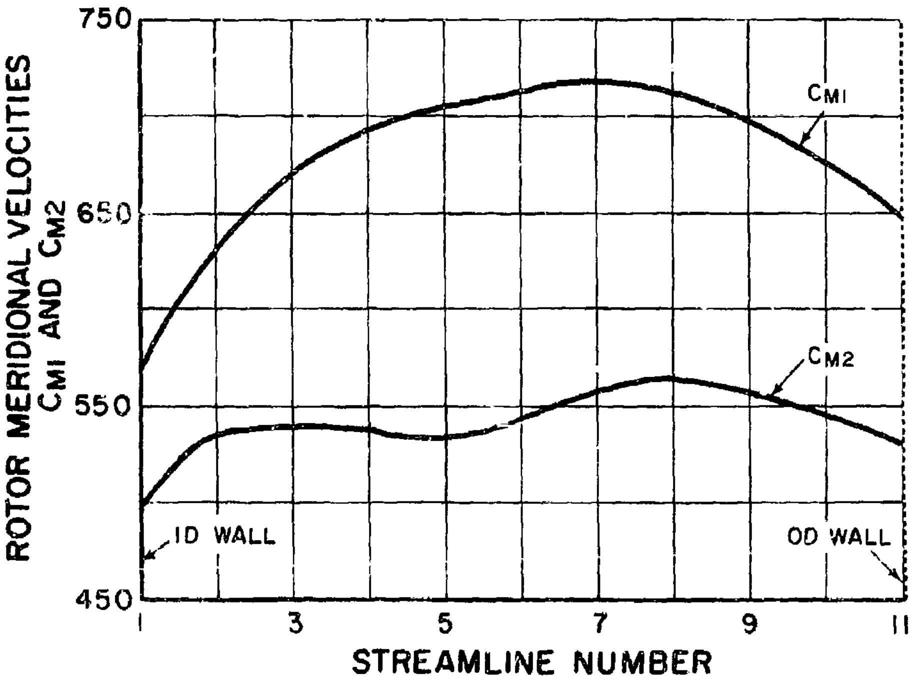

STF219 FAN AERODYNAMIC DESIGN STAGE ONE ROTOR MERIDIONAL VELOCITIES

Figure 2A-7

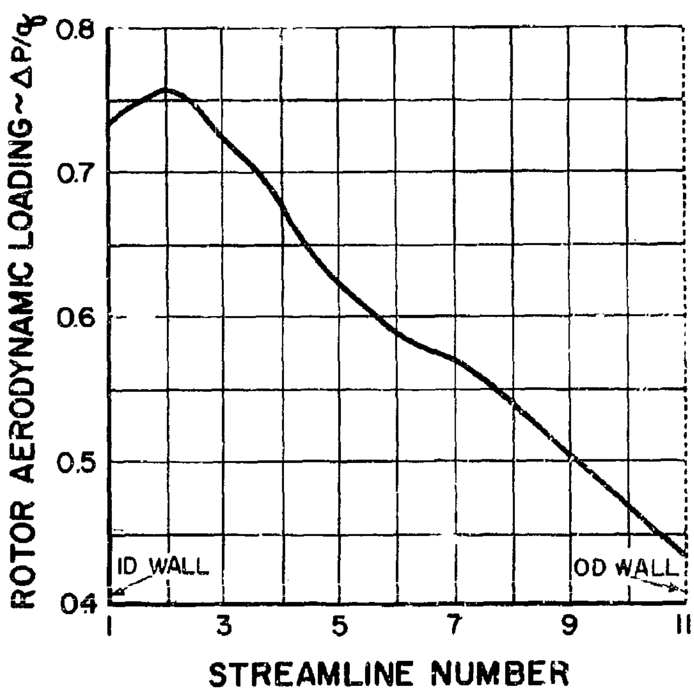

STF219 FAN AERODYNAMIC DESIGN STAGE ONE ROTOR AERODYNAMIC LOADING ($\Delta P/q$)

Figure 2A-8

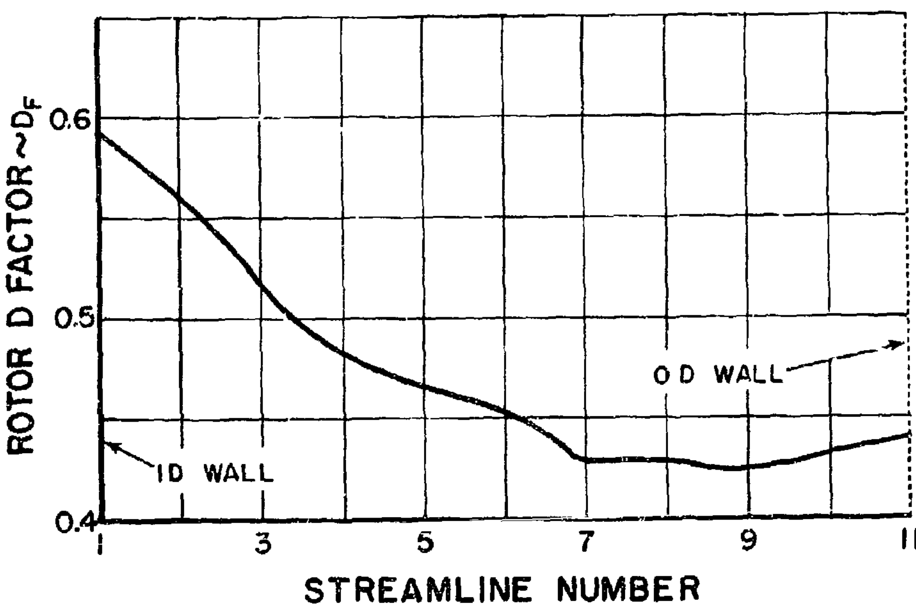

STF219 FAN AERODYNAMIC DESIGN STAGE ONE ROTOR "D" FACTOR

Figure 2A-9

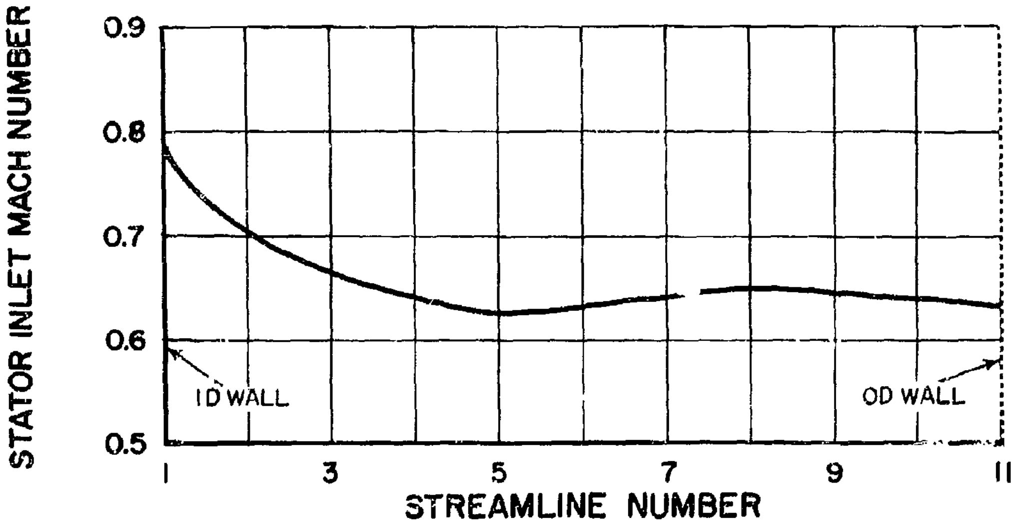

STF219 FAN AERODYNAMIC DESIGN STAGE ONE STATOR INLET MACH NUMBER

Figure 2A-10

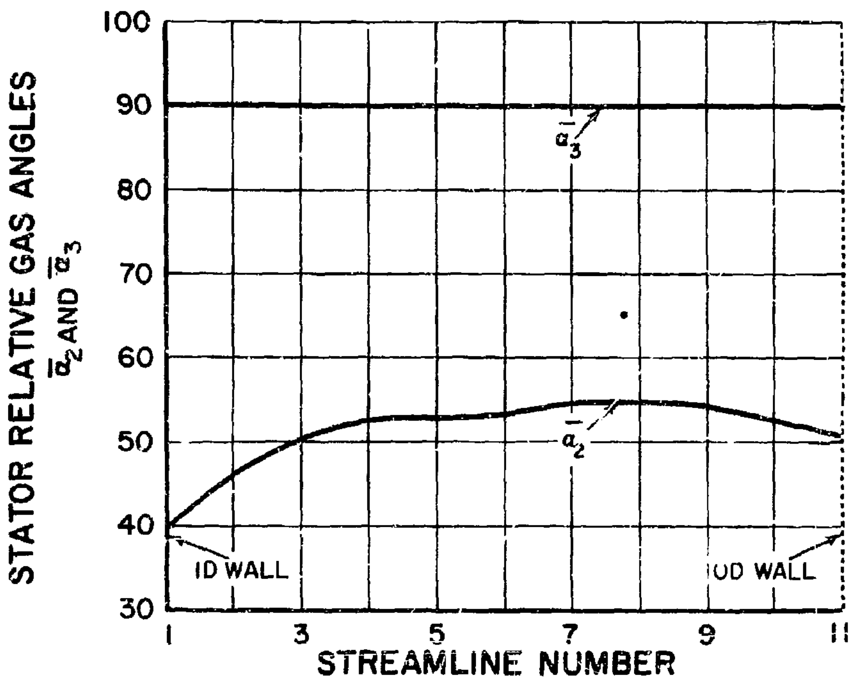

STF219 FAN AERODYNAMIC DESIGN STAGE ONE STATOR RELATIVE GAS ANGLES

Figure 2A-11

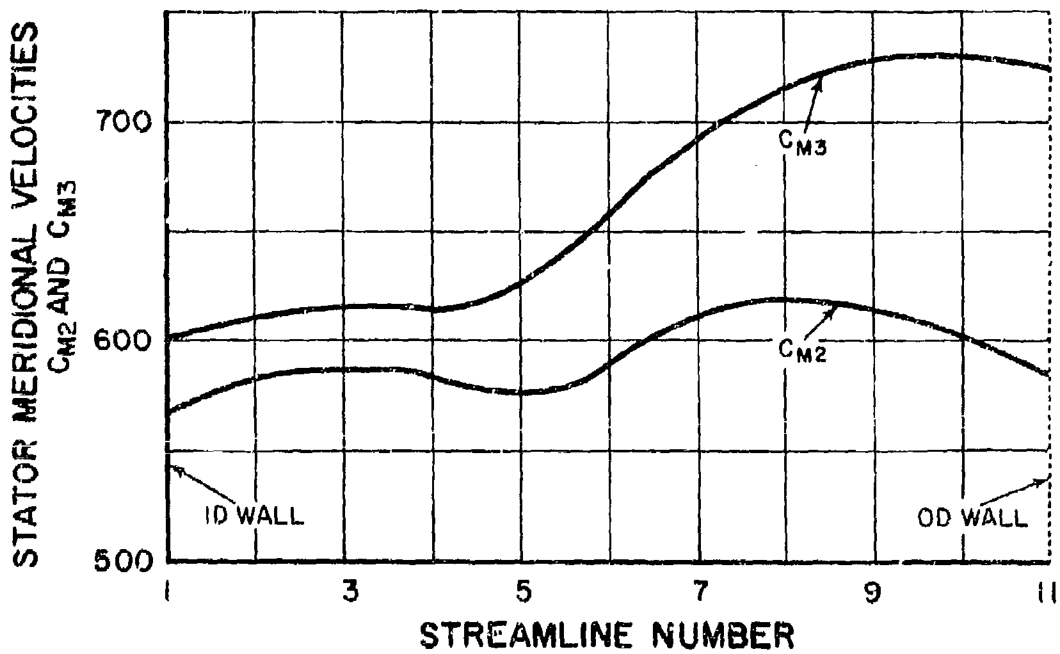

STF219 FAN AERODYNAMIC DESIGN STAGE ONE STATOR MERIDIONAL VELOCITIES

Figure 2A-12

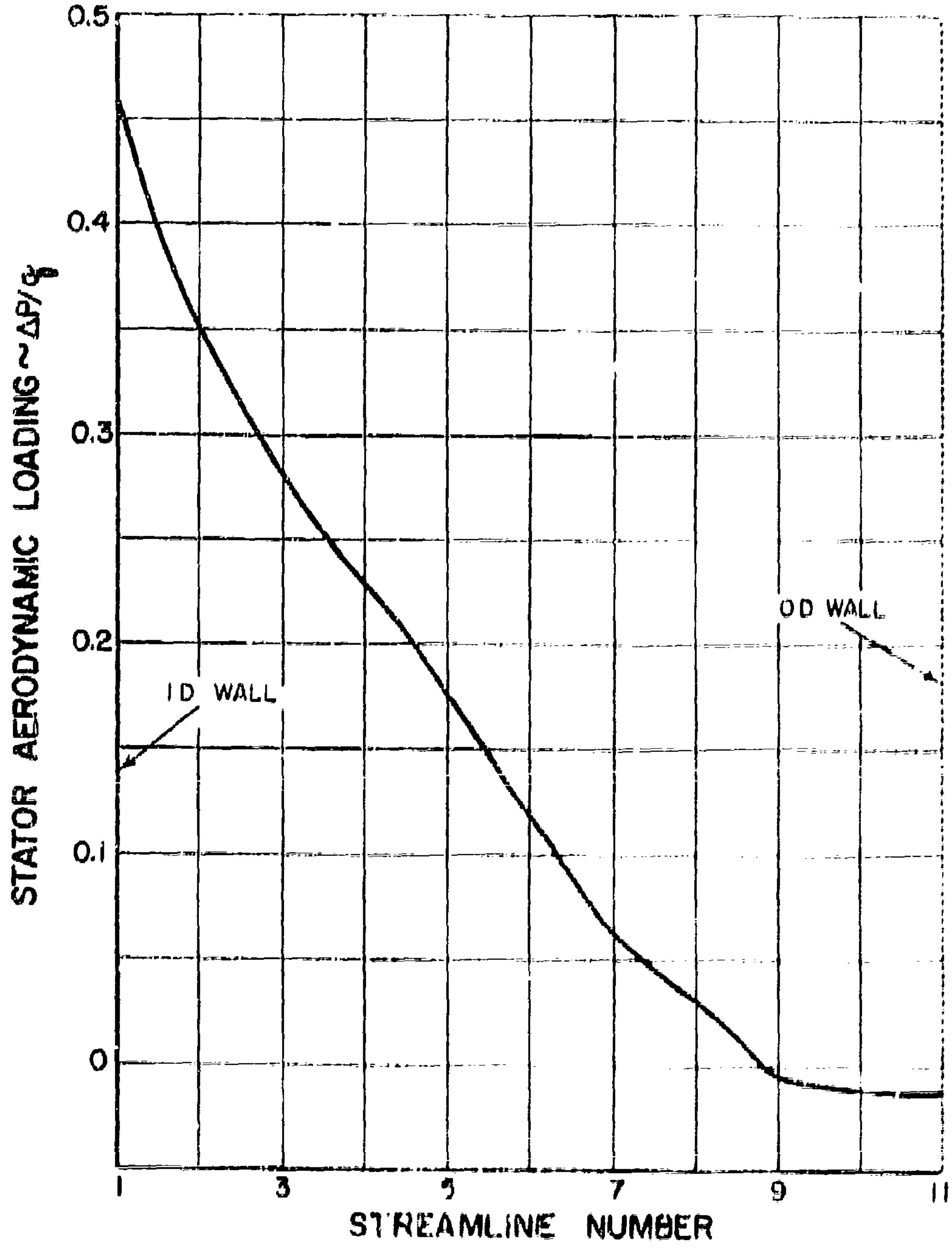

STF219 FAN AERODYNAMIC DESIGN STAGE ONE STATOR AERODYNAMIC LOADING (ΔP/q)

Figure 2A-13

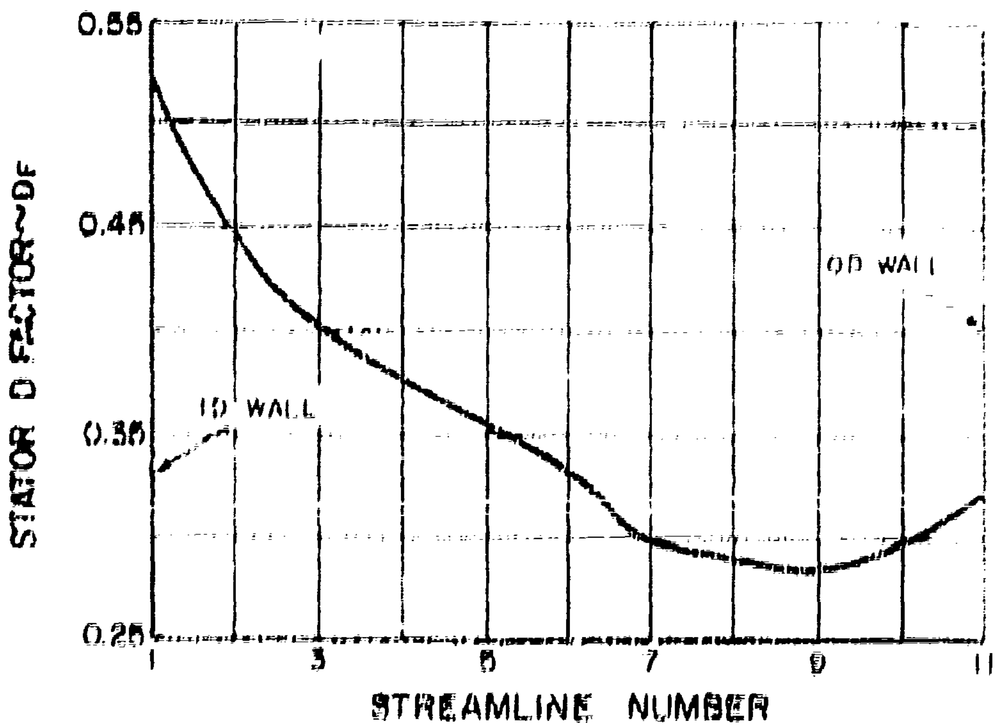

STF 219 FAN AERODYNAMIC DESIGN STAGE ONE STATOR "D" FACTOR

Figure 2A-14

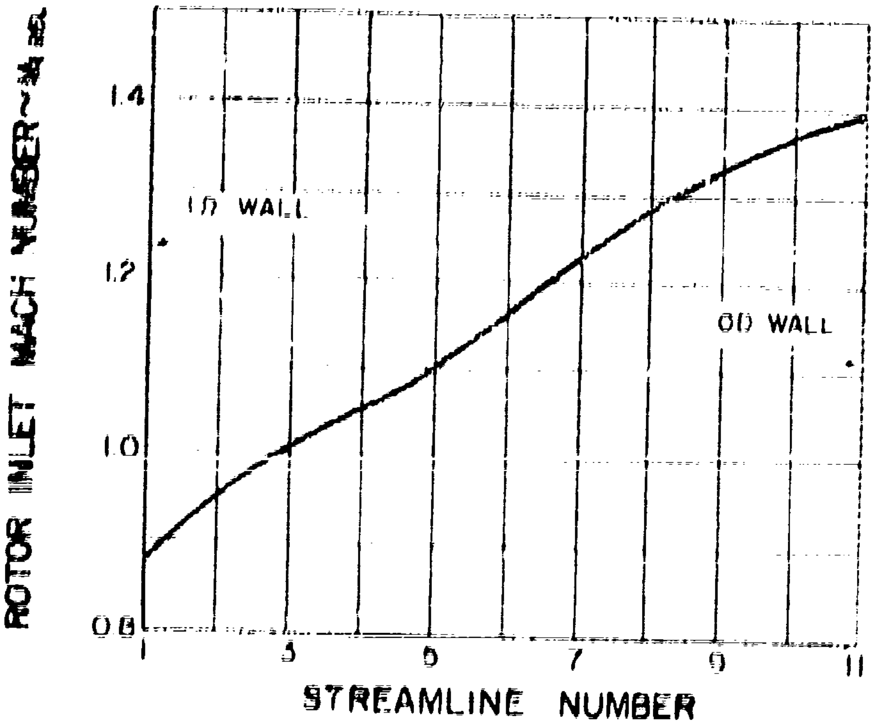

STF 219 FAN AERODYNAMIC DESIGN STAGE TWO ROTOR INLET MACH NUMBER

Figure 2A-15

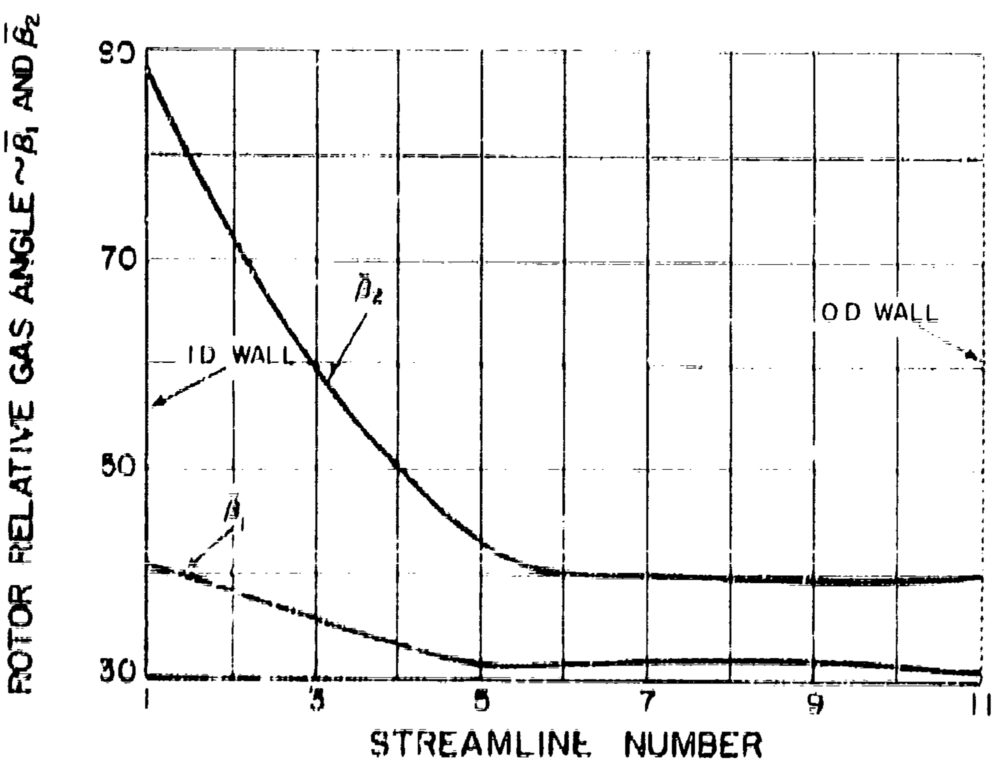

STF 219 FAN AERODYNAMIC DESIGN STAGE TWO ROTOR RELATIVE GAS ANGLES

Figure 3A-16

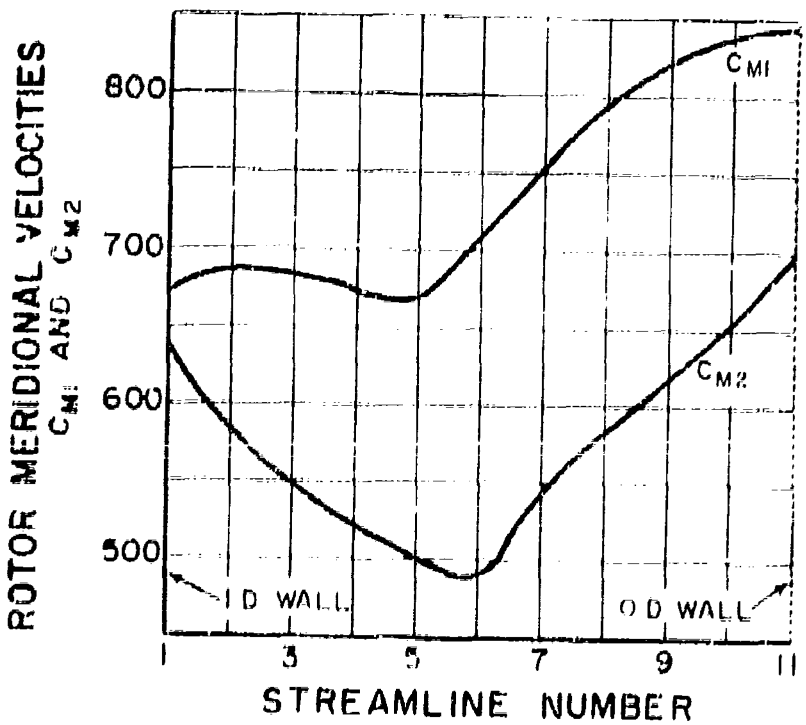

STF219 FAN AERODYNAMIC DESIGN STAGE 1 ROTOR MERIDIONAL VELOCITIES

Figure 6.2A-17

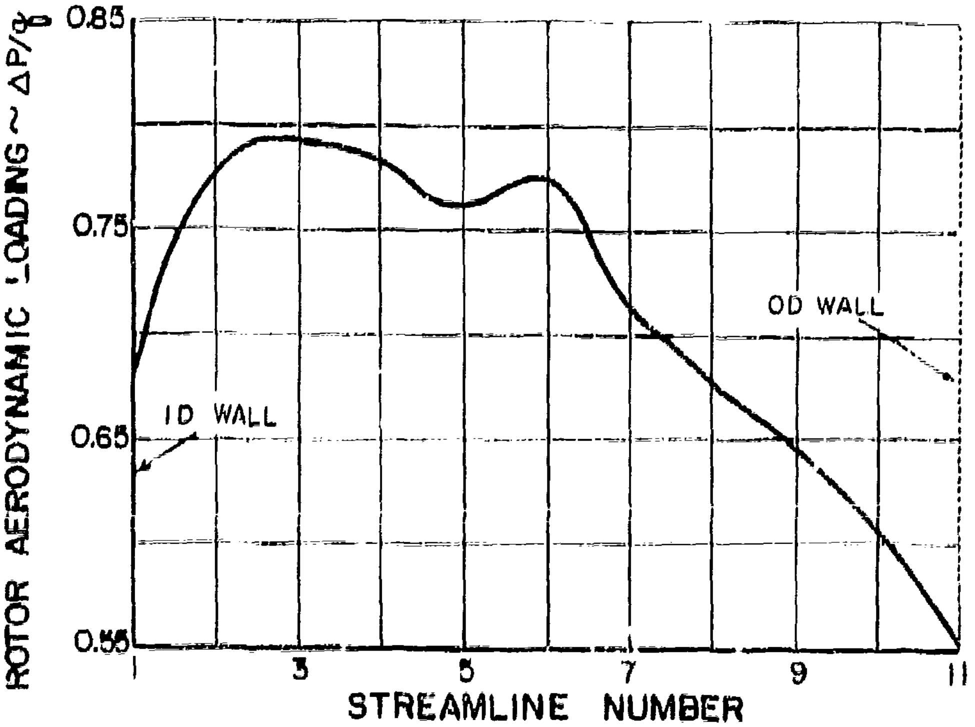

STF219 FAN AERODYNAMIC DESIGN STAGE TWO ROTOR AERODYNAMIC LOADING ΔP/q

Figure 2A-18

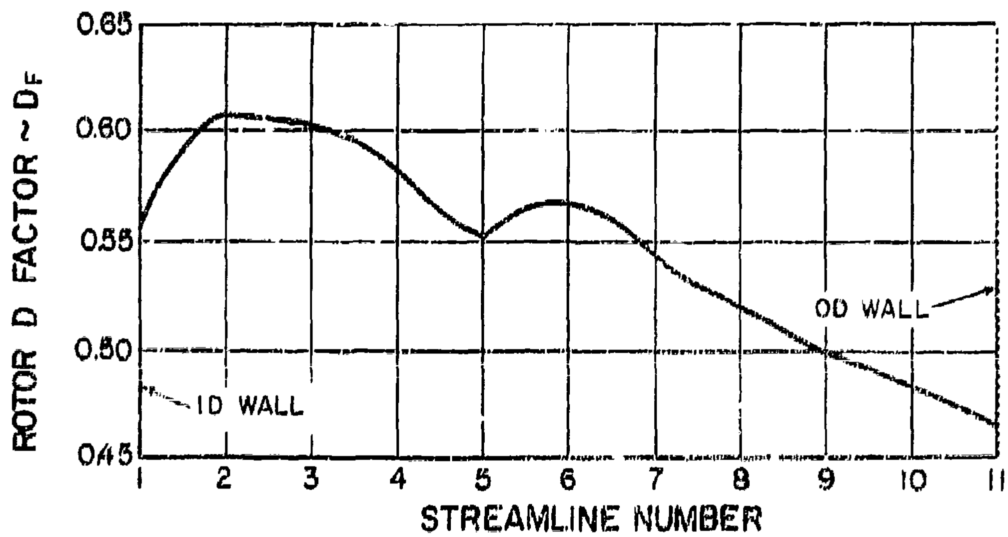

STF219 FAN AERODYNAMIC DESIGN STAGE TWO ROTOR "D" FACTORS

Figure 2A-19

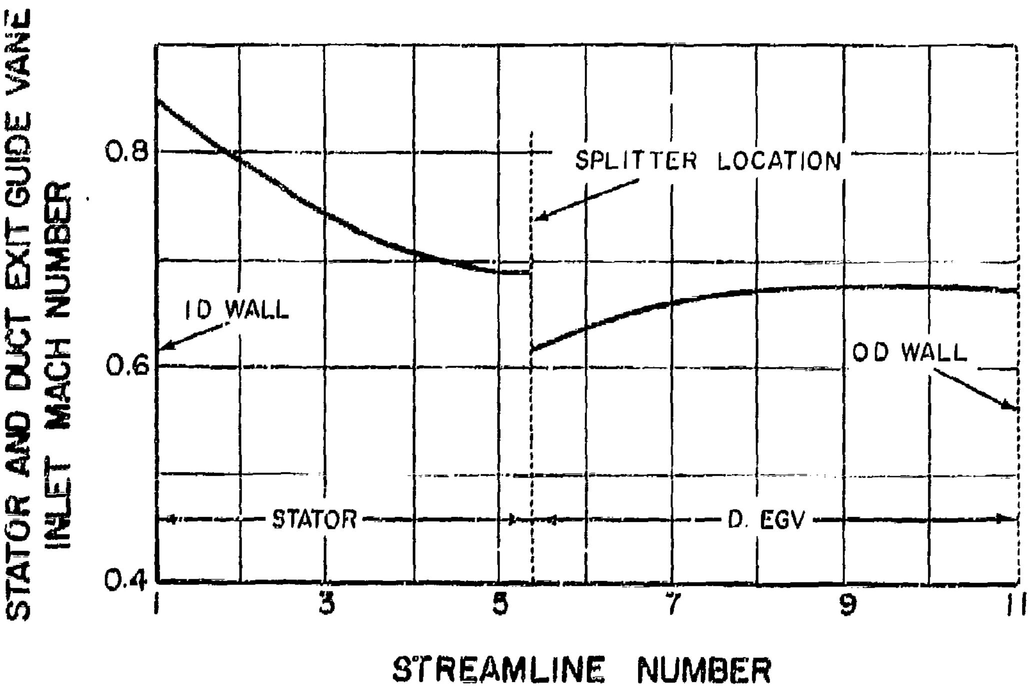

STF219 FAN AERODYNAMIC DESIGN STAGE TWO STATOR AND DEGV INLET MACH NUMBER

Figure 2A-20

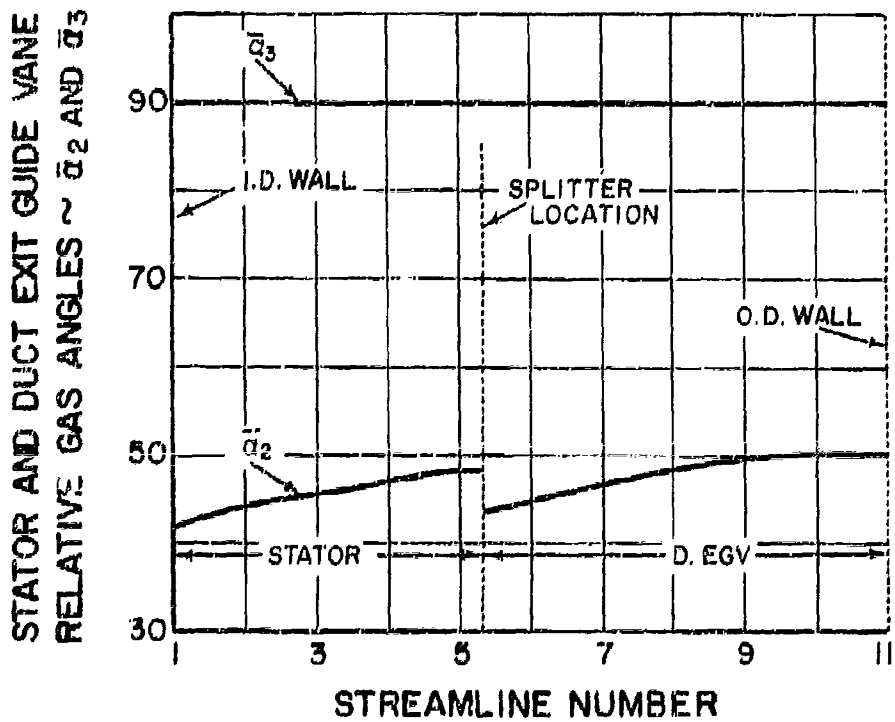

STF219 FAN AERODYNAMIC DESIGN STAGE TWO STATOR AND DEGV RELATIVE GAS ANGLES

Figure 2A-21

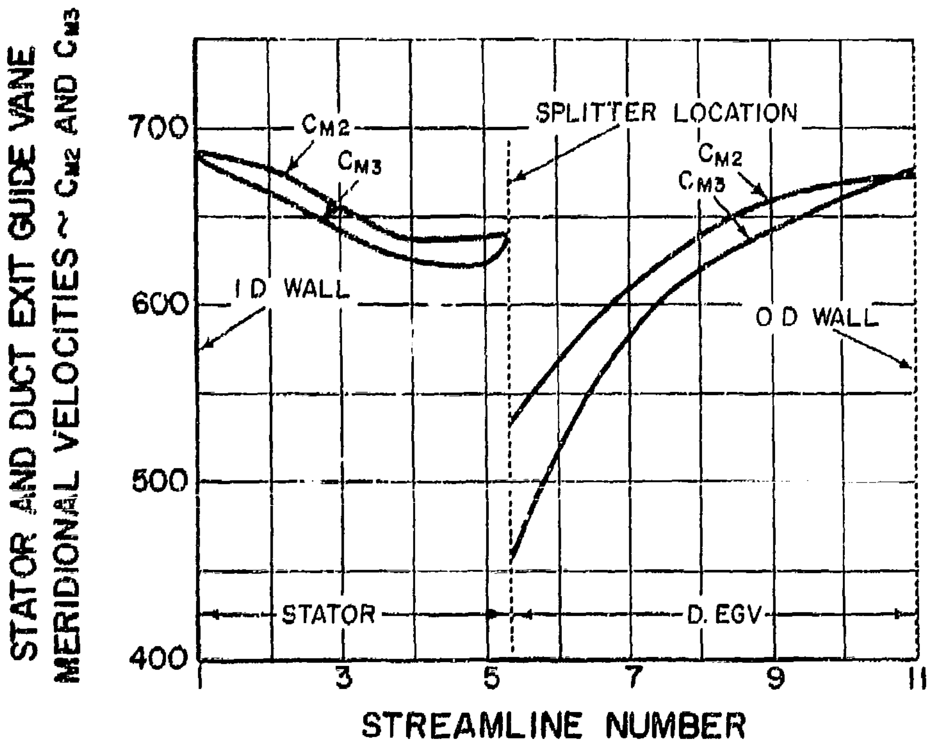

STF219 FAN AERODYNAMIC DESIGN STAGE TWO STATOR AND DEGV MERIDIONAL VELOCITIES

Figure 2A-22

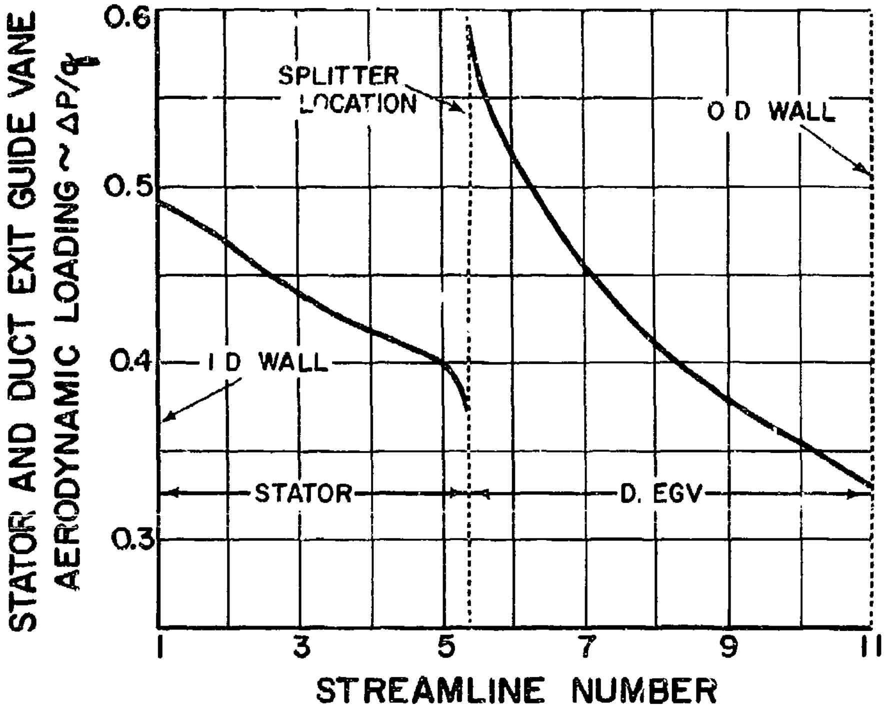

STF219 FAN AERODYNAMIC DESIGN STAGE TWO STATOR ANL DEGV AERODYNAMIC LOADING

Figure 2A-23

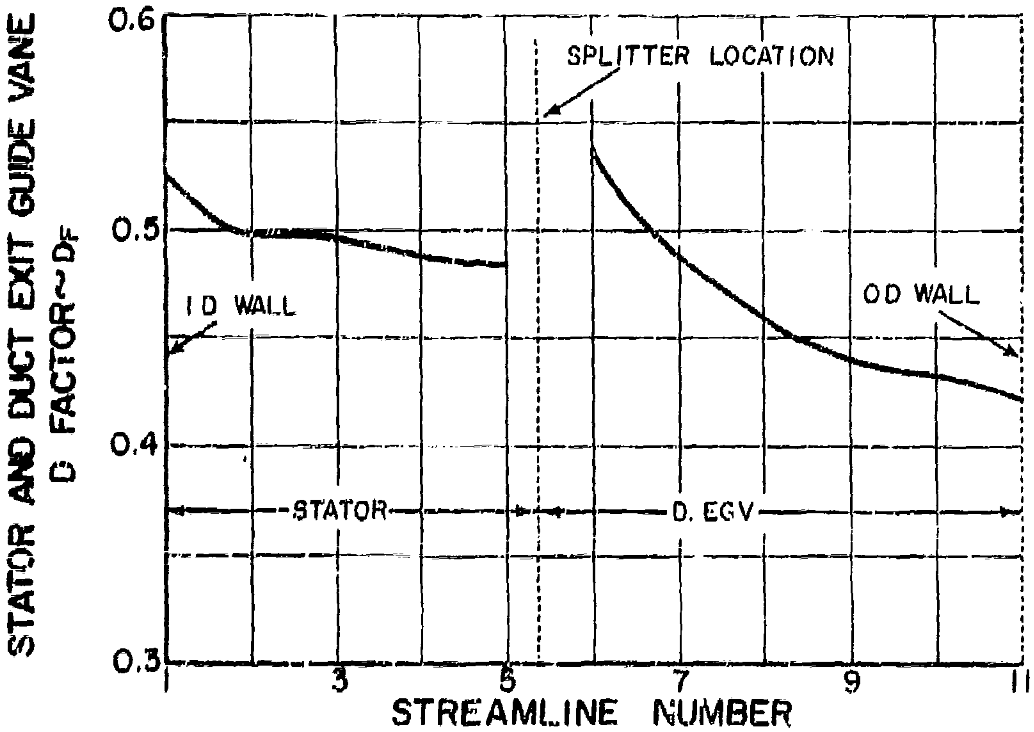

STF219 FAN AERODYNAMIC DESIGN STAGE TWO STATOR AND DEGV "D" FACTOR

Figure 2A-24

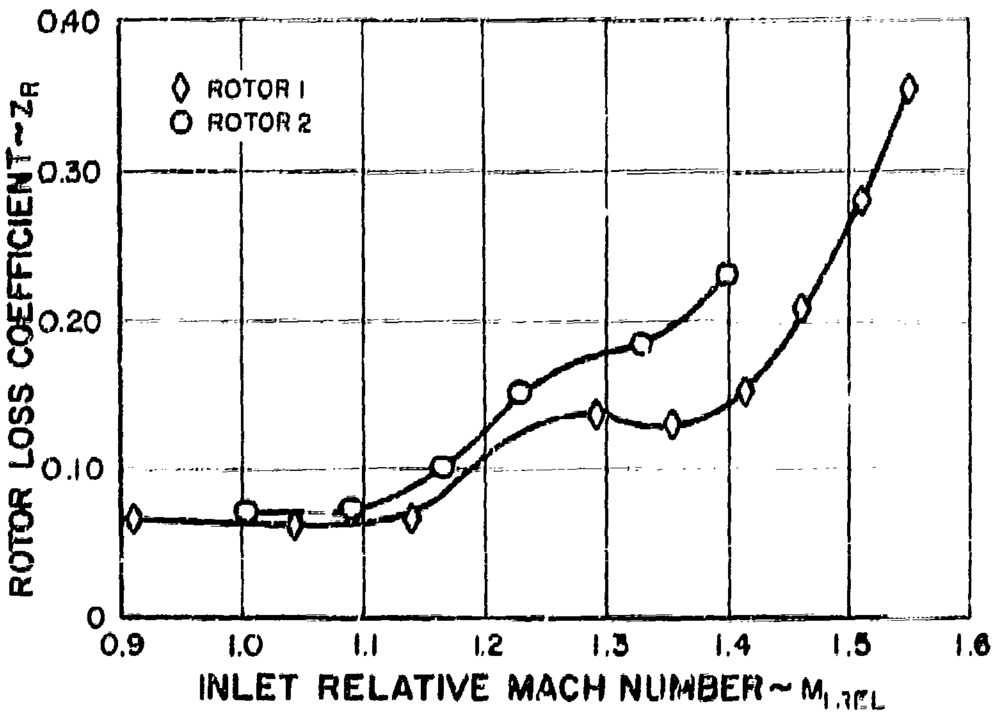

STF219 FAN AERODYNAMIC DESIGN ROTOR LOSS COEFFICIENT VS. INLET RELATIVE MACH NUMBER

Figure 2A-25

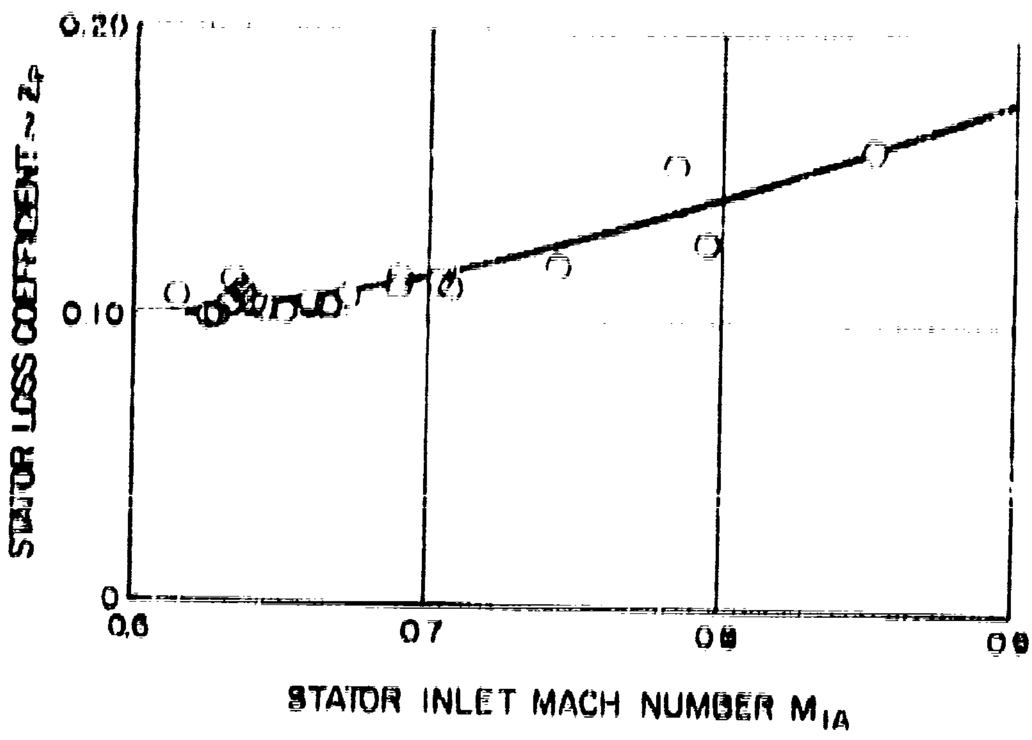

STF219 FAN AERODYNAMIC DESIGN STATOR LOSS COEFFICIENT VS. STATOR INLET MACH NUMBER

Figure 7A-26

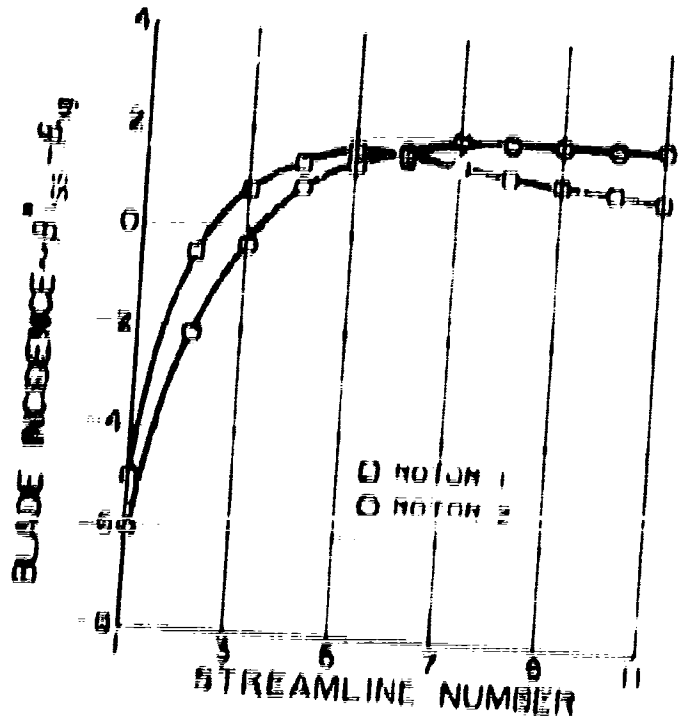

JTF 219 FAN AERODYNAMIC DESIGN ROTOR INCIDENCE

Figure 2A-27

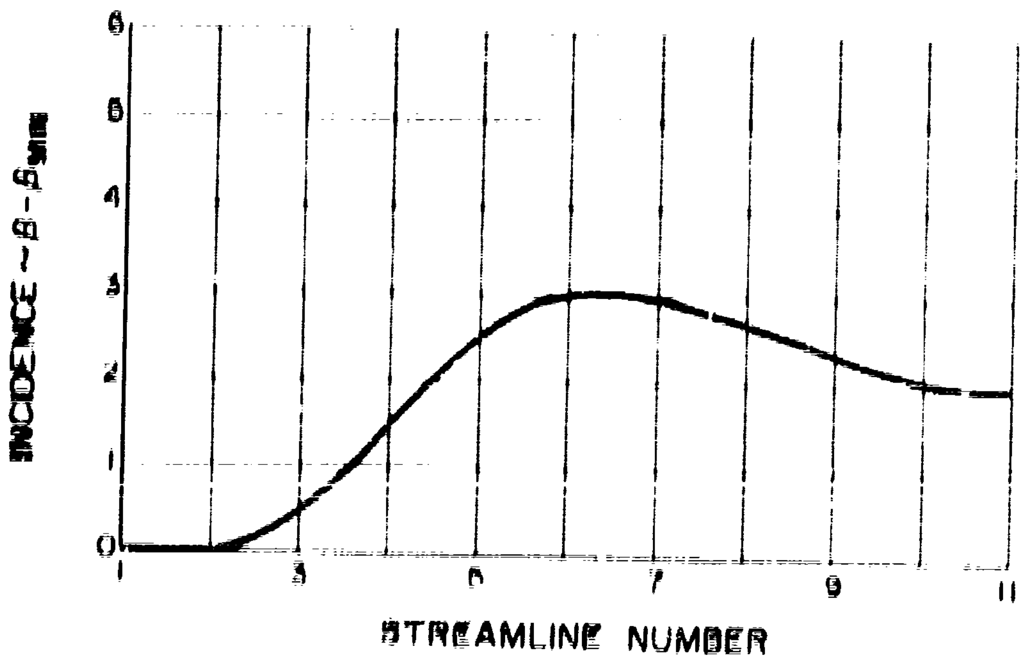

STF219 FAN AERODYNAMIC STATOR ONE INCIDENCE - DIFFERENCE BETWEEN GAS ANGLE AND MINIMUM LOSS ANGLE

Figure [illegible]

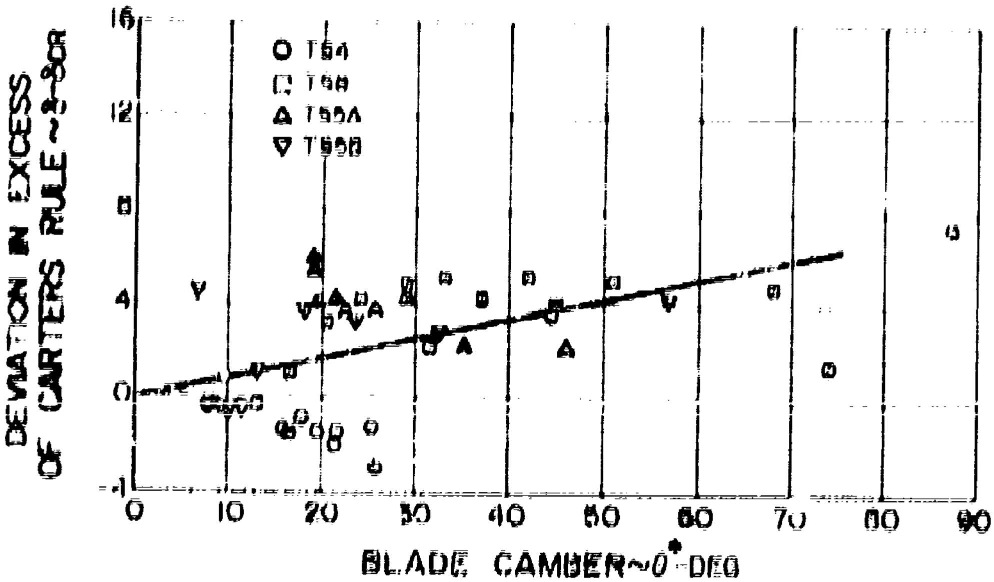

STF 219 FAN AERODYNAMIC DEVIATION IN EXCESS OF CARTER'S RULE VS BLADE CAMBER*

Figure AA-29

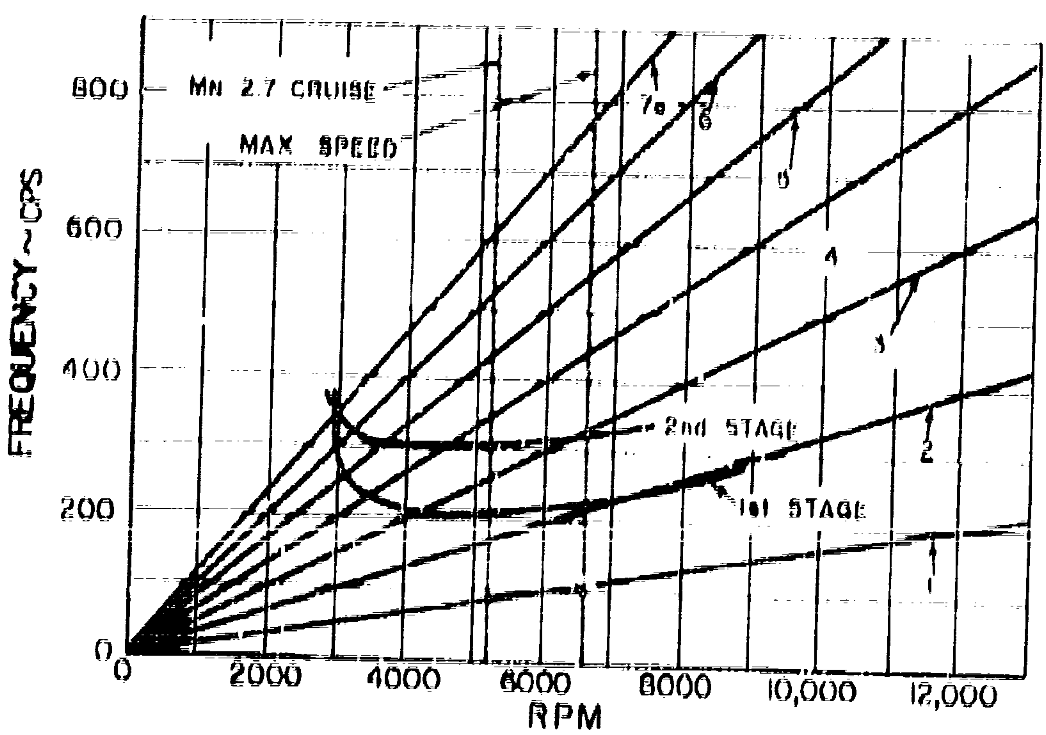

STF219 FAN RESONANCE DIAGRAMS

Figure 2A-10

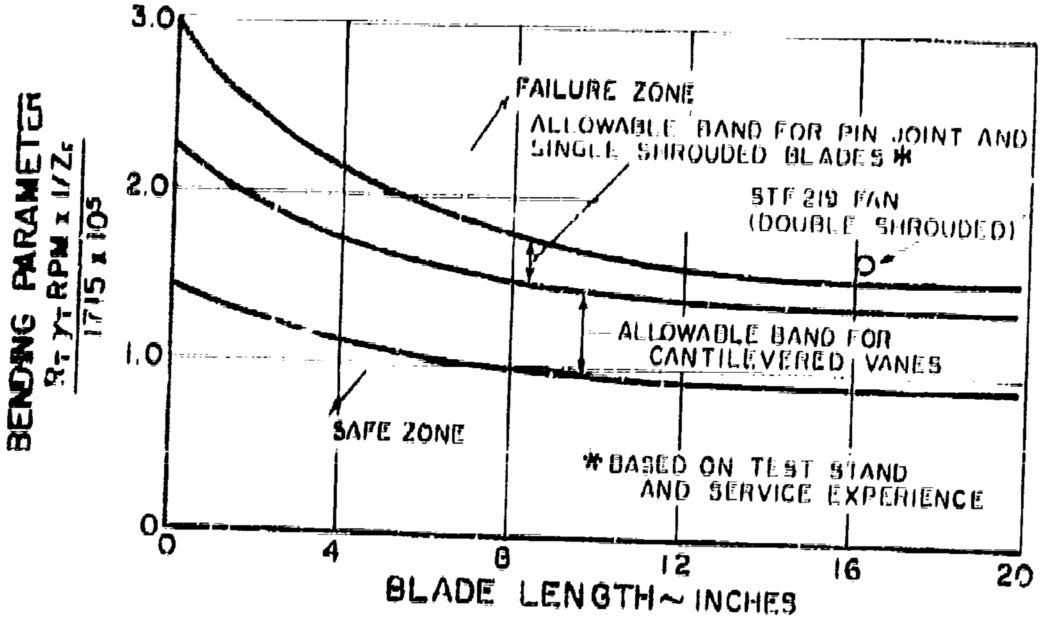

BLADE INGESTION PARAMETER VS. BLADE LENGTH

Figure 6A-11

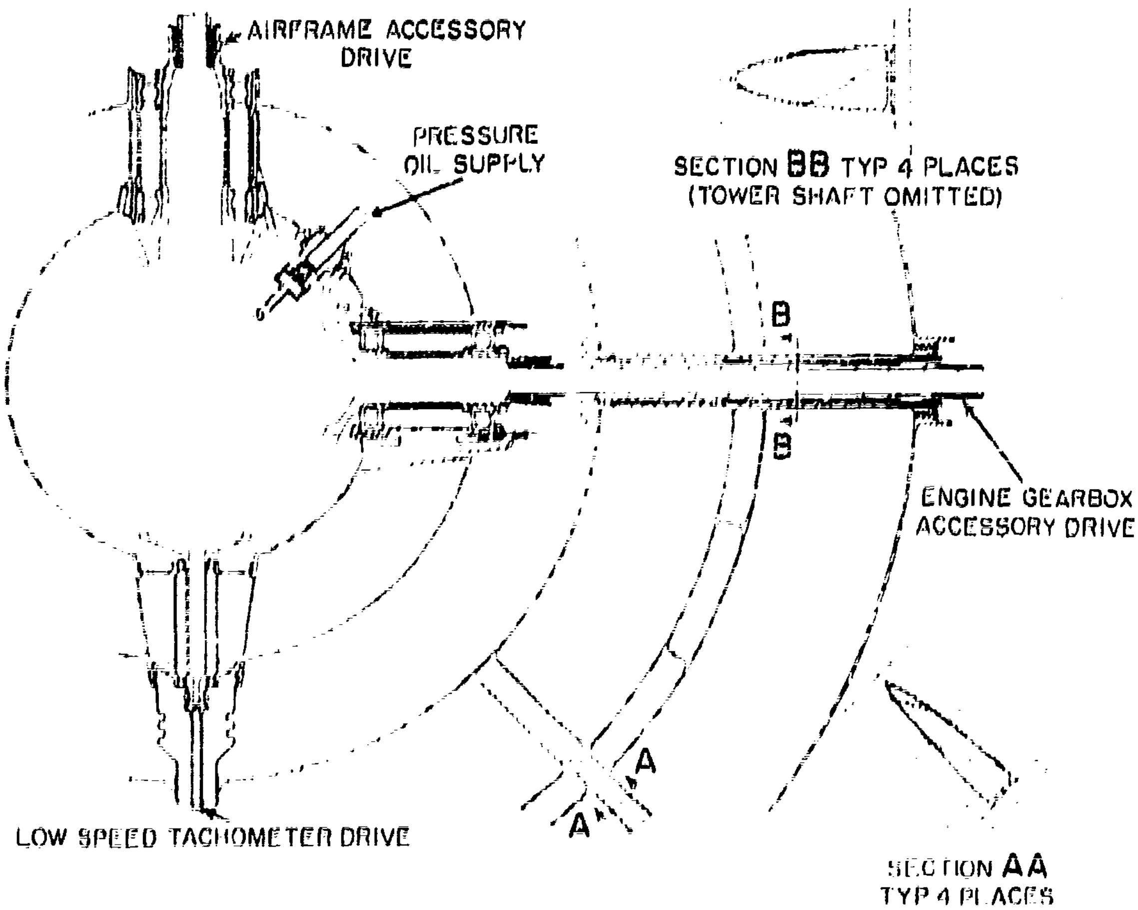

INTERMEDIATE CASE AND ACCESSORY DRIVE ARRANGEMENT (LOOKING AFT)

Figure 2A-12

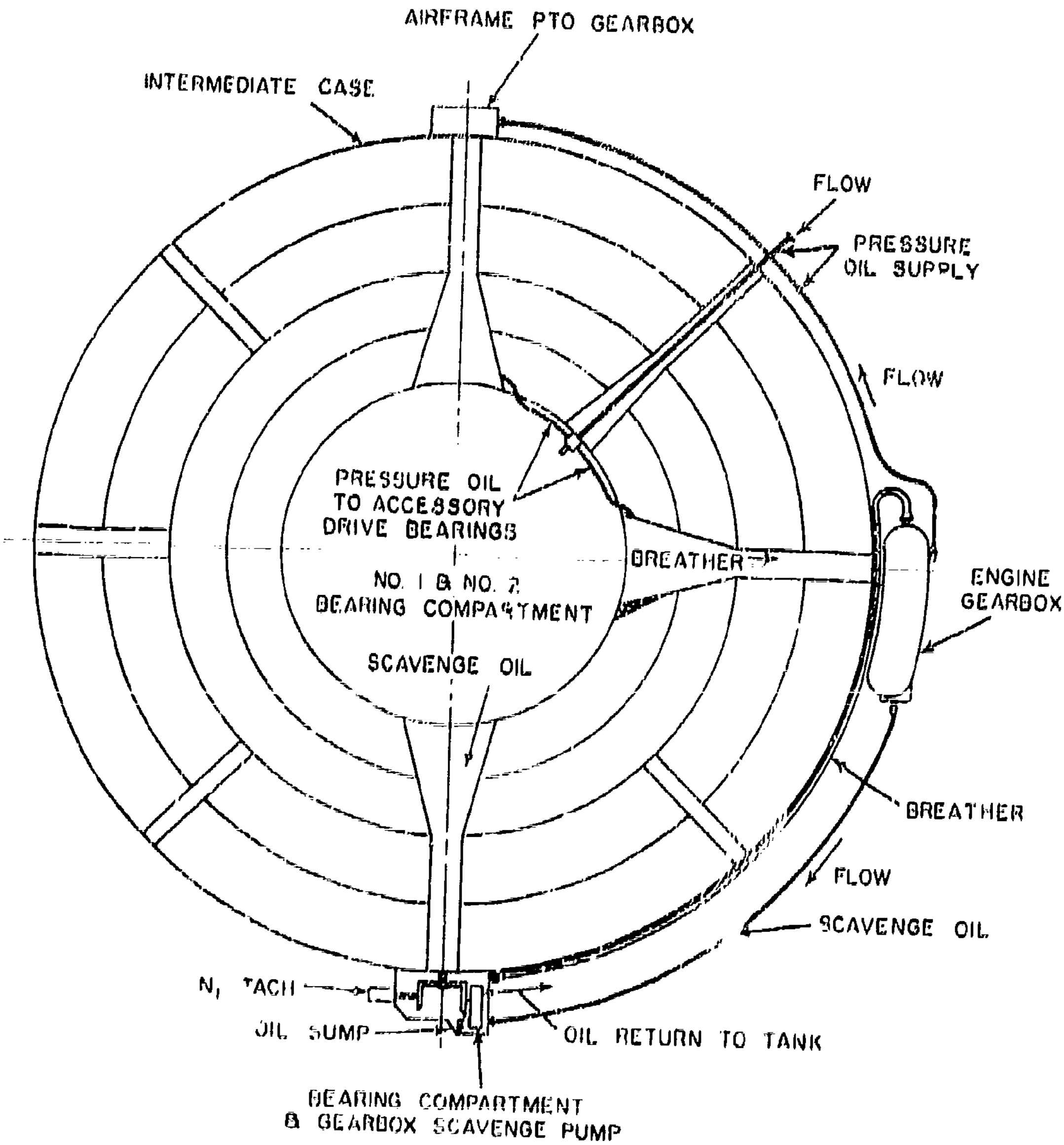

NO. 1 AND NO. 2 BEARING COMPARTMENT OILING AND SCAVENGE SCHEMATIC

Figure 2A-33

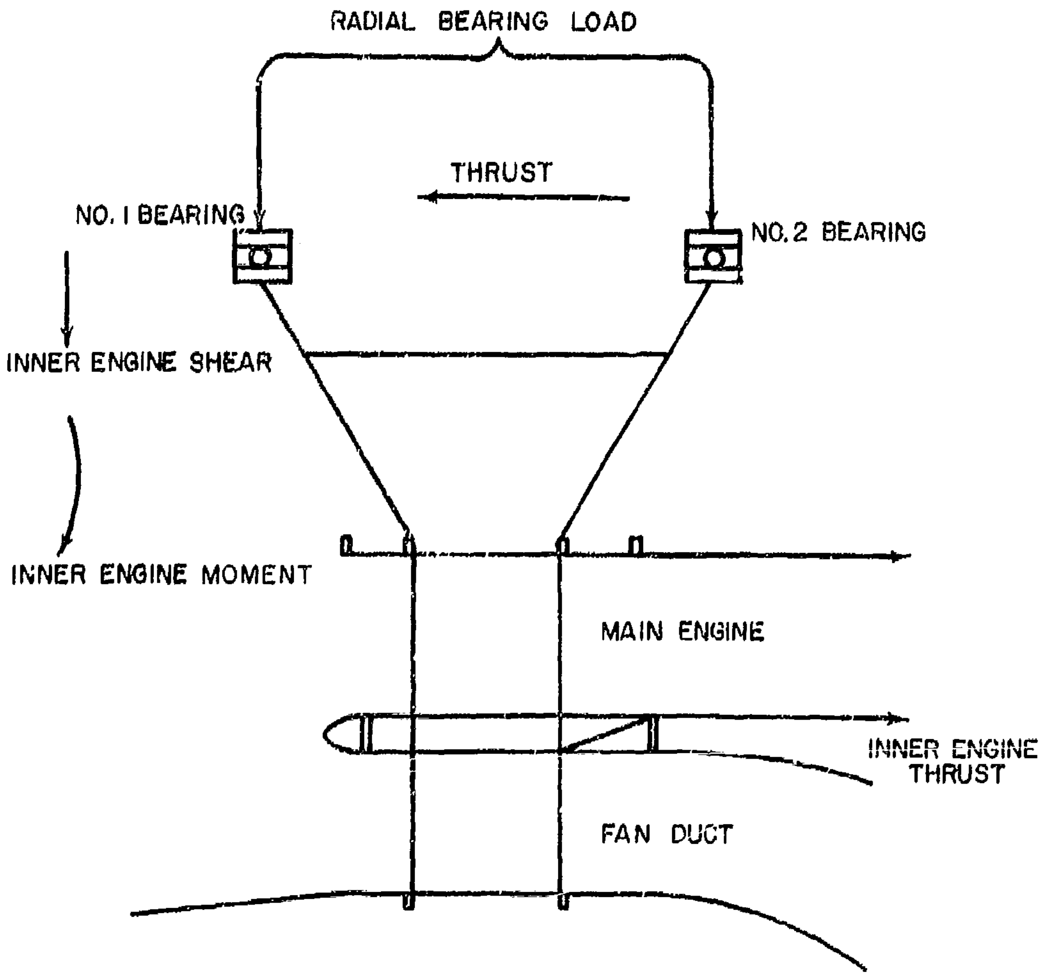

THE INTERMEDIATE CASE IS SUBJECTED TO THE LOADING SHOWN ABOVE
LOADS ARE INTRODUCED BY THE THRUST AND RADIAL LOAD OF THE Ist AND 2nd BEARINGS, THE CANTILEVERED INNER ENGINE, AND TANGENTIAL GAS LOADING OF THE STRUTS

INTERMEDIATE CASE LOADING

Figure 2A-34

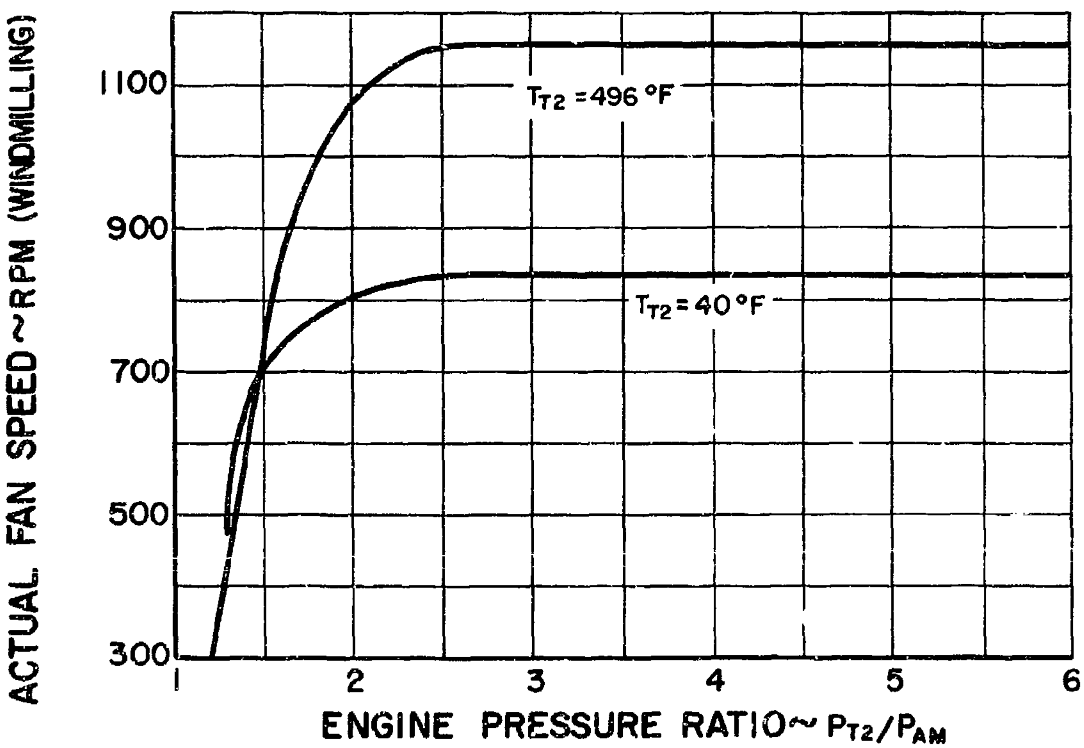

STF219 WINDMILLING PREDICTED FAN SPEED WHEN COMPRESSOR ROTATES AT CONSTANT 2000 RPM

Figure 2A-35

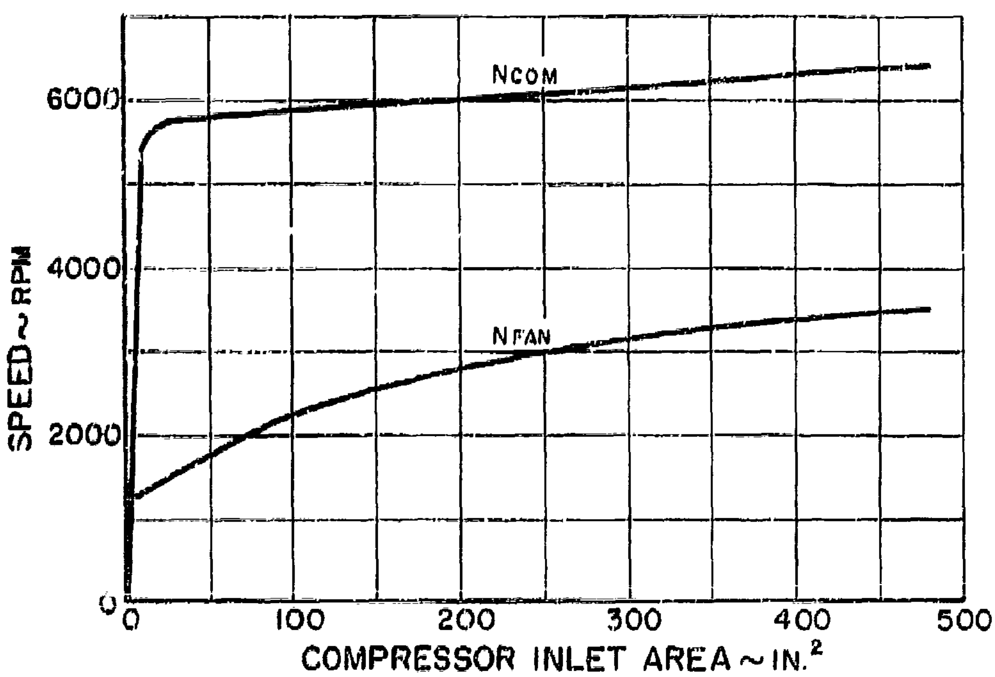

STF219 1900°F TURBOFAN AT Mn - 2.7 AT 65,000 FEET - ESTIMATED WINDMILLING SPEED

Figure 2A-36

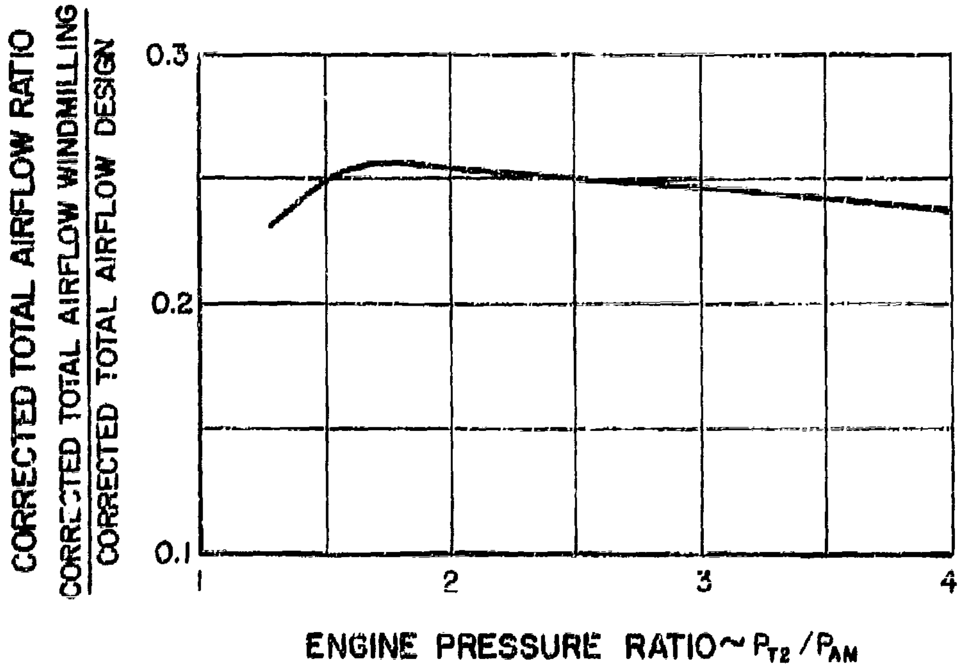

STF219 1900°F TURBOFAN CORRECTED TOTAL AIRFLOW RATIO FOR A COMPRESSOR INLET AREA WHICH VARIES TO MAINTAIN 2000 RPM

Figure 2A-37

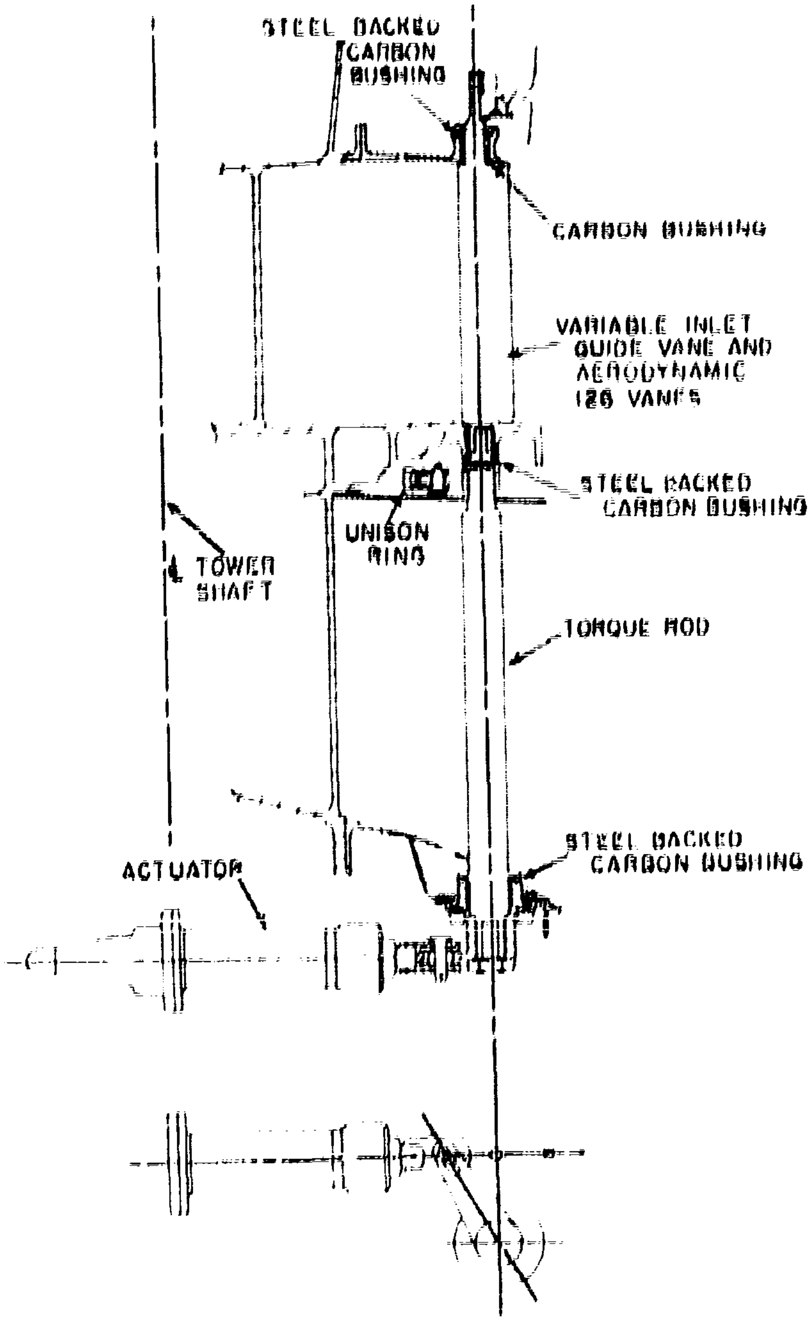

STF219 VARIABLE INLET GUIDE VANE AND AERODYNAMIC BRAKE

Figure 2A-38

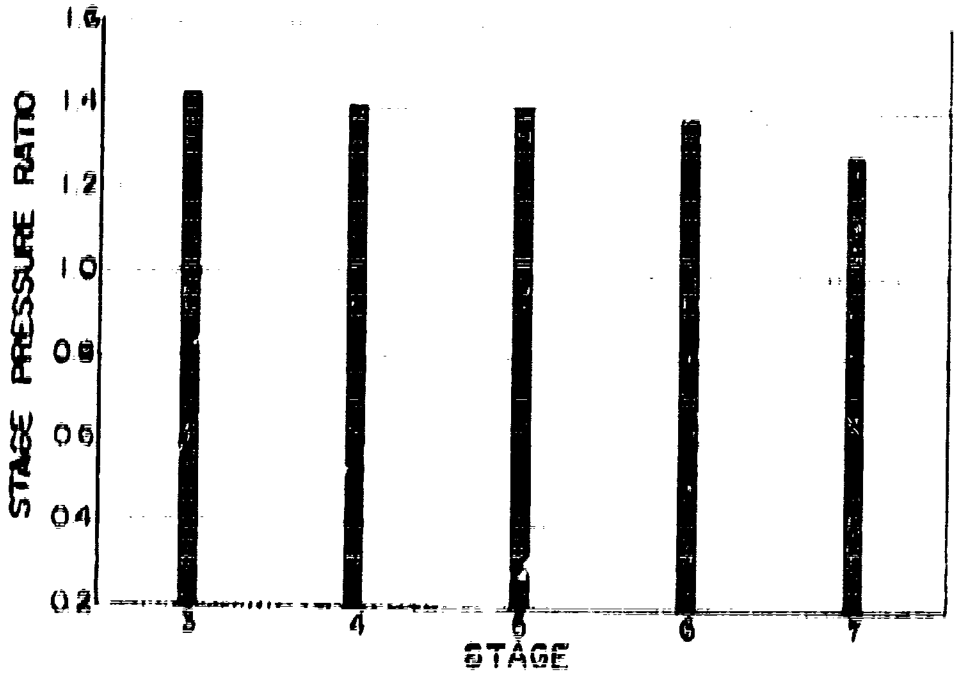

STF219 HIGH PRESSURE COMPRESSOR STAGE PRESSURE RATIO DISTRIBUTION

Figure 2A-39

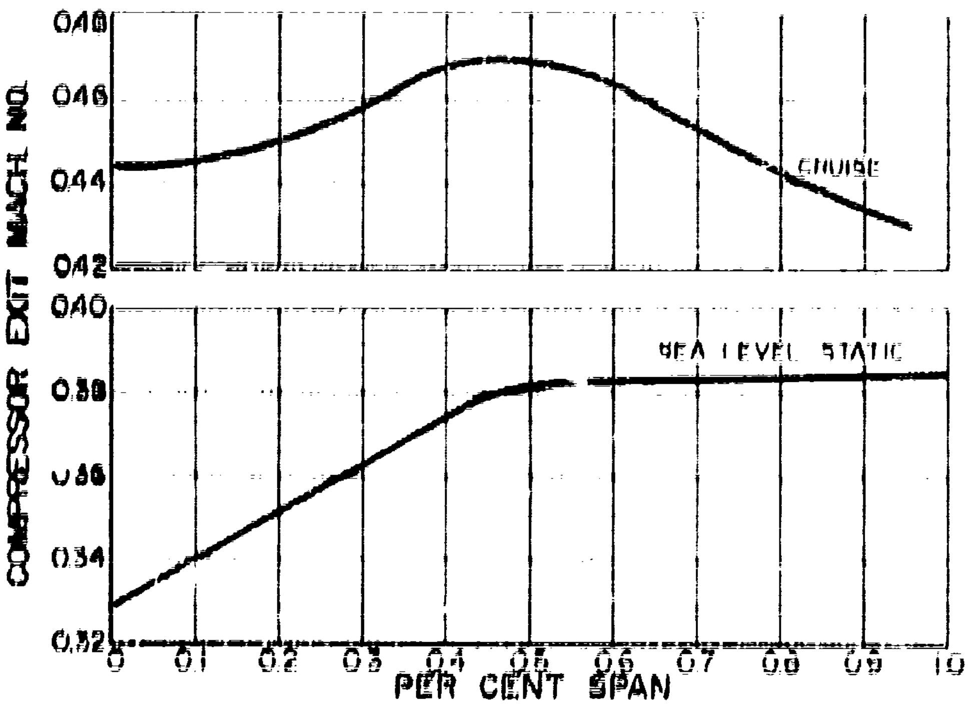

STF219 HIGH PRESSURE COMPRESSOR EXIT PROFILES

Figure 2A-40

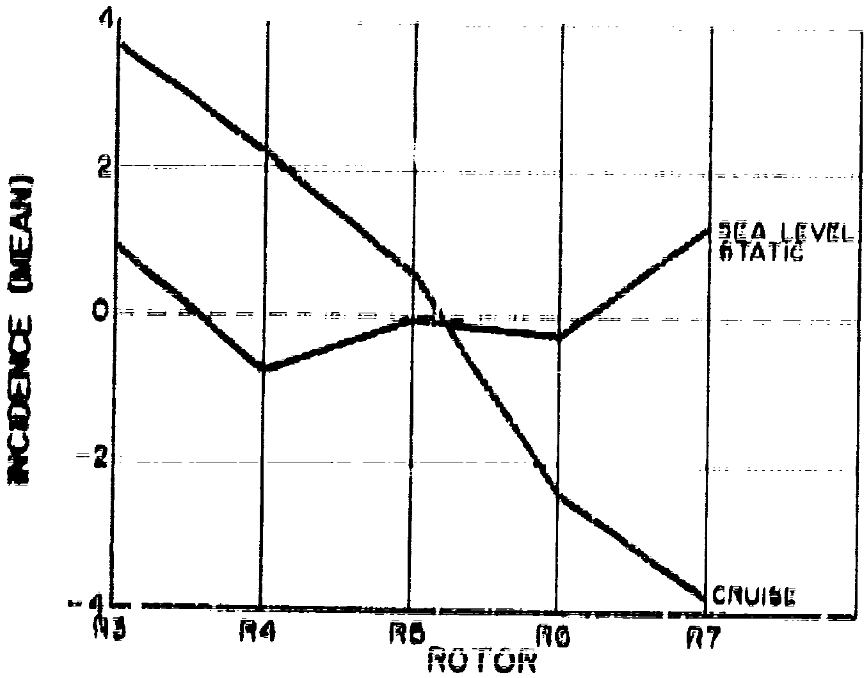

STF219 MID-SPAN INCIDENCES AT PART SPEED AND FULL SPEED

Figure 2A-41

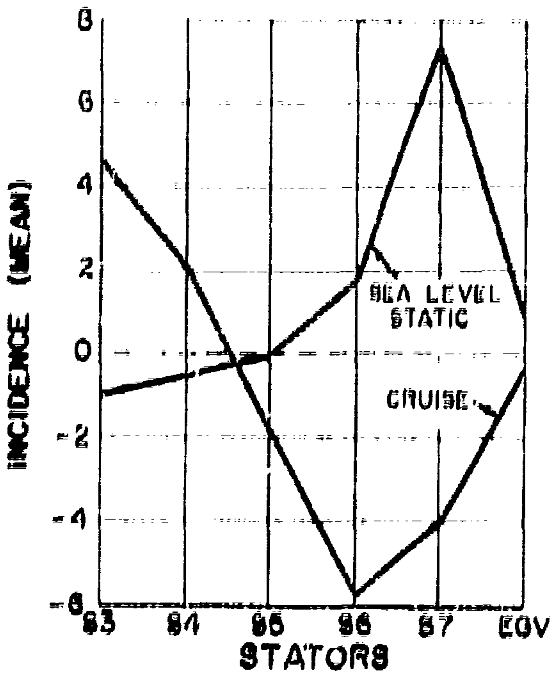

STF219 MID-SPAN INCIDENCES AT PART SPEED AND FULL SPEED

Figure 2A-42

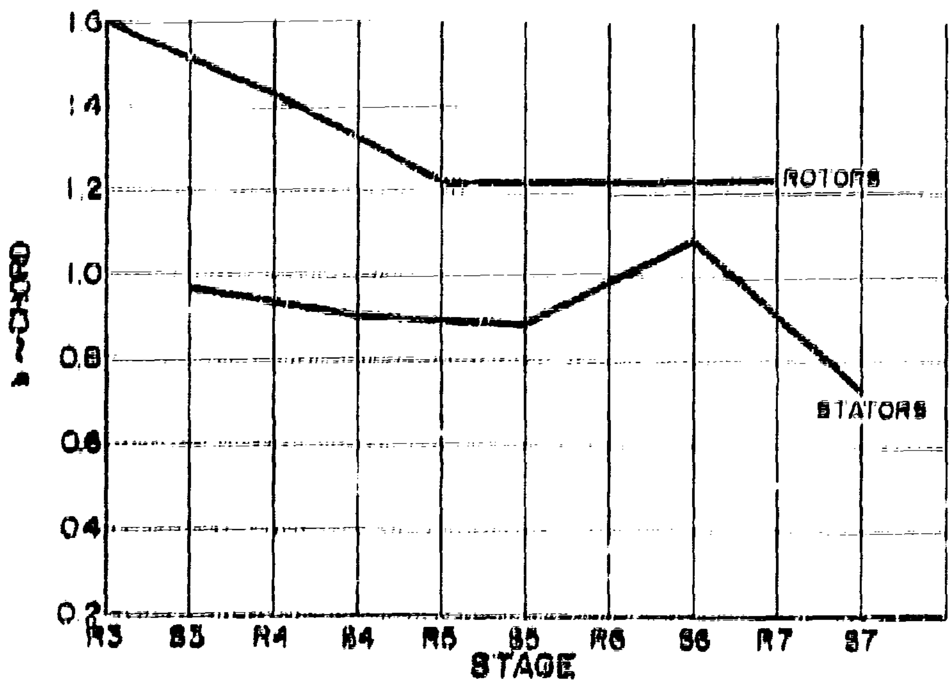

STF219 COMPRESSOR FINAL CHORD SELECTION

Figure 2A-43

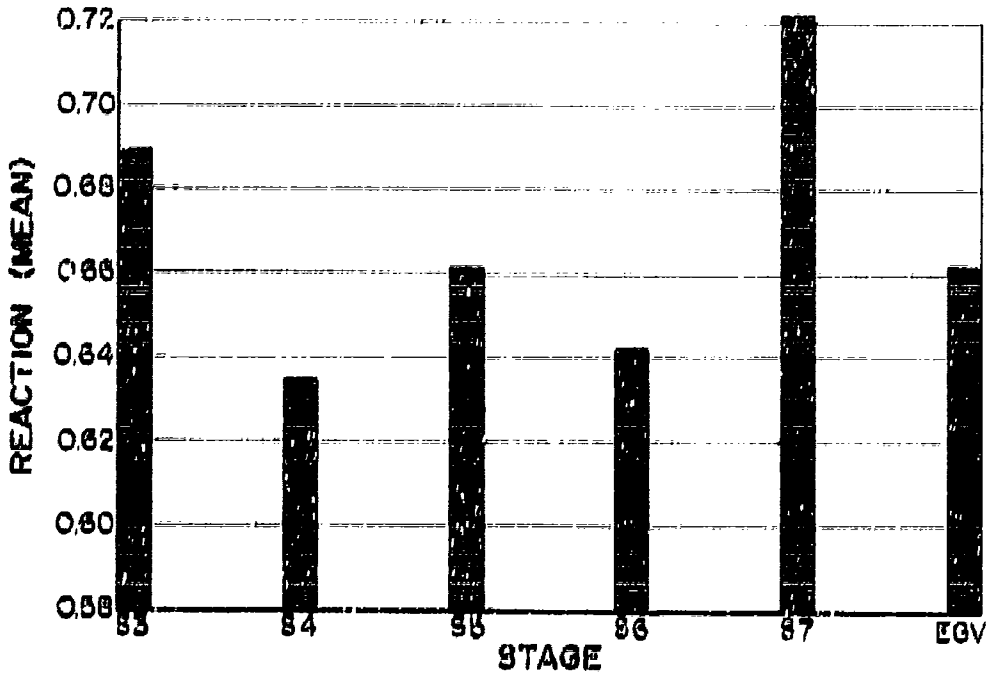

STF219 STAGE REACTION DISTRIBUTION

Figure 2A-44

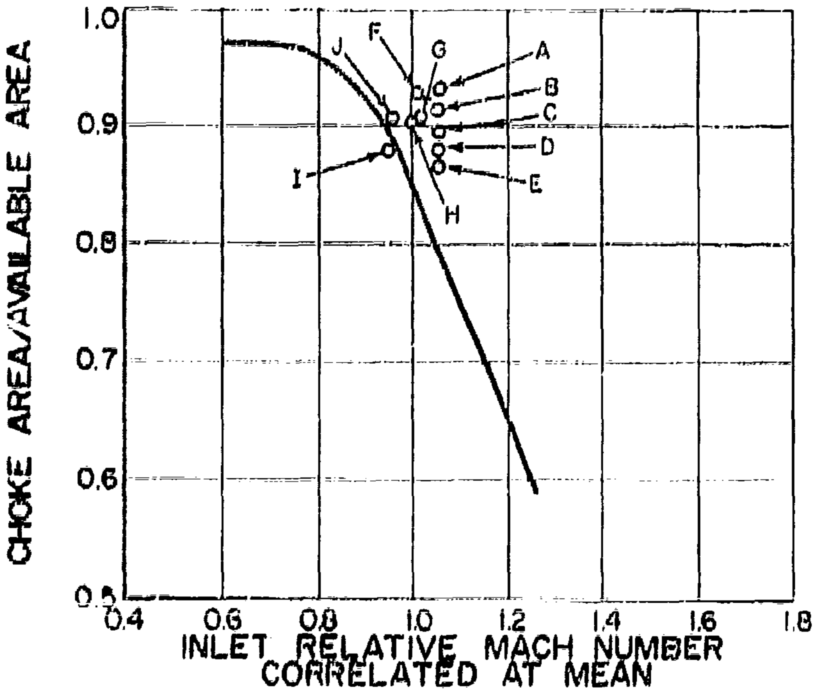

STF219 HIGH PRESSURE COMPRESSOR CHOKE PARAMETERS

Figure 2A-45

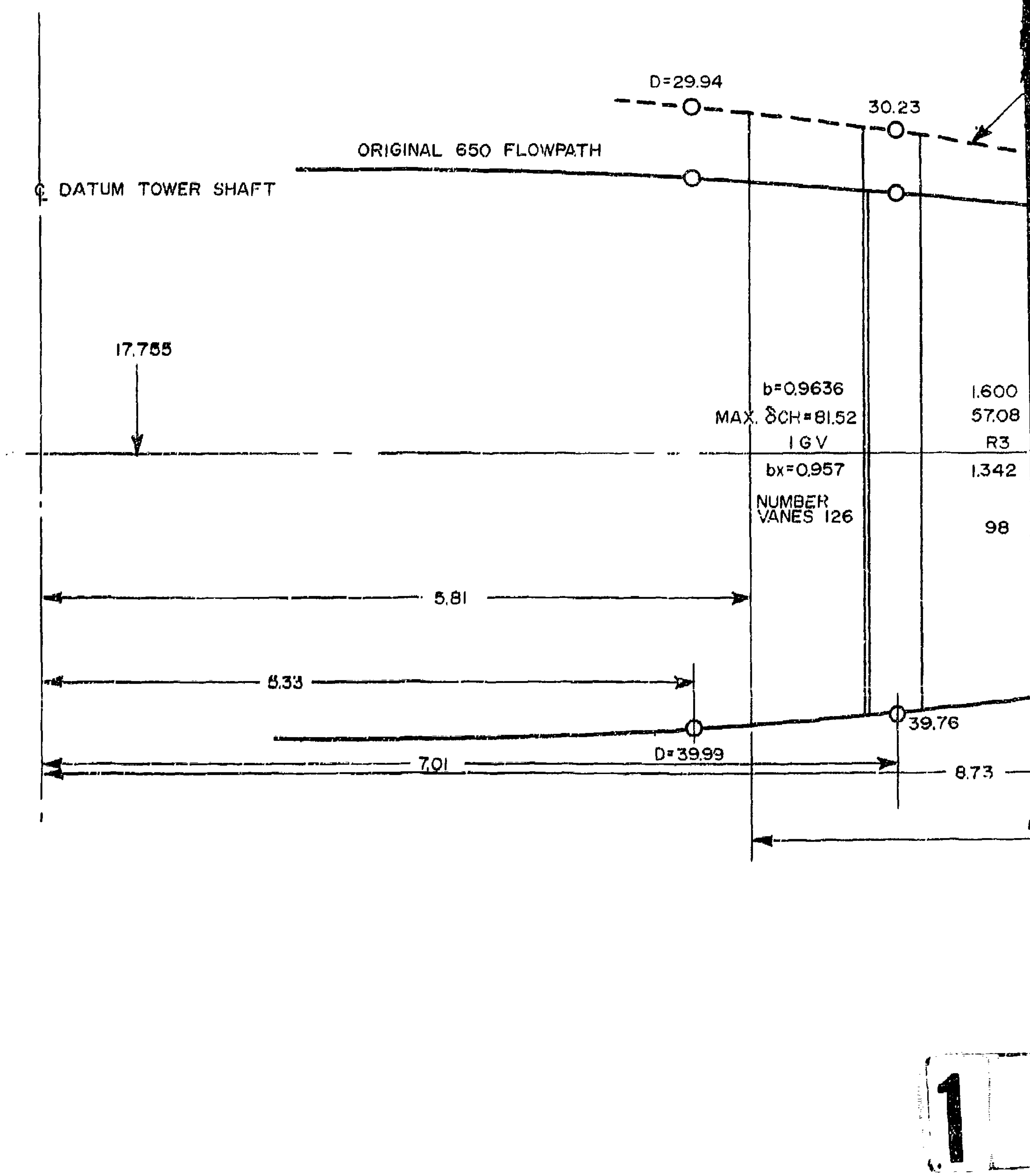
D=29.94
30.23
ORIGINAL 650 FLOWPATH
℄ DATUM TOWER SHAFT
17.755
b=0.9636
MAX. δCH=81.52
IGV
bx=0.957
NUMBER VANES 126
1.600
57.08
R3
1.342
98
5.81
6.33
39.76
D=39.99
7.01
8.73
1

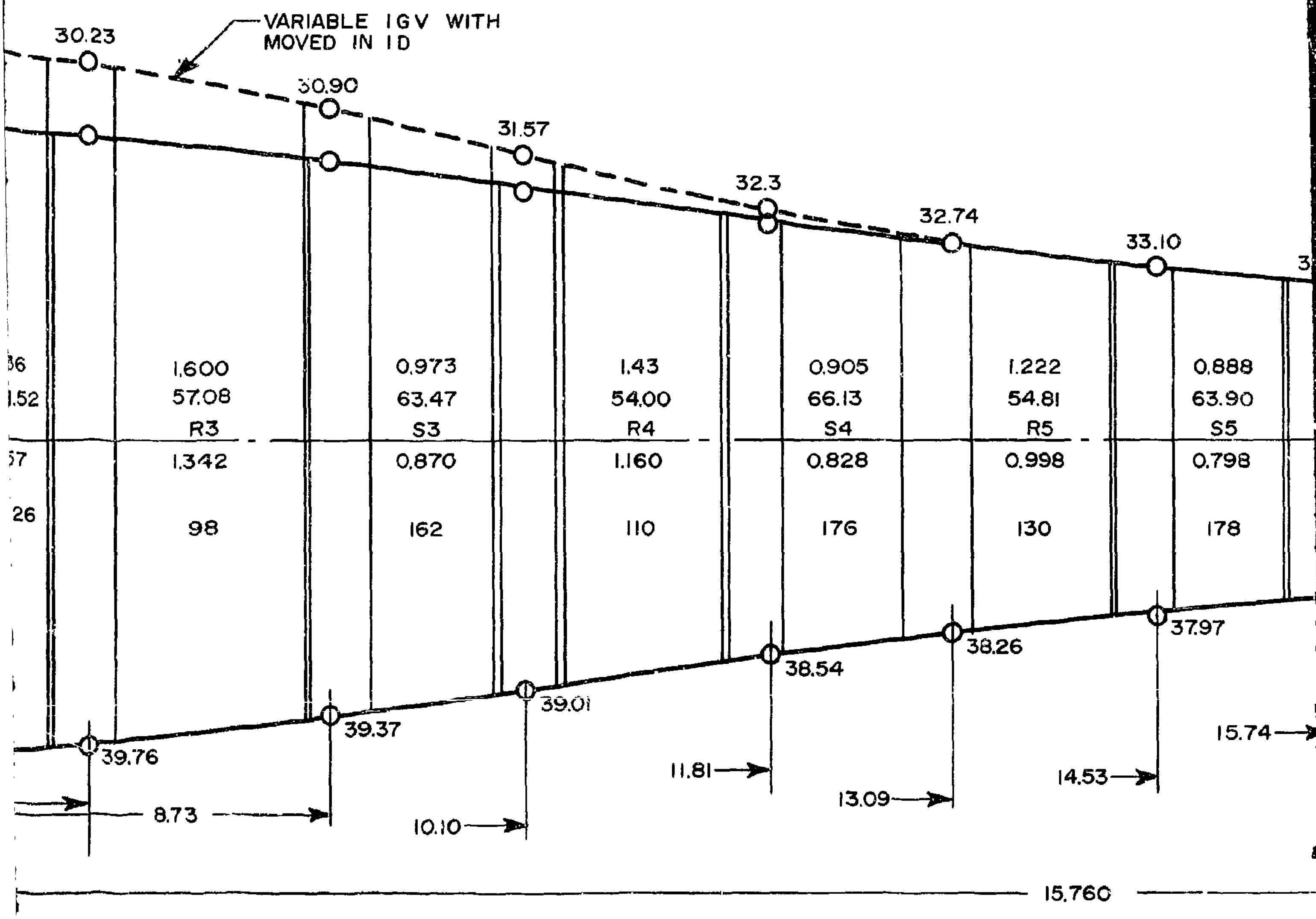

VARIABLE IGV WITH
MOVED IN ID
30.23
30.90
31.57
32.3
32.74
33.10
3
36
1.52
57
26
1.600
57.08
R3
1.342
98
0.973
63.47
S3
0.870
162
1.43
54.00
R4
1.160
110
0.905
66.13
S4
0.828
176
1.222
54.81
R5
0.998
130
0.888
63.90
S5
0.798
178
39.76
39.37
39.01
38.54
38.26
37.97
8.73
10.10
11.81
13.09
14.53
15.74
15.760

2

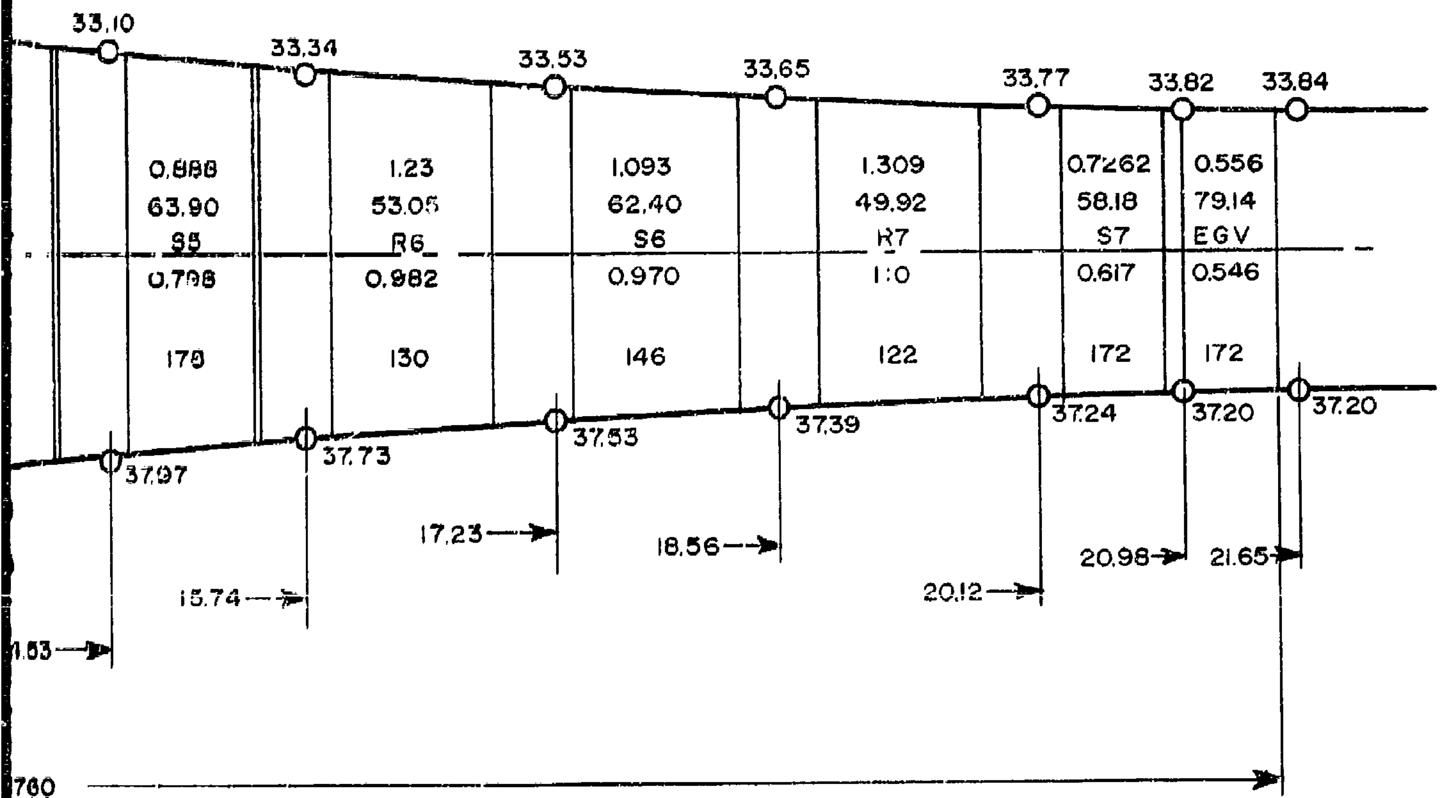

STF219 HIGH PRESSURE COMPRESSOR FLOW PATH

Figure 2A-46

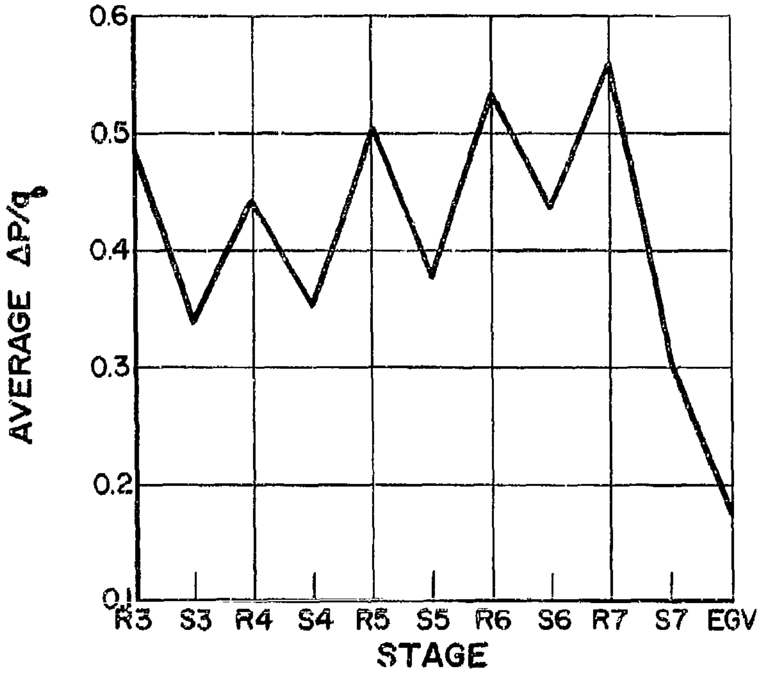

STF219 HIGH PRESSURE COMPRESSOR AERODYNAMIC LOADING ($\Delta P/q$)

Figure 2A-47

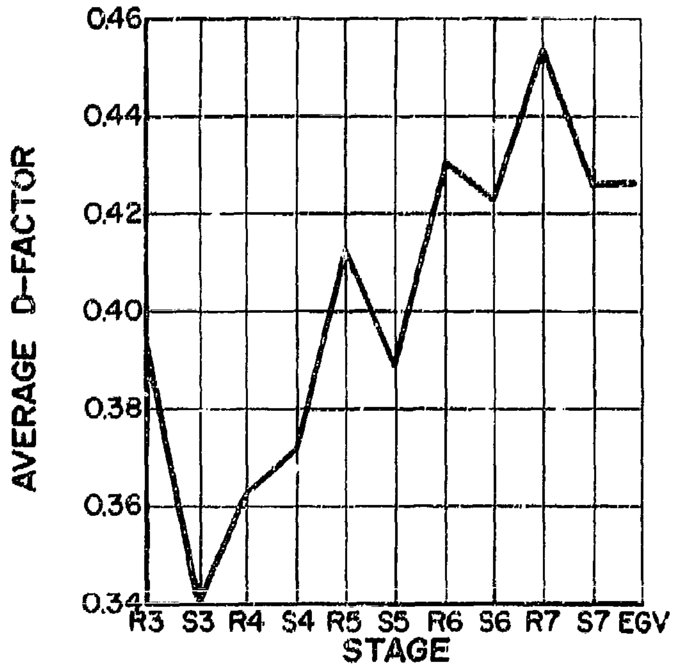

STF219 HIGH PRESSURE COMPRESSOR "D" FACTOR

Figure 2A-48

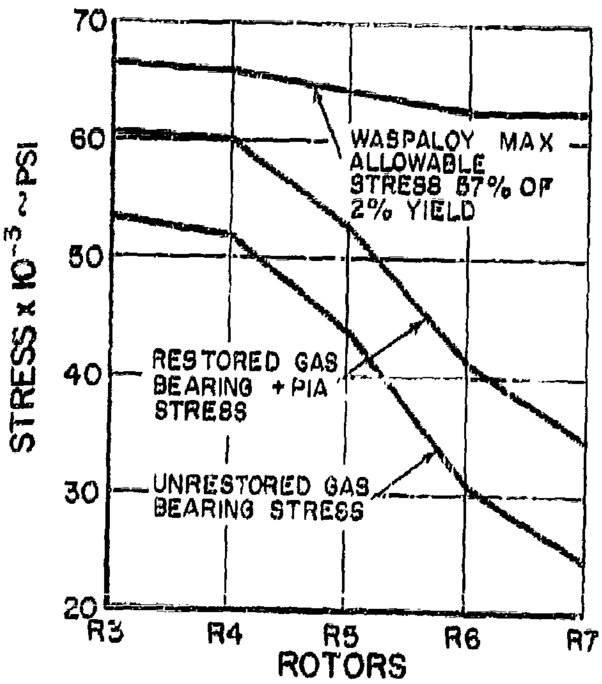

STF219 HIGH PRESSURE COMPRESSOR ROTOR STRESSES

Figure 2A-49

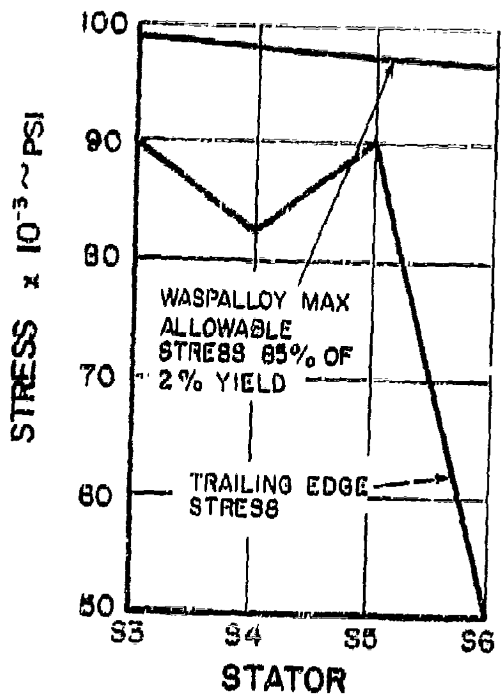

STF219 HIGH PRESSURE COMPRESSOR STATOR STRESSES

Figure 2A-50

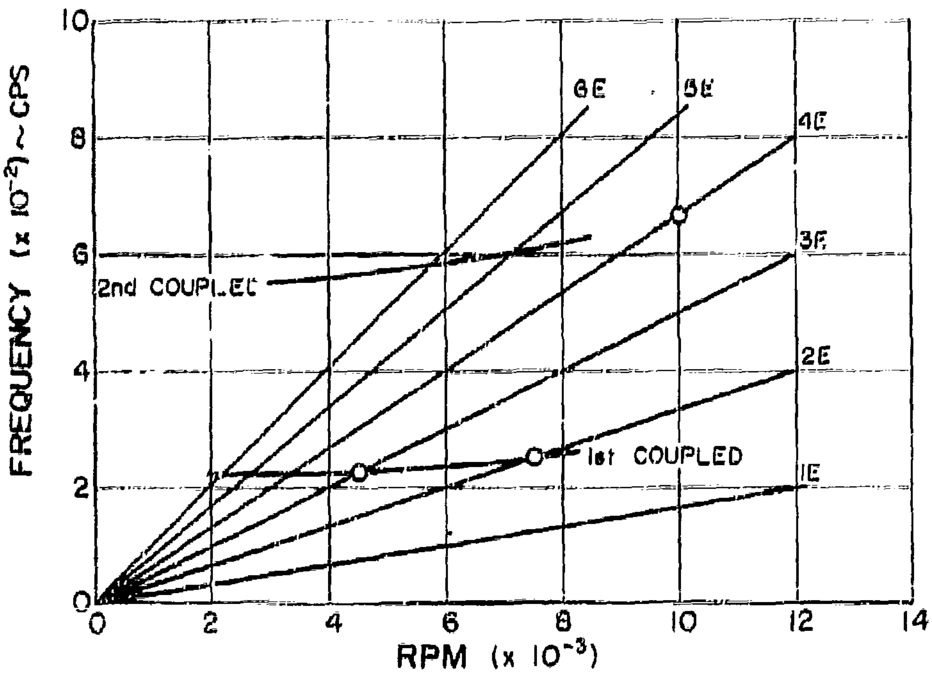

STF219 HIGH PRESSURE COMPRESSOR STAGE ONE BLADED DISK FREQUENCY AT 6400 RPM

Figure 2A-51

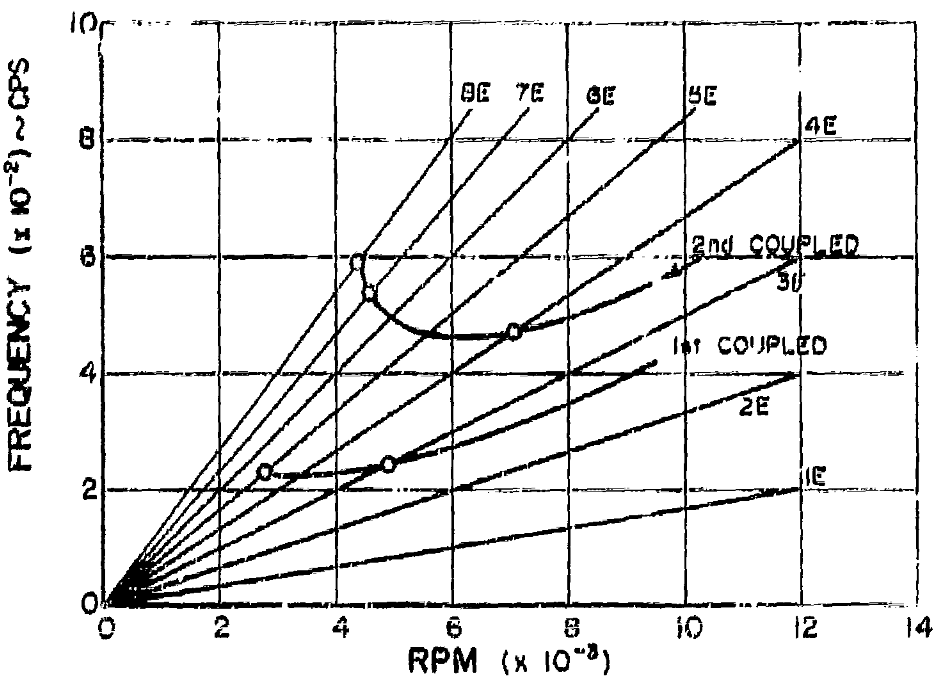

STF219 HIGH PRESSURE COMPRESSOR STAGE THREE COUPLED BLADE-DISK FREQUENCY

Figure 2A-52

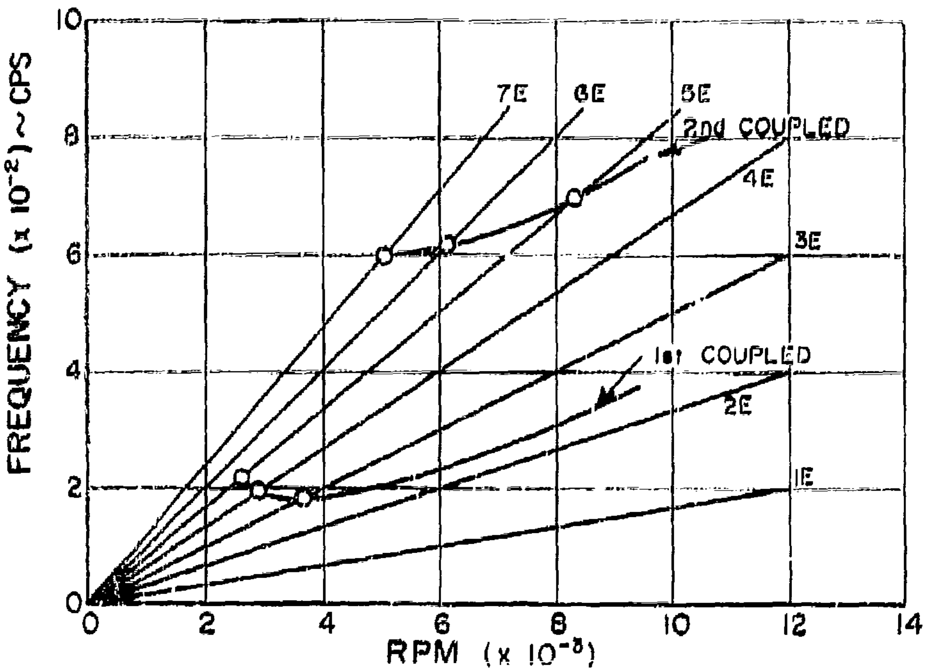

STF219 HIGH PRESSURE COMPRESSOR STAGE FIVE COUPLED BLADE-DISK FREQUENCY

Figure 2A-53

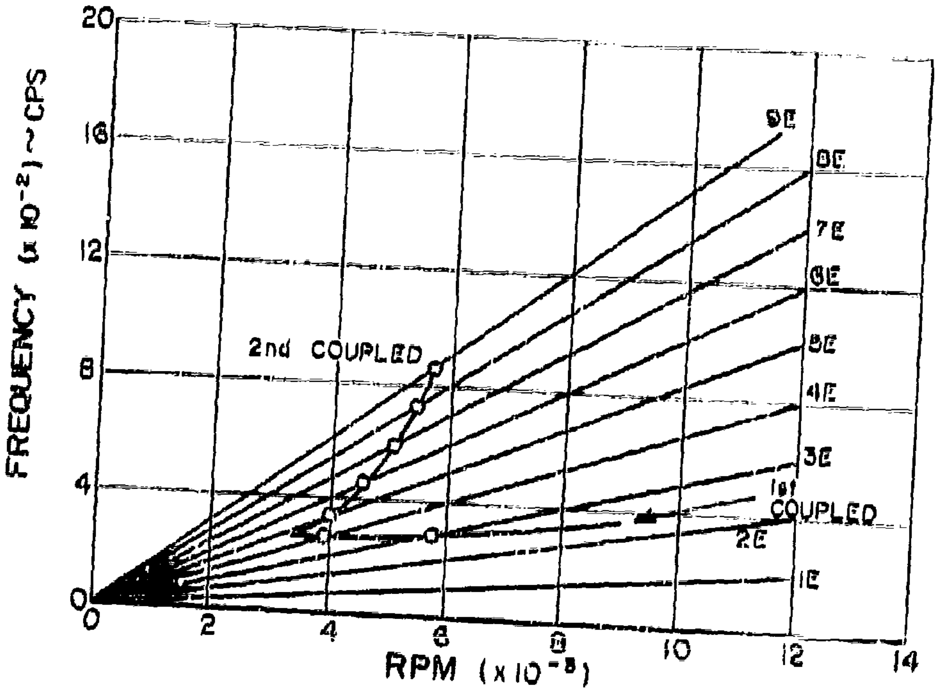

STF219 HIGH PRESSURE COMPRESSOR STAGE SEVEN COUPLED BLADE-DISK FREQUENCY

Figure 2A-54

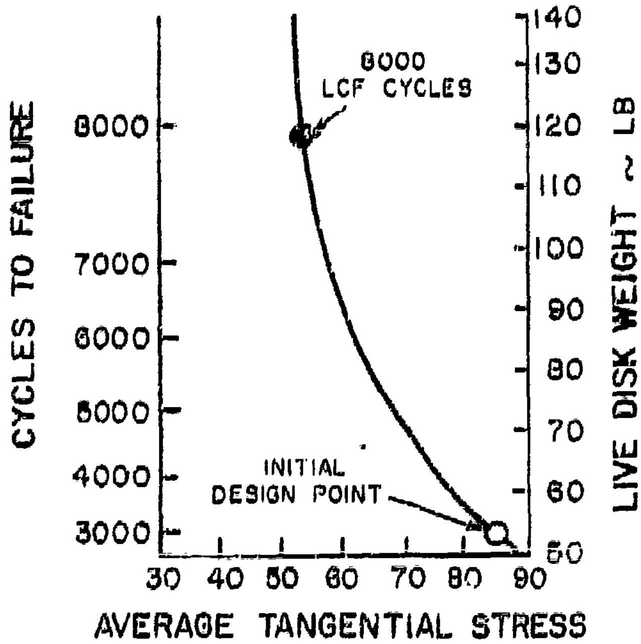

STF219 HIGH PRESSURE COMPRESSOR STAGE FOUR AVERAGE TANGENTIAL STRESS LEVEL VS. DISK THICKNESS

Figure 2A-55

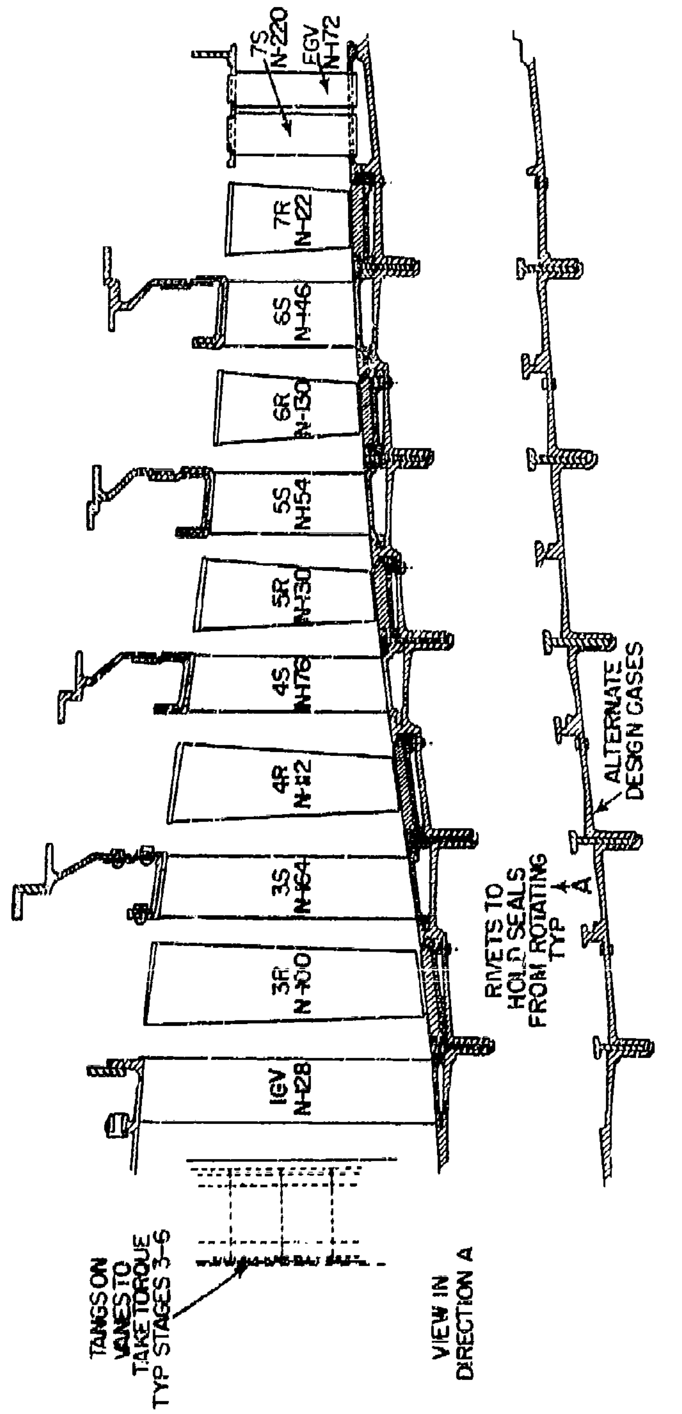

STF219 INITIAL DESIGN STUDY - COMPRESSOR CASE AND STATOR CONSTRUCTION

Figure 2A-56

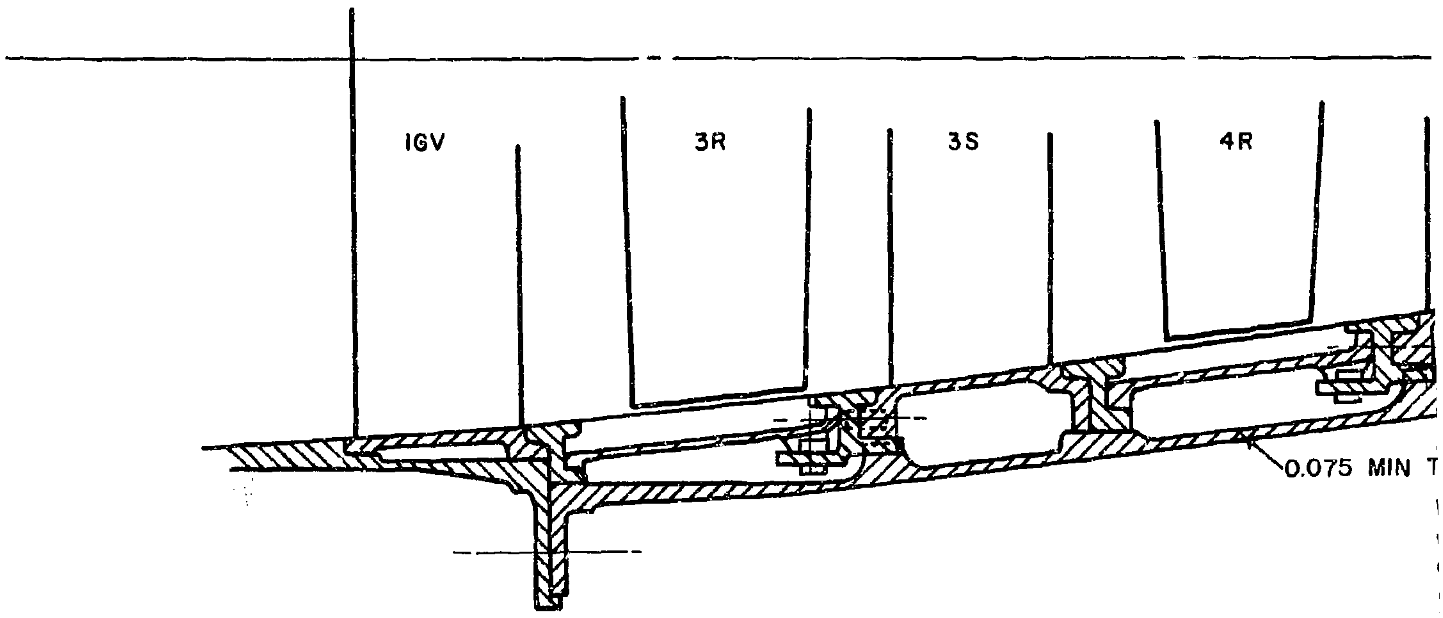

1

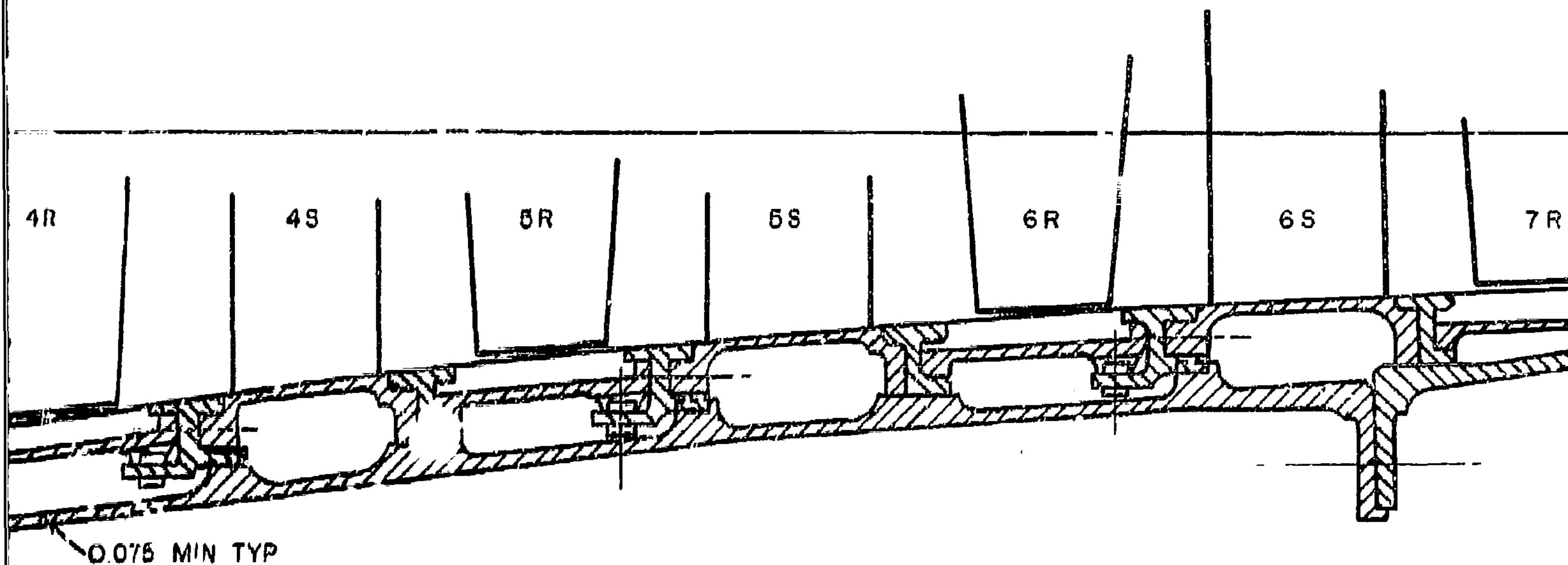

STF219 INITIAL DESIGN STUDY - HIGH P
CASE AND STATOR CONSTRUCTION

Figure 2A-57

2

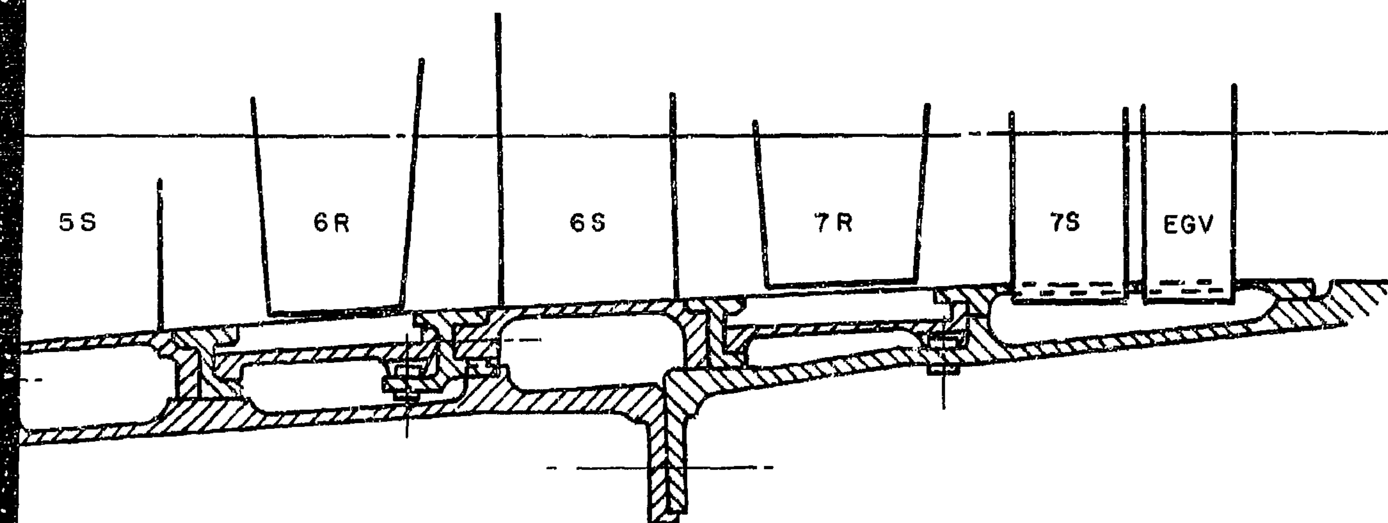

MACHINED VANES

STF... NITIAL DESIGN STUDY - HIGH PRESSURE COMPRESSOR CASE AND STATOR CONSTRUCTION

Figure 2A-57

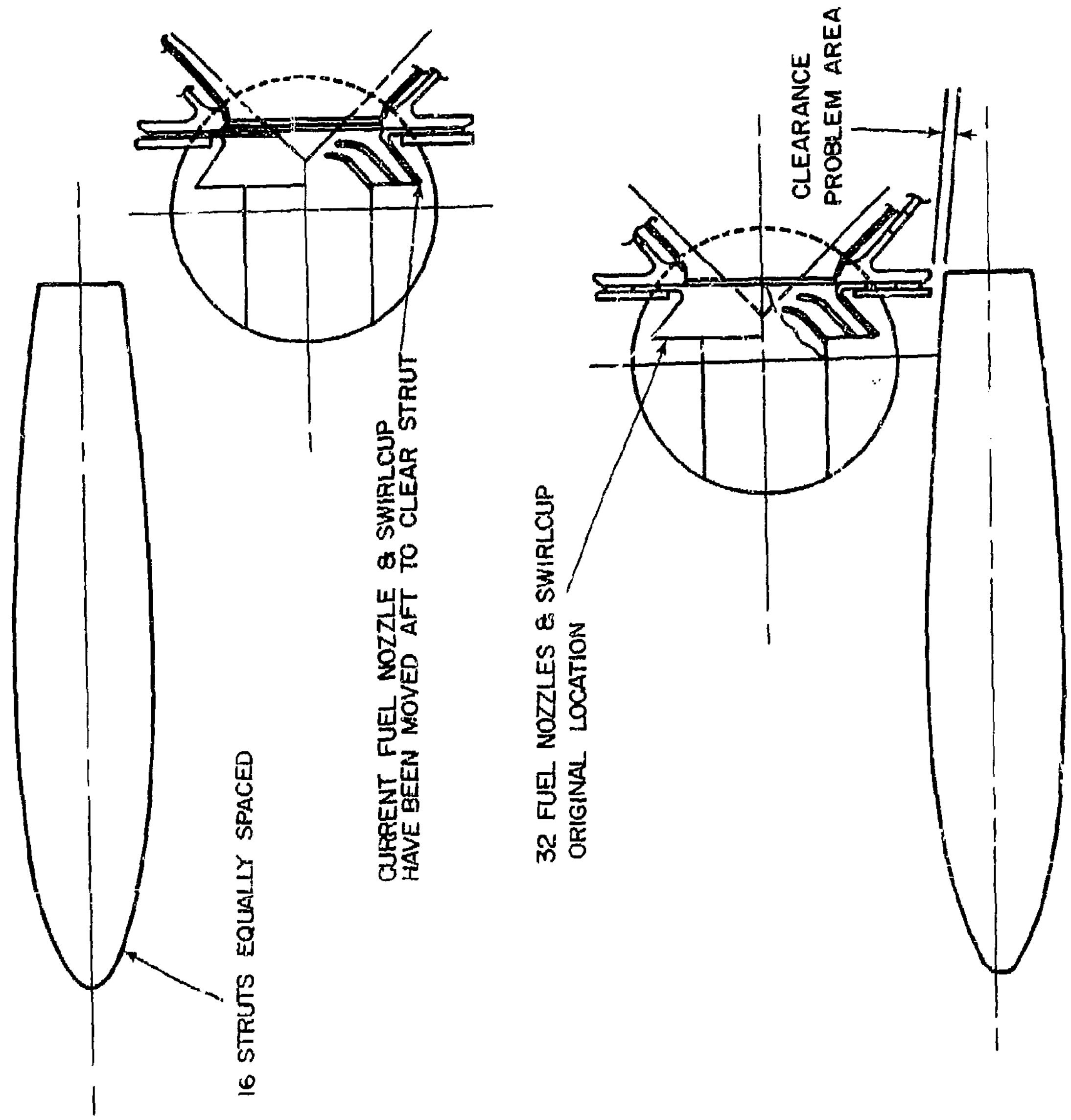

STF219 INITIAL DESIGN STUDY - DIFFUSER CASE STRUT LOCATION

Figure 2A-58

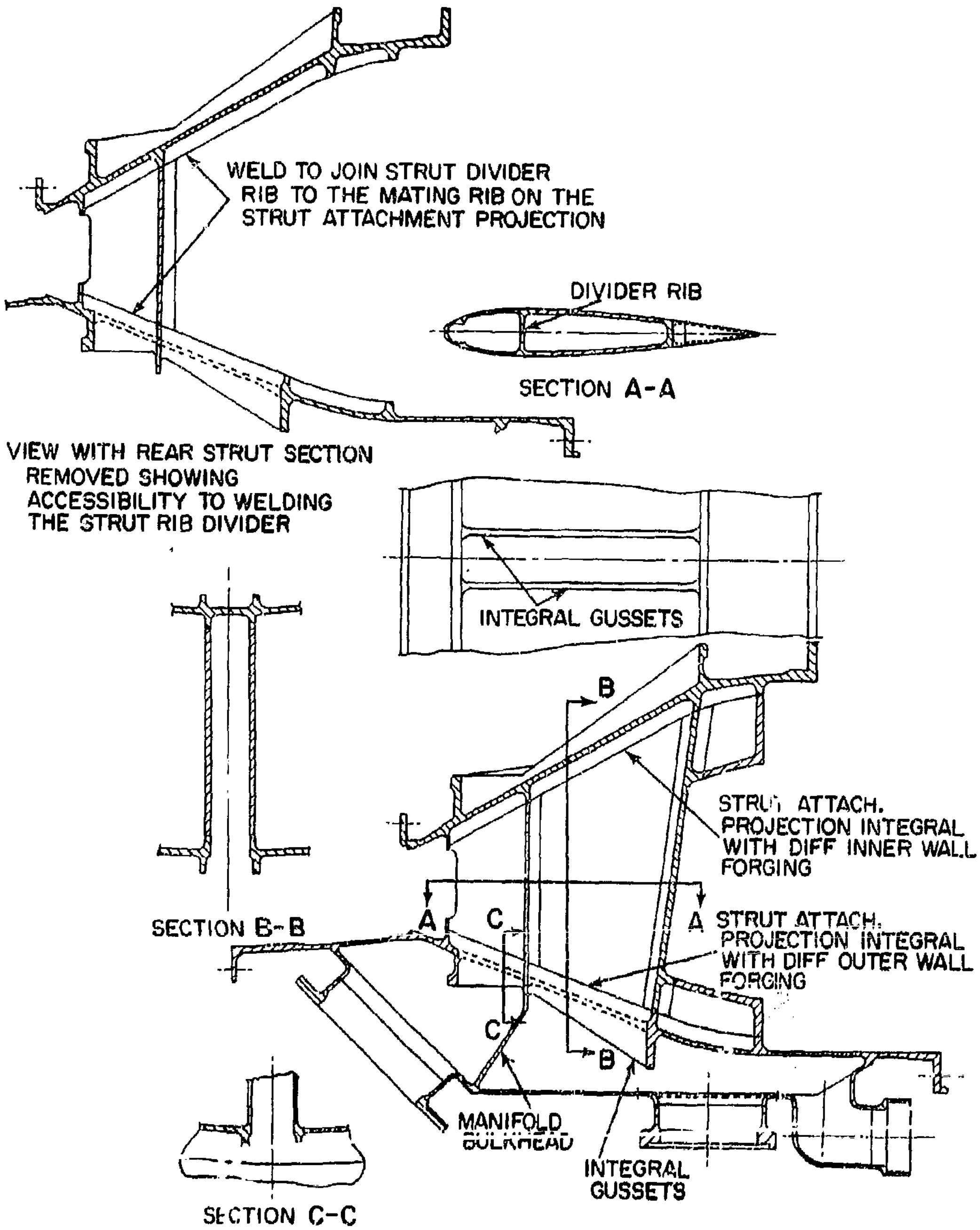

STF219 DIFFUSER CASE FABRICATION TECHNIQUES CONSIDERED IN EARLY DESIGN STUDIES

Figure 2A-59

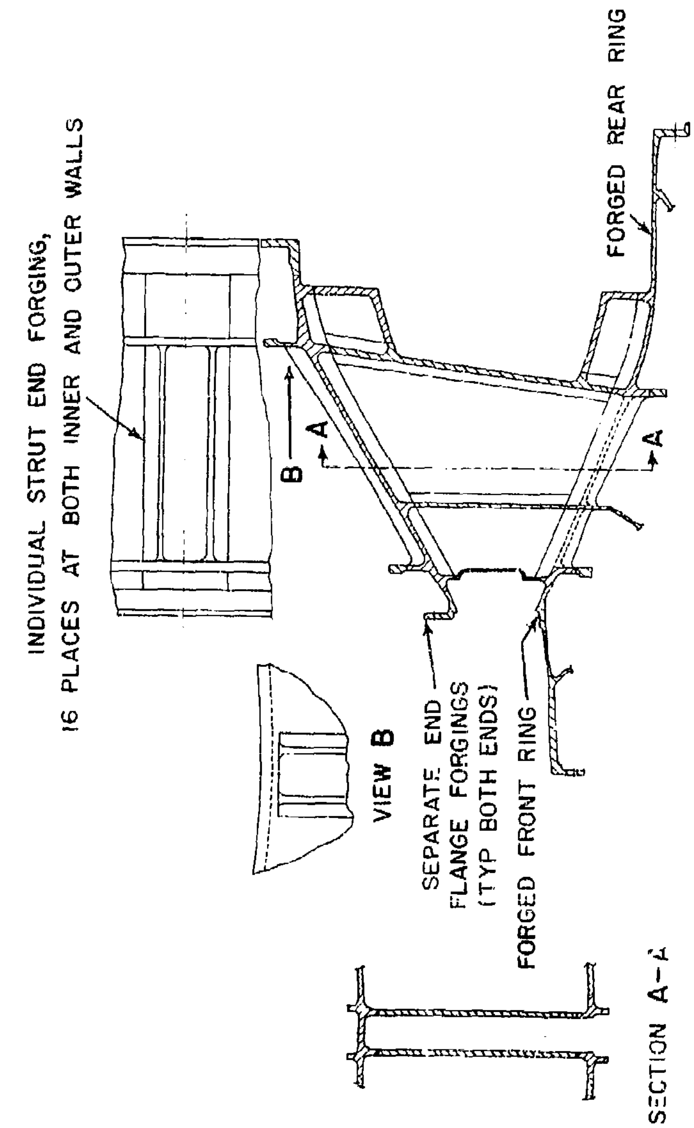

STF219 DIFFUSER CASE FABRICATION TECHNIQUES CONSIDERED IN EARLY DESIGN STUDIES

Figure 2A-60

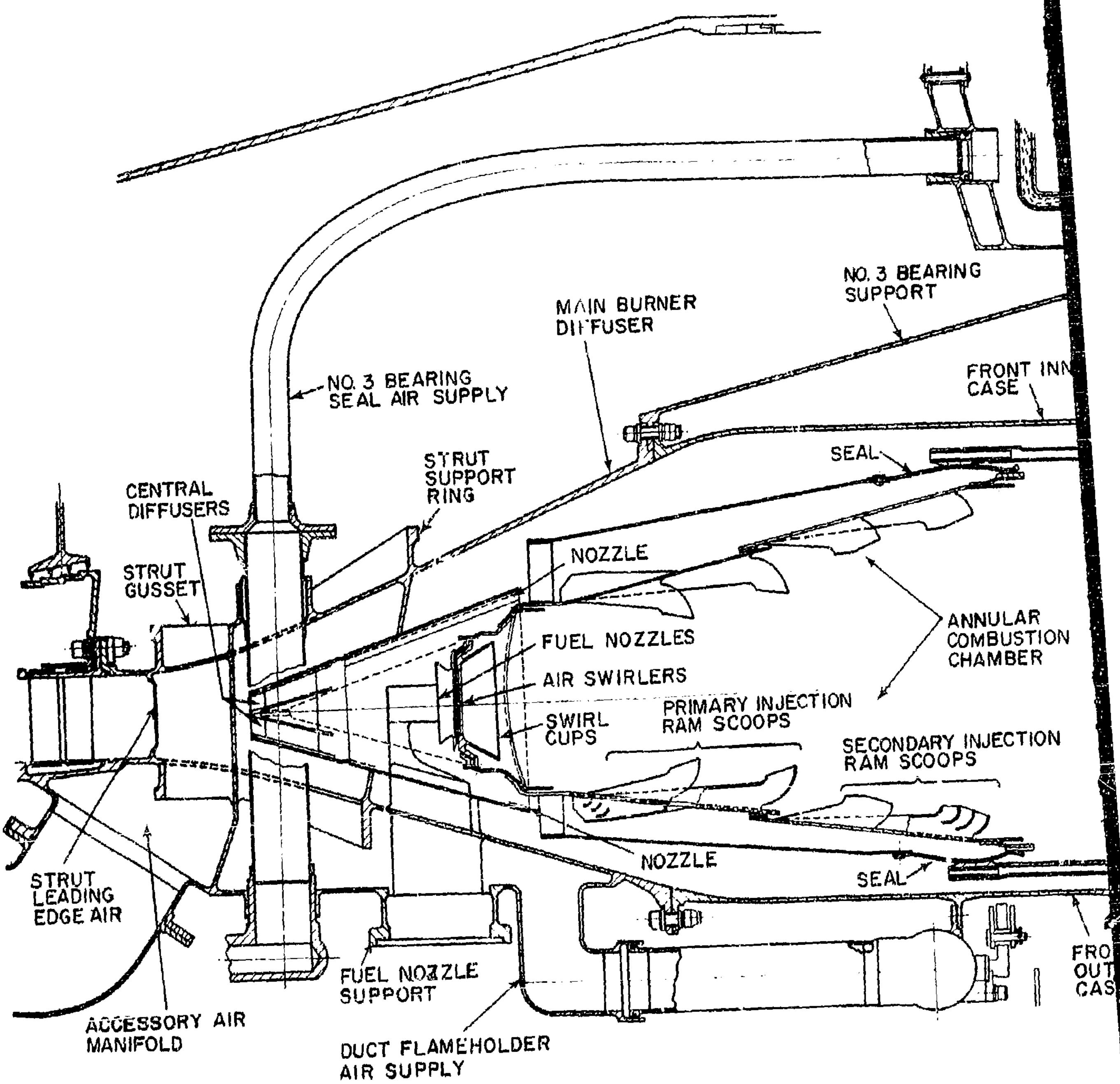

STF219 MAIN COMBUS

1

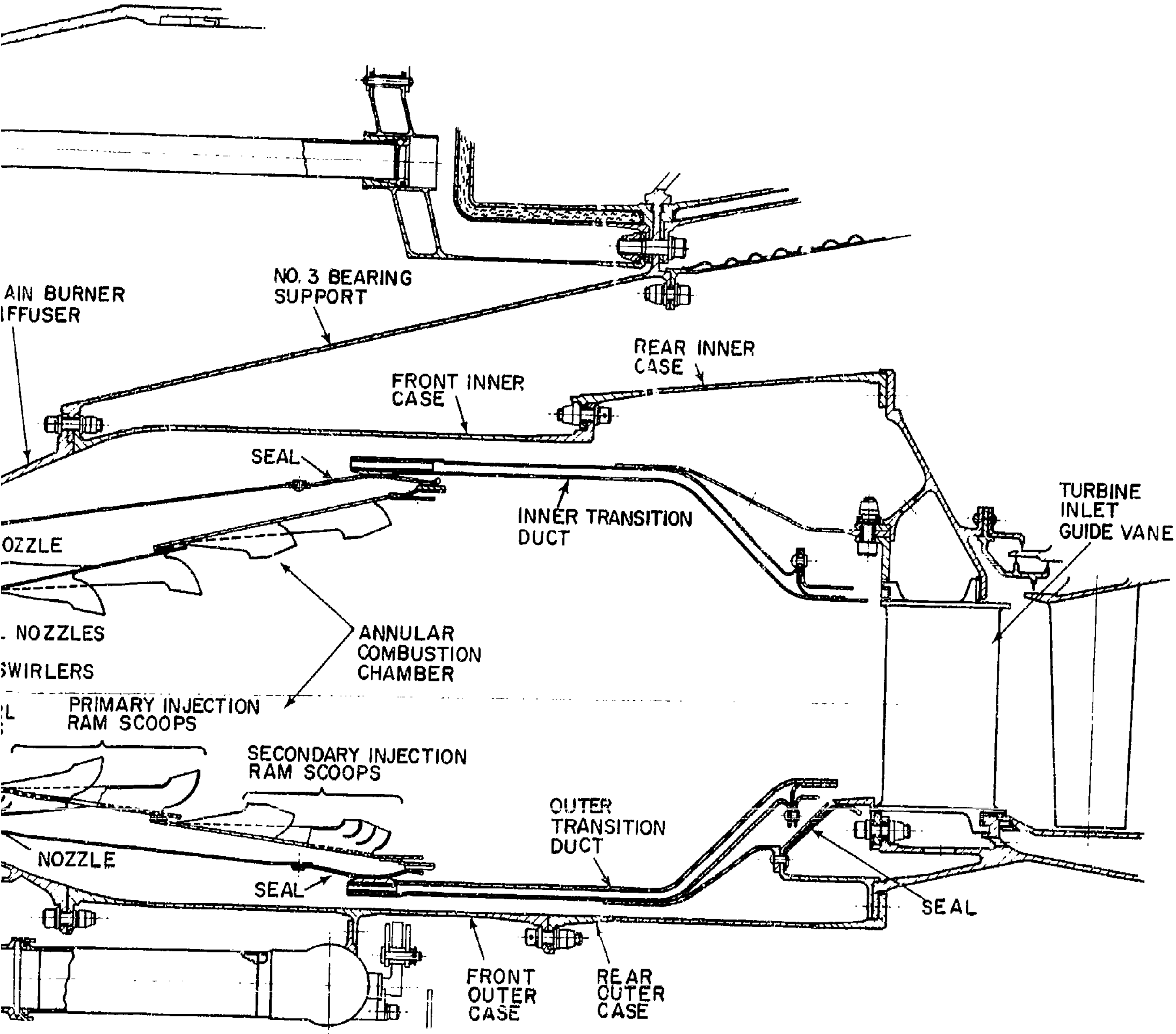

2

STF219 MAIN COMBUSTION CHAMBER SECTION

Figure 2A-61

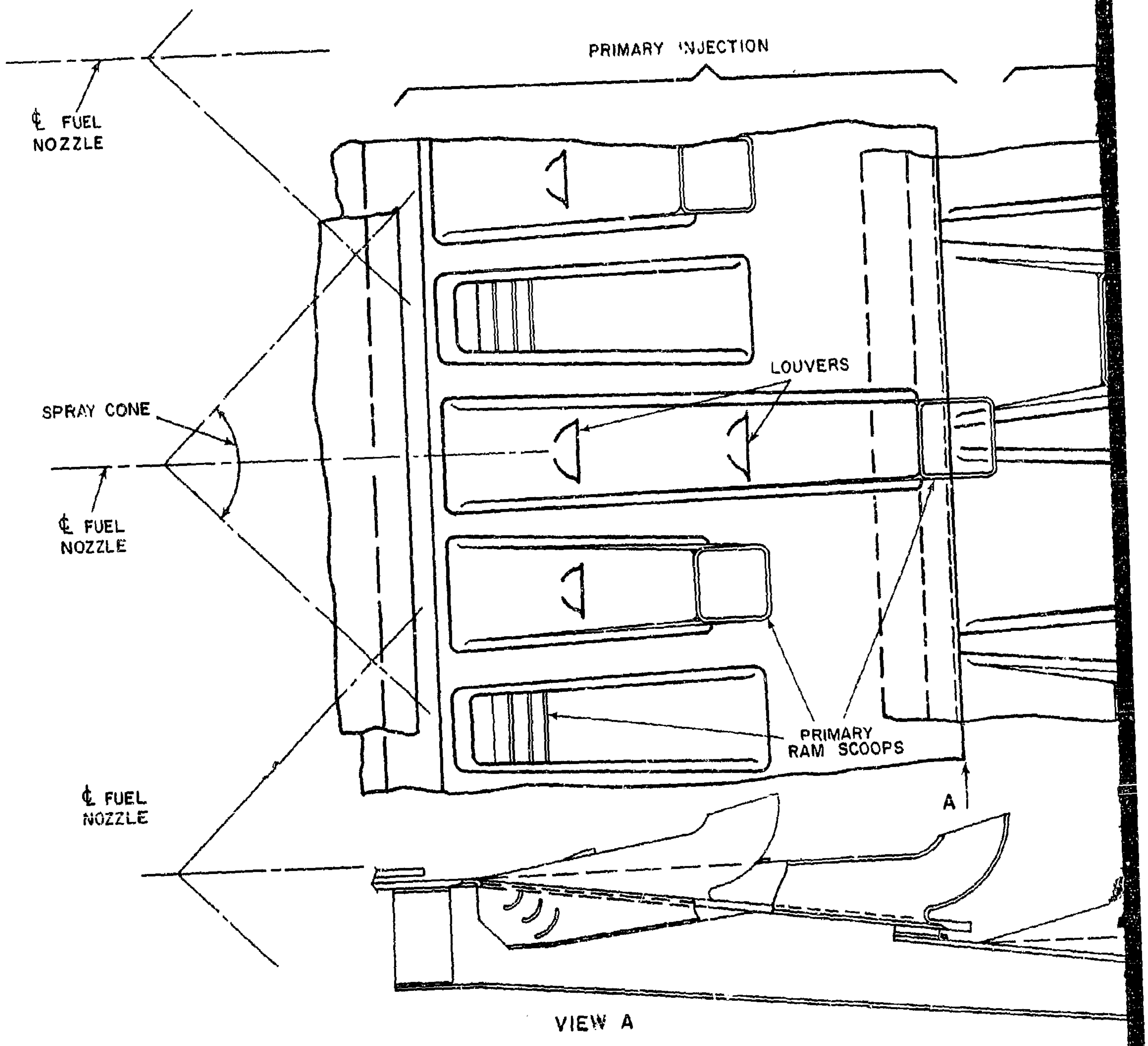

STF219 MAIN COMBUSTION CHAMBE
OF SCOOP WITH FILM-COOLED LOU

Figure 2A-

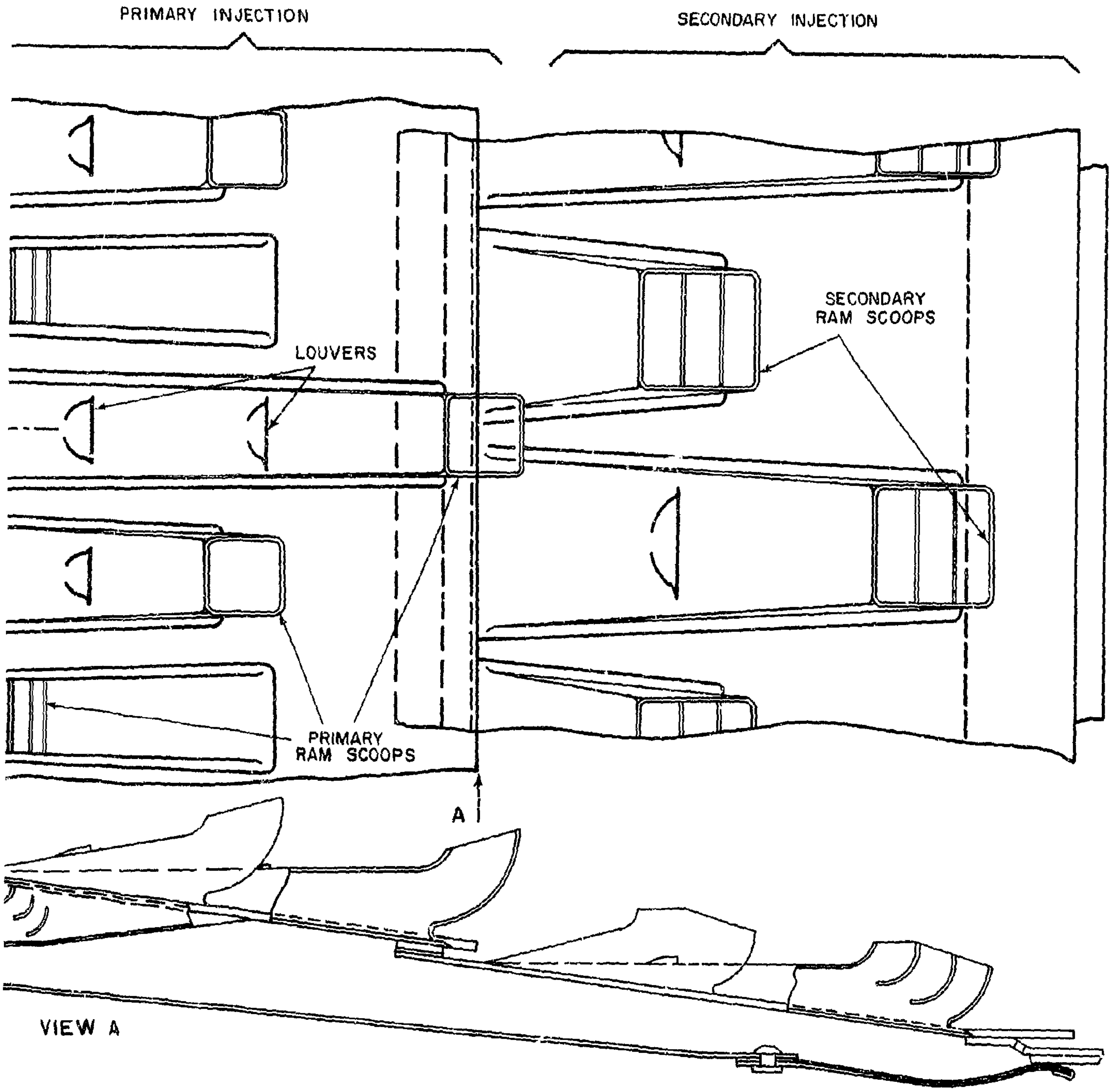

STF219 MAIN COMBUSTION CHAMBER SECTION - DETAILED SECTION OF SCOOP WITH FILM-COOLED LOUVERS

Figure 2A-62

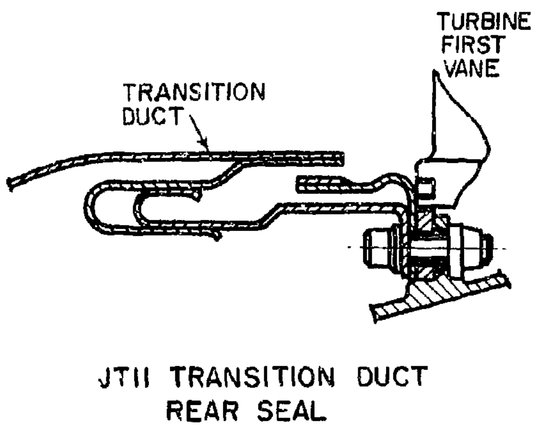

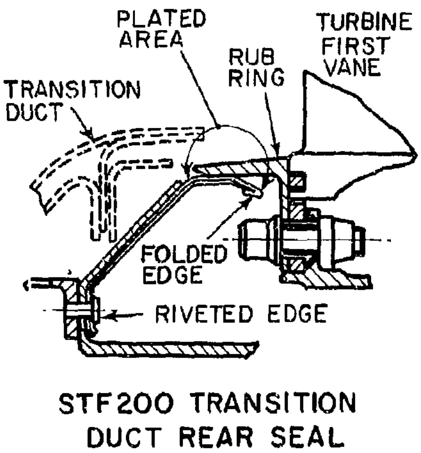

SEALS STUDIED FOR USE IN STF219 ANNULAR COMBUSTION CHAMBER

Figure 2A-63

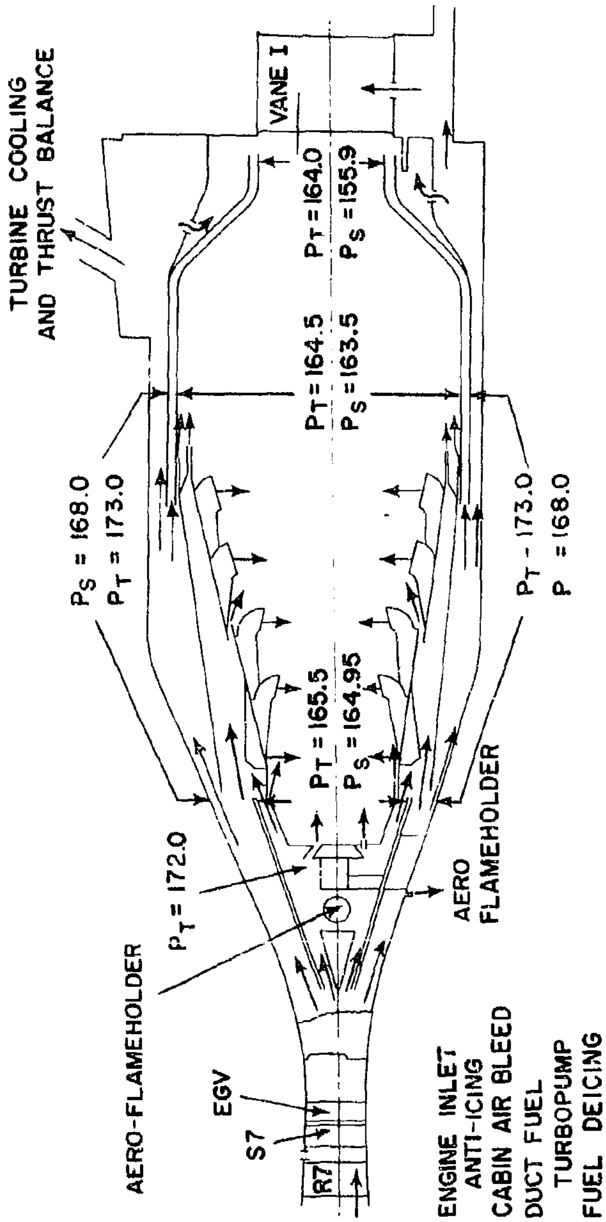

STF219 ESTIMATED PRESSURE THROUGH COMBUSTION CHAMBER - SEA LEVEL TAKE-OFF

Figure 2A-64

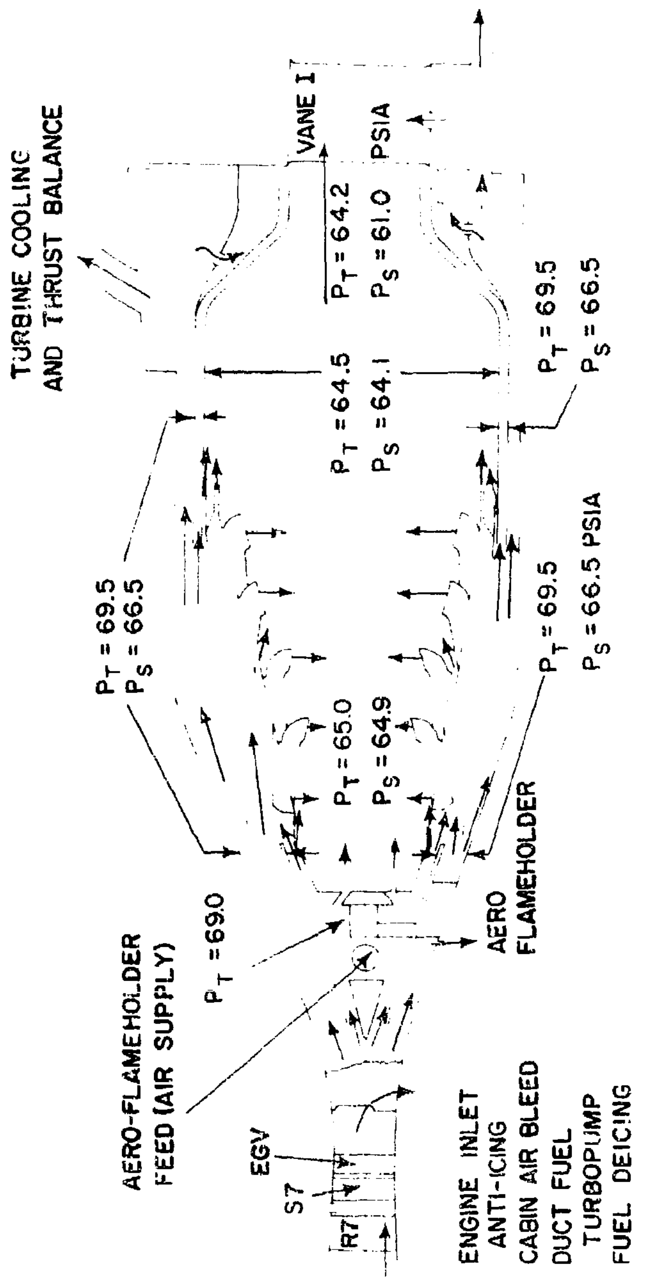

STF219 ESTIMATED PRESSURES THROUGH COMBUSTION CHAMBER - ALTITUDE CRUISE

Figure 2A-65

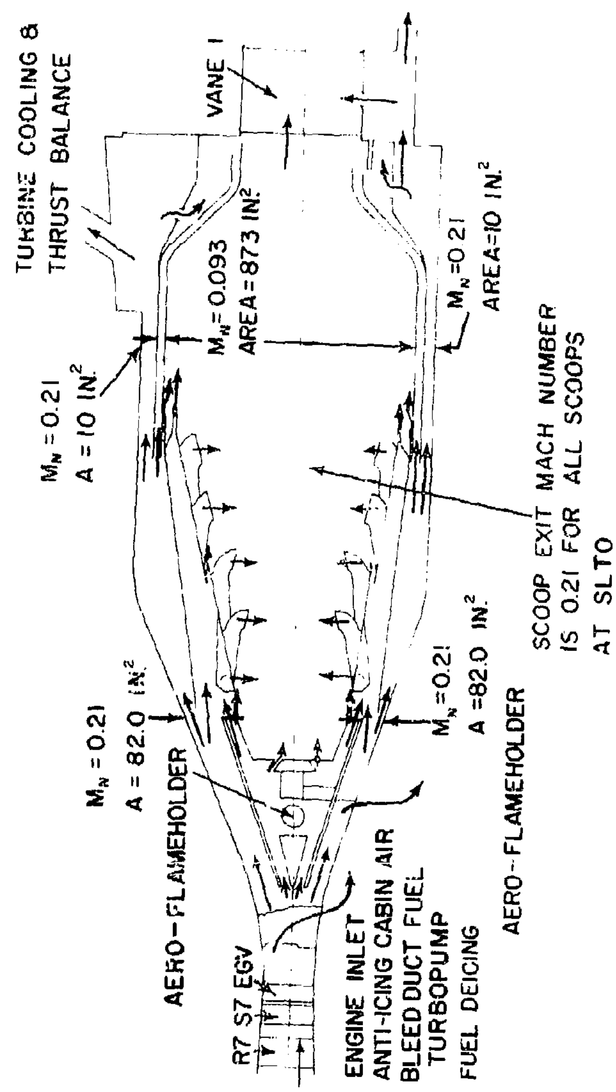

STF219 ESTIMATED COMBUSTION CHAMBER MACH NUMBERS AND FLOW AREAS

Figure 2A-66

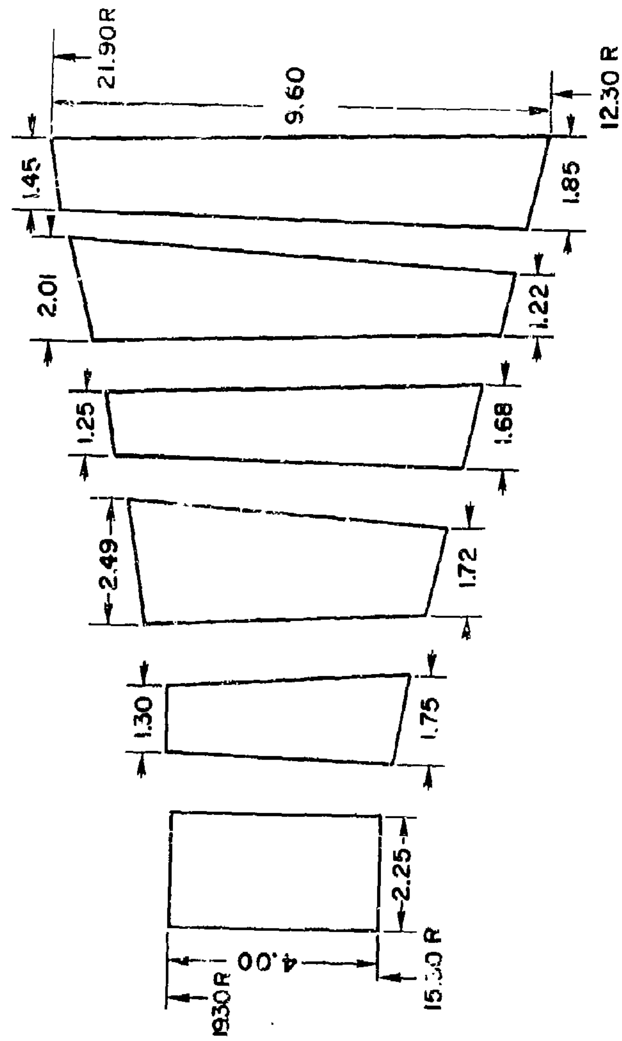

STF219 TURBINE FLOWPATH

Figure 2A-67

Stage	1	2	3
Vane			
Inlet Velocity (ft/sec)	577.9	1063.	997.1
Inlet Mach number at 1900°F	-	0.5153	0.5079
Axial Velocity	577.9	963.1	933.6
Swirl Velocity	-	450.	350.
Gas Inlet Angle (deg.)	90.0	64.96	69.45
Exit Velocity (ft/sec)	2100.8	1569.2	1516.0
Exit Mach number	0.97[illegible]1	0.7796	0.7935
Axial Velocity (ft/sec)	800.4	941.5	996.3
Swirl Velocity (ft/sec)	1942.4	1255.4	1142.7
Gas Exit Angle (deg.)	22.39	36.87	41.08
Blade			
Inlet Relative Velocity (ft/sec)	1926.6	1028.3	1041.8
Inlet Relative Mach number	0.4958	0.5109	0.5453
Axial Velocity (ft/sec)	800.4	941.5	996.3
Relative Swirl Velocity (ft/sec)	710.6	413.5	304.4
Inlet Wheel Speed (ft/sec)	1231.7	841.9	838.3
Inlet Relative Gas Angle (deg.)	48.4	66.29	73.01
Exit Relative Velocity (ft/sec)	1926.6	1510.4	1709.0
Exit Relative Mach number	0.9339	0.7694	0.9341
Axial Velocity (ft/sec)	963.1	933.6	1179.7
Relative Swirl Velocity (ft/sec)	1668.6	1187.3	1236.6
Exit Wheel Speed (ft/sec)	1218.6	837.3	836.6
Exit Relative Gas Angle (deg.)	29.99	38.18	43.65
Stage Work (Btu/lb)	113.4	53.0	51.0

TURBINE MEAN LINE AERODYNAMICS AT 1900°F CRUISE CONDITION

Figure 2A-68

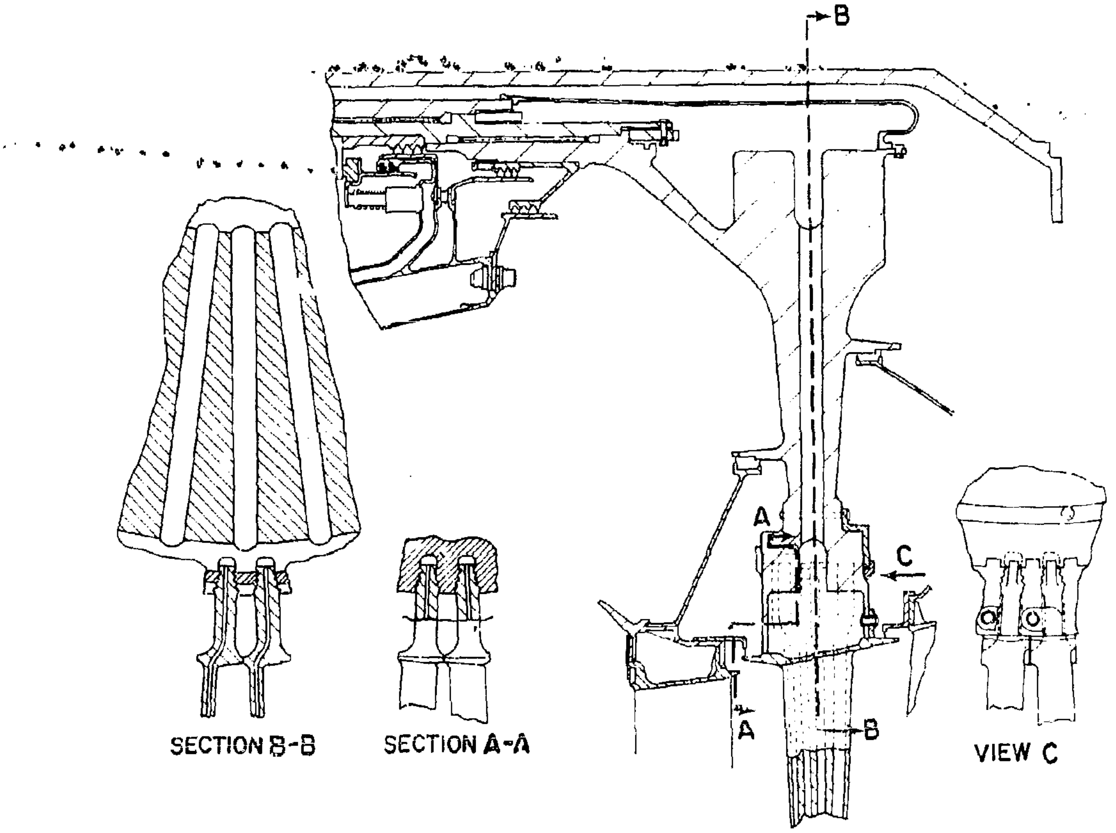

STF219 TURBINE BLADE COOLING SCHEME

Figure 2A-69

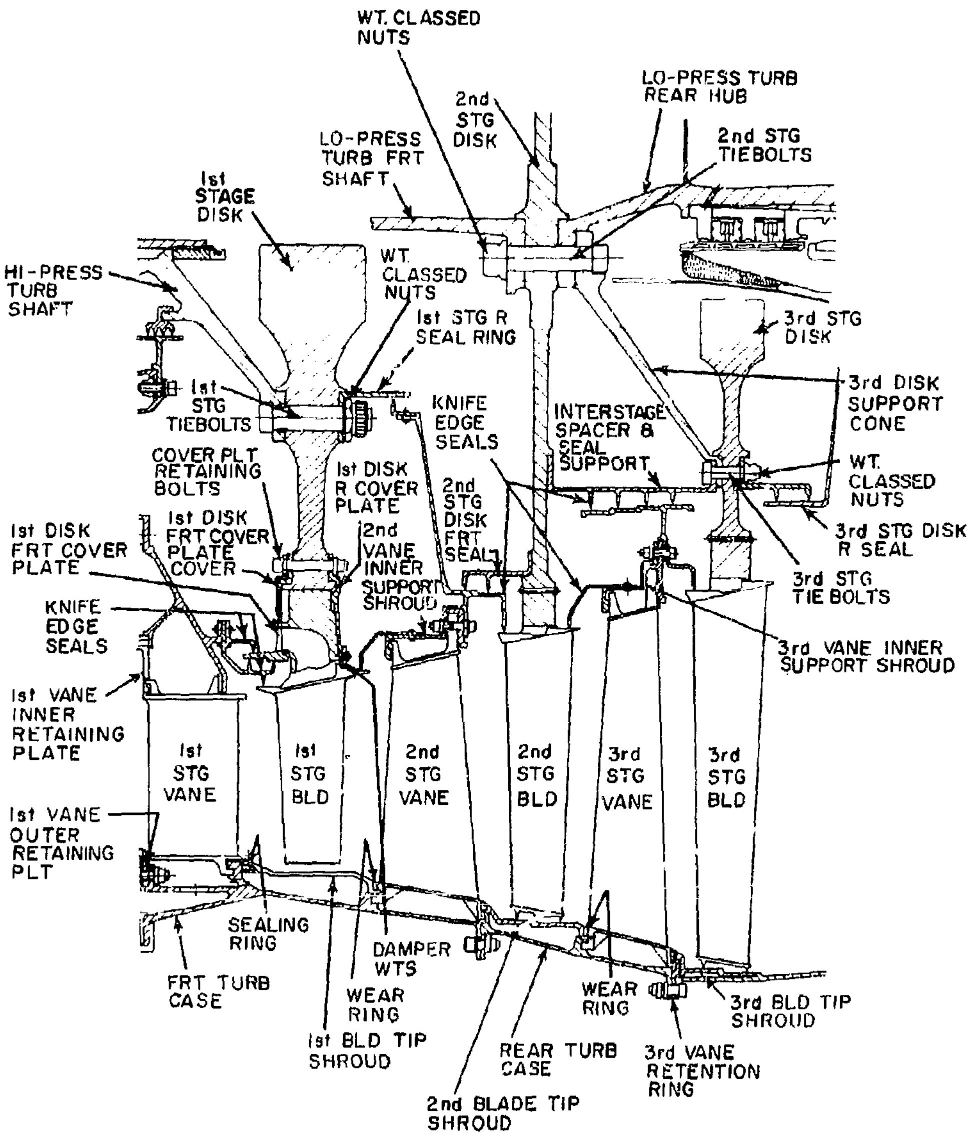

STF219 TURBINE BLADE COOLING SCHEME EVOLVED FROM J58 ENGINE EXPERIENCE

Figure 2A-70

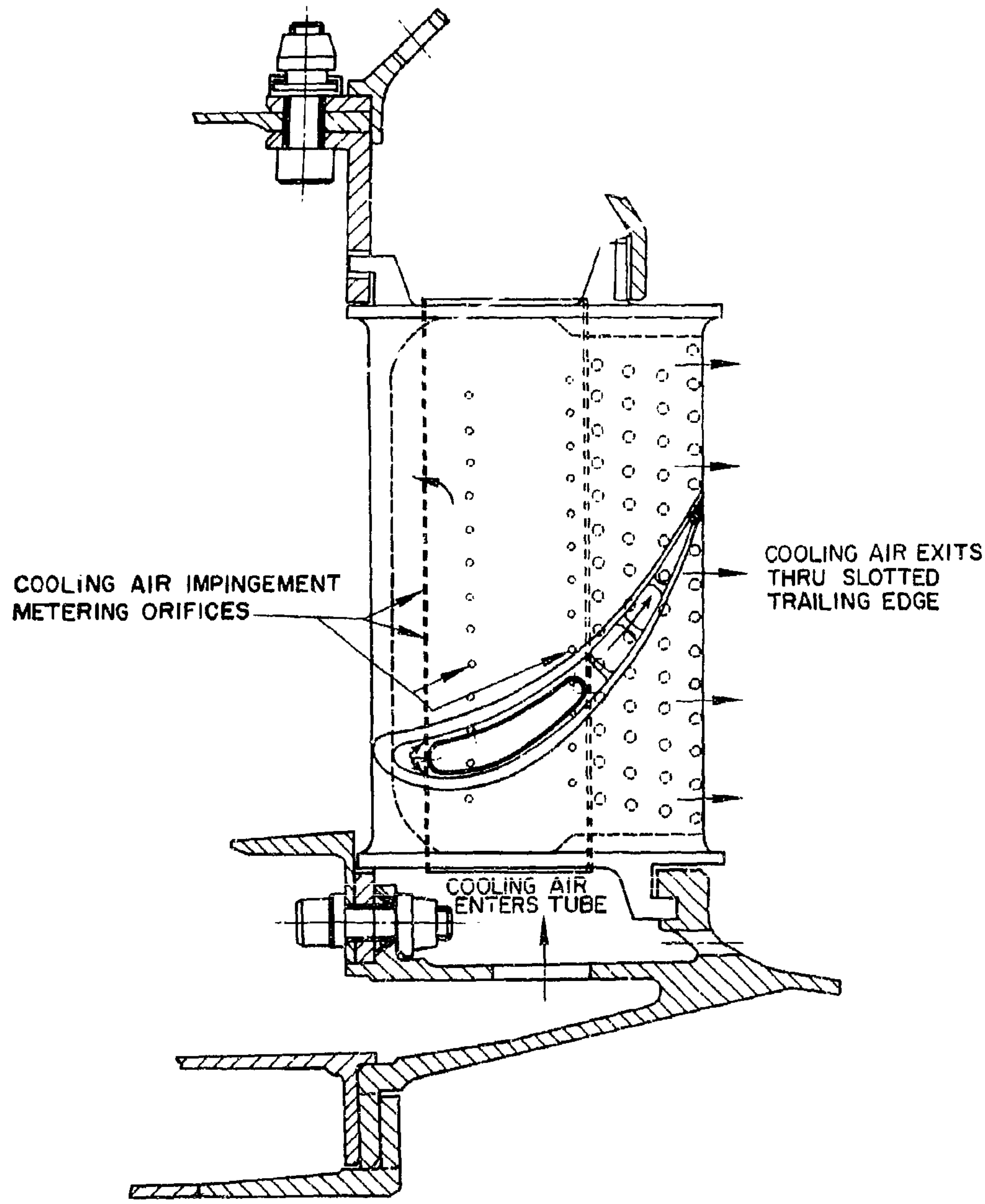

STF219 FIRST STAGE VANE ATTACHMENT AND COOLING SCHEME

Figure 2A-71

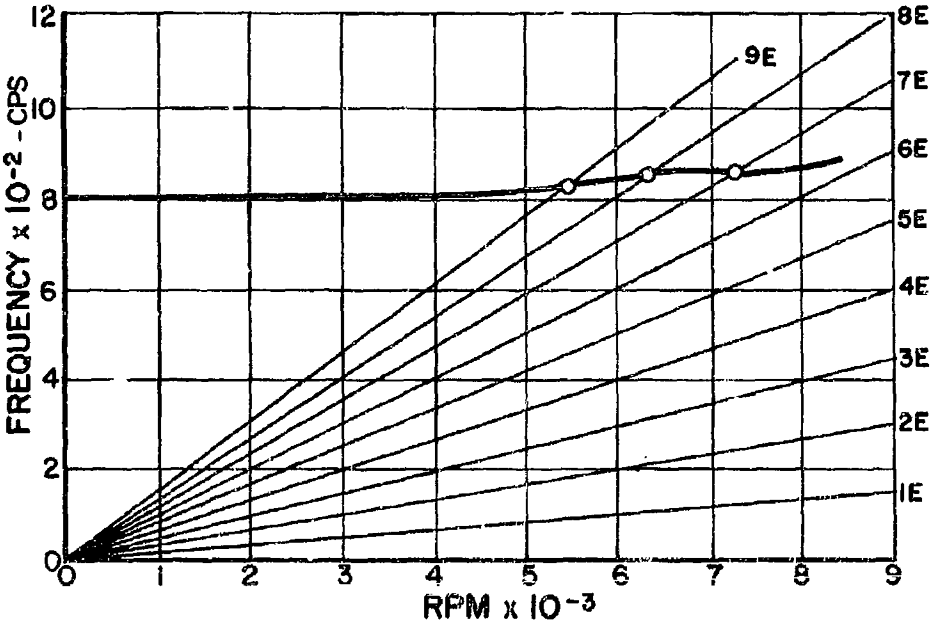

STF219 FIRST STAGE BLADE AND DISK COUPLED VIBRATIONS MODE

Figure 2A-72

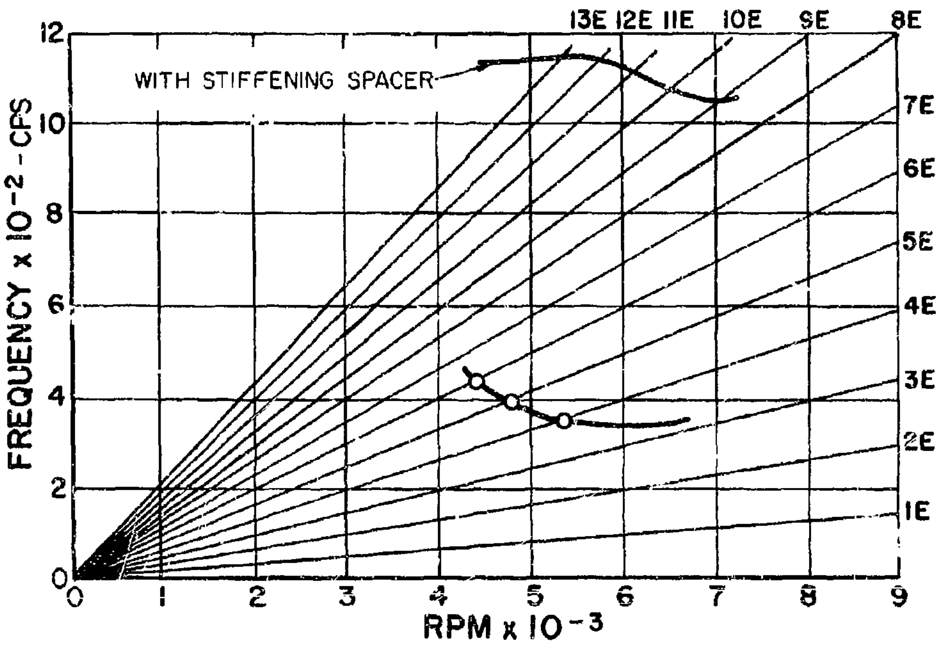

STF 219 SECOND STAGE DISK BLADE COUPLED FREQUENCIES

Figure 2A-73

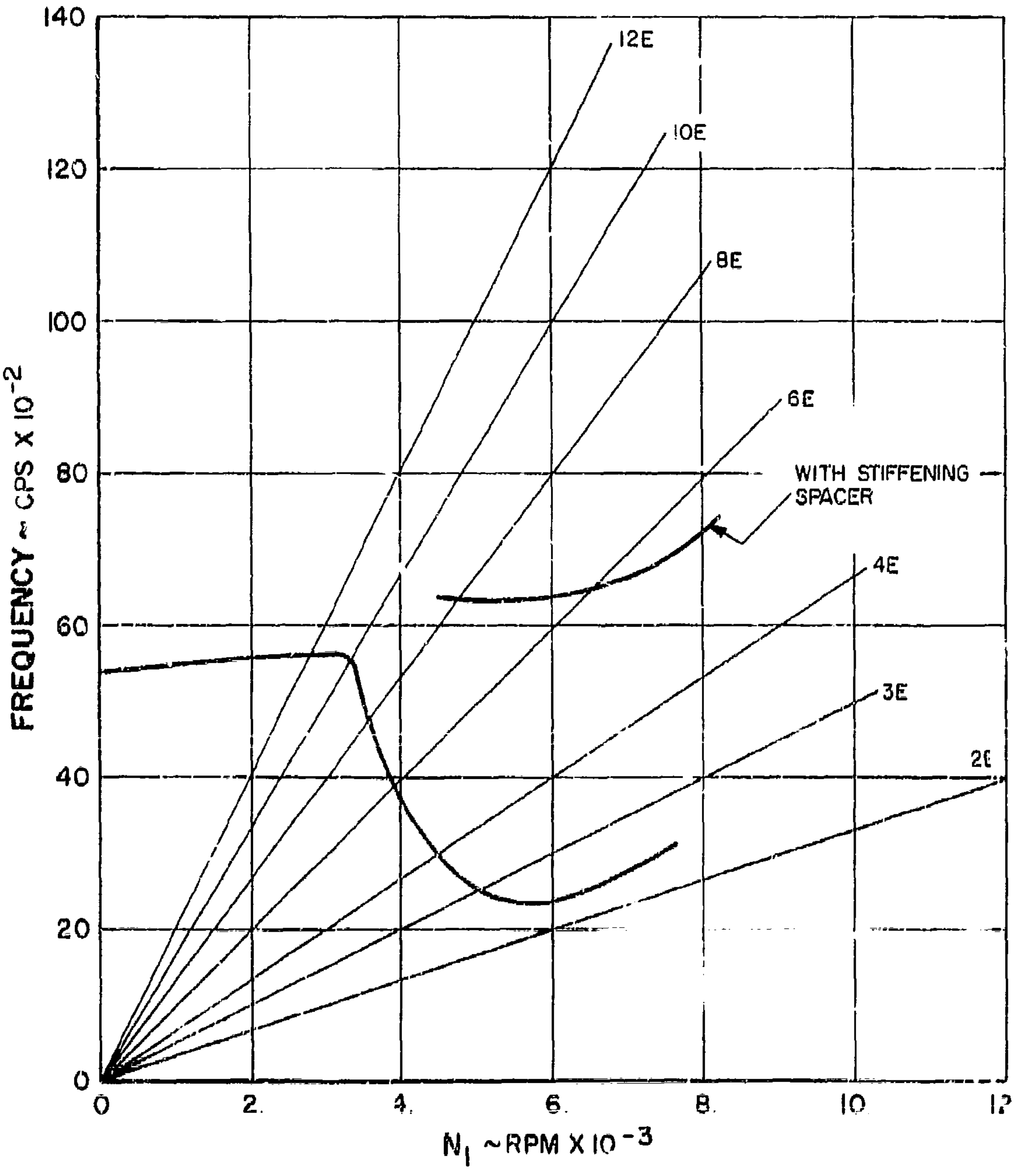

STF219 THIRD STAGE DISK BLADE COUPLED FREQUENCIES

Figure 2A-74

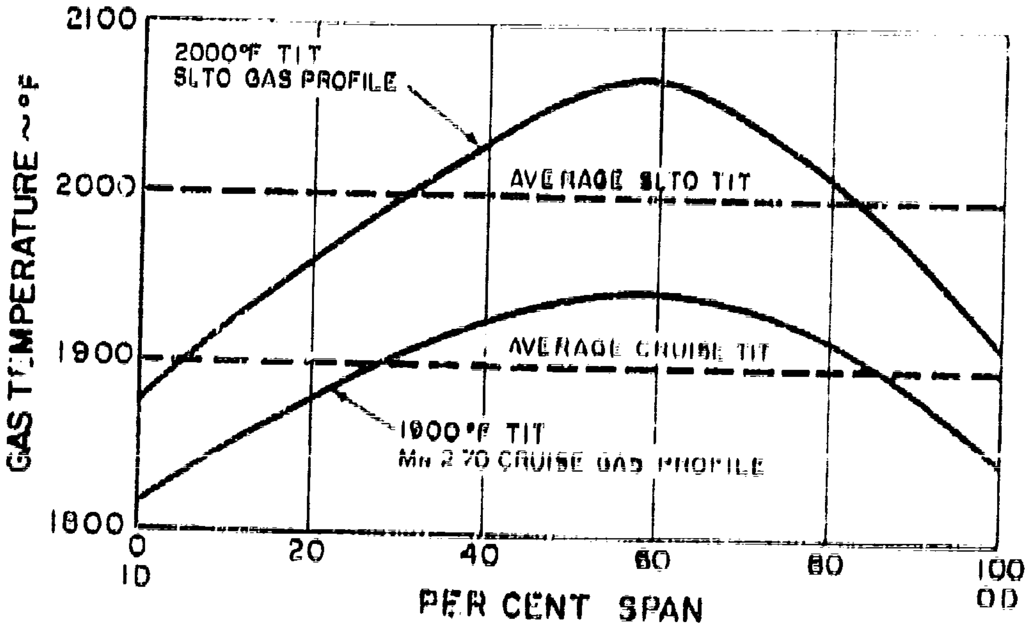

BURNER TEMPERATURE PROFILES VS AVERAGE RADIAL PROFILE

Figure 2A-75

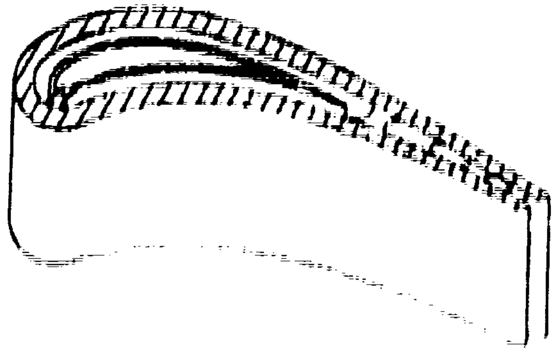

VANE DESIGN - INITIAL (2000°F) RATING

Figure 7A-[illegible]

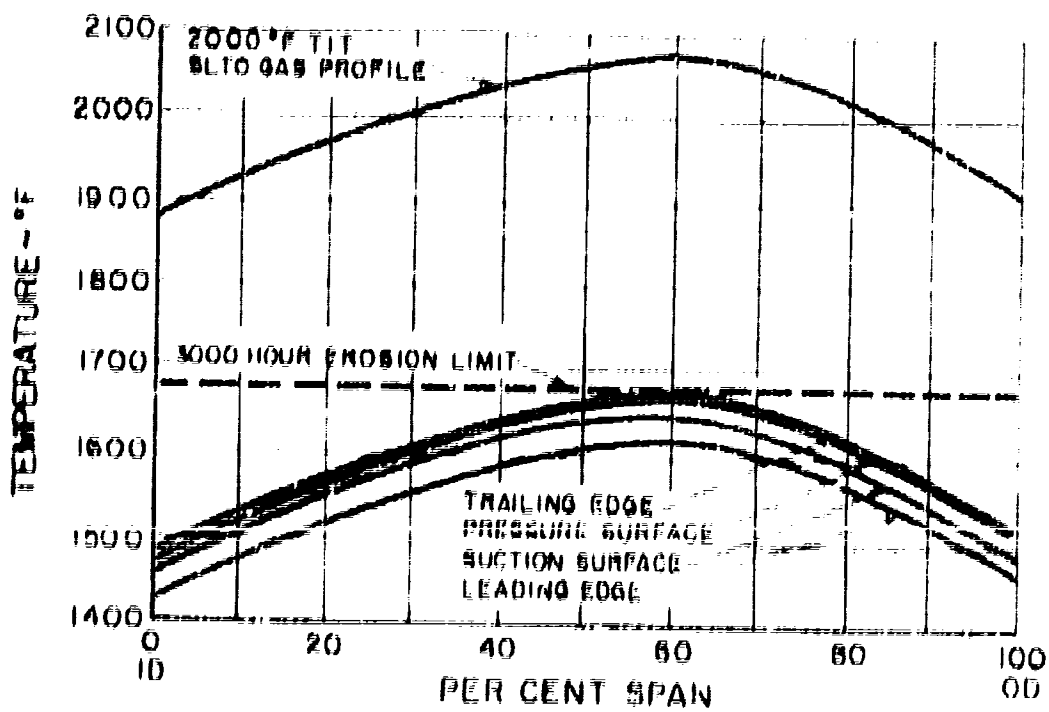

SPANWISE GRADIENT FOR THE INITIAL ENGINE

Figure [illegible]

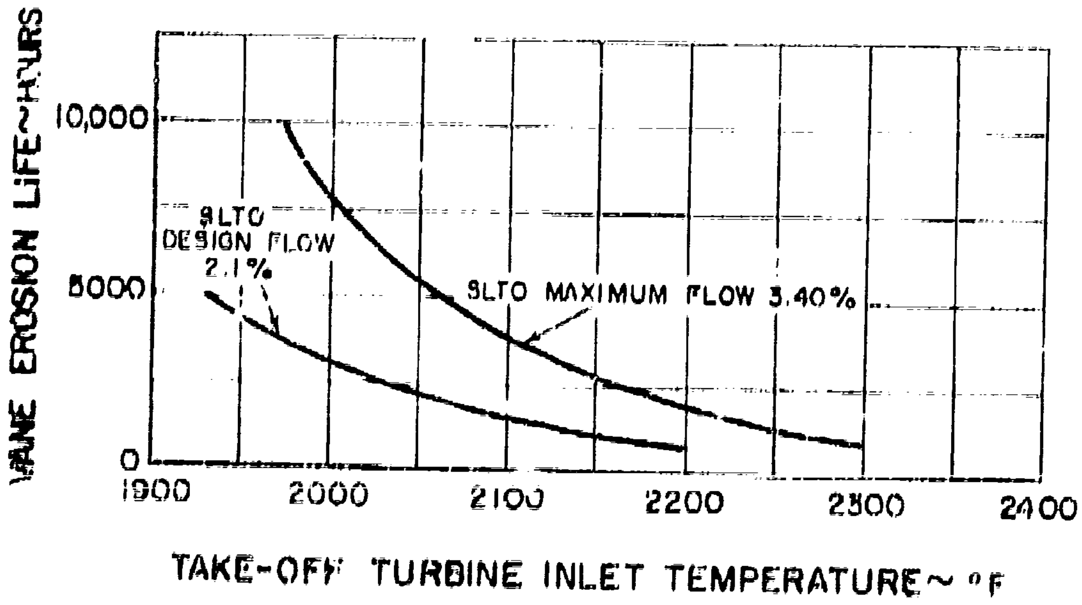

GROWTH CAPABILITY FOR THE INITIAL ENGINE

Figure 2A-78

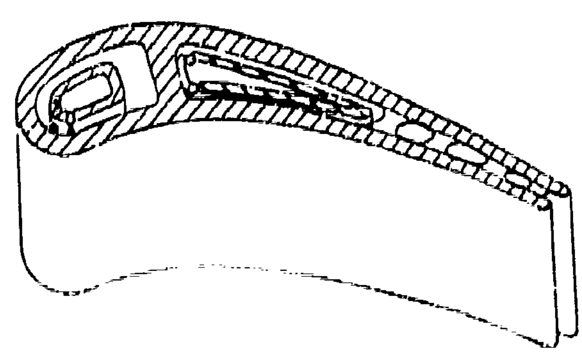

VANE DESIGN - BASIC (2400°F) RATING

Figure 2A-7[illegible]

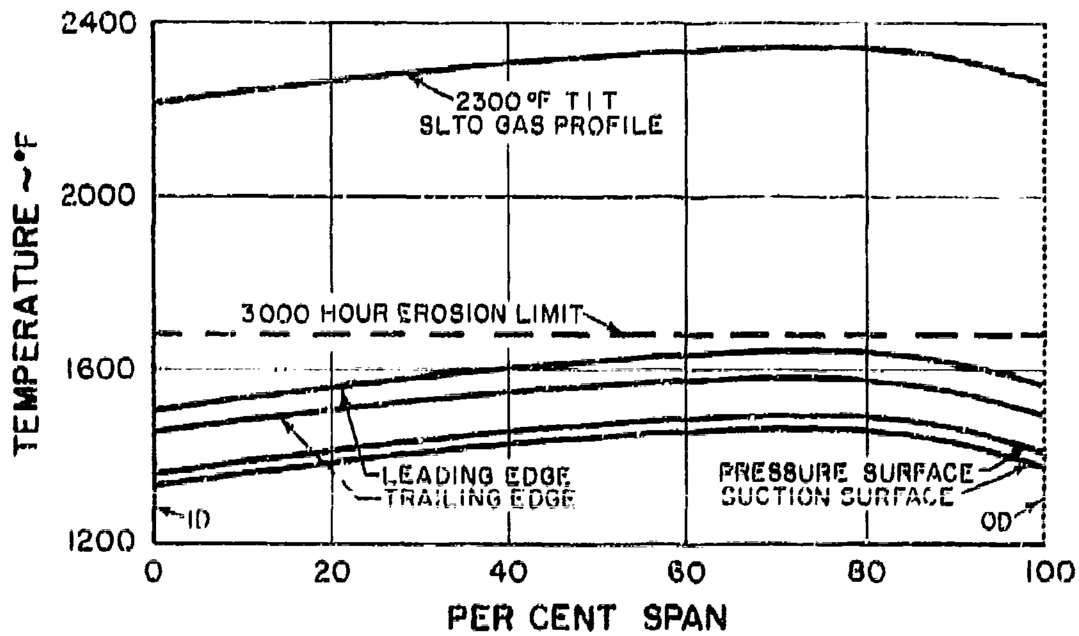

SPANWISE GRADIENT FOR THE BASIC RATING

Figure 2A-80

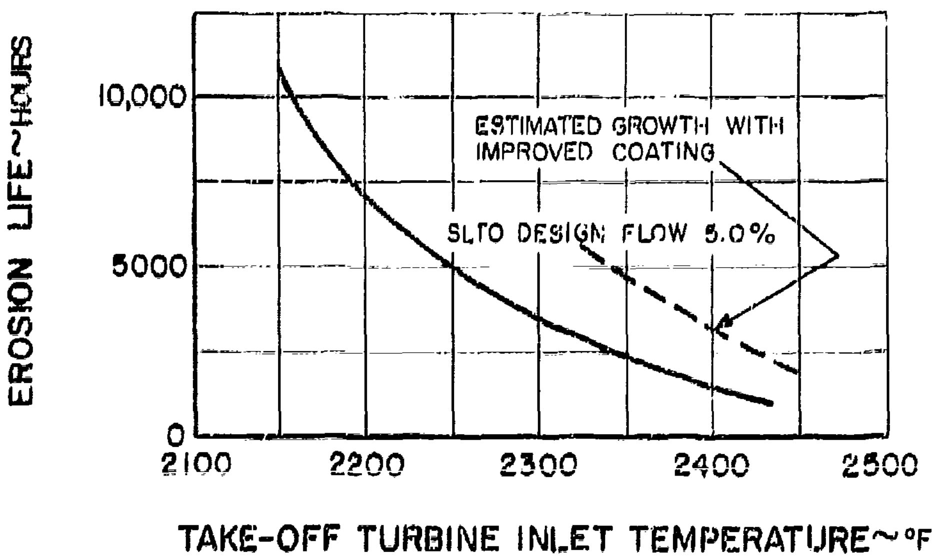

GROWTH CAPABILITY FOR THE BASIC RATING

Figure 2A-81

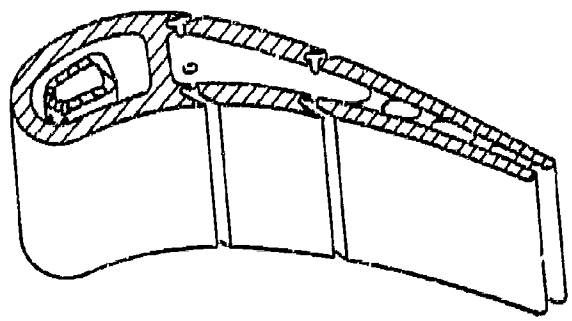

ALTERNATE BASIC RATING ENGINE VANE DESIGN

Figure 2A-82

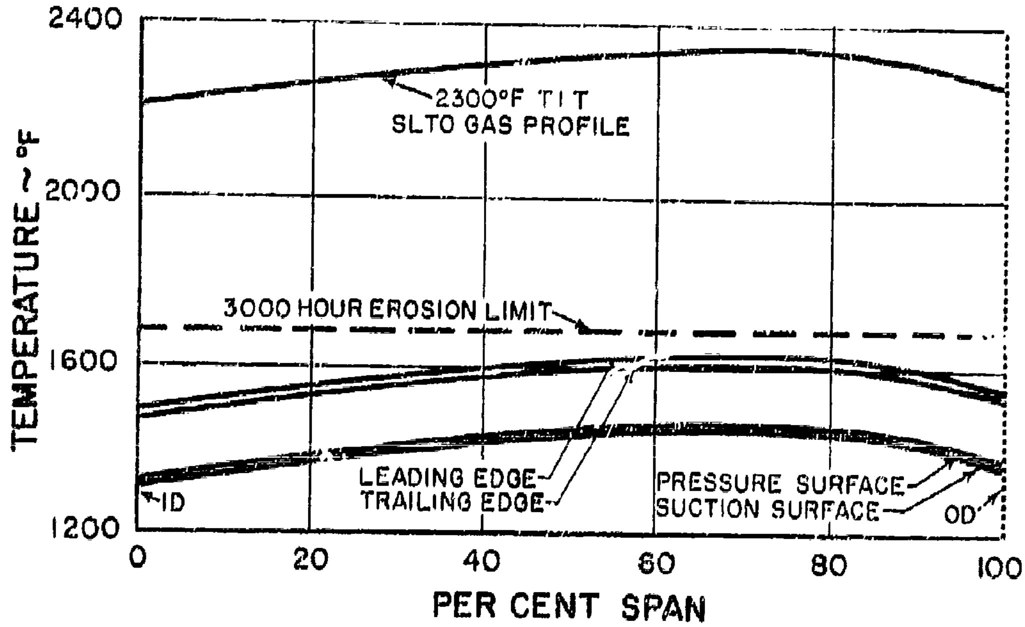

SPANWISE GRADIENT FOR THE ALTERNATE VANE

Figure 2A-83

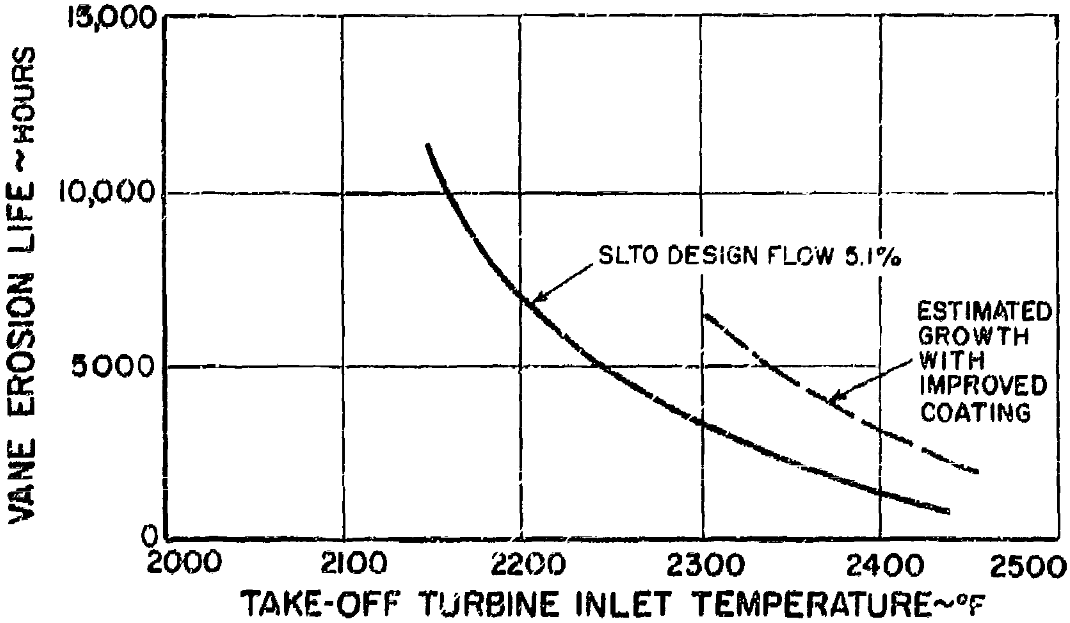

BASIC RATING CAPABILITY FOR THE ALTERNATE VANE

Figure 2A-84

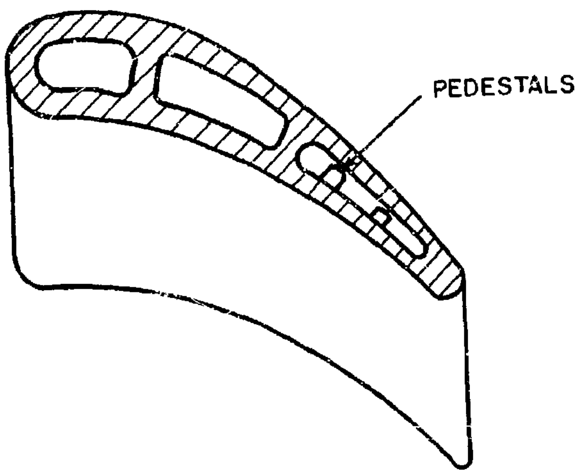

BLADE DESIGN FOR THE INITIAL RATING

Figure 2A-85

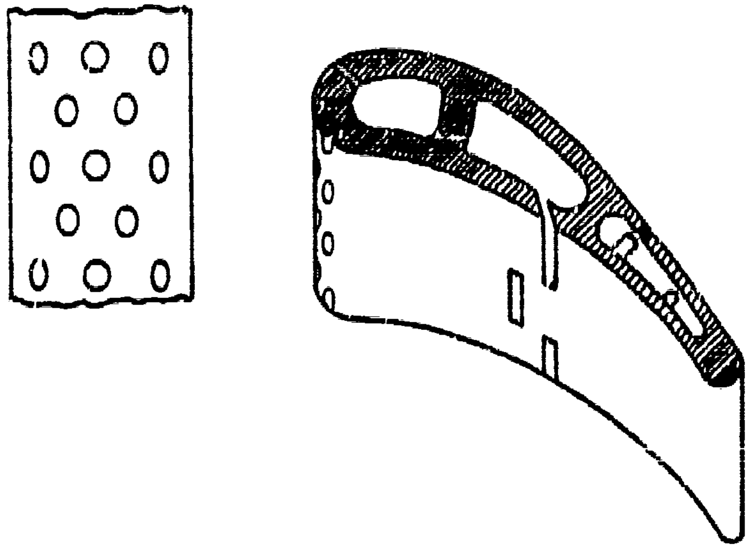

BASIC RATING ENGINE BLADE DESIGN

Figure 2A-86

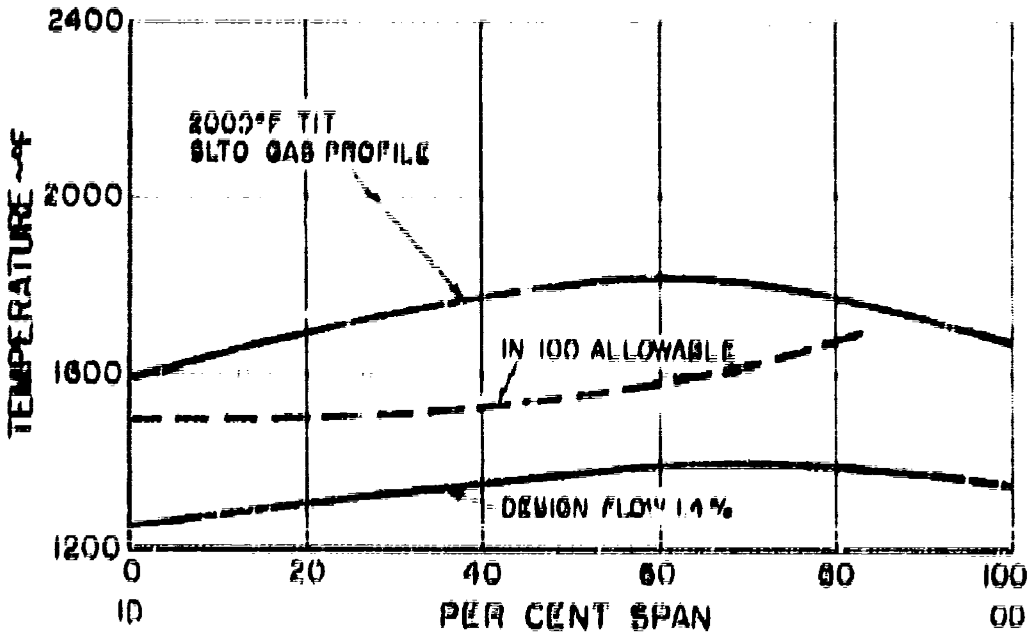

SPANWISE GRADIENT FIRST STG BLADE - INITIAL RATING

Figure 2A-87

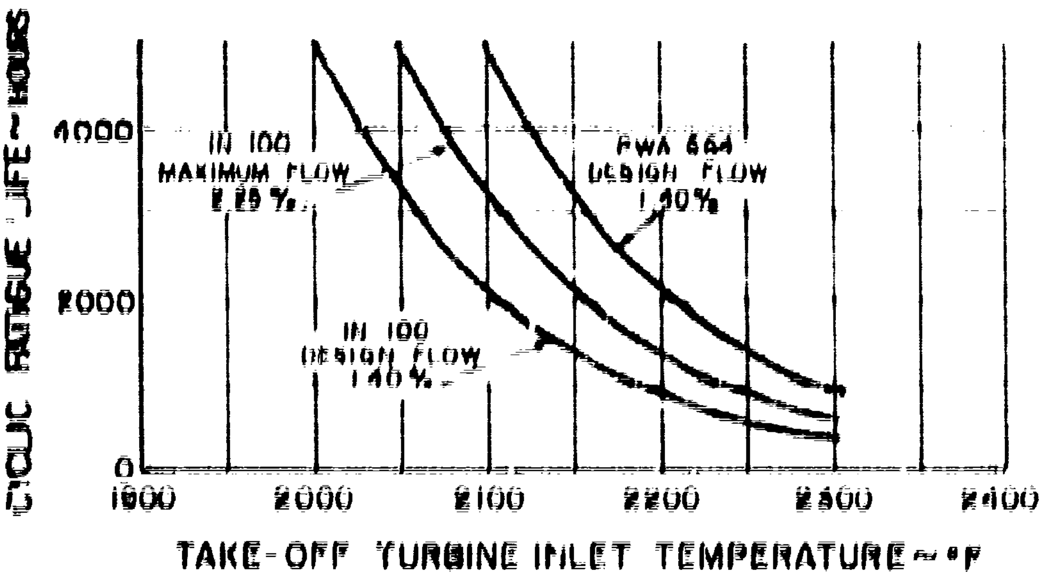

GROWTH CAPABILITY OF THE INITIAL RATING CONFIGURATION
- FIRST STAGE BLADE

Figure 7A-[illegible]

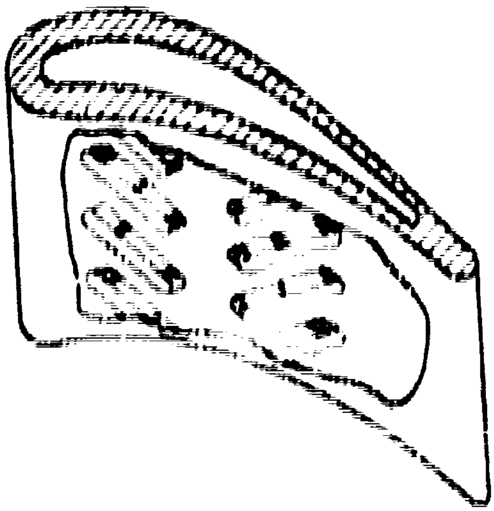

ALTERNATE INITIAL RATING ENGINE BLADE DESIGN — 1st STAGE

Figure 7A-[illegible]

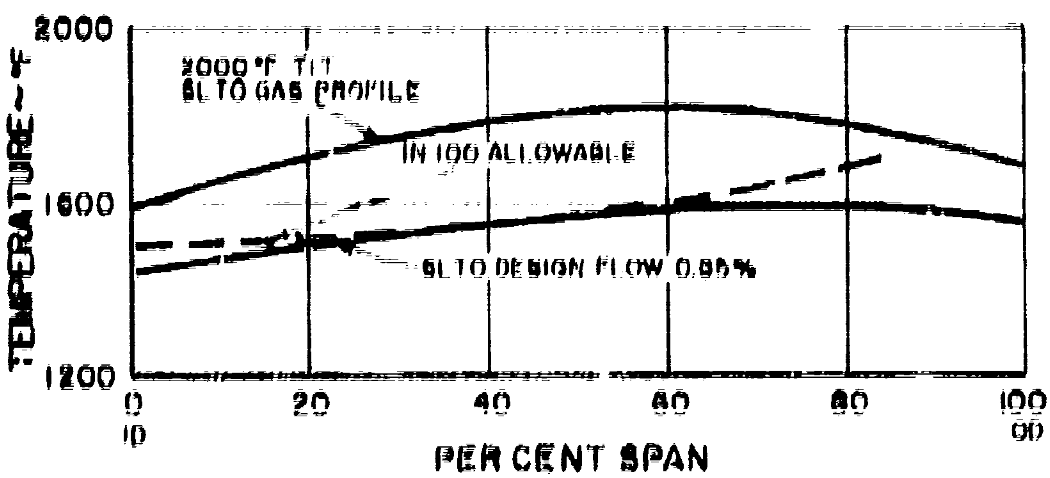

SPANWISE GRADIENT FOR THE INITIAL RATING ENGINE – FIRST STAGE BLADE

Figure 7A-90

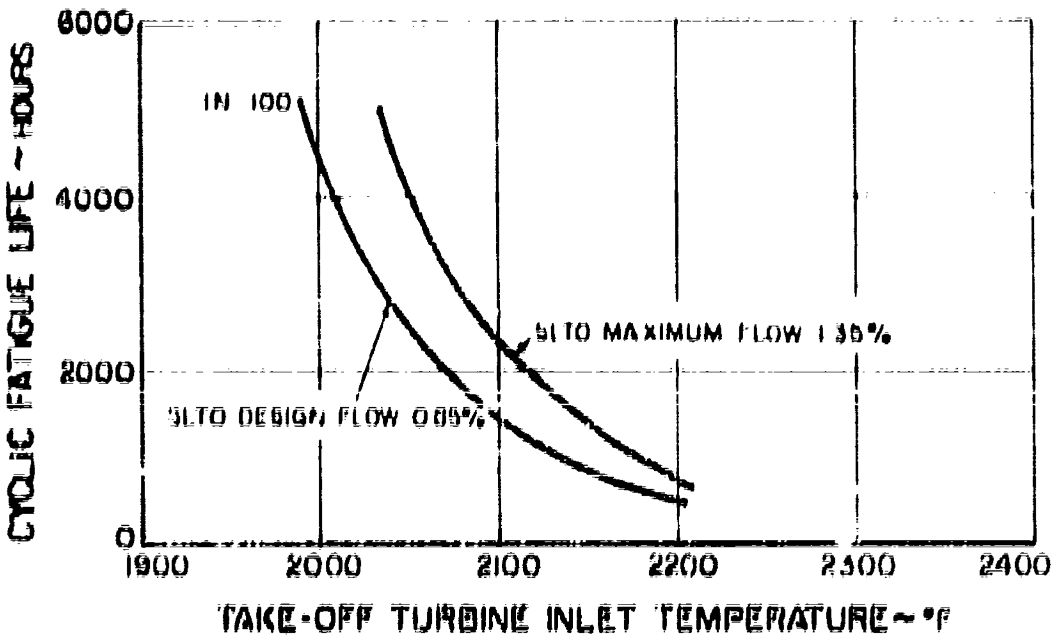

GROWTH CAPABILITY FOR THE INITIAL RATING ENGINE - FIRST STAGE BLADE

Figure 2A-91

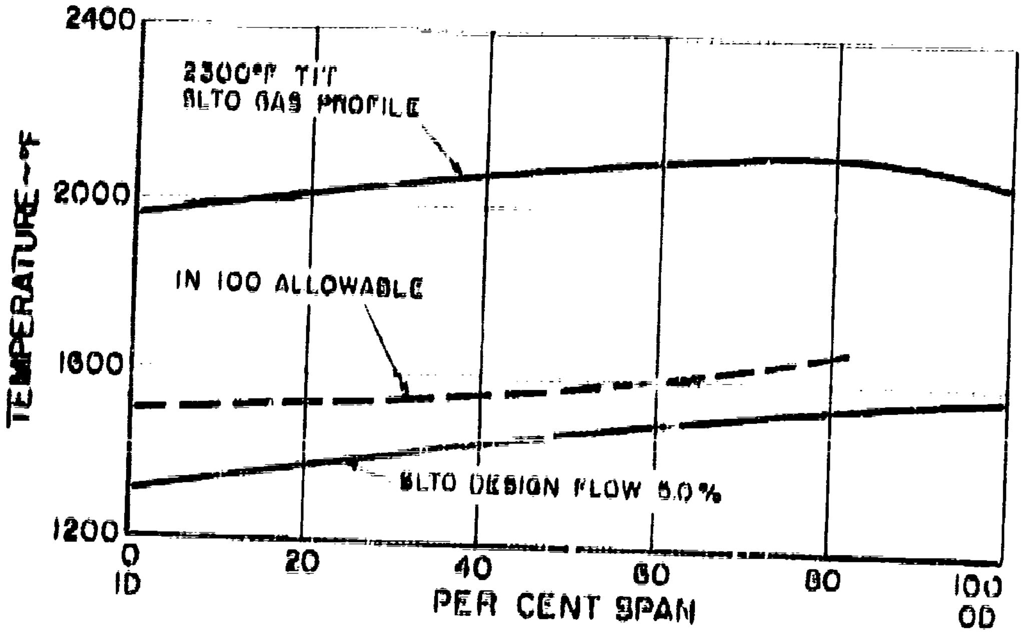

SPANWISE GRADIENT FOR THE BASIC RATING — FIRST STAGE BLADE

Figure 2A-92

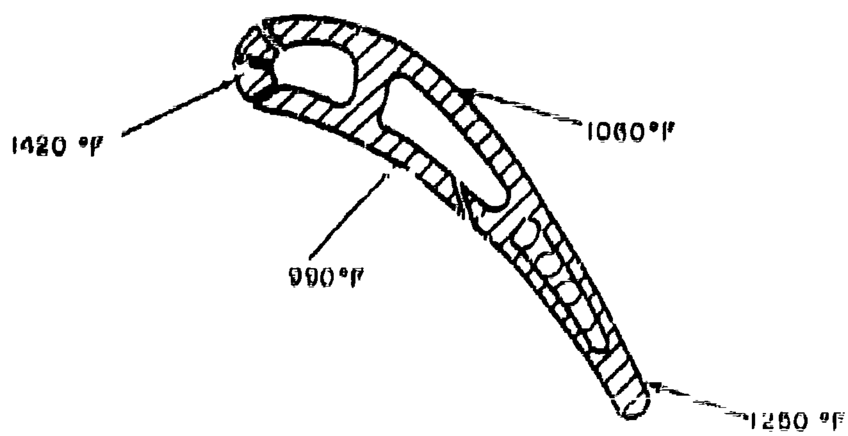

CHORDWISE GRADIENT FOR THE BASIC RATING - FIRST STAGE BLADE

Figure 2A-93

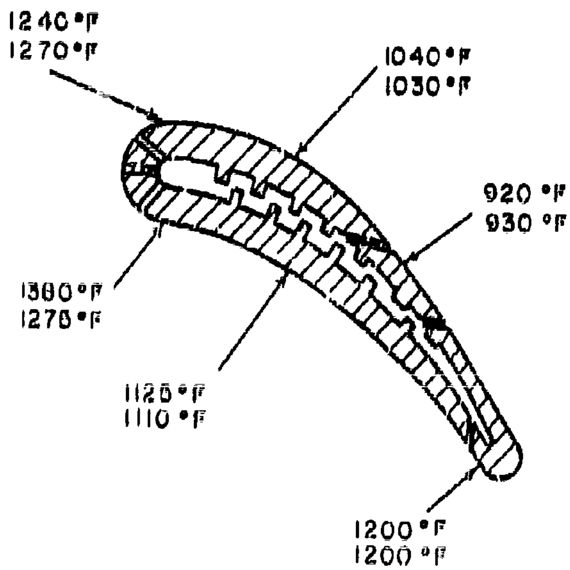

TRANSIENT THERMAL GRADIENTS ON THE TURBINE DEVELOP MENT ENGINE

Figure 2A-94

This page intentionally blank

Figure 2A-95

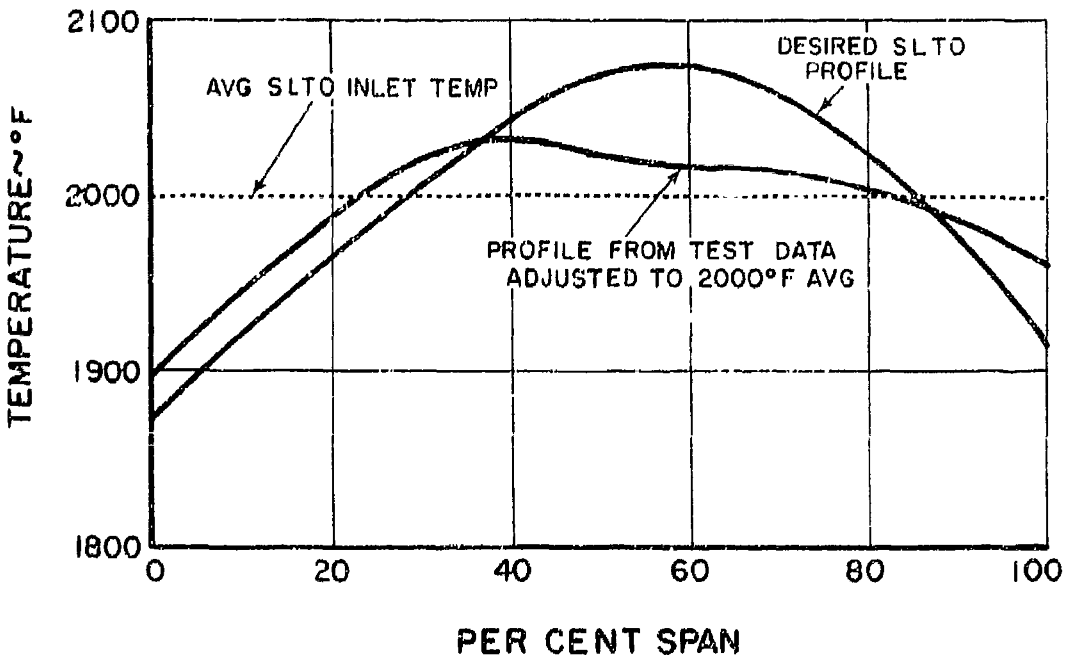

COMPARISON OF RADIAL TEMPERATURE PROFILES

Figure 2A-97

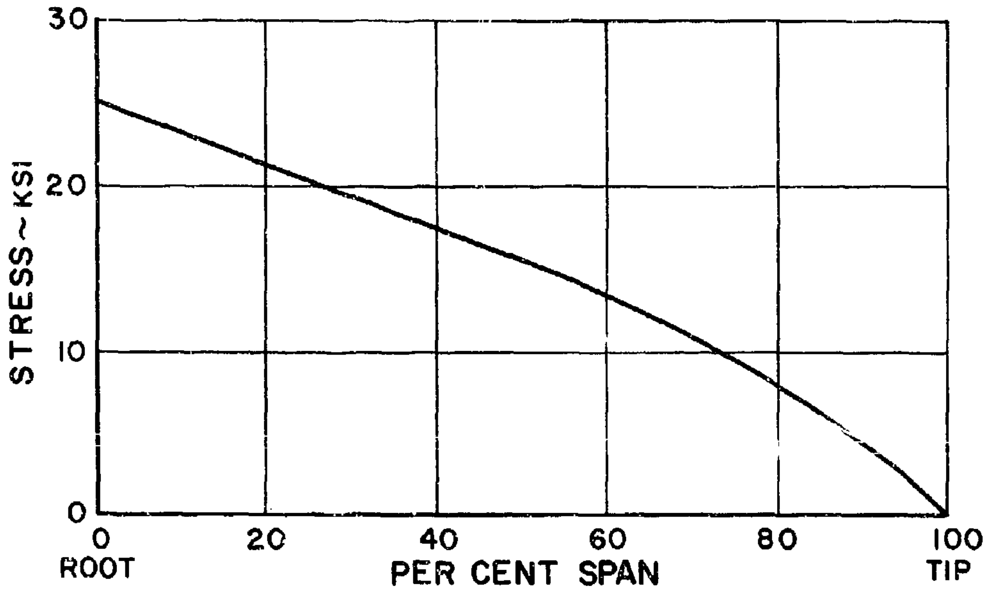

FIRST BLADE STRESS DISTRIBUTION - INITIAL RATING

Figure 2A-98

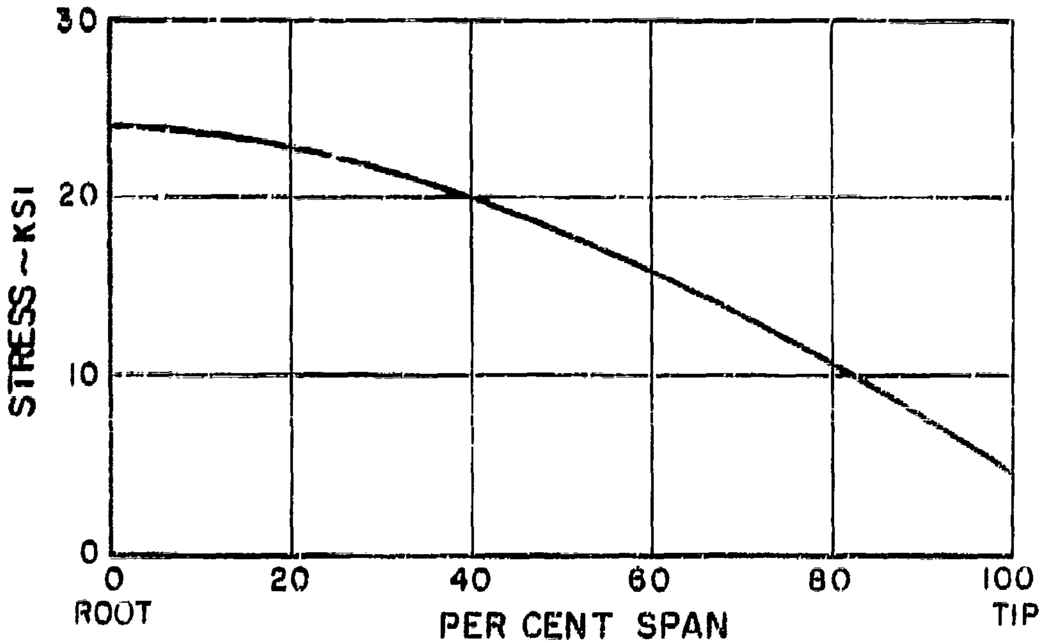

SECOND BLADE STRESS DISTRIBUTION - INITIAL RATING

Figure 2A-99

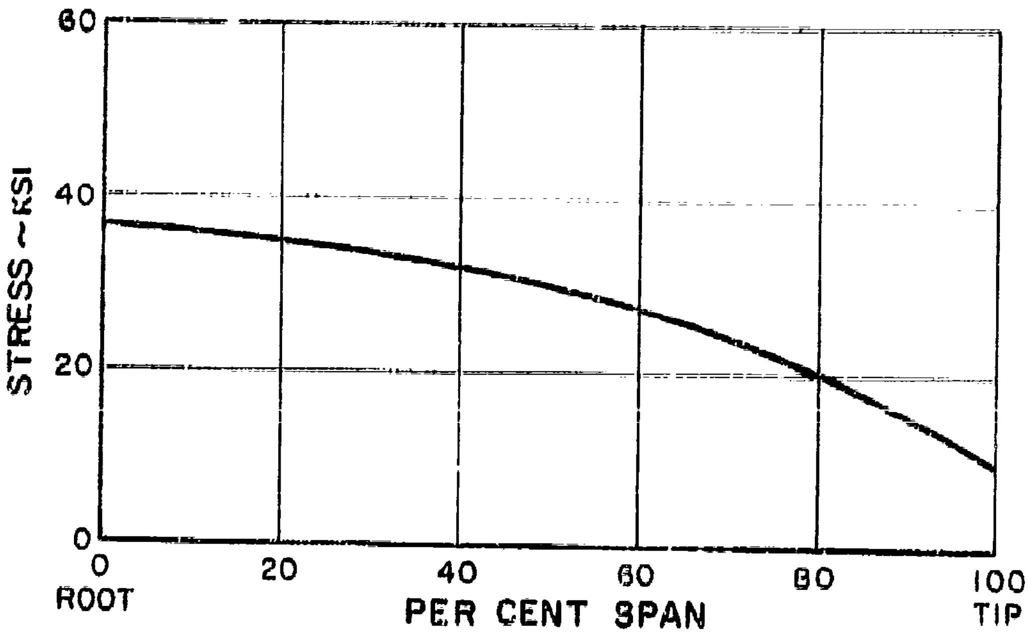

THIRD BLADE STRESS DISTRIBUTION - INITIAL RATING

Figure 2A-100

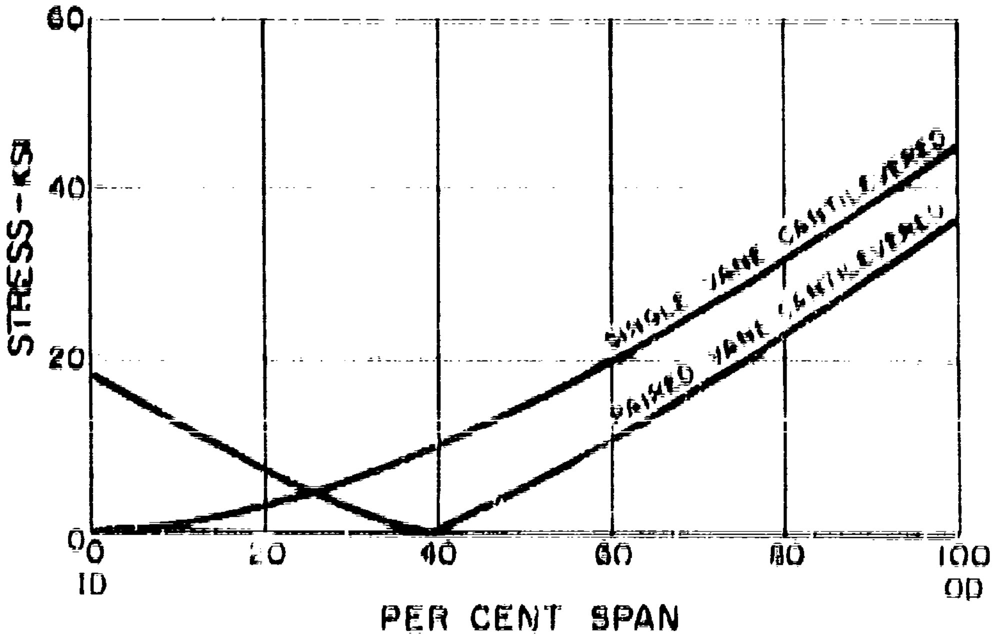

FIRST STAGE VANE STRESS DISTRIBUTION - INITIAL RATING

Figure 2A-101

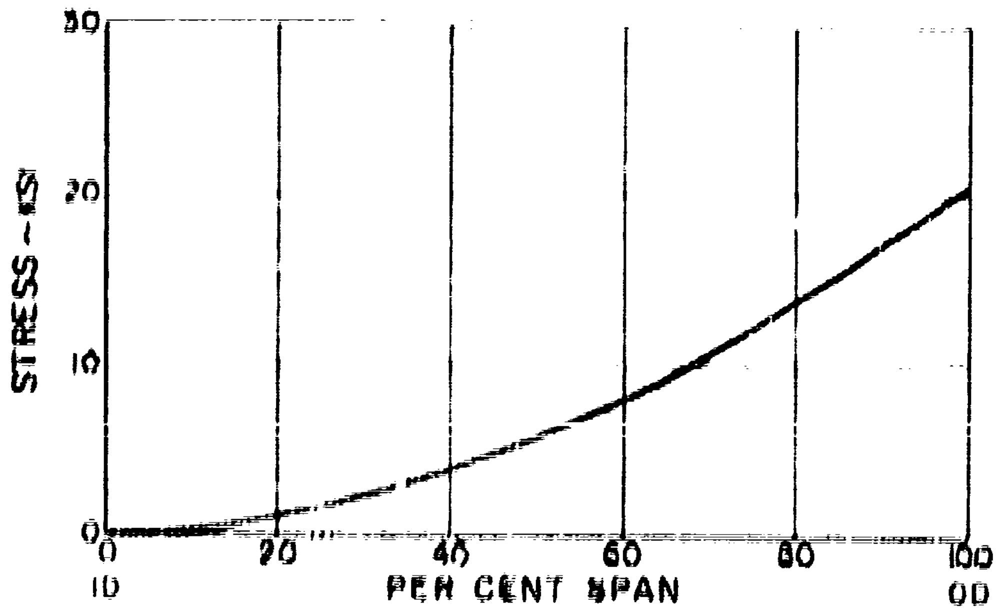

SECOND STAGE VANE STRESS DISTRIBUTION – INITIAL RATING

Figure 7A-102

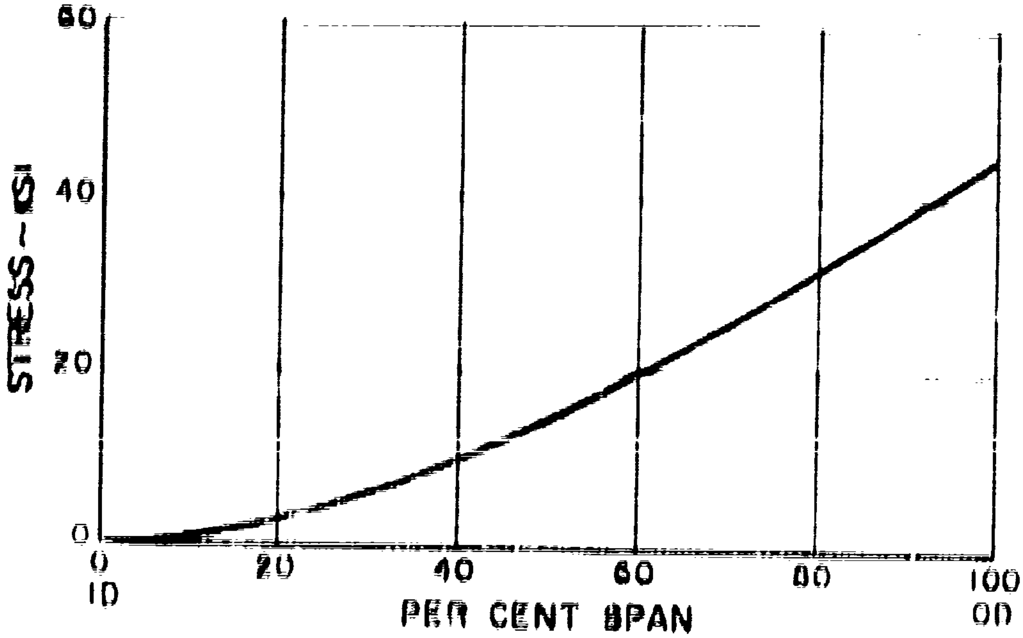

THIRD STAGE VANE STRESS DISTRIBUTION INITIAL RATING

Figure 2A 103

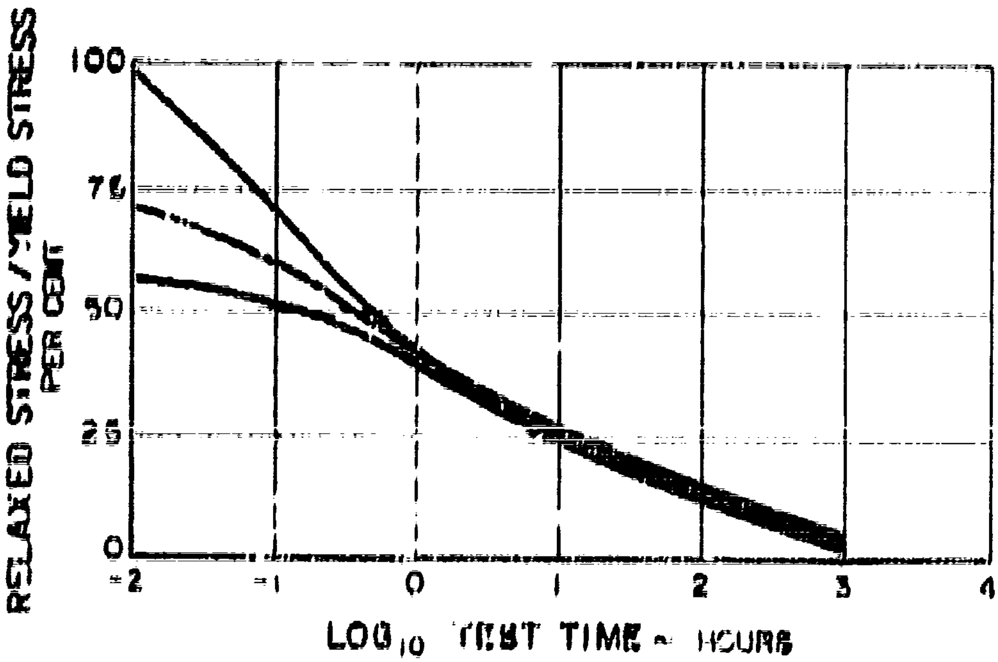

SUPER ALLOY RELAXATION CURVE

Figure 7A-104

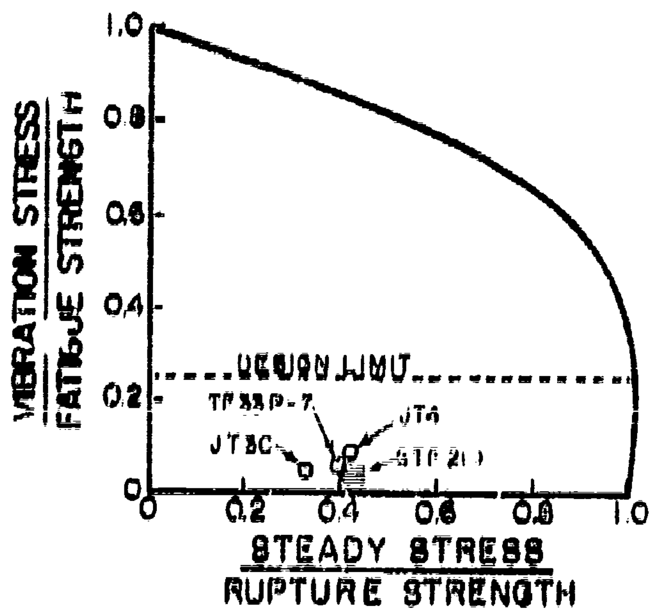

GOODMAN DIAGRAM, TYPICAL TURBINE BLADE MATERIAL

Figure 2A-105

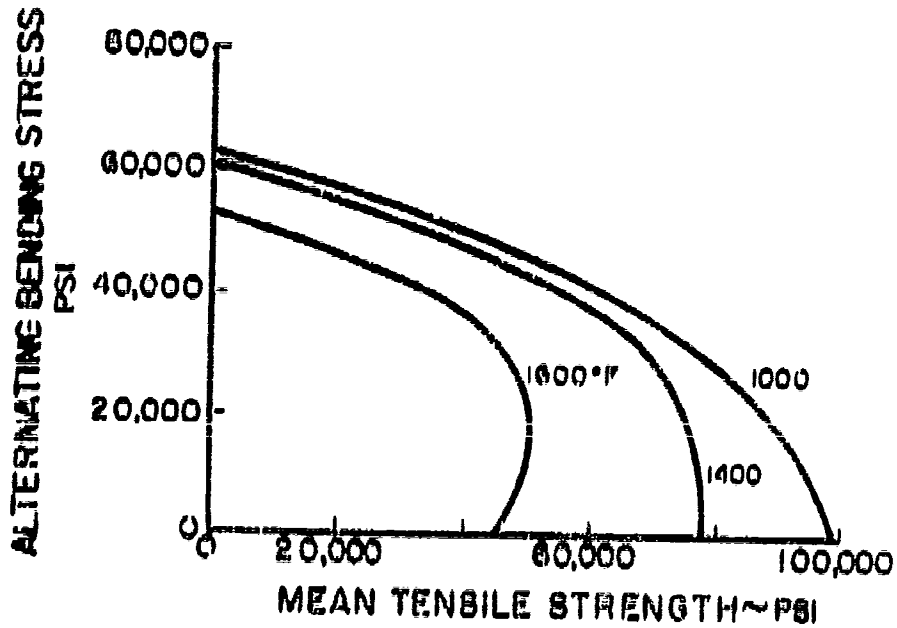

GOODMAN DIAGRAM, UNNOTCHED U-700, SHOWING TEMPERATURE DEPENDENCE

Figure 2A-106

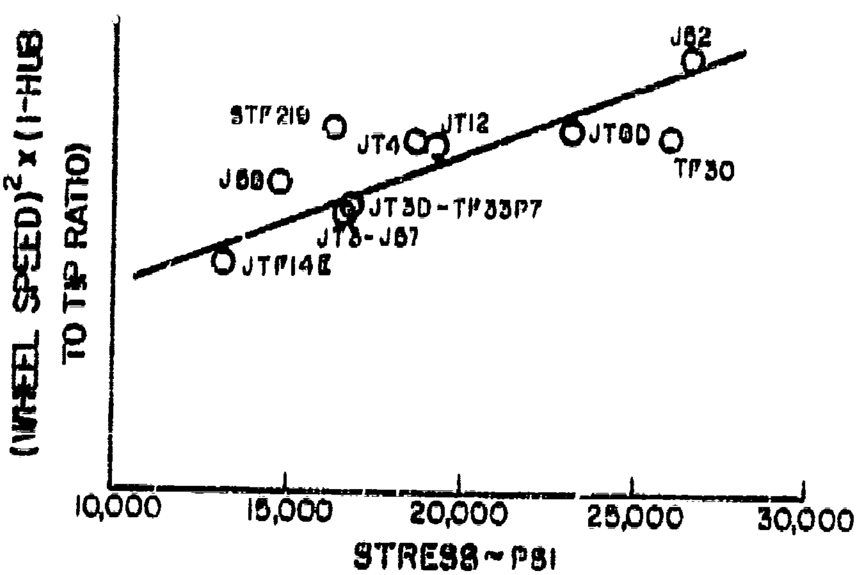

MIDSPAN CENTRIFUGAL STRESS

Figure 2A-107

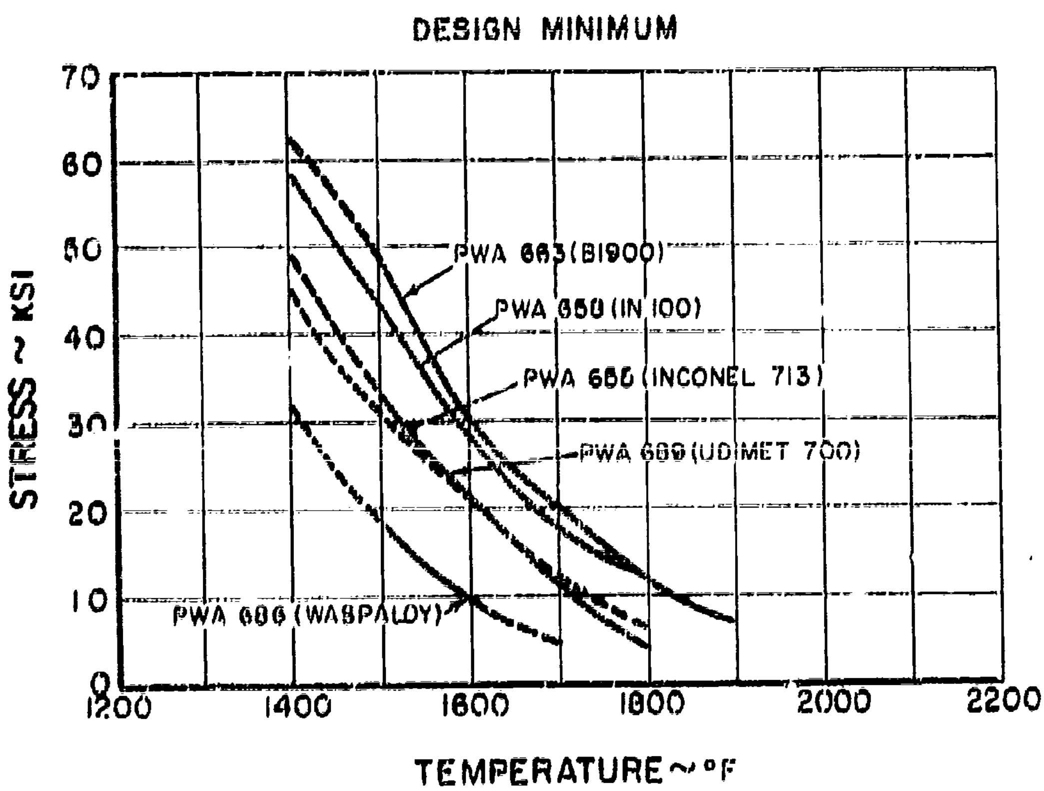

COMPARISON OF CREEP STRENGTH TEMPERATURE MARGIN

Figure 2A-108

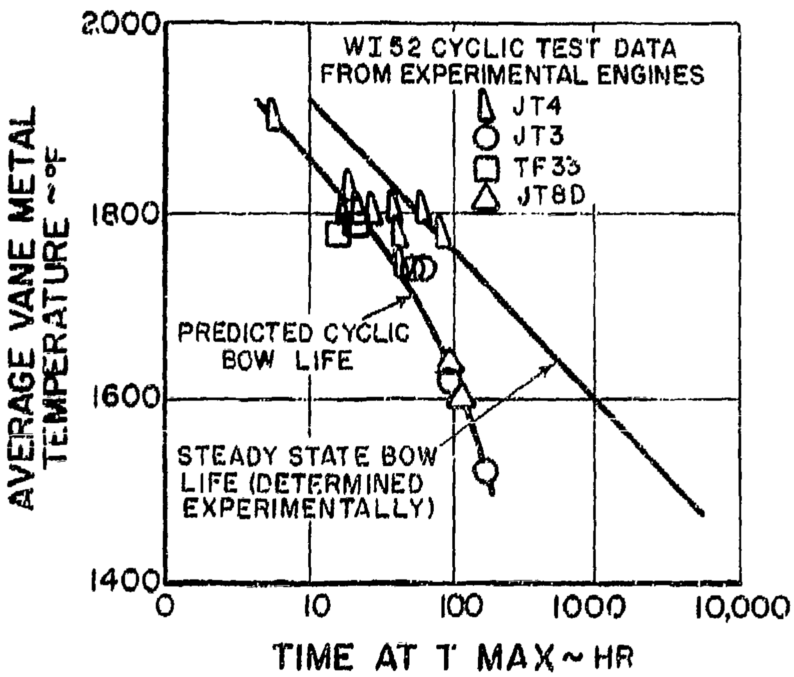

TRAILING EDGE BOW PREDICTIONS AND TEST VALUES

Figure 2A-109

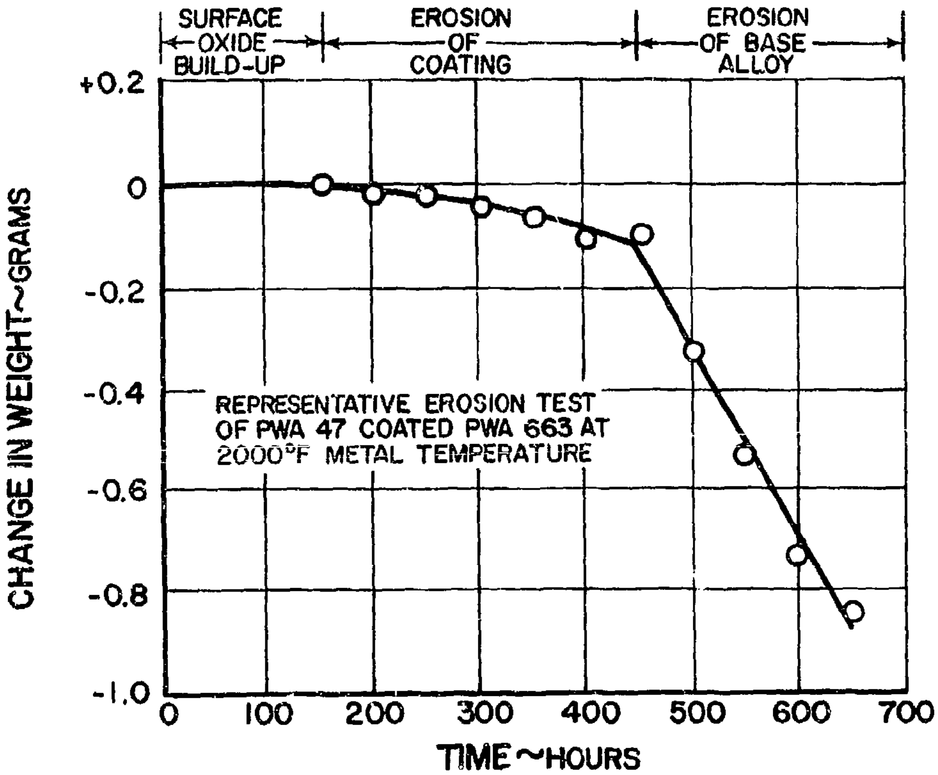

WEIGHT LOSS PLOT FOR COATED B-1900 EROSION TEST

Figure 2A-110

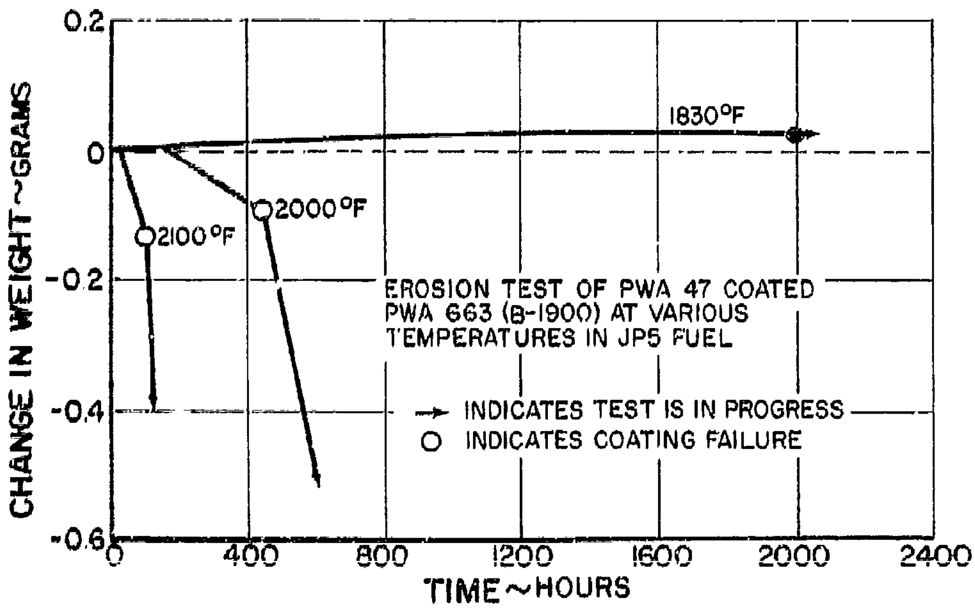

TEMPERATURE DEPENDENCE OF RATE OF EROSION

Figure 2A-111

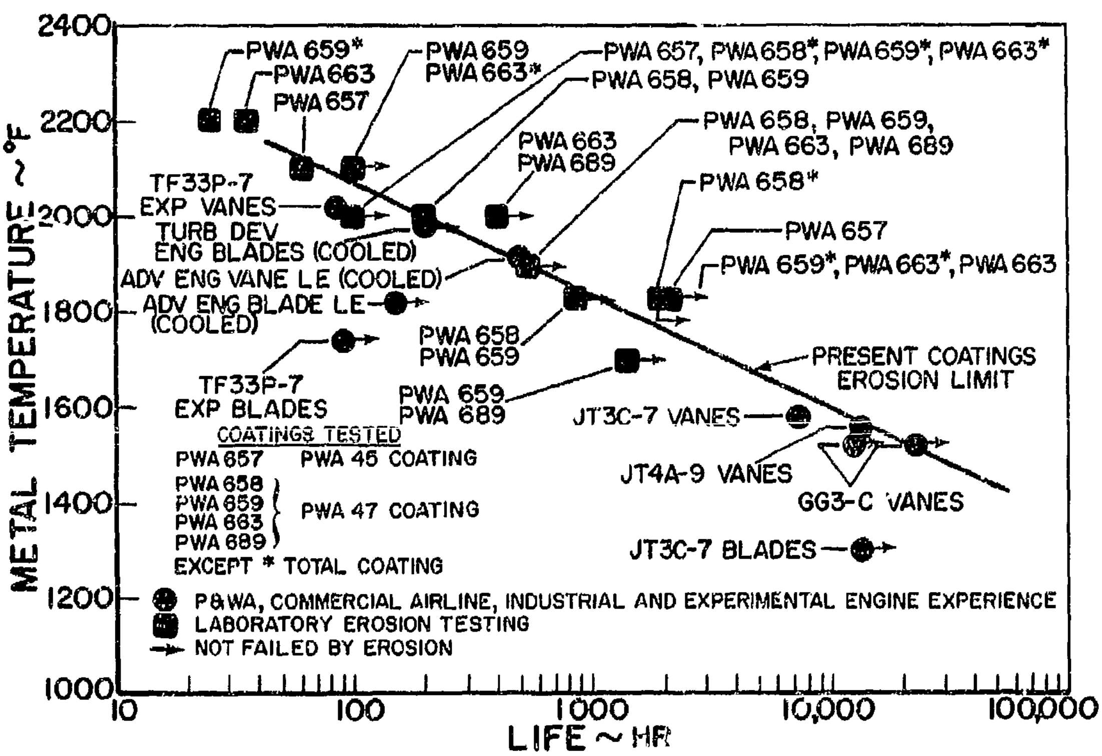

EROSION LIMITS FOR COATED TURBINE MATERIALS

Figure 2A-112

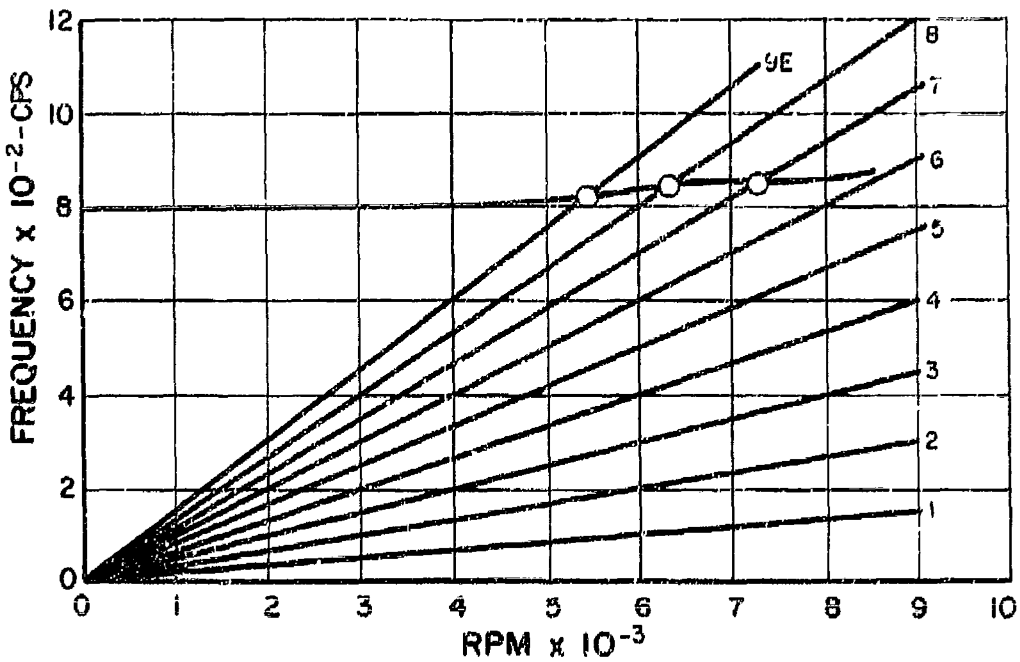

FIRST STAGE TURBINE BLADED-DISK FREQUENCY

Figure 2A-113

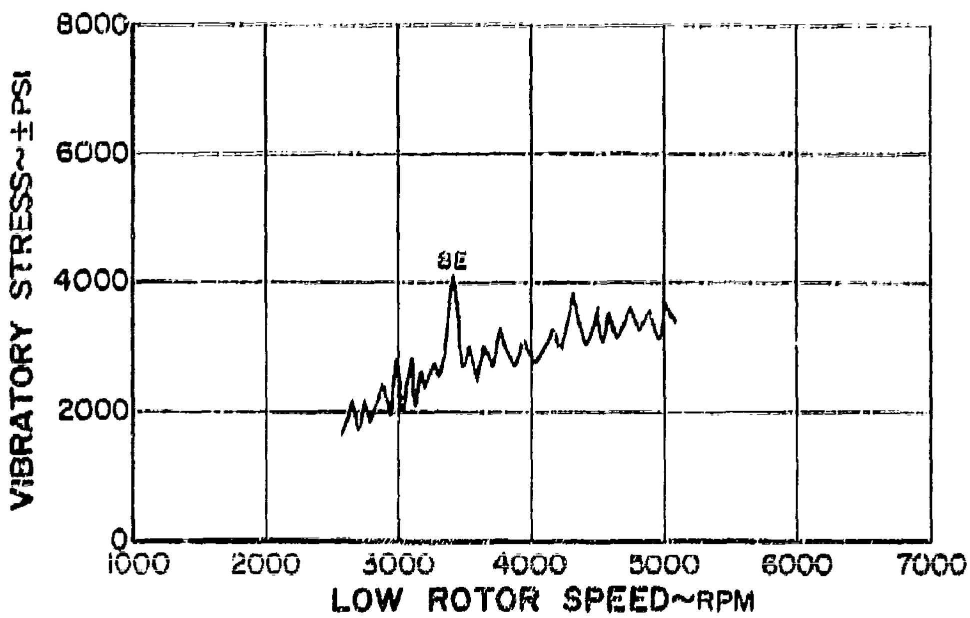

TURBINE BLADE VIBRATORY STRESS

Figure 2A-114

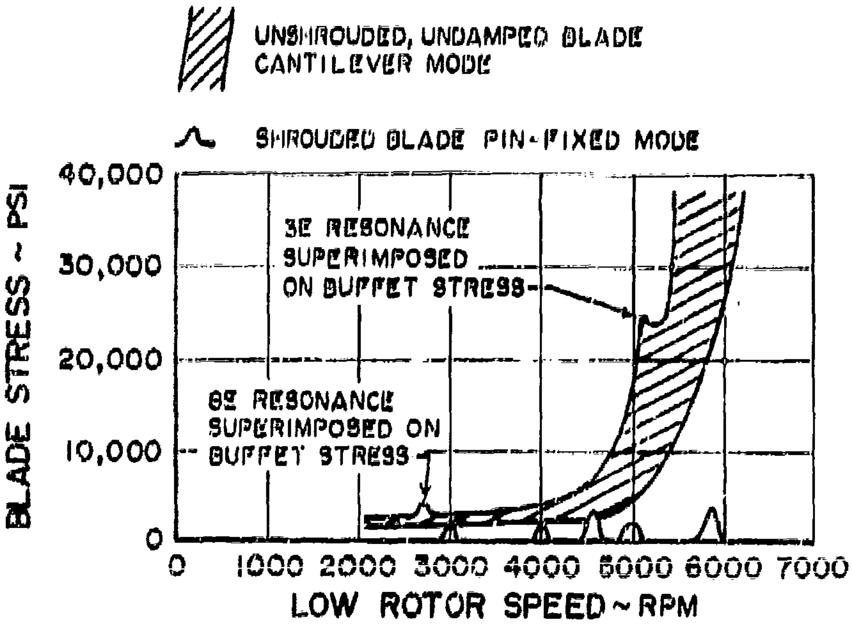

STRESS LEVELS JT3C SHROUDED AND UNSHROUDED BLADES

Figure 2A-115

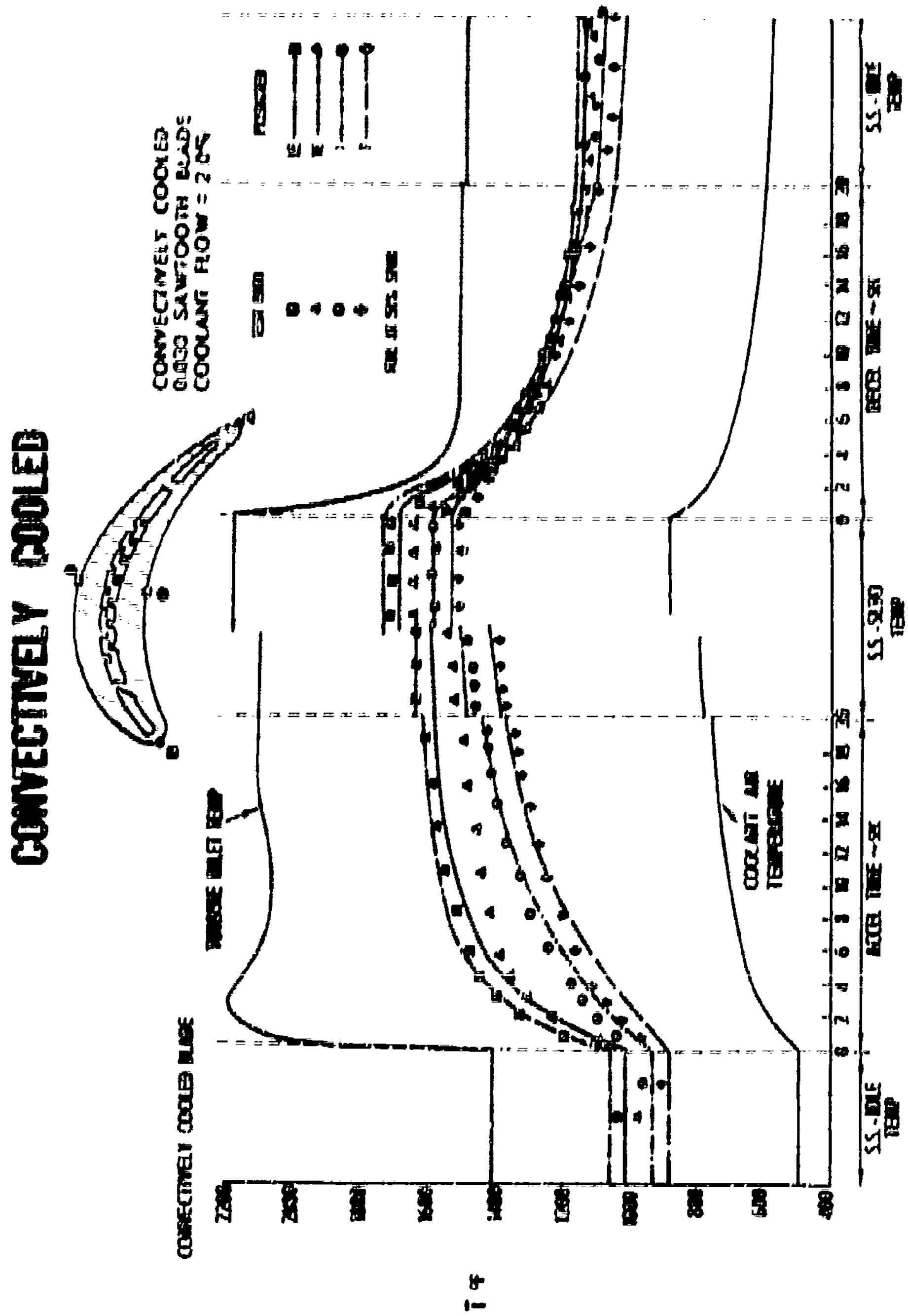

TRANSIENT TEMPERATURES ON CONVECTIVELY COOLED BLADES SHOWING PREDICTED AND ACTUAL VALUES

Figure 2A-116

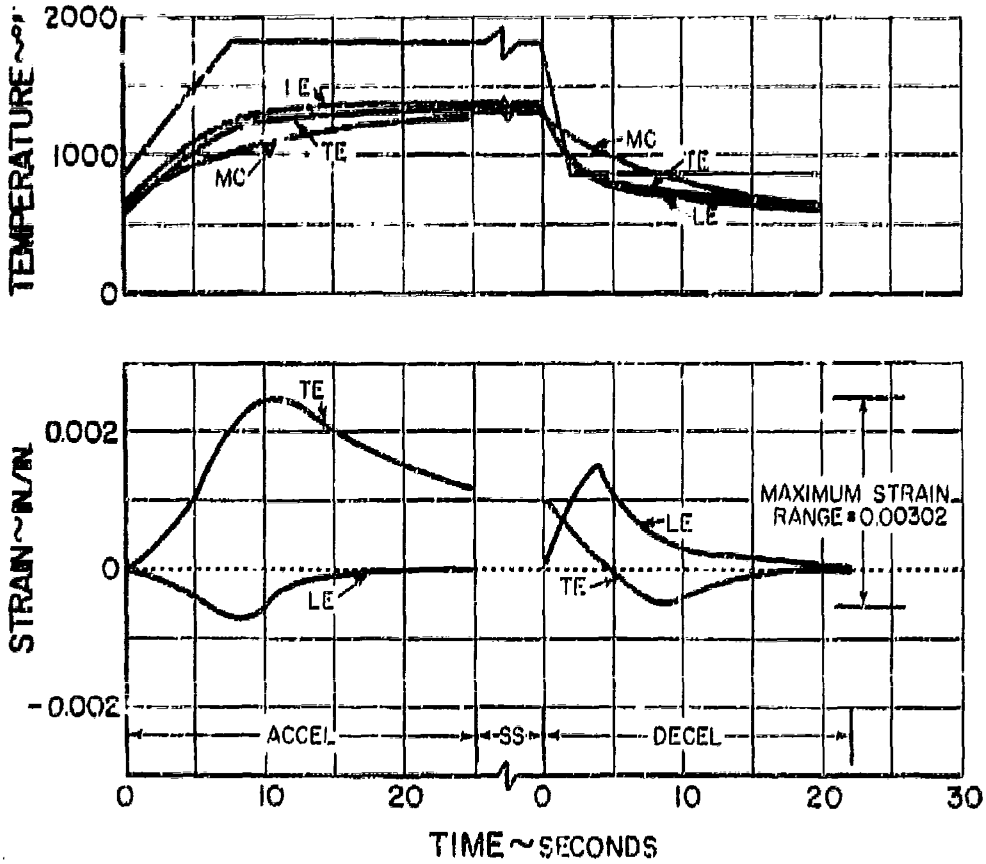

FIRST STAGE TURBINE BLADE STRAIN RANGE

Figure 2A-117

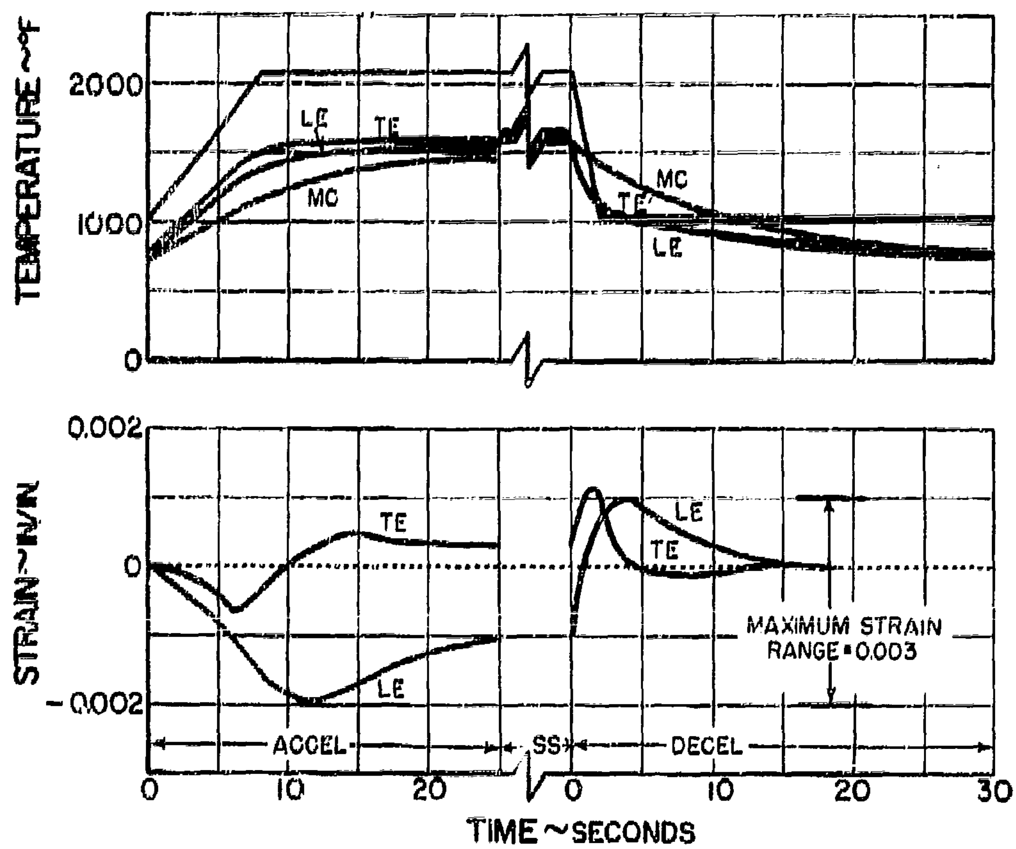

FIRST STAGE TURBINE VANE STRAIN RANGE

Figure 2A-118

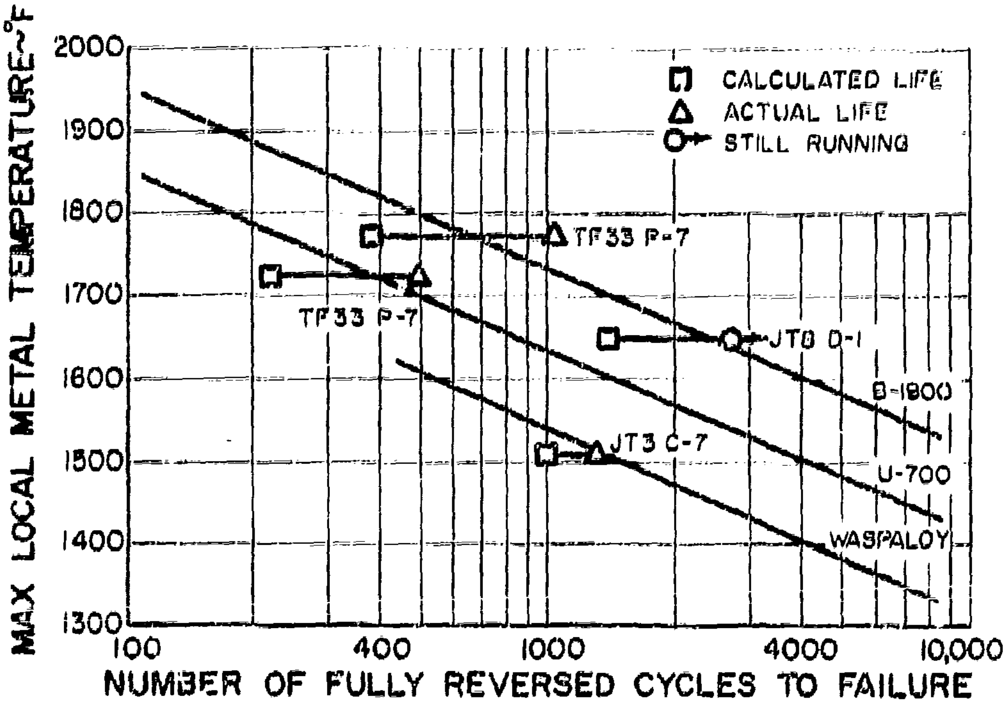

ENGINE SUBSTANTIATION OF FATIGUE STRENGTH OF TURBINE BLADE ALLOYS

Figure 2A-119

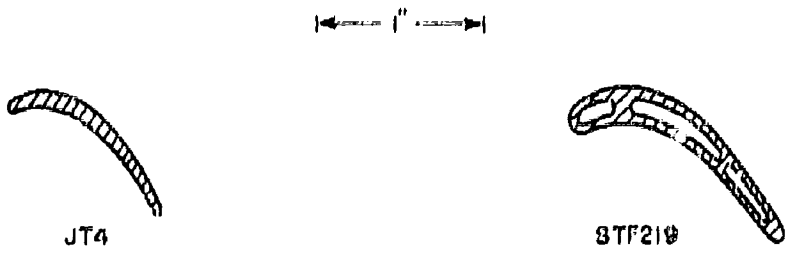

FIRST STAGE BLADE TIP SECTION

Figure 2A-120

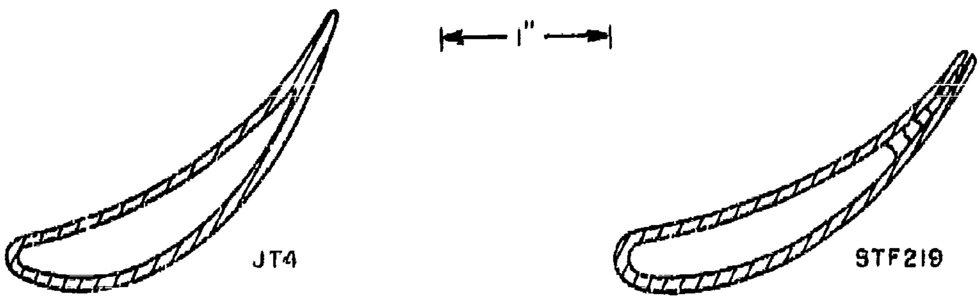

FIRST STAGE VANE TIP SECTION

Figure 2A-121

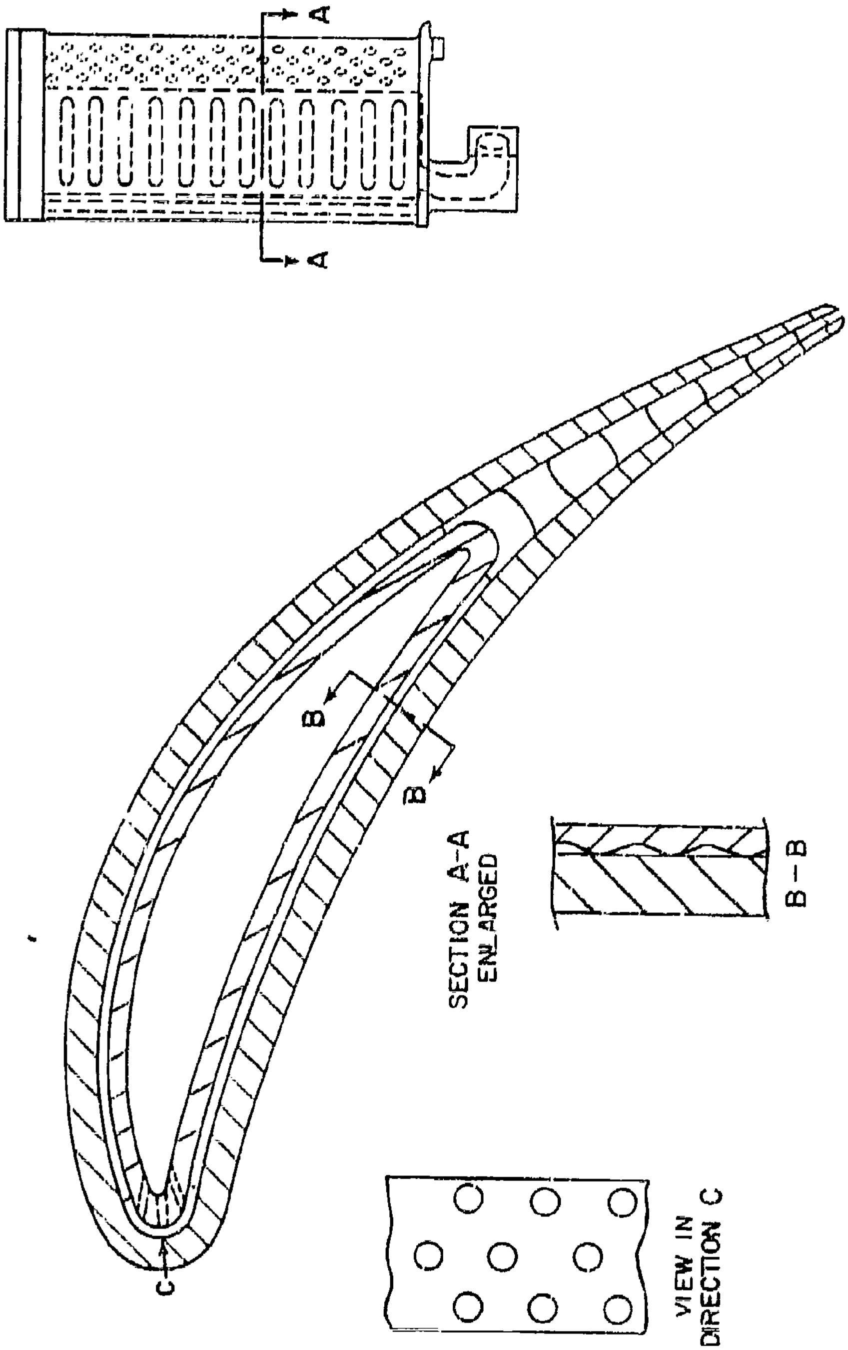

FIRST TURBINE VANE GEOMETRY - INITIAL (2000°F) RATING

Figure 2A-122

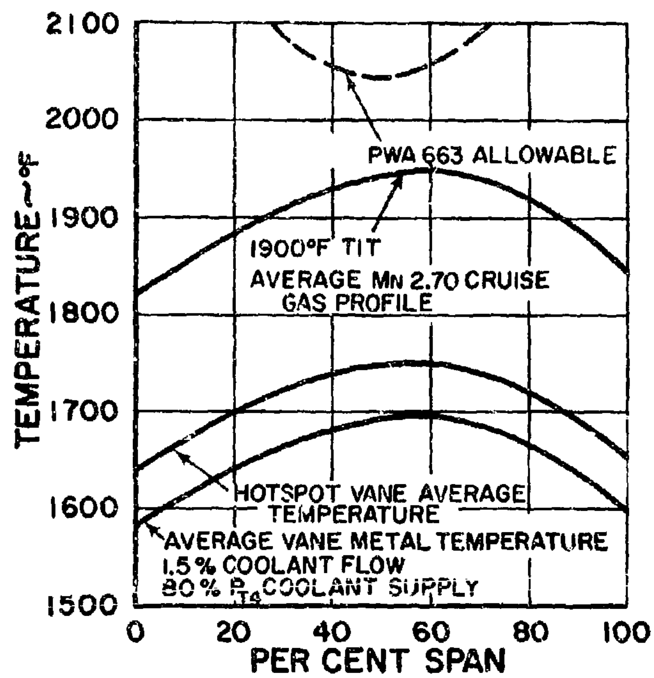

FIRST TURBINE VANE SPANWISE TEMPERATURE DISTRIBUTION

Figure 2A-123

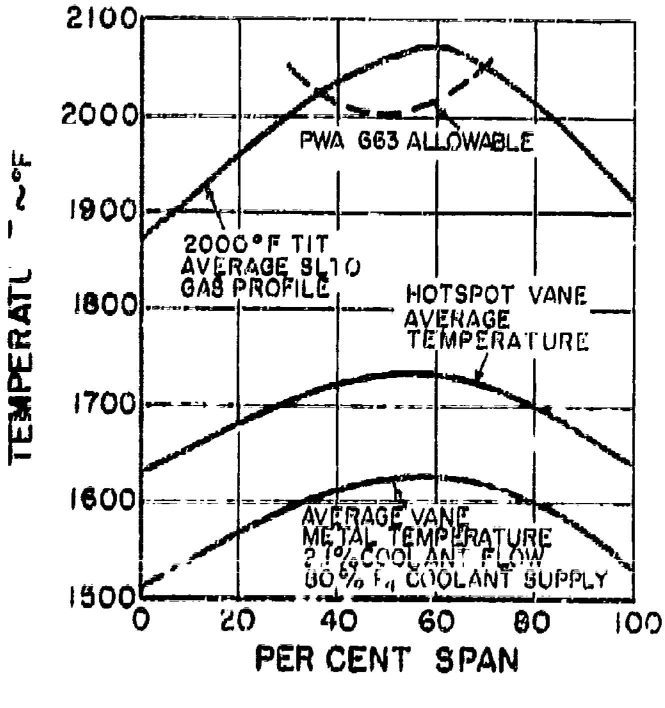

FIRST TURBINE VANE SPANWISE TEMPERATURE DISTRIBUTION

Figure 2A-124

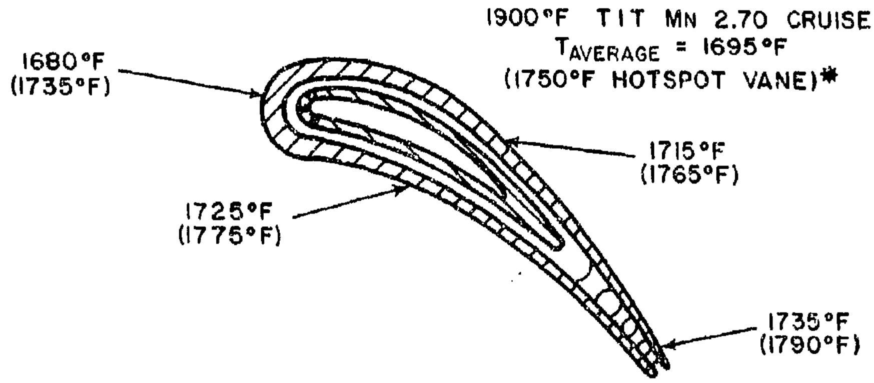

*BRACKETS INDICATE HOTSPOT VANE CONDITIONS

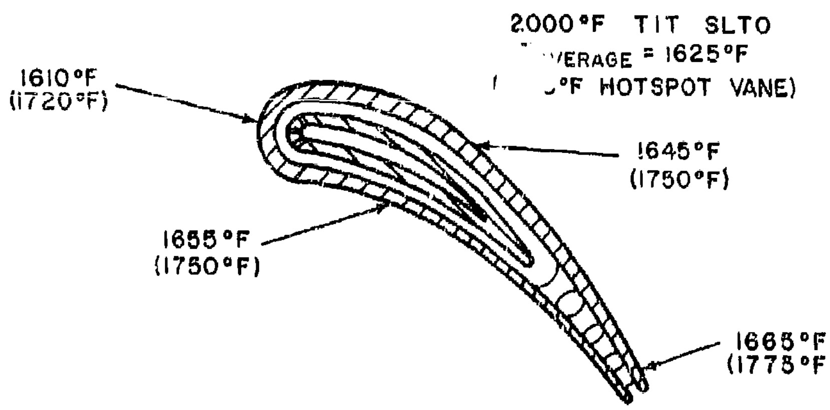

TURBINE VANE MIDSPAN LOCAL METAL TEMPERATURE

Figure 2A-125

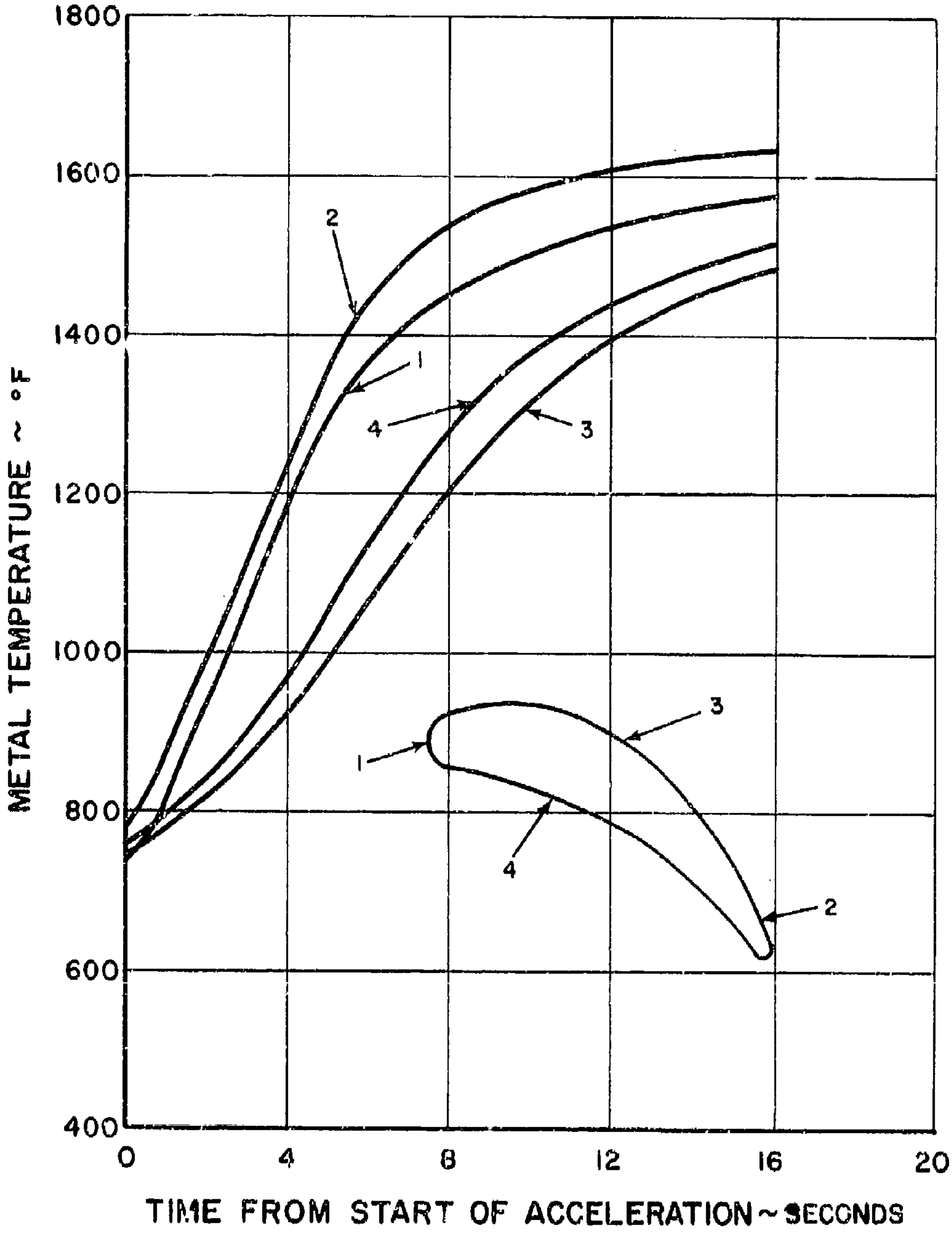

FIRST VANE TYPICAL TRANSIENT RESPONSE

Figure 2A-125

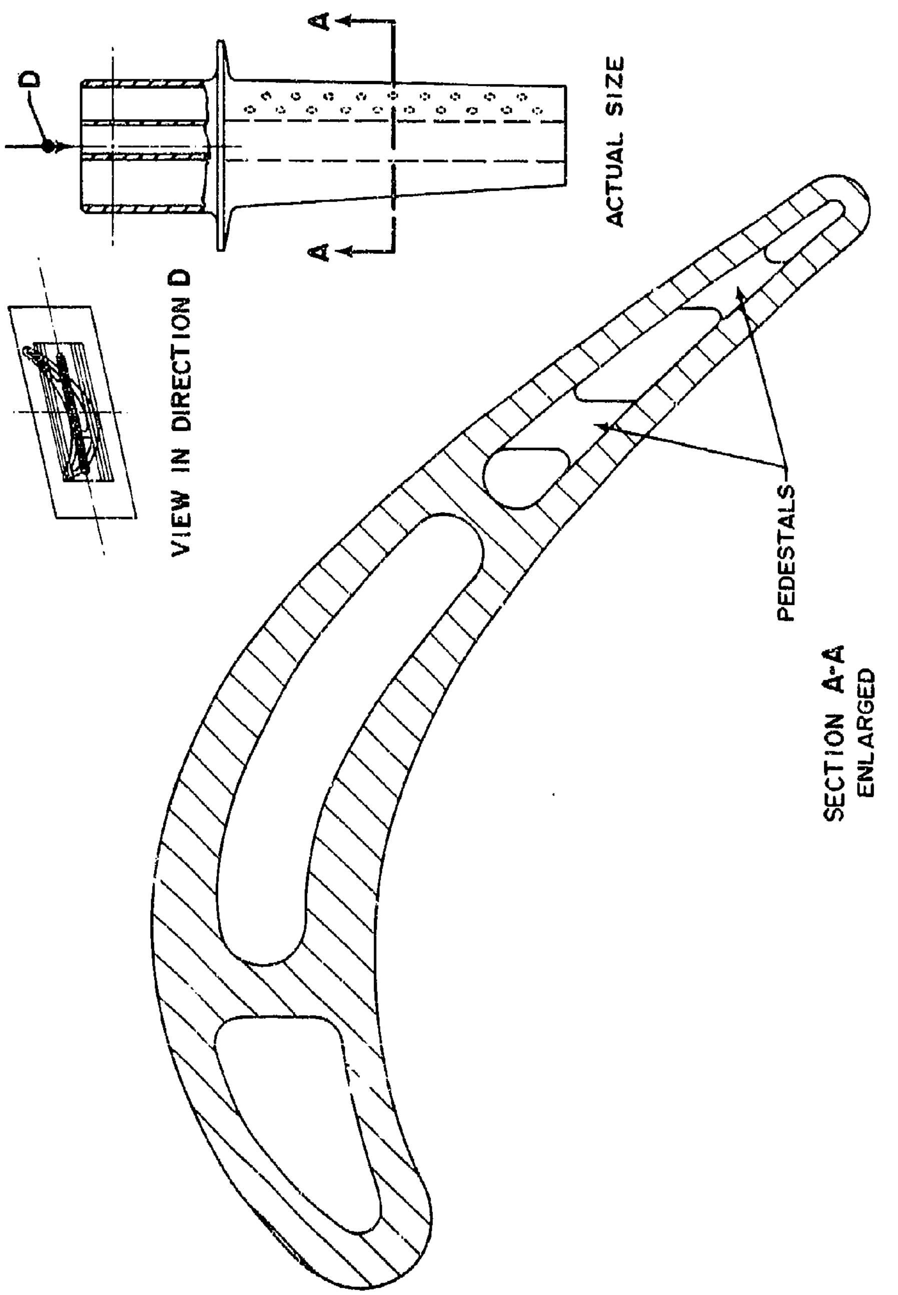

FIRST TURBINE, THREE CAVITY BLADE SECTION - INITIAL (2000°F) DESIGN

Figure 2A-127

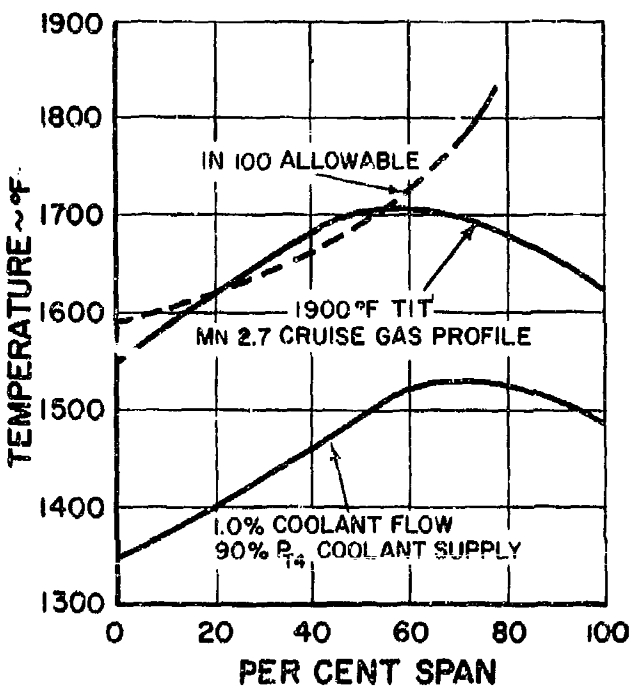

FIRST TURBINE, THREE CAVITY BLADE SPANWISE TEMPERATURE DISTRIBUTION

Figure 2A-128

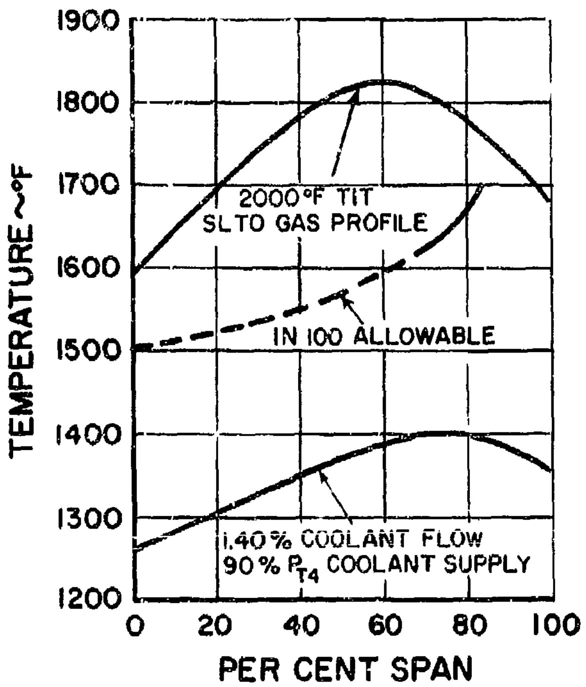

FIRST TURBINE, THREE CAVITY BLADE SPANWISE TEMPERATURE DISTRIBUTION

Figure 2A-129

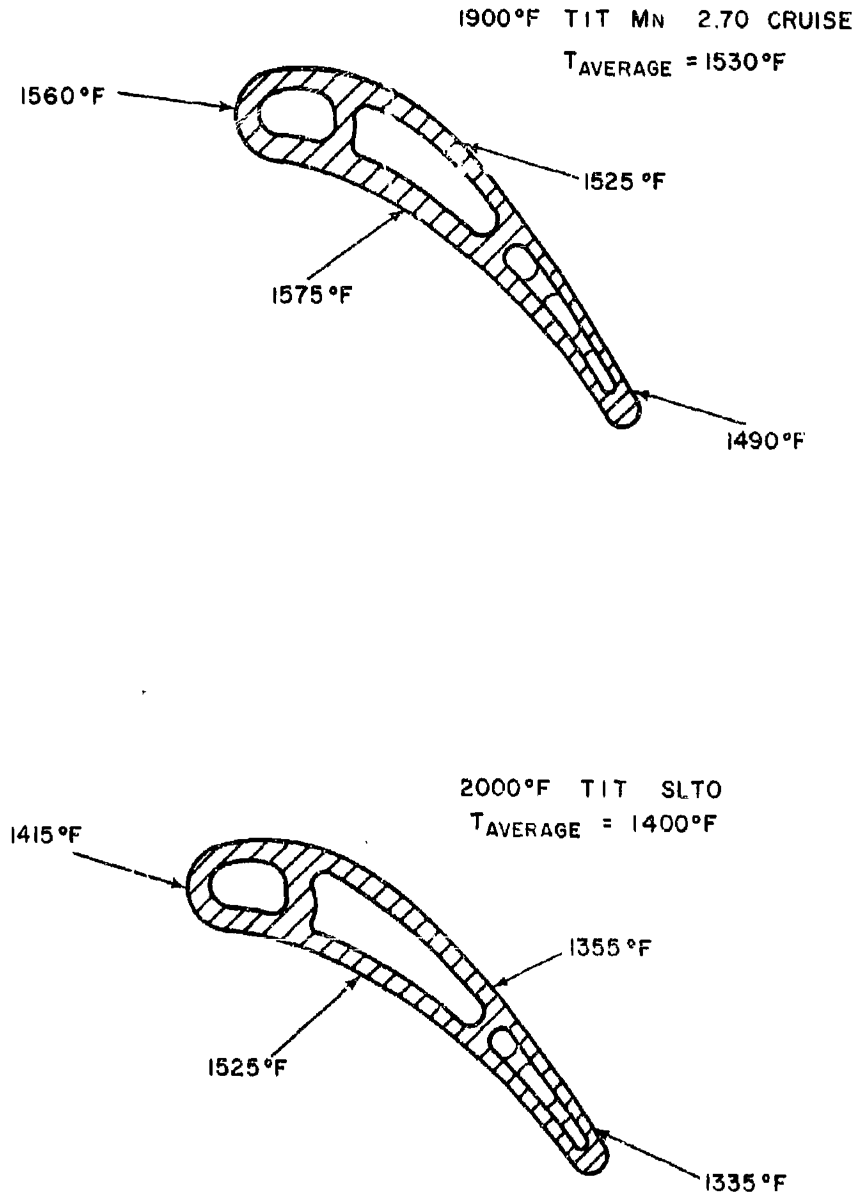

FIRST TURBINE, THREE CAVITY BLADE SPANWISE TEMPERATURE DISTRIBUTION

Figure 2A-130

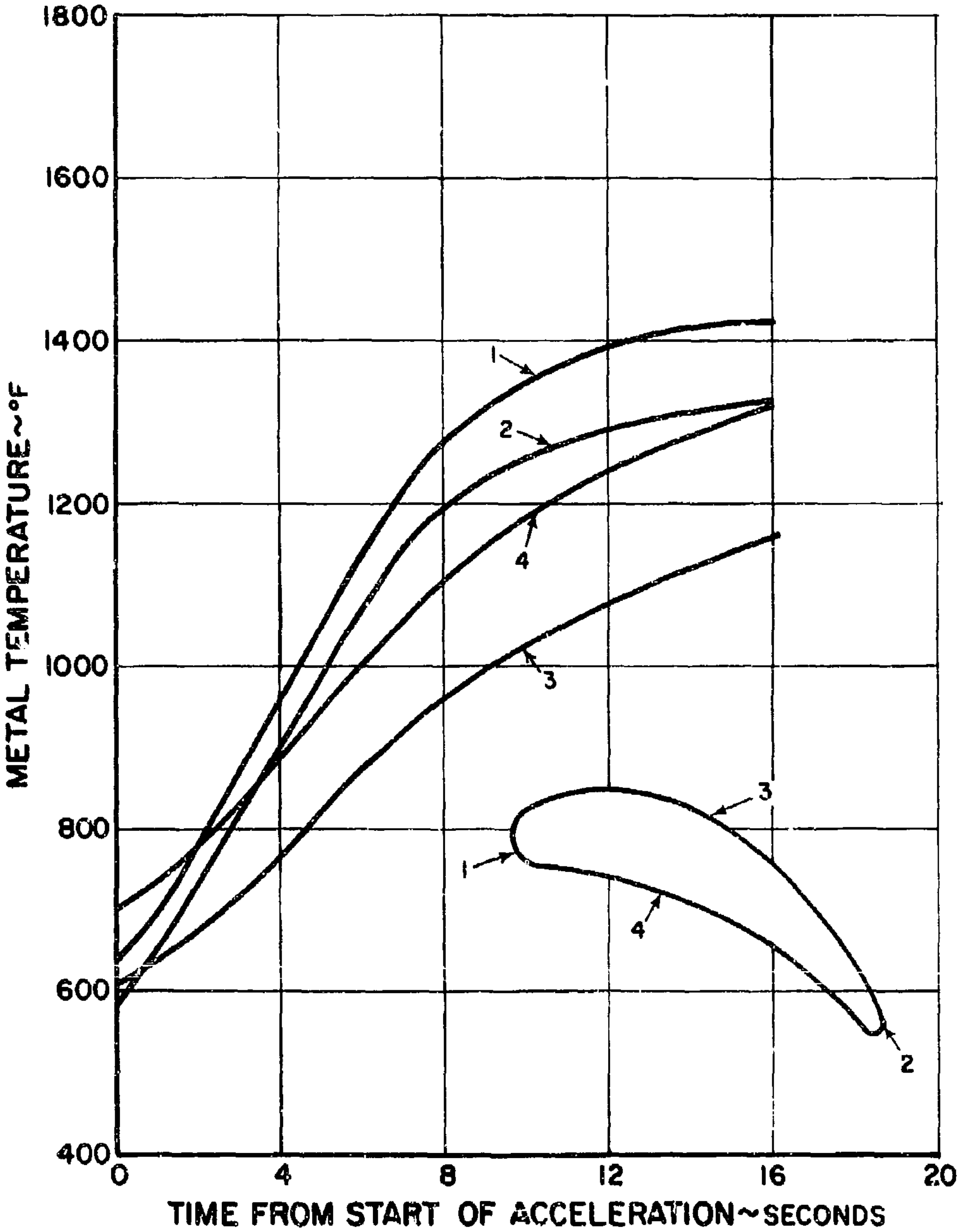

CONVECTIVELY COOLED FIRST TURBINE BLADE - TRANSIENT RESPONSE

Figure 2A-131

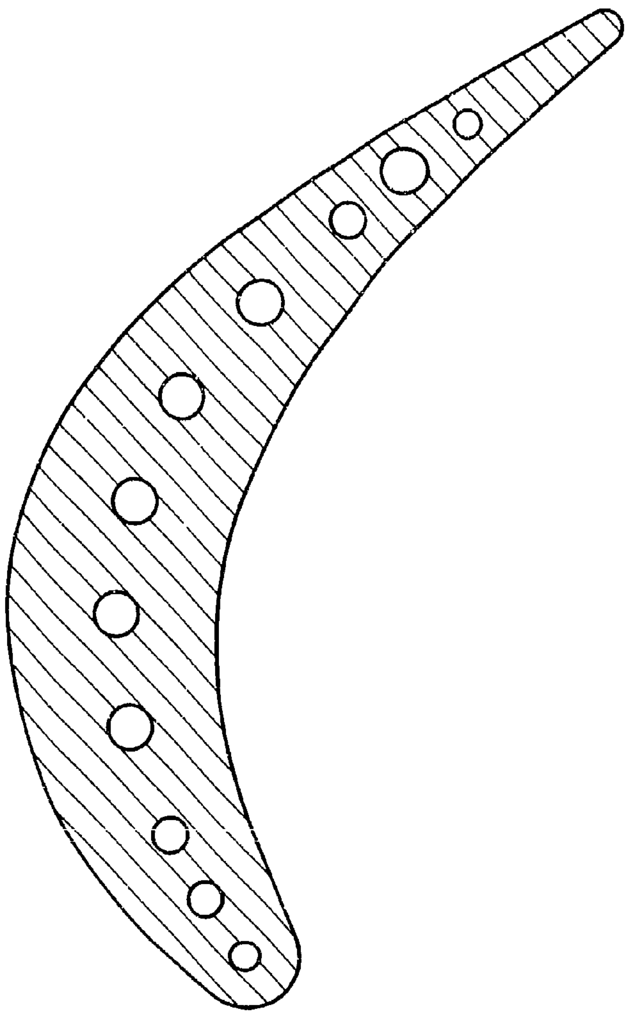

ELEVEN HOLE BLADE MIDSPAN CROSS SECTION

Figure 2A-132

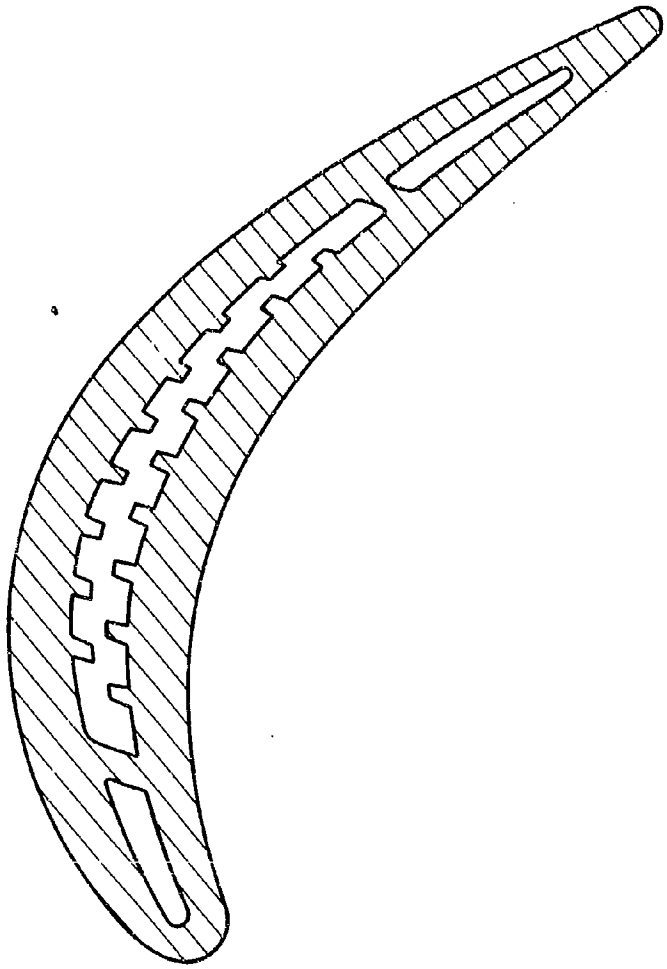

0.020 SAWTOOTH BLADE

Figure 2A-133

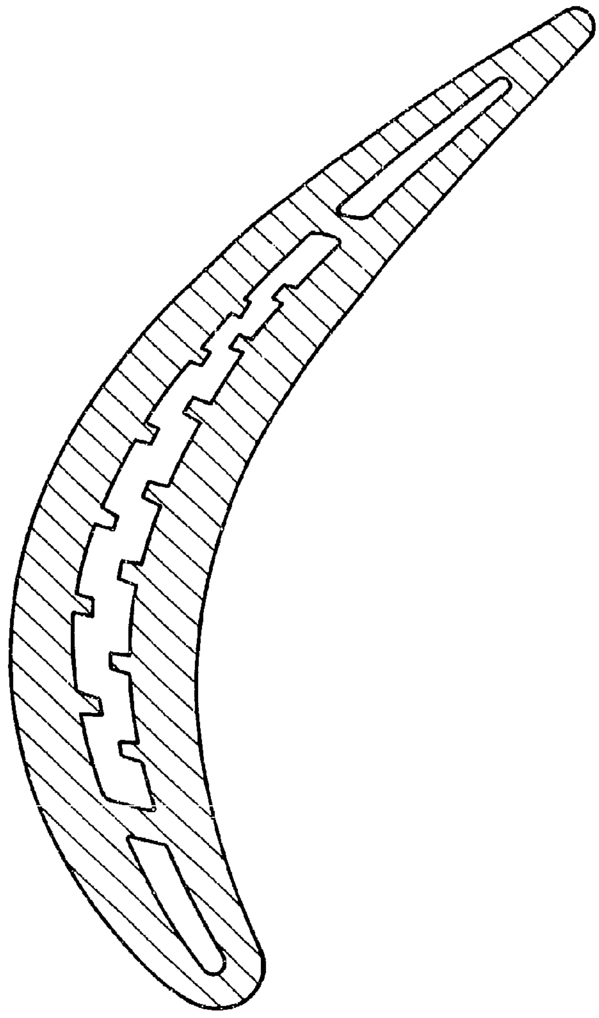

0.030 SAWTOOTH BLADE

Figure 2A-134

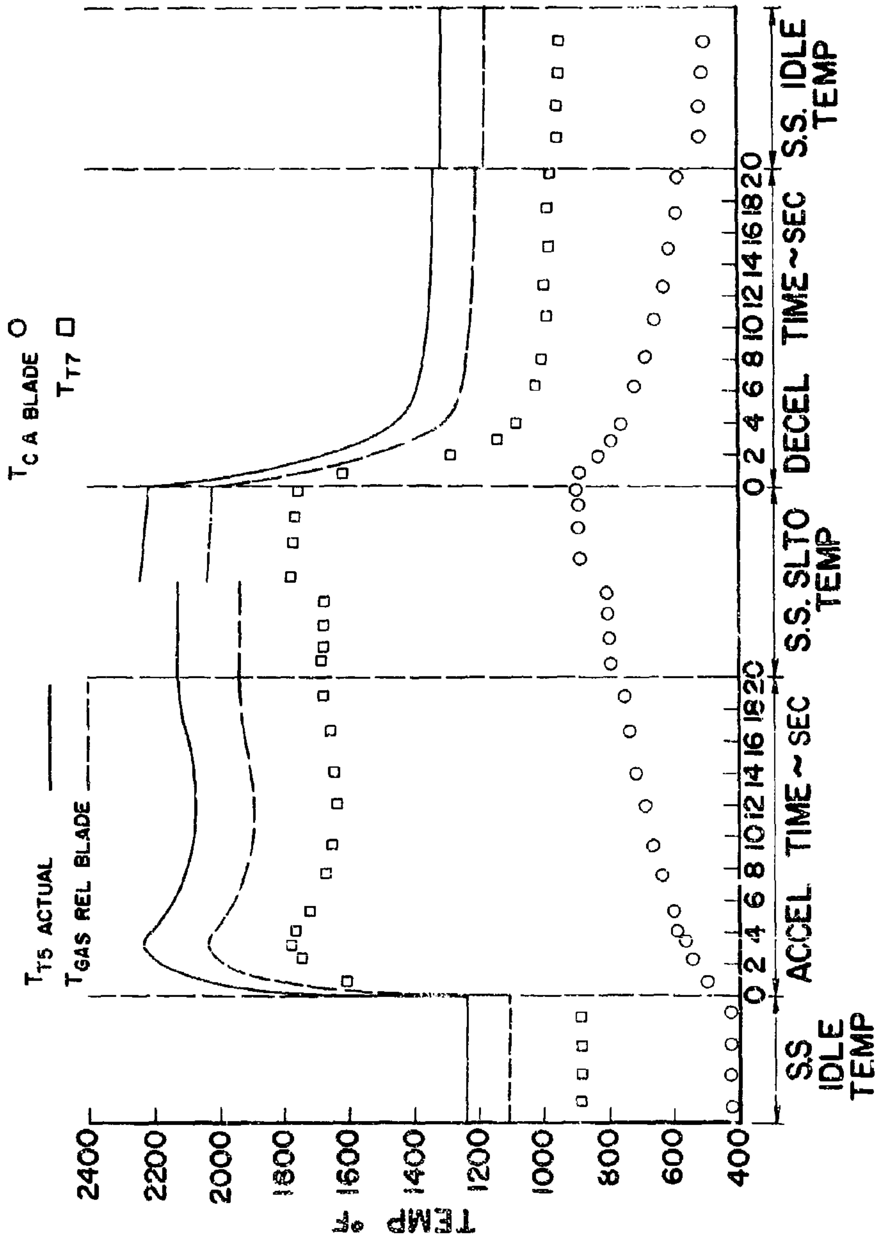

TYPICAL CYCLING TEST DATA - HIGH TEMP. TURBINE DEVELOPMENT TEST ENGINE

Figure 2A-135

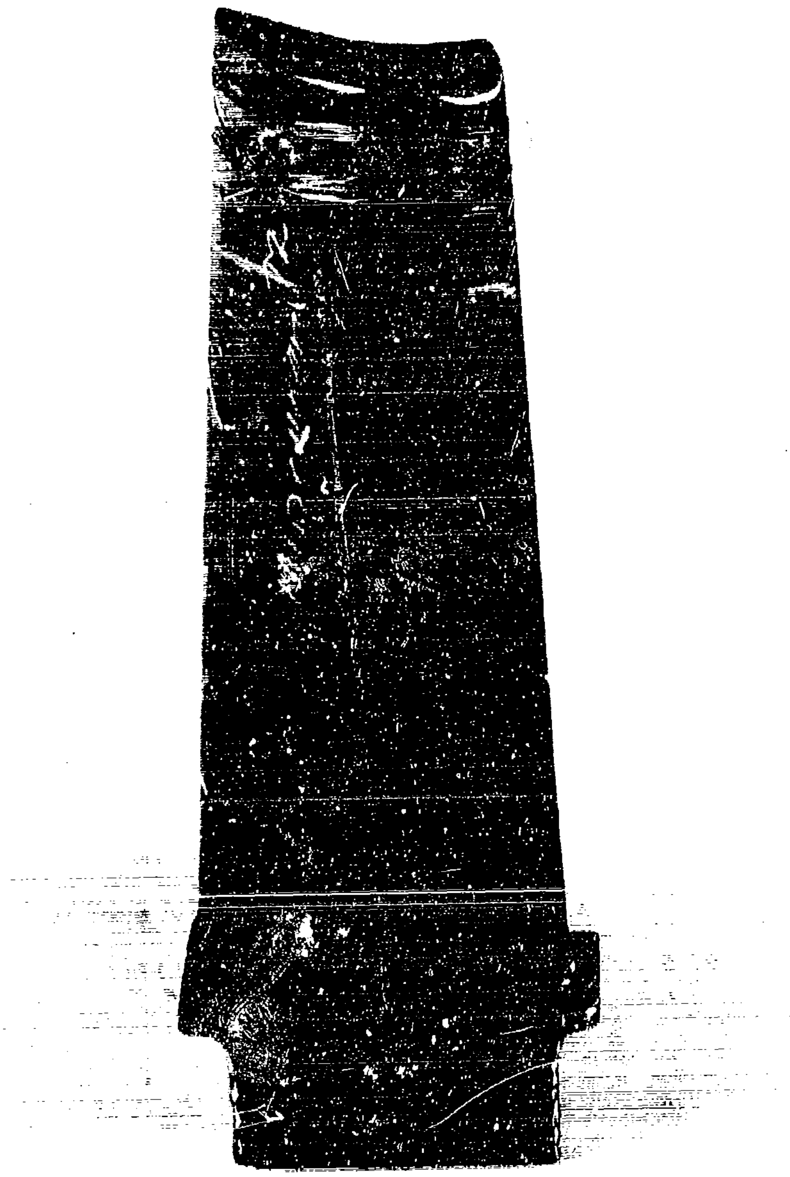

INSTRUMENTED BLADE

Figure 2A-136

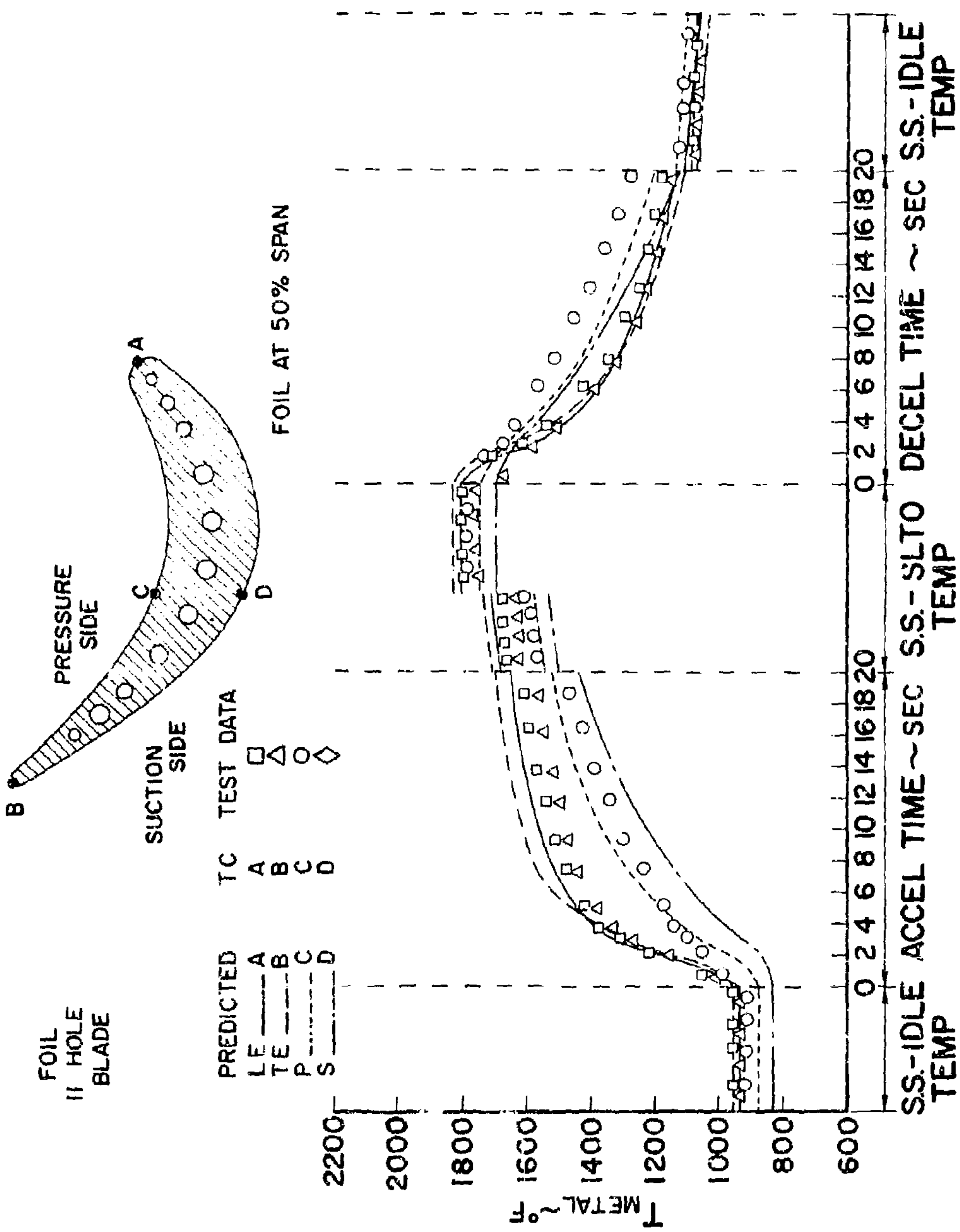

ELEVEN HOLE BLADE TEST DATA

Figure 2A-137

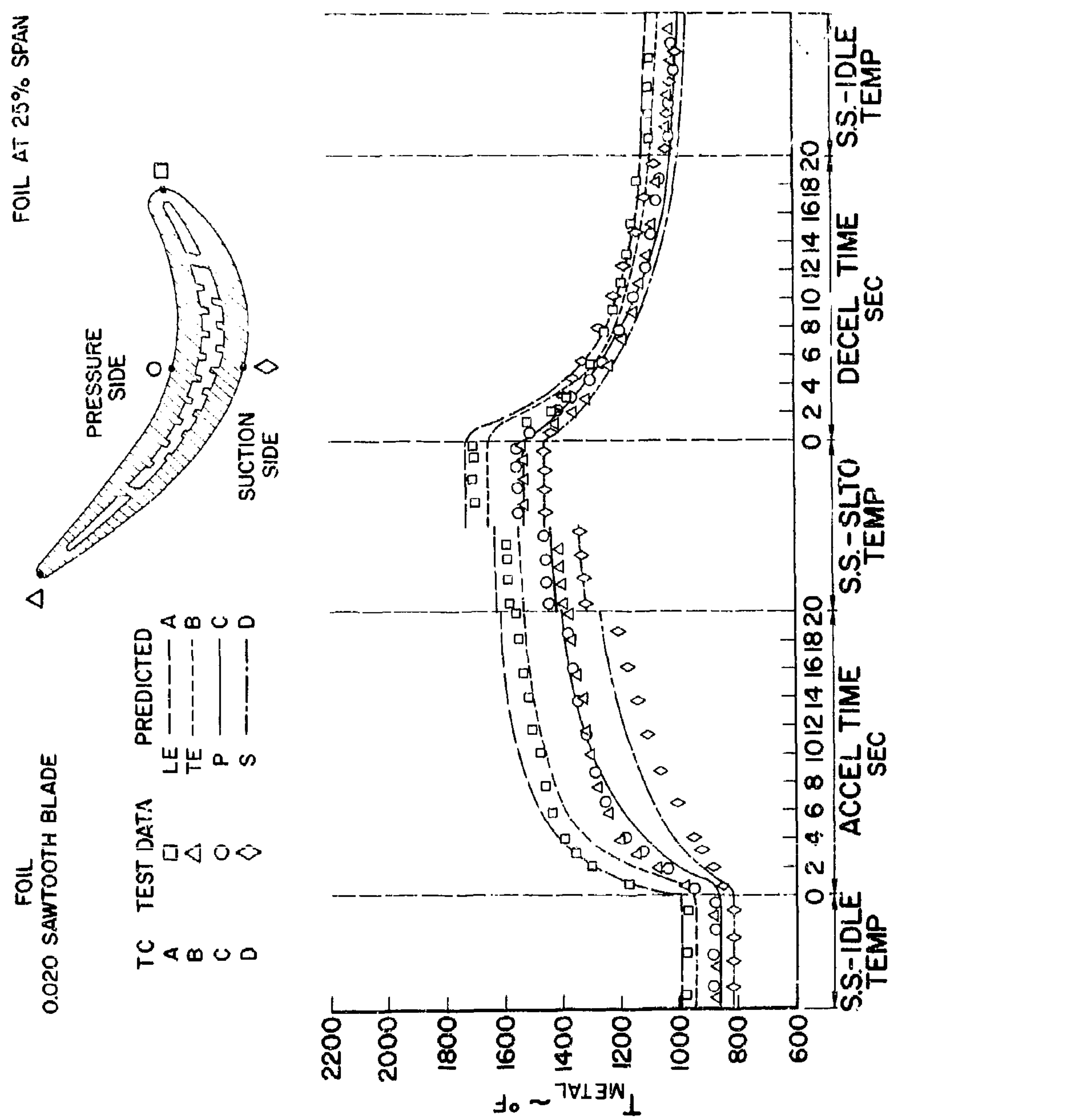

0.020 SAWTOOTH BLADE TEST DATA

Figure 2A-138

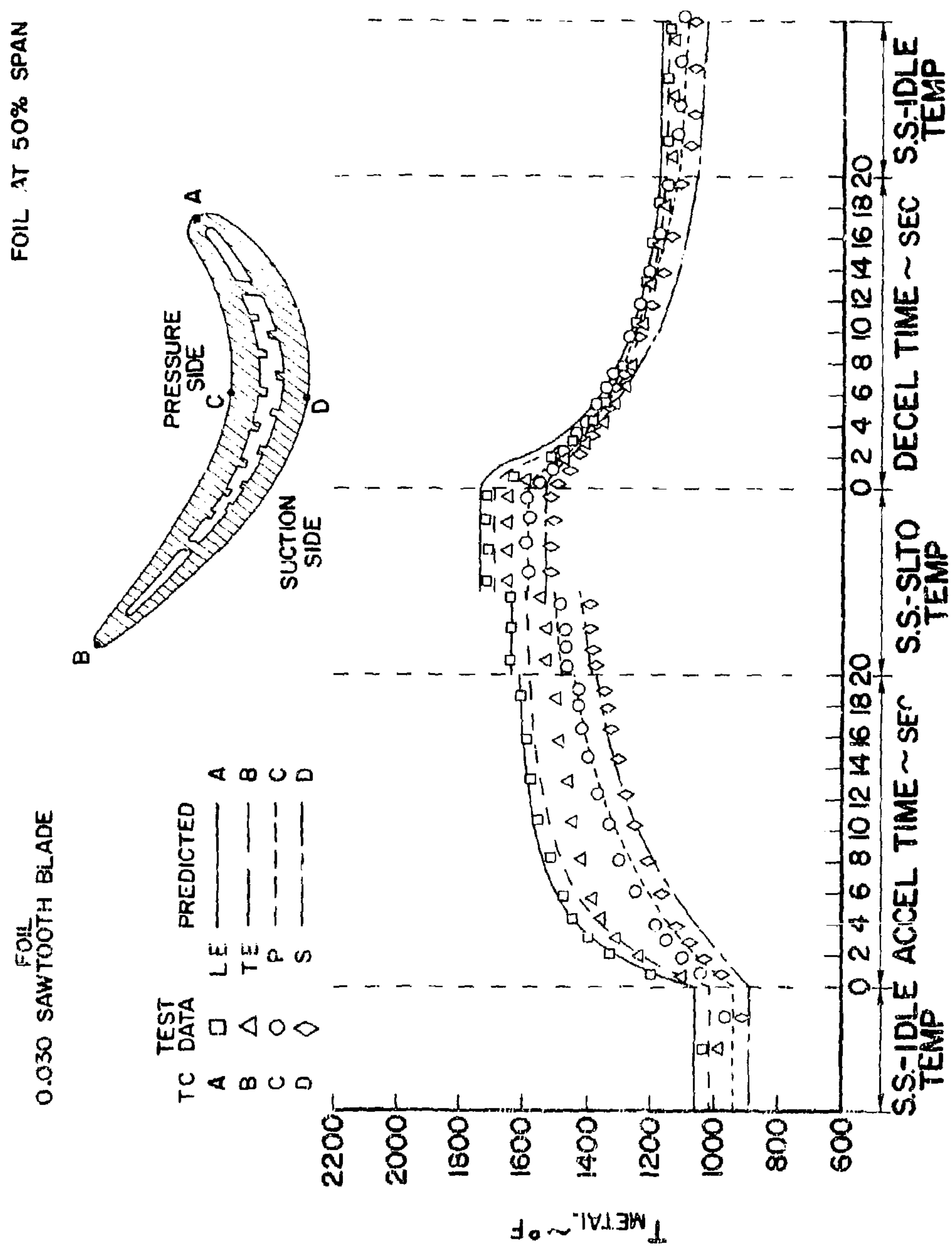

0.030 SAWTOOTH BLADE TEST DATA

Figure 2A-139

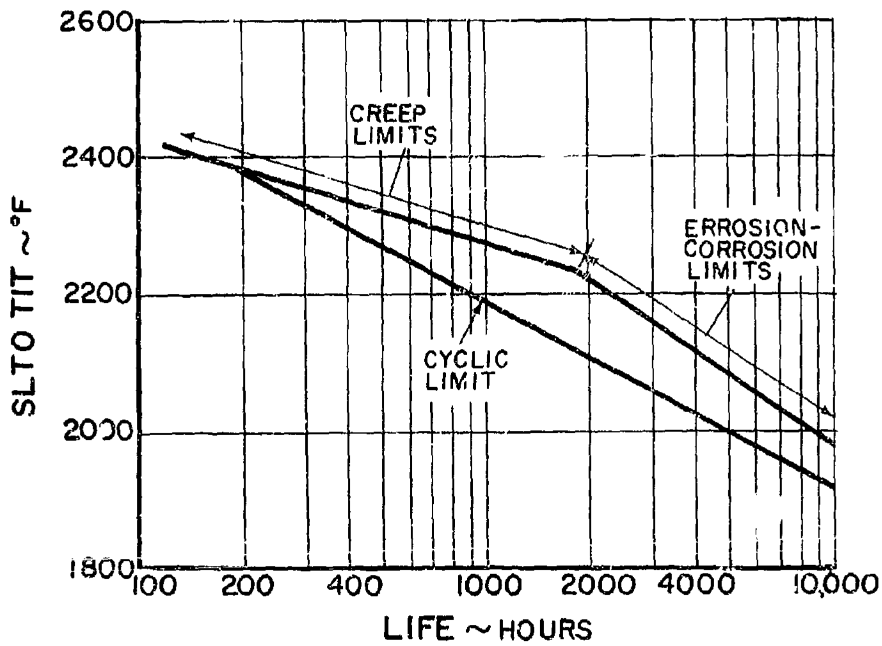

CONVECTIVELY COOLED BLADES LIFE LIMITS

Figure 2A-140

As-Cast Mar M 200 Stress Rupture Data

Heat	Condition	Temp.	Stress	Time to Rupture	Elong.	R. A.	Remarks
P5624	as-cast	1200	115 ksi	8.1 hrs.	7%	28.5%	
P5526	as-cast	1200	115	289.7	discontinued		Notched K_t 3.8
P5625	as-cast	1400	92	0.7	6.6	27	
P5626	as-cast	1400	92	329.6	discontinued		Notched K_t 3.8
A-64	as-cast	1400	95	73.1	0.4	2.2	
P5417	as-cast	1400	95	9.0	2.1	4.4	
P5417	as-cast	1400	95	15.0	-	-	Notched K_t 3.8
A-64	as-cast	1400	110	2.4	2	6	
P5417	as-cast	1600	60	5.7	1.2	2.0	
P5417	as-cast	1600	60	167.6	-	-	Notched K_t 3.8
A-64	as-cast	1600	60	66.8	1.0	6.0	
A-64	as-cast	1600	65	26.1	1.0	4.0	
P5423	as-cast	1800	27.5	69.2	6.45	13.8	
P5424	as-cast	1800	27.5	29.2	3.0	3.0	
P5424	as-cast	1800	27.5	67.2	2.0	5.0	Porosity in gage section
P5425	as-cast	1800	27.5	74.6	5.0	7.0	
P5425	as-cast	1800	27.5	69.3	7.0	6.0	
P5417	as-cast	1800	25	45	8.5	17.5	
P5417	as-cast	1800	25	305.2	discontinued	-	Notched K_t 3.8
XA137	as-cast	1800	25	36.3	4.2	16.5	
A-80	as-cast	1800	24	252.3	4.1	4.8	

MAR M200 STRESS RUPTURE DATA

Figure 2A-141

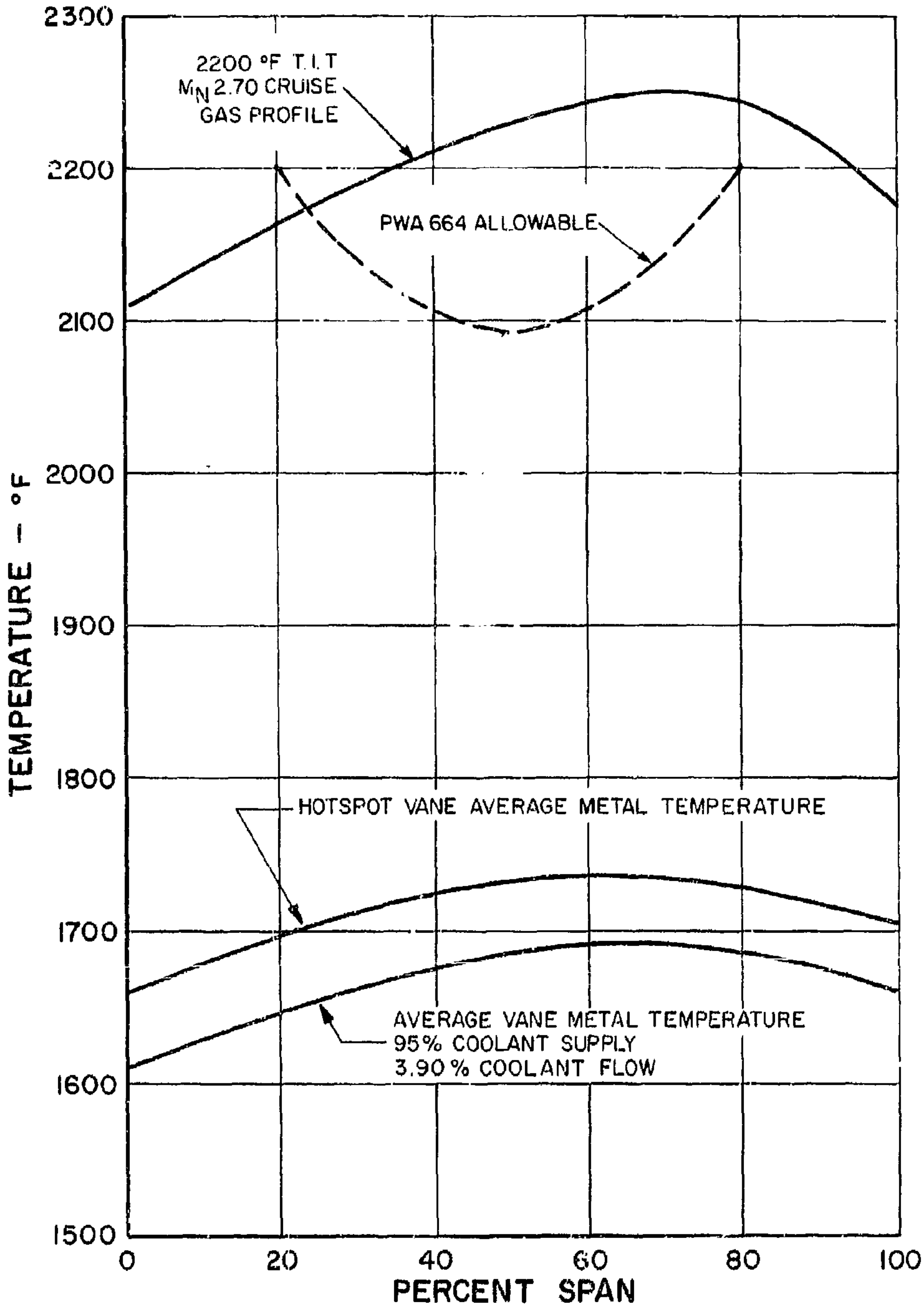

CREEP LIMIT TEMPERATURE MARGIN, FIRST STAGE VANE

Figure 2A-142

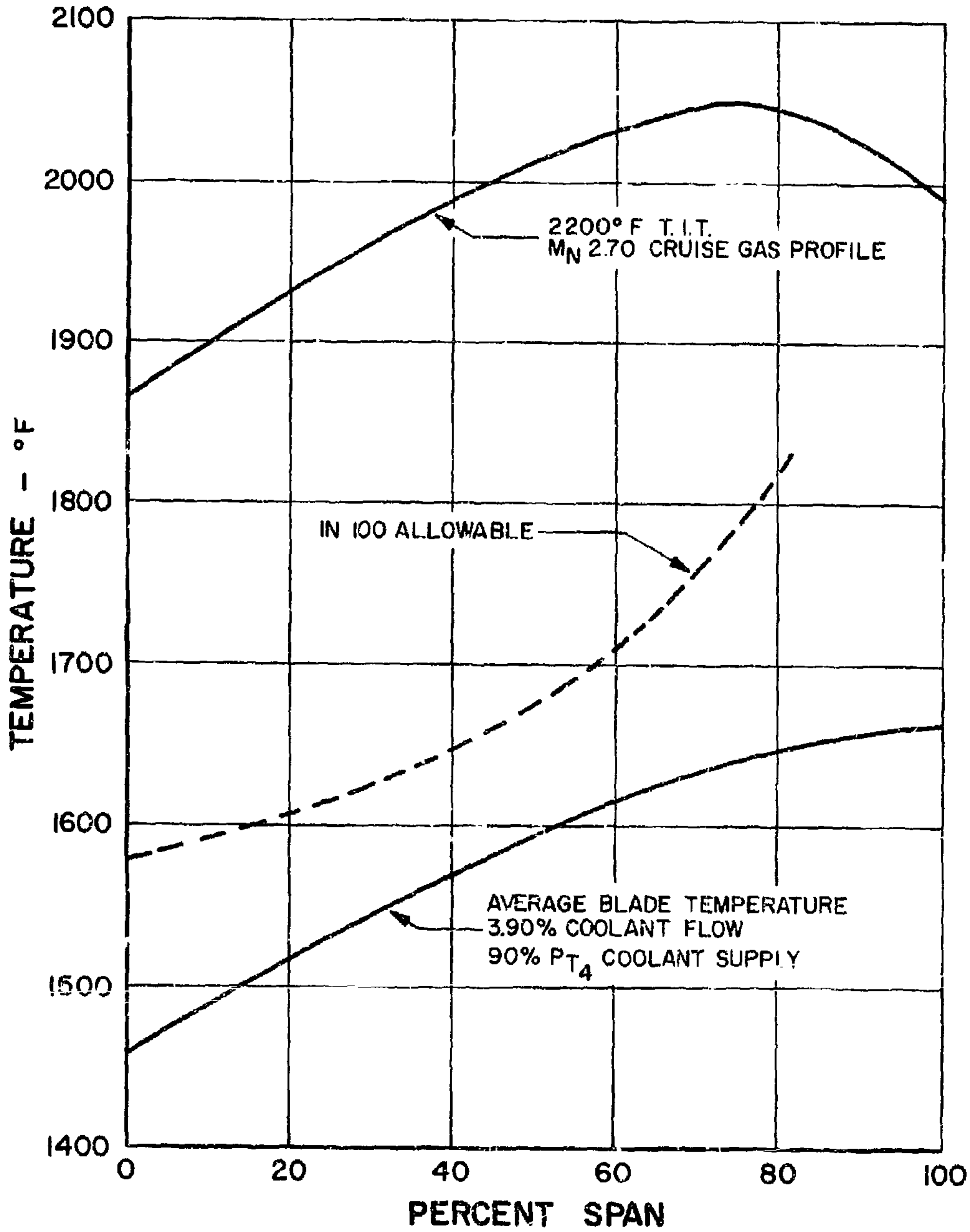

CREEP LIMIT TEMPERATURE MARGIN, FIRST STAGE BLADE

Figure 2A-143

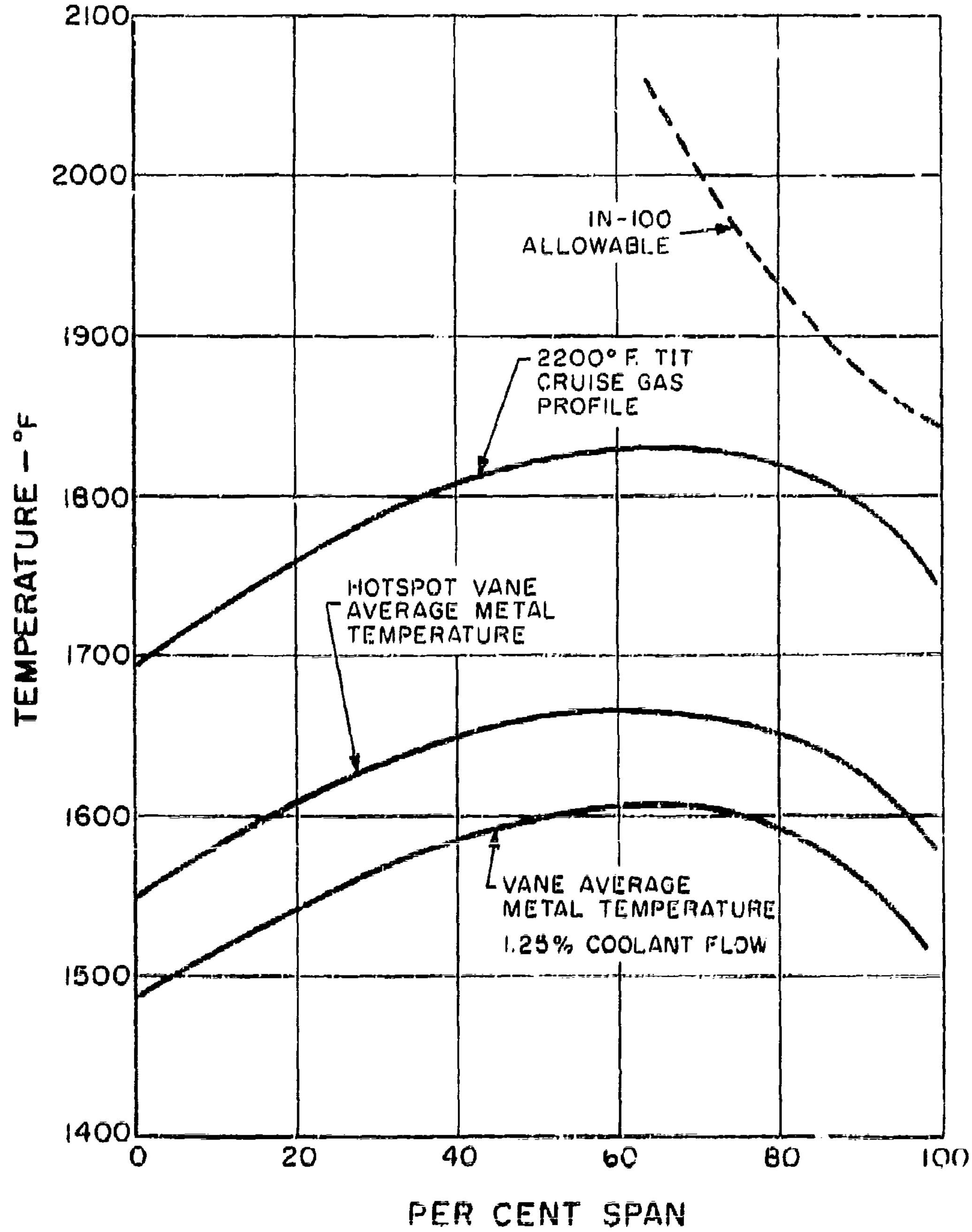

CREEP LIMIT TEMPERATURE MARGIN, SECOND STAGE VANE

Figure 2A-144

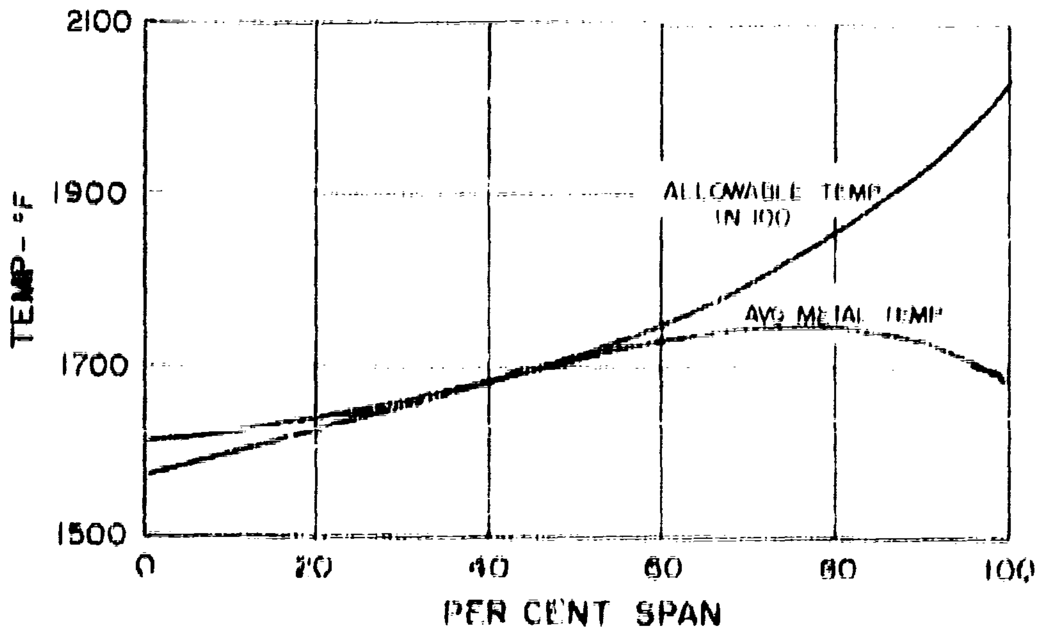

CREEP LIMIT TEMPERATURE MARGIN, SECOND STAGE BLADE

Figure 2A-148

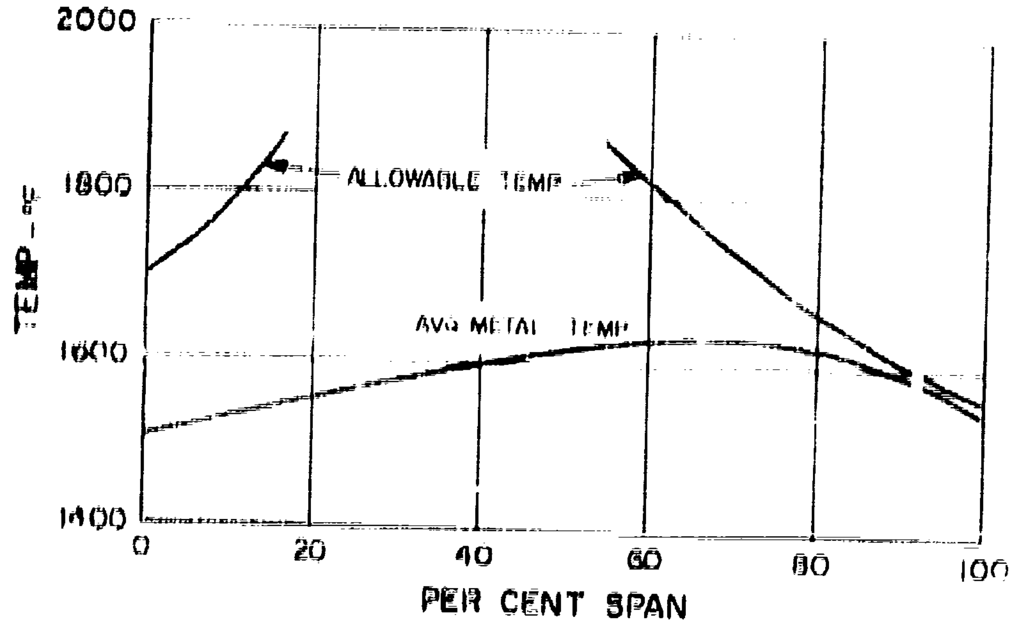

CREEP LIMIT TEMPERATURE MARGIN, THIRD STAGE VANE

Figure 2A-146

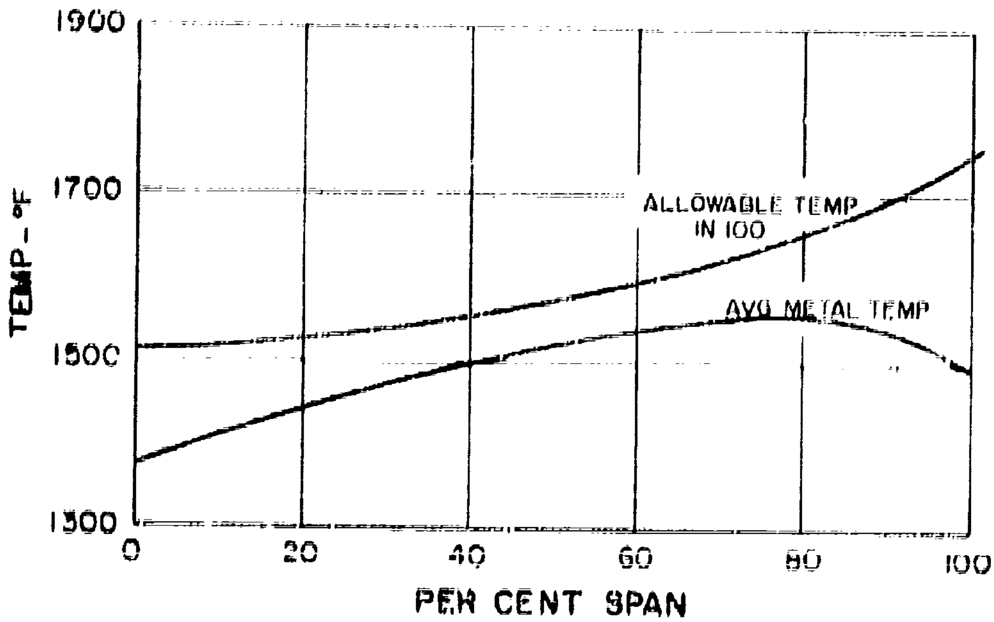

CREEP LIMIT TEMPERATURE MARGIN, THIRD STAGE BLADE

Figure 2A-147

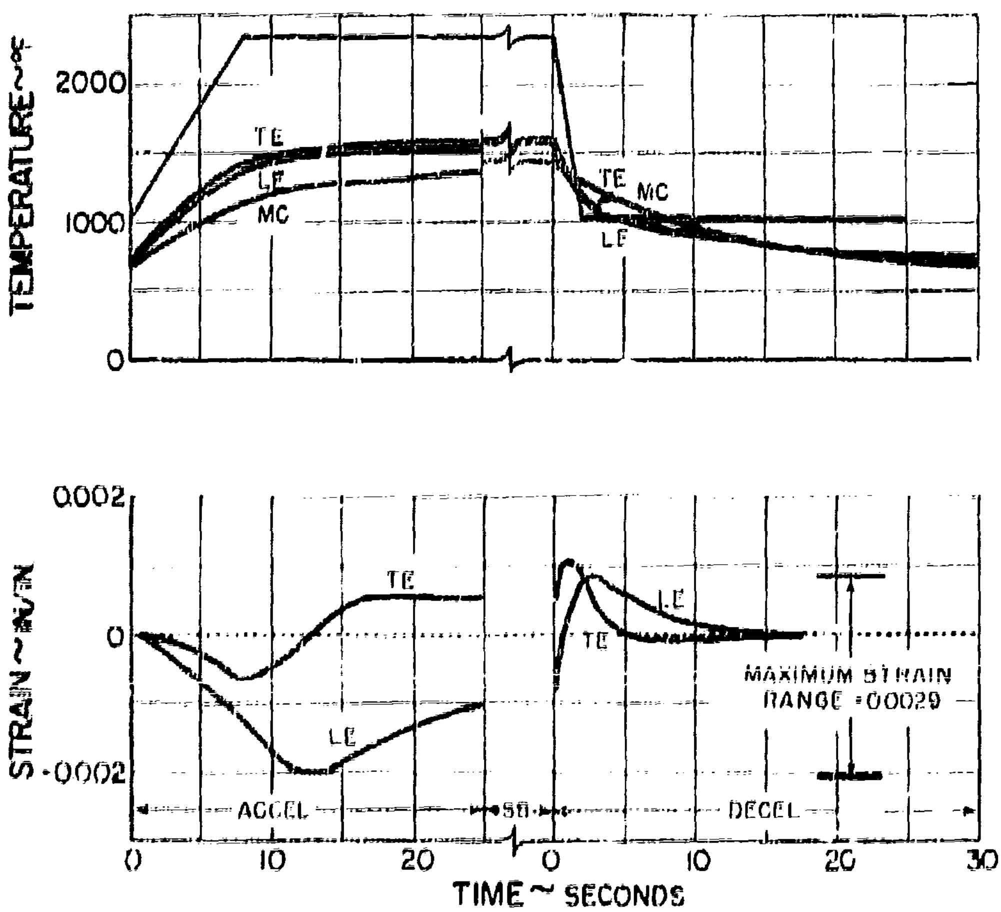

TRANSIENT RESPONSE FIRST STAGE VANE, 2300°F TIT

Figure 2A-148

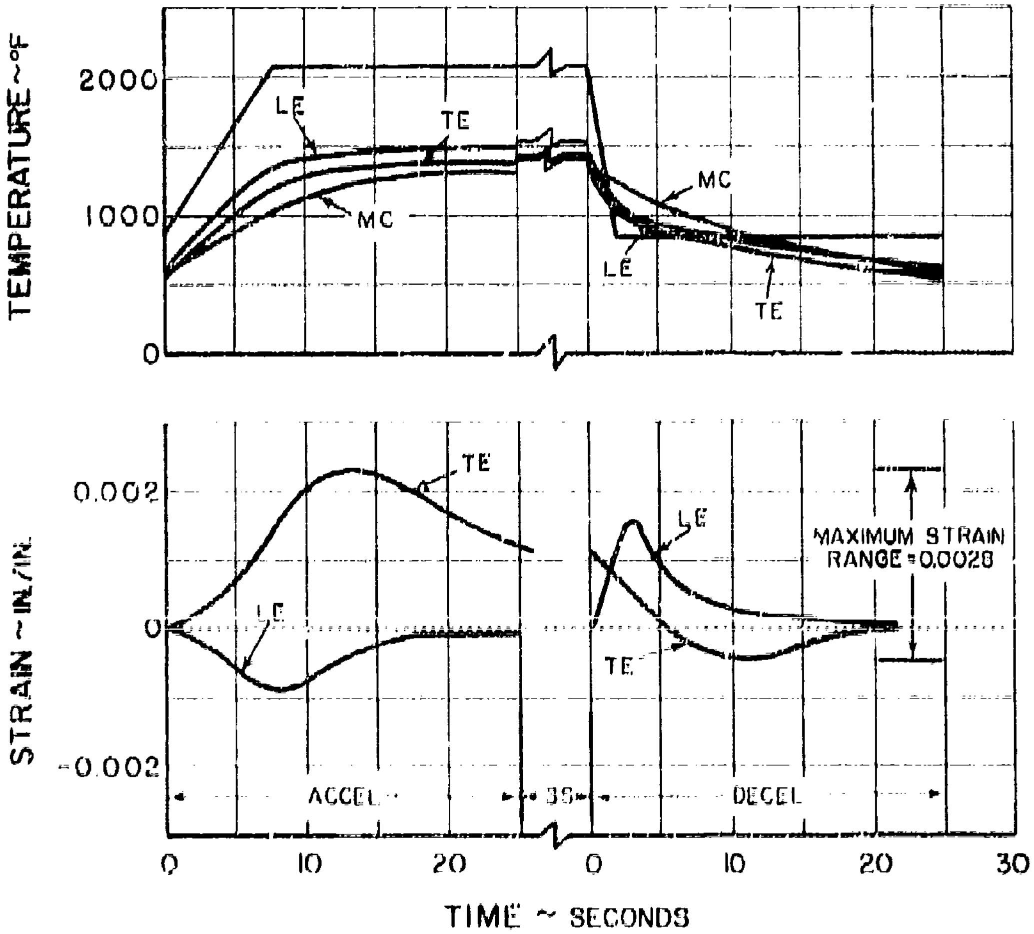

TRANSIENT RESPONSE FIRST STAGE BLADE, 2300°F TIT

Figure 2A-150

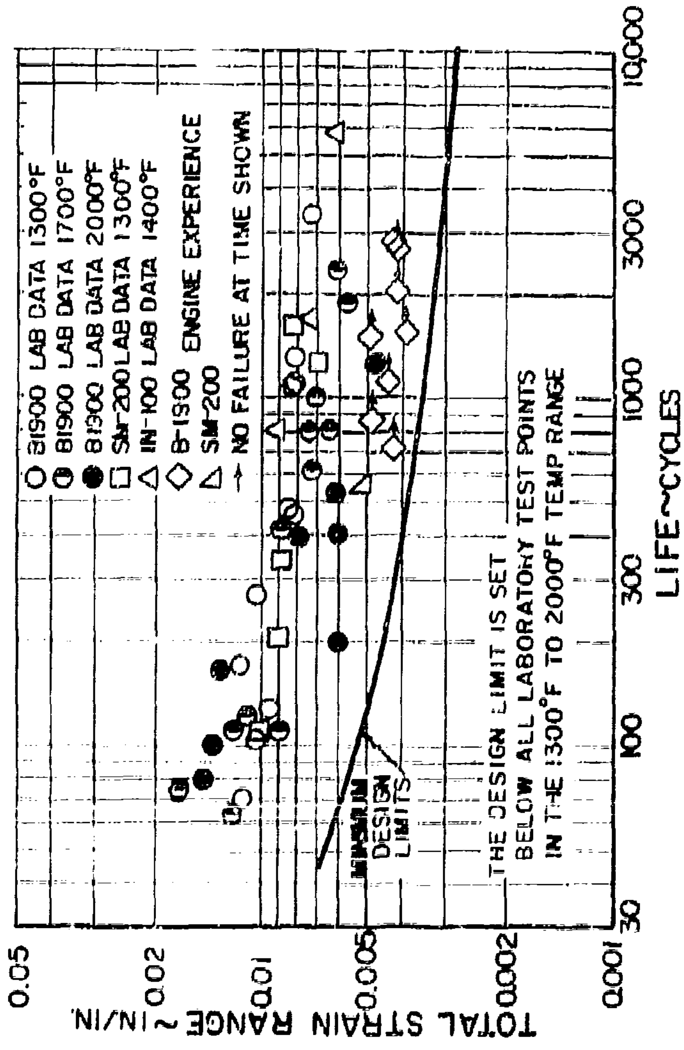

STRAIN S-N CURVE FOR TURBINE SUPER ALLOYS

Figure 2A-151

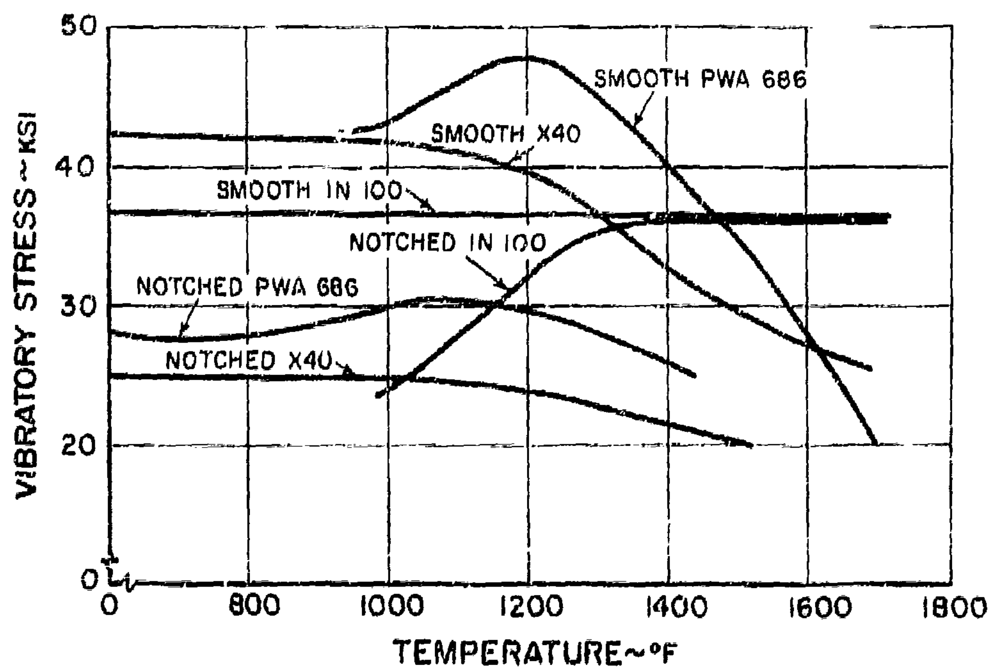

RUNOUT FATIGUE STRENGTHS OF NOTCHED AND SMOOTH TURBINE MATERIALS

Figure 2A-152

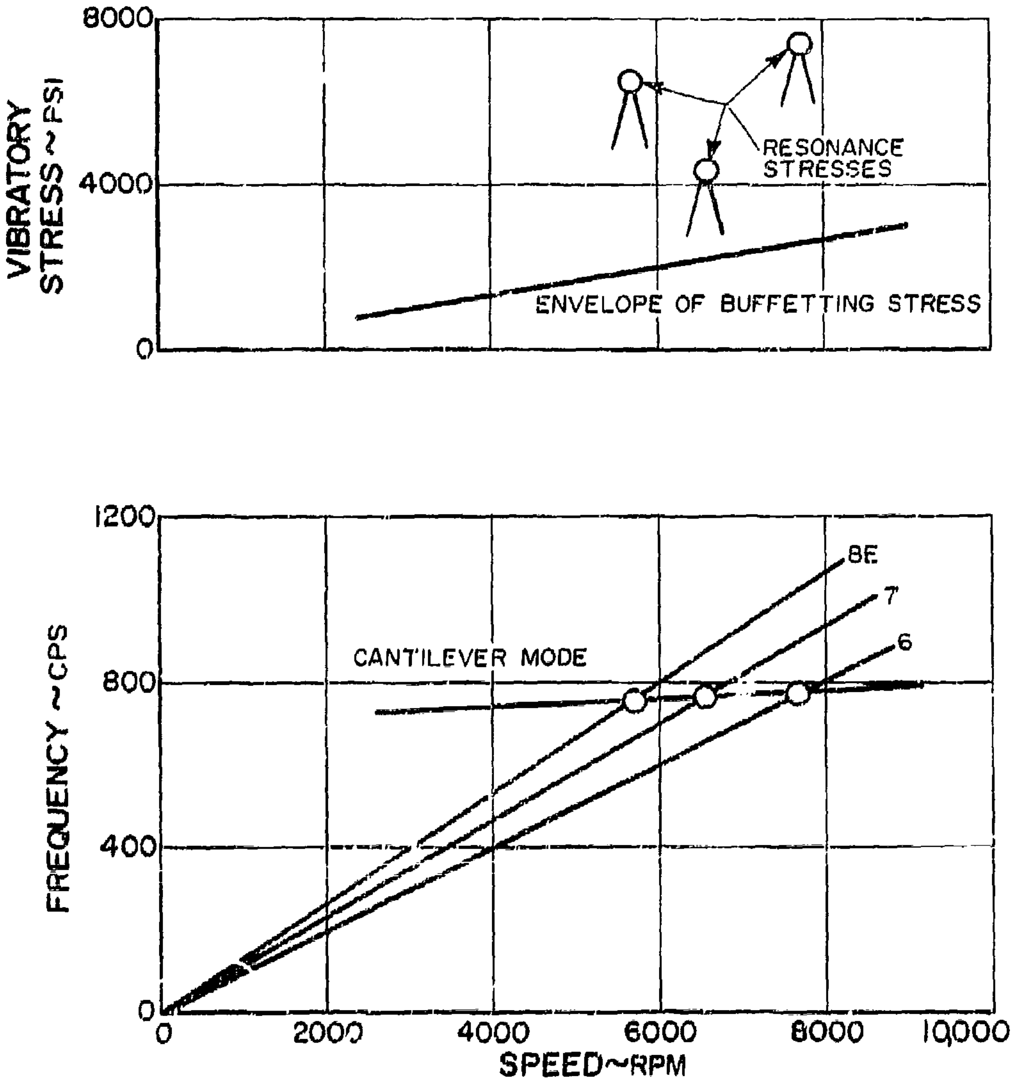

JT4 VIBRATION SURVEYS

Figure 2A-153

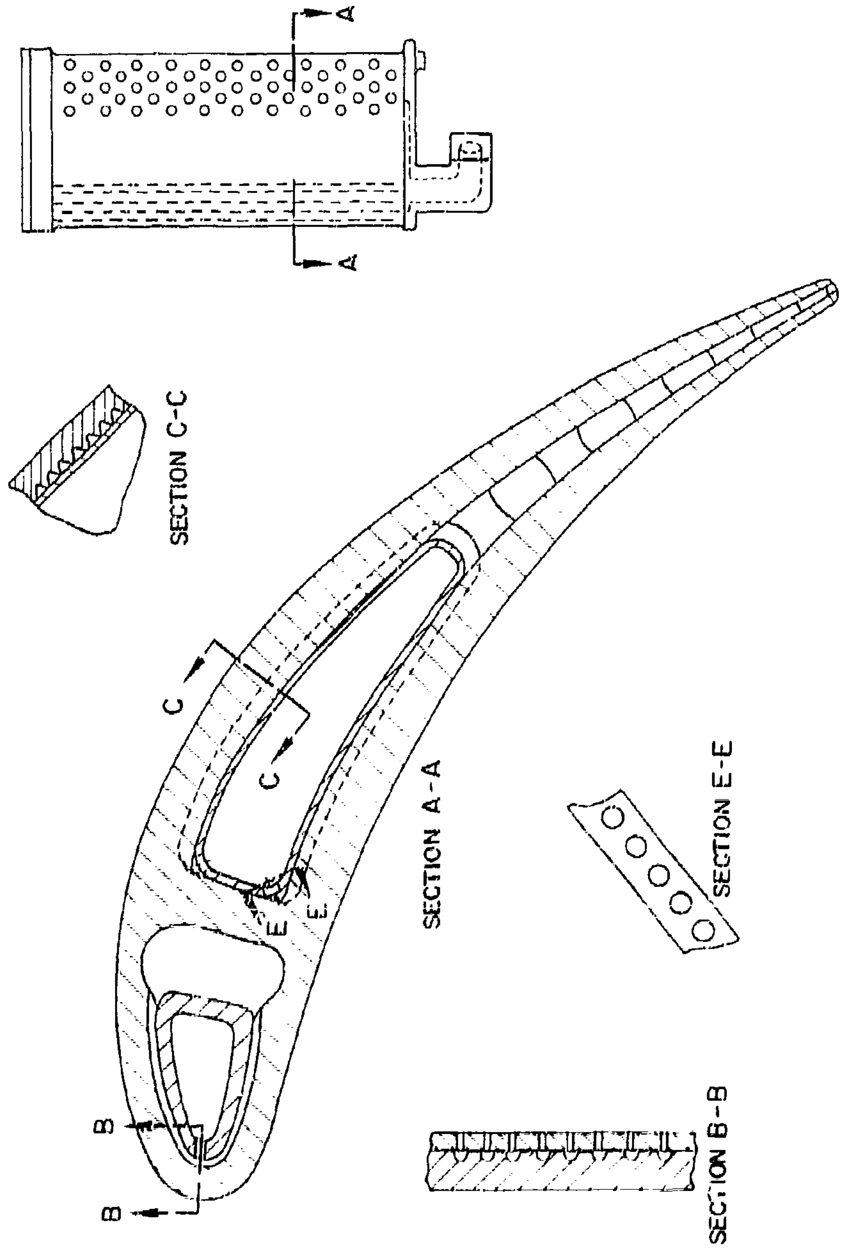

FIRST STAGE BASIC ENGINE VANE GEOMETRY

Figure 2A-154

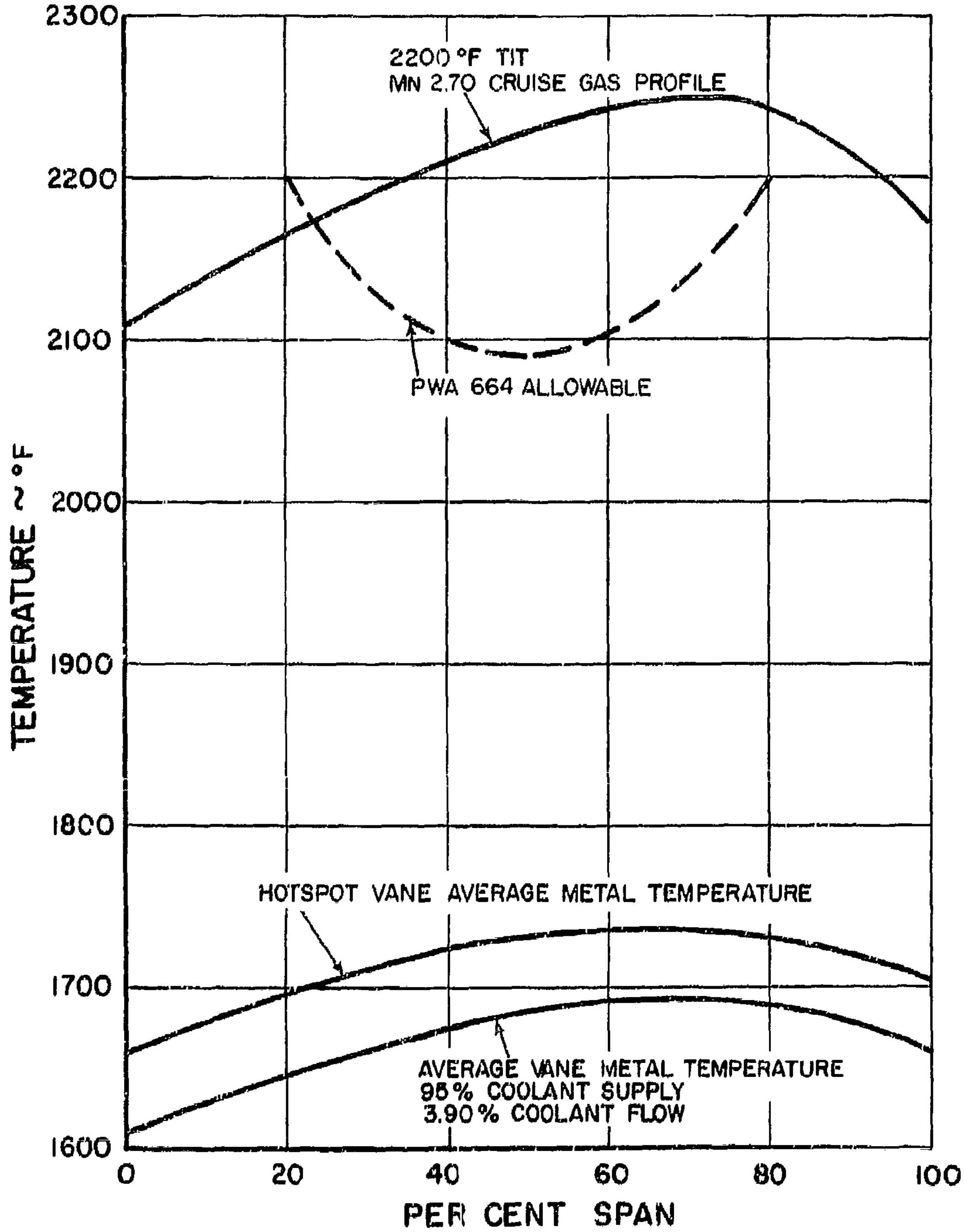

AVERAGE VANE TEMPERATURE

Figure 2A-155

FIRST TURBINE IMPINGEMENT VANE
QUARTER TIP METAL TEMPERATURES

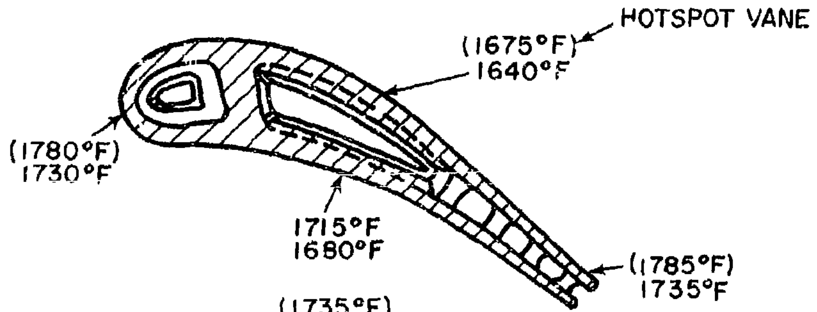

$T_{AVERAGE} = \frac{(1735°F)}{1690°F}$

3.9% COOLANT FLOW
95 % P_{T4} COOLANT SUPPLY

LOCAL METAL TEMPERATURE (75% SPAN)

Figure 2A-156

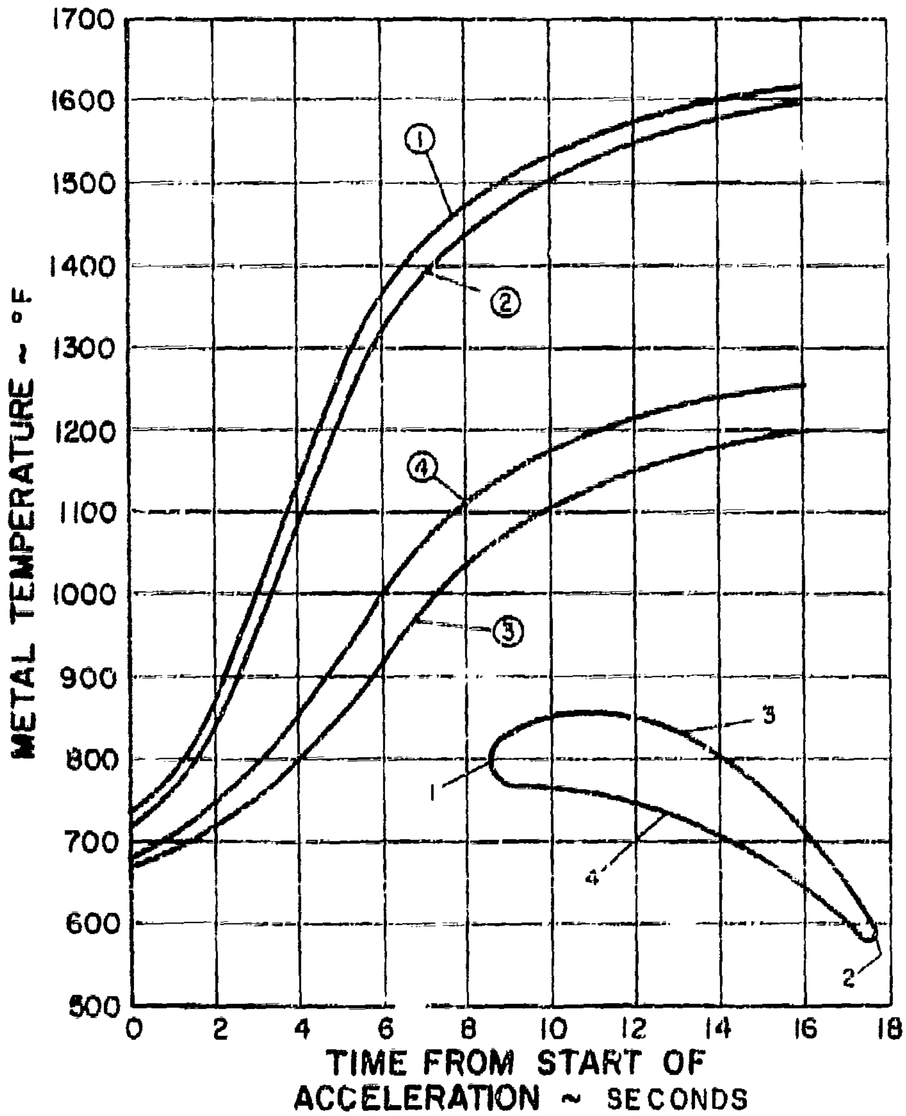

FIRST STAGE VANE TRANSIENT TEMPERATURE, 2300°F TIT-SLTO

Figure 2A-157

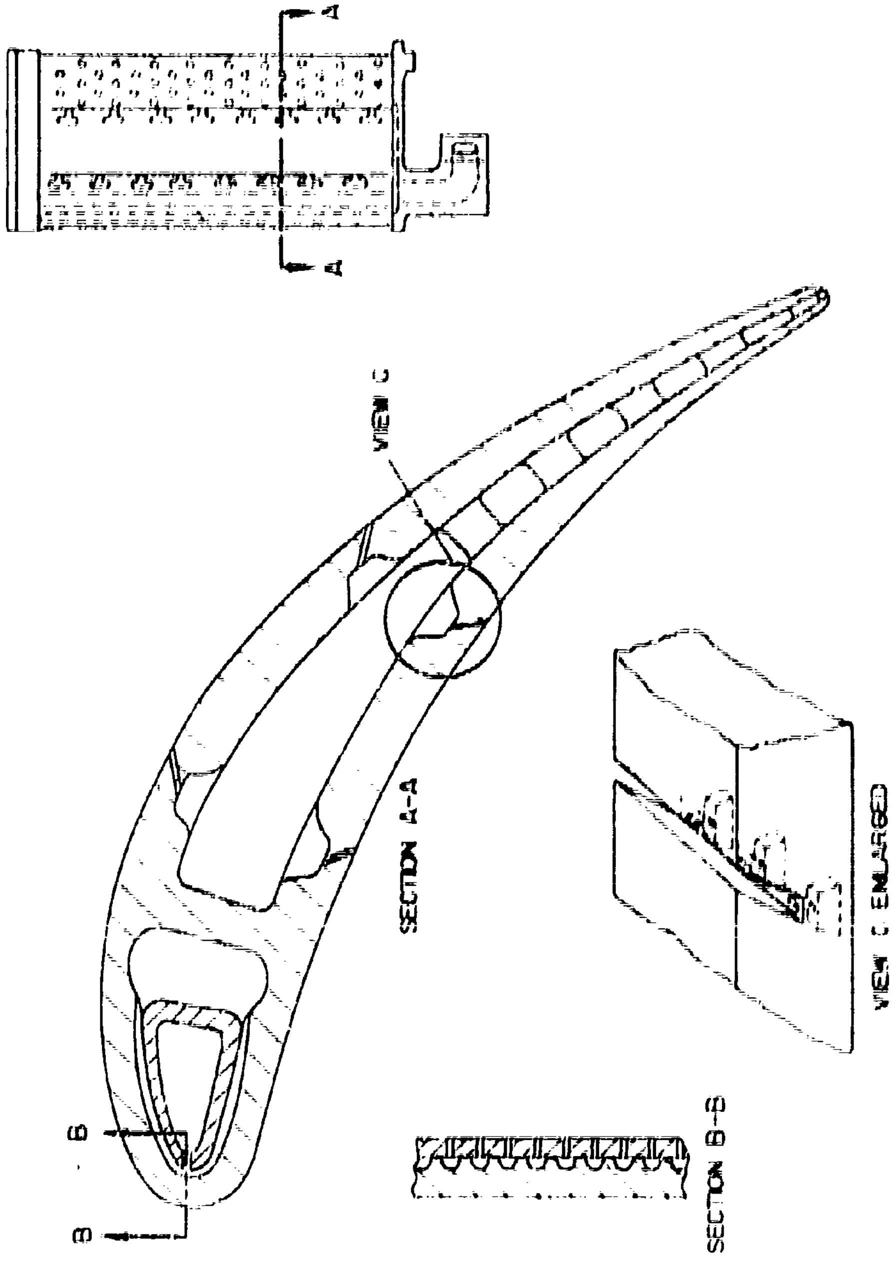

FIRST STAGE BASIC ENGINE VANE GEOMETRY

Figure 2A-158

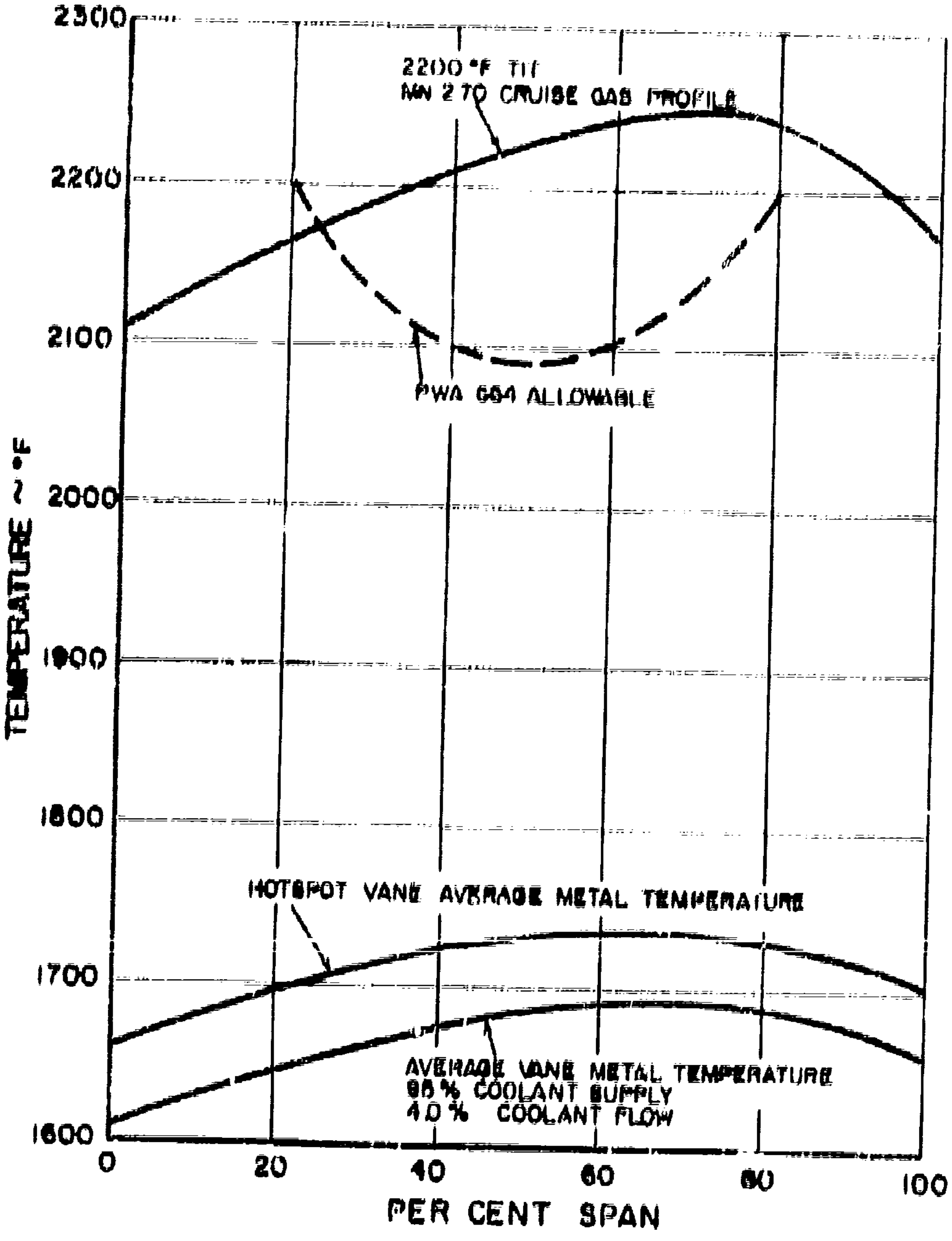

AVERAGE VANE TEMPERATURE

Figure 2A-159

FIRST TURBINE IMPINGEMENT VANE
QUARTER TIP METAL TEMPERATURES

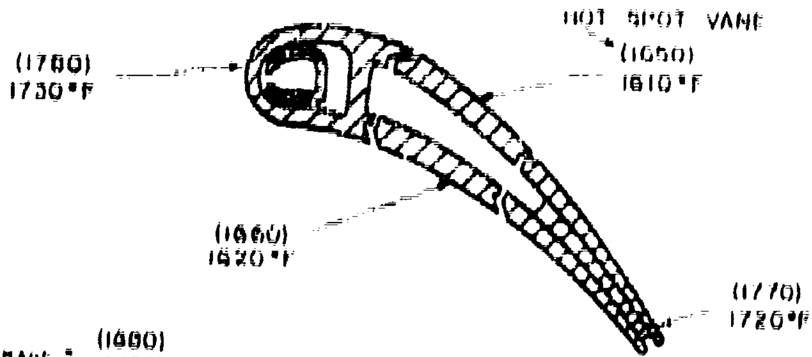

$T_{AVERAGE}$ = (1690)
1645°F

4.0% COOLANT FLOW
99% P_{T4} COOLANT SUPPLY

FIRST TURBINE IMPINGEMENT COOLED VANE
LOCAL METAL TEMPERATURES AT 2200°F CRUISE

LOCAL METAL TEMPERATURES (75% SPAN) – MN 2.7

Figure 2A-160

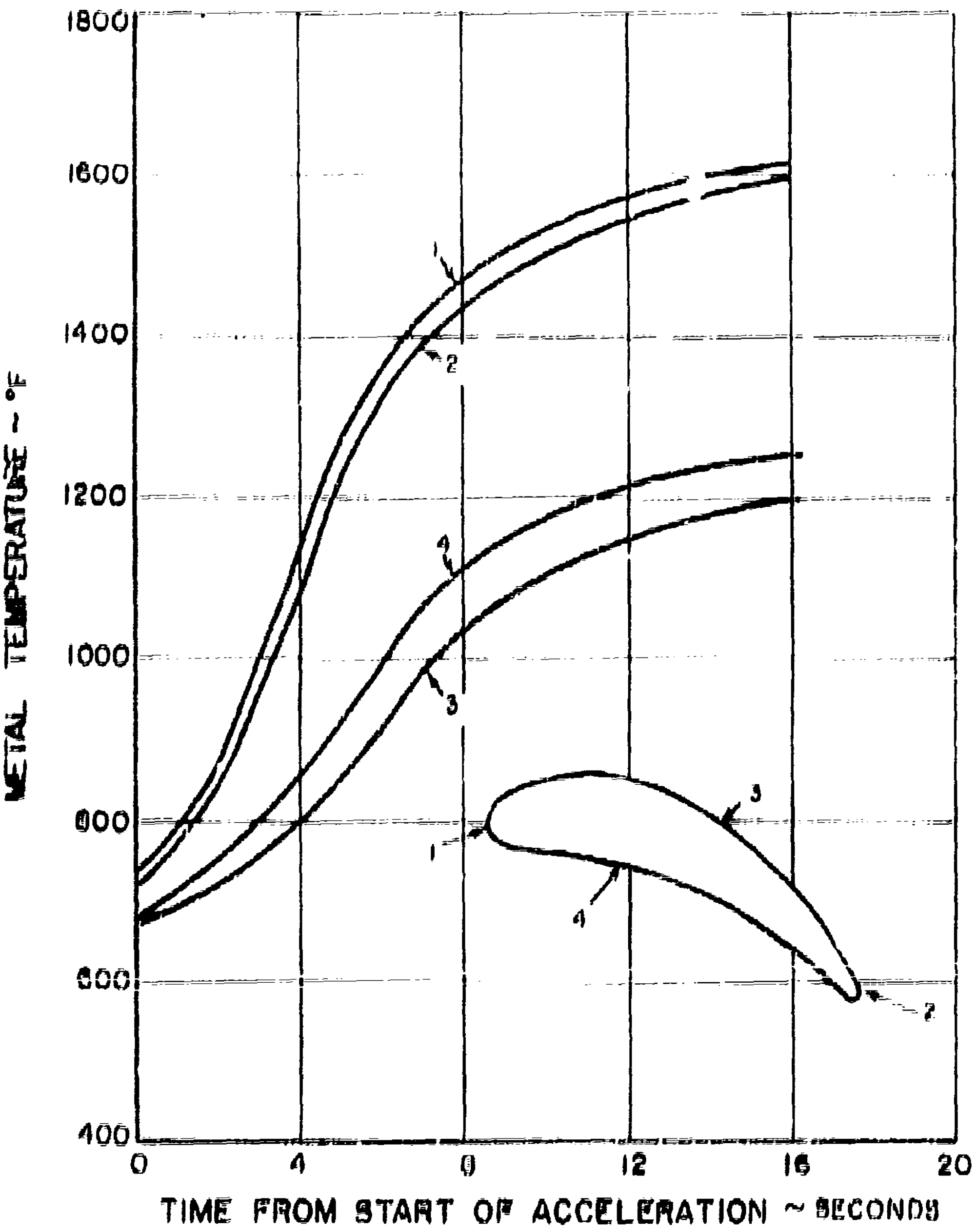

VANE TEMPERATURE RESPONSE - TRANSIENT ACCELL. SLTO - 2300°F RATING

Figure 2A-161

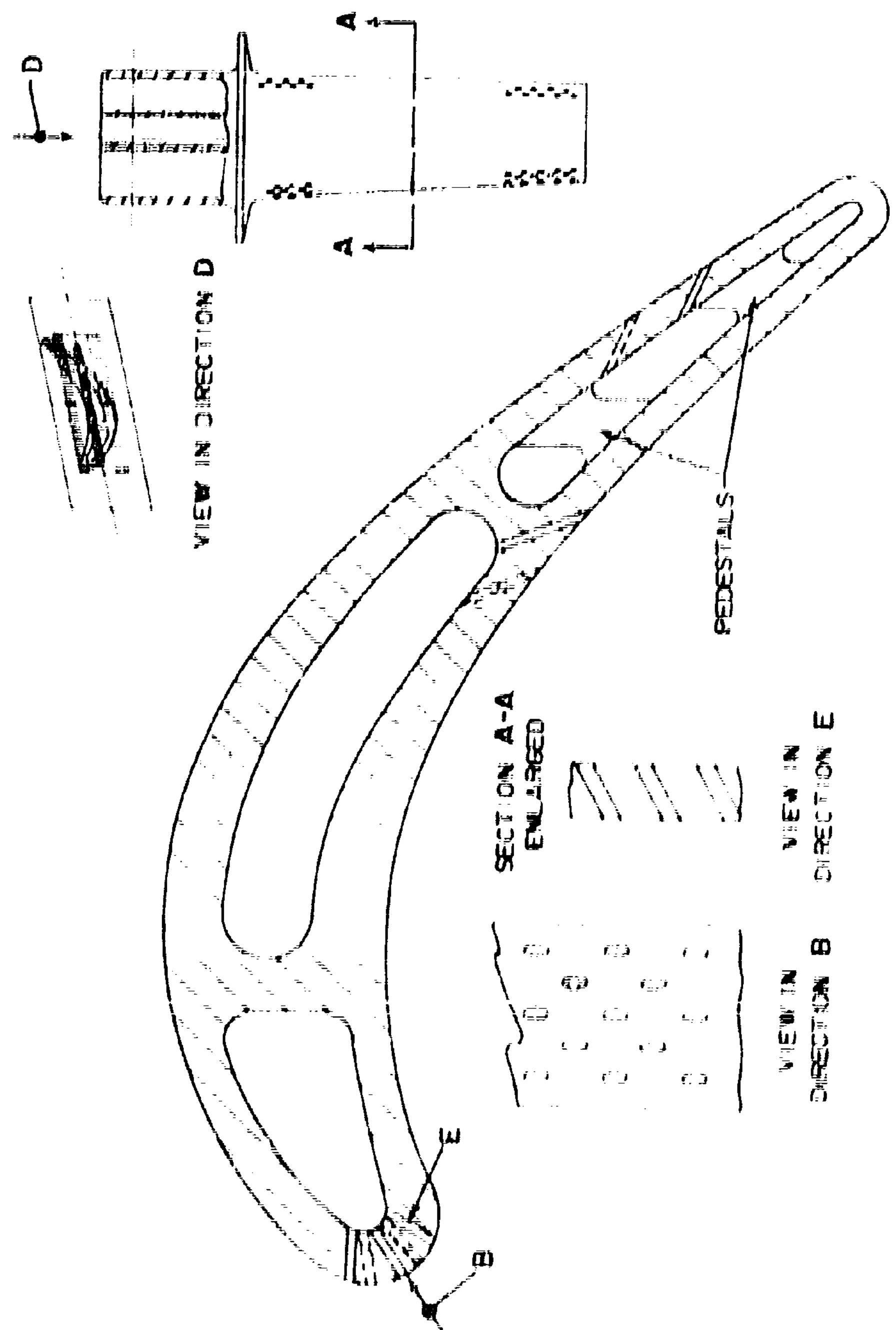

FIRST STAGE BLADE GEOMETRY - 2300°F RATING

Figure 2A-162

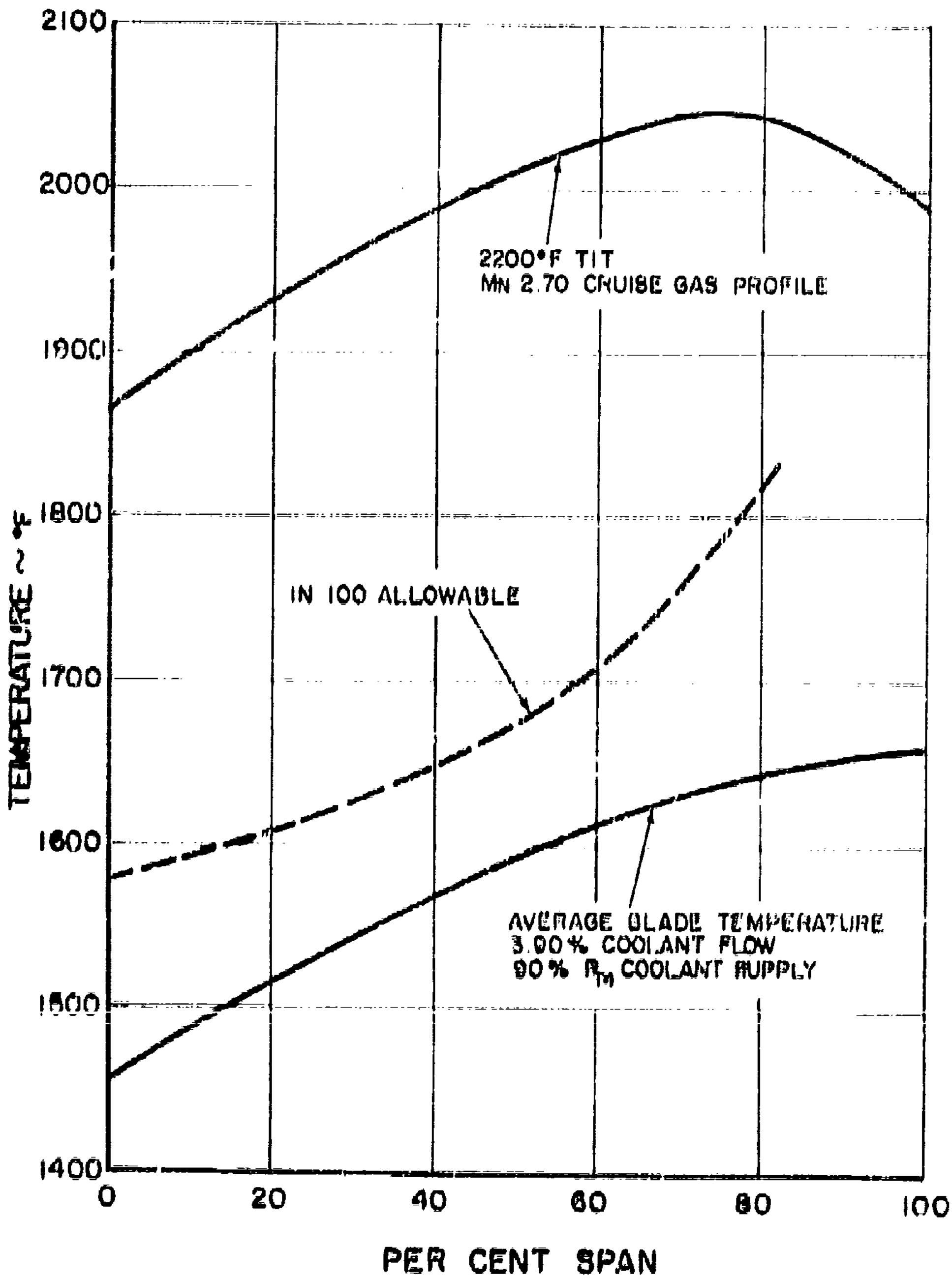

AVERAGE BLADE TEMPERATURES - FIRST STAGE BLADE

Figure 2A-163

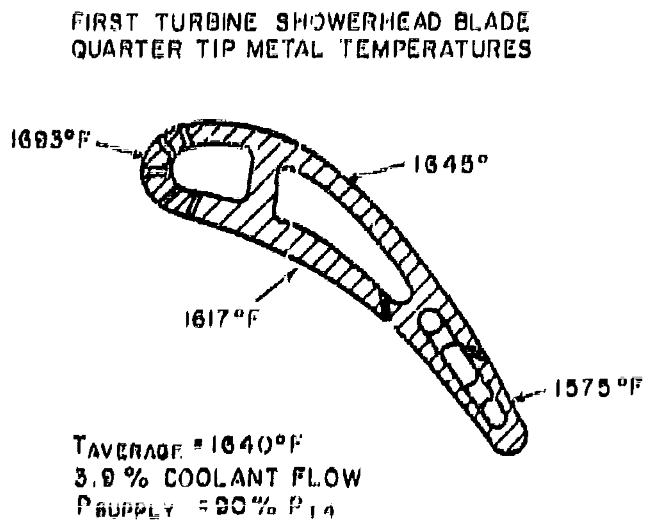

LOCAL BLADE TEMPERATURES (50% SPAN) - FIRST STAGE BLADE

Figure 2A-164

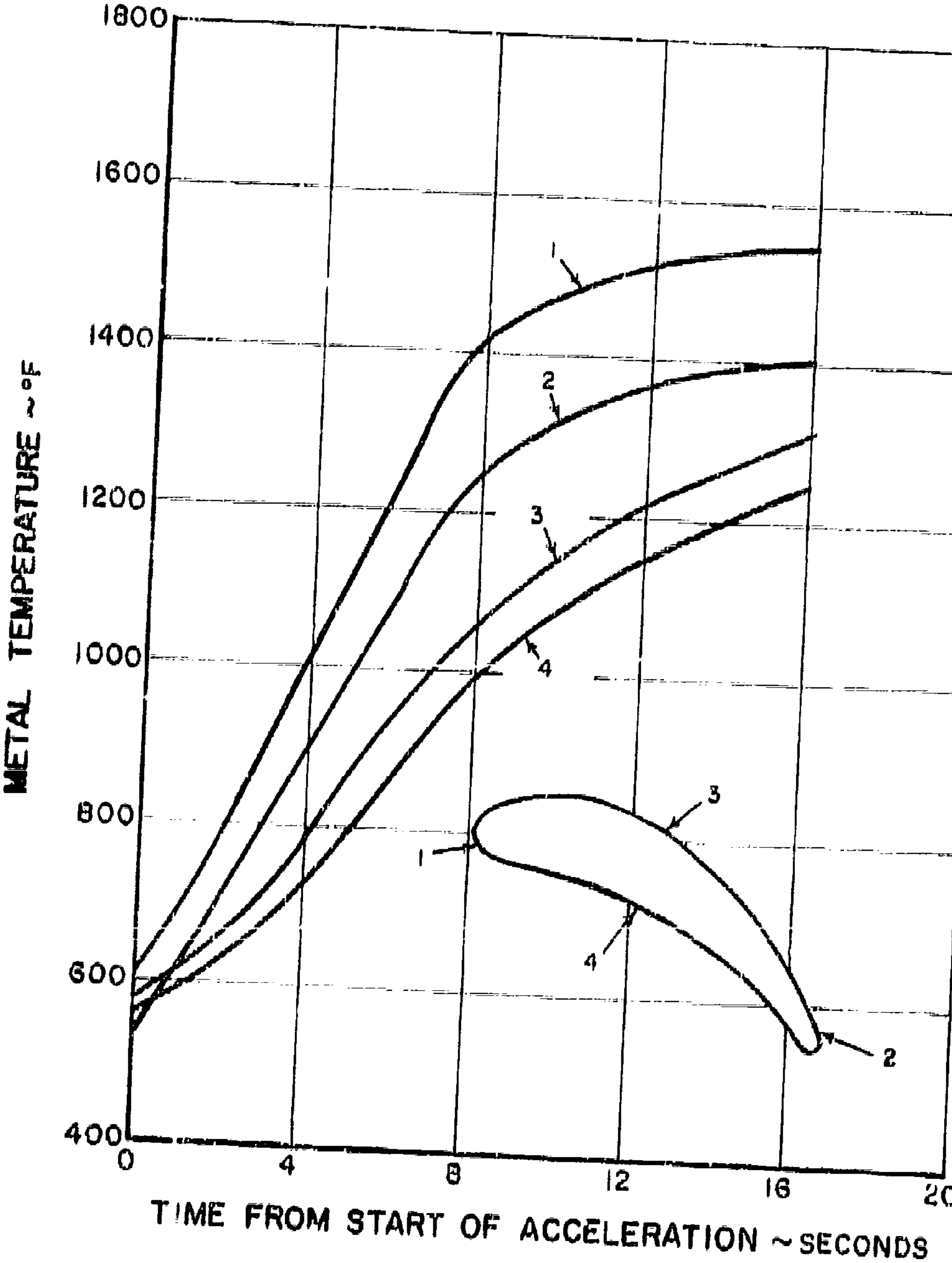

BLADE TEMPERATURE RESPONSE TRANSIENT ACCELL. SLTO,, 2300°F

Figure 2A-165

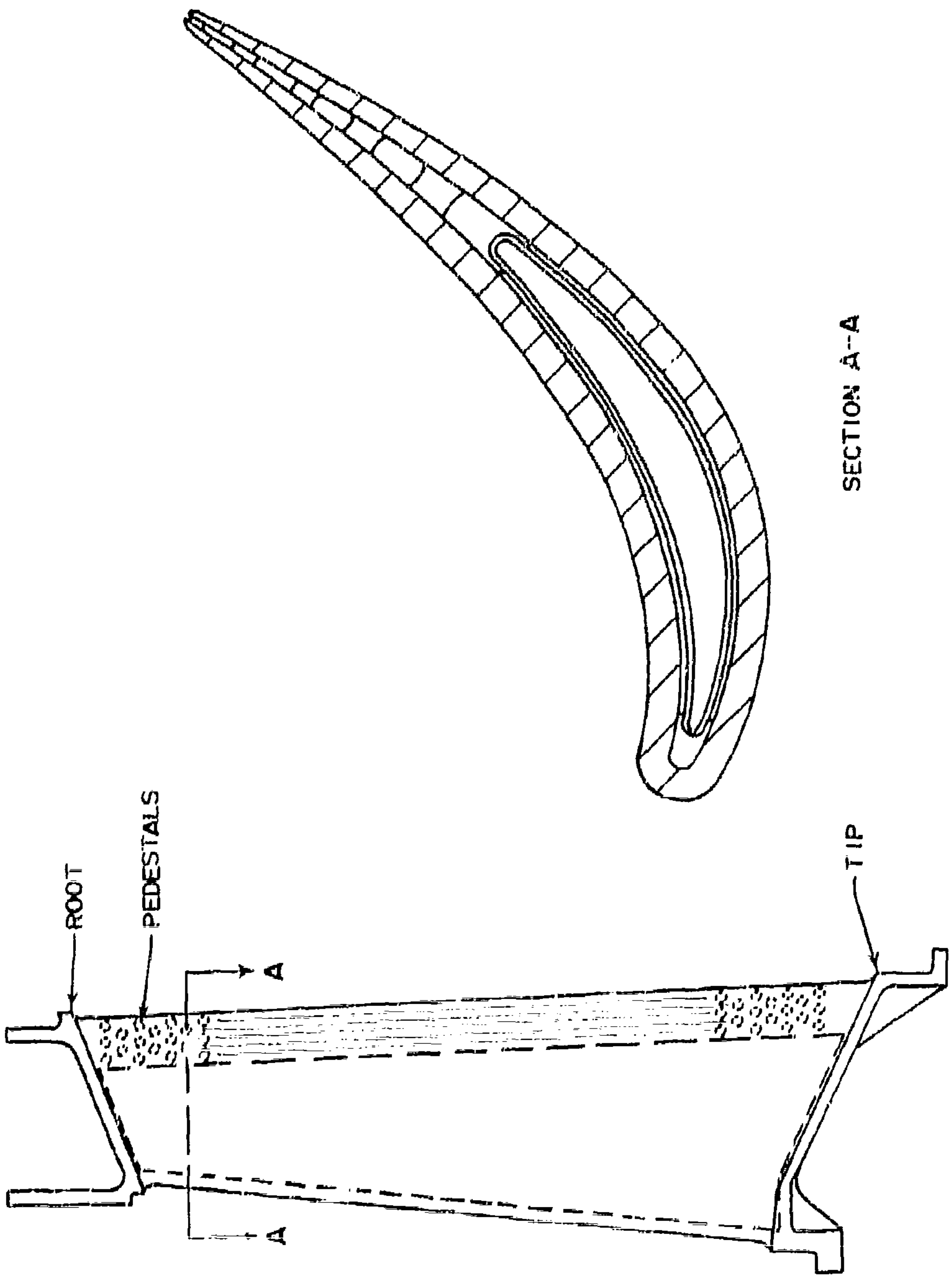

SECOND TURBINE VANE GEOMETRY - 2300°F RATING

Figure 2A-166

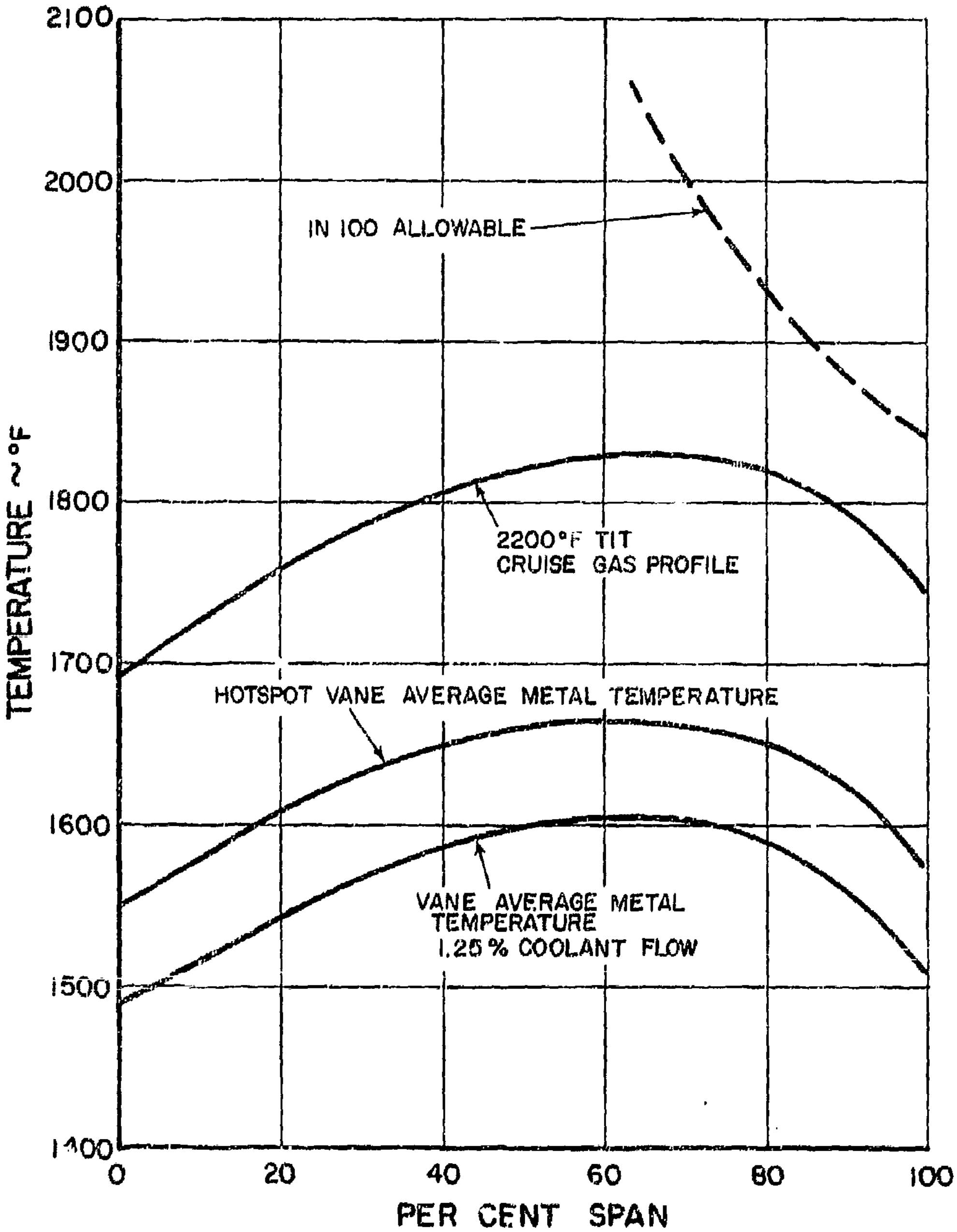

AVERAGE SECOND STAGE VANE TEMPERATURES

Figure 2A-167

2200°F TIT CRUISE 2nd TURBINE VANE
$T_{M\ AVERAGE}$ = 1600°F (1660°F)

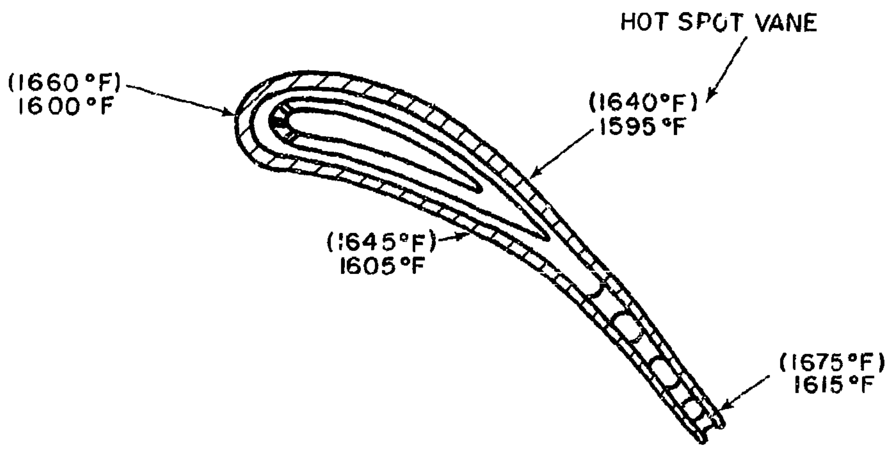

SECOND STAGE VANE MAXIMUM METAL TEMPERATURE

Figure 2A-168

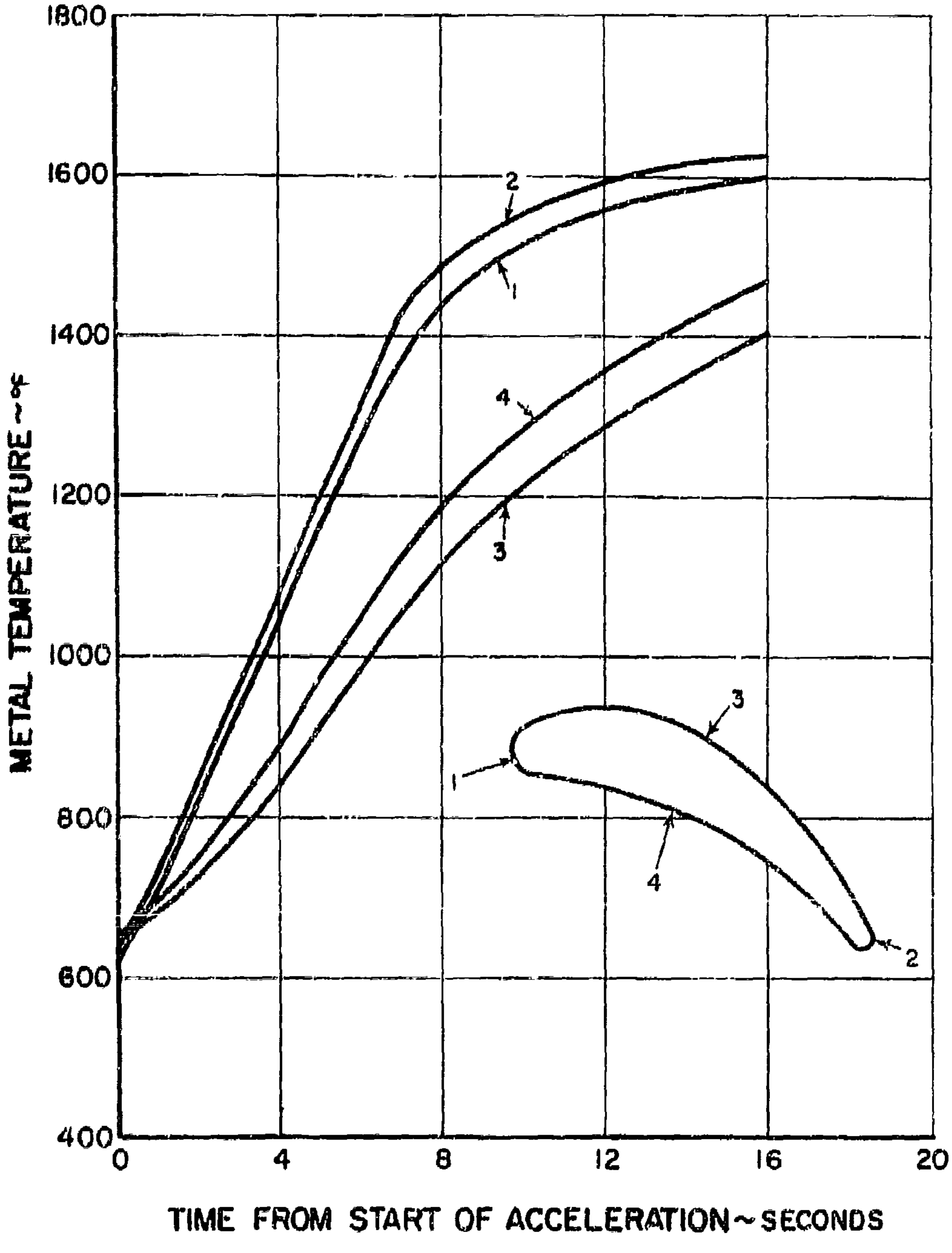

TYPICAL TRANSIENT GRADIENTS, SECOND STAGE VANE - ACCELL. SLTO - 2300°F

Figure 2A-169

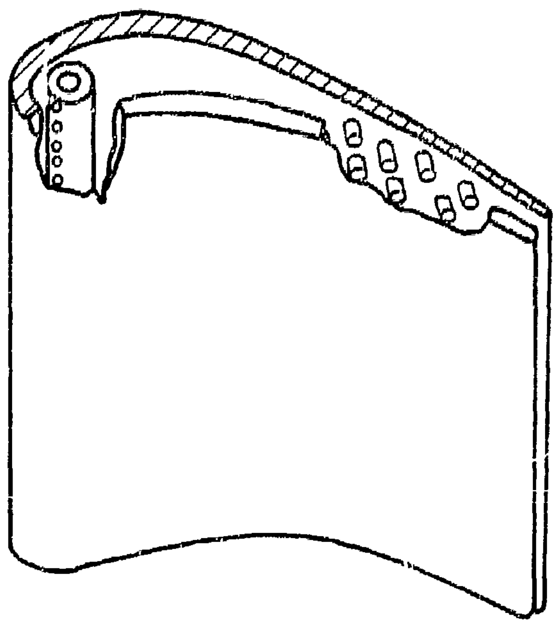

VANE DESIGN, IMPINGEMENT COOLED LEADING EDGE AND CONVECTIVELY COOLED TRAILING EDGE

Figure 2A-170

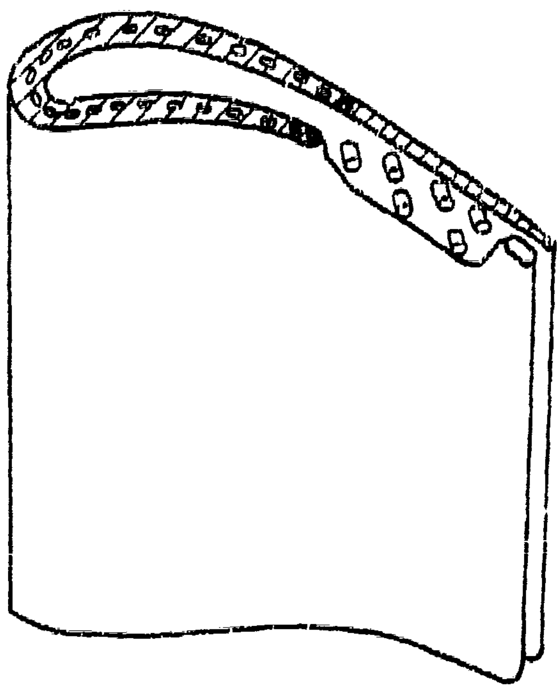

VANE DESIGN, RADIAL HOLE CONVECTIVELY COOLED LEADING EDGE AND CONVECTIVELY COOLED TRAILING EDGE

Figure 2A-171

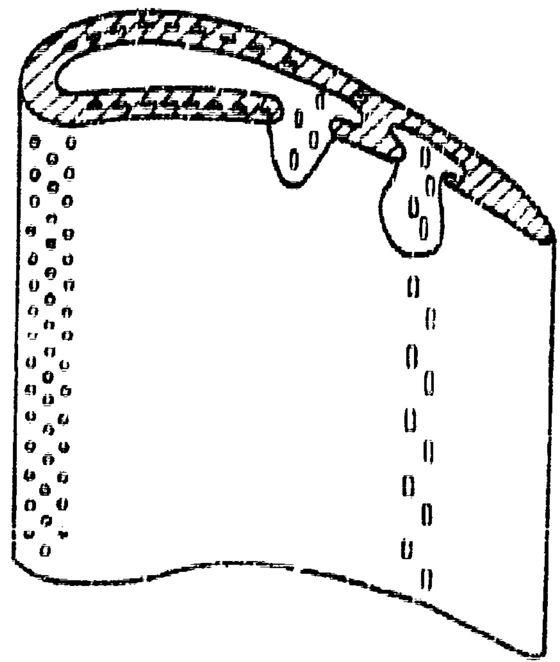

VANE DESIGN, SHOWERHEAD LEADING EDGE AND FILM COOLED TRAILING EDGE

Figure 2A-177

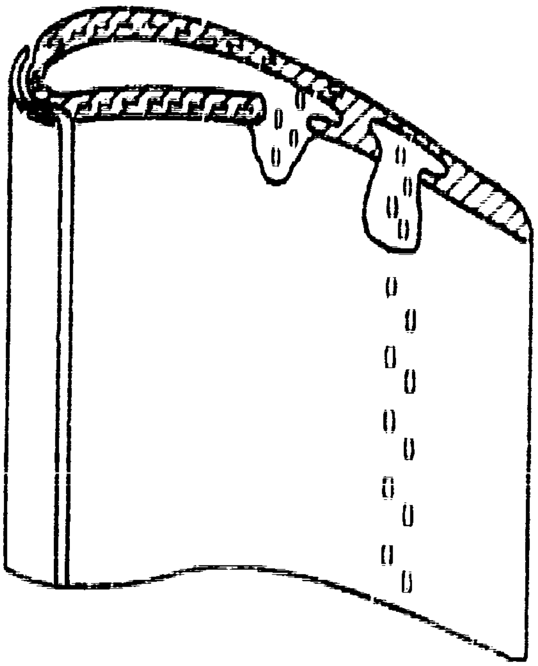

VANE DESIGN, DETACHED LEADING EDGE AND FILM COOLED TRAILING EDGE

Figure 2A-173

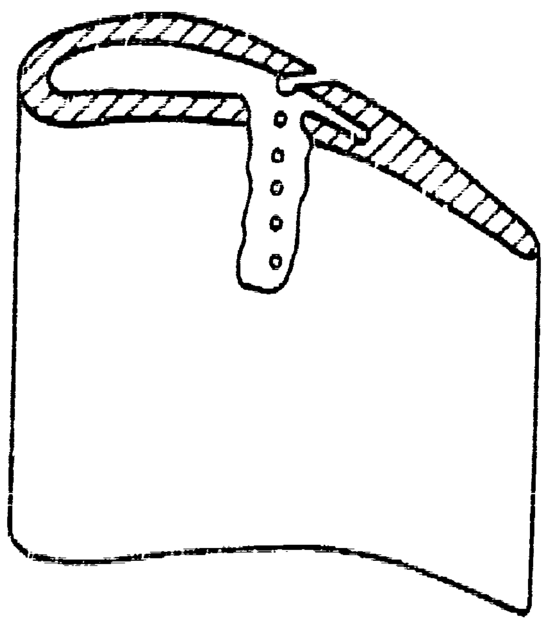

VANE DESIGN, FILM COOLED TRAILING EDGE

Figure 2A-174

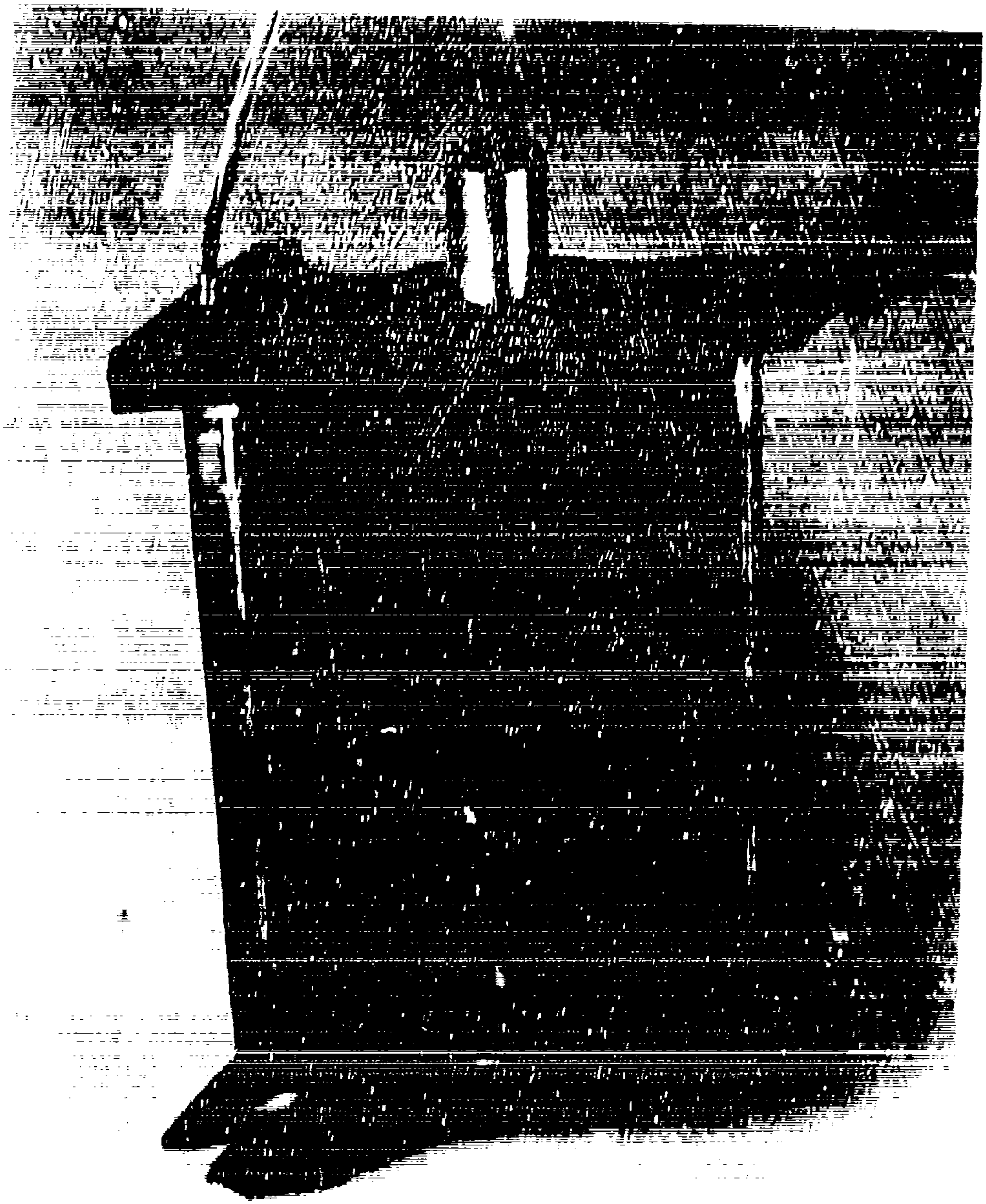

TYPICAL THERMOCOUPLED VANE

Figure 2A-175

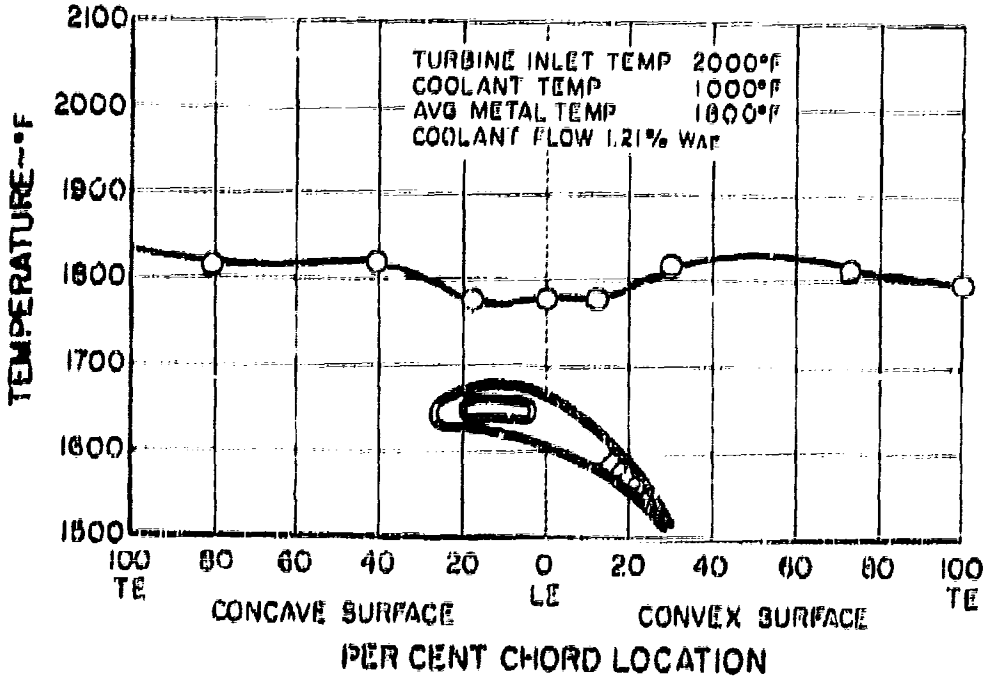

FIRST TURBINE VANE METAL TEMPERATURE

Figure 2A-176

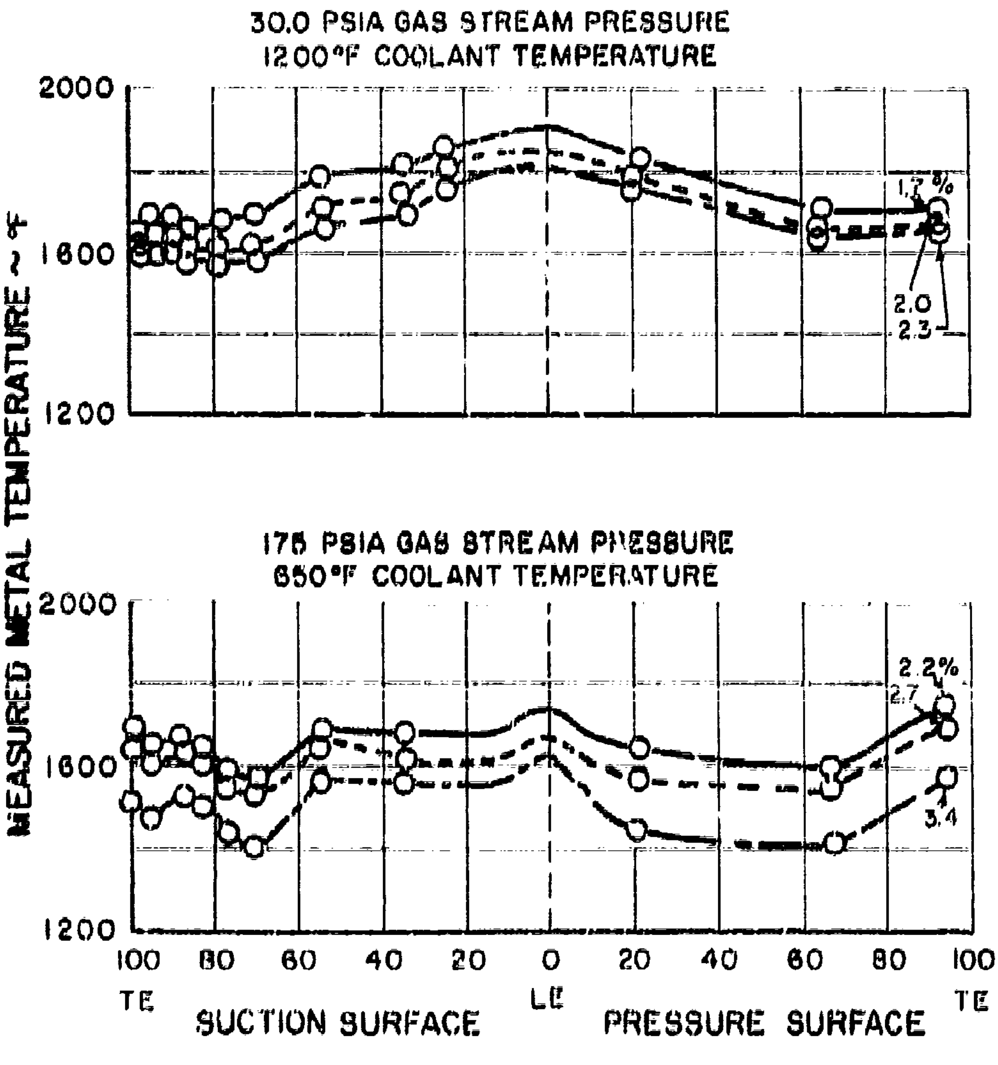

PEDESTAL T.E. VANE DATA - 2300°F GAS TEMP

Figure 2A-176A

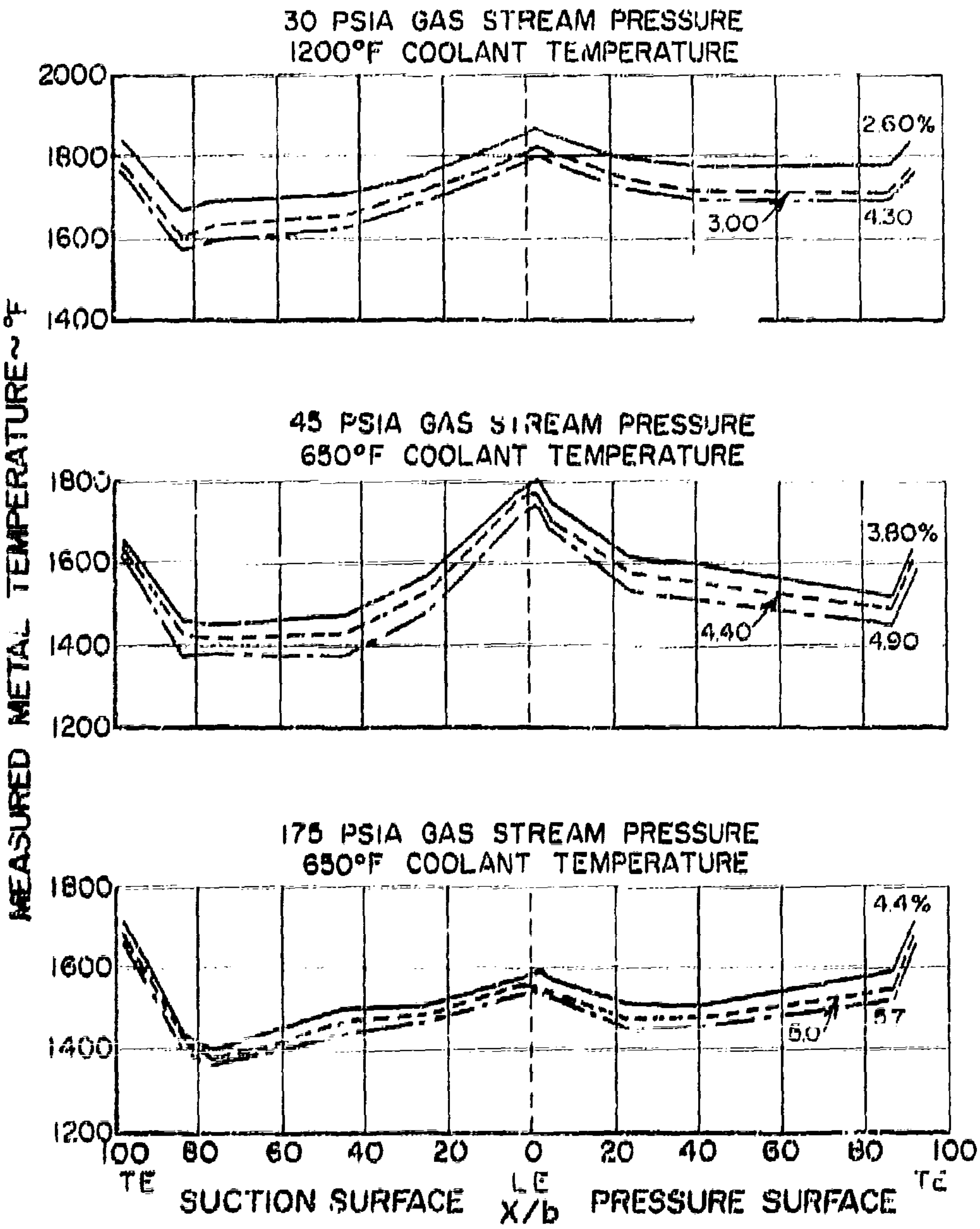

SHOWERHEAD VANE METAL TEMPERATURE VS CHORD - 2300°F GAS TEMP

Figure 2A-177

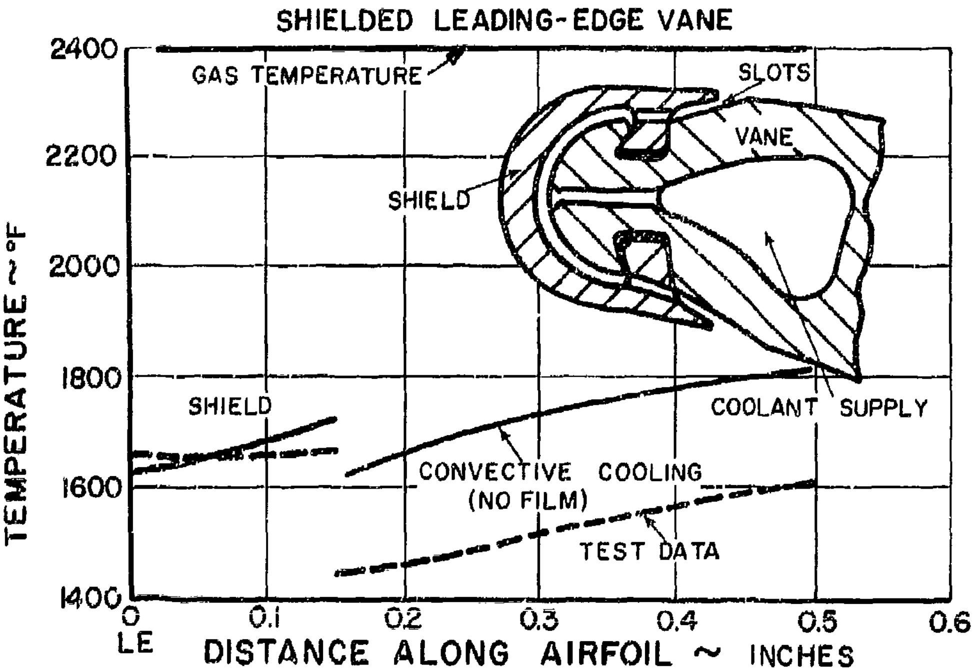

FILM COOLED AIRFOIL TEST RESULTS

Figure 2A-178

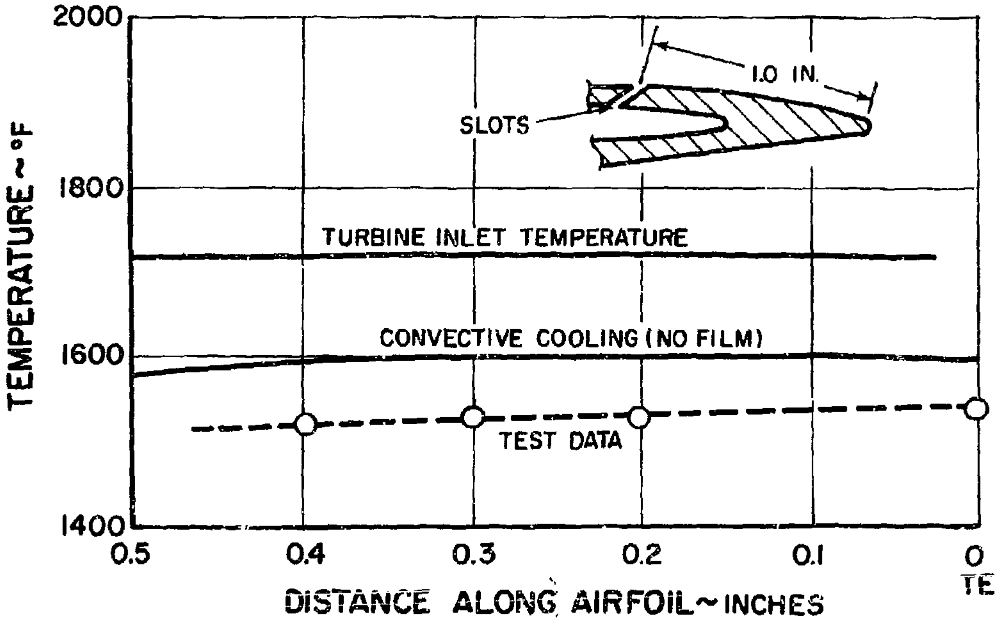

FILM COOLED AIRFOIL TEST RESULTS, VANE TRAILING EDGE FILM COOLING

Figure 2A-179

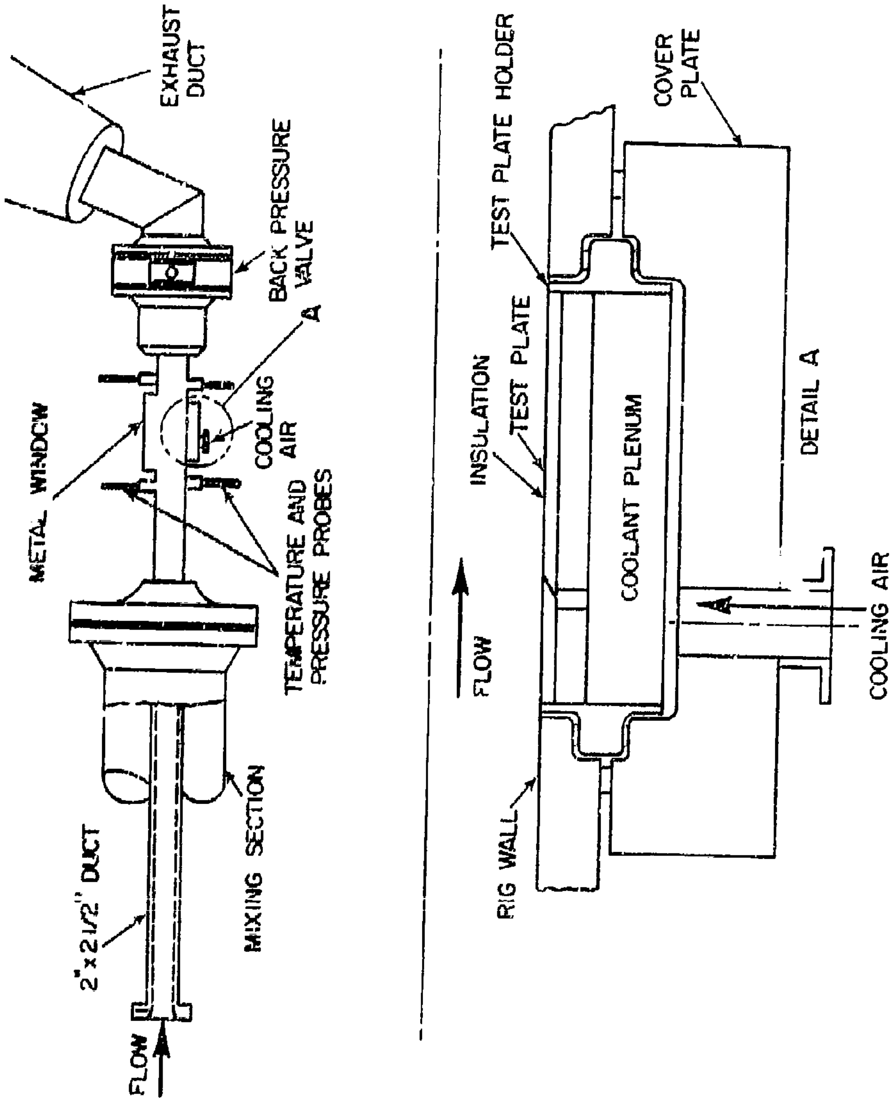

FLAT PLATE TEST RIG -- SCHEMATIC

Figure 2A-180

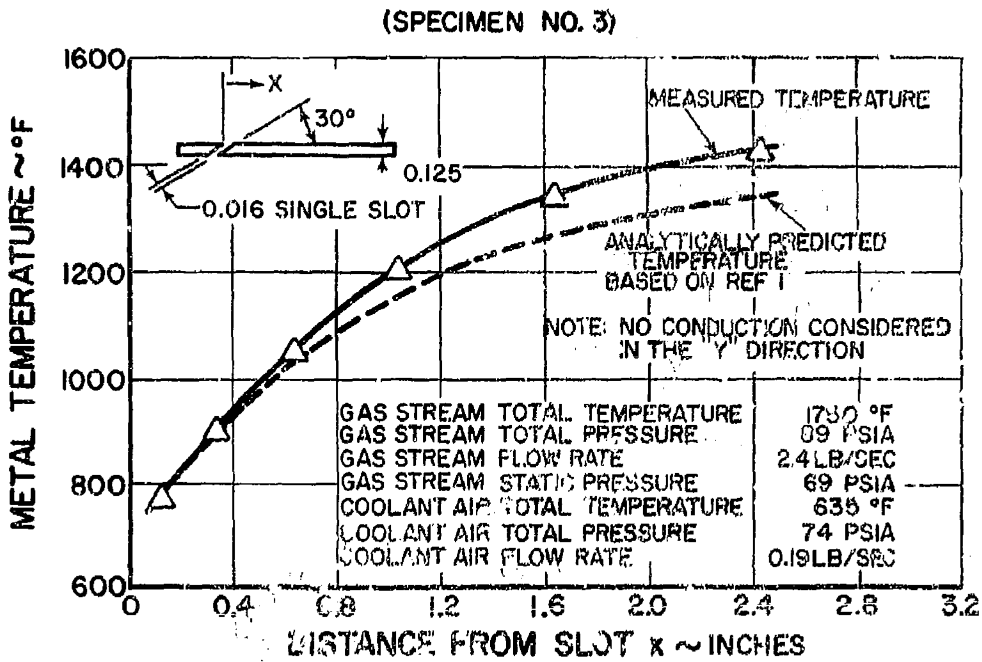

COMPARISON OF METAL TEMPERATURES BASIC FILM COOLING RIG

Figure 2A-181

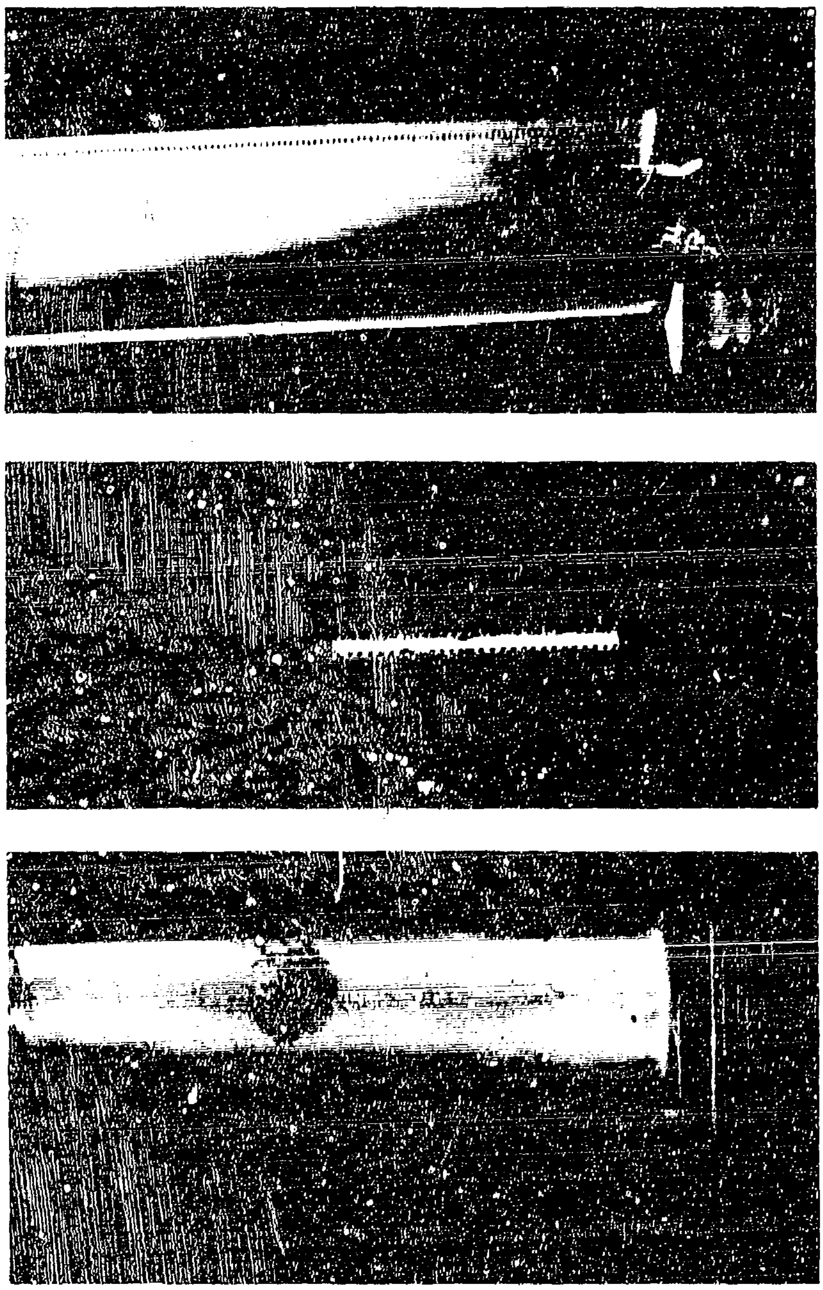

FILM COOLED BLADE, .008 DIAMETER HOLES

Figure 2A-182

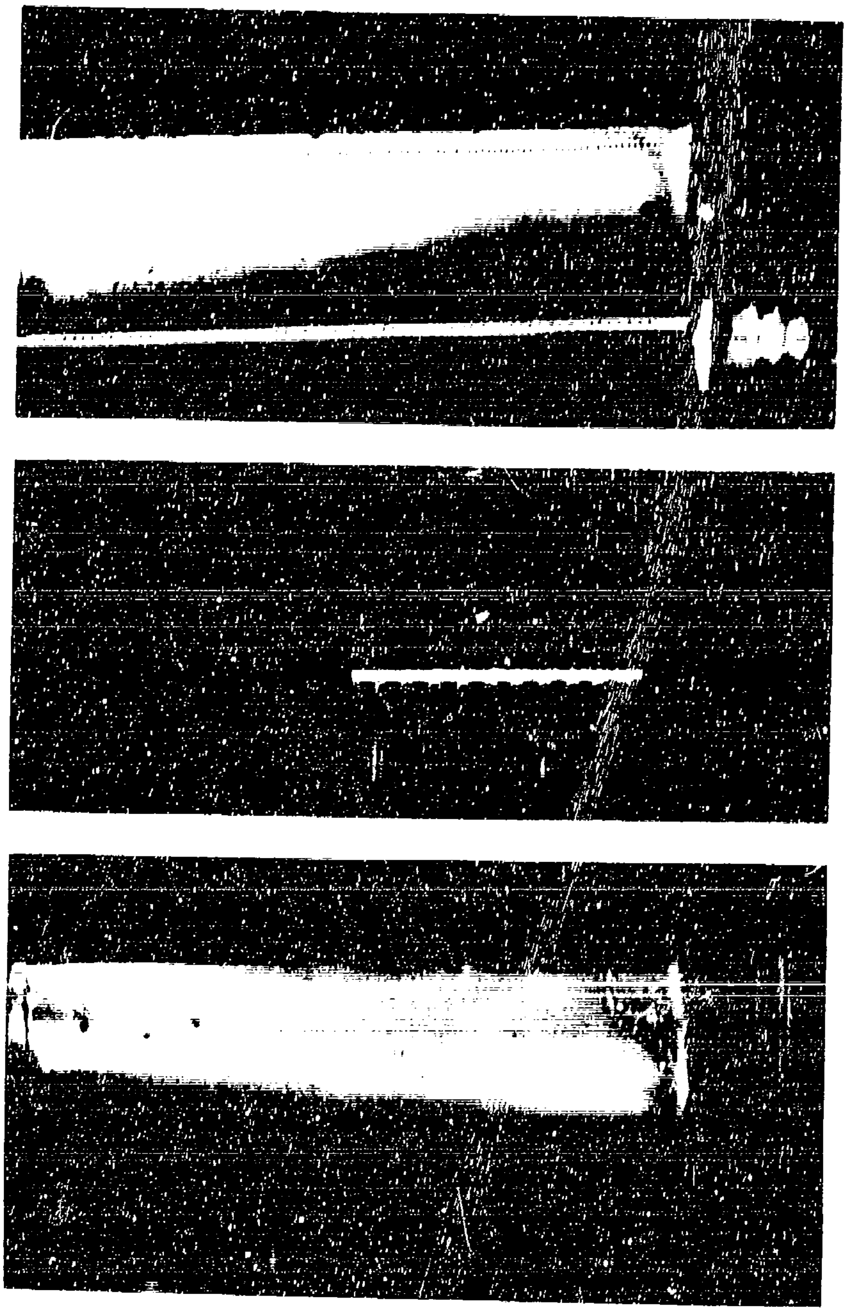

FILM COOLED BLADE, .013 DIAMETER HOLES, 30°

Figure 2A-183

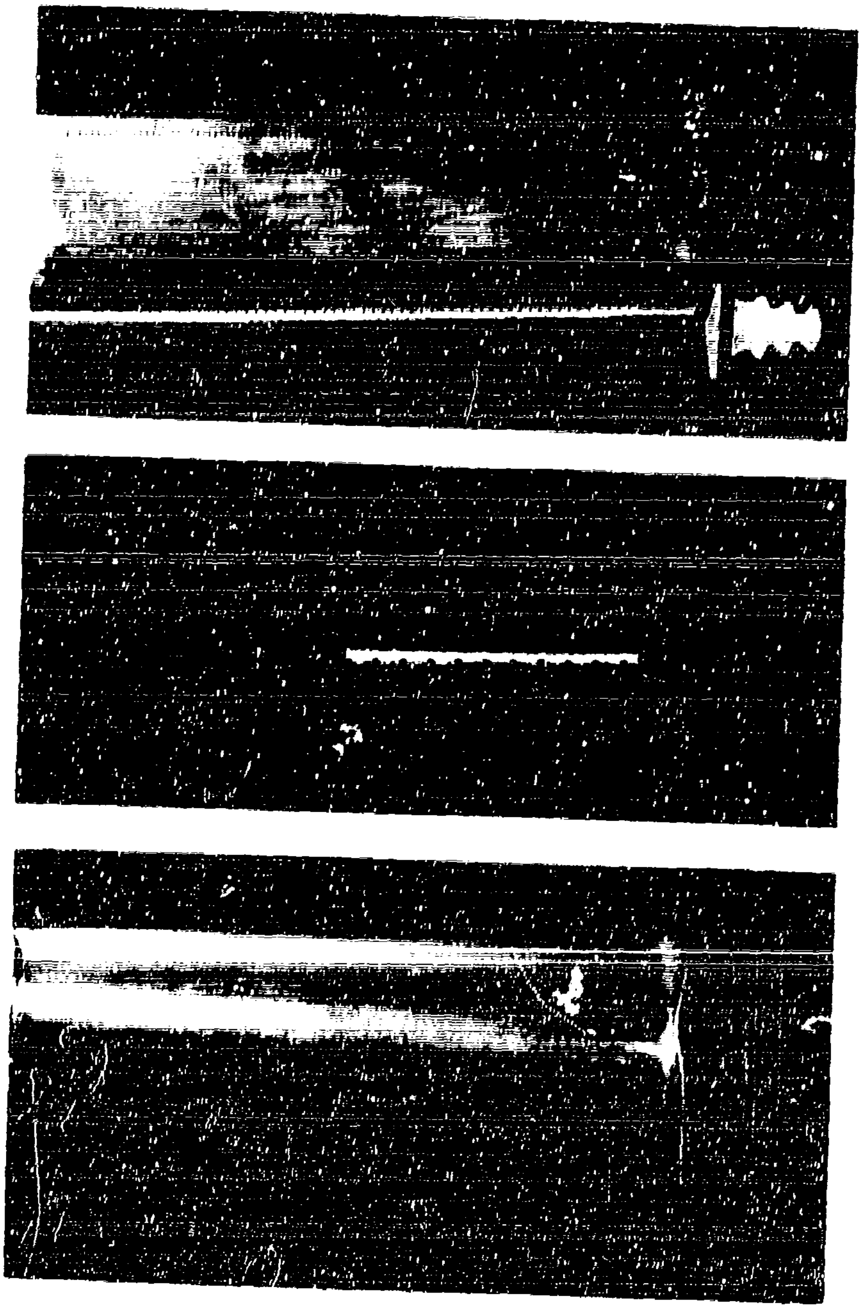

FILM COOLED BLADE, .013 DIAMETER HOLES, 90°

Figure 2A-184

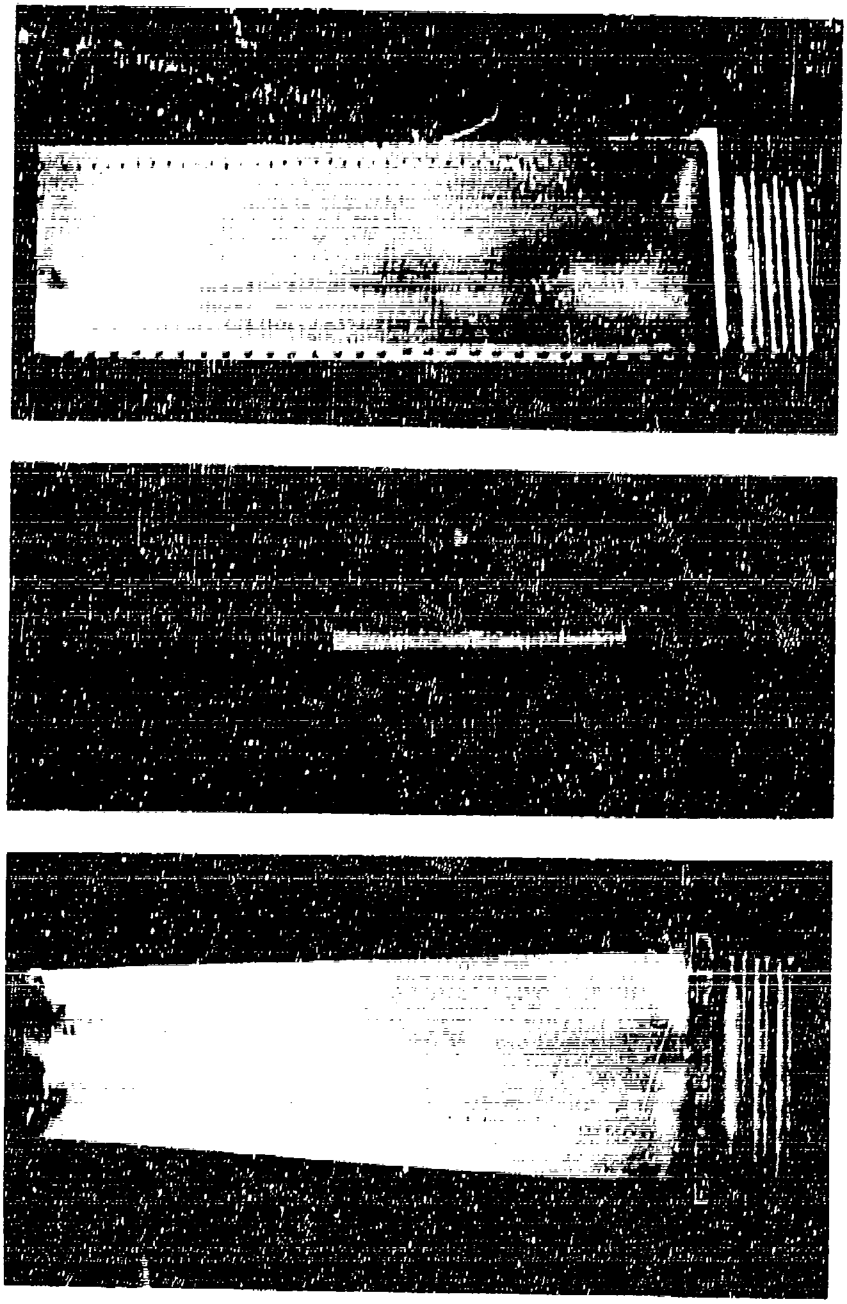

FILM COOLED BLADE, .030 DIAMETER HOLES, 30°

Figure 2A-185

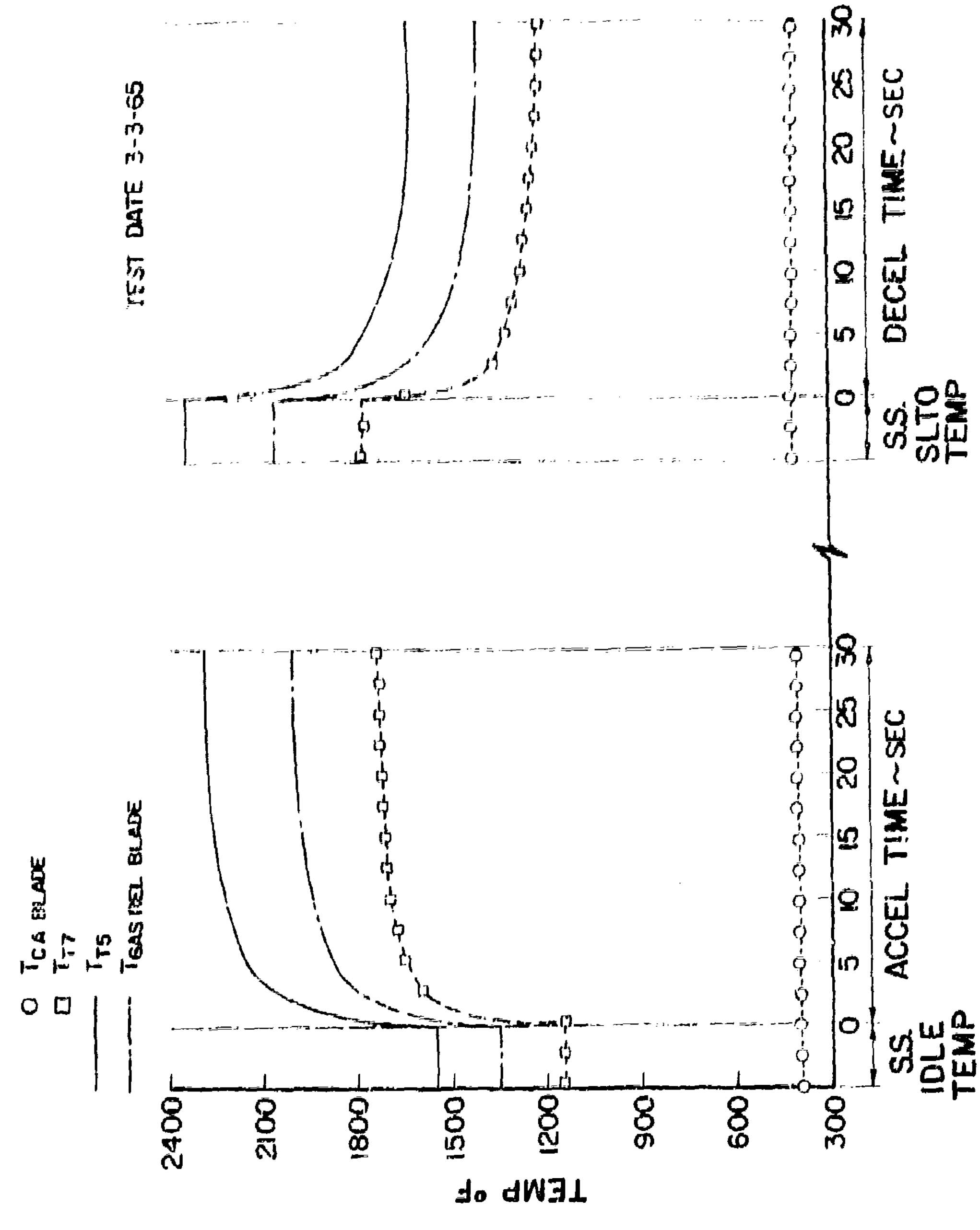

JT4 TURBINE INLET TEMPERATURE VARIATION - HIGH TEMPERATURE DEVELOPMENT ENGINE

Figure 2A-186

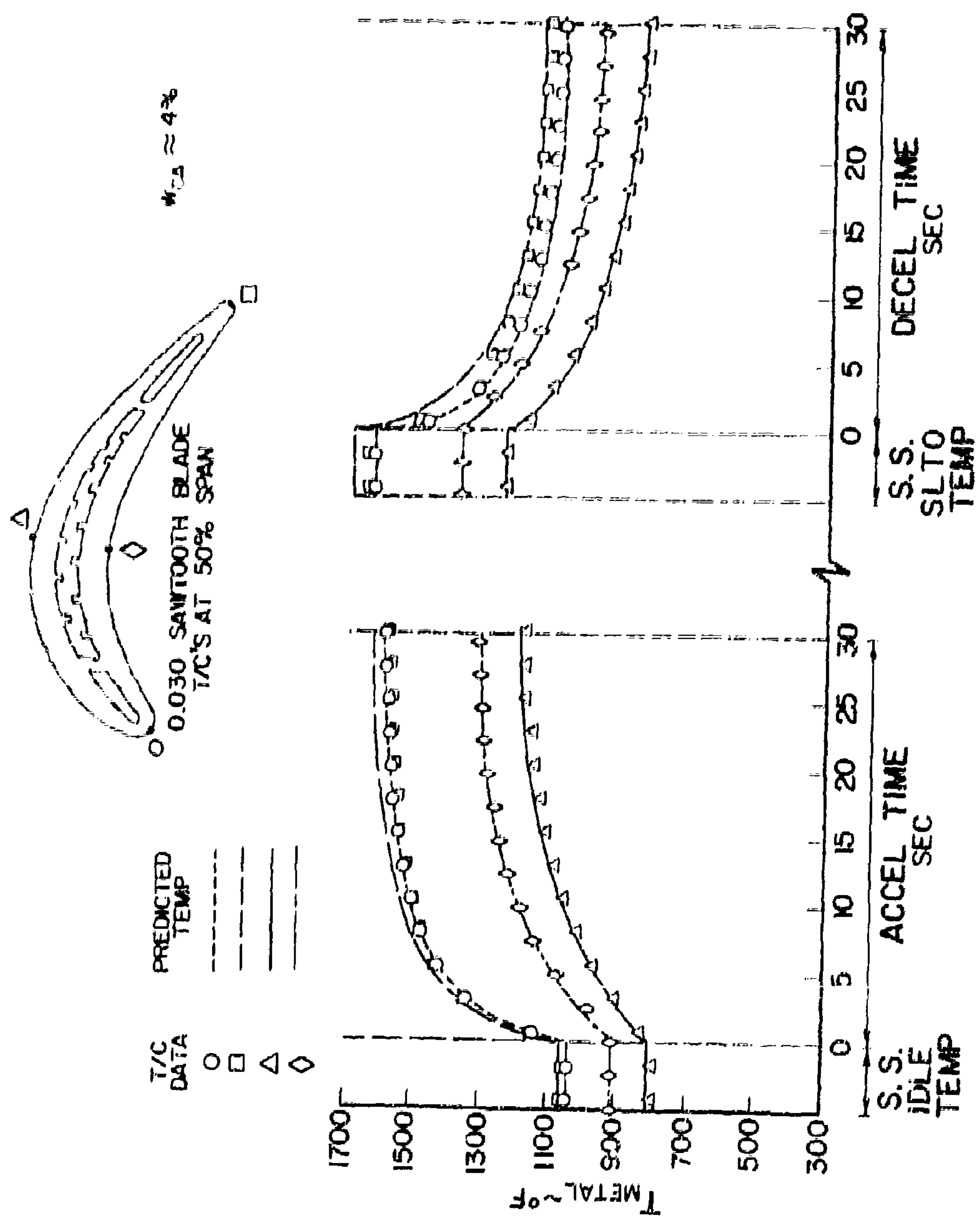

CONVECTIVELY COOLED TURBINE BLADE TEST RESULTS – HIGH TEMP DEVELOPMENT ENGINE

Figure 2A-187

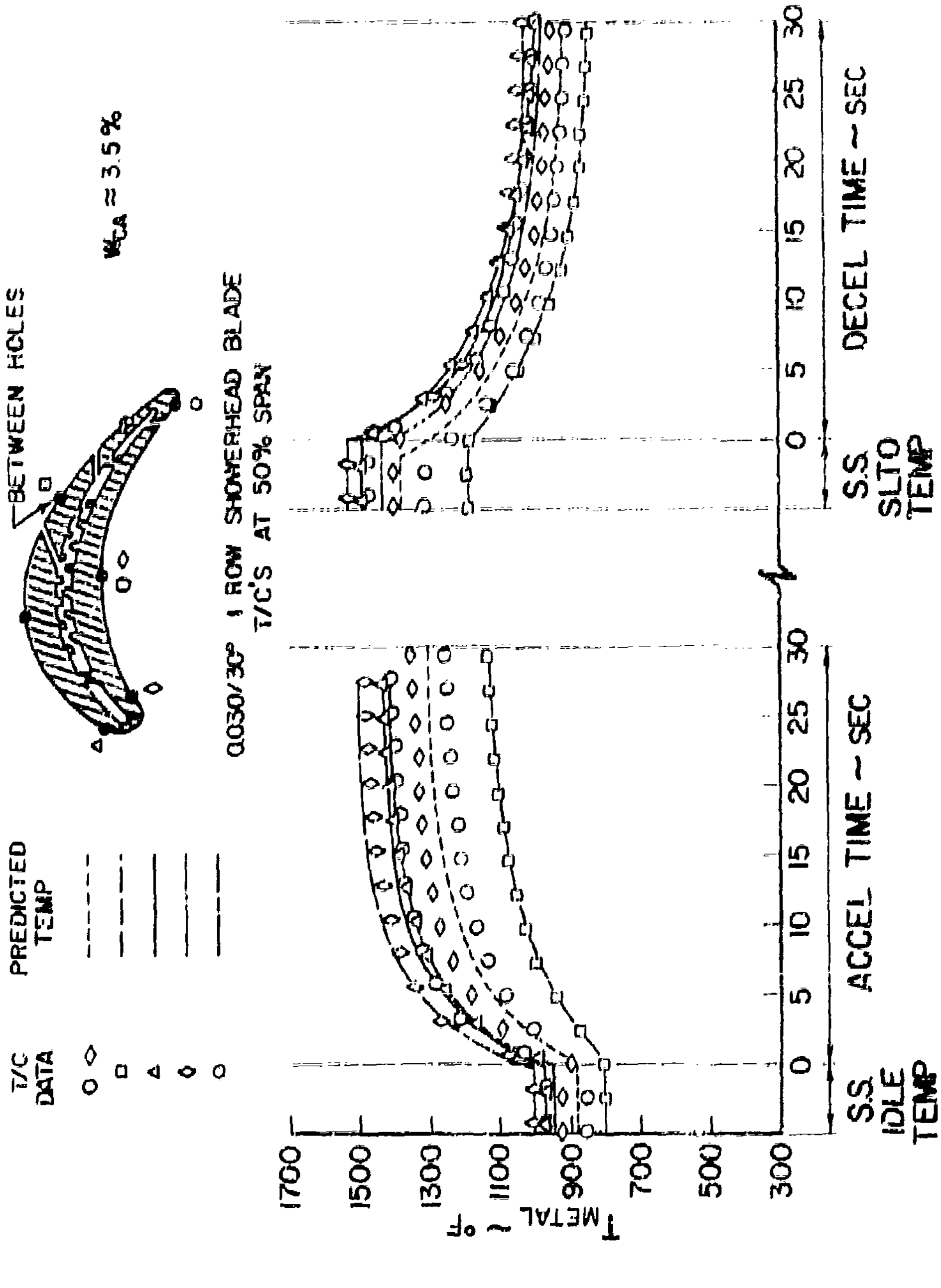

FILM COOLED TURBINE BLADE TEST RESULTS - HIGH TEMP DEVELOPMENT ENGINE

Figure 2A-188

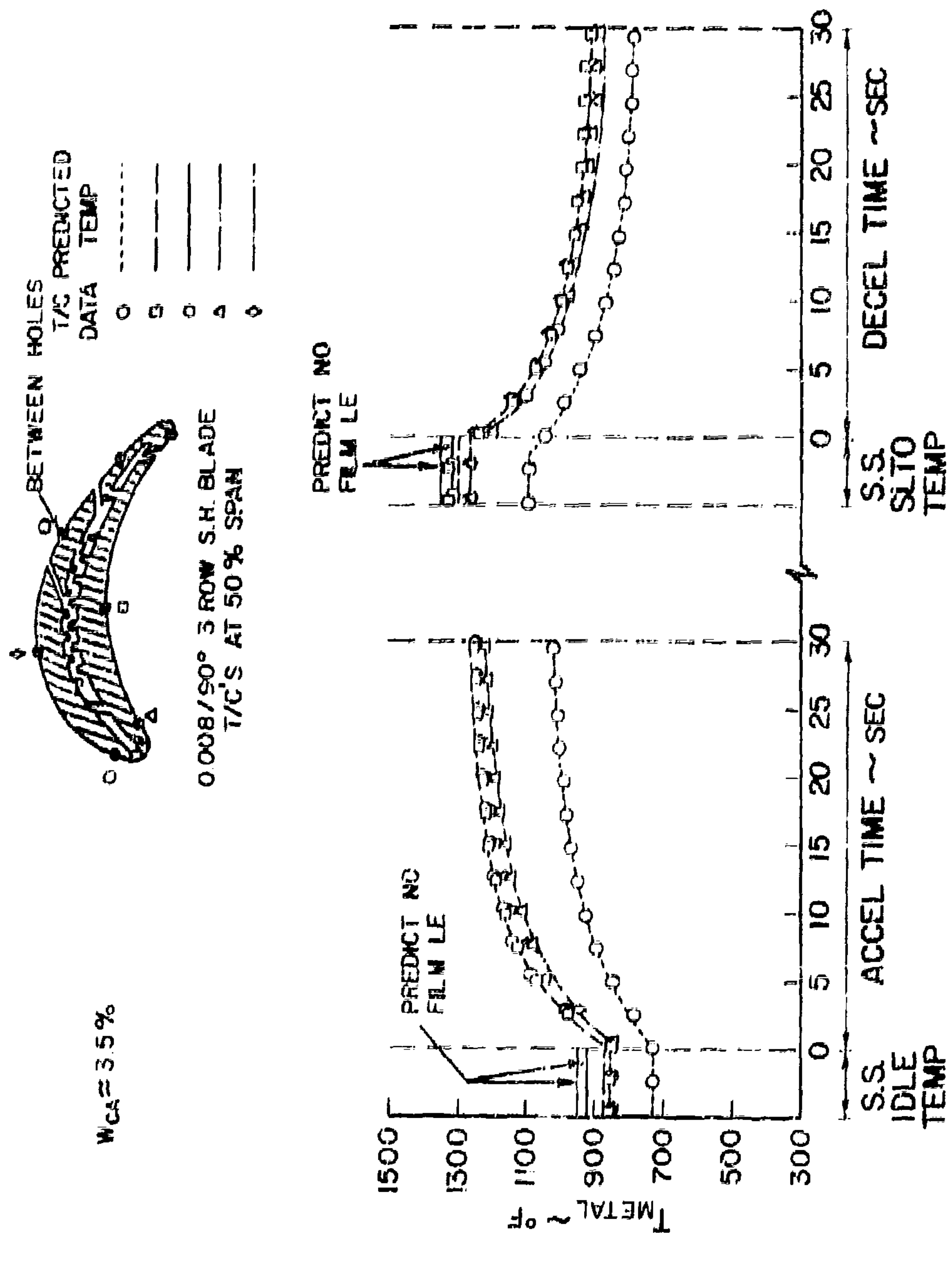

FILM COOLED BLADE TEST RESULTS - HIGH TEMP DEVELOPMENT ENGINE

Figure 2A-189

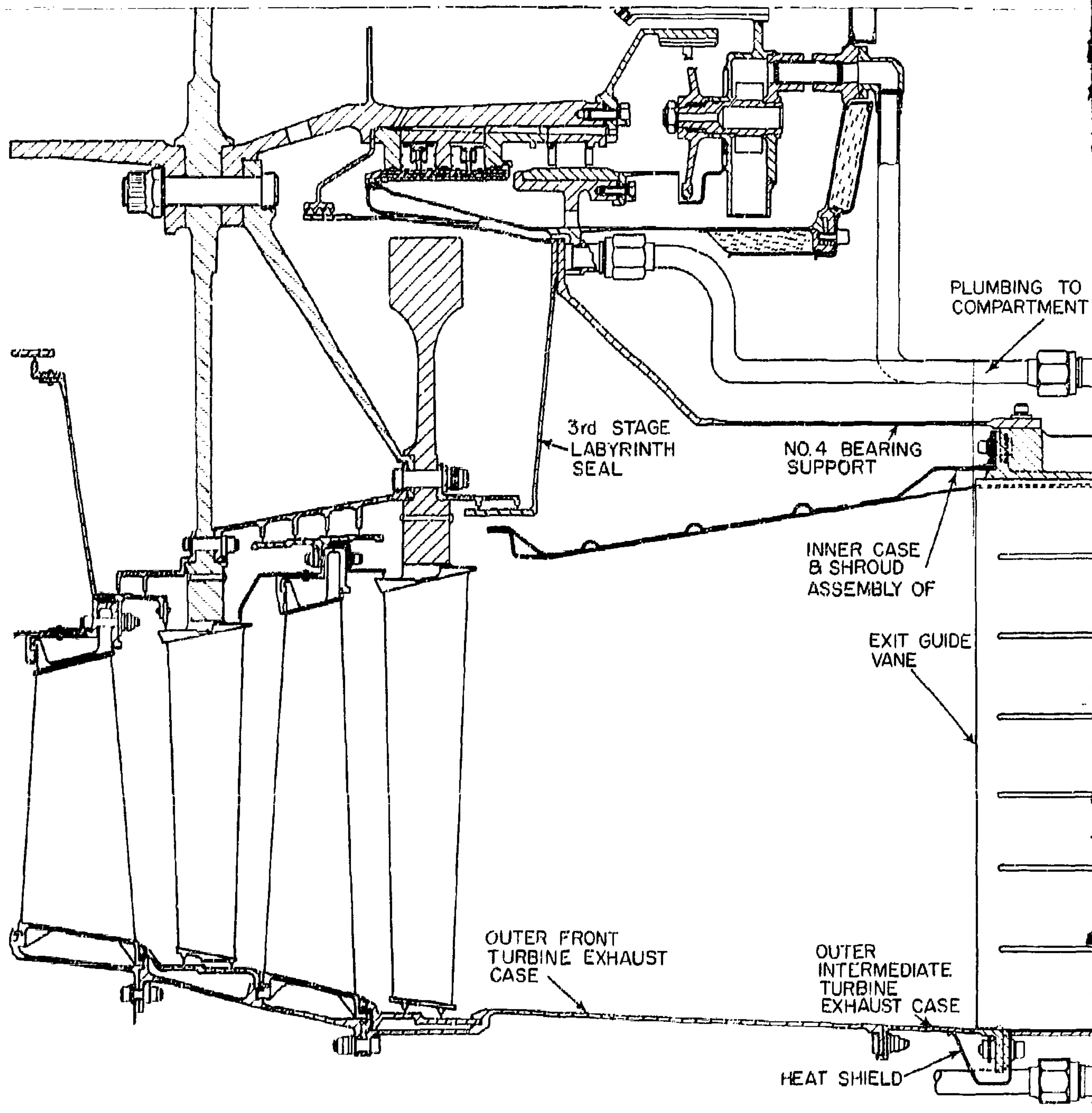
PLUMBING TO COMPARTMENT
3rd STAGE LABYRINTH SEAL
NO.4 BEARING SUPPORT
INNER CASE & SHROUD ASSEMBLY OF
EXIT GUIDE VANE
OUTER FRONT TURBINE EXHAUST CASE
OUTER INTERMEDIATE TURBINE EXHAUST CASE
HEAT SHIELD

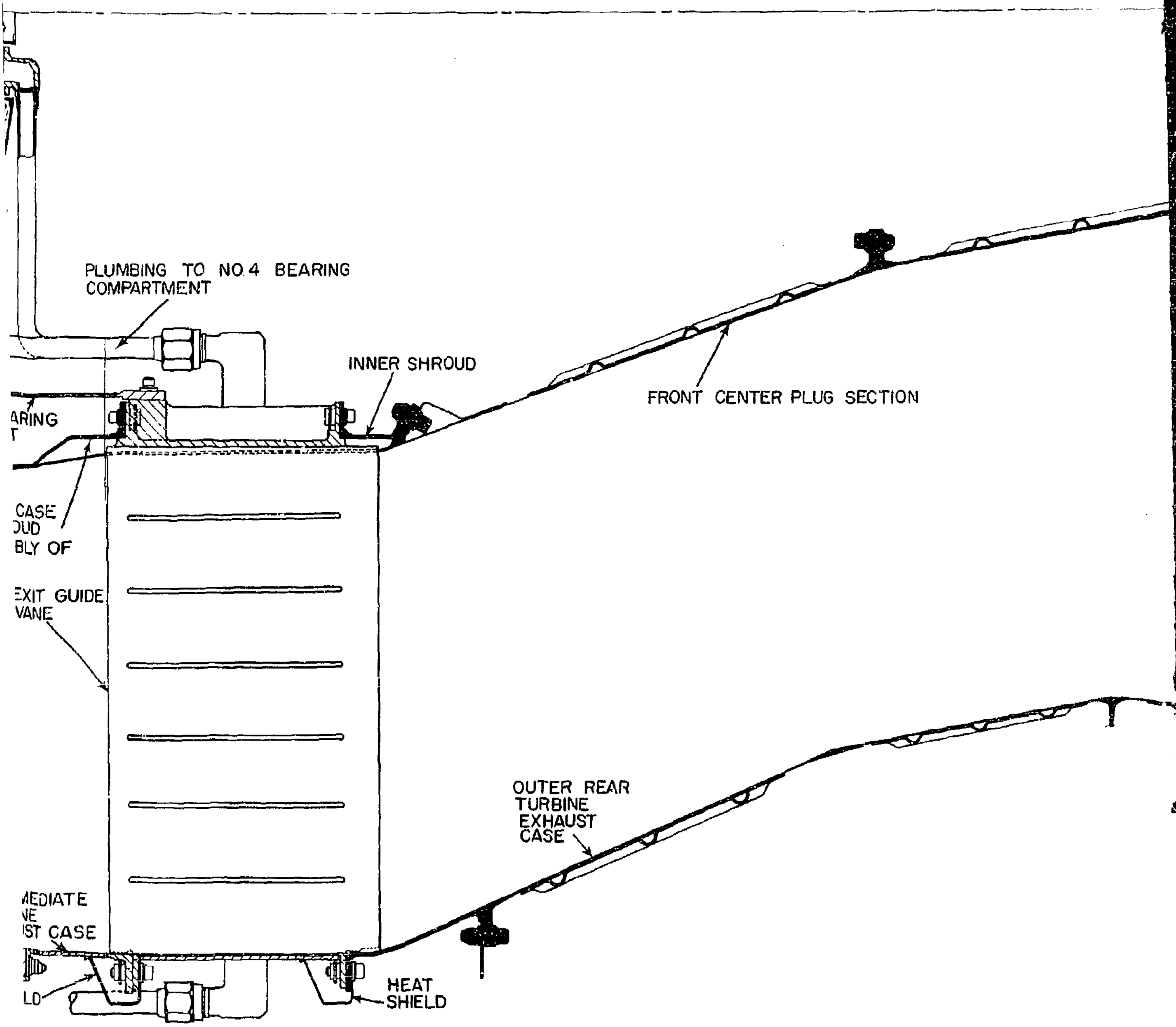

PLUMBING TO NO.4 BEARING COMPARTMENT
INNER SHROUD
FRONT CENTER PLUG SECTION
ARING
CASE
OUD
BLY OF
EXIT GUIDE VANE
OUTER REAR TURBINE EXHAUST CASE
MEDIATE
IST CASE
LD
HEAT SHIELD

2

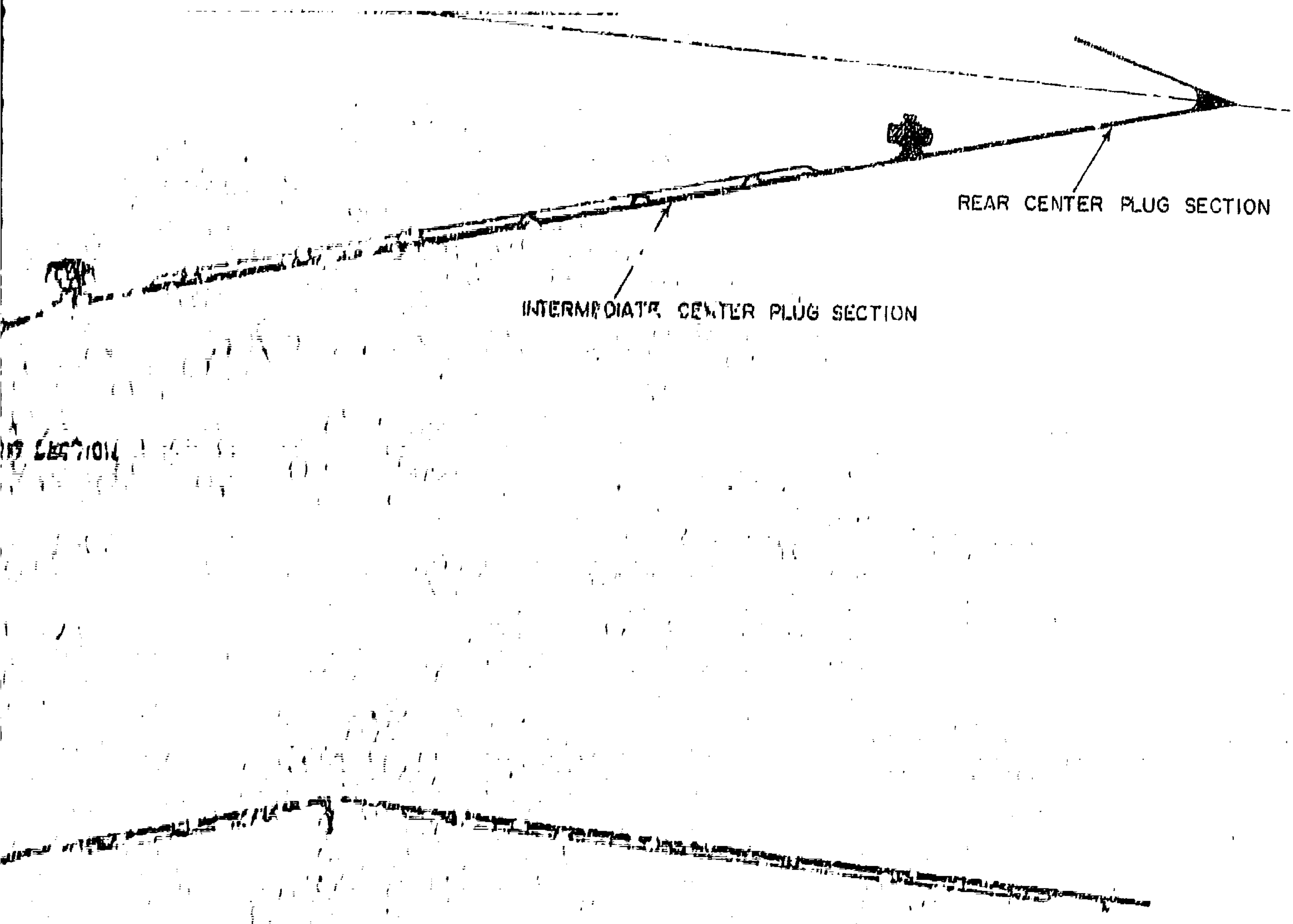

3

TURBINE EXHAUST SECTION

Figure 2A-190

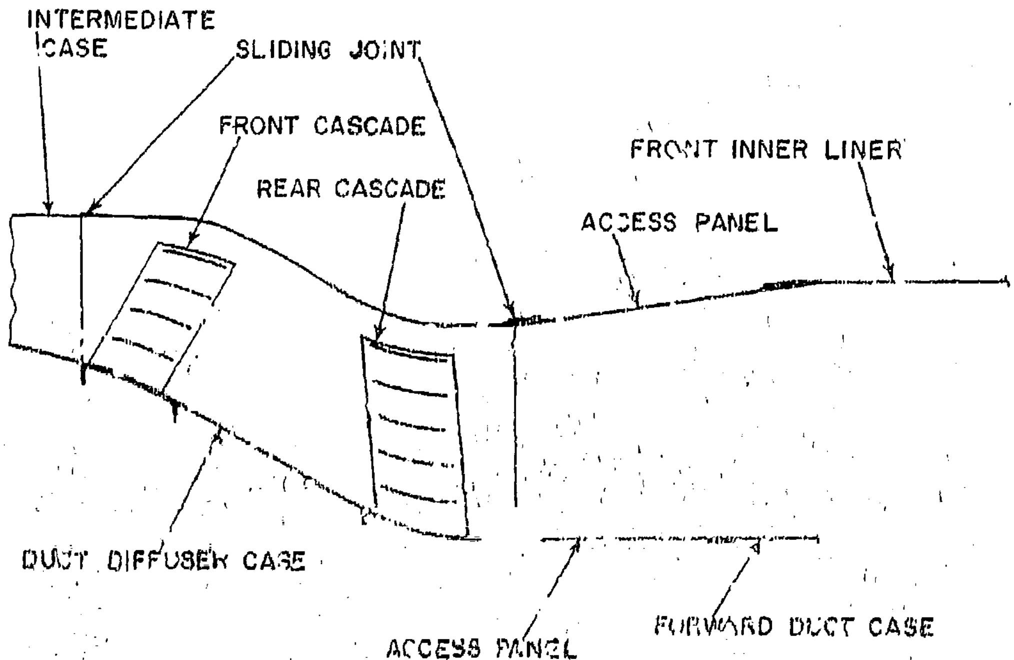

DUCT HEATER DIFFUSER SCHEMATIC

Figure 2A-197

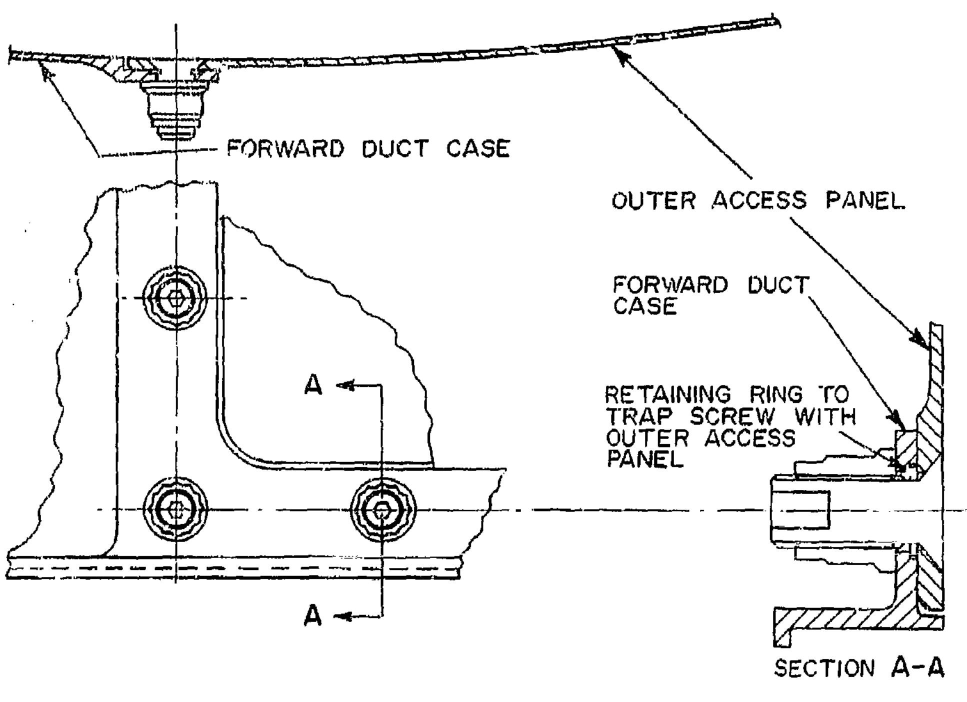

DUCT HEATER ACCESS PANEL

Figure 2A-192

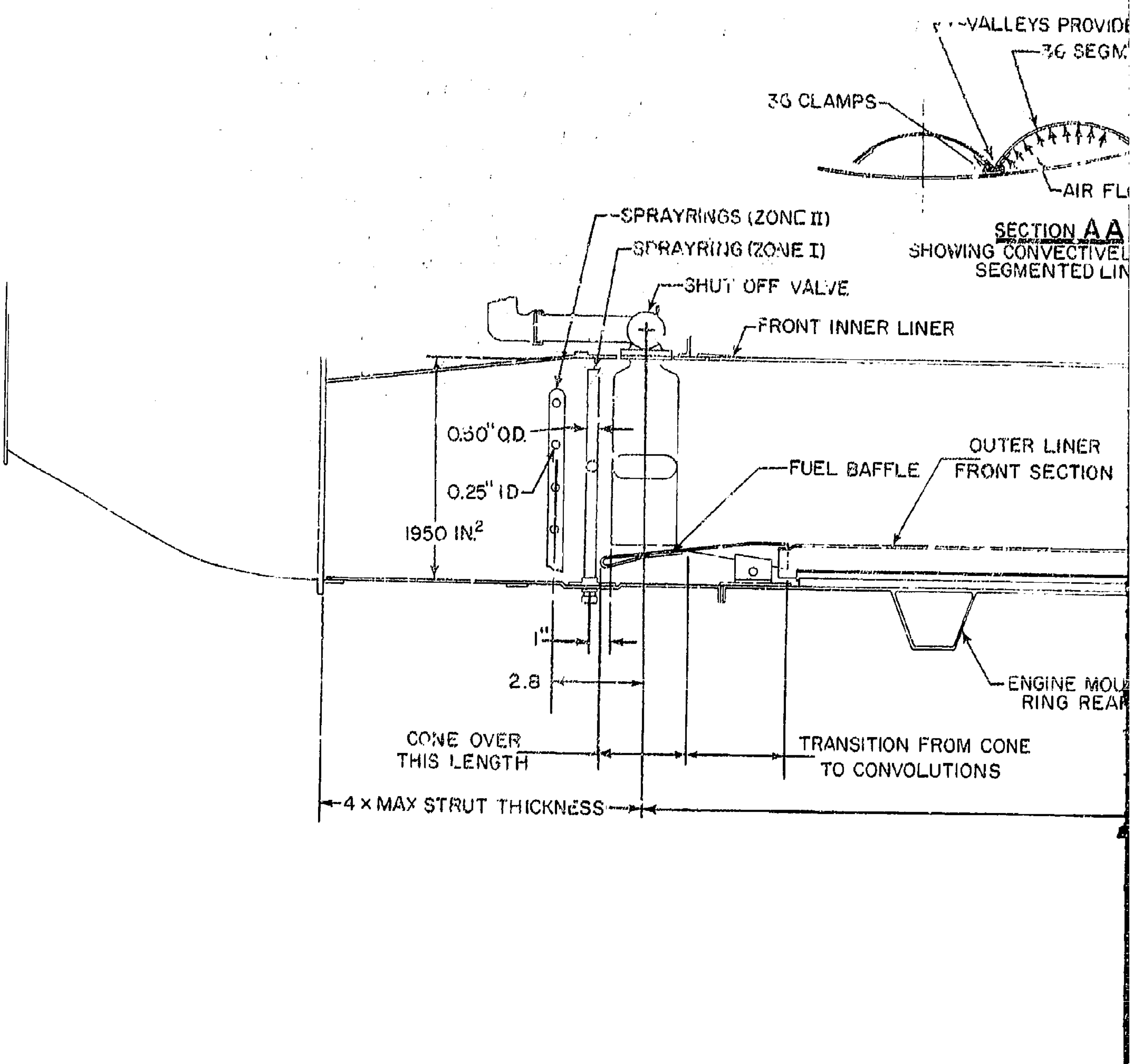
VALLEYS PROVIDE
36 SEGM
36 CLAMPS
AIR FL
SECTION AA
SHOWING CONVECTIVEL
SEGMENTED LIN
SPRAYRINGS (ZONE II)
SPRAYRING (ZONE I)
SHUT OFF VALVE
FRONT INNER LINER
0.50" O.D.
0.25" I.D.
1950 IN.²
FUEL BAFFLE
OUTER LINER
FRONT SECTION
1"
2.8
ENGINE MOU
RING REAR
CONE OVER
THIS LENGTH
TRANSITION FROM CONE
TO CONVOLUTIONS
4 × MAX STRUT THICKNESS

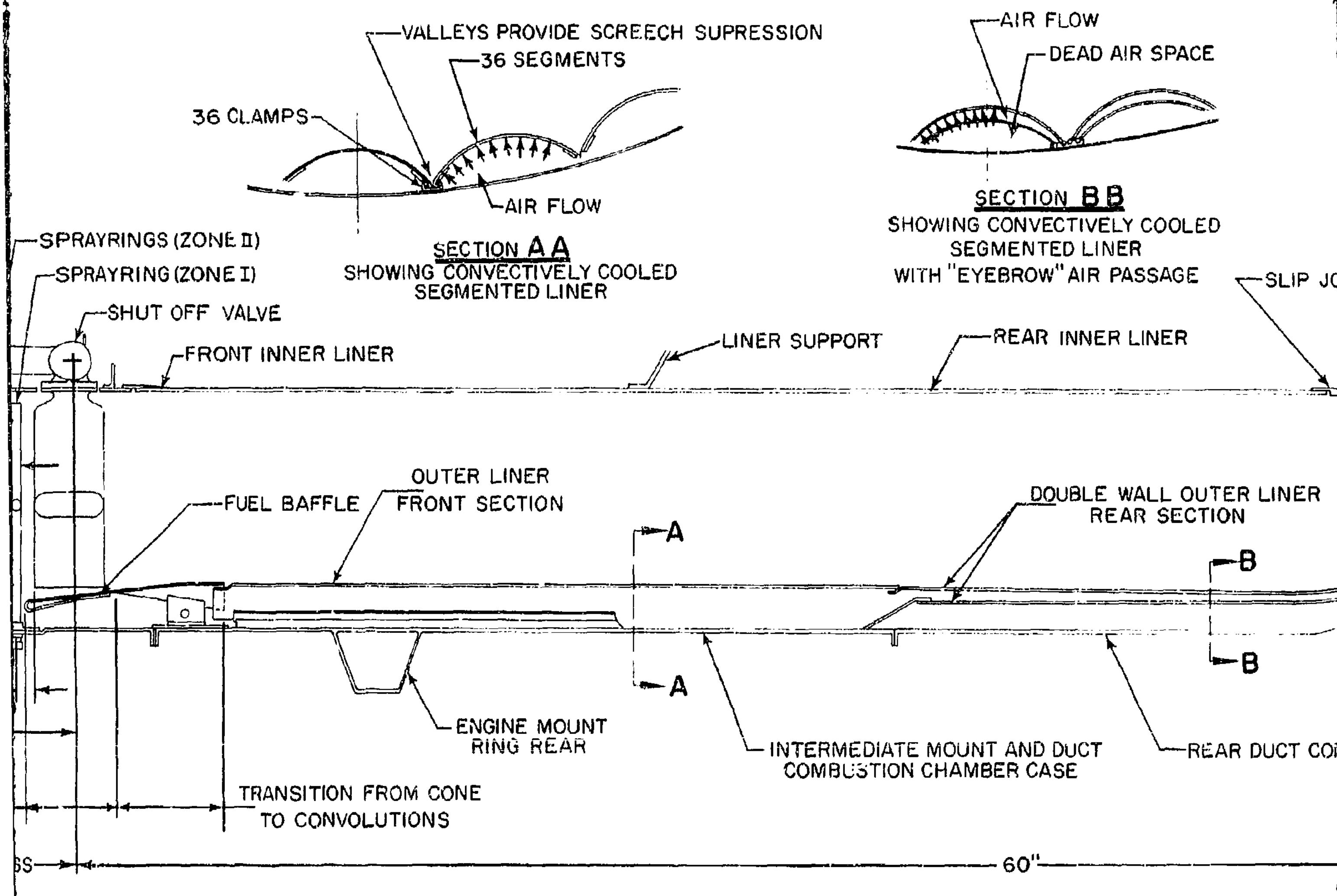

DUCT HEATER SCHEMATIC

Figure 2A-193

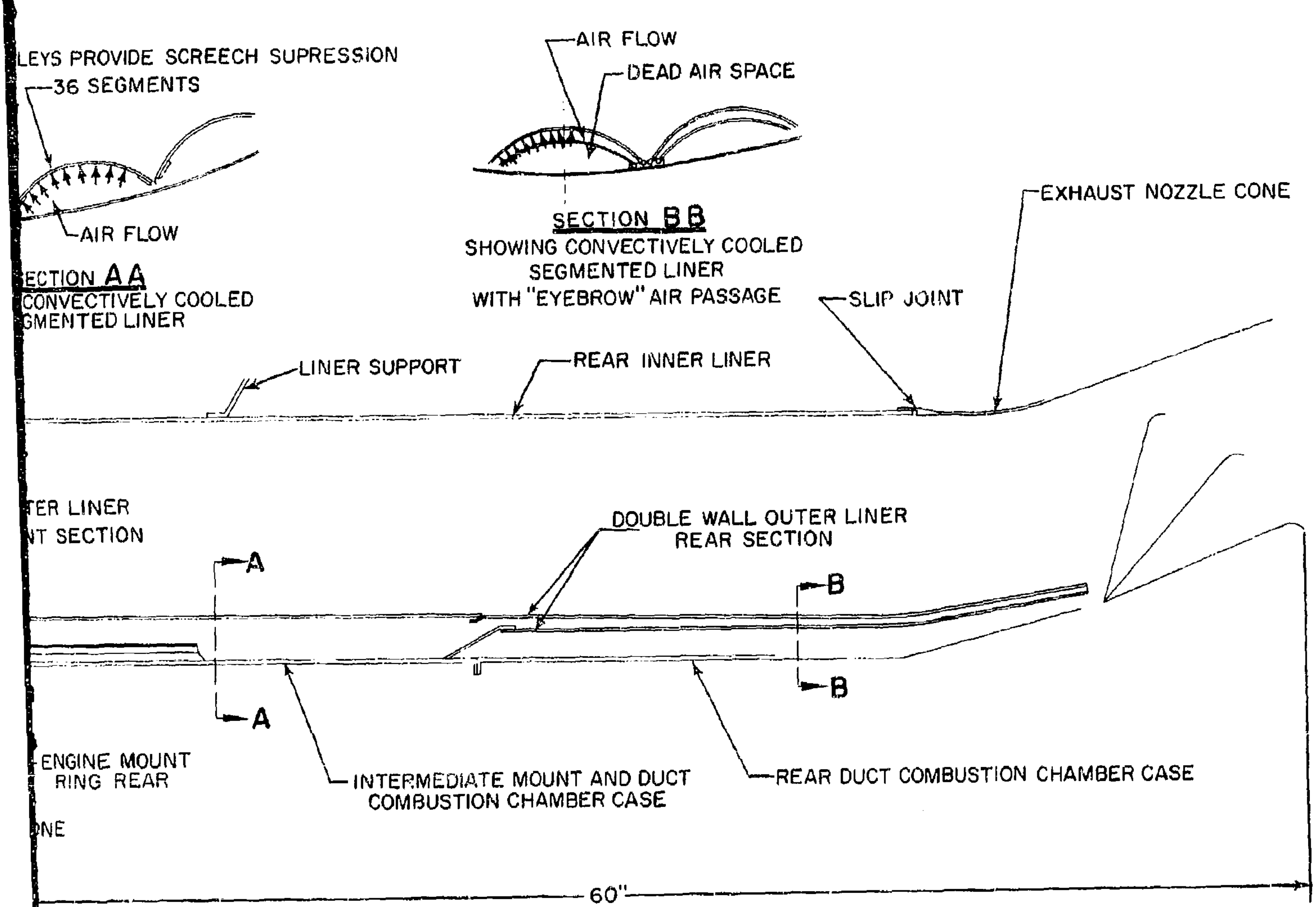

DUCT HEATER SCHEMATIC

Figure 2A-193

3

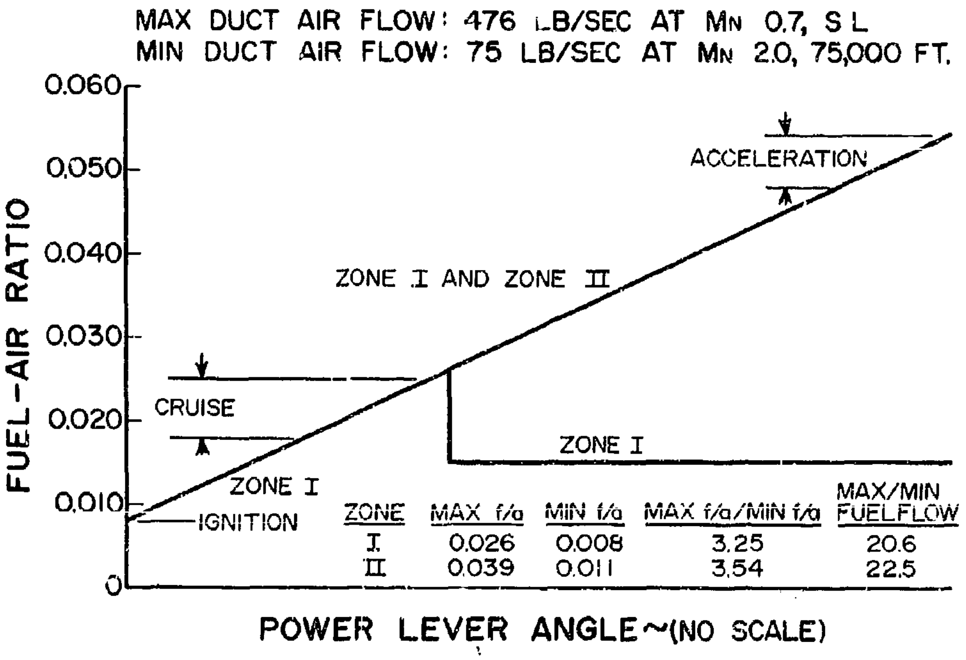

FUEL-AIR RATIO vs. POWER LEVER ANGLE

Figure 2A-194

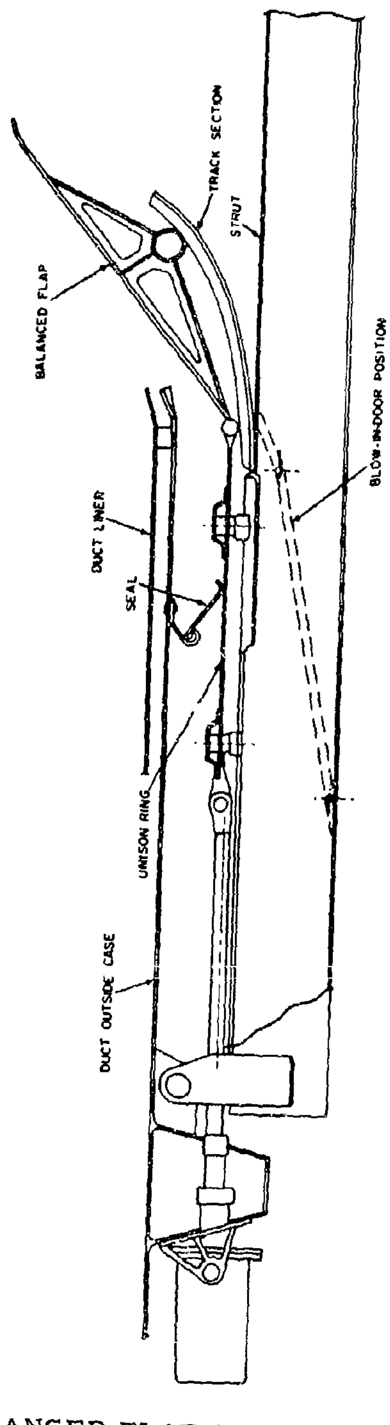

BALANCED FLAP SYSTEM SCHEMATIC

Figure 2A-195

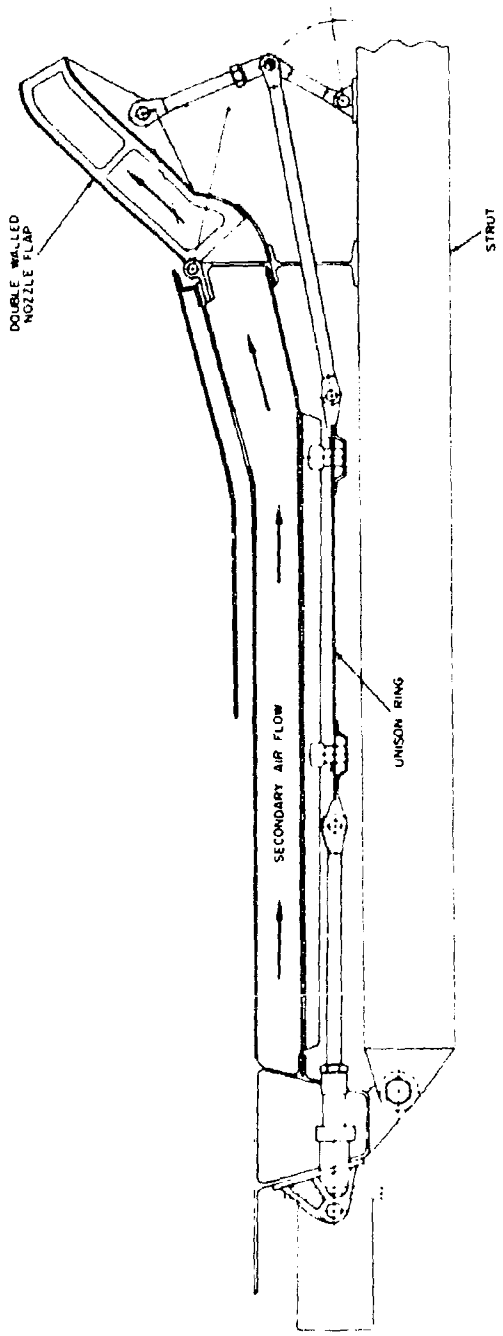

SECONDARY AIR TO PRIMARY NOZZLE SCHEMATIC

Figure 2A-196

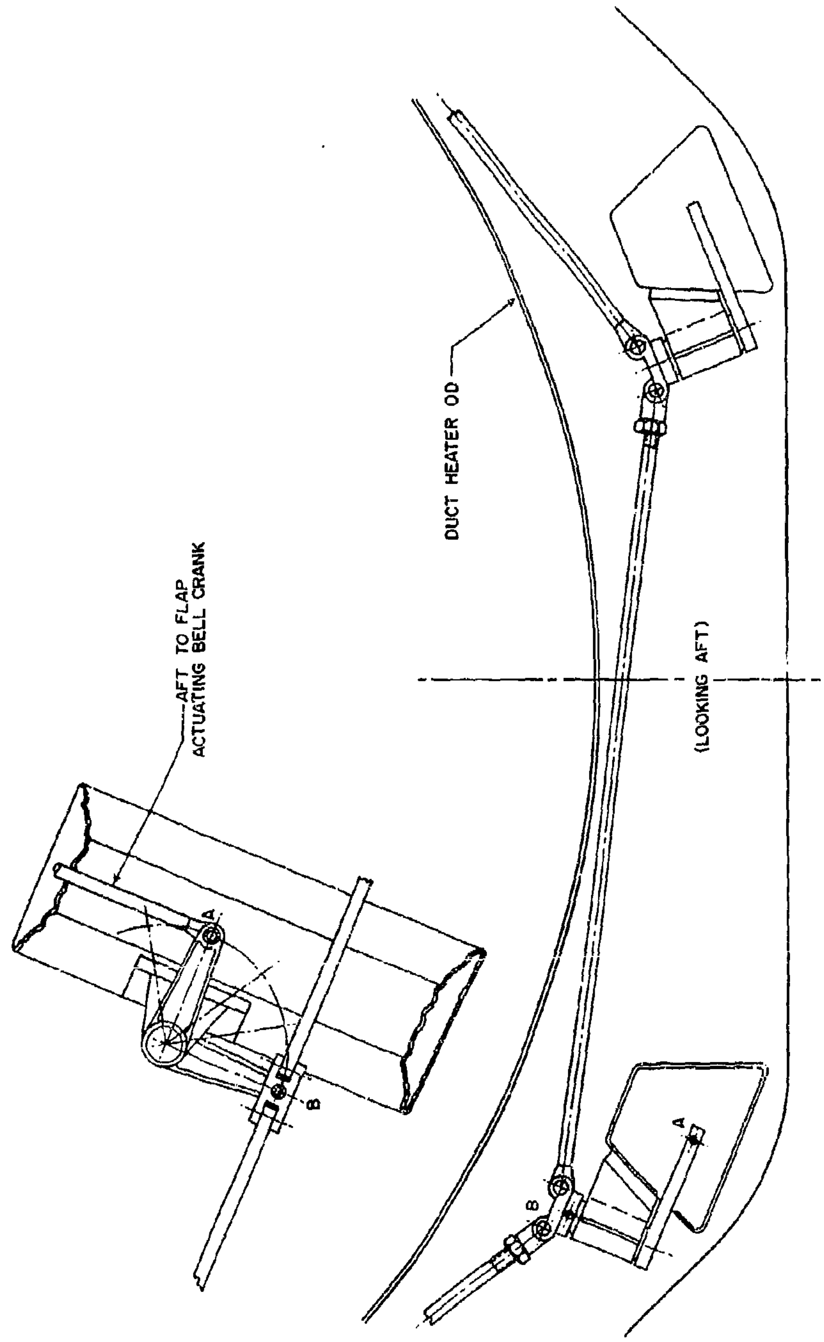

BELLCRANK FLAP SYNCHRONIZATION SCHEMATIC

Figure 2A-197

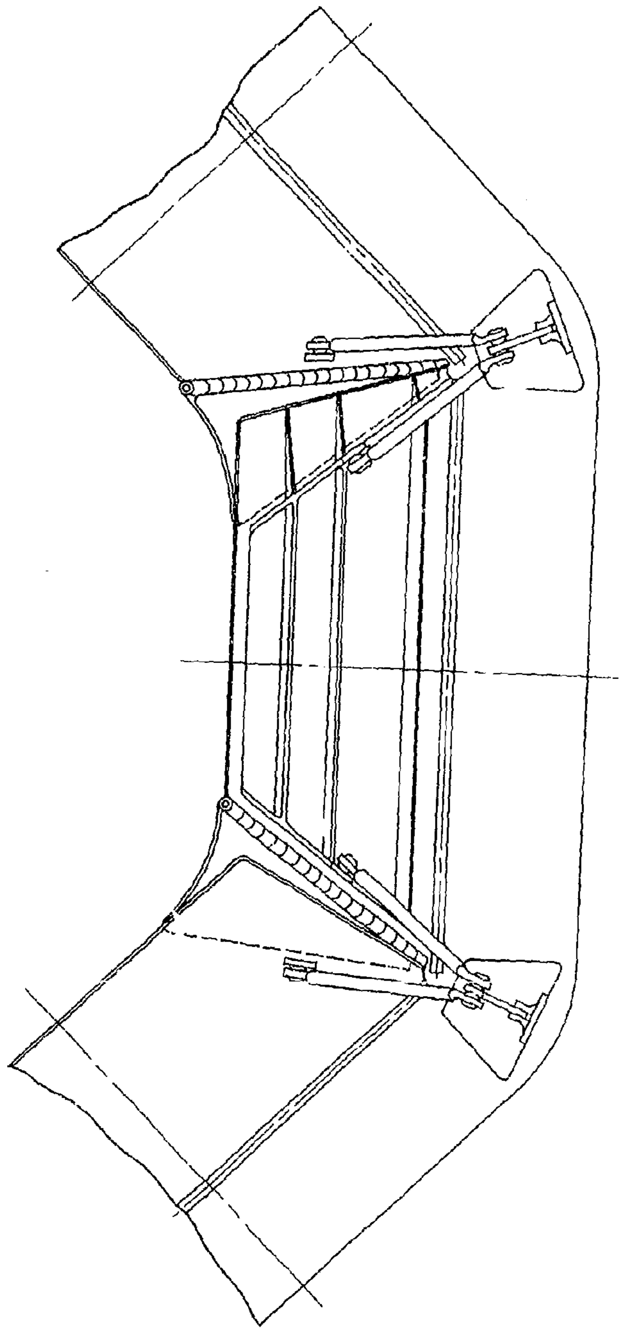

HINGED FLAP SEAL ARRANGEMENT LOOKING FORWARD

Figure 2A-198

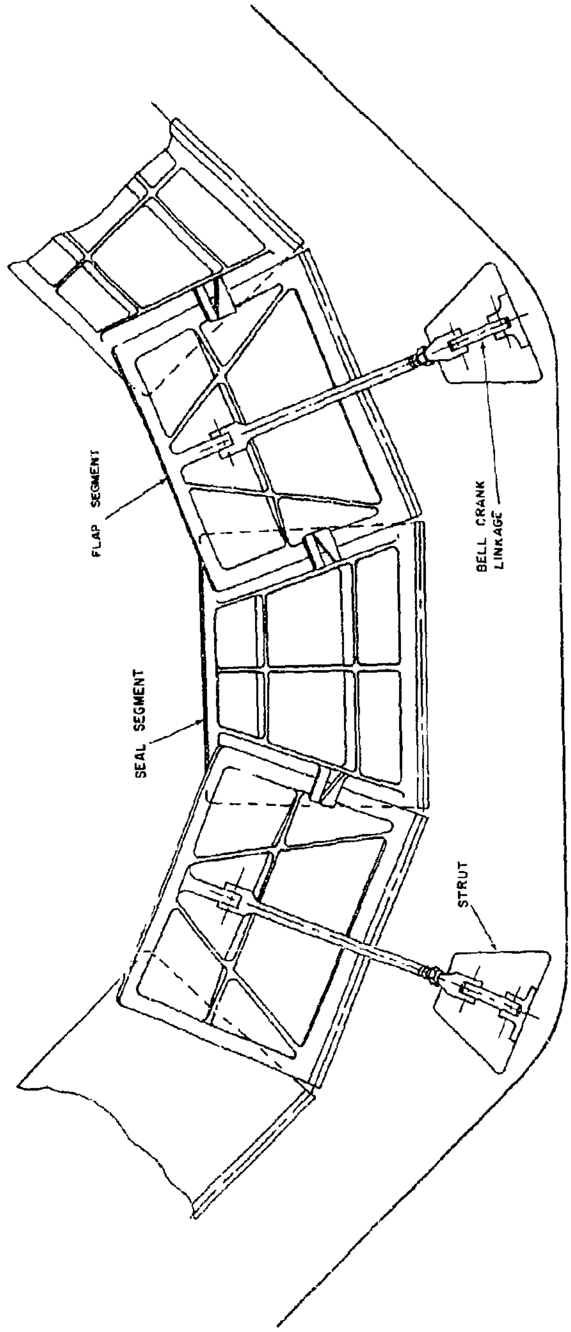

SIXTEEN SIDED NOZZLE FLAP ARRANGEMENT LOOKING FORWARD

Figure 2A-199

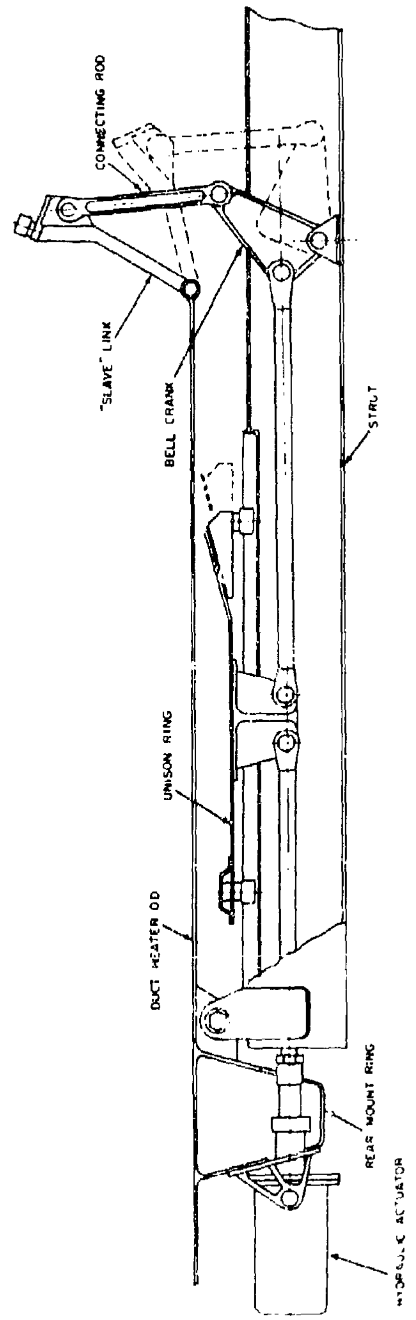

DUCT HEATER NOZZLE LINKAGE LONGITUDINAL SECTION

Figure 2A-200

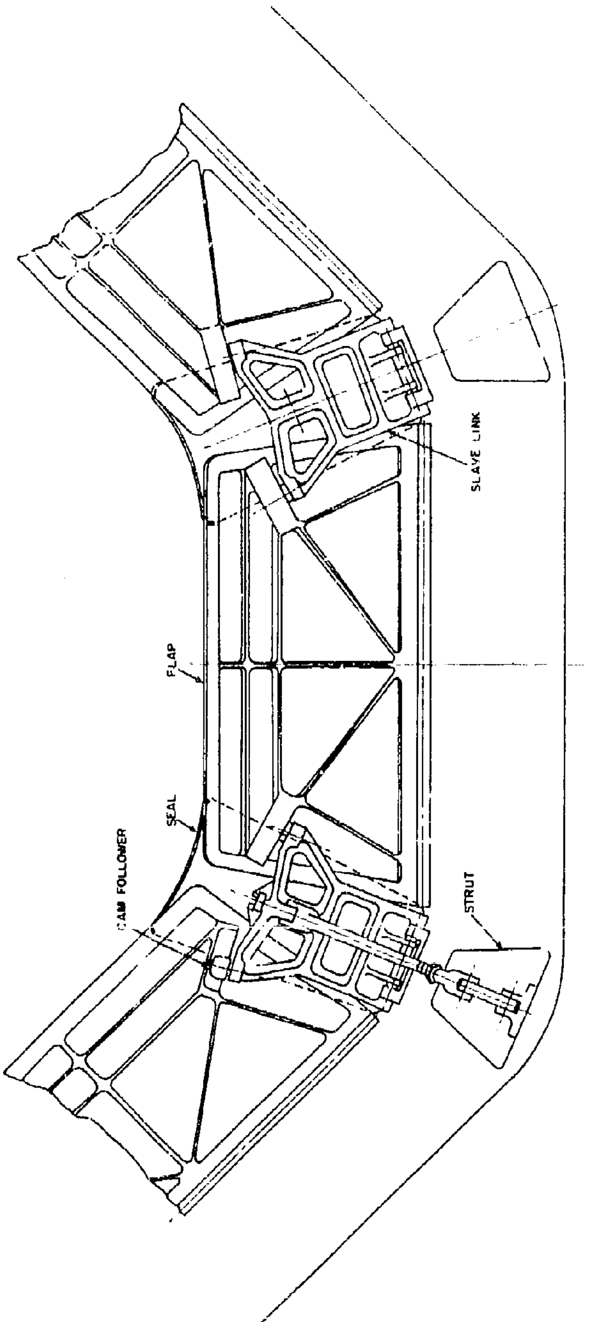

DUCT HEATER NOZZLE ASSEMBLY LOOKING FORWARD

Figure 2A-201

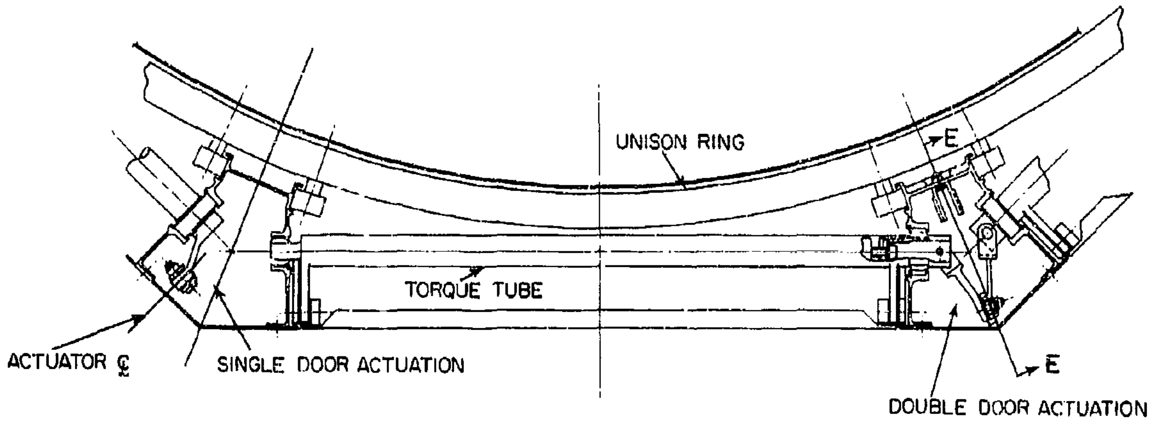

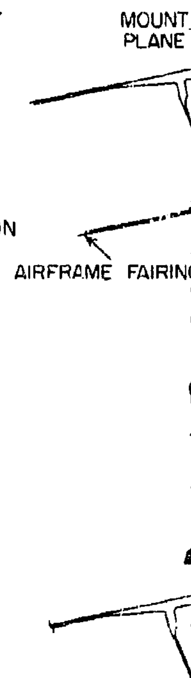

SECTION D-D
ROTATED 22 1/2°
BLOW-IN-DOOR ACTUATION

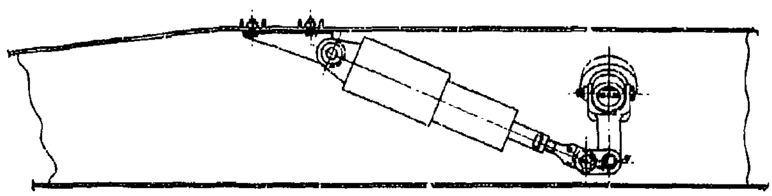

SECTION E-E
ROTATED 22 1/2°

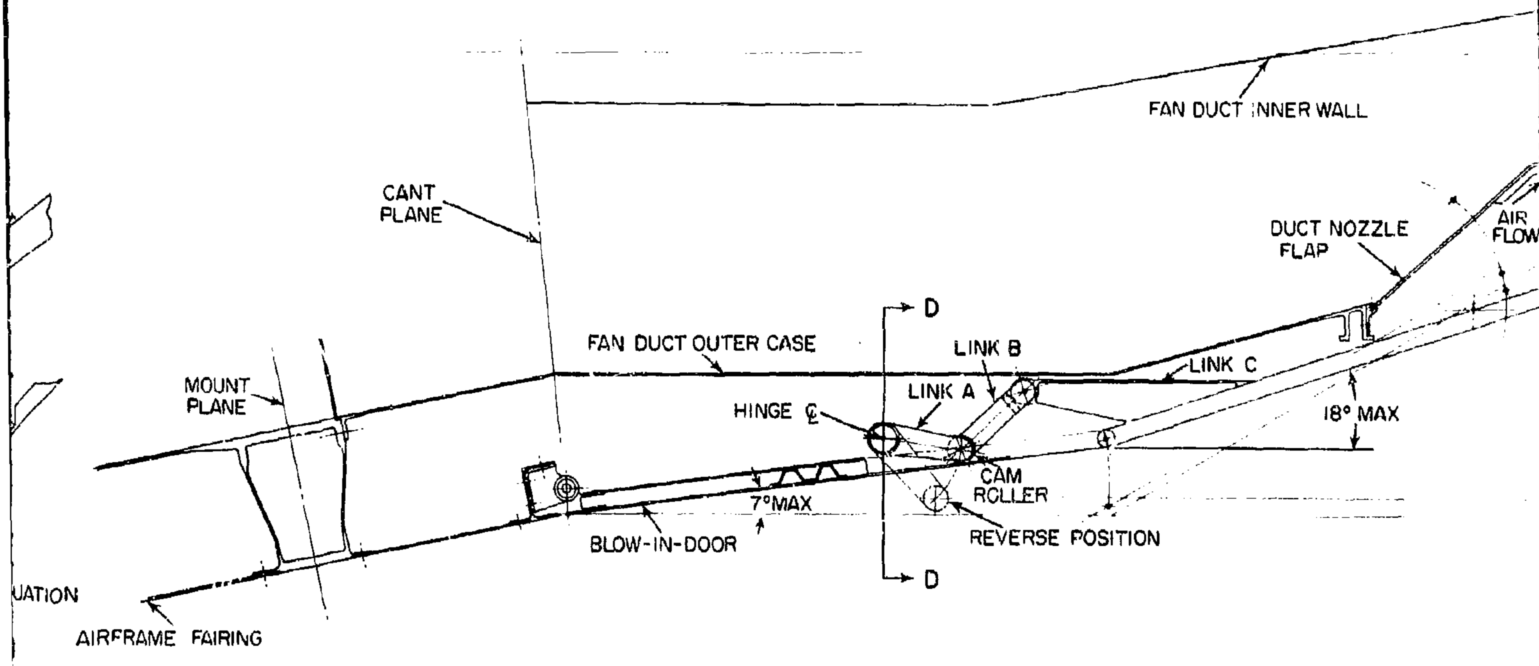

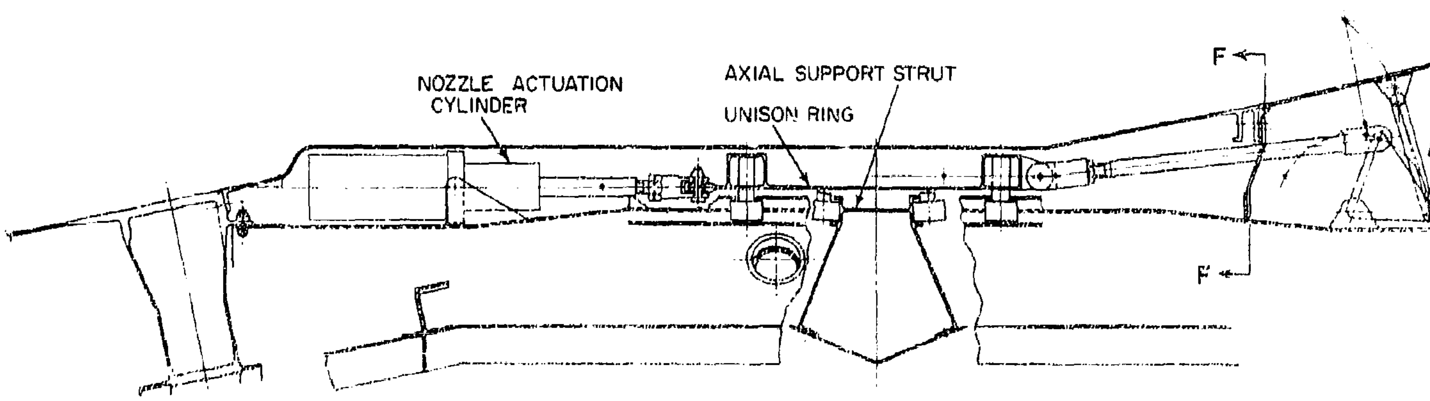

SECTION B-B
(PARTIAL SECT)

2

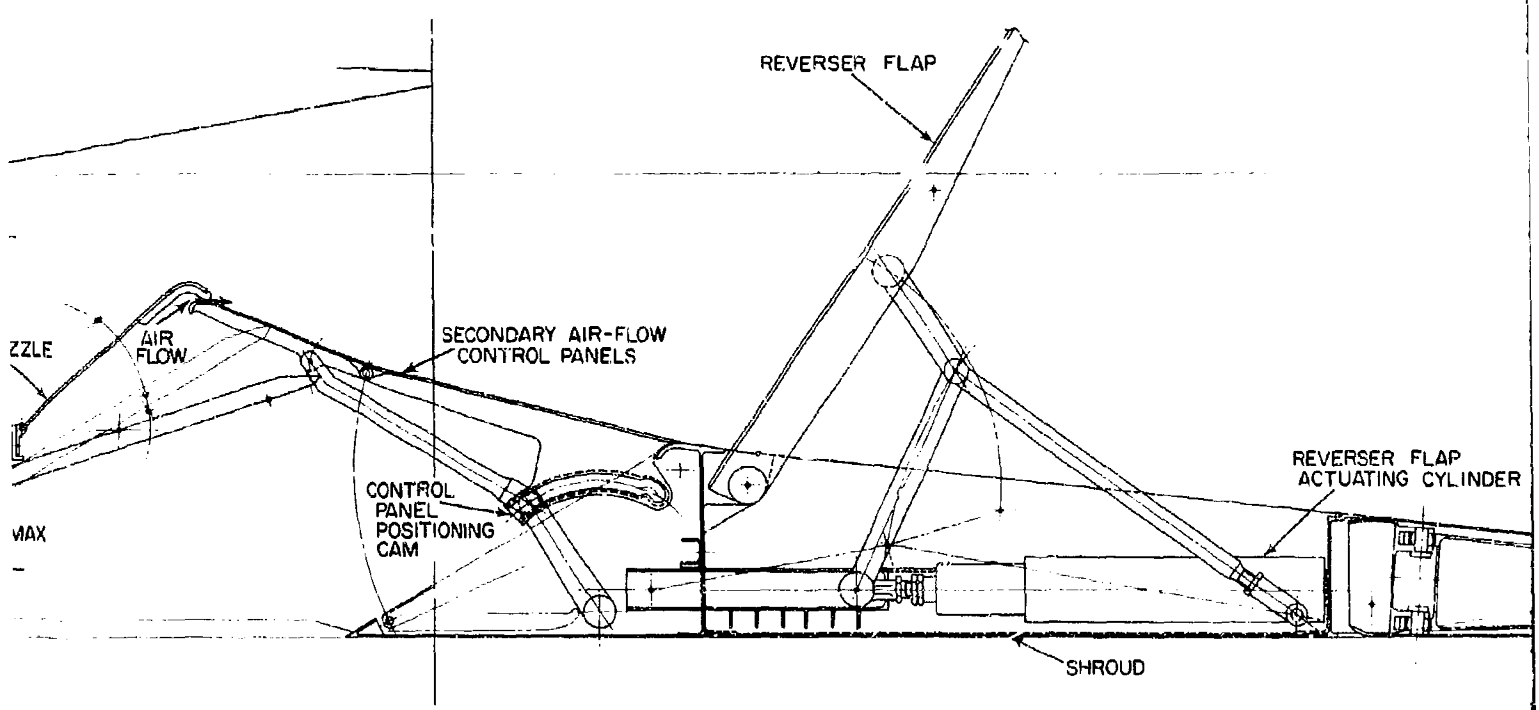

SECTION A-A
(PARTIAL SECT)

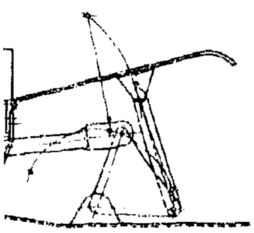

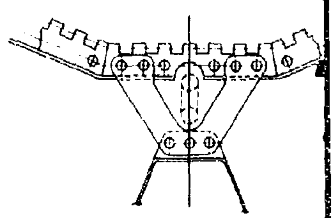

VIEW F-F

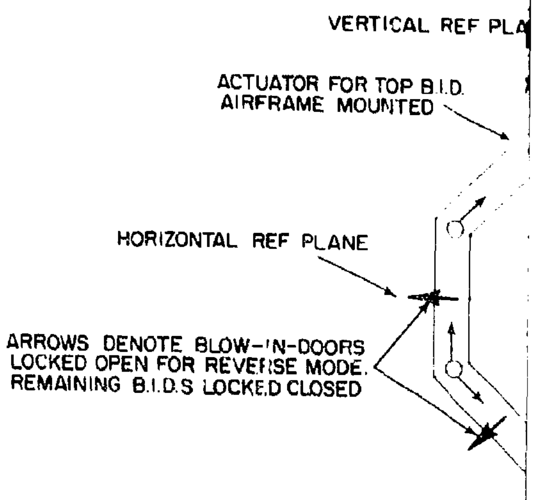

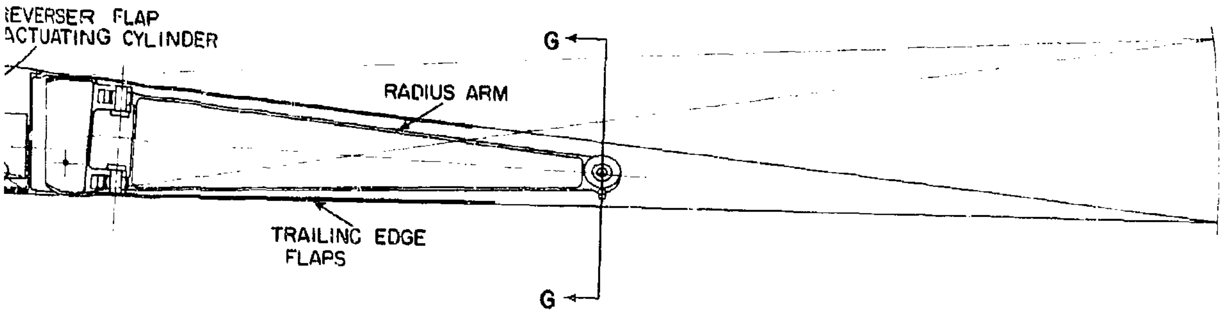

RE

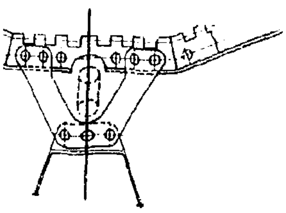

VIEW F-F

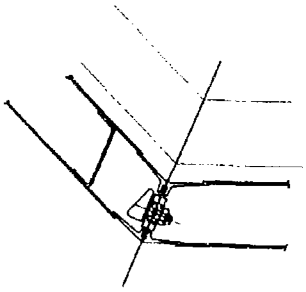

SECTION G-G

OCTAGONAL EJEC

Figure 2

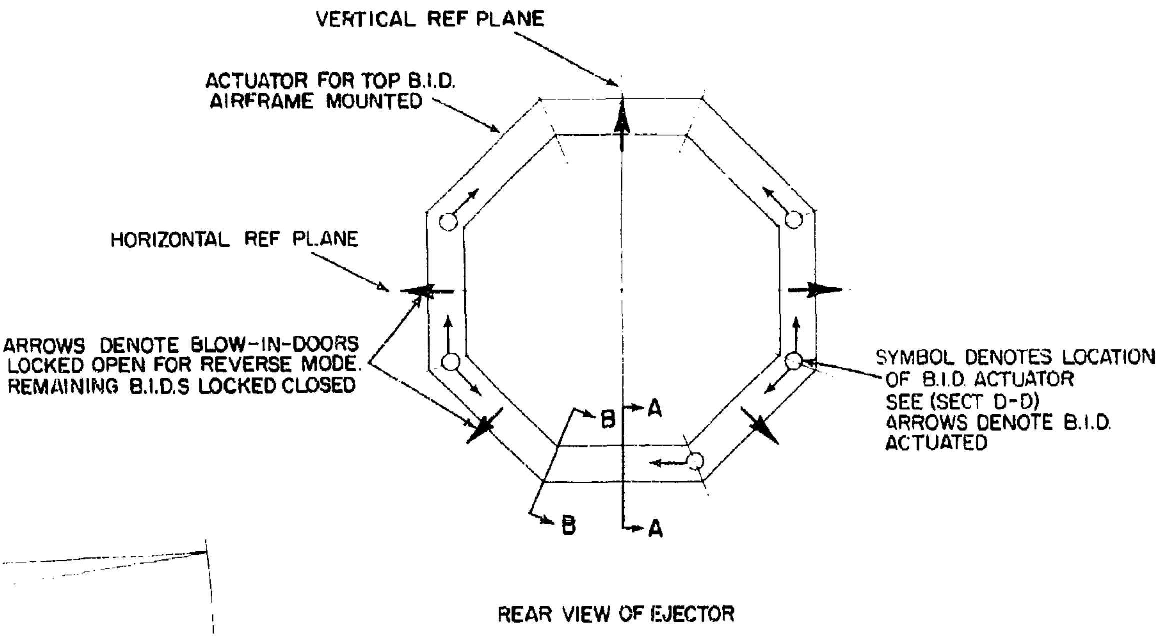

OCTAGONAL EJECTOR FOR BOEING

Figure 2A-202

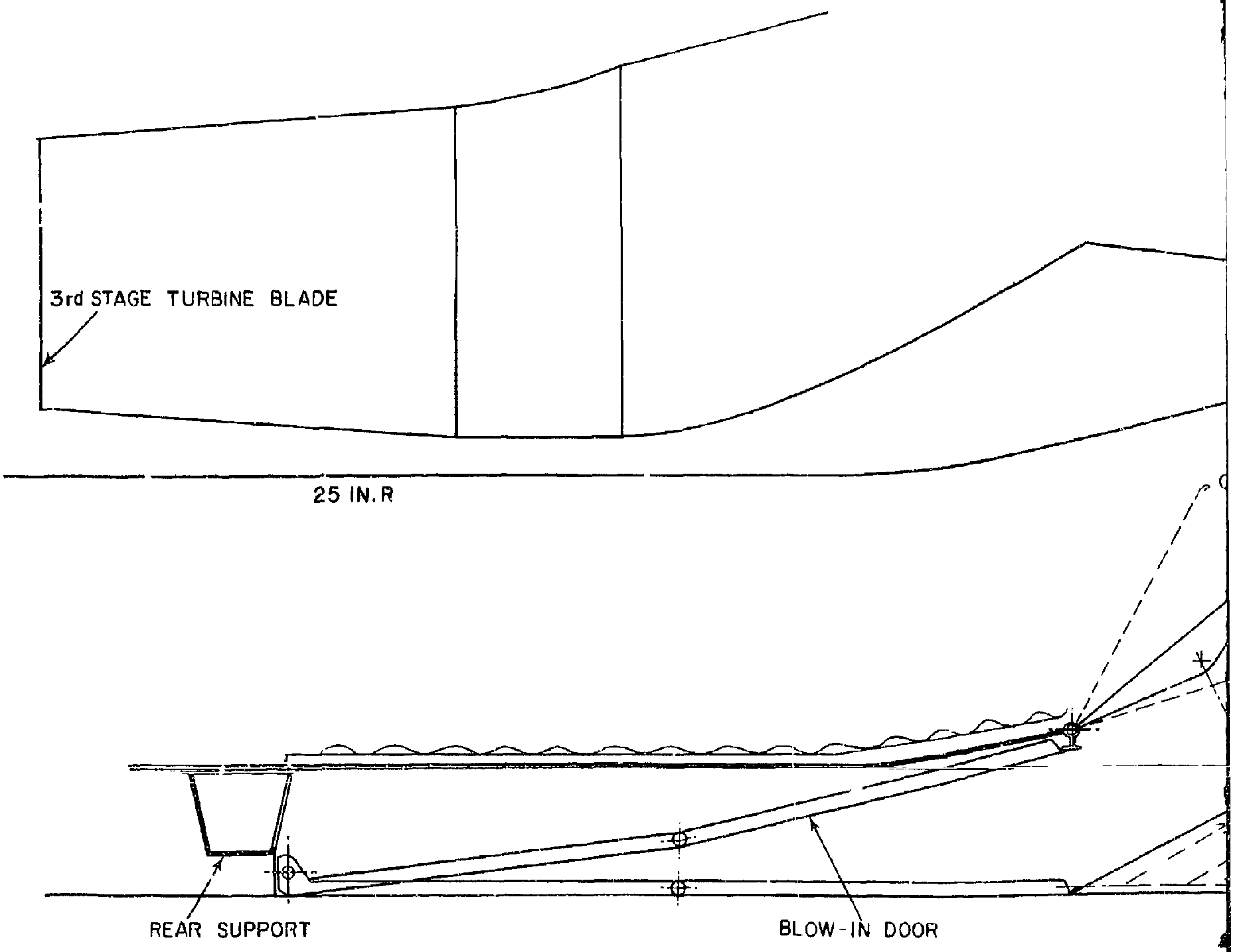

1

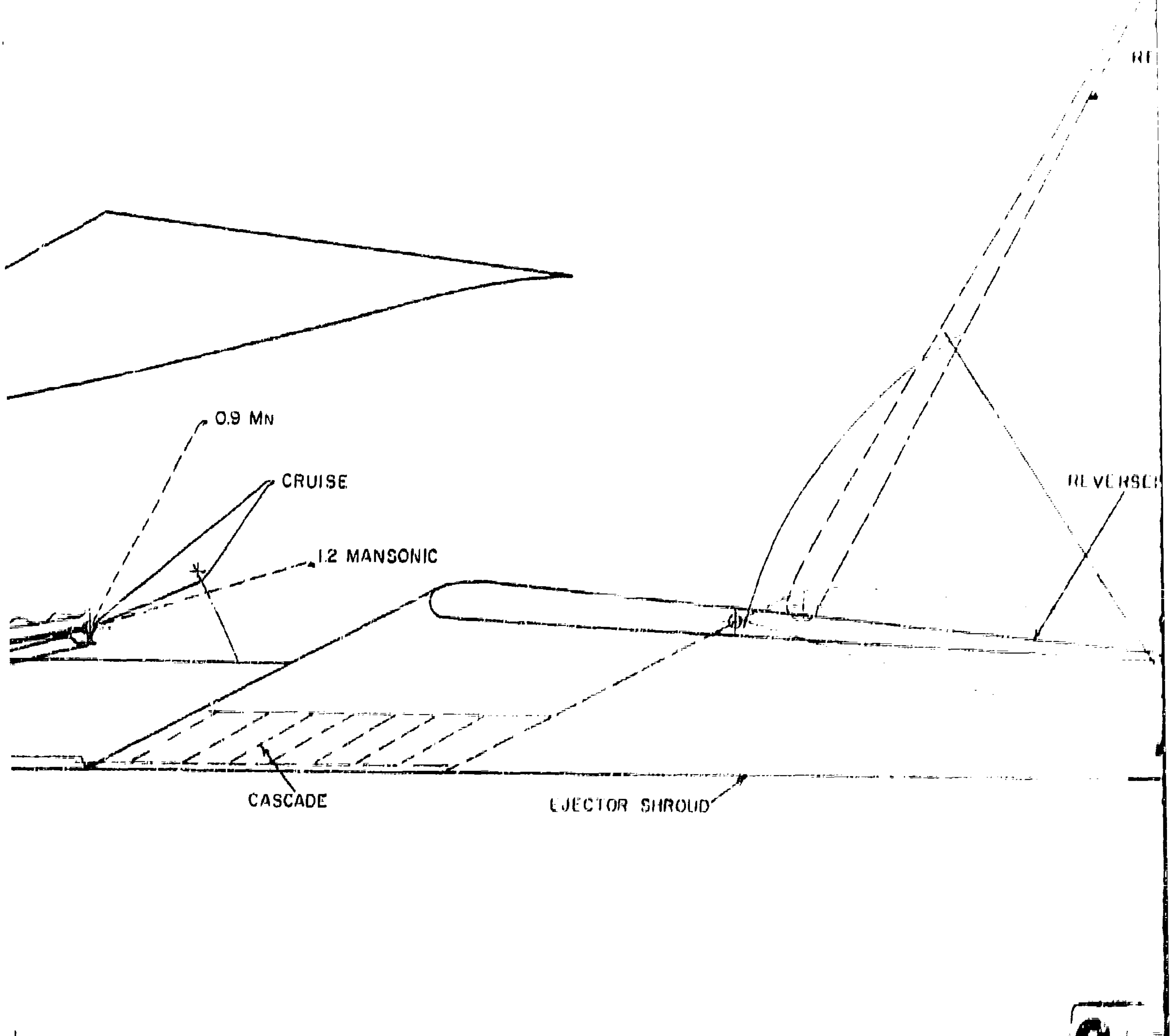

2

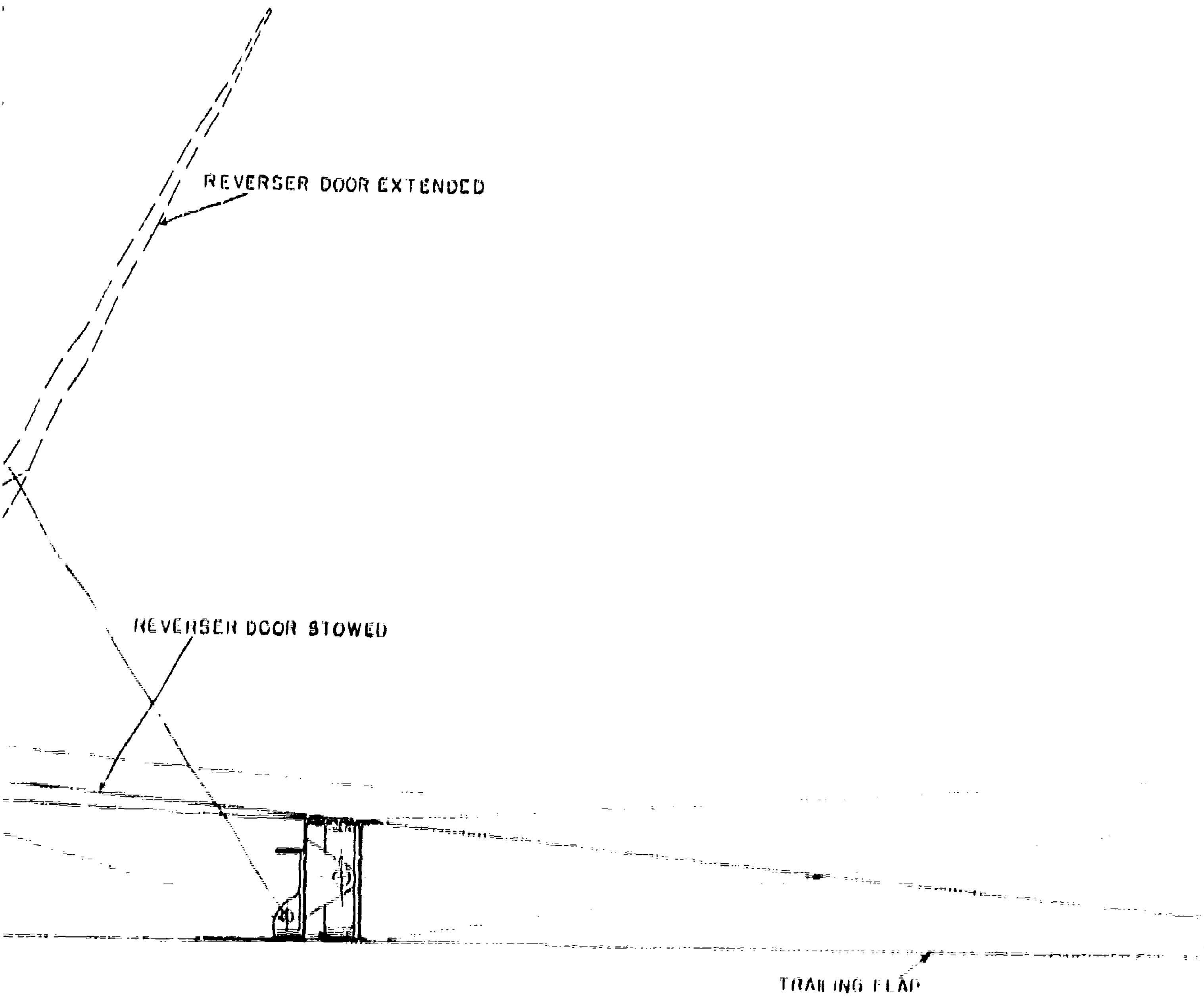

OCTAGONAL EJECTOR-TRANSLATING

Figure 2A-203

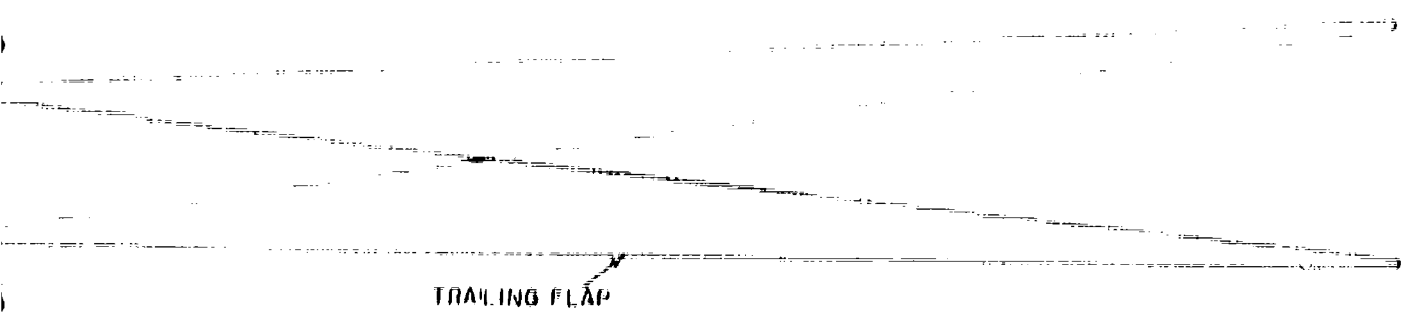

OCTAGONAL EJECTOR-TRANSLATING SHROUD

Figure 2A-203

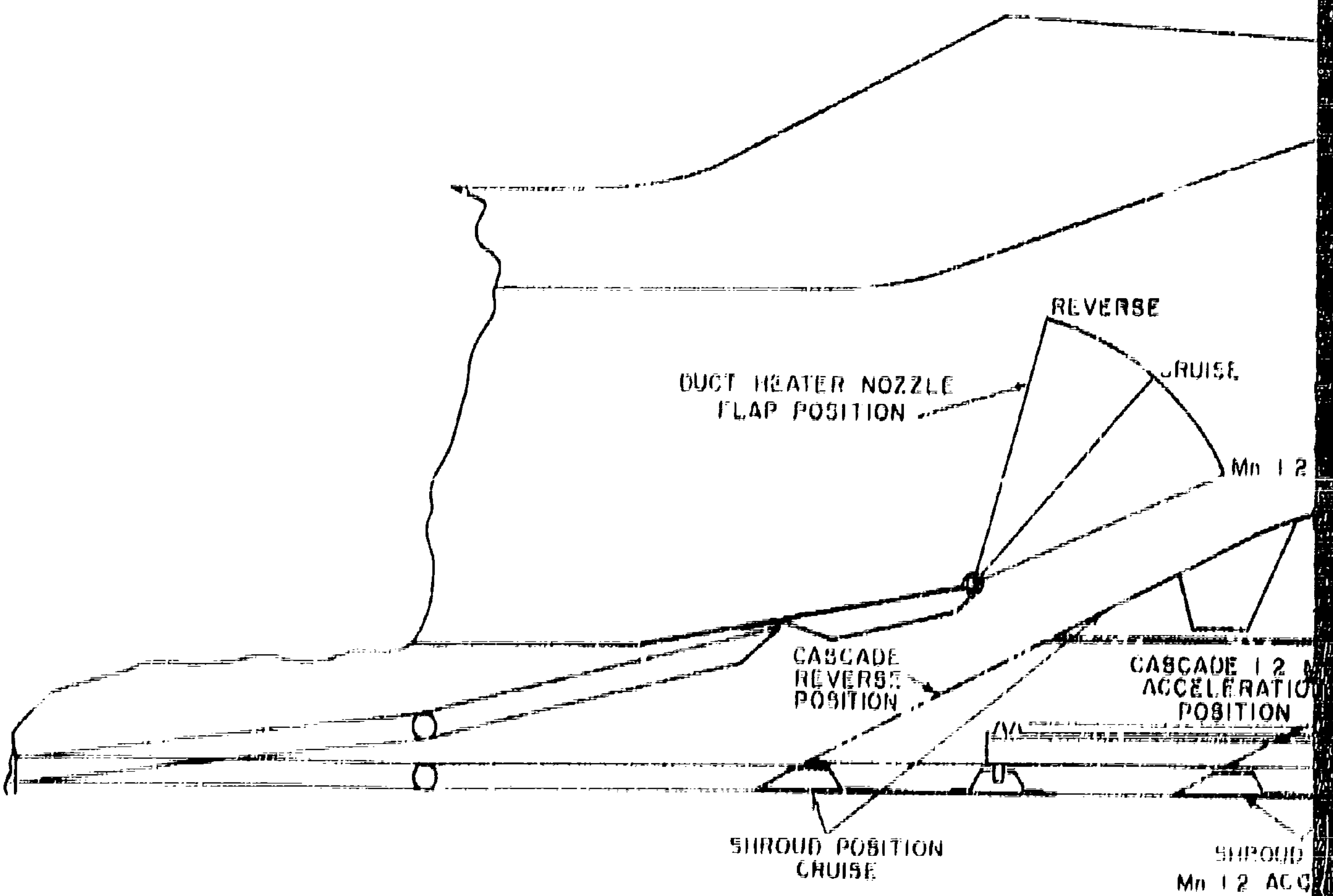
REVERSE
CRUISE
DUCT HEATER NOZZLE FLAP POSITION
Mn 1.2
CASCADE REVERSE POSITION
CASCADE 1.2 M ACCELERATIO POSITION
SHROUD POSITION CRUISE
SHROUD Mn 1.2 ACC

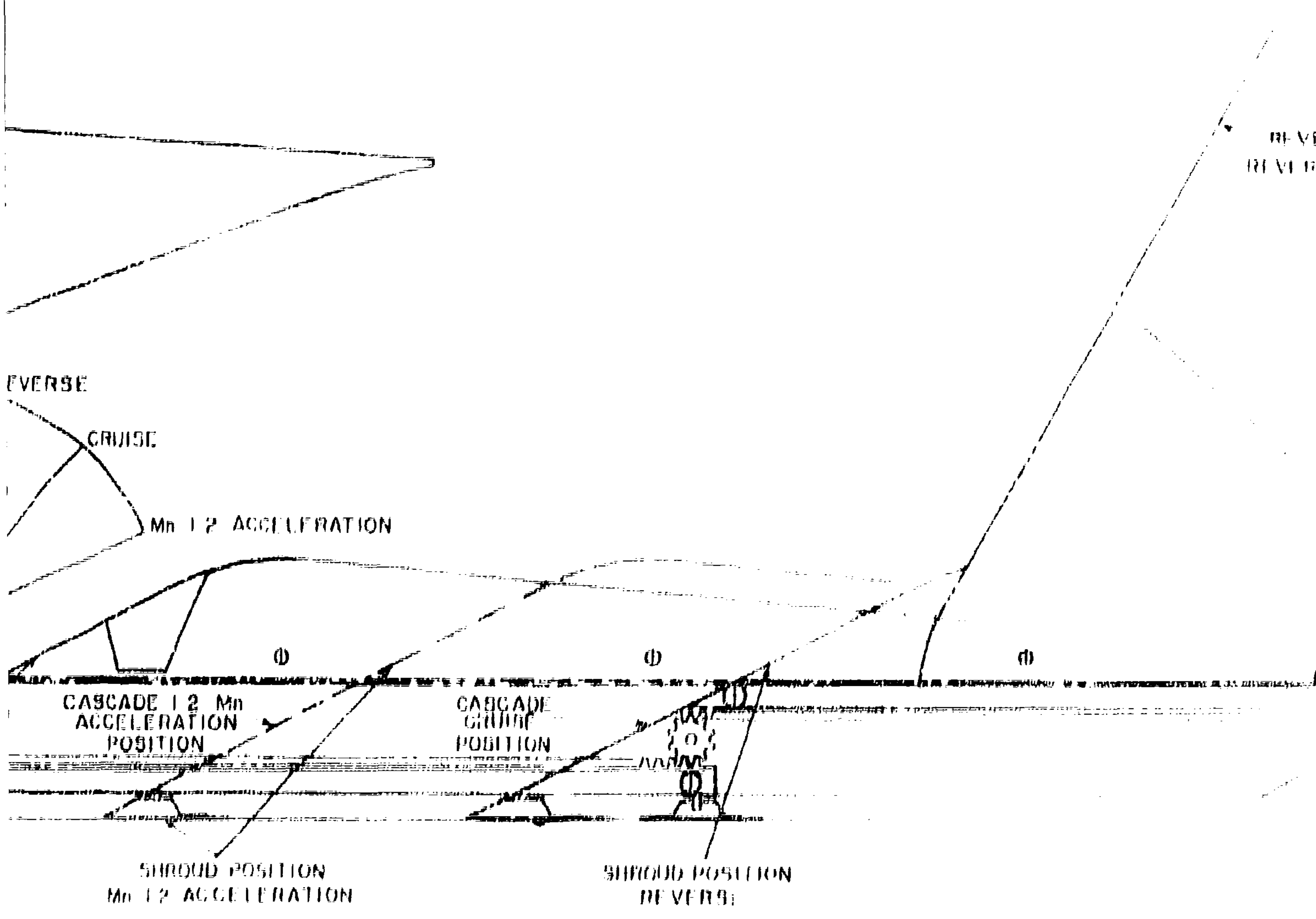

EVERSE
CRUISE
Mn 1.2 ACCELERATION
CASCADE 1.2 Mn
ACCELERATION
POSITION
CASCADE
CRUISE
POSITION
SHROUD POSITION
Mn 1.2 ACCELERATION
SHROUD POSITION
REVERSE

2

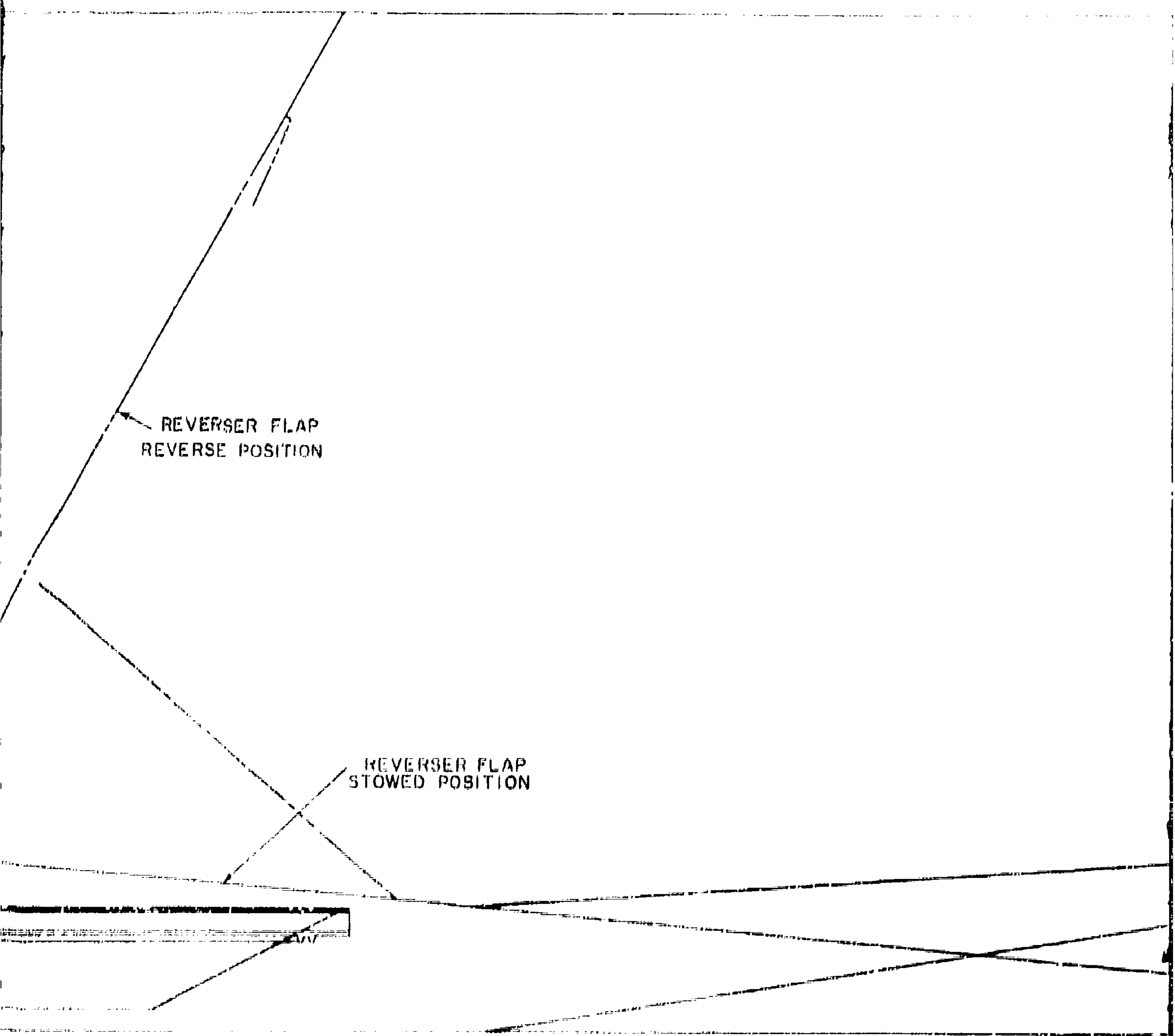
REVERSER FLAP
REVERSE POSITION
REVERSER FLAP
STOWED POSITION

CASCADE EJ

3

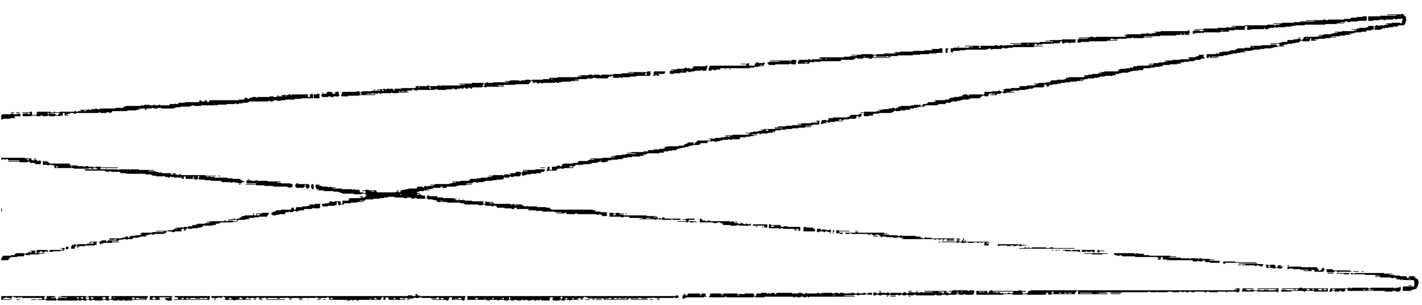

CASCADE EJECTOR-TRANSLATING SHROUD

Figure 2A-204

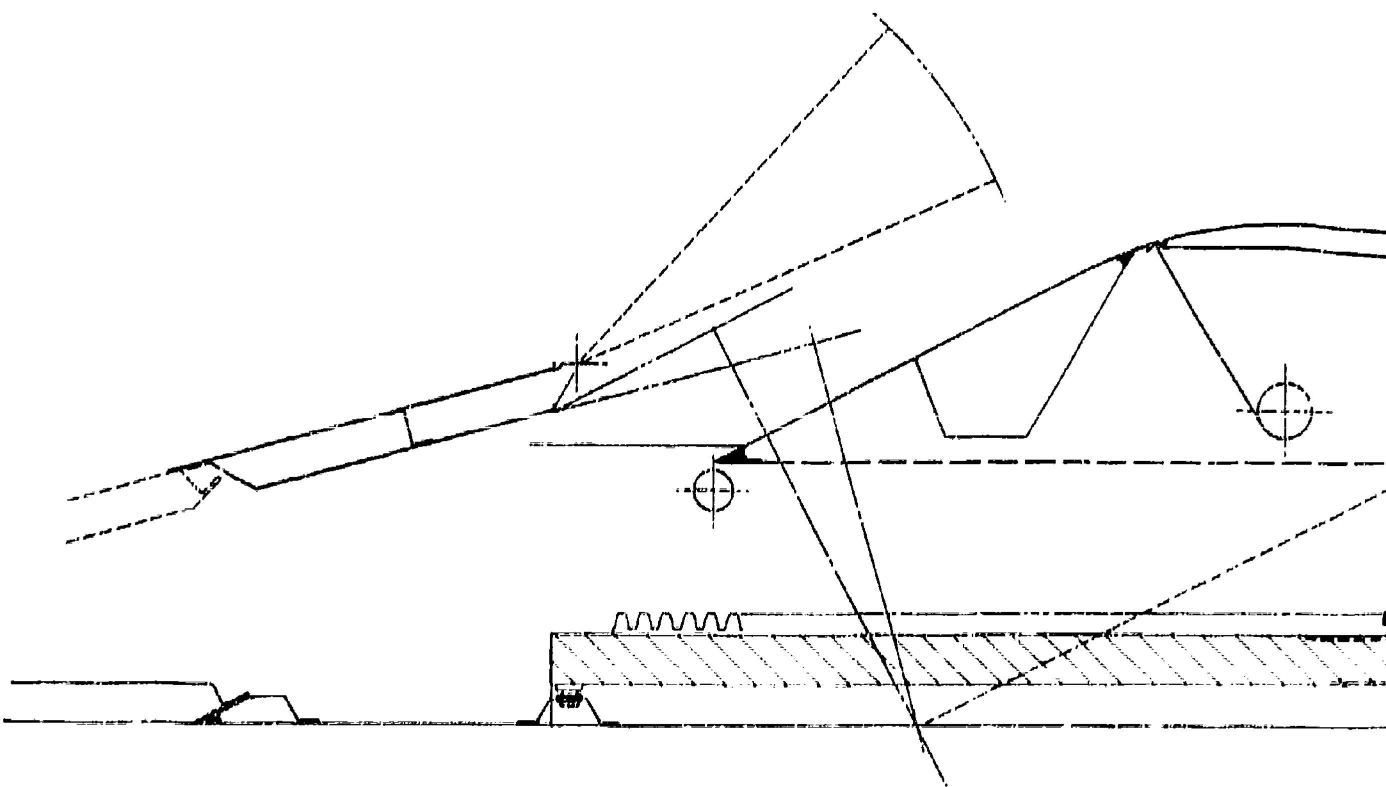

1

TRANSLATING SHROUD EJECTOR
DETAILS OF RACK AND PINION
SYSTEM FOR TRANSLATING
CASCADE ASSEMBLY

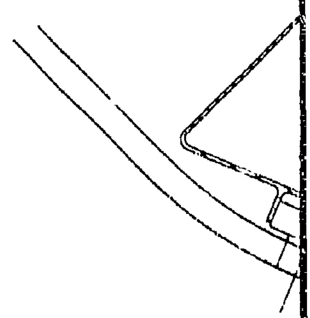

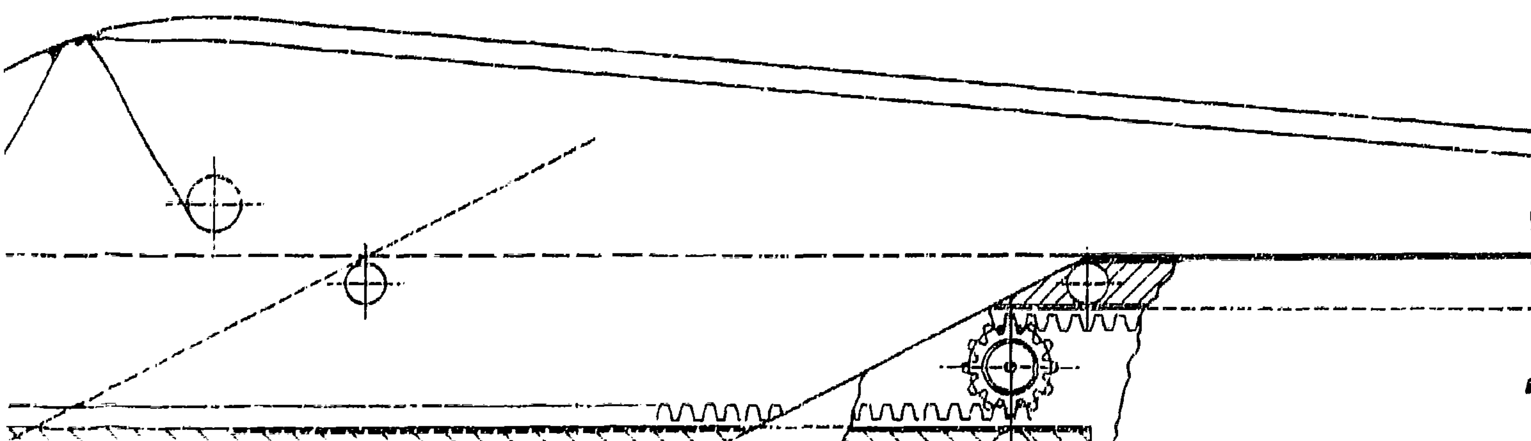

SECTION A-A

2

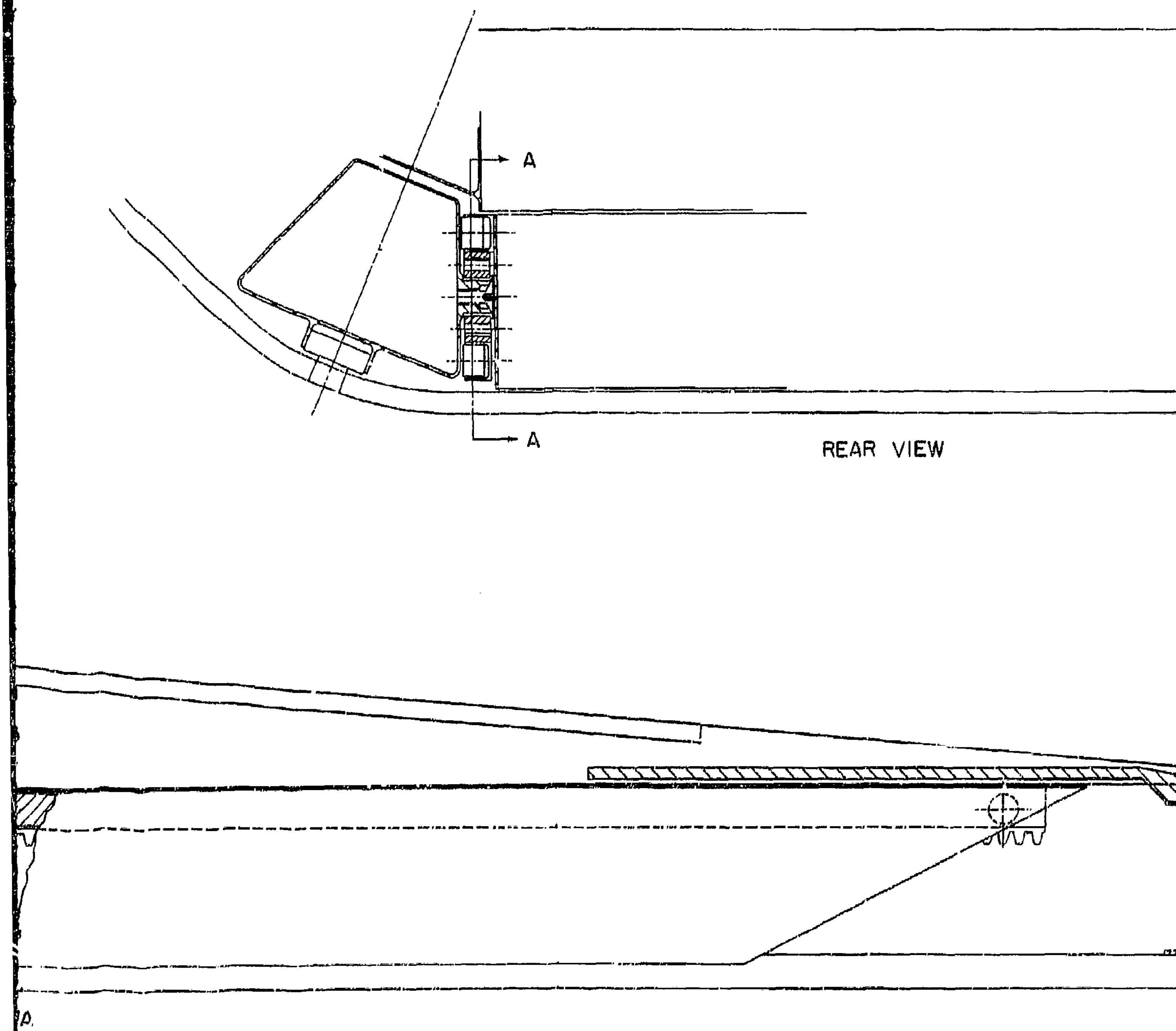

RACK AND PINION DETAILS-TRANSLATING SHR

Figure 2A-205

3

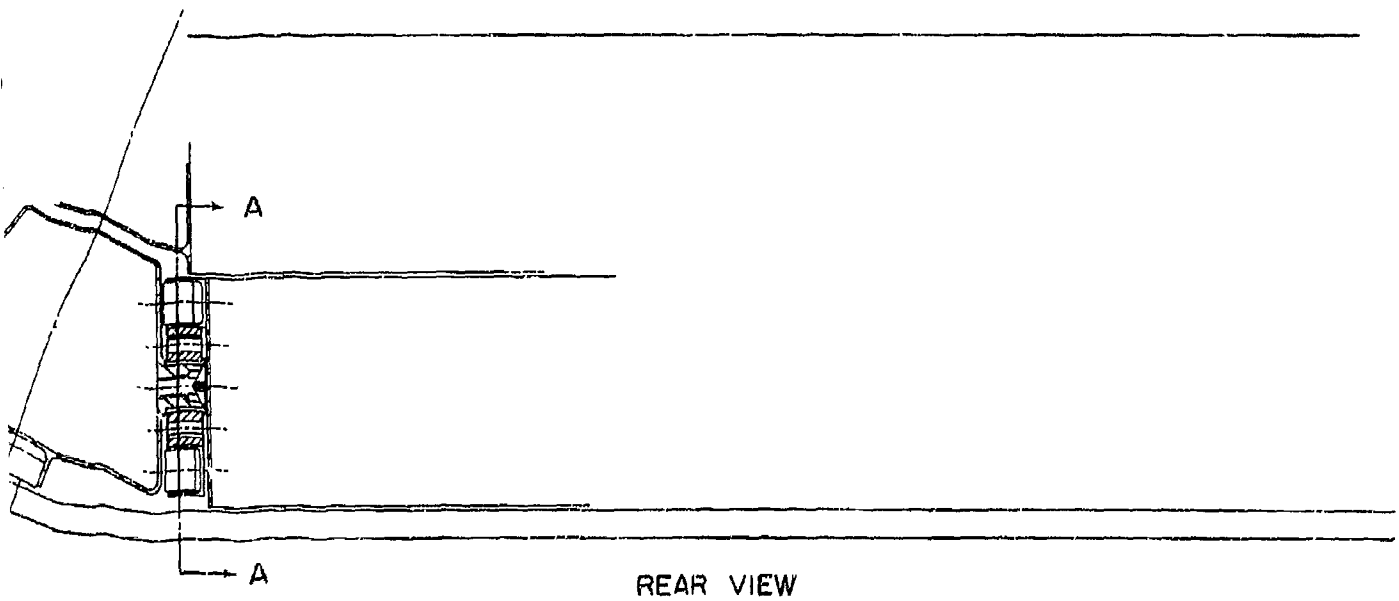

REAR VIEW

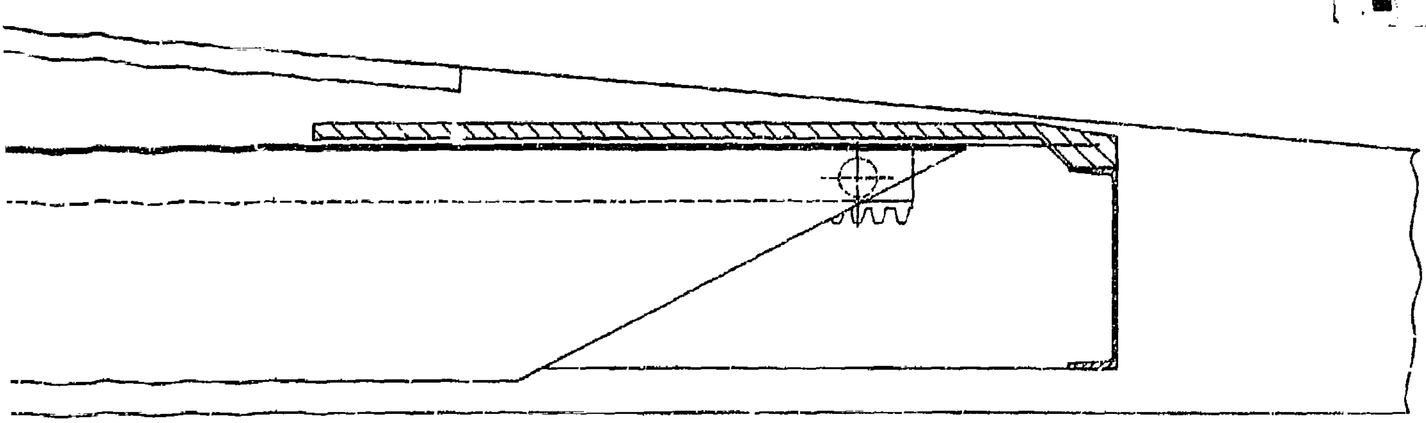

RACK AND PINION DETAILS-TRANSLATING SHROUD

Figure 2A-205

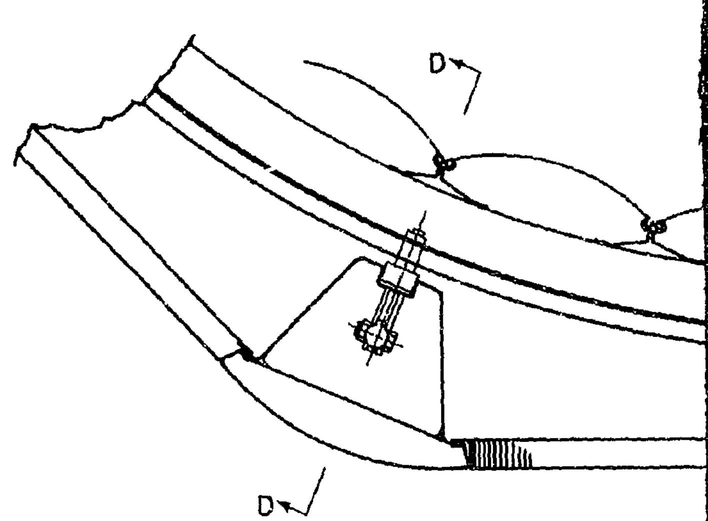

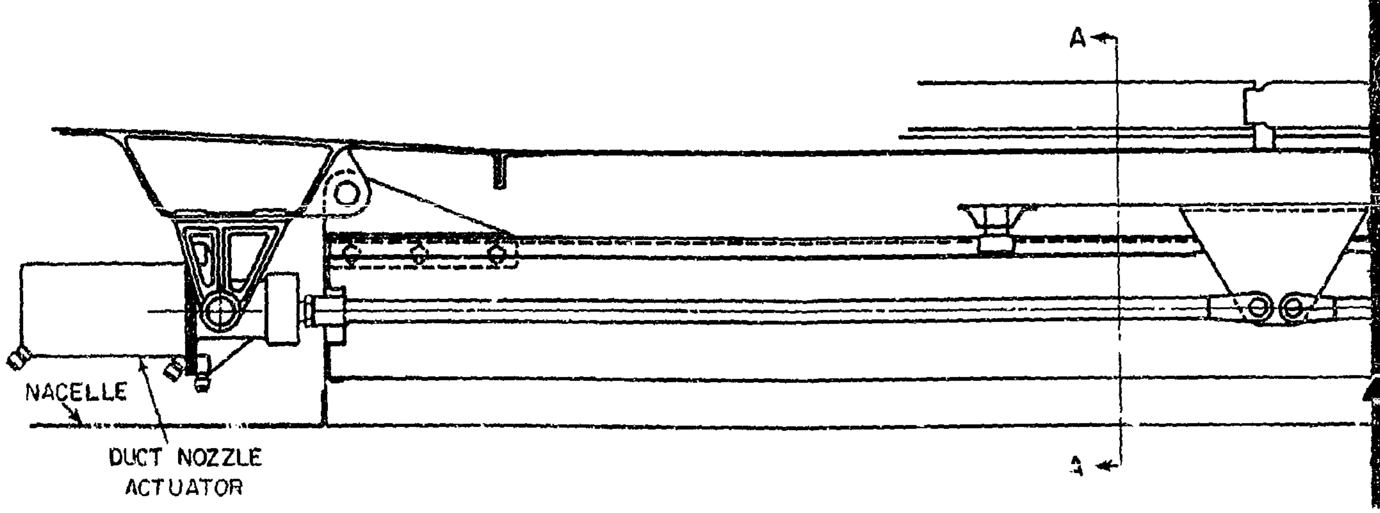

1

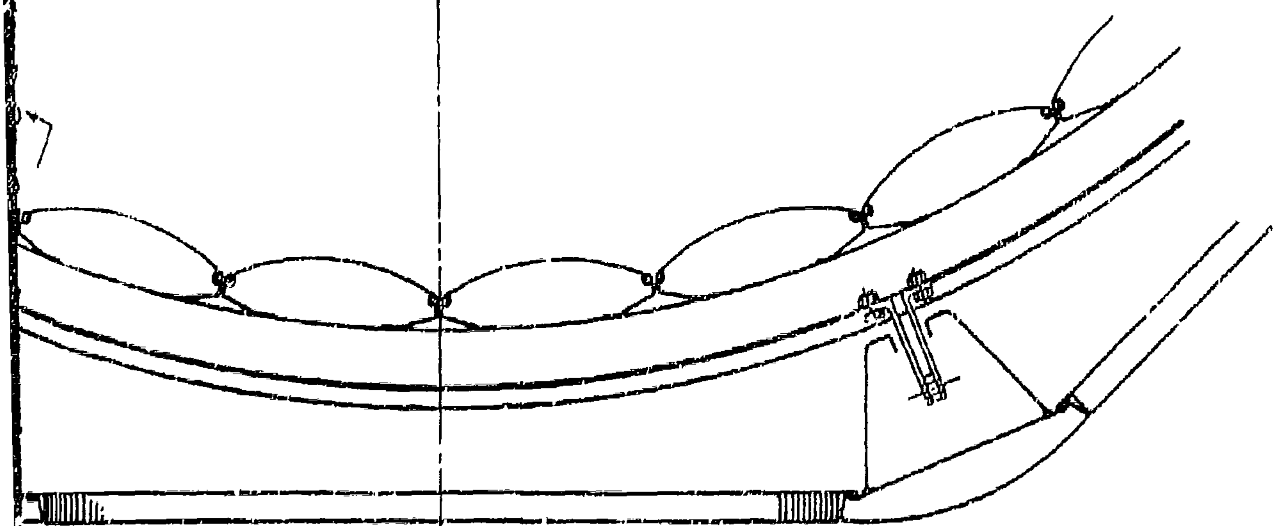

SECTION A-A
THROUGH DUCT HEATER

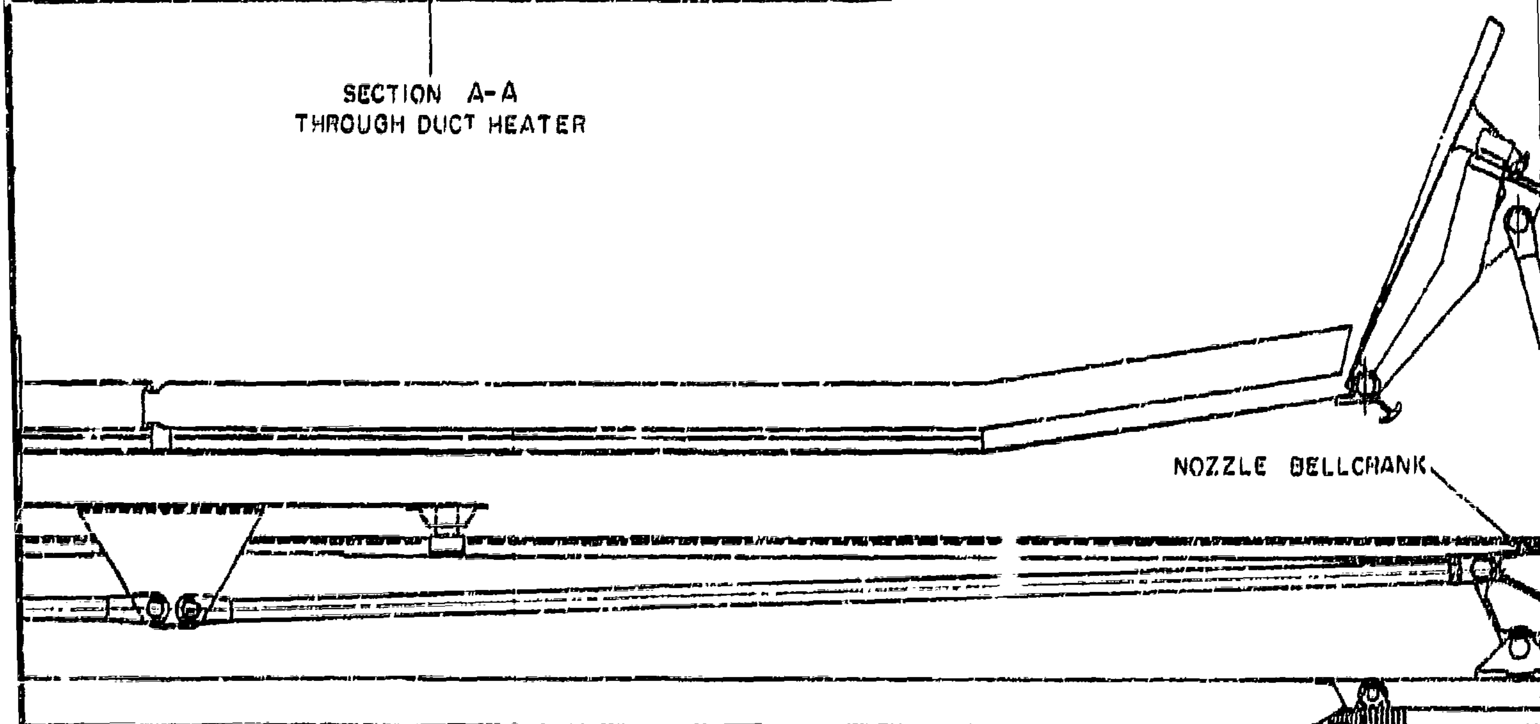

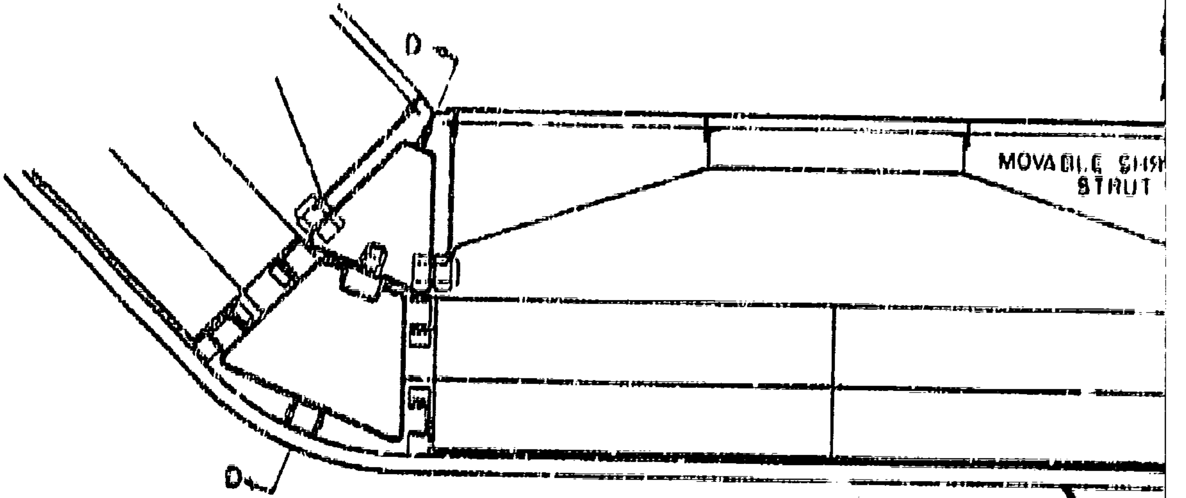

SECTION B-B
THROUGH EJECTOR

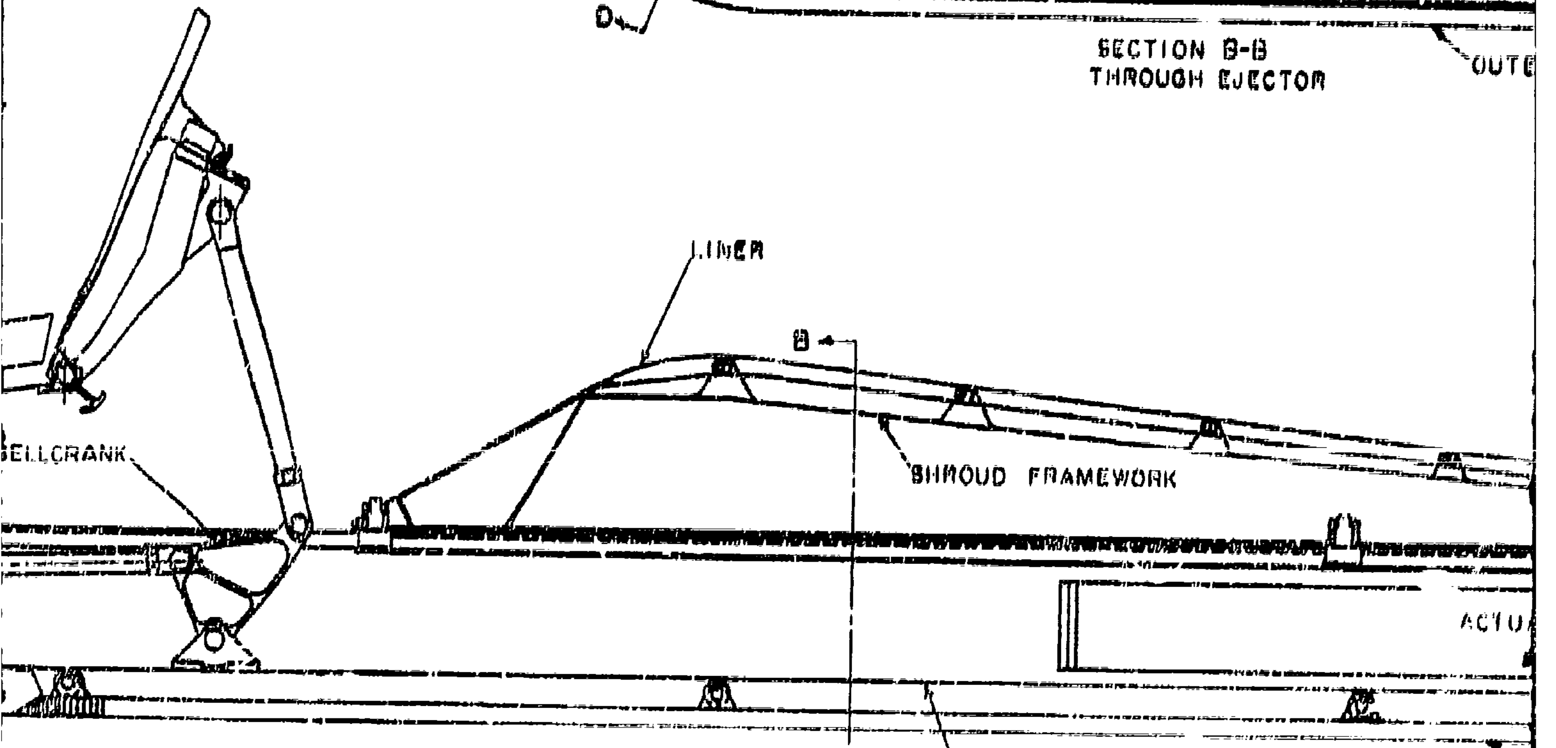

SECTION D-D
LONGITUDINAL SECTION THROUGH STINGS
(ACROSS CORNERS)

B

FIXED STRUTS
(STATIONARY FRAMEWORK)

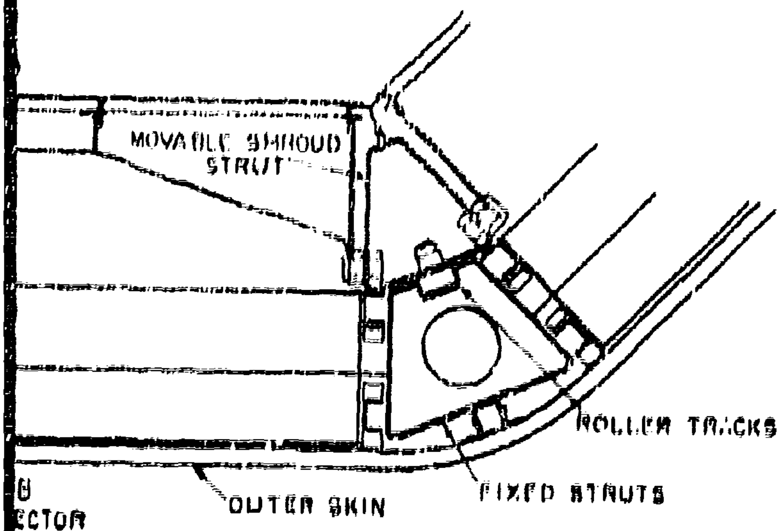
MOVABLE SHROUD STRUT
ROLLER TRACKS
OUTER SKIN
FIXED STRUTS
ECTOR

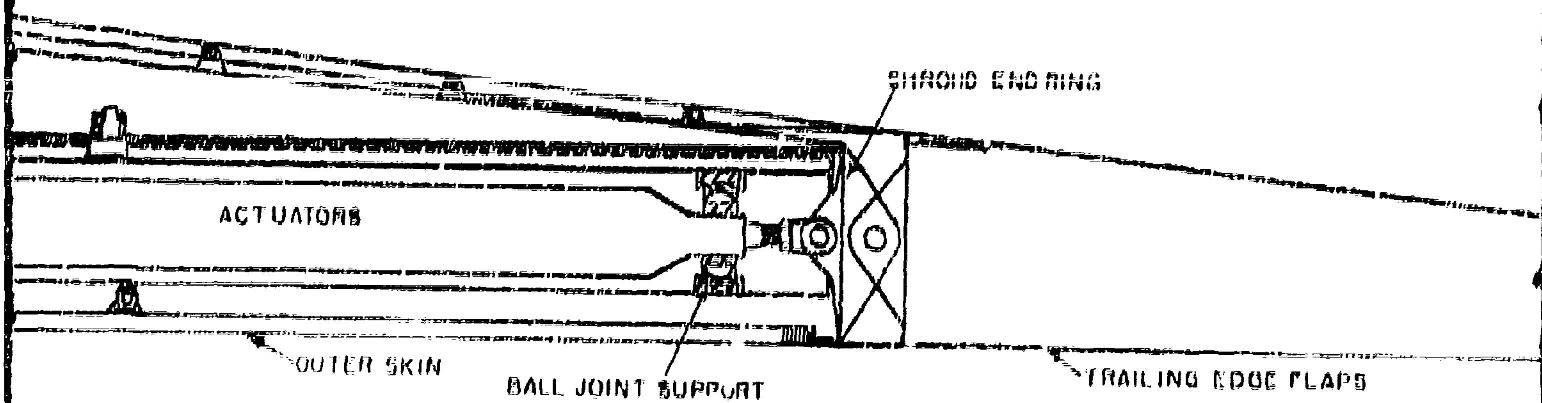
SHROUD END RING
ACTUATORS
OUTER SKIN
BALL JOINT SUPPORT
TRAILING EDGE FLAPS

4

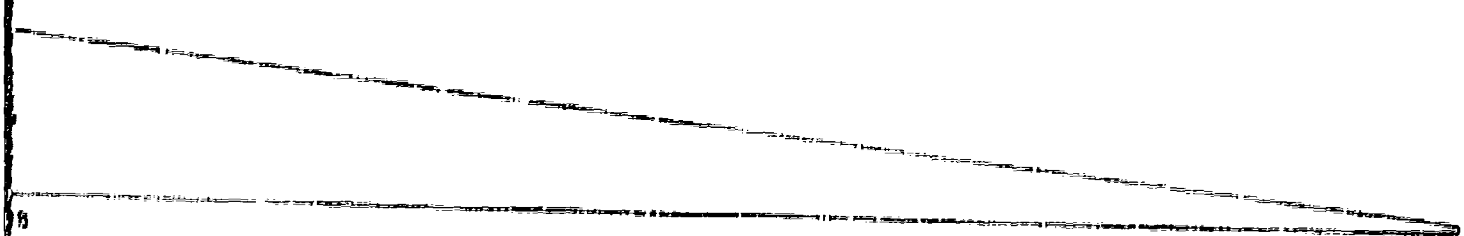

ACTUATION SYSTEM DETAILS-TRANSLATING SHROUD

Figure 2A-206

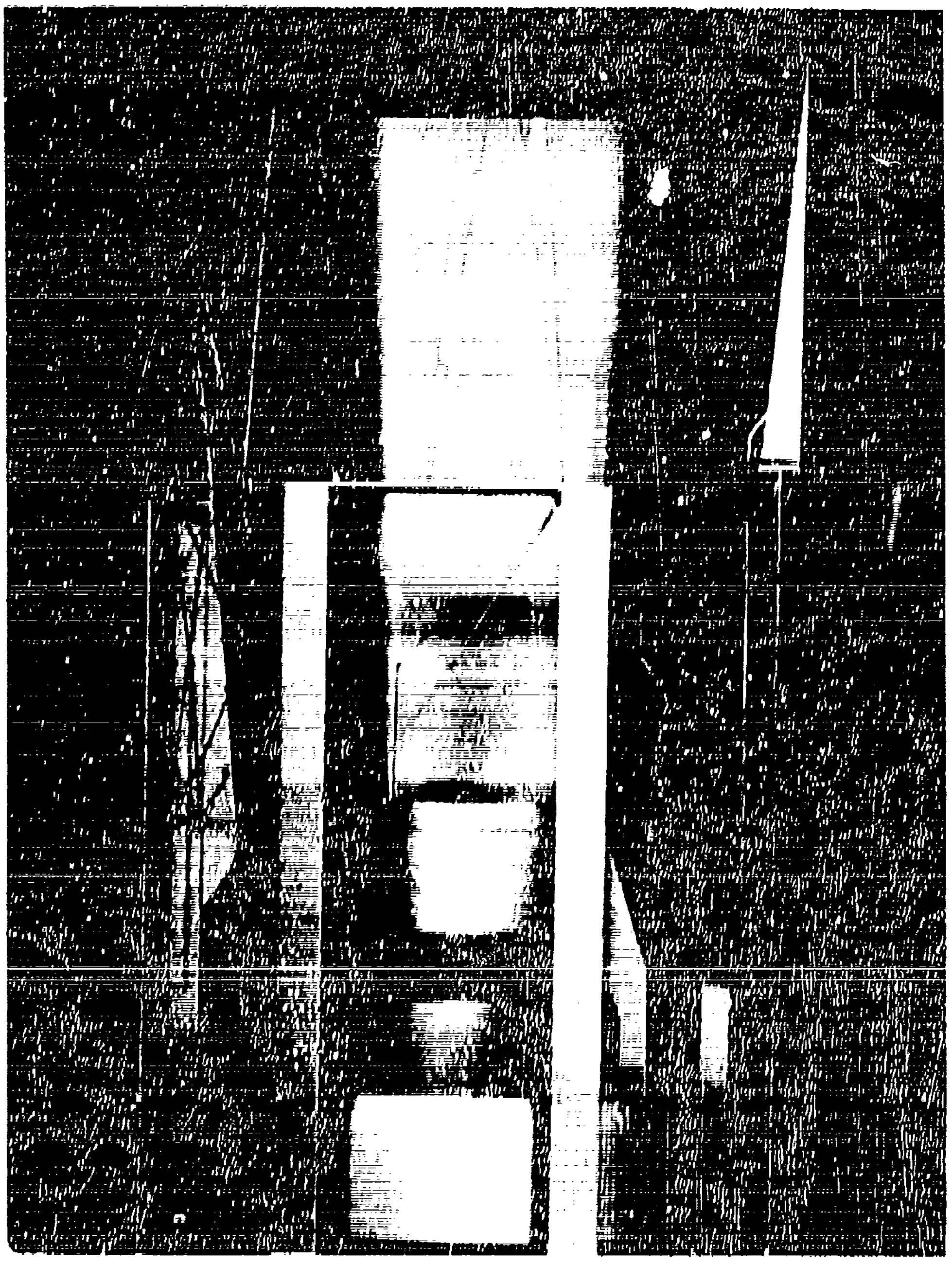

MODEL OF TRANSLATING CASCADE - CRUISE POSITION

Figure 2A-207

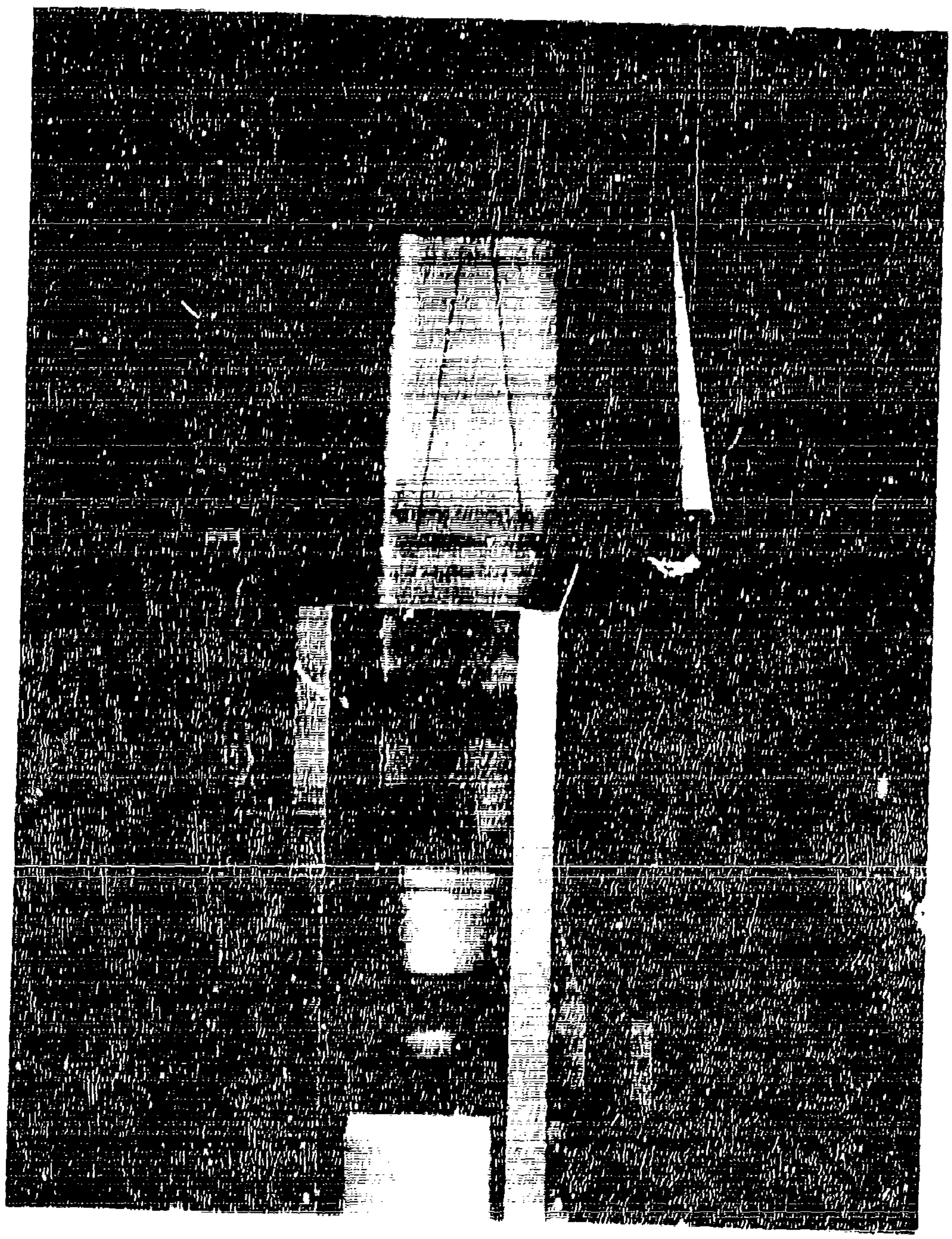

MODEL OF TRANSLATING CASCADE - LOWER POSITION

Figure 7A-208

MODEL OF TRANSLATING CASCADE - REVERSE POSITION

Figure 2A-209

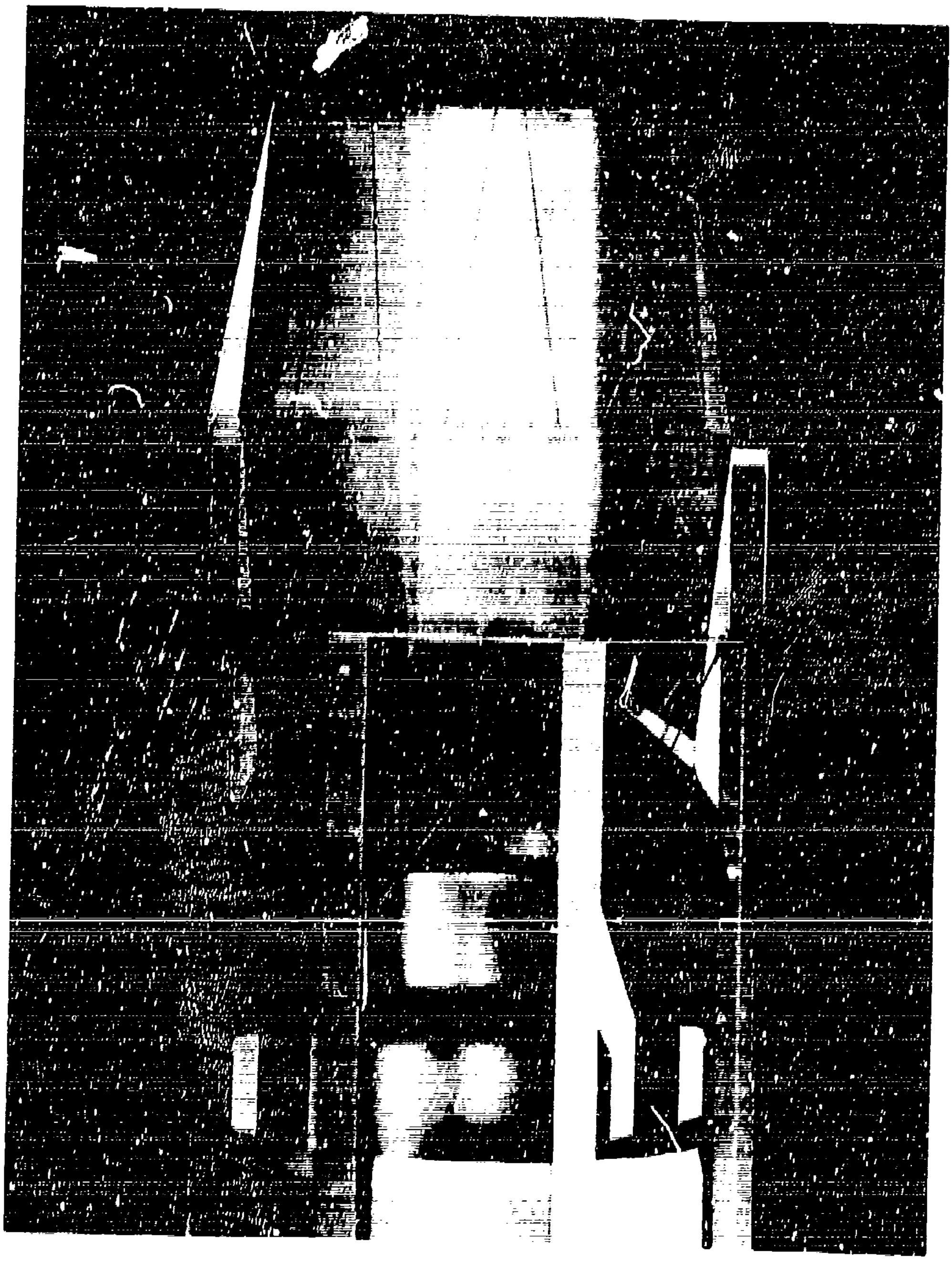

MODEL OF TRANSLATING CASCADE - REVERSE POSITION

Figure 2A-210

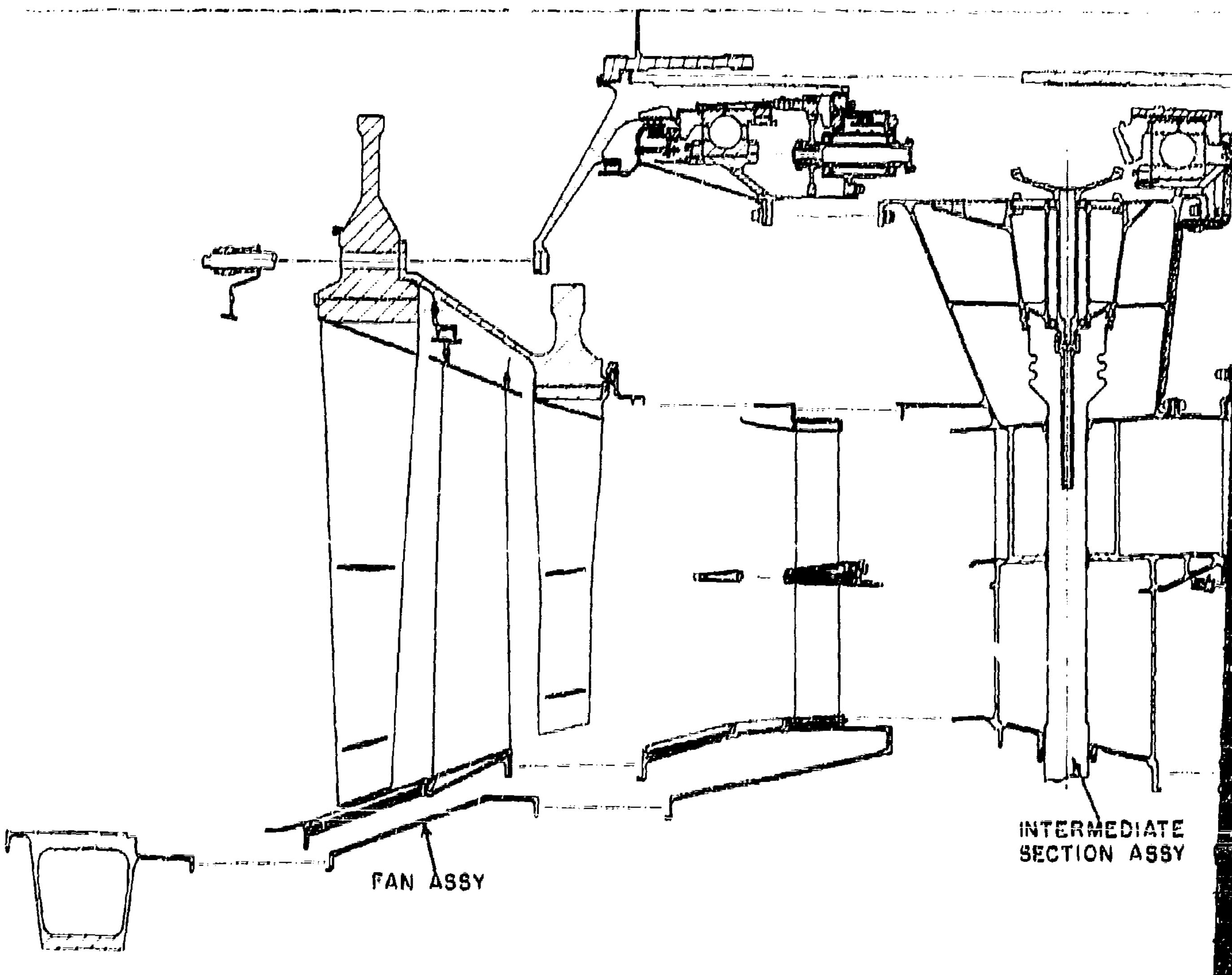
INTERMEDIATE
SECTION ASSY
FAN ASSY

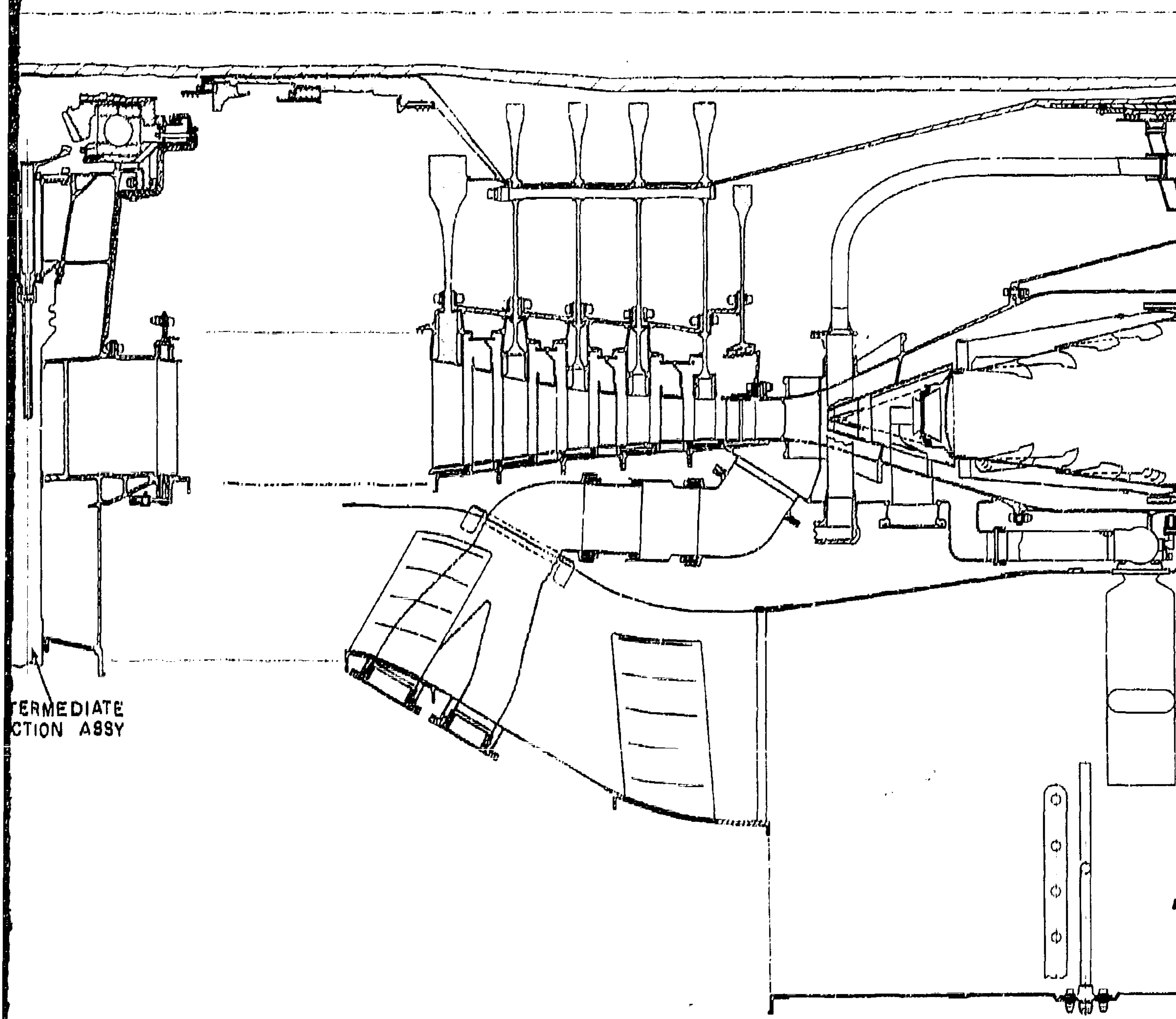

2

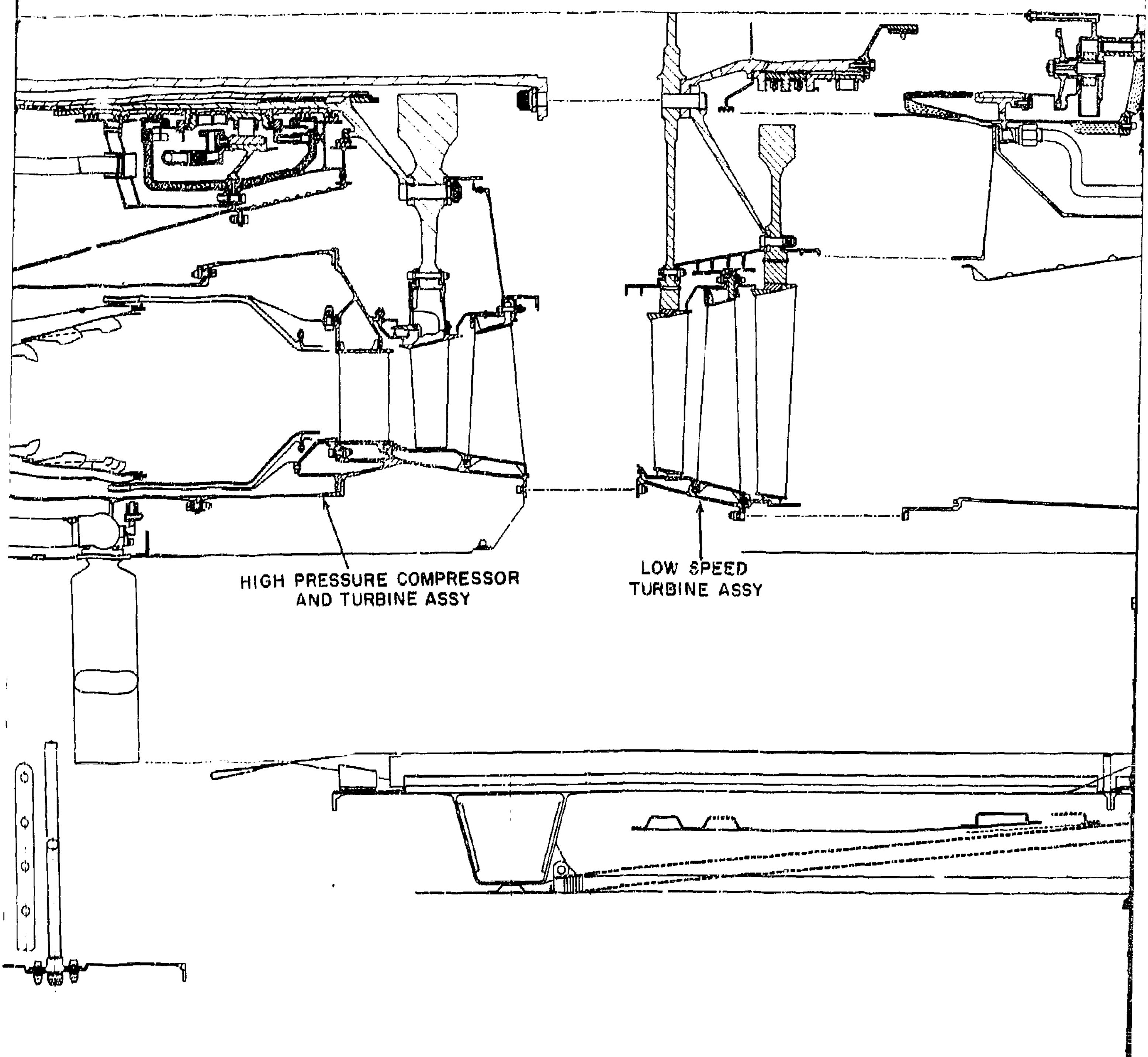
HIGH PRESSURE COMPRESSOR
AND TURBINE ASSY
LOW SPEED
TURBINE ASSY

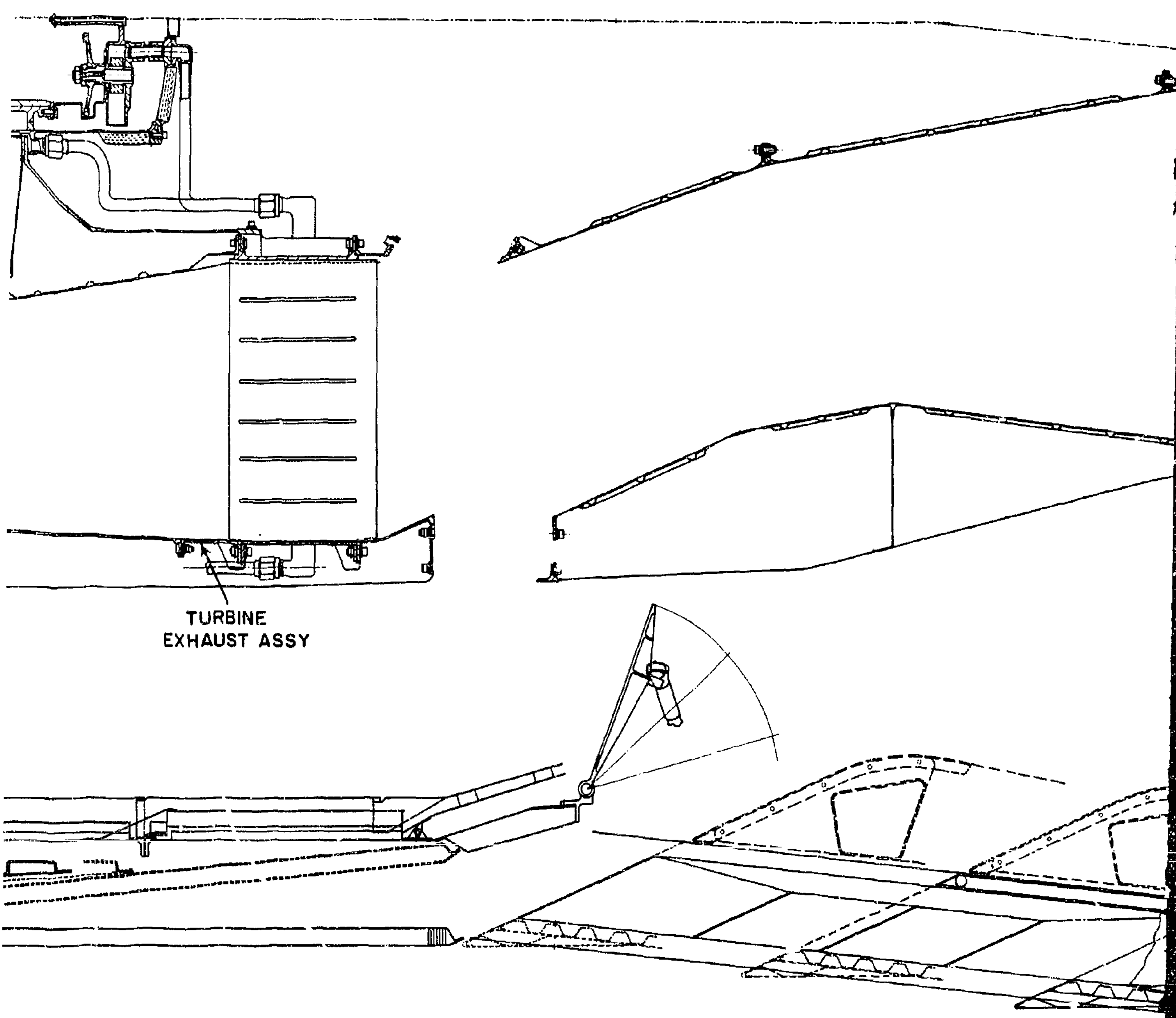

4

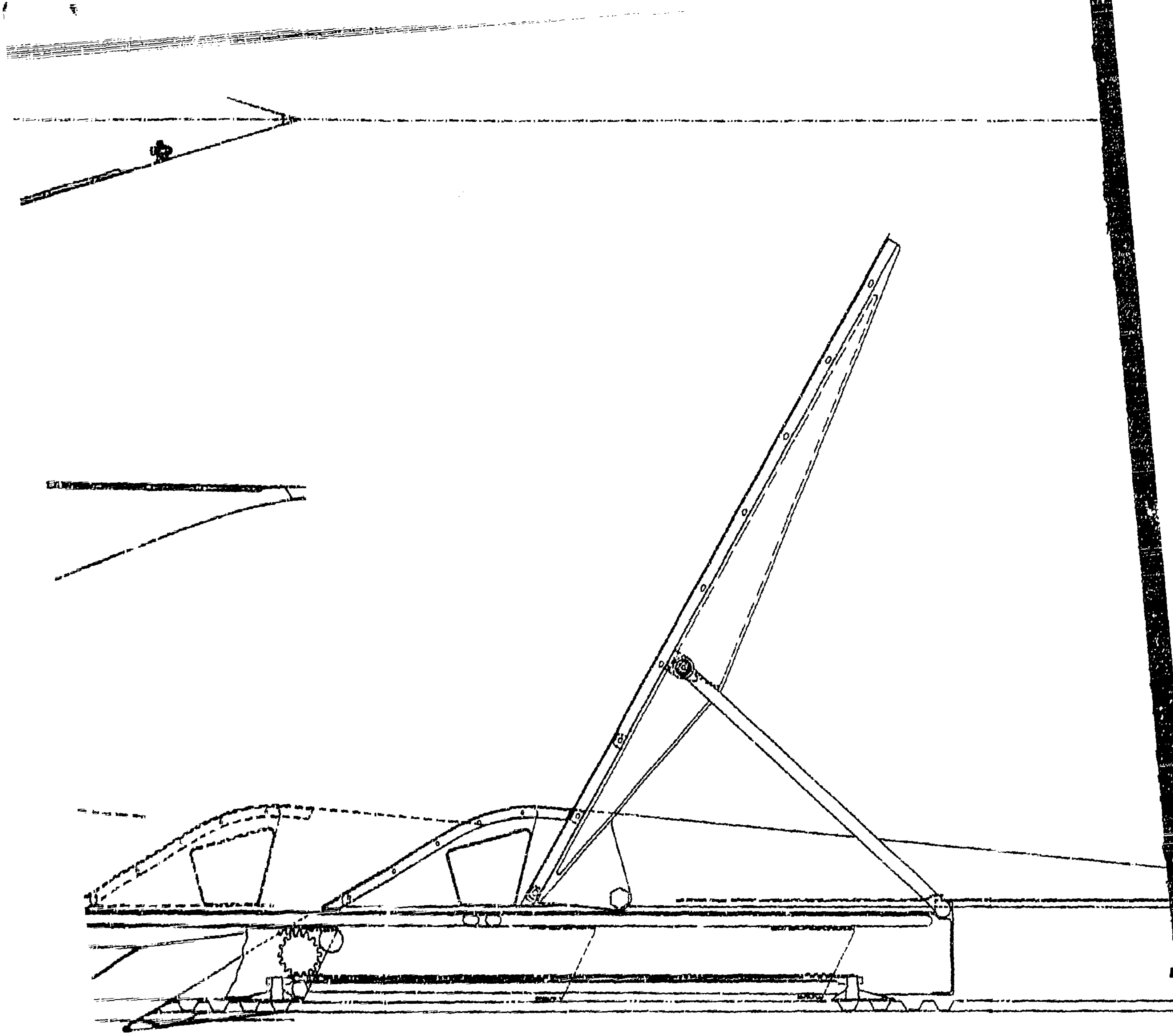

5

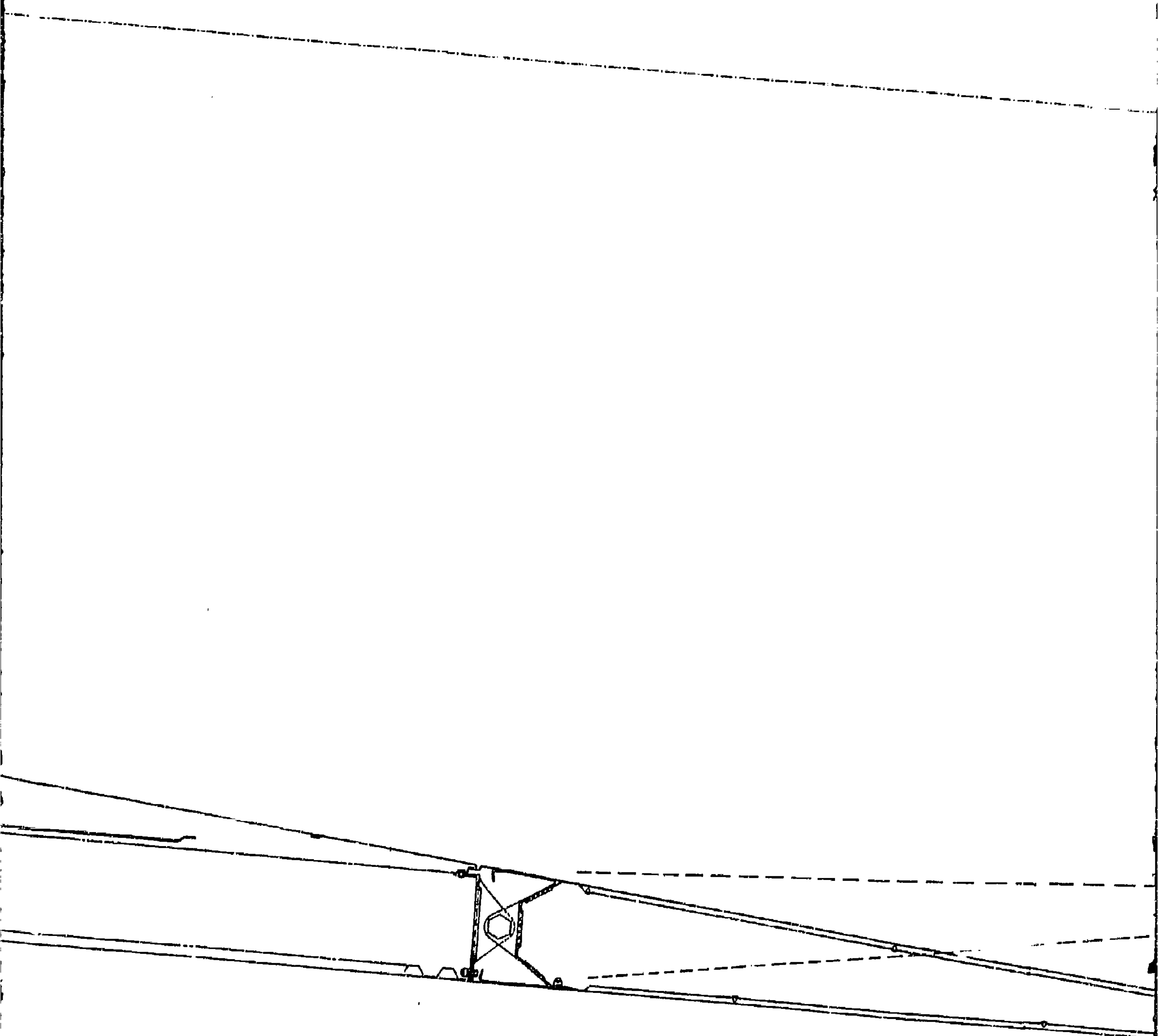

ASSEMBLY OF MAJ

Figure 2A

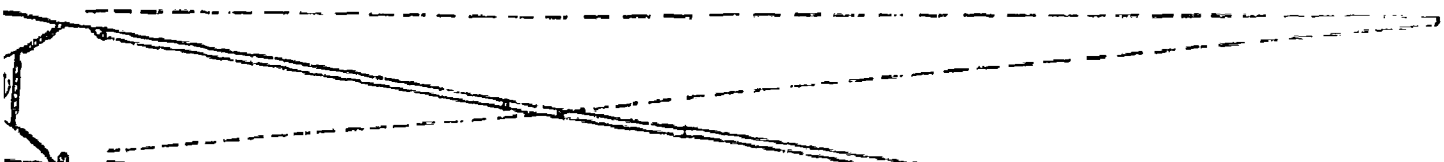

ASSEMBLY OF MAJOR COMPONENTS

Figure 2A-211

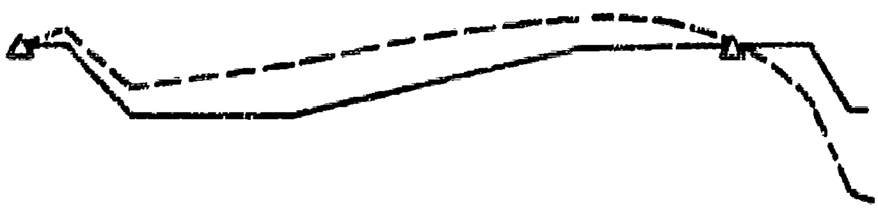

STIFF BEARING - FIRST MODE - 124% OF ROTOR SPEED

Figure 2A-212

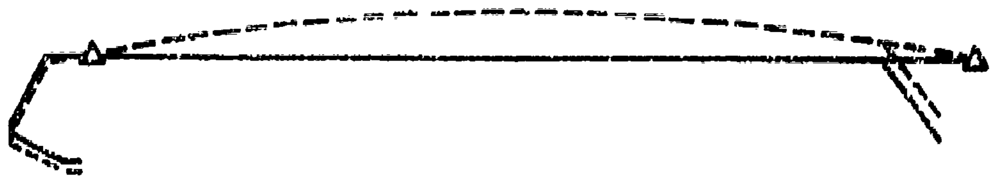

STIFF BEARING - FIRST MODE - 120% OF ROTOR SPEED

Figure 2A-213

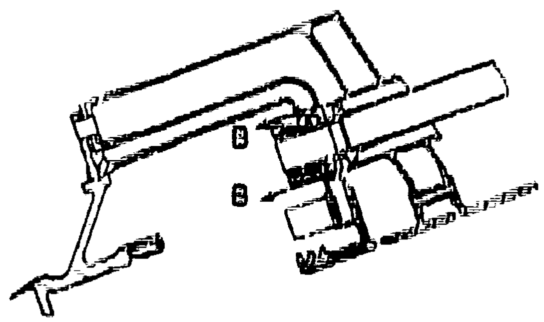

SECT. C-C BREATHER LINE

SECT. B-B

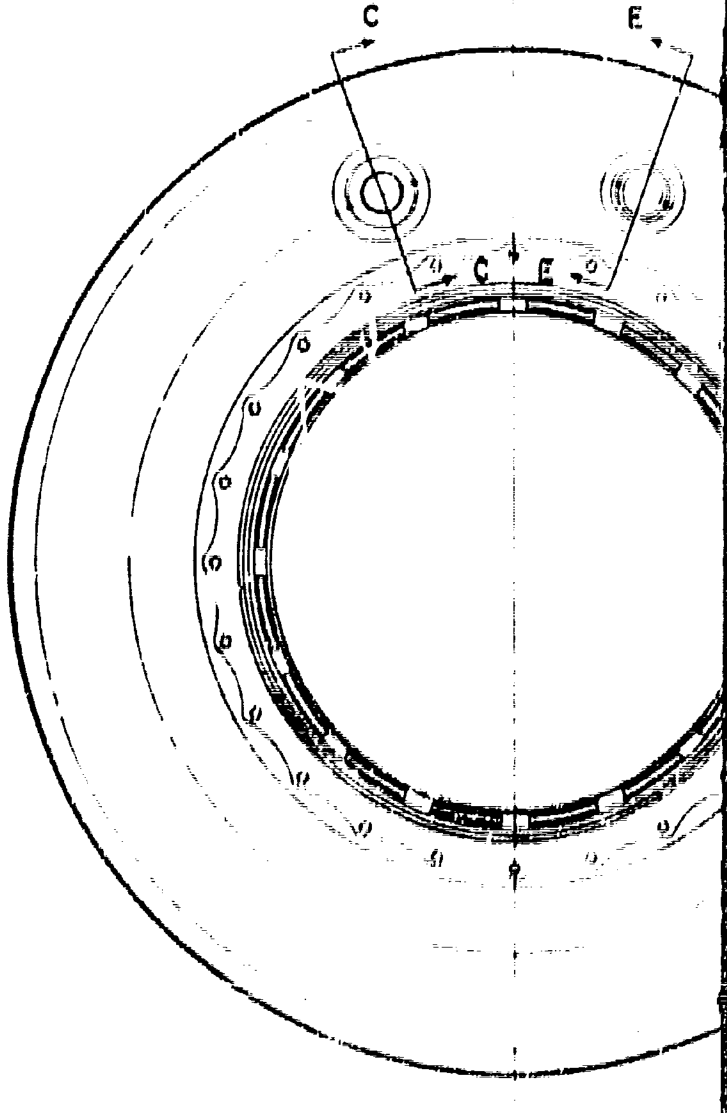

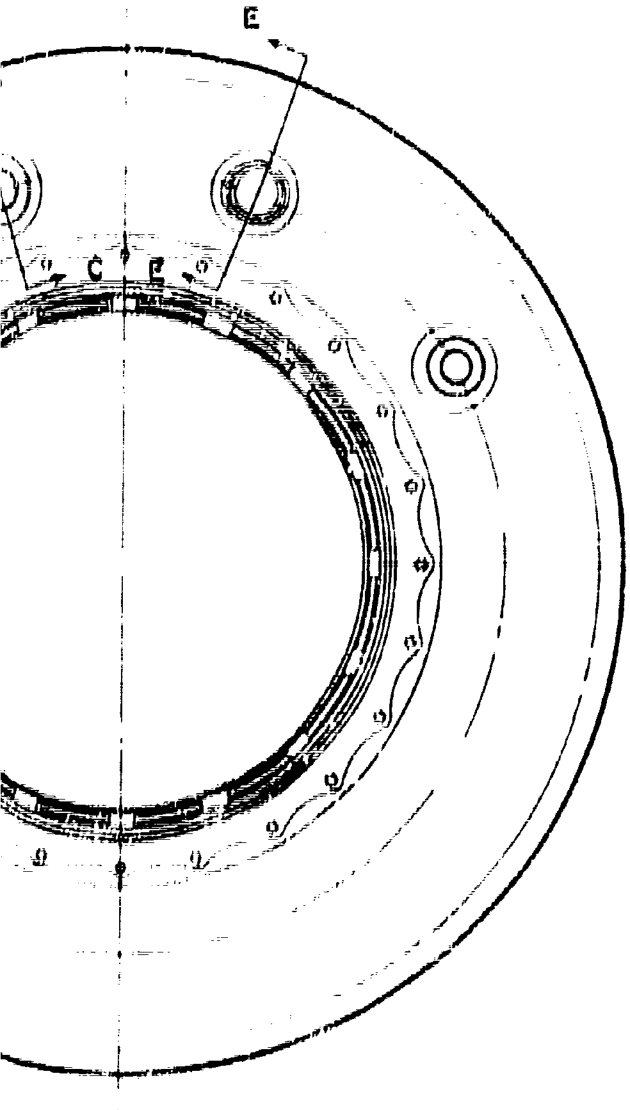

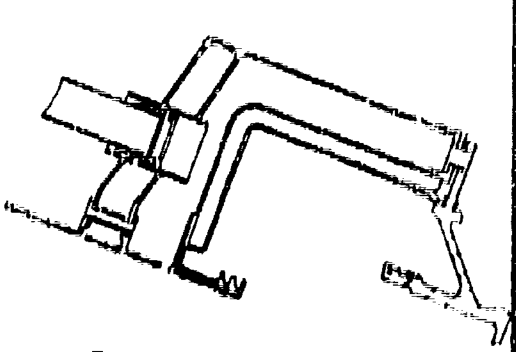

SECT. E - E SHOWING LABYRINTH SEAL COMPARTMENT VENT LINE CONNECTION

2

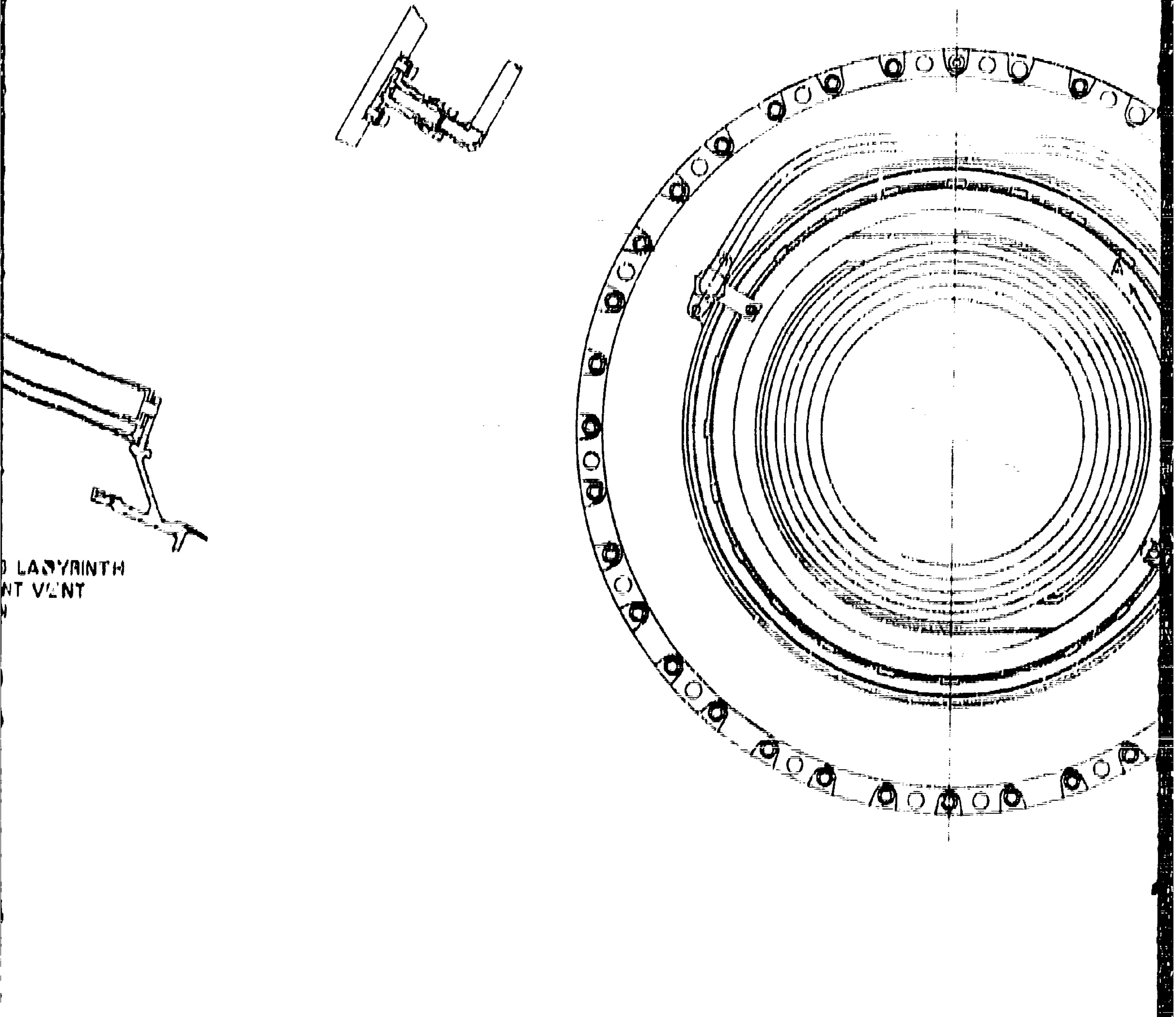

3

CONFIDENTIAL

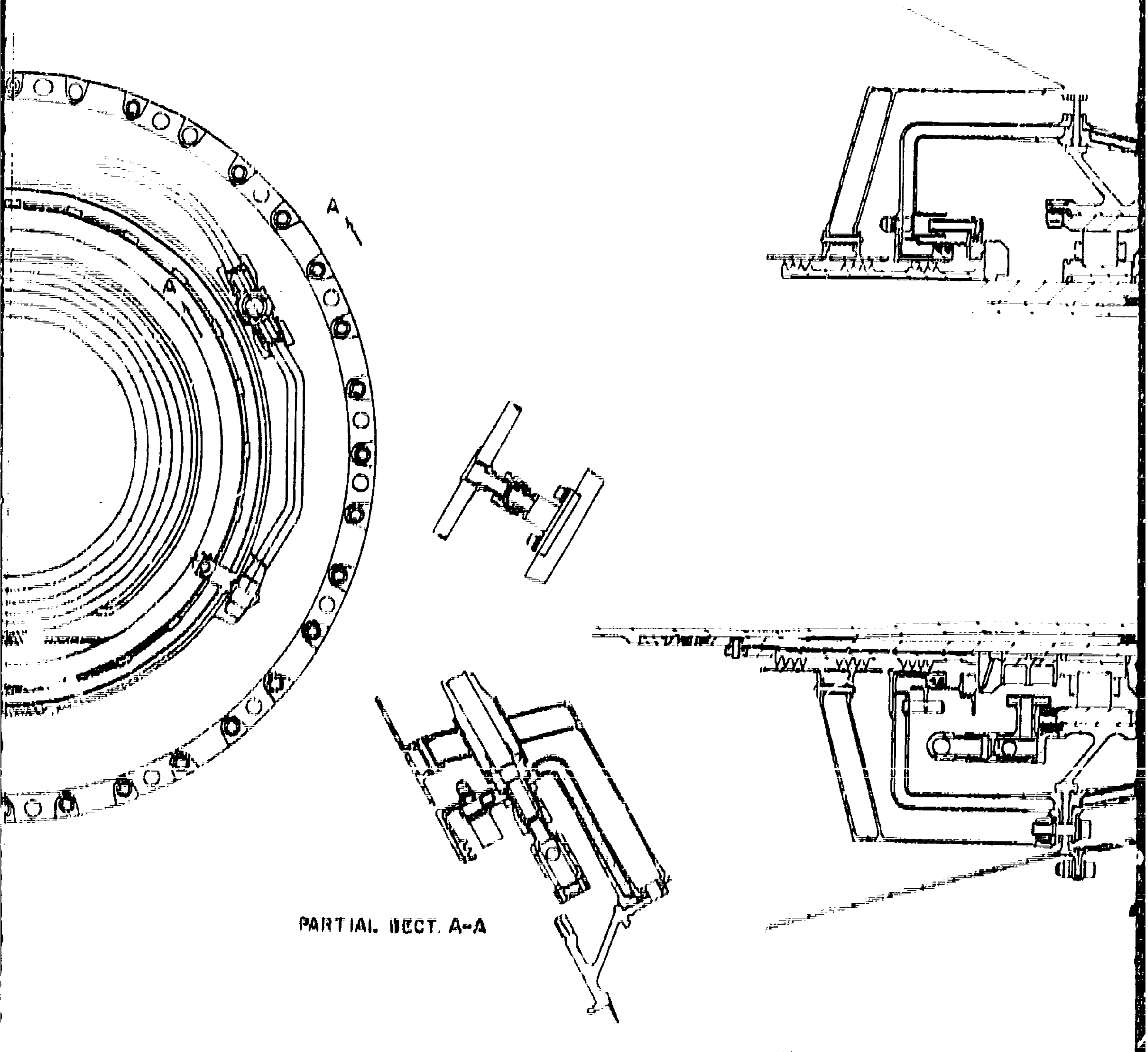

NUMBER 4 BEARING COMPARTM

Figure 2A-214

CONFIDENTIAL

4

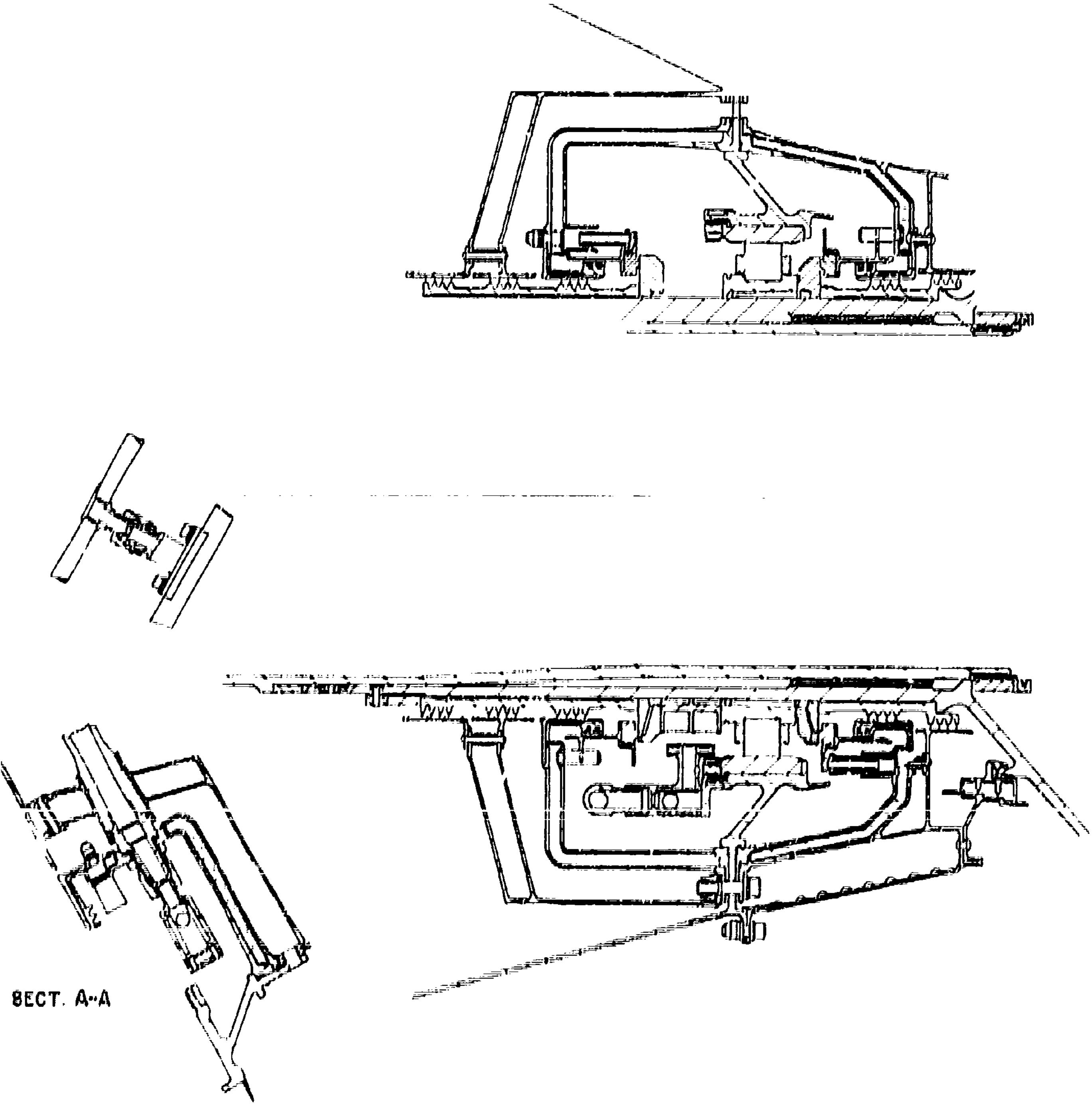

5

NUMBER 3 BEARING COMPARTMENT

Figure 2A-214

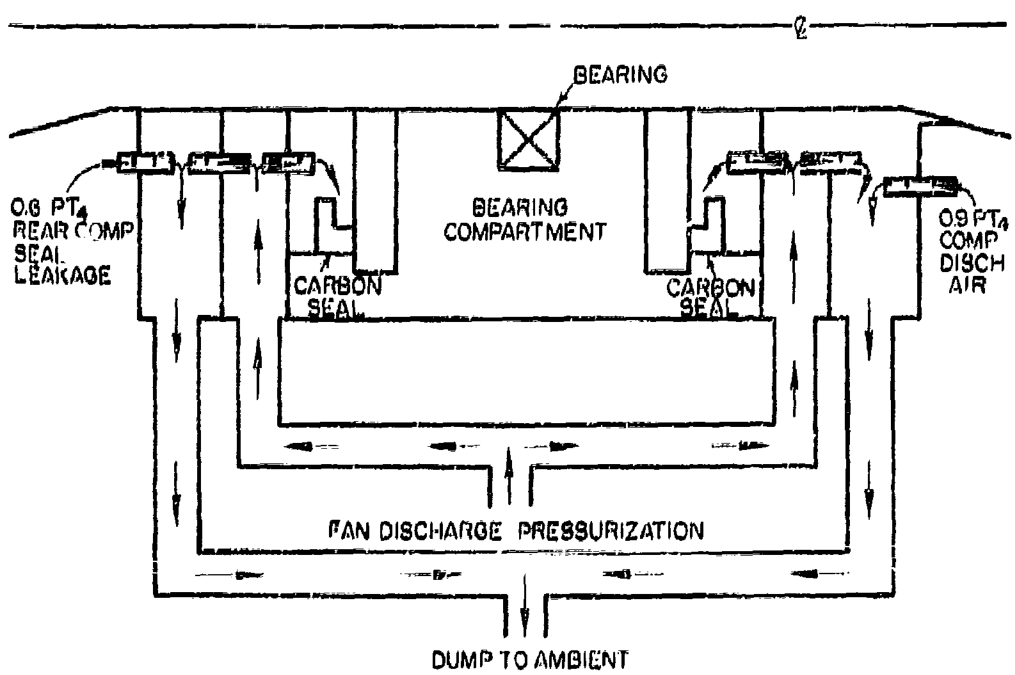

COMPARTMENT AIR COOLING - NUMBER 3 BEARING

Figure 2A-215

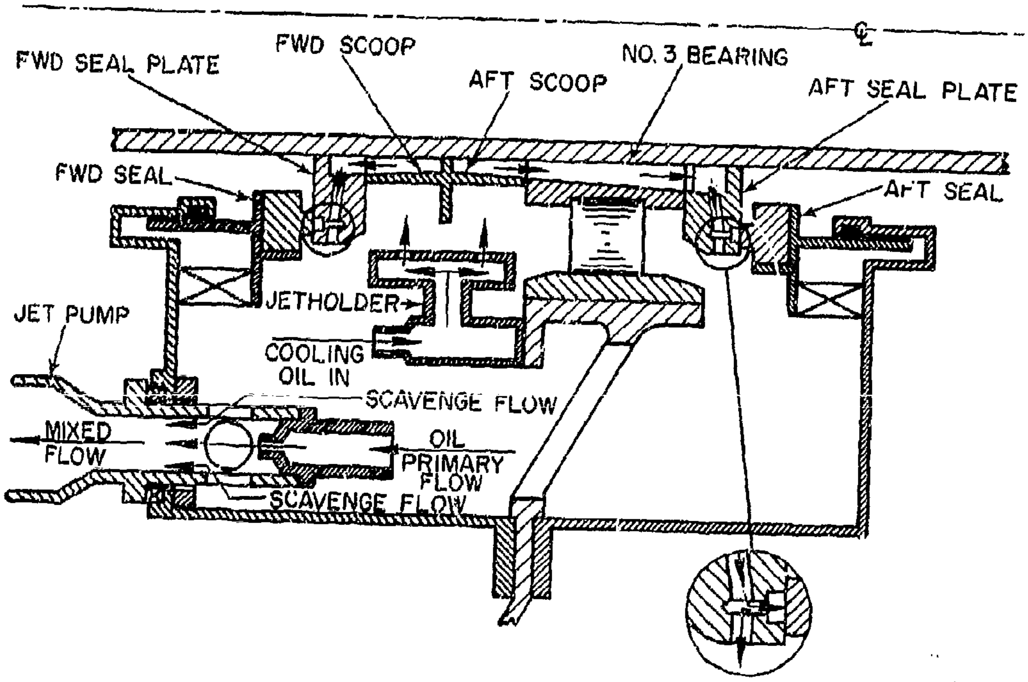

COMPARTMENT OIL FLOW - NUMBER 3 BEARING

Figure 2A-216

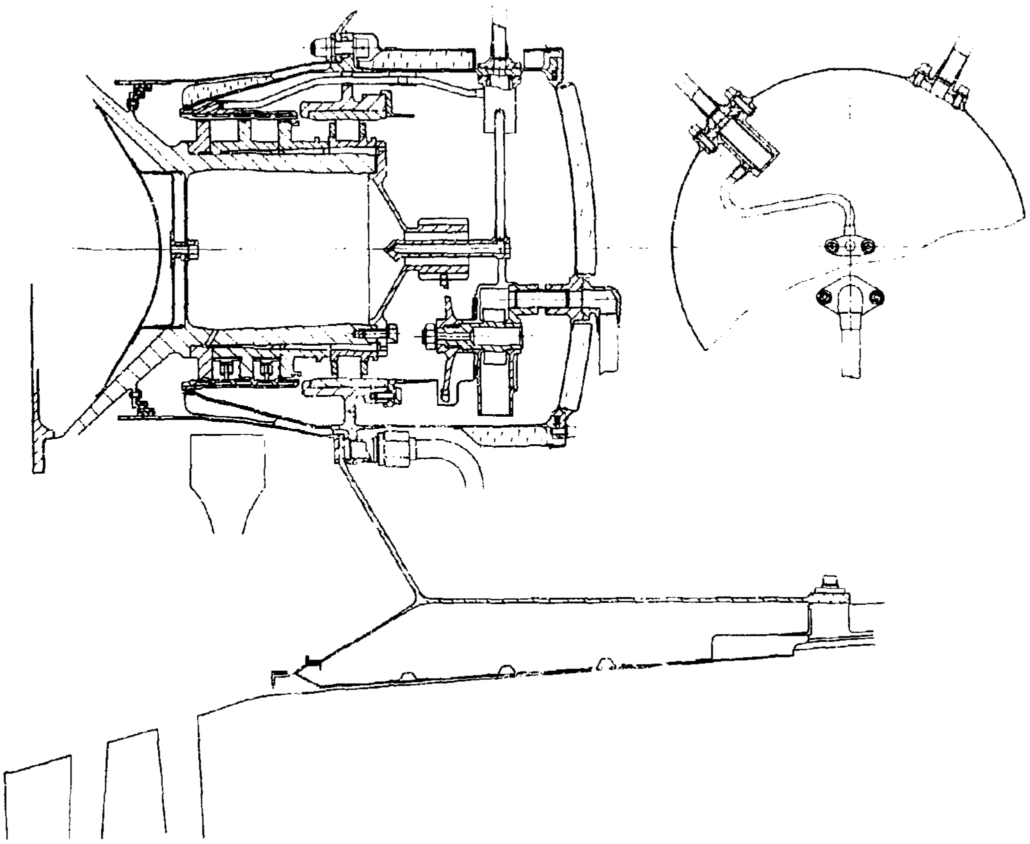

NUMBER 4 BEARING COMPARTMENT

Figure 2A-217

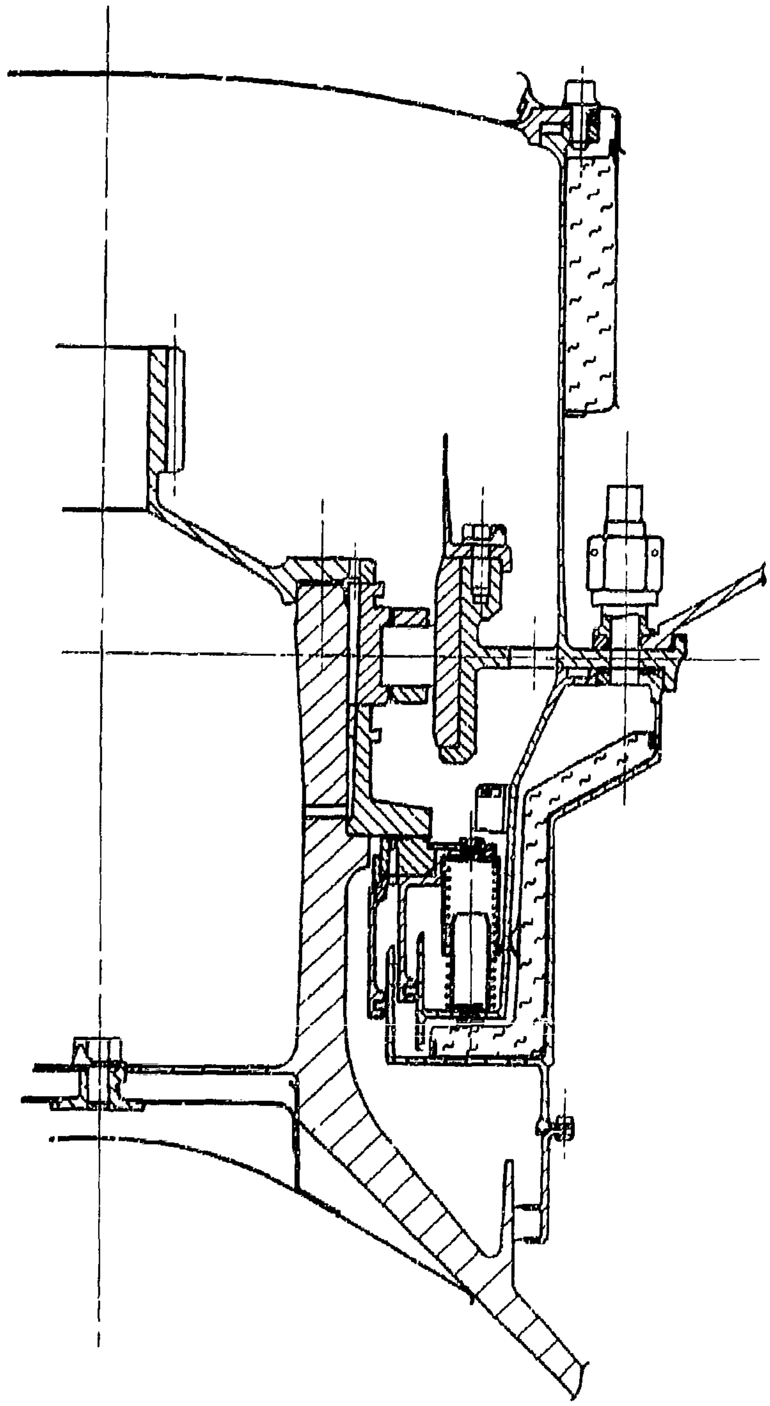

HYDROSTATIC SEAL SCHEMATIC

Figure 2A-218

SYSTEM FEATURES AND CONSIDERATIONS	SYSTEM A	B	C	D	E
Low Rotor					
Thrust Direction	Positive	Positive	Negative	Negative	Negative
Thrust Range	20,000	14,000	10,000	10,000	10,000
	Unacceptable	Fair	Good	Good	Good
Minimum Thrust Point (Skid Limit)	Cruise	Cruise	Transonic	Transonic	Transonic
Thrust Reversal During Idle Descent	Yes	Yes	No	No	No
Sensitivity To Bias Pressure (P_6)	Excellent	Good	Poor	Fair	Fair
Trim Capability (Relocation of Key Seals)	Fair	Good	Poor	Excellent	Excellent
High Rotor					
Thrust Direction	Negative	Negative	Negative	Negative	Negative
Thrust Range	5,000	5,000	5,000	5,000	7,000
	Excellent	Excellent	Excellent	Excellent	Excellent
Minimum Thrust Point	Transonic	Transonic	Transonic	Transonic	Transonic
Thrust Reversal During Idle Descent	No	No	No	No	No
Sensitivity toBias Pressure (P_4)	Excellent	Excellent	Excellent	Excellent	Excellent
Trim Capability (Relocation of Key Seals)	Excellent	Excellent	Good	Fair	Fair
Mechanical Requirements					
Overall Simplicity	Excellent	Good	Good	Fair	Poor
Vent Line Requirements For #3 Brg. Compartment	Moderate	Moderate	High	Low	Low
Vent System Required For #2 Brg. Compartment	Yes	Yes	Yes	Yes	No
Vent to Fan Duct to Reduce P_4 Bias Pressure	No	No	No	Perhaps	Yes
Intershaft Seal Required	No	No	No	Yes	Yes
Baffle From Fan Hub to Low Shaft Required	No	Yes	Yes	Yes	No
Holes Required in Low Rotor Shaft	No	No	No	No	Yes
Holes Required in Compressor Disk Webs	No	No	No	No	Yes
Performance Considerations					
High Pressure Compressor Discharge Leakage Loss	Low	Low	Moderate	High	High
Fan Discharge Leakage Loss	Low	Moderate	Moderate	Moderate	High
Radial Inflow to High Pressure Compressor Inlet	Moderate	Moderate	High	Low/Moderate	Low
Ground Rules Satisfied	2, 3, 4	2, 3, 4	1, 2, 3	1, 2, 3, 4	1, 2, 3, 4, 5

SUMMARY OF PROPOSED THRUST BALANCE SYSTEMS

Figure 2A-219

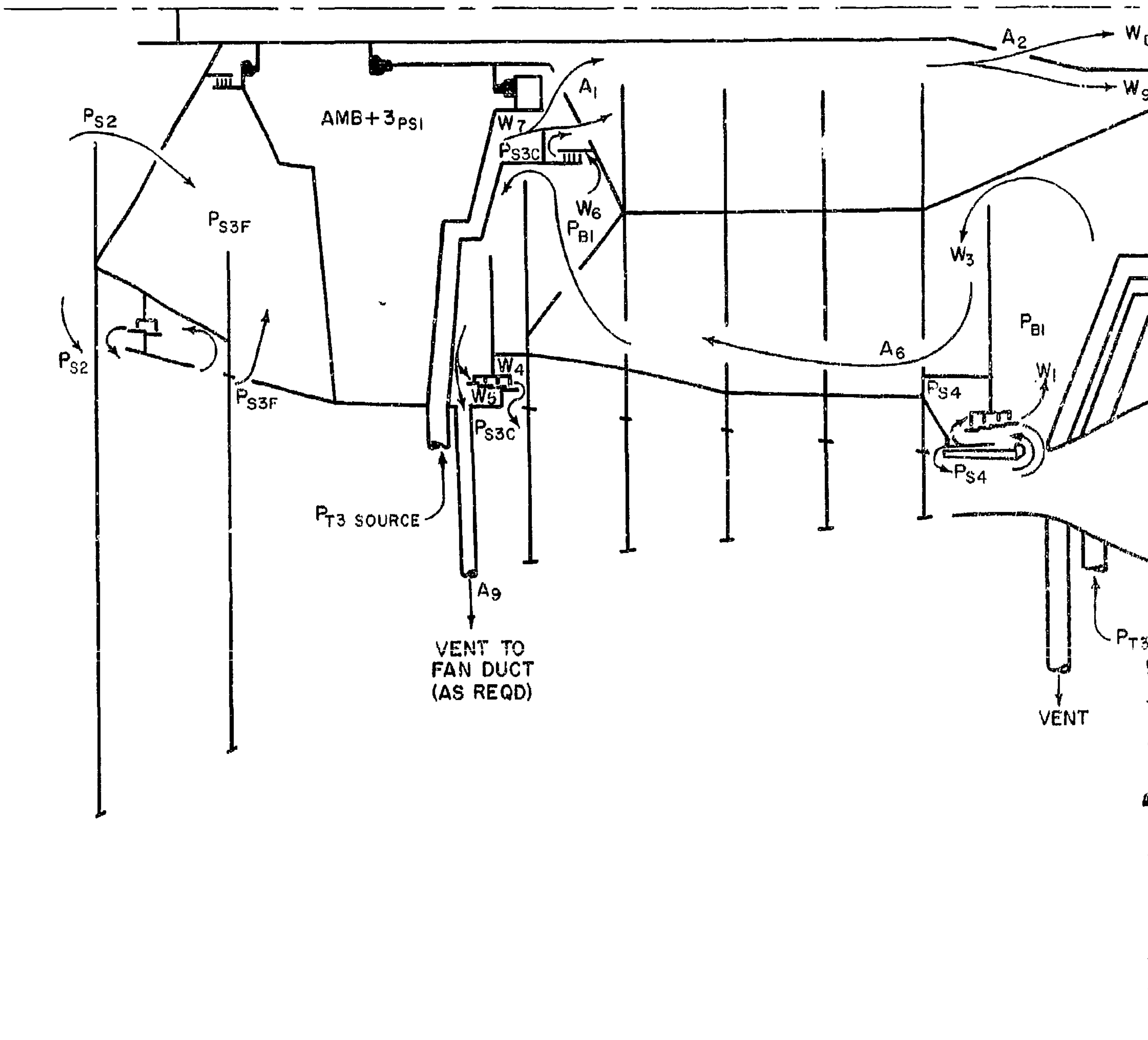

A_2
W_0
W_9
A_1
P_{S2}
AMB+3 PSI
W_7
P_{S3C}
W_6
P_{B1}
P_{S3F}
W_3
P_{B1}
A_6
P_{S2}
W_4
W_5
P_{S4}
W_1
P_{S3F}
P_{S3C}
P_{S4}
P_{T3} SOURCE
A_9
P_{T3}
VENT TO
FAN DUCT
(AS REQD)
VENT

1

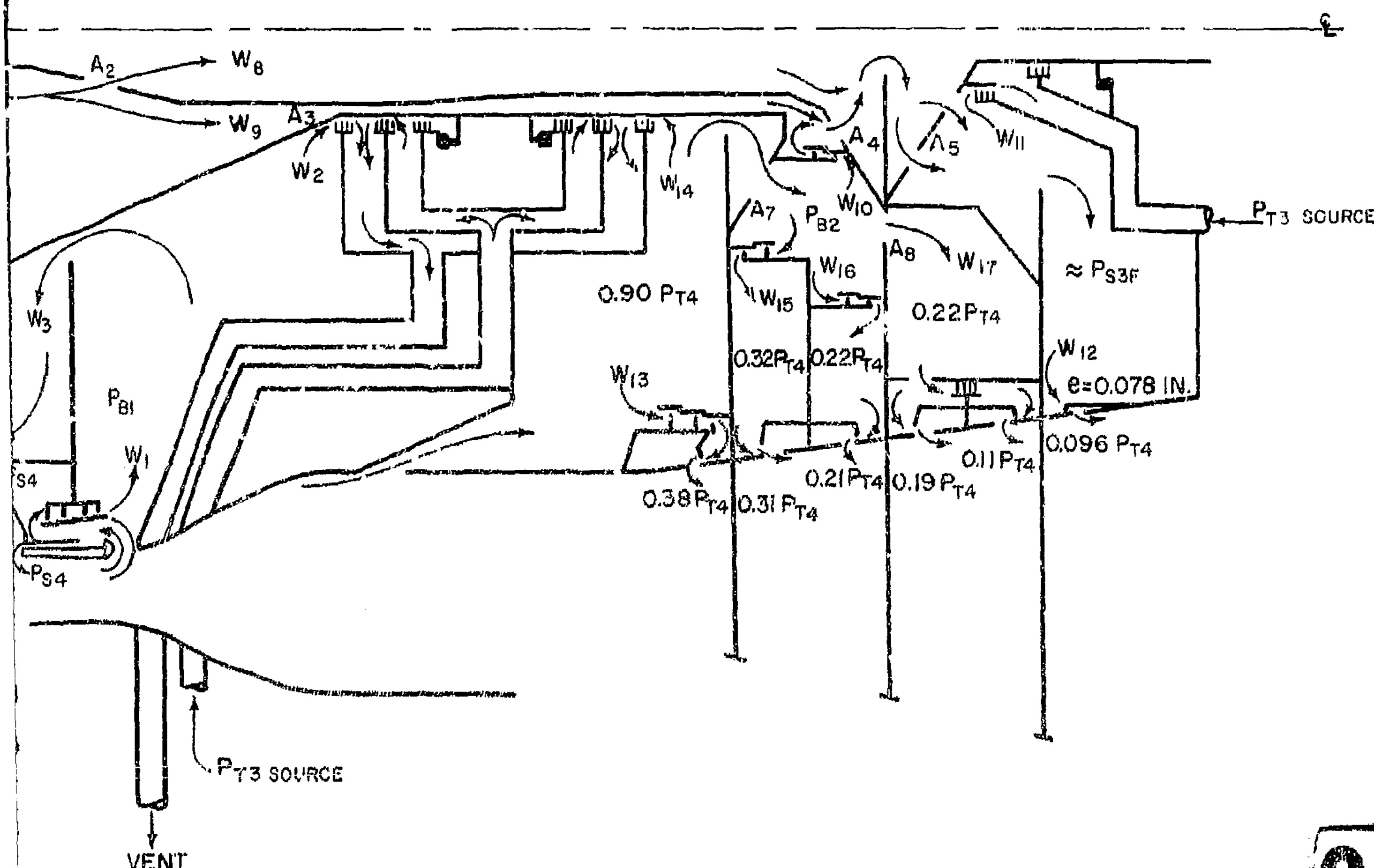

2

SECONDARY FLOW SCHEMATIC - SYSTEM E

Figure 2A-220

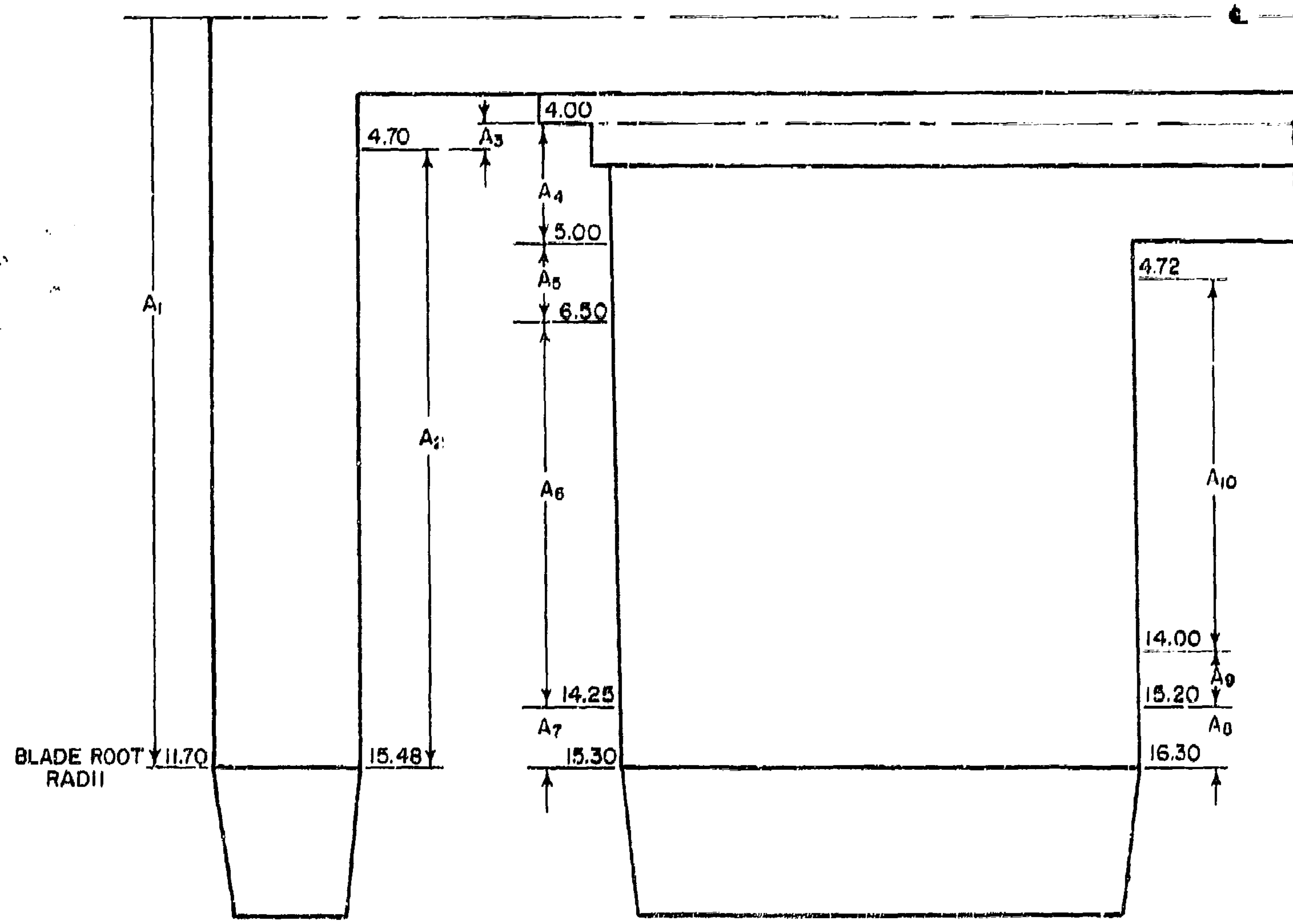

AREAS							
A_1	430.0	A_8	109.0	A_{15}	501.0	A_{22}	160.5
A_2	683.0	A_9	110.0	A_{16}	86.0	A_{23}	83.6
A_3	19.1	A_{10}	545.0	A_{17}	13.3	A_{24}	18.6
A_4	28.2	A_{11}	429.0	A_{18}	179.5	A_{25}	14.6
A_5	54.2	A_{12}	153.0	A_{19}	263.5	A_{26}	377.0
A_6	505.0	A_{13}	46.0	A_{20}	61.6	A_{27}	12.1
A_7	97.5	A_{14}	25.6	A_2	32.4	A_{28}	26.4

P_1	P
P_2	P
P_3	AN
P_4	AR
P_5	P
P_6	P
P_7	P

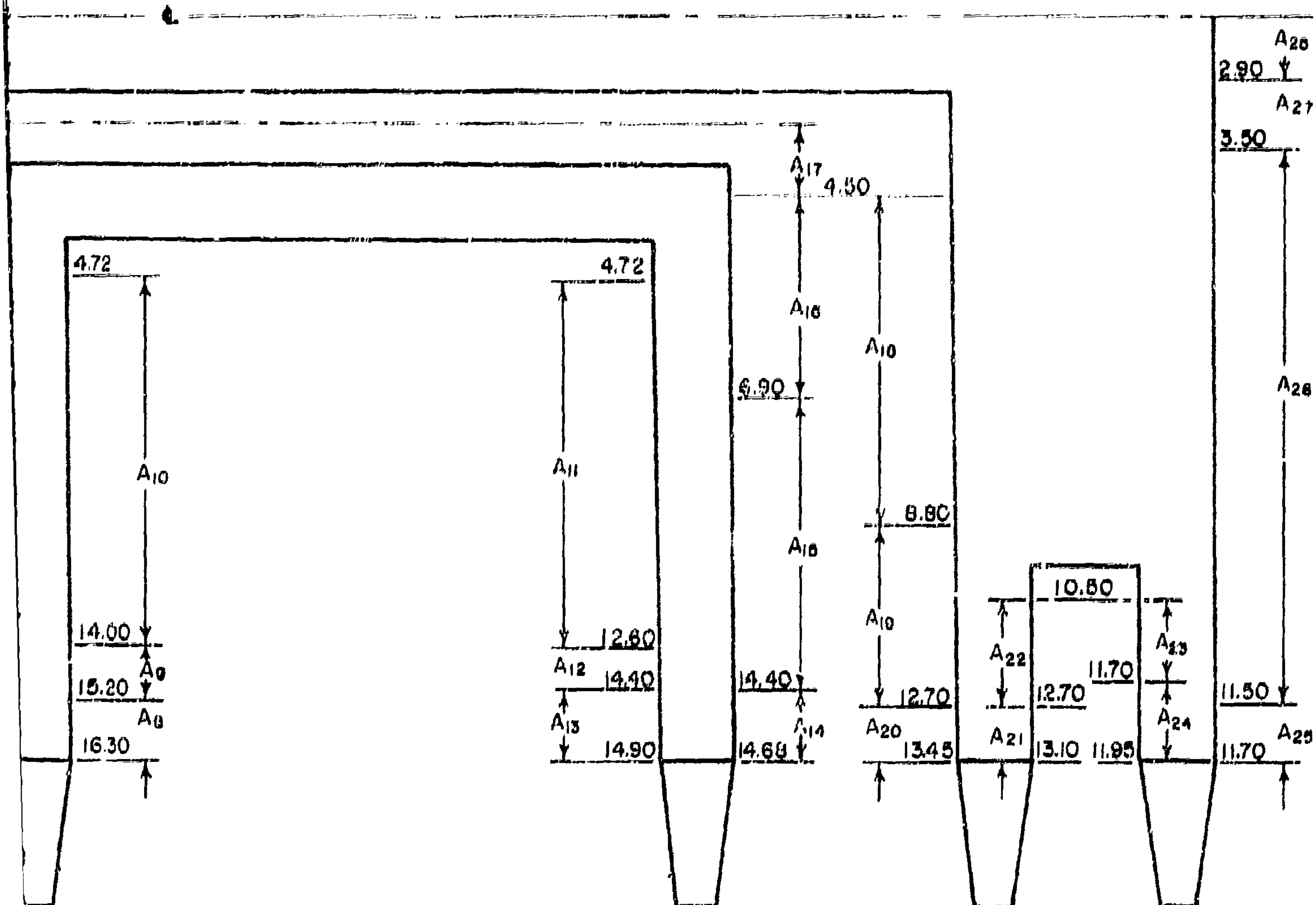

PRESSURES							
P_1	P_{B2}	P_8	P_{S4}	P_{15}	$0.32\ P_{T4}$	P_{22}	$0.21\ P_{T4}$
P_2	P_{B3} FAN	P_9	P_{B4}	P_{16}	P_{B2}	P_{23}	$0.13\ P_{T4}$
P_3	AMB +3	P_{10}	P_{B1}	P_{17}	P_{B3} FAN	P_{24}	$0.11\ P_{T4}$
P_4	AMB +3	P_{11}	$0.90\ P_{T4}$	P_{18}	P_{B2}	P_{25}	$0.096\ P_{T4}$
P_5	P_{B3} COMP	P_{12}	$0.44\ P_{T4}$	P_{19}	$0.22\ P_{T4}$	P_{26}	P_{B3} FAN
P_6	P_{B1}	P_{13}	$0.38\ P_{T4}$	P_{20}	$0.21\ P_{T4}$	P_{27}	P_{T3}
P_7	P_{B3} COMP	P_{14}	$0.31\ P_{T4}$	P_{21}	$0.19\ P_{T4}$	P_{28}	AMB + 3

P_{B1} – HIGH ROTOR BIAS PRESSURE
P_{B2} – LOW ROTOR BIAS PRESSURE

THRUST BALANCE SCHEMATIC - SYSTEM E

Figure 2A-221

2

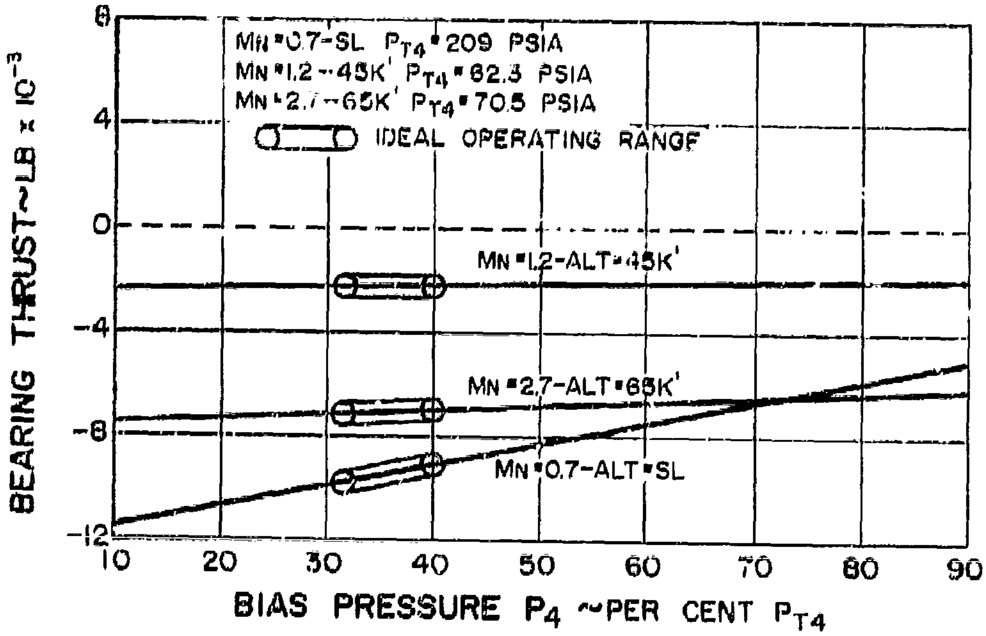

HIGH ROTOR THRUST vs. BIAS PRESSURE - SYSTEM E

Figure 2A-222

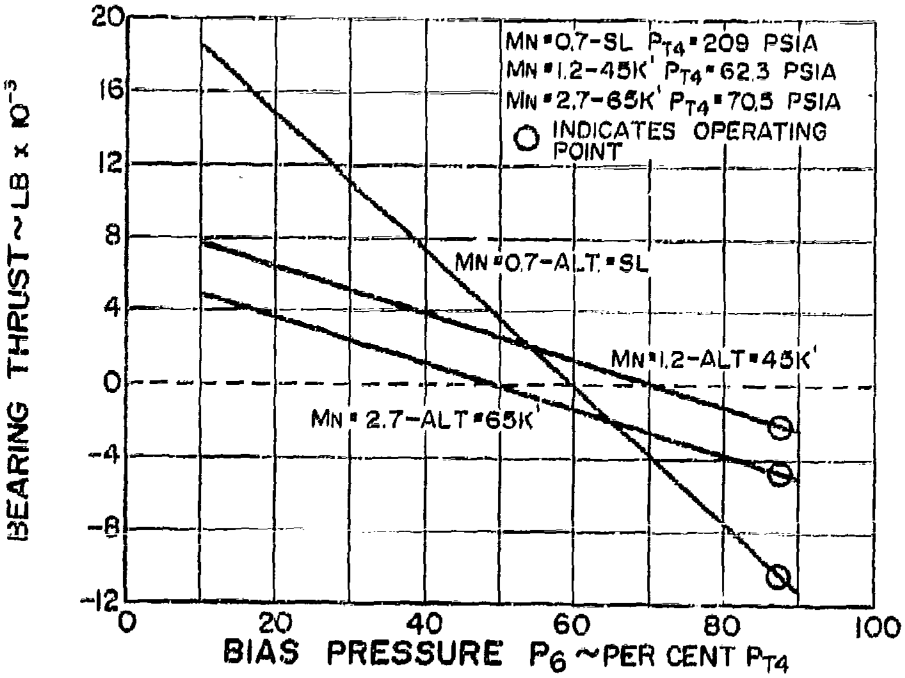

LOW ROTOR THRUST vs BIAS PRESSURE - SYSTEM E

Figure 2A-223

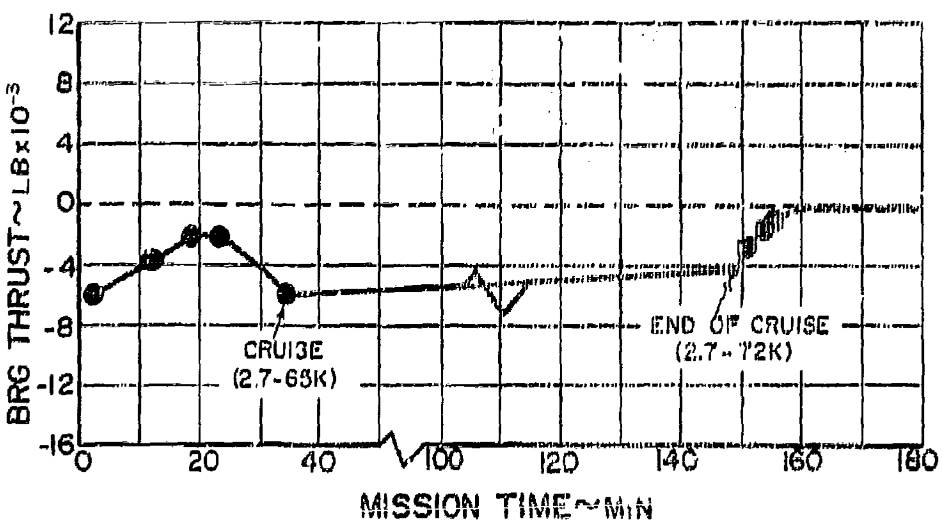

HIGH ROTOR BEARING THRUST vs. MISSION TIME

Figure 2A-224

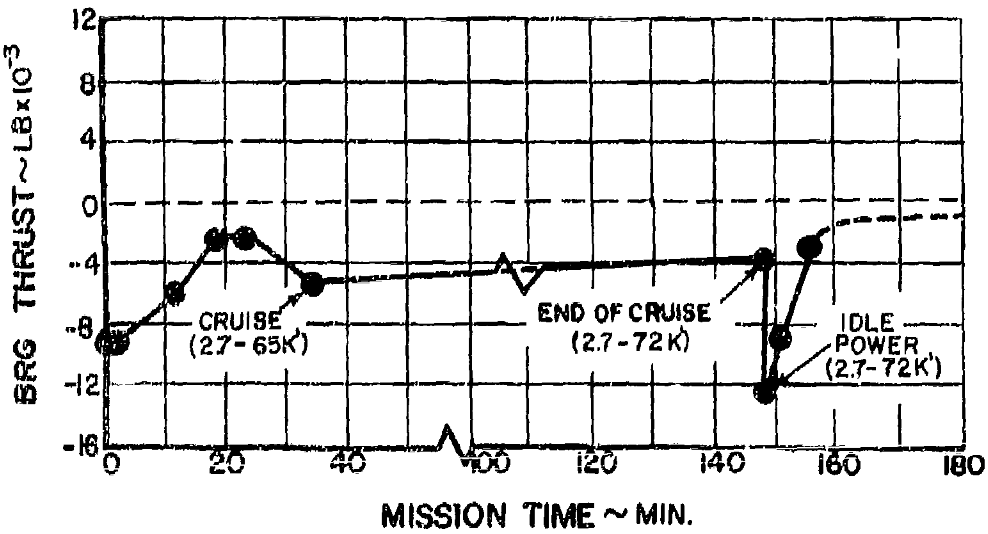

LOW ROTOR BEARING THRUST vs. MISSION TIME

Figure 2A-225

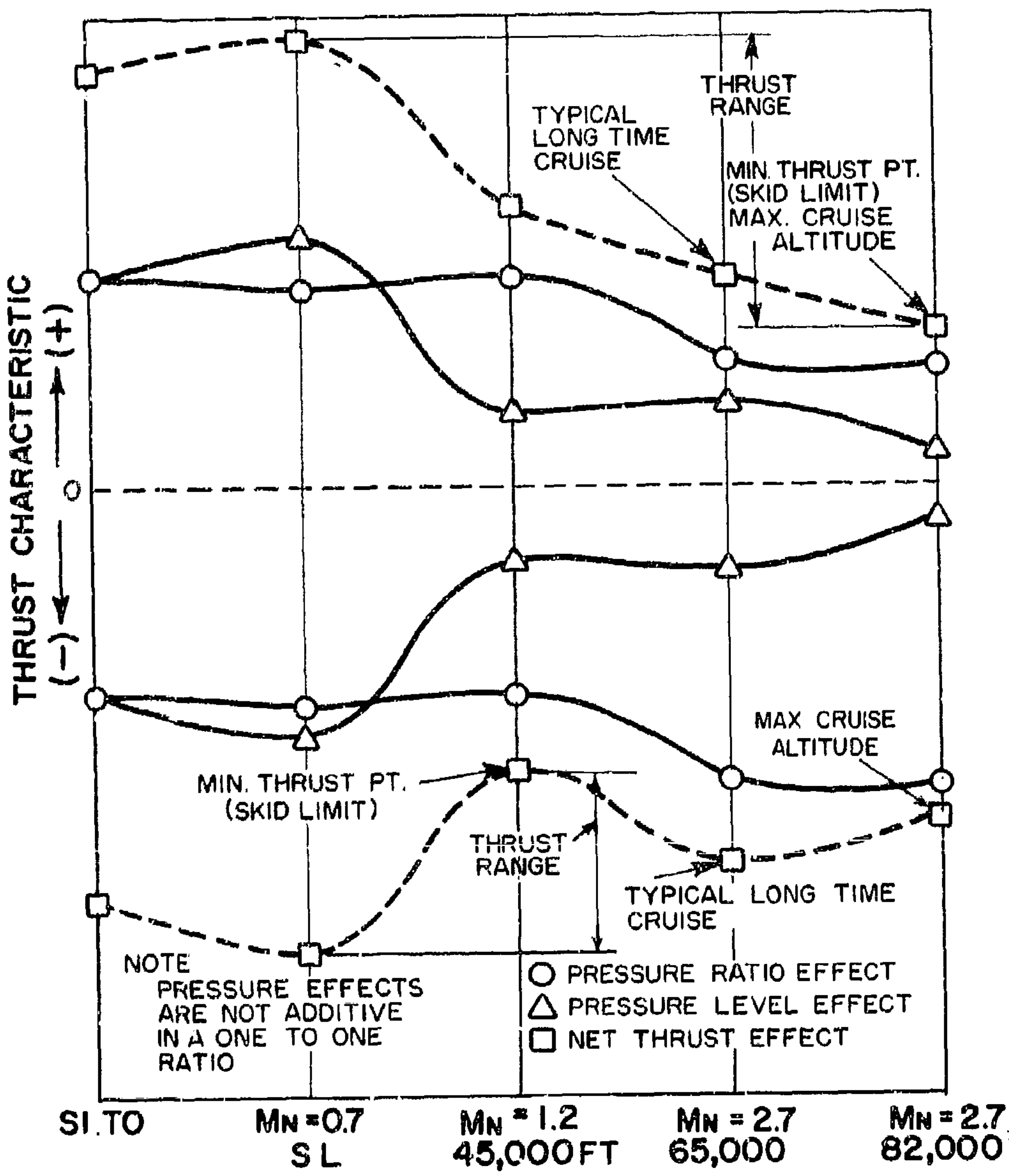

FUNDAMENTAL THRUST vs. CLIMB CHARACTERISTIC

Figure 2A-226

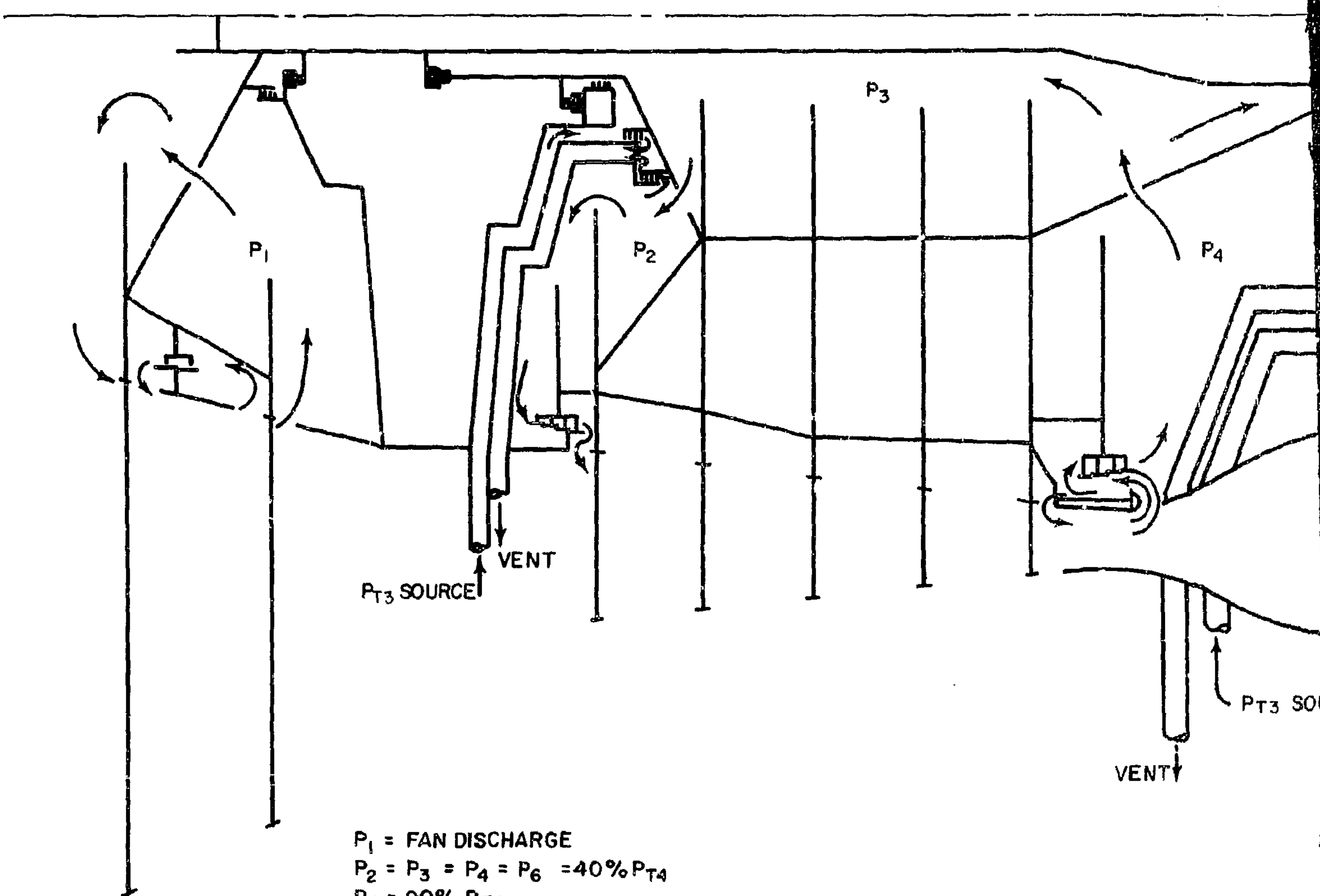

P_1 = FAN DISCHARGE
$P_2 = P_3 = P_4 = P_6 = 40\% P_{T4}$
$P_5 = 90\% P_{T4}$
P_7 > TURBINE EXIT PRESSURE

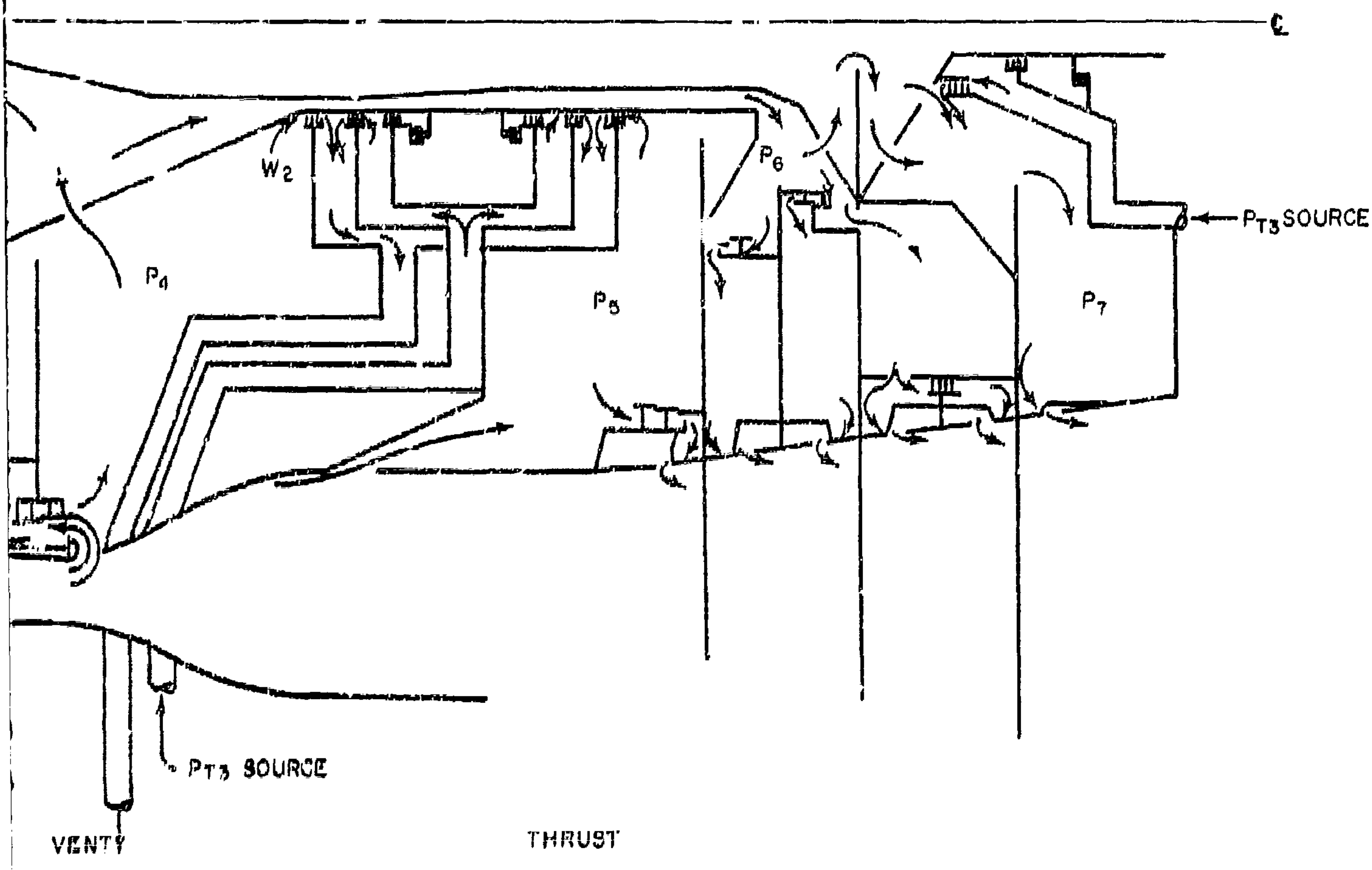

	THRUST	
DESIGN PT	HIGH ROTOR	LOW ROTOR
MN = 0.7 SL	-7000	+22,000
MN = 1.2 45,000 FT	-2000	+ 7000
MN = 2.7 65,000 FT	- 6000	+ 2000

2

THRUST BALANCE AND FLOW SCHEMATIC - SYSTEM A

Figure 2A-227

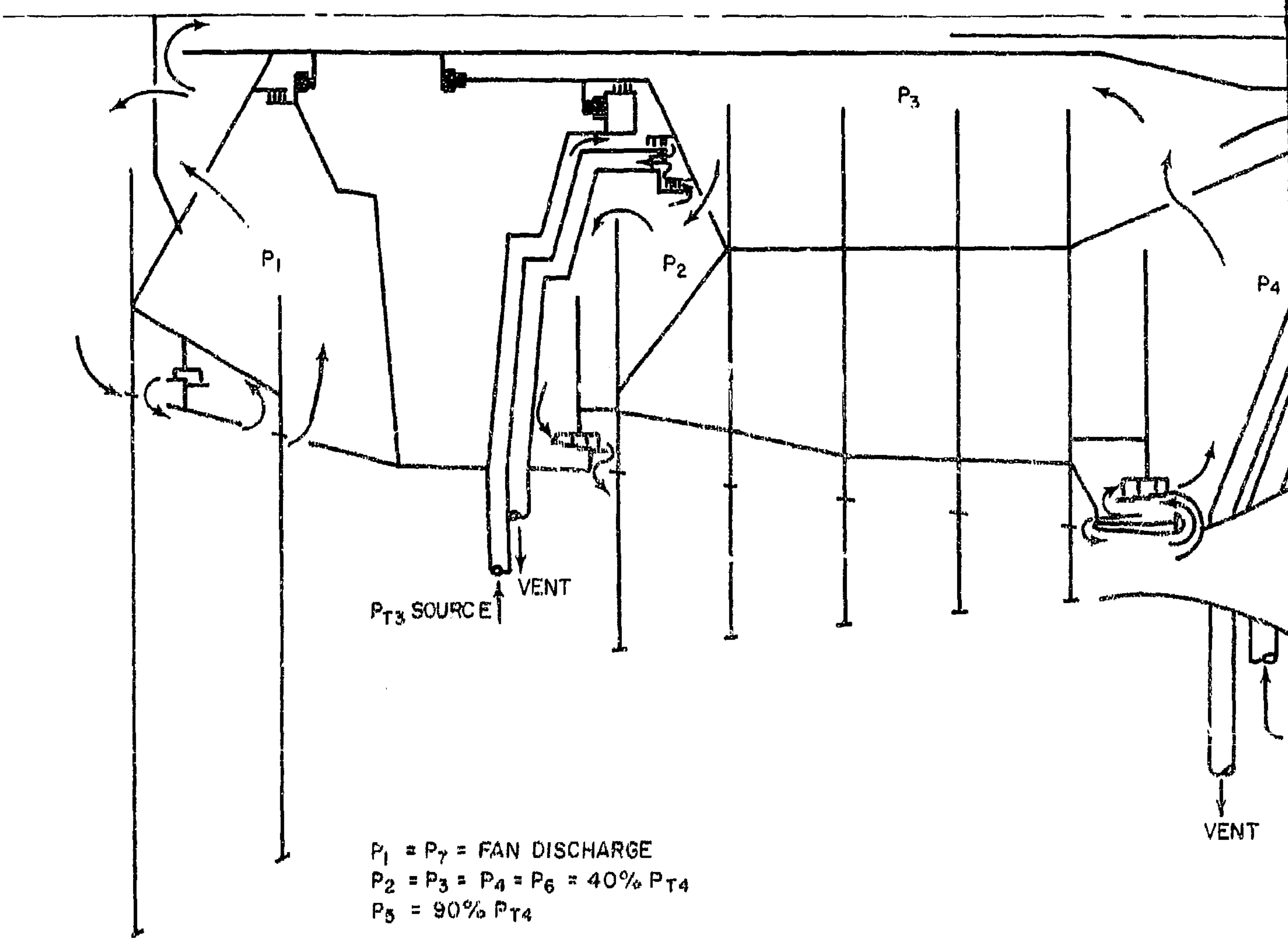

P_1
P_2
P_3
P_4
VENT
P_{T3} SOURCE
VENT
$P_1 = P_7 =$ FAN DISCHARGE
$P_2 = P_3 = P_4 = P_6 = 40\% \; P_{T4}$
$P_5 = 90\% \; P_{T4}$

1

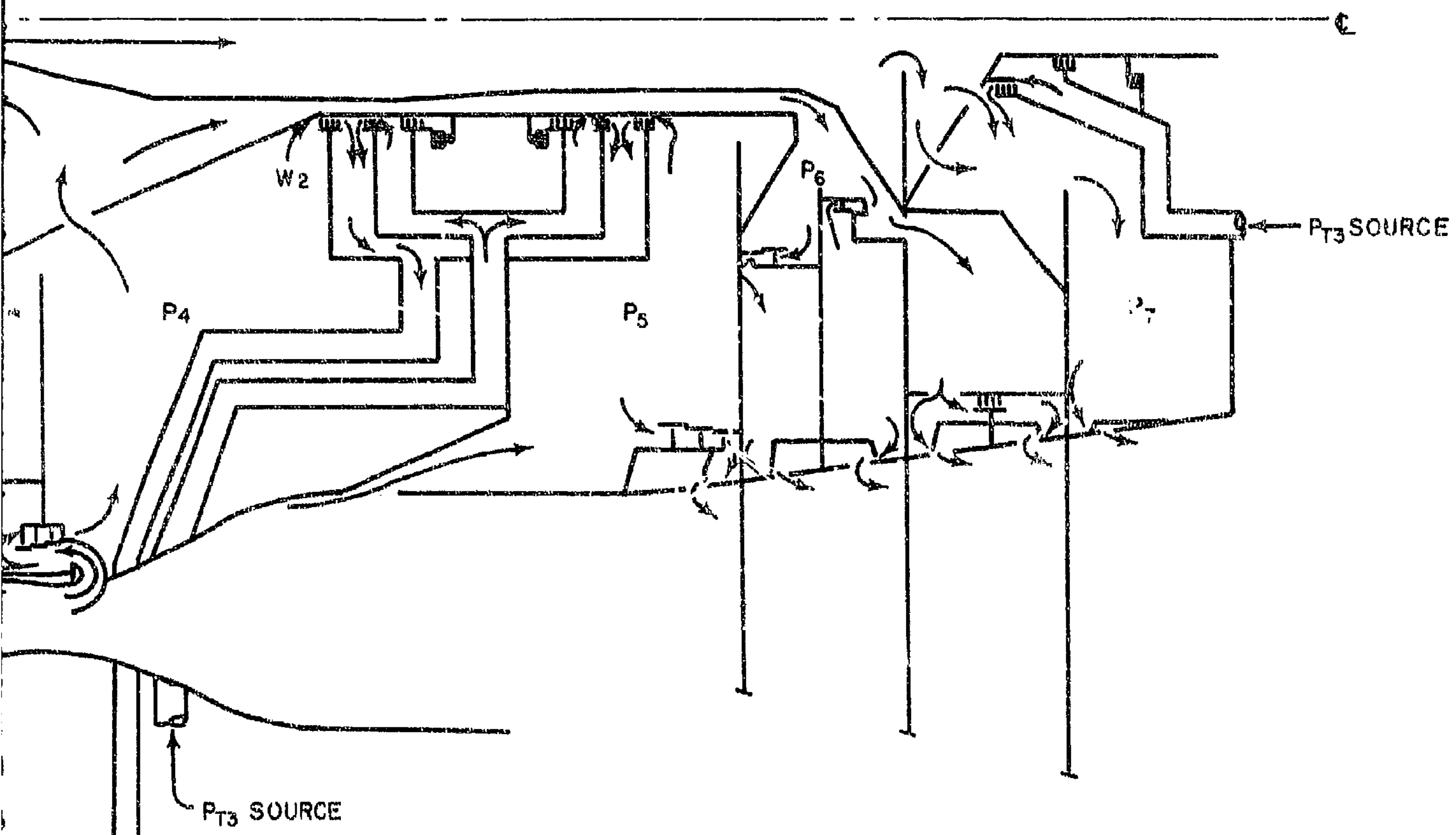

DESIGN PT	THRUST HIGH ROTOR	THRUST LOW ROTOR
MN = 0.7 SL	-7000	+15,000
MN = 1.2 45,000 FT	-2000	+ 4500
MN = 2.7 65,000 FT	-6000	+ 2000

2

THRUST BALANCE AND FLOW SCHEMATIC - SYSTEM B

Figure 2A-228

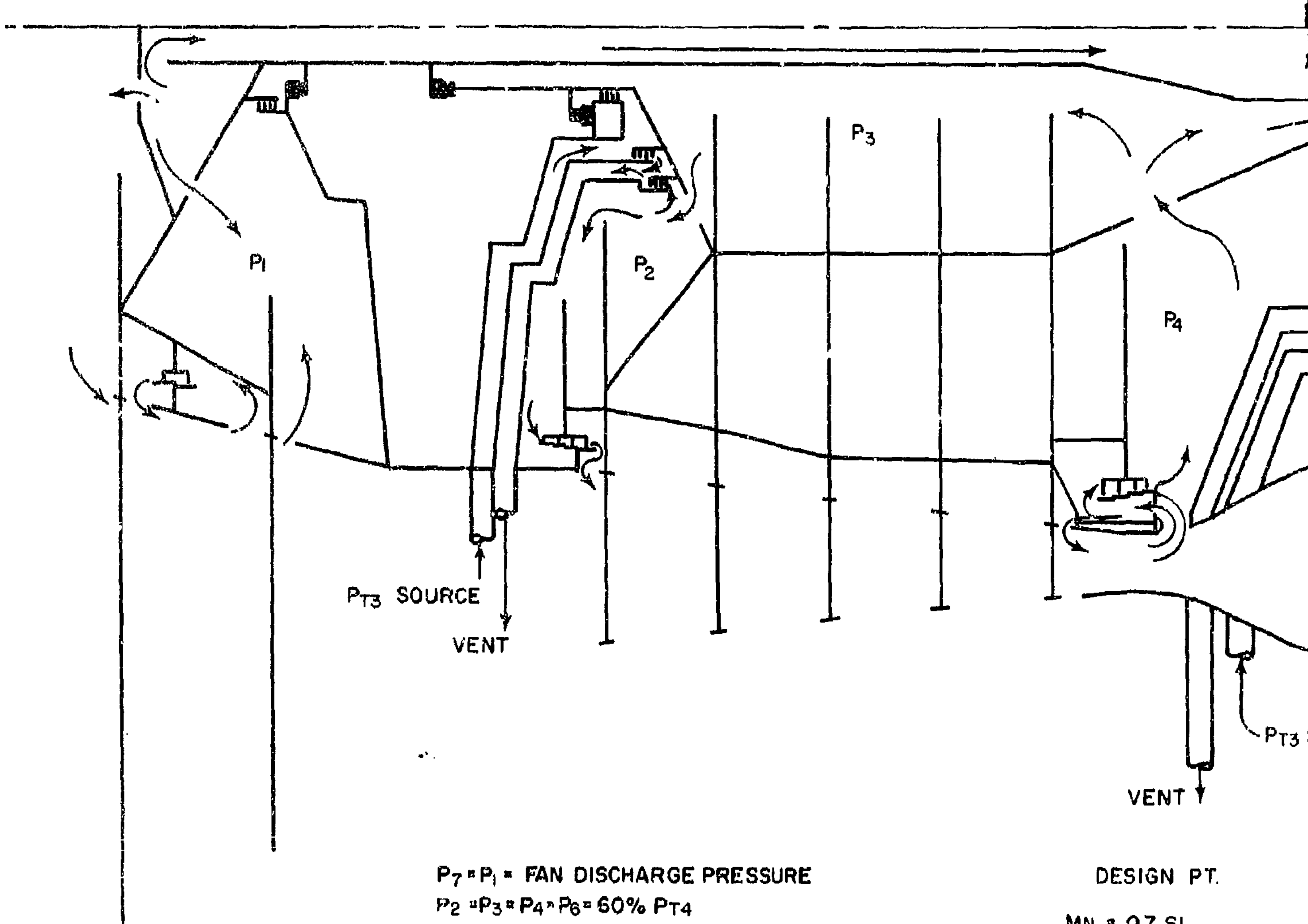

$P_7 = P_1 =$ FAN DISCHARGE PRESSURE
$P_2 = P_3 = P_4 = P_6 = 60\% \ P_{T4}$
$P_5 = 90\% \ P_{T4}$

DESIGN PT.

MN = 0.7 SL
MN = 1.2 45,000 FT
MN = 2.7 65,000 FT

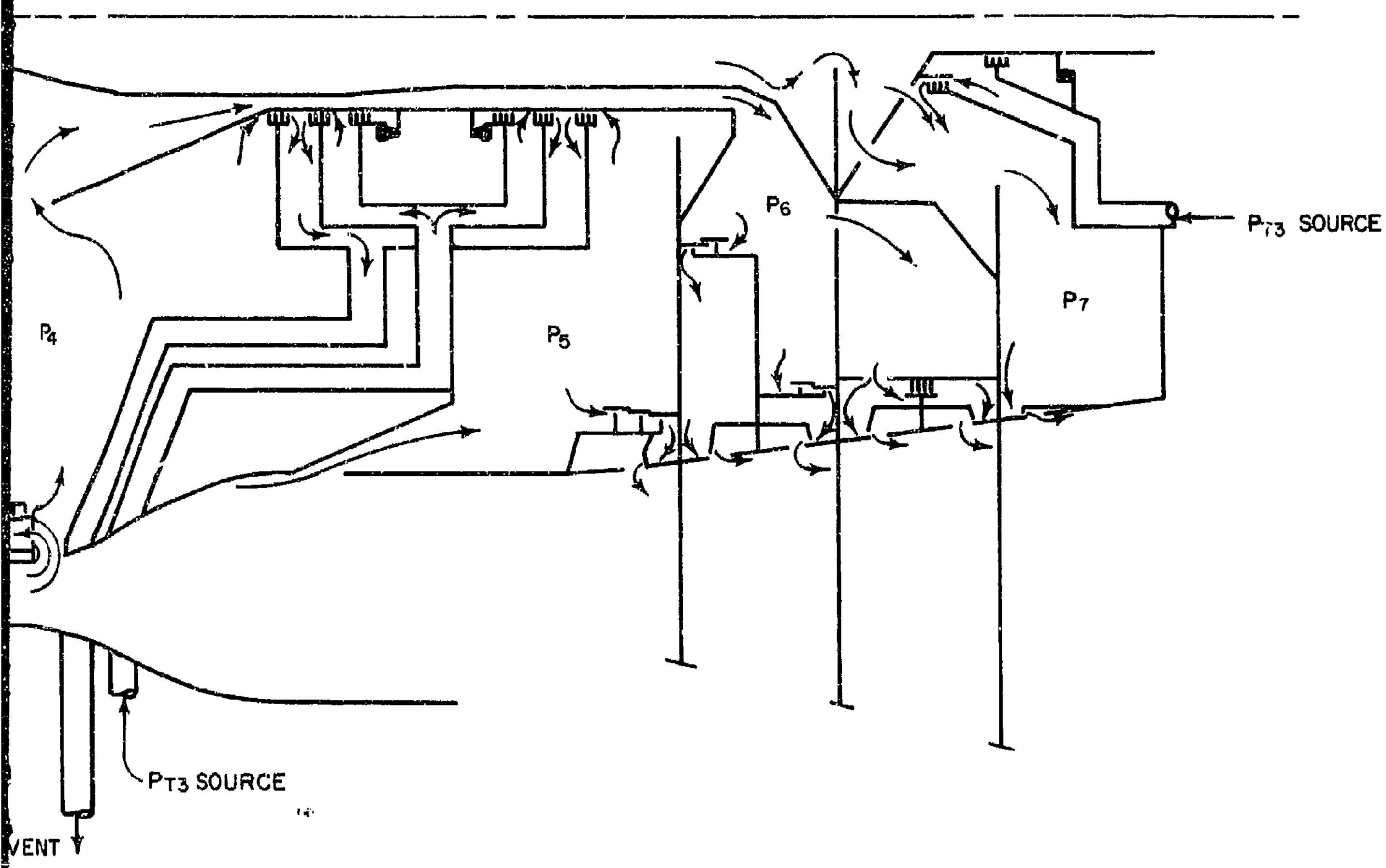

	THRUST	
IGN PT.	HIGH ROTOR	LOW ROTOR
.7 SL	7000	12,000
.2 45,000 FT	2000	2000
.7 65,000 FT	6000	5000

THRUST BALANCE AND FLOW SCHEMATIC - SYSTEM C

Figure 2A-229

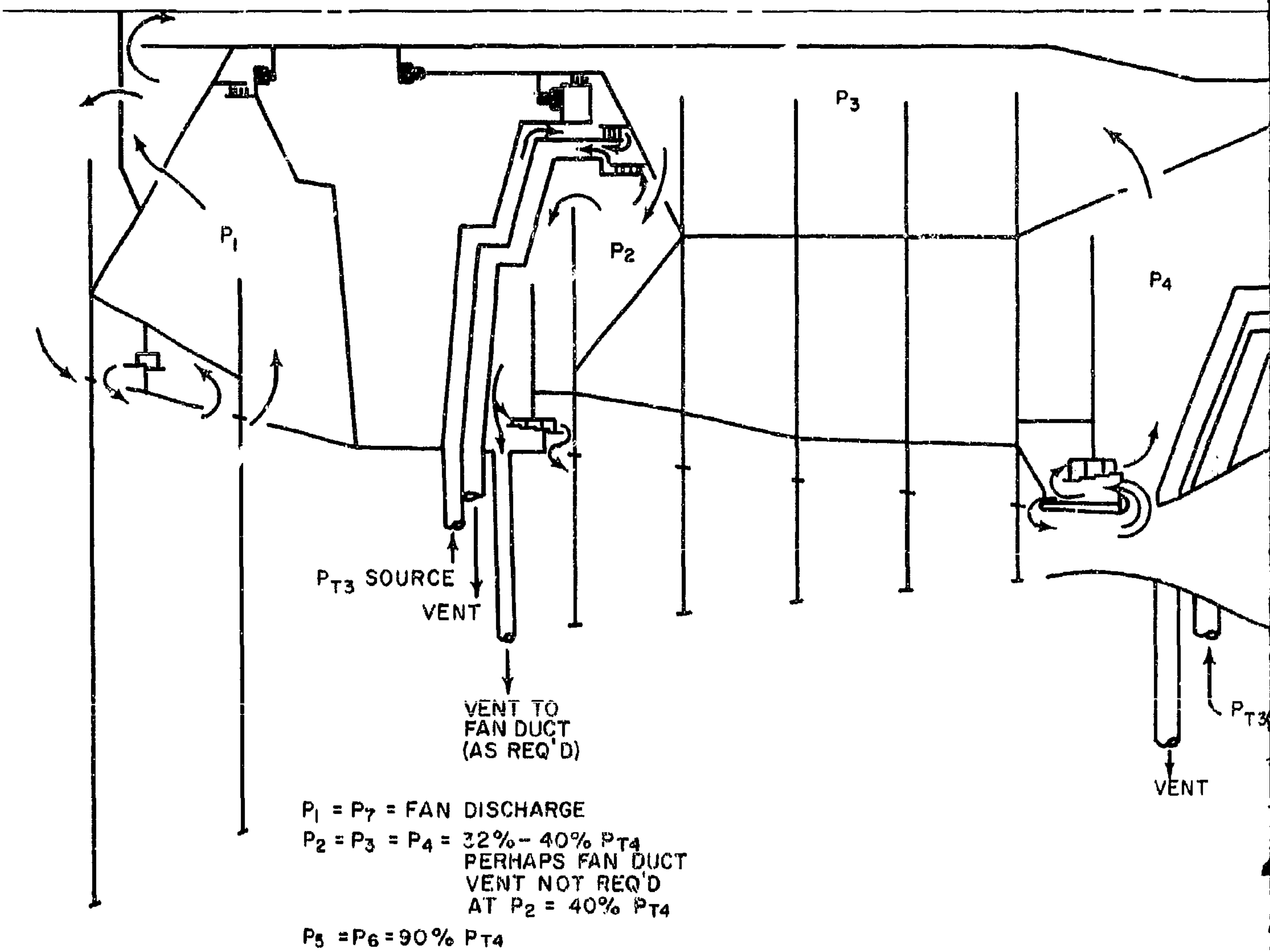
P3
P1
P2
P4
PT3 SOURCE
VENT
VENT TO
FAN DUCT
(AS REQ'D)
PT3
VENT
P1 = P7 = FAN DISCHARGE
P2 = P3 = P4 = 32%– 40% PT4
PERHAPS FAN DUCT
VENT NOT REQ'D
AT P2 = 40% PT4
P5 = P6 = 90% PT4

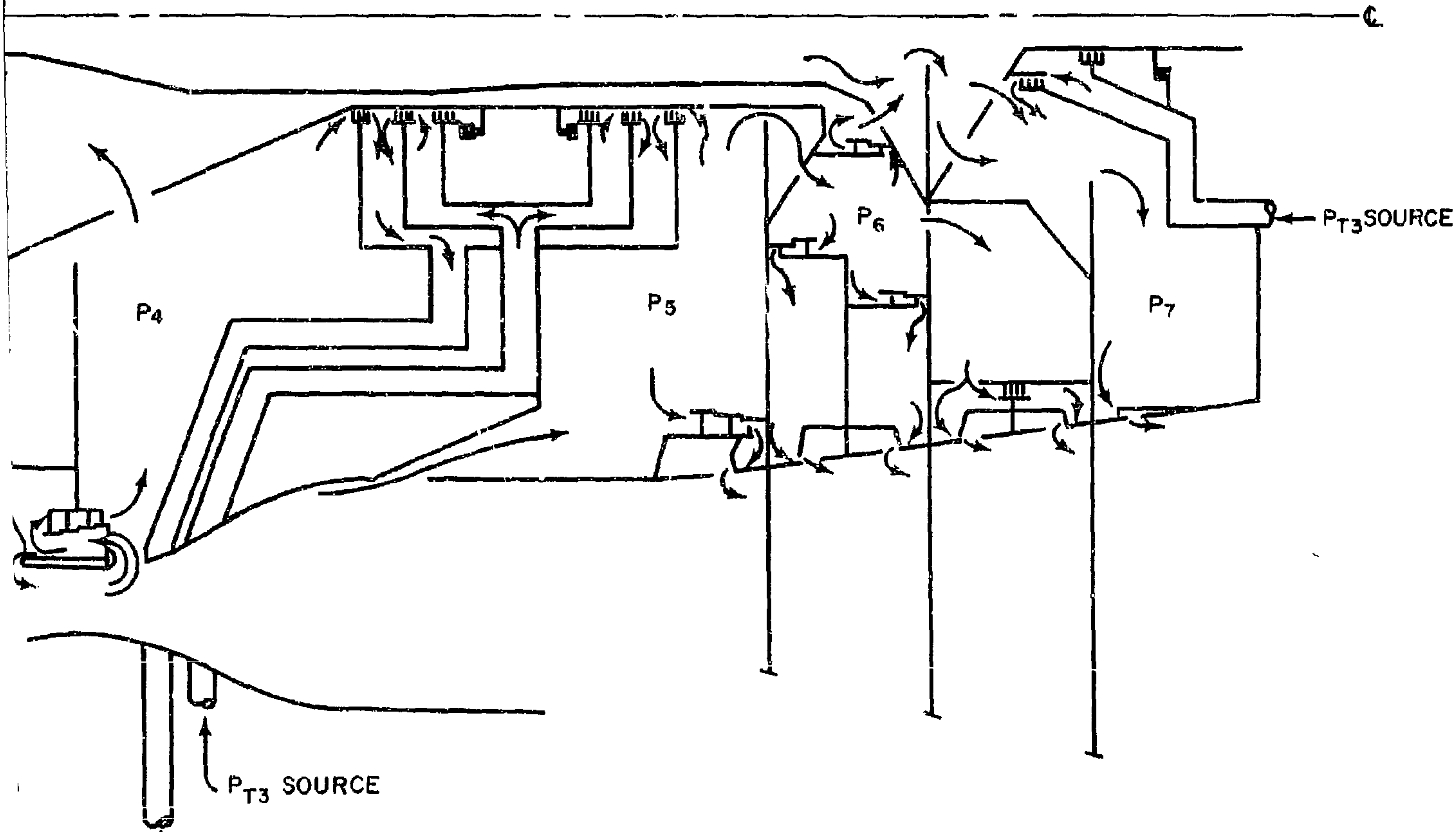

DESIGN PT	THRUST HIGH ROTOR	LOW ROTOR
M_N = 0.7 S L	7000	12,000
M_N = 1.2 45,000	2000	2000
M_N = 2.7 65,000	6000	5000

2

THRUST BALANCE AND FLOW SCHEMATIC - SYSTEM D

Figure 2A-230

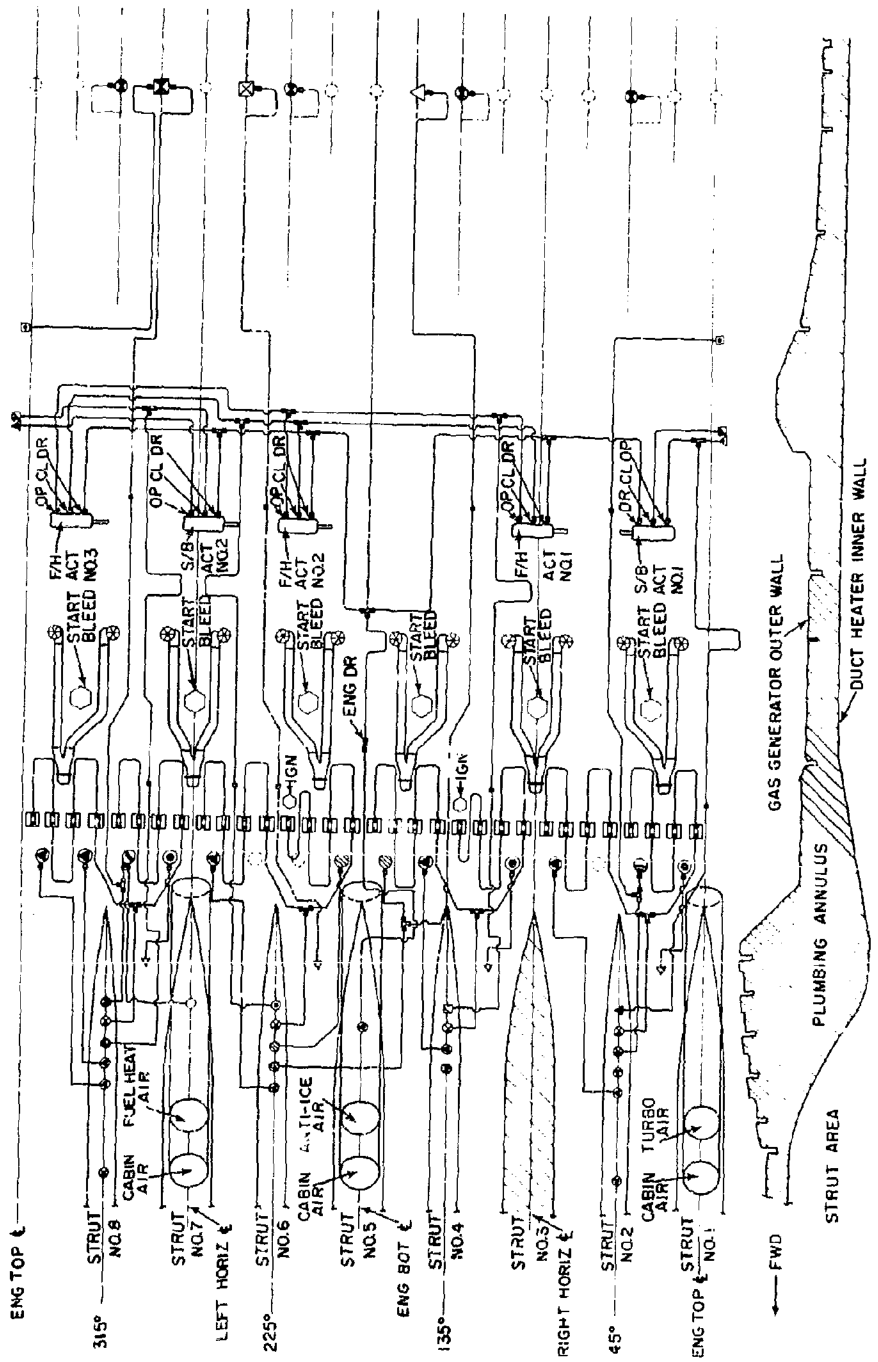

FLOW SYSTEM SCHEMATIC - FAN DUCT DIFFUSER STRUTS

Figure 2A-231

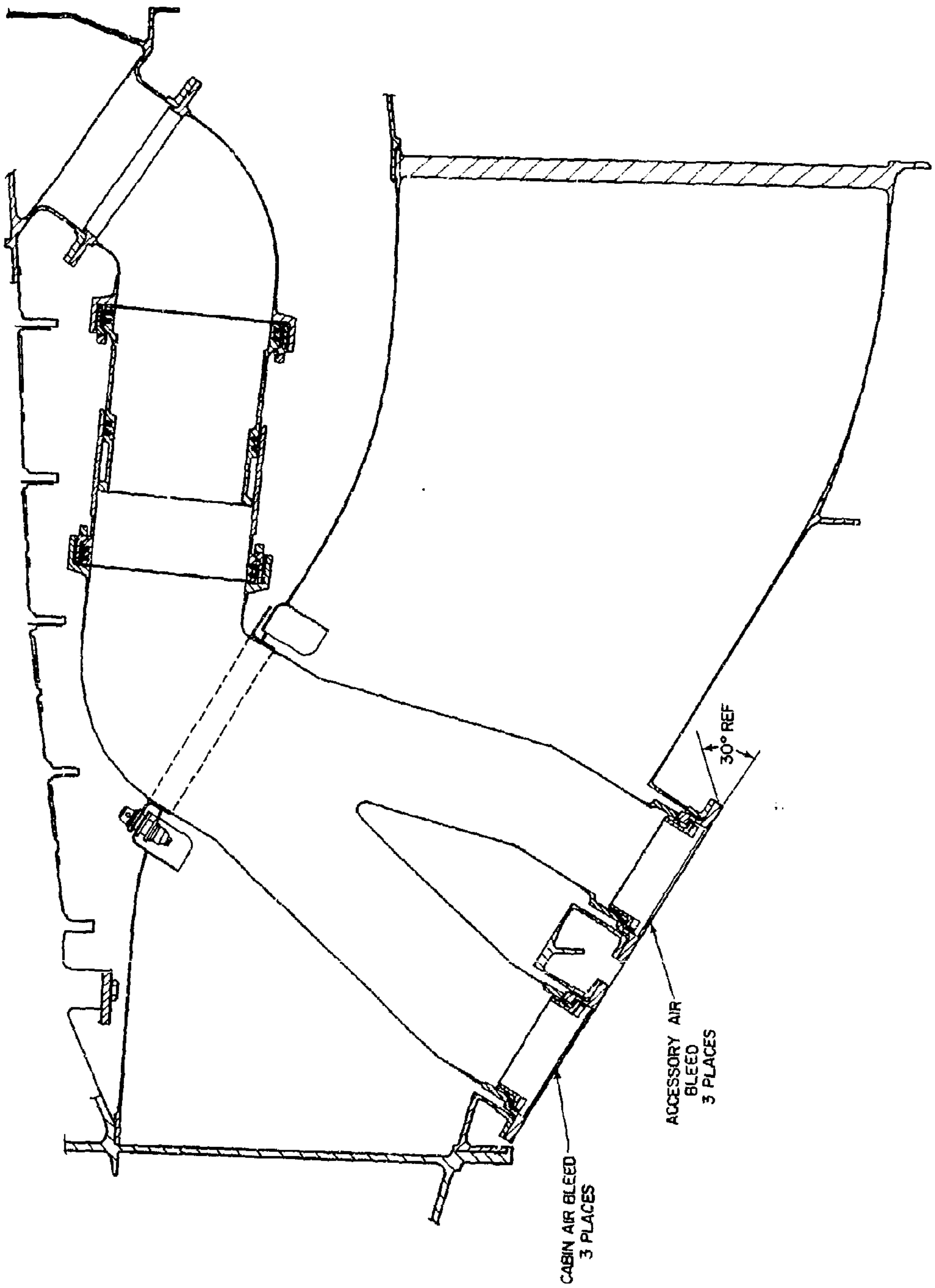

AIR BLEED FROM DIFFUSER CASE TO OUTER CASE

Figure 2A-232

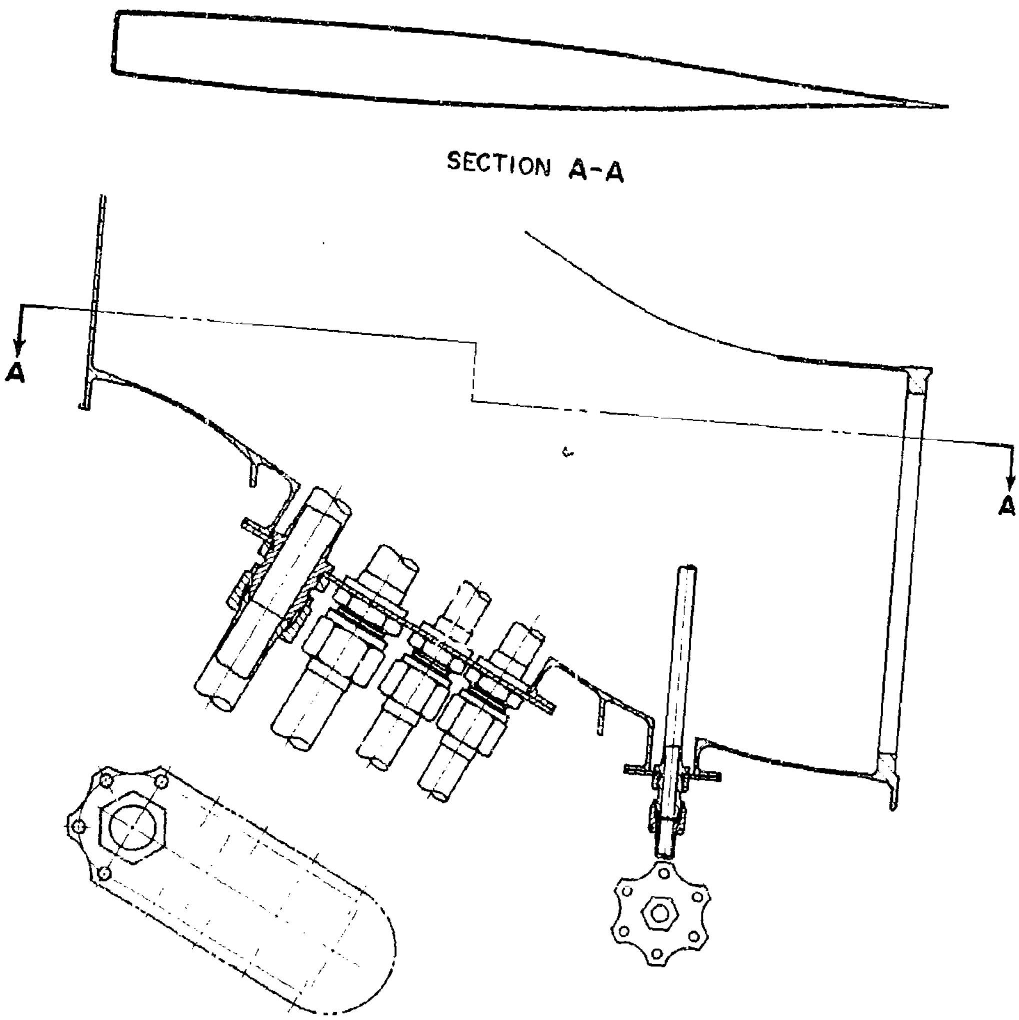

TYPICAL STRUT CONNECTIONS FOR LINES

TYPICAL STRUT CONNECTIONS FOR LINES

Figure 2A-233

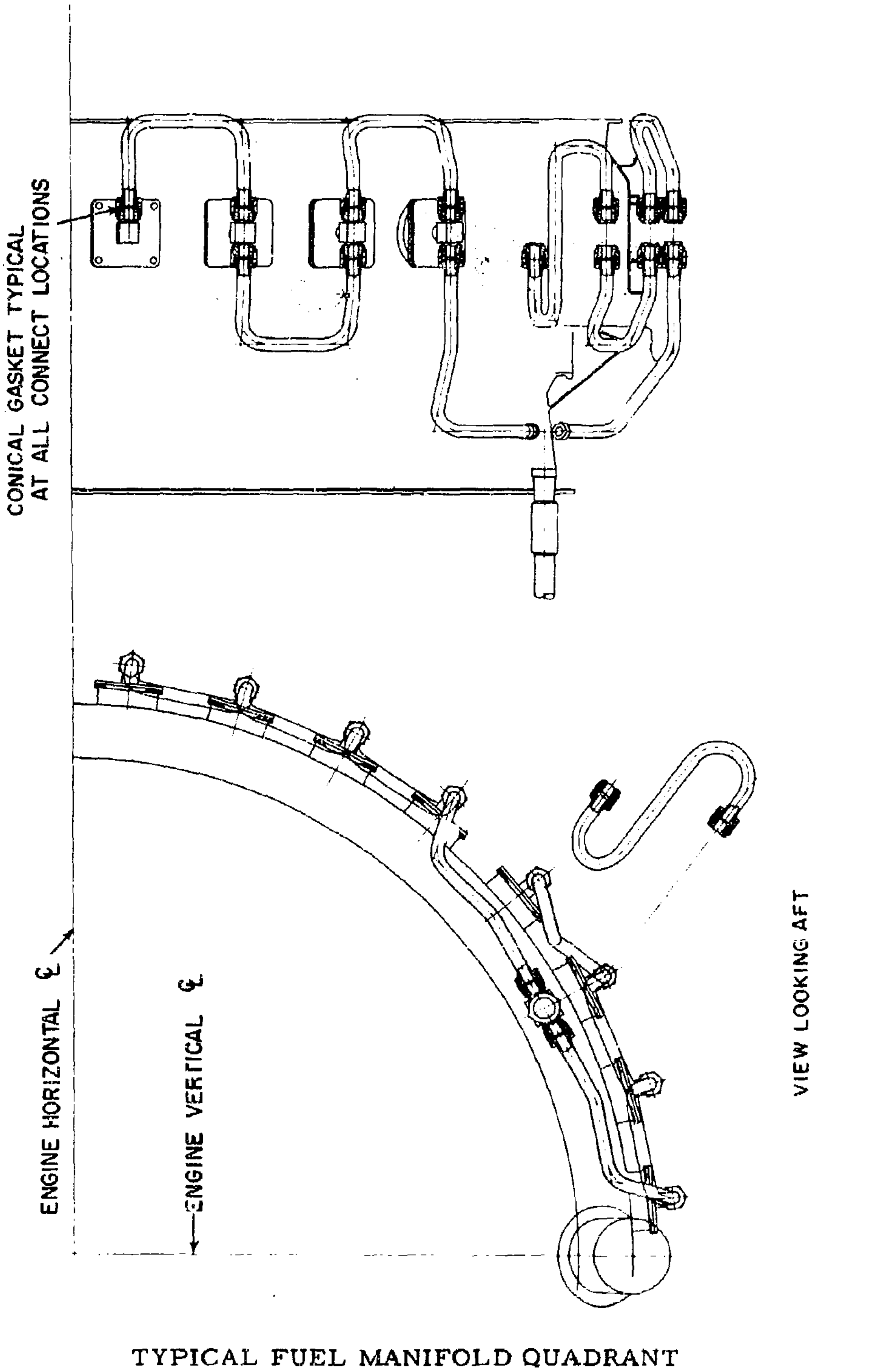

TYPICAL FUEL MANIFOLD QUADRANT

Figure 2A-234